NASA SP-393

THE STUDY OF COMETS

Part 2

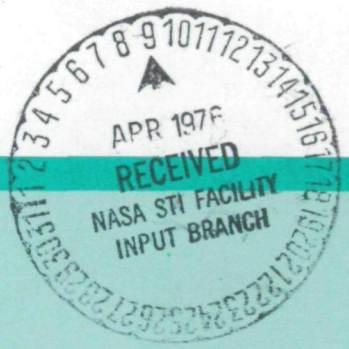

A conference held at
GODDARD SPACE FLIGHT CENTER
Greenbelt, Maryland
October 28–November 1, 1974

NATIONAL AERONAUTICS AND SPACE ADMINISTRATION

NASA SP-393

THE STUDY OF COMETS

Part 2

The Proceedings of IAU Colloquium No. 25,
Co-Sponsored by COSPAR,
and held at Goddard Space Flight Center,
Greenbelt, Maryland, October 28–November 1, 1974

Edited by:

B. Donn, *Goddard Space Flight Center*
M. Mumma, *Goddard Space Flight Center*
W. Jackson, *Howard University*
M. A'Hearn, *University of Maryland*
R. Harrington, *U.S. Naval Observatory*

Scientific and Technical Information Office 1976
NATIONAL AERONAUTICS AND SPACE ADMINISTRATION
Washington, D.C.

For sale by the Superintendent of Documents,
U.S. Government Printing Office, Washington, D.C. 20402

CONTENTS

CONTENTS (Continued)

CONTENTS (Continued)

CONTENTS (Continued)

CONTENTS (Continued)

CONTENTS (Continued)

CONTENTS (Continued)

A CONTINUING CONTROVERSY: HAS THE COMETARY NUCLEUS BEEN RESOLVED?

Zdenek Sekanina

I. COMETARY ACTIVITY AT LARGE HELIOCENTRIC DISTANCES

Barnard (1891) appears to have been the first to recognize the significance of systematic observations of comets at large distances from the sun. His successful tracing of two 1889 comets to heliocentric distances over 5 and even 6 a.u. caused him to notice that some of the short-period comets might be within the reach of the Lick Observatory's 36-inch refractor throughout their entire orbits around the sun. Although it is clear nowadays that the short-period comets would be a good deal fainter at comparable distances than the two nearly parabolic comets referred to by Barnard, his original idea proved basically correct, except for the necessity of using photographic plates. Periodic Comet Encke was probably detected near aphelion during Barnard's lifetime, in September 1913 (Barnard 1914a; Marsden and Sekanina 1974). Undisputed images of the comet just several days off aphelion were obtained in 1972 (Roemer 1972; McCrosky and Shao 1972).

Barnard's emphasis on the observation of distant comets stemmed primarily from his apprehension of the importance of precise positional determinations at large heliocentric distances for orbital studies. This attitude completely prevailed until the mid-20th century, although interest in the physical processes in comets at large distances emerged from time to time, usually in connection with a discovery of a peculiarly behaving comet far from the sun.

A study of the tails of two distant comets by Osterbrock (1958) was a significant step forward, primarily because it showed that the two comets, Baade 1955 VI and

Haro-Chavira 1956 I, behaved in the same way and therefore were not cases of yet other exceptional objects (such as, e.g., P/Schwassmann-Wachmann 1; or, a few years after the two comets, Humason 1962 VIII). Indeed, Roemer (1962), in her excellent paper reviewing the progress in the study of physical processes in comets at large heliocentric distances, pointed out that tails of the type displayed by the two comets observed by Osterbrock are rather common among the distant comets and that these comets have still other characteristic properties. I have recently interpreted Osterbrock's results (Sekanina 1973) to indicate that new comets on the incoming branch of their orbit show definite signs of a surprisingly high activity at distances up to about 15 a.u. or more, and that substances that vaporize from the comets at the required rates at such large distances must be equivalent to or more volatile than solid methane. This information is derived unambiguously from the dynamics of the rather heavy particles – most probably "dirty" icy grains – that constitute the tails and heads of the distant comets and that are also responsible for the comets' pure reflection-type spectra, such as the one observed by Walker (1958) in Comet Baade.

II. LARGE-SCALE PHOTOGRAPHS OF COMETS FAR FROM THE SUN

Independent evidence on the significant activity of many – and not only new – comets at large heliocentric distances comes from large-scale photographs. They show that a number of comets display definite traces of a coma at distances up to 8 a.u.; the image of Comet Stearns 1927 IV (which was by no means a new comet) was still diffuse at a record distance of 11 a.u. (Van Biesbroeck 1933). Furthermore, it is not difficult to demonstrate that the actual solid nucleus is not observed even on plates on which the cometary image looks essentially stellar. In the following, we use the photographic

"nuclear" magnitudes by Roemer whenever available, both because they are internally consistent and because they are generally fainter and therefore, it is believed, closer to the brightness of the actual nucleus than are the nuclear magnitudes by any other observer.

As an example of the observed variations in the nuclear magnitudes with heliocentric distance, we have plotted in Fig. 1 the light curves of two new comets of large perihelion distance observed by Roemer (Jeffers 1956; Roemer 1956; Roemer and Lloyd 1966). If the cometary images referred to the solid nucleus, their brightness should, of course, be inversely proportional to the square of the heliocentric distance. Meanwhile, however, at distances r from the sun ranging from 4.6 to 6.1 a.u., Comet Humason 1959 X – described by Roemer as essentially stellar, nearly stellar, or sharply condensed on most plates – basically followed a r^{-4} law. Comet Haro-Chavira 1956 I also fitted a r^{-4} law after perihelion (at distances of 5.6 to 7.8 a.u.), while the preperihelion observations showed the comet to be substantially brighter and suggested that it may have actually started fading intrinsically even before reaching perihelion. The r^{-2} law is also totally incompatible with Roemer's postperihelion nuclear magnitudes for Comets Baade 1955 VI (r^{-3} law between 3.9 and 7.8 a.u.), Wirtanen 1957 VI (r^{-6} for the primary nucleus between 4.6 and 7.3 a.u. and r^{-4} for the secondary nucleus from 4.6 to 6.9 a.u.), and Gehrels 1971 I (r^{-4} between 5.4 and 7.1 a.u.). The first of these three comets was new, the second was most probably new, and the third was positively not new (Marsden and Sekanina 1973).

In a rather surprising contrast to Roemer's nuclear magnitudes, Van Biesbroeck's (1930a, 1933) considerably brighter estimates of the "total" magnitude of the above-mentioned Comet Stearns did follow a r^{-2} law except in the immediate neighborhood of

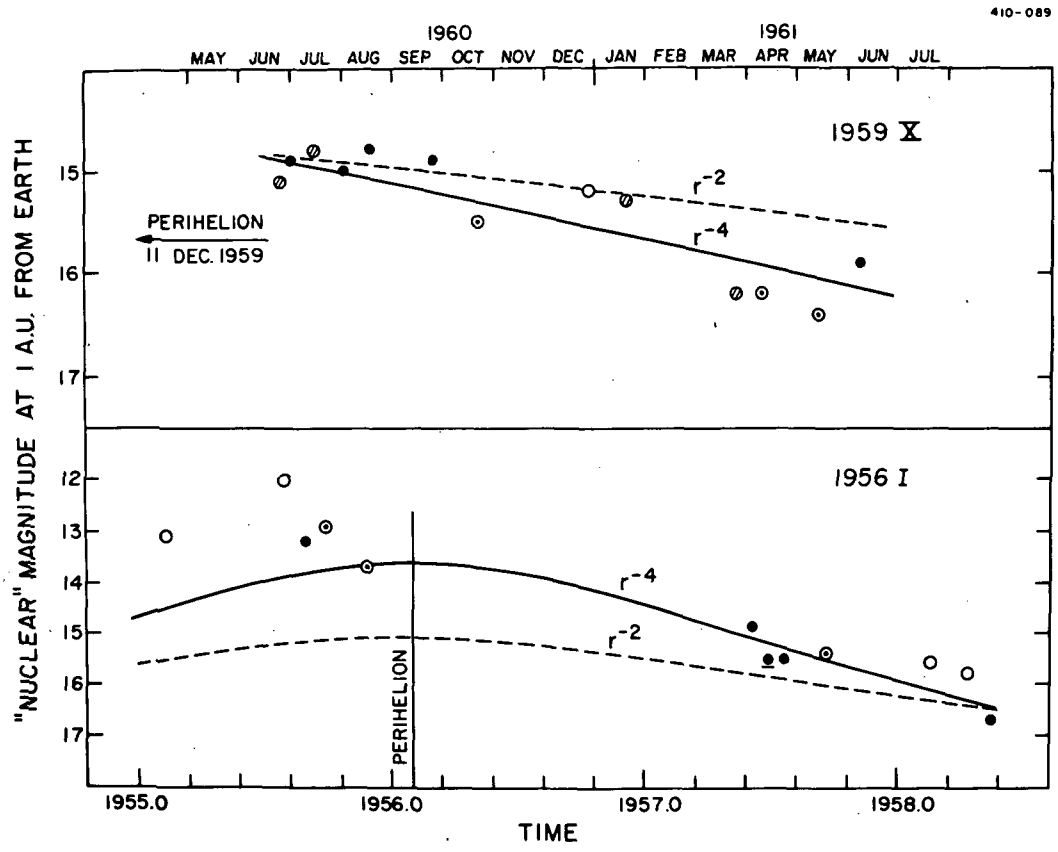

Fig. 1. "Nuclear" magnitudes by Roemer of Comets 1959 X and 1956 I, reduced to a unit geocentric distance, versus time. Observations before 1956 were made with the 36-inch Crossley refractor of the Lick Observatory, and those after 1956, with the 40-inch Ritchey-Chrétien reflector of the Flagstaff Station of the U.S. Naval Observatory. Observations with the 20-inch Carnegie astrograph of the Lick Observatory have not been used here, in order to avoid a possible instrumental effect. The various symbols correspond to Roemer's description of the cometary image on plates: underlined circle – stellar image; solid circles – practically or essentially or nearly stellar image; shaded circles – practically no coma, sharply or strongly condensed image; circled dots – well-condensed or condensed image, nuclear condensation; open circles – other description, usually mentioning the presence of a coma, or no comment on the image.

perihelion (Fig. 2). It appears, therefore, that neither an essentially star-like appearance nor a r^{-2} brightness law alone guarantees that the solid nucleus has actually been resolved.

Recent nuclear magnitude estimates of Comet Kohoutek 1973f by Roemer from her large-scale plates suggest that even the simultaneous presence of a practically stellar image and of the inverse-square power law at large heliocentric distances does not imply the detection of the solid nucleus. Preperihelion photographs of the comet at distances more than 2 a.u. from the sun (Roemer 1973a, b) show the comet to be nearly stellar, and Roemer's nuclear magnitudes fit the inverse-square power law with a precision better than $\pm 0.^{m}2$. Yet a postperihelion plate at 2.5 a.u. from the sun (Roemer 1974) shows that the nucleus is 3 magnitudes fainter intrinsically than it was before perihelion (see Table I for details).

The activity of comets at large heliocentric distances and the associated bias in the reported nuclear magnitudes have a profound effect on the determination of the sizes and reflectivities of cometary nuclei; this problem will be discussed in Sections IV and V.

III. EVAPORATION OF COMETARY NUCLEI

Delsemme (1972) pointed out that the empirical law used by Marsden (1969) for the nongravitational acceleration in the motion of P/Comet Schwassmann-Wachmann 2 strongly resembles the vaporization curve of water snow, derived from the steady-state equation at the cometary surface. Since the vaporization flux is obtained from

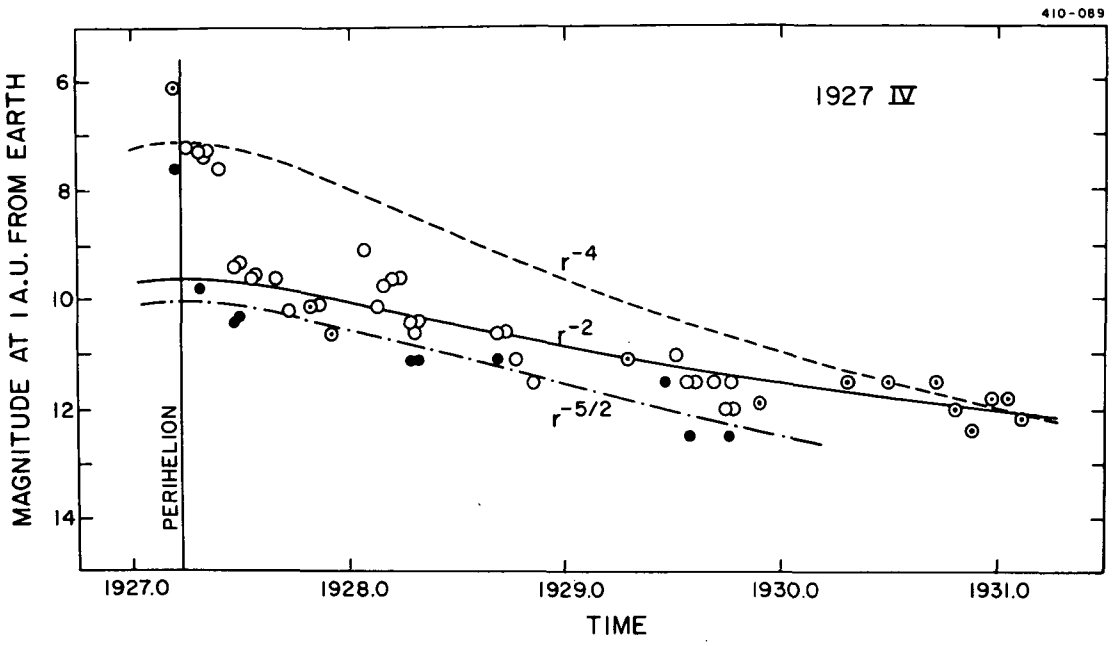

Fig. 2. "Total" and "nuclear" magnitudes of Comet 1927 IV, reduced to a unit geocentric distance, versus time. The observations were made by Van Biesbroeck at the Yerkes Observatory: open circles – total visual magnitudes with the 40-inch refractor; circled dots – total photographic magnitudes with the 24-inch reflector; solid circles – nuclear magnitudes, all visual except for the preperihelion one, which is photographic. The observed nucleus was seldom described as star-like in appearance, and the comet's image was still diffuse in 1931.

Table 1
"Nuclear" magnitudes of Comet Kohoutek 1973*f* (observations by Roemer 1973a, b, 1974).

Date	Location in Orbit	Distance from Sun (a.u.)	Phase Angle	Nuclear Magnitude*			Description
				No phase effect	Lambert phase law	Moon's phase law	
1973 Apr. 4	before perihelion	4.4	12°	10.7	10.7	10.4	nearly stellar condensation in trace of coma
Apr. 28	before perihelion	4.2	14	10.9	10.9	10.6	sharply condensed nucleus
Sept. 29	before perihelion	2.1	13	10.6	10.6	10.3	nearly stellar nuclear condensation
1974 Apr. 26	after perihelion	2.5	14	13.7	13.7	13.4	

*Reduced to unit heliocentric and geocentric distances by the inverse-square power law.

the equation numerically, and since no analytical form is available, we suggested the following empirical formula to fit the variations in the normalized vaporization rate with heliocentric distance r (Marsden et al. 1973):

$$g(r) = \alpha \left(\frac{r}{r_0}\right)^{-m} \left[1 + \left(\frac{r}{r_0}\right)^{n}\right]^{-k} , \qquad (1)$$

where m, n, k, and r_0 are parameters of the vaporization curve and α is the normalizing factor.

Although the above expression was originally intended to fit a particular vaporization curve, a study of a large number of vaporization curves for a rapidly rotating nucleus (constant vaporization flux over the nuclear surface) later revealed remarkable properties of formula (1):

A. The exponents m, n, and k are practically independent of the absorptivity κ of the cometary nucleus for solar radiation, its emissivity ϵ for reradiation, and the latent heat of vaporization L.

B. The scaling distance r_0 (in a.u.) is the following simple function of κ, ϵ, and L:

$$r_0 = 370\ L^{-2}\ \kappa^{1/2}\ \epsilon^{-0.56} , \qquad (2)$$

where L is in kcal mole^{-1} (L_{H_2O} is taken equal to 11.4 kcal mole^{-1}).

The above results should be complemented by three additional remarks:

C. Formula (1) also applies to the average vaporization rate from a nonrotating nucleus (with no evaporation from the dark side) if r_0 from equation (2) is multiplied by a factor of $2^{1/2}$, and to the vaporization rate from the subsolar point of the nonrotating nucleus if r_0 is multiplied by a factor of 2.

D. A very important relation has now been found to exist between the fraction of the solar energy absorbed by the nucleus that is spent for snow vaporization (E_{vap}) and the fraction that is reradiated back to space (E_{rad}). Analysis of a large number of vaporization curves indicates that the ratio E_{rad}/E_{vap} is a virtually exclusive function of the rate of variation in the vaporization flux with heliocentric distance, thus depending only on the ratio r/r_0. Inspection of these vaporization curves indicates that the logarithmic gradient w of the vaporization flux Z,

$$w = - \frac{d(\ln Z)}{d(\ln r)} \quad , \tag{3}$$

is related to E_{rad}/E_{vap} by

$$\frac{E_{rad}}{E_{vap}} = 0.604\ (w - 2)^{1.05} \tag{4}$$

for $w \lesssim 4$, and by

$$\frac{E_{rad}}{E_{vap}} = 0.522\ (w - 2)[1 + 0.105\ (w - 2)] \tag{5}$$

for $w \lesssim 8$. This remarkable relationship is actually a logical extension of the physical interpretation of the scaling distance r_0 submitted by Marsden et al. (1973).

E. The logarithmic gradient w calculated from the empirical formula (1) converges to m + nk when $r \gg r_0$, whereas the steady-state equation indicates that for $r \gg r_0$, gradient $w \sim r^{1/2}$ and therefore diverges. Thus it is preferable to replace g(r) at distances substantially exceeding r_0 by

$$h(r) = \beta \exp\left(-br^{1/2}\right) \quad , \tag{6}$$

where

$$b = \left(\frac{\ell\sigma\epsilon}{Q\kappa}\right)^{1/4} \left(\frac{L}{R_g}\right) \quad , \tag{7}$$

in which σ is the Stefan-Boltzmann constant, Q is the solar constant, R_g is the universal gas constant, and ℓ equals 4 for the rapidly rotating nucleus and 2 for a nonrotating nucleus. If formula (6) is used in relative terms and in conjunction with formula (1), the normalizing factor β can serve to adjust h(r) so that it matches g(r) at a particular distance $r_1 > r_0$, for which

$$\frac{d}{d(\ln r)} [\ln h(r)]_{r_1} = \frac{d}{d(\ln r)} [\ln g(r)]_{r_1} \quad ; \tag{8}$$

h(r) then replaces g(r) at $r > r_1$, and

$$\beta = g(r_1) \exp\left(br_1^{1/2}\right) \quad . \tag{9}$$

If formula (6) is used in absolute terms, β is determined by the vapor pressure of the vaporizing substance.

IV. THE DELSEMME-RUD METHOD

An ingenious method has recently been proposed by Delsemme and Rud (1973) to separate the cross-sectional area S of a cometary nucleus from its Bond albedo A_s for solar radiation. The vaporization cross section $(1 - A_s)S$ has been determined from the production rate of water at relatively small heliocentric distances on the assumption that water snow, the dominant component of cometary snows, controls the vaporization process at the nuclear surface. The vaporization cross section therefore also depends on the latent heat of vaporization of H_2O and on the intensity of the impinging solar energy. In their approach, however, it does not depend on the emissivity of the cometary nucleus for reradiation, because Delsemme and Rud have assumed that the radiative term of the steady-state equation can be neglected at the heliocentric distances under consideration ($\lesssim 0.8$ a.u.). The photometric cross section $A_s S$ has been established from Roemer's nuclear magnitudes (reduced to unit heliocentric and geocentric distances) and from a carefully discussed relation among the Bond albedo, the geometric albedo, and the phase law of the nucleus. Delsemme and Rud have thus obtained two equations, which can readily be solved for A_s and S:

$$(1 - A_s)S = c_1 \quad ,$$
$$A_s S = c_2 \quad . \tag{10}$$

Taking into account the systematic bias in the nuclear magnitudes of comets (Section II) and the generally not negligible contribution from E_{rad} (Section III), we can now modify Delsemme and Rud's formulas (10) as follows:

$$\pi\kappa R^2 = c_1 \left(1 + \frac{E_{rad}}{E_{vap}}\right) ,$$

$$\pi(1 - \kappa) R^2 = c_2 \times 10^{-0.4\Delta m} , \qquad (11)$$

where $R = (S/\pi)^{1/2}$ is the effective radius of the solid cometary nucleus, $\kappa = 1 - A_s$ (by definition), and $\Delta m > 0$ is the bias or contamination factor (in magnitudes) giving the difference between the actual magnitude of the nucleus and the nuclear magnitude by Roemer. We note that the E_{rad}/E_{vap} term produces an increase in both the nuclear radius R and the absorptivity κ (and, hence, a decrease in A_s), whereas the Δm factor implies an increase in κ but a decrease in R. We also remark that equation (11) contains four unknowns, κ (or A_s), R (or S), E_{rad}/E_{vap} (or, if a rotation model is specified, the emissivity ϵ, or the Bond albedo A_r, for reradiation), and Δm.

V. COMET BENNETT 1970 II

From a careful analysis of OAO-2 spectrometric and photometric observations of Comet Bennett, Keller and Lillie (1974) have recently concluded that the production rates of hydroxyl and atomic hydrogen are indeed consistent with the assumption that water controls the gas output at heliocentric distances ~1 a.u. They have also derived a production rate of water vapor from the nucleus of Comet Bennett of $(2.9 \pm 1.2) \times 10^{29}$ molecules s^{-1} at 1 a.u. and a variation in the production rate proportional to an inverse 2.3 ± 0.3 power of heliocentric distance between 0.77 and 1.26 a.u.

The new production rate compares very favorably with Delsemme and Rud's (1973) value of 4.4×10^{29} molecules s^{-1} at 0.8 a.u. from the sun, which was based on several investigations of hydrogen production only. At the same heliocentric distance, Keller and Lillie's determination gives 4.8×10^{29} with the $r^{-2.3}$ law and 4.5×10^{29} with the r^{-2} law used by Delsemme and Rud. The $r^{-2.3 \pm 0.3}$ law implies that $E_{rad}/E_{vap} = 0.17$ [see eq. (4)] with a lower limit of 0.0 and an upper limit of 0.35. Equations (11) now contain three unknowns and can be solved for κ and R with the bias factor as a parameter.

We have retained c_2, determined by Delsemme and Rud with the Lambert phase law, and used Keller and Lillie's results to derive the average value of $\pi\kappa R^2 = 19.3$ km^2, as well as its limits, 9.7 km^2 (for $E_{rad}/E_{vap} = 0$ and H_2O production of 1.7×10^{29} molecules s^{-1} at 1 a.u.) and 31.5 km^2 ($E_{rad}/E_{vap} = 0.35$ and H_2O production of 4.1×10^{29}). The dependence of the solution of equations (11) on Δm is exhibited in Fig. 3. The two corrections to κR^2 suggested by Delsemme and Rud have not been applied here, since they are rather uncertain and do not alter the results significantly. We note, however, that in their sum, they would tend to decrease both R and κ somewhat. [The corrections are, respectively, due to evaporation of volatile substances adsorbed on water snow (which increases c_1) and to the fact that water can be transported away from the nucleus not only by evaporation but also in the form of icy grains (which decreases c_1).]

Figure 3 also compares the solution of equations (11) with Delsemme and Rud's results and with the nuclear size derived by Sekanina and Miller (1973) from the photometric study of the type II tail of Comet Bennett.

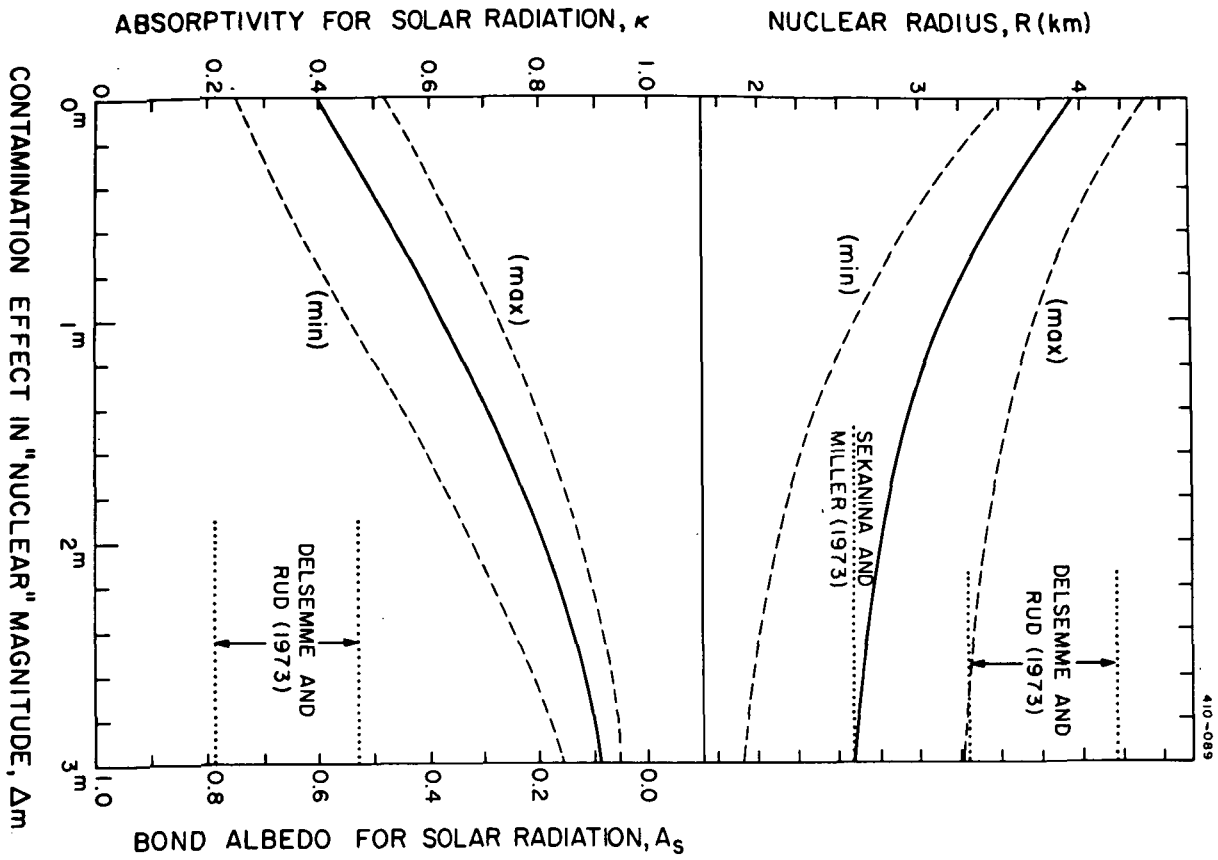

Fig. 3. Comet Bennett 1970 II. Nuclear radius (top) and surface absorptivity and Bond albedo for solar radiation (bottom) versus the contamination effect in the nuclear magnitude Δm (i.e., the difference between the magnitude of the actual nucleus and the observed nuclear magnitude). The dashed curves give the upper and lower limits. The results by Delsemme and Rud (1973) and by Sekanina and Miller (1973) are shown for comparison.

The high albedo A_s, deduced by Delsemme and Rud, appears to be incompatible with Whipple's (1950) "dirty-snowball" model of the cometary nucleus in general and with the high contents of dust observed in Comet Bennett in particular. It came as a surprise even to the authors themselves. And Keller and Lillie (1974) comment that their results would be more consistent with a lower albedo and that Delsemme and Rud may have underestimated the effect of dust.

While this controversy may lead to other interpretations in the future, once production rates of water are known for a greater number of comets, the present discussion of equations (11) indicates that in the case of Comet Bennett, we can bring A_s from over 0.6 down to 0.1 or 0.2 if we accept that the brightness of the actual solid nucleus is some 2 to 3 magnitudes below the level measured by Roemer's nuclear magnitudes. At the same time, allowance for this effect also cuts the nuclear radius from nearly 4 km down to less than 3 km and thus brings it into considerably better agreement with the Sekanina-Miller determination. We note that this determination implies an H_2O production rate, which, according to Keller and Lillie, is in excellent agreement with the OAO observations.

The possibility of a 2- to 3-magnitude bias in Roemer's nuclear magnitudes cannot, in general, be excluded in light of the results of Section II. To be more specific, we list in Table II the nuclear magnitudes of Comet Bennett. The last three entries, used by Delsemme and Rud to calculate A_sS, are indeed very consistent with the inverse square law of light reflection. So is, however – at least when the Lambert phase law is applied – the first entry, which is affected by a significant contribution from the coma. This appears to remind us of Van Biesbroeck's observational series of Comet Stearns (Fig. 2).

Table II

"Nuclear" magnitudes of Comet Bennett 1970 II (postperihelion observations by Roemer; see Marsden 1971, 1972a).

Date	Distance from Sun (a.u.)	Phase Angle	Nuclear Magnitude*			Description
			No phase effect	Lambert phase law	Moon's phase law	
1970 June 1	1.6	29°	12.5	12.4	11.7	not clear photometric resolution from coma
July 2	2.0	23	12.0	11.9	11.4	central condensation embedded in coma
July 27	2.4	22	11.8	11.7	11.2	sharply condensed
Sept. 26	3.2	18	12.6	12.5	12.1	rather sharp, faint coma
Nov. 25	3.9	14	12.5	12.5	12.2	sharp, nearly stellar, trace of coma
1971 Jan. 20	4.5	13	12.4	12.4	12.1	well condensed, possibly trace of coma

*Reduced to unit heliocentric and geocentric distances by the inverse-square power law.

The Lambert phase law is probably a more realistic approximation than is the moon's phase law even for a dust-rich surface of an icy-conglomerate nucleus. Nevertheless, we point out that because the moon's law would imply a lower c_2 in equations (11), its effect would be identical with that of an additional Δm correction: Compared to the figures resulting from the Lambert law, the nuclear size would go down, whereas absorptivity κ would go up (and, hence, A_s down).

All the above considerations are independent of the adopted model of nuclear rotation. The emissivity of the nucleus for reradiation could be calculated only if the nuclear spin were known. For two adopted models, the rapidly rotating nucleus and the nonrotating nucleus, the emissivity ϵ is plotted versus Δm in Fig. 4. It turns out that ϵ is almost completely indeterminate, mainly because E_{rad} is very poorly known. (Note that $E_{rad} = 0$ is equivalent to $\epsilon = 0$.)

Comet Tago-Sato-Kosaka 1969 IX, also studied by Delsemme and Rud, has not been included here. The production rate of water for this comet has been assessed from the number density of OH, which itself is only an order-of-magnitude estimate (Code 1971). We therefore feel that $(1 - A_s)S$ is not known sufficiently well to justify the type of study explored in the case of Comet Bennett. It seems, however, that the law of variation in H_2O production with heliocentric distance, $r^{-2.9\pm0.2}$, may be reasonably well established for Comet Tago-Sato-Kosaka from the relative OH densities (Delsemme 1973). Then the ratio E_{rad}/E_{vap} near 0.9 a.u. from the sun comes out to be as high as 0.54 ± 0.12, which restricts the absorptivity for solar radiation to $\kappa \lesssim 0.6$ for a rapidly rotating nucleus ($A_s \gtrsim 0.4$) and to $\kappa \lesssim 0.3$ for a nonrotating nucleus ($A_s \gtrsim 0.7$). It also implies that emissivity ϵ must be near unity ($A_r \simeq 0$).

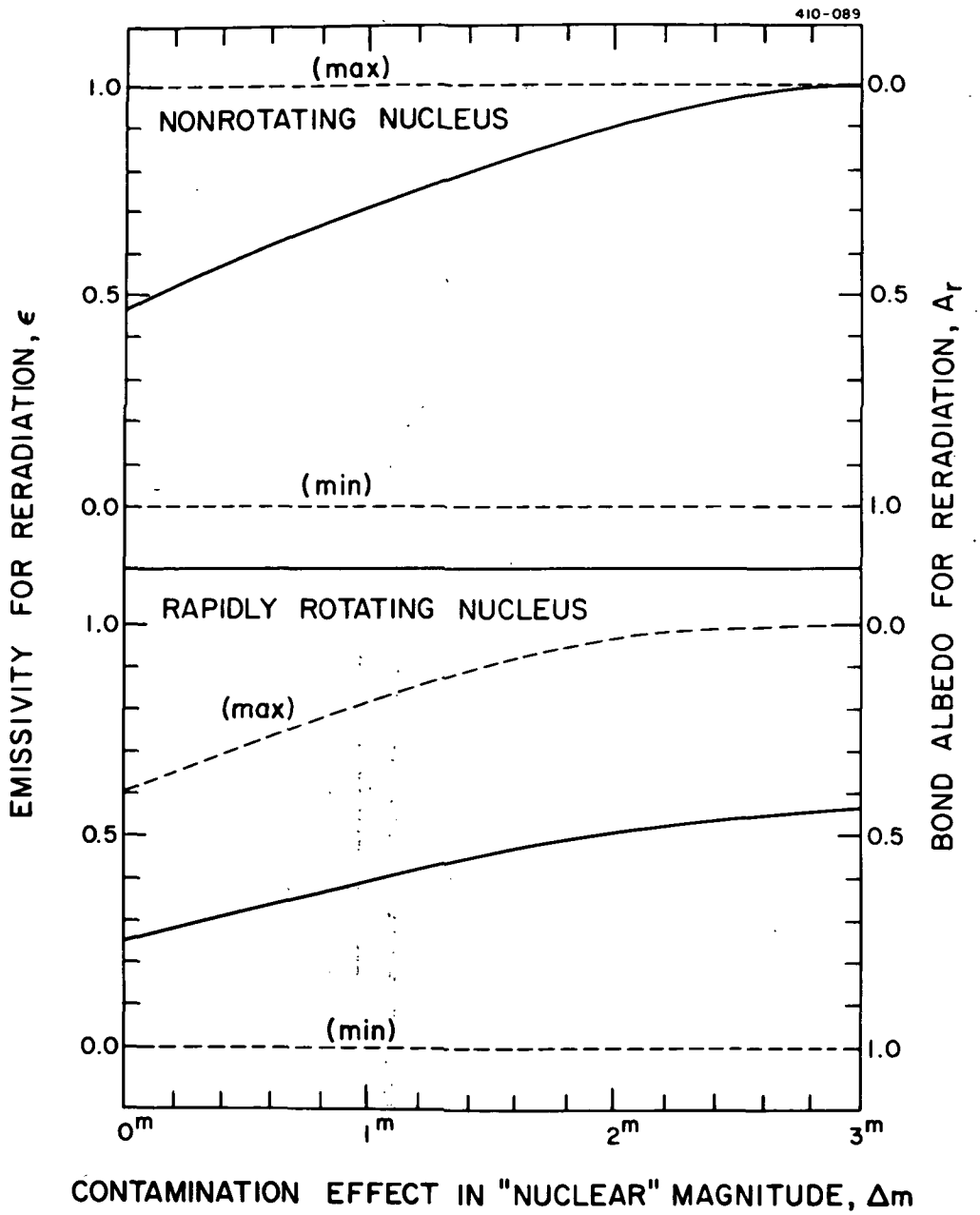

Fig. 4. Comet Bennett 1970 II. The surface emissivity and Bond albedo for reradiation from the nucleus versus the contamination effect in the nuclear magnitude Δm, on the assumption of a nonrotating nucleus (top) and a rapidly rotating nucleus (bottom). The probable upper and lower limits (dashed curves) indicate that the emissivity is, in either case, virtually entirely indeterminate.

Table III lists the nuclear magnitudes of Comet Tago-Sato-Kosaka reported by Roemer. When the Lambert phase law is applied, the observations suggest that the brightness of the nuclear condensation varies more slowly with heliocentric distance than required by the law of reflection. The last two entries, used by Delsemme and Rud to compute A_sS, are $0^m.6$ brighter than the first entry, which corresponds to 1.1 a.u. from the sun.

VI. ACTIVITY OF SHORT-PERIOD COMETS AT LARGE HELIOCENTRIC DISTANCES

Uncritical identification of the actual brightness of a solid cometary nucleus with nuclear magnitude can cause a severe misinterpretation of the evolution of short-period comets.

Kresák (1973) recently proposed a classification for nuclei of short-period comets, relying heavily on two basic models I recently formulated (Sekanina 1969, 1971, 1972a). The two, a core-mantle model and a coreless one, were postulated in order to interpret physically the systematic long-term variations in the magnitude of the nongravitational effects, which were established for a number of short-period comets by Marsden and his collaborators (for an updated table of nongravitational parameters, see Marsden et al. 1973).

Kresák found evidence that the nuclei of periodic comets captured by Jupiter from orbits well beyond 3 a.u. fade appreciably during a few revolutions after capture; he concluded that the fading is due to a decrease in the nuclear albedo and is associated

Table III

"Nuclear" magnitudes of Comet Tago-Sato-Kosaka 1969 IX (postperihelion observations by Roemer; see Marsden 1971).

Date	Distance from Sun (a.u.)	Phase Angle	Nuclear Magnitude*			Description
			No phase effect	Lambert phase law	Moon's phase law	
1970 Feb. 3	1.1	69°	15.0	14.3	13.1	condensed
Feb. 13	1.3	52	15.4 pv	15.0 pv	14.0 pv	well condensed
Mar. 7	1.6	37	14.3	14.1	13.3	nearly stellar
Apr. 6	2.1	26	13.8	13.7	13.1	sharply condensed, but not stellar
May 4	2.5	19	13.8	13.7	13.3	small, sharply condensed

*Reduced to unit heliocentric and geocentric distances by the inverse-square power law.

with the rapid removal of a thin envelope of high-reflectivity icy grains covering the massive core of dark meteoric material.

We point out that this hypothesis strongly contradicts the dynamical evidence based on a study of the nongravitational effects. P/Brooks 2, the most outstanding case in Kresák's Fig. 5 (showing a fading parameter), leads the population of short-period comets sorted by the magnitude of the nongravitational effects (see Table I of Marsden et al. 1973). Its mass loss inferred from the dynamical results comes out so very large that only the direct surface evaporation of the comet's snows – the most effective mechanism of gas production – gives theoretical mass-loss rates at least moderately consistent with the well-established observational data. A nucleus with the icy mantle just removed, such as Kresák suggested for P/Brooks 2 and similar comets, cannot supply the required production of gas, because a substantial portion of the solar radiation absorbed by the nucleus should be spent on heating the surface-insulating layer of meteoric material before any evaporation could commence. And even then, the production of gas, which would have to proceed by diffusion through the porous matrix, would barely be able to exert any detectable nongravitational effect at distances near or beyond 2 a.u.

The above reasoning also applies to P/Schwassmann-Wachmann 2, which Kresák does not classify as a recent incomer on account of Belyaev's (1967) orbital calculations suggesting that this comet was around before 1735. Marsden (1966, 1973a) does not, however, find any substantial changes in the comet's motion for at least 2 1/2 centuries before its capture in 1926. It appears, therefore, that no definite conclusion can be reached about the comet's orbital history by running its motion so long into the past.

The contradiction between the photometric and the dynamical lines of evidence, which makes Kresák's interpretation totally unacceptable, can be readily removed when the brightness data he gathered on short-period comets at large heliocentric distances are not referred to the solid nucleus. This possibility is strengthened by a rather striking resemblance between the observed fading of the recently captured short-period comets and that of the new comets. However, since a "new" short-period comet of the P/Brooks 2 type must have moved in orbits with perihelia between 3 and 6 a.u. for a rather extensive period of time in the past, it should have lost virtually all the highly volatile substances (e.g., carbon monoxide or methane) from its outer layer a long time ago. However, such a comet may have retained some supplies of moderately or subnormally volatile materials (with latent heat of vaporization in excess of, say, 6000 to 8000 cal $mole^{-1}$ but below water snow's 11000 cal $mole^{-1}$), which thus were "enriching" the surface mixture dominated presumably by water snow. After the comet's capture by Jupiter into an orbit of smaller perihelion distance ($q < 3$ a.u.), appreciable amounts of the "enriching" components should start evaporating from the nucleus along with, for the first time, water snow. Stimulated by the evaporating gases, a rather bright icy-grain halo should develop at larger heliocentric distances during the first revolutions in the new, short-period orbit. The halo must rapidly subside at smaller distances from the sun, since the vaporization lifetime of icy grains there drops drastically (Delsemme and Miller 1971; Sekanina 1973).

In the particular case of P/Brooks 2, the observed effect may have been enhanced by the comet's splitting shortly before its discovery, whereby extensive areas of the nuclear interior, potentially rich in highly volatile substances, might have added dramatically to the total momentum of the escaping gas and thus to the extent and brightness of the halo.

Since high vaporization rates point to large nongravitational forces, and since the progressive depletion of the more volatile components of the snow mixture implies, in addition to the gradual subsidence in the brightness and extension of the halo, a progressive decrease in the nongravitational effects in the motion of such a "new" short-period comet during the revolutions just after the capture, the presented interpretation explains, at least qualitatively, the dynamical behavior of such a comet, along with its photometric behavior.

The vaporization curve (vaporization flux versus heliocentric distance) of the "enriched" mixture should differ from that of water snow (unless the latter controls the mixture, as in the case of solid hydrates). Since the variation in the nongravitational forces in the motions of P/Brooks 2 and P/Schwassmann-Wachmann 2 has been found essentially consistent with the vaporization law of water snow (Marsden et al. 1973), yet another interpretation may exist. The alternative is based on the premise that dirty snow should evaporate more rapidly than pure snow of the same chemical composition, simply because the impurities of dark meteoric material would lower the effective surface reflectivity and thus increase the absorbing power of the nucleus for solar radiation (Marsden et al. 1973). If most fine dust is essentially confined to a narrow outer layer of the nucleus, the surface reflectivity should increase when the layer is removed by evaporation, and the vaporization flux should drop accordingly. Note that this mechanism implies a less conspicuous halo at large distances from the sun than did the enriched-mixture model, which could account for the absence of the initial peak in the extreme distance of P/Schwassmann-Wachmann 2 in Kresák's Fig. 5. In conjunction with the high observed level of the nongravitational effects, this mechanism also implies a distinctly smaller size of the cometary nucleus. In any case,

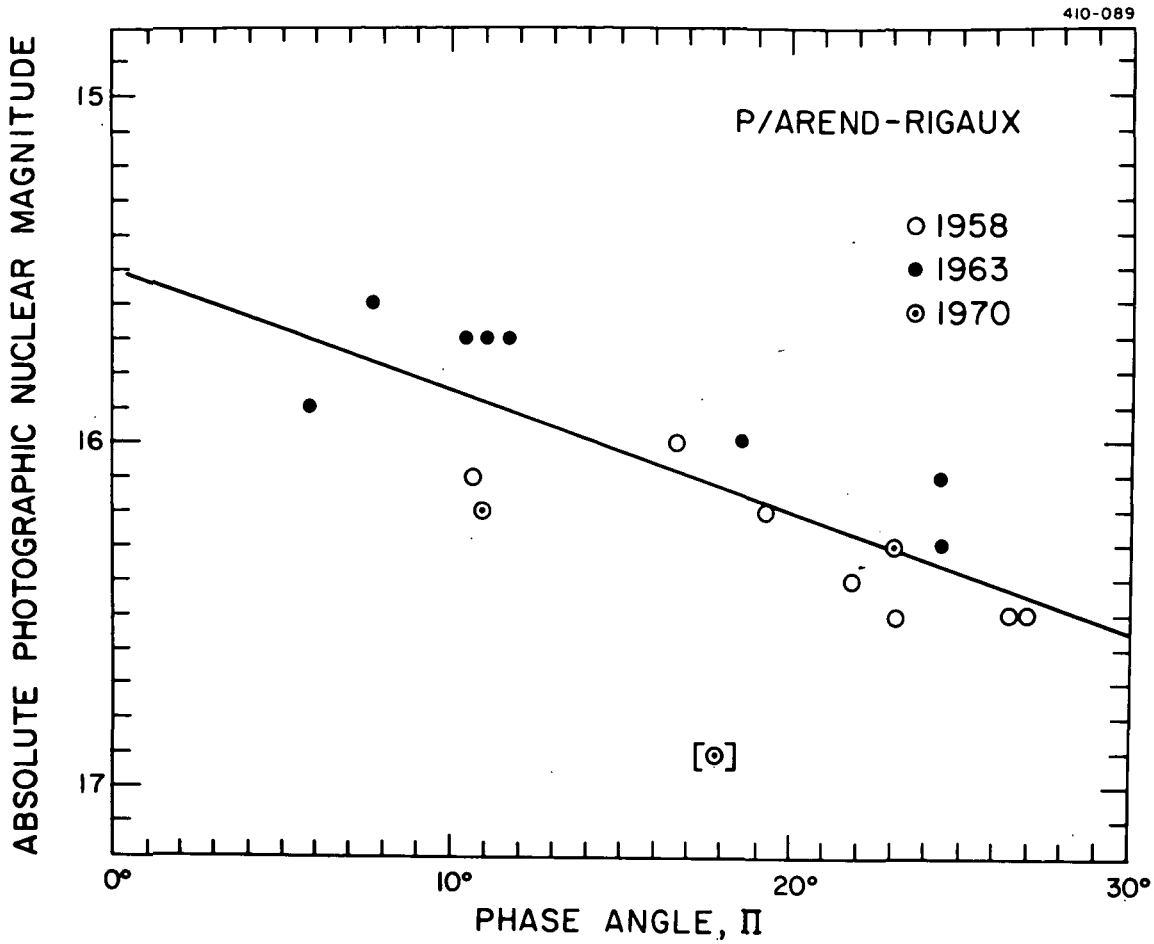

Fig. 5. Phase effect in the absolute brightness of P/Arend-Rigaux. Magnitude estimates of the stellar image of the comet were made by Roemer and reduced here to unit heliocentric and geocentric distances by using the standard inverse-square power law. In 1958, the observations were made after perihelion, and in 1963 and 1970, before perihelion. The solid line is the least-squares fit $15.^{m}50 + 0.^{m}035\Pi$. The bracketed observation, inconsistent with the fit (and not included in the solution), is the 1970 recovery observation.

however, either version fits the observed behavior of the new incomers to the short-period comets considerably better than does the interpretation based on albedo variations.

The nuclear sizes derived by Kresák (1973) and listed in his Table II must be considered totally incorrect, because of his misinterpretation of the nuclear magnitudes and also since, judging from his figures, he mistakenly used the Bond albedo instead of the geometric albedo in his photometric formula for the nuclear radius (the intended kind of albedo is not specified in the paper).

VII. P/AREND-RIGAUX AND P/NEUJMIN 1. PHASE EFFECT IN THE BRIGHTNESS OF A COMETARY NUCLEUS

Marsden (1968, 1969) called attention to two short-period comets whose motions appear to be completely free from nongravitational effects: P/Arend-Rigaux and P/Neujmin 1. He pointed out that the two are usually entirely stellar in appearance and that they are strong candidates for a type of objects that are presumably in transition from comet to asteroid.

P/Arend-Rigaux was systematically observed by Roemer at its three most recent apparitions (Roemer 1965; Roemer and Lloyd 1966; Marsden 1971). The comet was virtually always perfectly stellar. Its brightness is known to follow closely the inverse-square power law and to show a well-pronounced asteroidal-type phase effect (Marsden 1973a). My least-squares solution, based on 17 observations by Roemer in the range of phase angles from 6° to 27° (Fig. 5), gives a value of $15.^{m}50 \pm 0.^{m}12$ for the opposition photographic magnitude of the comet, reduced to 1 a.u. from the

sun and 1 a.u. from the earth. The phase term can be written in the form $B\Pi$, where Π is the phase angle in degrees and $B = +0^{m}.035 \pm 0^{m}.006$. The mean residual is $\pm 0^{m}.18$, and the phase curve is symmetrical with respect to perihelion. Only the 1970 recovery observation fails to fit the phase law, being $0^{m}.8$ too faint. Understandably, no opposition effect can be detected in Fig. 5; in the light curves of most asteroids, the opposition effect does not show up at phase angles exceeding 5° even when high-sensitive photoelectric techniques are used.

We conclude that considerable evidence supports the view that the nucleus of P/Arend-Rigaux has actually been detected, which indicates that the nuclei of defunct or almost defunct comets can be photographically resolved. The above photometric data suggest that the nucleus of P/Arend-Rigaux is about 2 km in radius if its geometric albedo is assumed to be near 0.1.

P/Neujmin 1 was not observed by Roemer. However, during its discovery apparition in 1913, the comet was observed extensively and a search in the literature has revealed fine sets of visual-magnitude estimates obtained by three of the most experienced observers of that time (Barnard 1915; Graff 1914; Van Biesbroeck 1914). In September 1913, the comet was consistently reported to display very slight traces of a coma and/or a tail "attached" to a stellar nucleus (see, e.g., Barnard 1914b); later, the comet was perfectly stellar (Barnard 1915). However, occasional fluctuations in the brightness of the nucleus were noticed in September and October (Banachiewicz 1914; Graff 1914). The brightness estimates of the nucleus reduced with the inverse-square power law show a rather large scatter in September. In its "quiescent" phase, the brightness of the comet's nucleus follows the inverse-square

power law closely and shows phase variations similar to those experienced by P/Arend-Rigaux (Fig. 6).

In 1931, P/Neujmin 1 was perfectly stellar, and a series of photographic magnitudes by Van Biesbroeck (1933) suggests a phase effect virtually identical with the one established from the 1913 observations. In 1948 and 1966, the comet was poorly observed. Van Biesbroeck (1950) secured a few plates at Yerkes and McDonald on which the comet's image was not quite stellar. The magnitude derived from the 1948 Yerkes plates, made with the same telescope as in 1931, is perfectly consistent with the 1931 phase curve, whereas the magnitudes from 1948 McDonald plates and from two of Pereyra's (1966) plates exposed during the comet's next return (stellar images) are only fairly consistent with the curve. Four more plates were obtained in a 10-day span at Boyden Observatory in 1966 (Andrews 1966). They show the comet diffuse, yet generally fainter than the above photographic observations would indicate (three of them would cluster at $\Pi = 9°$, absolute magnitude $13^{m}.5$ in Fig. 6; the fourth is 1 magnitude brighter and would fit the curve within $0^{m}.1$).

Least-squares solutions to the linear phase law, $A + B\Pi$, forced through the sets of magnitude estimates of Fig. 6, have given, respectively, the following values for the opposition magnitude A, reduced to unit heliocentric and geocentric distances, and the phase coefficient B (mag per degree): $11^{m}.42 \pm 0^{m}.12$, $+0.032 \pm 0.006$ (Barnard's visual magnitudes in 1913); $11^{m}.84 \pm 0^{m}.12$, $+0.027 \pm 0.008$ (Van Biesbroeck, visual, 1913); $12^{m}.16 \pm 0^{m}.14$, $+0.055 \pm 0.019$ (Graff, visual, 1913; B very uncertain because of a small range in Π); and $12^{m}.52 \pm 0^{m}.18$, $+0.034 \pm 0.013$ (Van Biesbroeck, photographic, 1931). The mean residuals ranged from $\pm 0^{m}.11$ to $\pm 0^{m}.18$. While the

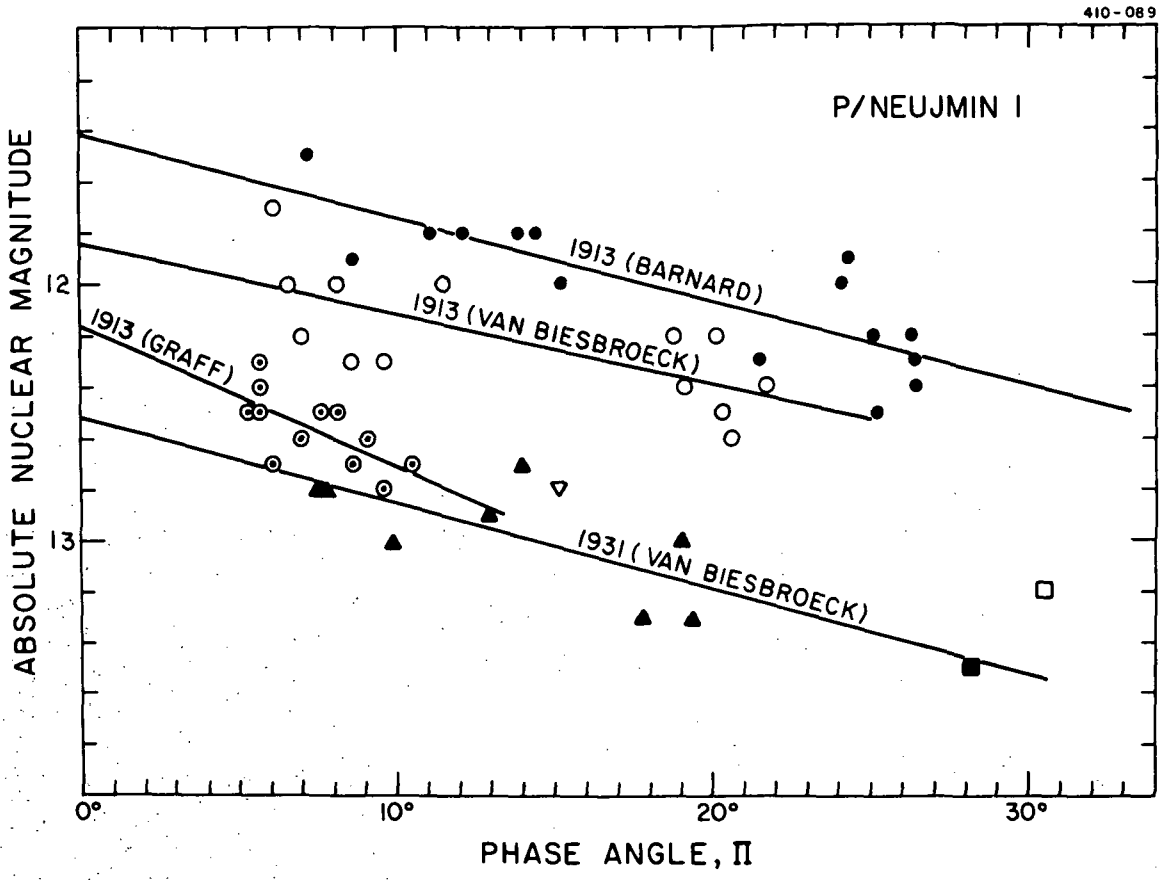

Fig. 6. Phase effect in the absolute (cf. caption to Fig. 5) brightness of P/Neujmin 1. Visual-magnitude estimates of the comet in its "quiescent" phase in 1913 come from Barnard (solid circles), Van Biesbroeck (open circles), and Graff (circled dots). Photographic magnitudes plotted were obtained by Van Biesbroeck with the 24-inch reflector of the Yerkes Observatory in 1931 (solid triangles), and with the 82-inch reflector of the McDonald Observatory (open square) and the 24-inch (solid square) in 1948, and by Pereyra with the 60-inch reflector at Bosque Alegre, Argentina, in 1966 (open triangle). The straight lines are the least-squares fits of the linear phase law forced through the sets of data. The 1913 and 1931 observations were made after perihelion, and the 1948 and 1966 ones, before perihelion.

discrepancies in the zero point among the three observers in 1913 apparently reflect the differences in their photometric scales, the discrepancy between the 1913 (visual) and the later (photographic) observations must, by and large, be due to the color index of the comet.

Analyzing Barnard's and his own 1913 magnitude estimates of P/Neujmin 1, Van Biesbroeck (1930b) did not consider the phase effect and concluded that the brightness of the comet varied in proportion to r^{-5}. However, his 1931 photographic magnitudes show practically no dependence on heliocentric distance when the phase effect is neglected (Fig. 7). This is so because in 1913 the comet, while receding from the sun, was moving away from opposition over most of the period of observation, whereas in 1931 it was moving toward opposition. Thus, the phase effect accelerated the comet's fading in 1913 but offset it in 1931. This peculiar coincidence of circumstances demonstrates the intricacy encountered when an attempt is made to interpret a comet's light curve.

VIII. PERIODIC COMET ENCKE

I suggested (Sekanina 1969, 1972a) that the long-term decrease in the magnitude of the nongravitational effects in the motion of P/Encke can be interpreted as an indication of the comet's progressive deactivation but not of its disintegration, and I predicted that the comet should eventually become asteroidal in appearance. Thus, P/Encke is perhaps currently evolving through a phase that might have been experienced in the past by P/Arend-Rigaux and P/Neujmin 1.

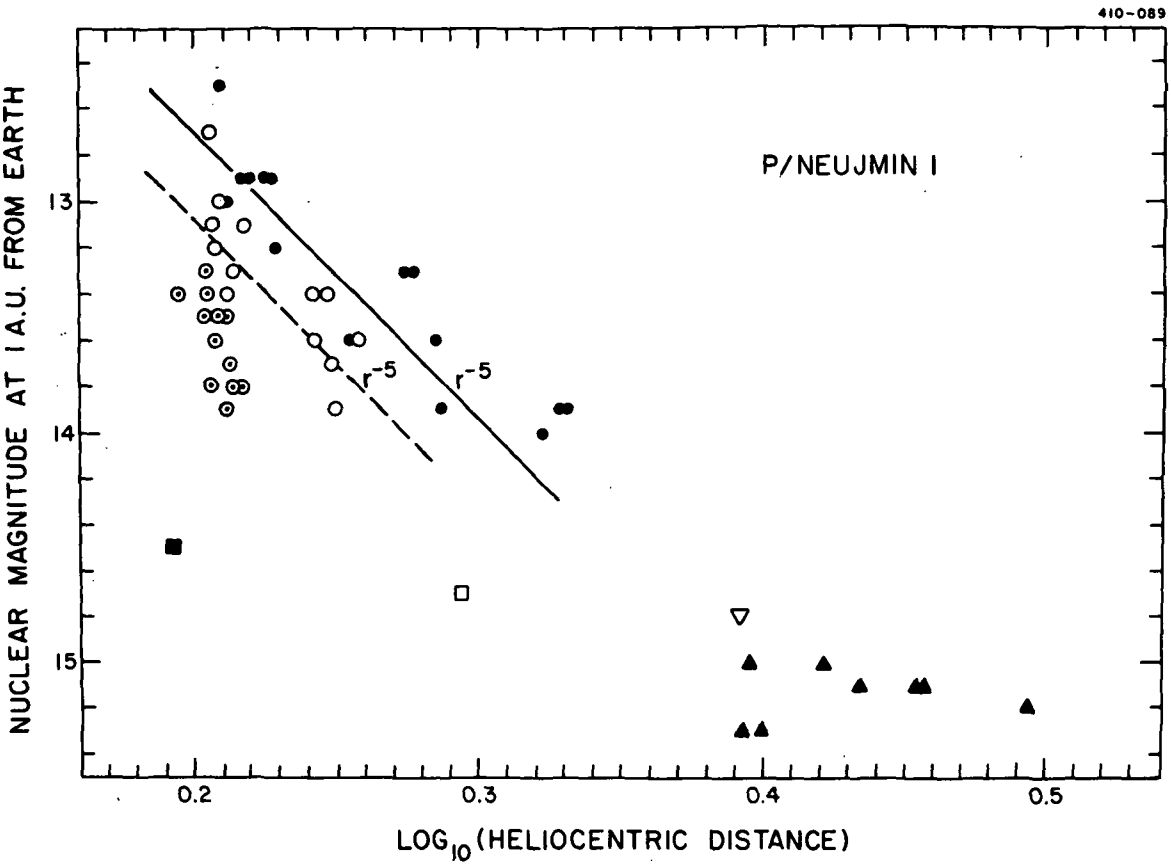

Fig. 7. Phase effect in the magnitudes of P/Neujmin 1 misinterpreted as a variation with heliocentric distance. Observations are the same as those in Fig. 6. Note the fictitious strong ($\sim r^{-5}$) brightness dependence in 1913 (comet receded from the sun and from opposition), as opposed to the equally fictitious brightness independent of heliocentric distance in 1931 (comet receded from the sun but approached opposition). The solid and dashed lines, respectively, are Van Biesbroeck's (1930b) formal fits (ignoring the phase effect) to Barnard's and his own 1913 magnitude estimates.

The deactivation hypothesis is strongly supported by the very low production rate of atomic hydrogen, established for P/Encke by Bertaux et al. (1973) from the OGO-5 observations of the comet's Lyman-alpha emission. Indeed, Delsemme and Rud (1973) concluded that the observed production rate rules out a possibility that water snow could cover the whole surface of the nucleus (or even its significant fraction) and at the same time control the production rate of hydrogen. However, Delsemme and Rud's conclusion depends on Roemer's nuclear magnitude of P/Encke near its aphelion in 1972. We have collected and plotted in Fig. 8 all Roemer's 1957-1974 observations of the comet (Roemer 1965; Roemer and Lloyd 1966; Marsden 1971, 1972a, 1973b, 1974a, b). Although some indication for a phase effect might be present, Fig. 8 does not allow any straightforward conclusion on the character of the phase law or on the brightness of the actual solid nucleus. However, unlike P/Arend-Rigaux, P/Encke seems to be generally fainter after perihelion. On the other hand, it was unusually bright when photographed near the 1972 aphelion.

It is most doubtful that a major part of the scatter in the nuclear brightness of the comet is due to changes in the reflectivity of the nuclear surface. The amplitude of the scatter, about 3 magnitudes, would imply variations in the geometrical albedo of 16:1. Very dark surfaces of the Martian satellites have a geometric albedo of about 0.05 (Masursky et al. 1972). On the other hand, Veverka (1973) concluded that the most probable geometric albedo of a smooth snow-covered object is 0.45 ± 0.1, but he added that large-scale surface roughness would tend to increase it somewhat. Indeed, the (visual) geometric albedo of Europa, the most richly water-frost-covered Galilean satellite (Pilcher et al. 1972), is now believed to be 0.68 (Jones and Morrison 1974). The two values, 0.05 and 0.68, are likely to approximate well the two limits

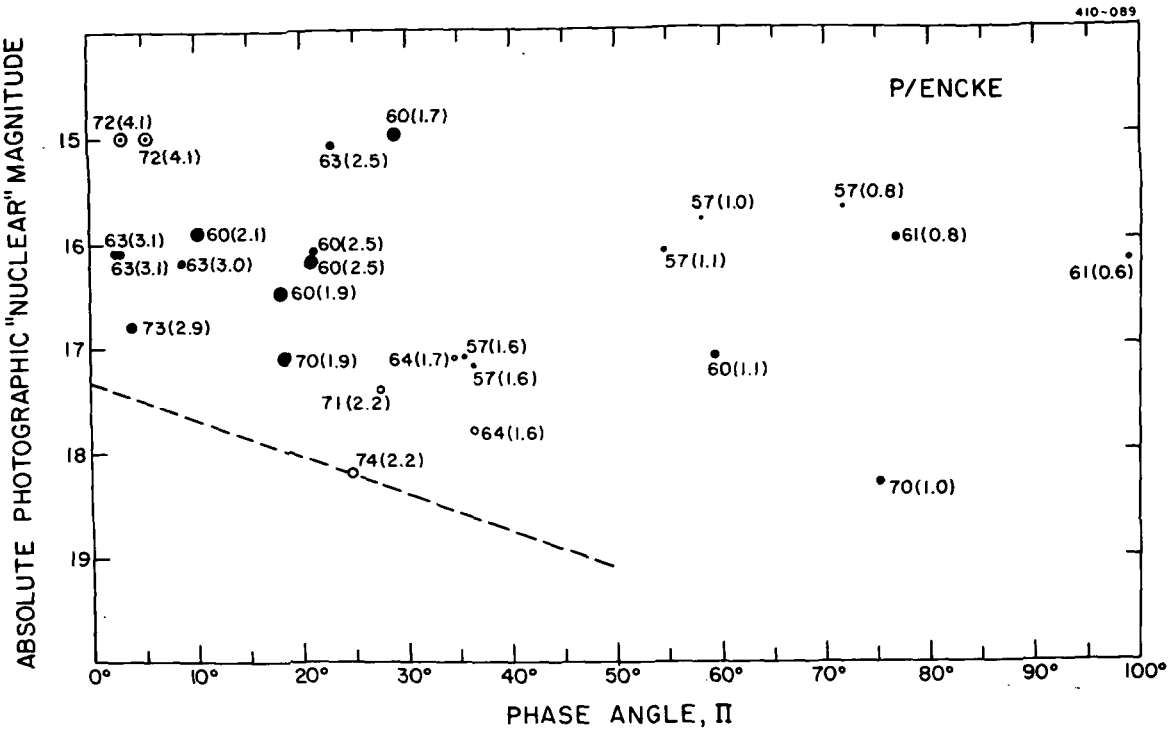

Fig. 8. Roemer's photographic "nuclear" magnitudes of P/Encke, reduced to unit heliocentric and geocentric distances by the inverse-square power law, versus phase angle Π. The size of the circles describes the comet's appearance: The largest ones refer to stellar images, and the smallest, to diffuse images. Solid circles – preperihelion observations; open circles – postperihelion; circled dots – near-aphelion. All postperihelion images were reported by Roemer to be weak. Each entry in the figure is further defined by the year of observation and the heliocentric distance in a.u. (in parentheses). For reference, the phase law established for P/Arend-Rigaux ($B = 0.^{m}035$ per degree) is plotted to fit the faintest brightness estimate.

for the geometric albedo of small bodies in the solar system. Their ratio gives a magnitude difference of $2.^{m}8$, matching almost exactly the magnitude amplitude of P/Encke. Naturally, it is most unlikely that the reflectivity of a single object, such as the nucleus of P/Encke, would periodically (once in 3.3 years) vary from one known extreme limit to the other. Consequently, the variations in the size and optical thickness of the icy-grain halo surrounding the nucleus must contribute significantly to the observed scatter.

If, on the other hand, we assume for the moment that the scatter is entirely due to the icy-grain halo, the whole surface of P/Encke should be covered by a snow mixture. Because of the very small nongravitational effects observed (Marsden and Sekanina 1974), such a snow mixture should be dominated and controlled by its least volatile component, i.e., presumably, water snow. In order that an unrealistically high Bond albedo ($\gtrsim$0.9) be avoided, the comet's vaporization and photometric cross sections should be of the same order of magnitude. With water snow controlling the production rate of hydrogen, the photometric cross section should be about 0.1 km^2 and the comet's radius therefore about 250 m. The corresponding brightness of the nucleus would range between magnitude 18 and 19 (at 1 a.u.). Furthermore, this assumption leads to a relative mass loss of the comet of as much as about 10% per revolution, slightly increasing with time (and to the associated nongravitational effects also increasing somewhat with time). Such a high value of mass loss is difficult to reconcile with the small observed nongravitational effects, unless evaporation from the comet's surface is allowed to be almost perfectly isotropic [the anisotropy factor defined by Sekanina (1969) would barely reach 10^{-3}]. Since the nongravitational effects have been found to decrease with time ever since the 1820s (Marsden and Sekanina

1974), rather than to increase as required by the above assumption, we have to accept further that they are due to a process other than progressive deactivation; systematic motions of the rotation axis of the nucleus (Marsden 1972b; Sekanina 1972b) have so far been the only alternative explanations suggested. But any appreciable effect of this kind requires a fair degree of anisotropy in the vaporization process – which is contrary to the above statement. The well-known asymmetric shape of the comet's head also implies some degree of anisotropy.

We do not find it possible to invalidate the Delsemme-Rud conclusion as to the extent of water-snow cover on P/Encke, even when the unknown radiative term in the vaporization-radiation equilibrium, neglected by Delsemme and Rud, is roughly accounted for.

It appears that a combined effect of the icy-grain halo and reflectivity changes of the comet's surface – the latter associated with the variable extent of the snow cover – is the most acceptable solution to the problem of scatter in the nuclear magnitudes of P/Encke. A particular result of my unpublished calculations of heat- and mass-transfer phenomena in a disperse medium might be of interest in this context. The disperse medium was assumed to be a spherical body composed of a porous matrix of meteoric material with water snow uniformly embedded in it, filling 40% of the whole volume. The object was allowed to move around the sun in the orbit of P/Encke, and temperature and snow-concentration distributions within the object were then calculated as functions of time, starting from the equilibrium conditions at aphelion. The variations in the snow concentration at the surface and at two depths, exhibited in Fig. 9, show completely different patterns. Whereas the subsurface supply of snow decreases very smoothly

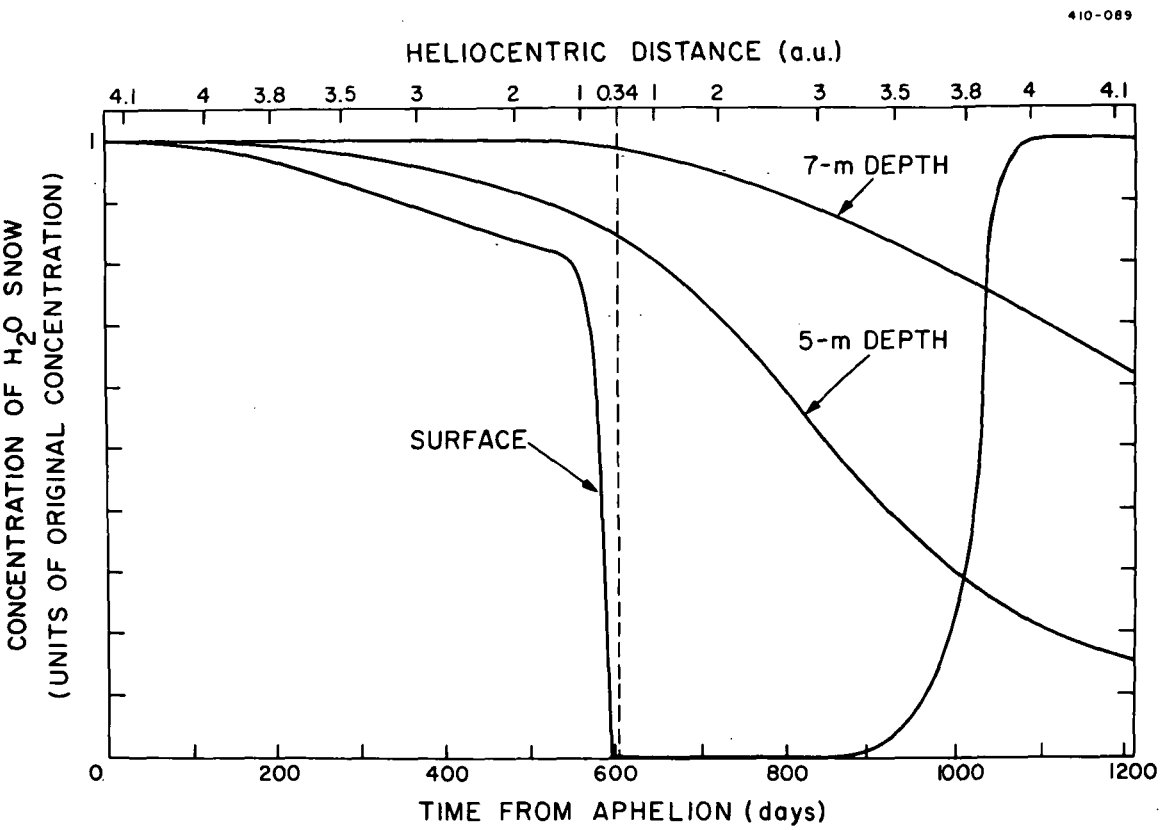

Fig. 9. Calculated mass transfer in a spherical body, moving in the orbit of P/Encke and composed of a porous matrix of meteoric material with water snow initially uniformly embedded: concentration of snow at the surface and at depths of 5 and 7 m as a function of the location in orbit (or of time from aphelion).

throughout the orbit, the surface concentration drops at an almost constant rate as the object approaches the sun until a distance of about 1 a.u. is reached. At that point, the rate of depletion of the surface reservoir starts increasing enormously; the depletion is virtually completed before perihelion. After perihelion, the surface remains practically snow-free until the object has receded to roughly 3 a.u. from the sun. Then, triggered both by temperature inversion (the surface is cooler than the underlying layers, thus facilitating recondensation of transferred vapor) and by a steep gradient in the concentration distribution of snow with depth, the replenishment mechanism restores the initial surface reservoir of snow even before aphelion.

As to the appearance of the object, it would be intrinsically bright near aphelion and on the incoming branch of the orbit because of the high reflectivity of the snow-covered surface and the presence of a small surrounding icy halo. At smaller distances ($\lesssim 1$ a.u.), the decreasing reflectivity of the surface, associated with a progressively diminishing extent of snow cover, is compensated by the increasing activity, so that the object would still look bright but more diffuse. When the surface supply of snow has been essentially depleted (around and after perihelion), the reflectivity will drop sharply (owing to the dark matrix exposed), the activity will cease, and the object will be at its faintest. With the gradual recovery of the snow supply on the surface, the brightness would increase again as the object approaches aphelion. We note that this rough qualitative description of the object's presumed photometric behavior bears a very definite resemblance to the observed appearance of the central condensation of P/Encke, as inferred from the brightness data of Fig. 8.

The described cycle in the object's evolution during one revolution around the sun is restricted only to its surface. The drop, in Fig. 9, in the snow supply beneath the surface by the time the revolution has been completed demonstrates the progressive overall deactivation process, which ultimately leads to the transition of an active comet into an asteroid (Section VII). While P/Encke is, of course, still a live comet, we feel that the available evidence is sufficient to conclude that this comet will inevitably approach the brink of the transition phase in the near future.

IX. FINAL REMARKS AND CONCLUSIONS

There is plenty of evidence that nearly parabolic comets are generally active at large heliocentric distances, where water-vapor pressure is negligibly low. The activity – particularly in the comets arriving from the Oort cloud – is conspicuously asymmetrical relative to perihelion. The substantial fading of nearly parabolic comets after their first passage near the sun, noticed by Oort (1950) from the distribution of "original" semimajor axes of cometary orbits and analyzed more quantitatively by Whipple (1962), is apparently an accumulated effect of the same process that causes the perihelion asymmetry. On an a priori assumption that the influx of new comets is a continuous process, Marsden and Sekanina (1973) have interpreted the fading of distant comets as being due to a rapid depletion of the most volatile substances during the first approach of the comets to the sun.

An important feature of the cometary activity at large heliocentric distances appears to be the formation of a rather dense cloud of presumably large icy grains that circulate in disarray and at very low velocities (lower than the velocity of escape from the comet?) in a circumnuclear space barely more than a few nuclear

diameters across. To a terrestrial observer, such a cloud of particles may look essentially stellar, particularly if the space density inside the cloud drops rapidly in the radial direction.

This qualitative interpretation is basically consistent with the observational evidence and suggests that the photometric images of comets far from the sun are contaminated by ejecta much more extensively than has generally been accepted. Thus, the nuclear magnitudes of comets, even at great distances from the sun and when derived from photographs taken with large instruments, give only an upper limit to the size of the solid nucleus. Until Delsemme and Rud (1973) came up with their method of comparing the vaporization cross section of the nucleus with its photometric cross section, no way existed to estimate numerically the contamination effect (i.e., the difference between the magnitude of the solid nucleus and the observed nuclear magnitude), because the surface reflectivity could not be separated from its geometric cross section (Roemer 1966).

The discussion of the Delsemme-Rud method, modified to incorporate the contamination effect as well as the contribution of the radiative term in the vaporization-radiation equilibrium, suggests that in the case of Comet Bennett 1970 II, the nucleus was probably 2 or perhaps even 3 magnitudes fainter than Roemer's nuclear magnitudes. When this effect is taken into account, the Bond albedo of the nucleus of this very dusty comet drops from a suspiciously high value of 0.6 to 0.7 down to a very comforting 0.1 to 0.2, and the size of the nuclear radius decreases from 3.8 to 2.6 or 2.8 km, thus becoming perfectly consistent with an independent determination (Sekanina and Miller 1973).

The formation of a dense cloud of icy grains around the nucleus of Comet Kohoutek 1973f was most probably responsible for the comet's excessive brightness at large heliocentric distances on the preperihelion branch of the orbit, which in turn resulted in the exaggerated brightness predictions for the near-perihelion period. Although the preperihelion nuclear brightness of the comet varied essentially according to the inverse-square power law, and in spite of the comet's nearly stellar appearance, the nuclear brightness after perihelion dropped intrinsically by 3 magnitudes, which implies a physically unacceptable reduction factor of 4 in the nuclear diameter or 16 in the geometric albedo. A moderate geometric albedo of 0.4 would give a nuclear radius of 10 km before perihelion, but only 2.5 km after perihelion. The available data on the production rate of hydrogen (Carruthers et al. 1974; Opal et al. 1974; Traub and Carleton 1974) and hydroxyl (Blamont and Festou 1974; Feldman et al. 1974) are, unfortunately, not easy to interpret, because of an apparently strong perihelion asymmetry and doubts as to whether water was indeed the parent molecule of the two species. Very tentatively, a nuclear radius of some 1 to 3 km can perhaps be inferred.

Uncritical identification of the nuclear magnitudes with the actual brightness of a cometary nucleus can cause a severe misinterpretation of the evolution of the short-period comets. We find it impossible to accept Kresák's (1973) explanation of the rapid fading in the nuclear magnitude of a recently captured short-period comet (of the P/Brooks 2 type) as being due to a decrease in the reflectivity of its nucleus. Instead, attributing the nuclear magnitude to a circumnuclear icy halo, gradually subsiding in brightness during the first revolutions after capture, is clearly preferable, because this interpretation is compatible with the parallel dynamical evidence on the large but rather dramatically decreasing nongravitational effects in the motion.

While the nuclear magnitudes appear to refer generally to a circumnuclear cloud of grains rather than to the nucleus itself, there is little doubt that Roemer's nuclear magnitudes of P/Arend-Rigaux do indeed refer to the solid nucleus of the comet. They satisfy the inverse-square power law, are symmetrical relative to perihelion, and display an asteroidal-type phase effect; furthermore, the comet's appearance is nearly always perfectly stellar, and its motion is free from nongravitational effects. Except for occasional minor flareups, P/Neujmin 1 is the only other comet that also satisfies the above conditions. The two comets appear to be in a transition phase from comet to minor planet (Marsden 1968, 1969).

The rather peculiar behavior of P/Encke is believed to suggest that the extent of the snow cover on the surface of the nucleus varies with the comet's position in orbit. Most of the surface – if not the whole – appears to be snow covered around aphelion and along much of the incoming branch of the orbit, whereas the surface might essentially be rid of snow near perihelion and along a significant portion of the outgoing branch of the orbit. This process is considered to be indicative of the comet's advanced phase of deactivation.

Recent calculations on the motions of the short-period comets and the results discussed in Sections VI to VIII have clear implications for the classification of cometary nuclei. First, we are now positive that the magnitude of the observed non-gravitational effects (and the transverse component, in particular) does not vary straightforwardly in proportion to the relative rate of the loss of mass from the nucleus. Second, an appreciable fraction of the mass lost by a short-period comet during the

first several revolutions after capture by Jupiter from a more distant orbit is apparently due to more volatile species than is the mass lost by "old" short-period comets. And third, we now have a very satisfactory correlation between the dynamical and the photometric characteristics of short-period comets at various phases of evolution.

We feel that the evidence for our classifying cometary nuclei into two basic types, described by the core-mantle and coreless (free-ice) models, respectively (Sekanina 1969, 1971, 1972a), has been strengthened by the recent progress. At the same time, the new results allow us to revise the plot, for the two models, of the mass-loss-related nongravitational effect in a comet's motion as a function of time (Fig. 1 of Sekanina 1971). The important change in the revised version (Fig. 10) is the addition of phase I, the early postcapture period, distinguished by a rather steep decrease in the nongravitational activity, as discussed in Section VI. The rest of the presumed evolution has been left virtually unchanged. Phase II, equivalent to phase E in Sekanina (1971), refers to the gradual evaporation of a thick icy envelope surrounding the meteoric matrix in the core of the nucleus. Whereas the coreless model continues to proceed in phase II until complete disintegration by evaporation, the core-mantle model starts a deactivation track (phase III) and ends up with complete depletion of the snow reservoir (phases V and VI). The precise character of evolution in the advanced phases, including the absolute rate of reduction of the nongravitational activity, might depend significantly on perihelion distance.

Obviously, the variations in the nongravitational effects in phases I and IV look very much alike, although they refer to two physically different mechanisms. Our present understanding of the nongravitational forces in short-period comets suggests

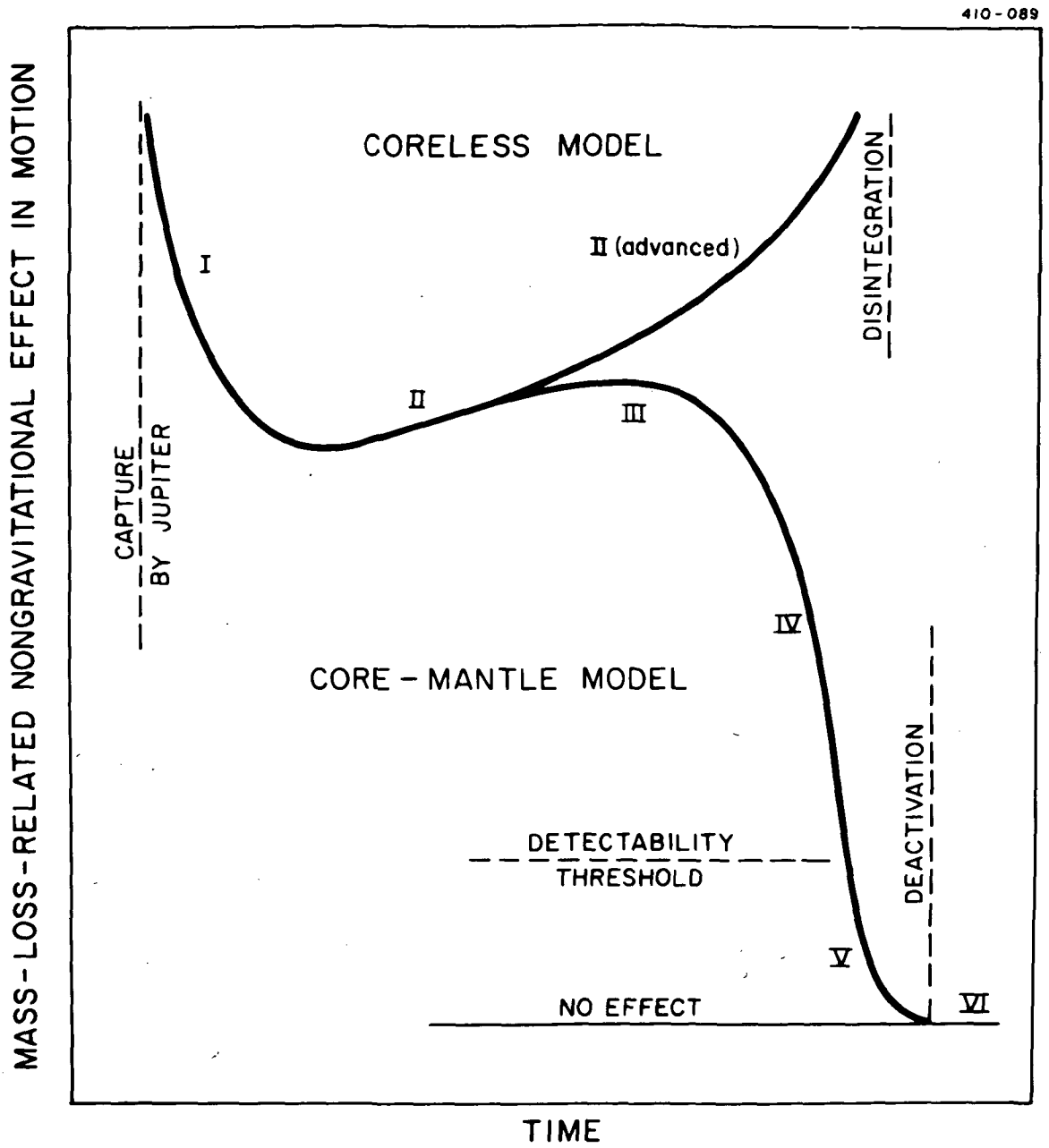

Fig. 10. Theoretical long-term variations in the magnitude of the mass-loss-related nongravitational effects on the motions of short-period comets with coreless and core-mantle nuclei.

the following probable locations in Fig. 10 of some of the well-studied comets: Phase I: P/Schwassmann-Wachmann 2, P/Brooks 2 (advanced?); Phase II: P/Borrelly, P/Tuttle; Phase II (advanced): P/Giacobini-Zinner?; Phase IV: P/Encke; and Phase V: P/Neujmin 1, P/Arend-Rigaux (advanced?).

In spite of all the progress in the physics of comets in recent years, the cometary nucleus still remains very much a mystery. Furthermore, there is little chance that observations from ground-based or even earth-orbiting stations could substantially improve our knowledge of the cometary nucleus. And so, we cannot escape the conclusion that deep-space missions to comets are by far our best hope for the future.

ACKNOWLEDGMENTS

This study could never have been undertaken without the availability of systematic brightness data accumulated through tireless efforts of several observers, primarily Dr. E. Roemer and the late Dr. G. Van Biesbroeck. Dr. B. G. Marsden has contributed informative discussions. This work was supported by grant NSG 7082 from the National Aeronautics and Space Administration.

REFERENCES

Andrews, A. D. (1966). Periodic Comet Neujmin 1 (1966a). IAU Circ. No. 1959.

Banachiewicz, T. (1914). Lichtschwankungen des Kometen 1913c (Neujmin). Astron. Nachr. 196, 249-250.

Barnard, E. E. (1891). Comets 1889 I and II, and some suggestions as to the possibility of seeing the short-period comets at aphelion. Astron. J. 10, 67-68.

Barnard, E. E. (1914a). Encke's Comet. On the possibility of photographing the comet at all points in its orbit. Pop. Astron. 22, 607-610.

Barnard, E. E. (1914b). Neujmin's Comet. Astron. Nachr. 196, 181-182.

Barnard, E. E. (1915). Observations of Comet 1913c (Neujmin). Astron. J. 28, 137-141.

Belyaev, N. A. (1967). Orbital evolution of Comets Neujmin 2 (1916 II), Comas Solá (1927 III), and Schwassmann-Wachmann 2 (1929 I) over the 400 years from 1660 to 2060. Soviet Astron. 11, 366-373.

Bertaux, J. L., Blamont, J. E., and Festou, M. (1973). Interpretation of hydrogen Lyman-alpha observations of Comets Bennett and Encke. Astron. Astrophys. 25, 415-430.

Blamont, J., and Festou, M. (1974). La comète de Kohoutek (1973f) observée en lumière de résonance du radical oxhydrile OH. Comptes Rendus 278 (Sér. B), 479-484.

Carruthers, G. R., Opal, C. B., Page, T. L., Meier, R. R., and Prinz, D. K. (1974). Lyman alpha imagery of Comet Kohoutek. Icarus (in press).

Code, A. D. (1971). Comments on OAO observations of Comets 1969g and 1969i. Trans. IAU 14B, 124.

Delsemme, A. H. (1972). Vaporization theory and non-gravitational forces in comets. In L'Origine du Système Solaire, Proc. Symp. Centre National de la Recherche Scientifique, Nice, ed. by H. Reeves, pp. 305-310.

Delsemme, A. H. (1973). The brightness law of comets. Astrophys. Lett. 14, 163-167.

Delsemme, A. H., and Miller, D. C. (1971). Physico-chemical phenomena in comets. III. The continuum of Comet Burnham (1960 II). Planet. Space Sci. 19, 1229-1257.

Delsemme, A. H., and Rud, D. A. (1973). Albedos and cross-sections for the nuclei of Comets 1969 IX, 1970 II and 1971 I. Astron. Astrophys. 28, 1-6. [Should be 1971 II.]

Feldman, P. D., Takacs, P. Z., Fastie, W. G., and Donn, B. (1974). Rocket ultraviolet spectrophotometry of Comet Kohoutek (1973f). Science 185, 705-707.

Graff, K. (1914). Über die Helligkeitsabnahme des Kometen 1913c (Neujmin). Astron. Nachr. 196, 250-252.

Jeffers, H. M. (1956). Observations of comets and asteroids. Astron. J. 61, 380-382.

Jones, T. J., and Morrison, D. (1974). Recalibration of the photometric/radiometric method of determining asteroid sizes. Astron. J. 79, 892-895.

Keller, H. U., and Lillie, C. F. (1974). The scale length of OH and the production rates of H and OH in Comet Bennett (1970 II). Astron. Astrophys. 34, 187-196.

Kresák, L. (1973). Short-period comets at large heliocentric distances. Bull. Astron. Inst. Czech. 24, 264-283.

Marsden, B. G. (1966). One hundred periodic comets. Science 155, 1207-1213.

Marsden, B. G. (1968). Comets and nongravitational forces. Astron. J. 73, 367-379.

Marsden, B. G. (1969). Comets and nongravitational forces. II. Astron. J. 74, 720-734.

Marsden, B. G. (1971). Comets in 1970. Quart. J. Roy. Astron. Soc. 12, 244-273.

Marsden, B. G. (1972a). Comets in 1971. Quart. J. Roy. Astron. Soc. 13, 415-435.

Marsden, B. G. (1972b). Nongravitational effects on comets: The current status. In The Motion, Evolution of Orbits, and Origin of Comets, Proc. IAU Symp. No. 45, ed. by G. A. Chebotarev, E. I. Kazimirchak-Polonskaya, and B. G. Marsden, D. Reidel Publ. Co., Dordrecht, Holland, pp. 135-143.

Marsden, B. G. (1973a). Private communication.

Marsden, B. G. (1973b). Comets in 1972. Quart. J. Roy. Astron. Soc. 14, 389-406.

Marsden, B. G. (1974a). Private communication.

Marsden, B. G. (1974b). Comets in 1973. Quart. J. Roy. Astron. Soc. (in press).

Marsden, B. G., and Sekanina, Z. (1973). On the distribution of "original" orbits of comets of large perihelion distance. Astron. J. 78, 1118-1124.

Marsden, B. G., and Sekanina, Z. (1974). Comets and nongravitational forces. VI. Periodic Comet Encke 1786-1971. Astron. J. 79, 413-419.

Marsden, B. G., Sekanina, Z., and Yeomans, D. K. (1973). Comets and nongravitational forces. V. Astron. J. 78, 211-225.

Masursky, H., Batson, R. M., McCauley, J. F., Soderblom, L. A., Wildey, R. L., Carr, M. H., Milton, D. J., Wilhelms, D. E., Smith, B. A., Kirby, T. B., Robinson, J. C., Leovy, C. B., Briggs, G. A., Duxbury, T. C., Acton, C. H., Jr., Murray, B. C., Cutts, J. A., Sharp, R. P., Smith, S., Leighton, R. B., Sagan, C., Veverka, J., Noland, M., Lederberg, J., Levinthal, E., Pollack, J. B., Moore, J. T., Jr., Hartmann, W. K., Shipley, E. N., de Vaucouleurs, G., and Davies, M. E. (1972). Mariner 9 television reconnaissance of Mars and its satellites: Preliminary results. Science 175, 294-305.

McCrosky, R. E., and Shao, C. Y. (1972). Periodic Comet Encke. IAU Circ. No. 2446.

Oort, J. H. (1950). The structure of the cloud of comets surrounding the solar system, and a hypothesis concerning its origin. Bull. Astron. Inst. Neth. 11, 91-110.

Opal, C. B., Carruthers, G. R., Prinz, D. K., and Meier, R. R. (1974). Comet Kohoutek: Ultraviolet images and spectrograms. Science 185, 702-705.

Osterbrock, D. E. (1958). A study of two comet tails. Astrophys. J. 128, 95-105.

Pereyra, Z. M. (1966). Periodic Comet Neujmin 1 (1966a). IAU Circ. No. 1963.

Pilcher, C. B., Ridgway, S. T., and McCord, T. B. (1972). Galilean satellites: Identification of water frost. Science 178, 1087-1089.

Roemer, E. (1956). Observations of comets. Astron. J. 61, 391-394.

Roemer, E. (1962). Activity in comets at large heliocentric distance. Publ. Astron. Soc. Pacific 74, 351-365.

Roemer, E. (1965). Observations of comets and minor planets. Astron. J. 70, 397-402.

Roemer, E. (1966). The dimensions of cometary nuclei. In Nature et Origine des Comètes, Proc. Coll. Int. Univ. Liège, pp. 23-28.

Roemer, E. (1972). Periodic Comet Encke. IAU Circ. Nos. 2435 and 2446.

Roemer, E. (1973a). Comet notes. Mercury 2, no. 4, 19-21.

Roemer, E. (1973b). Notes on Comet Kohoutek 1973f. Mercury 2, no. 5, 11.

Roemer, E. (1974). Comet Kohoutek (1973f). IAU Circ. No. 2671.

Roemer, E., and Lloyd, R. E. (1966). Observations of comets, minor planets, and satellites. Astron. J. 71, 443-457.

Sekanina, Z. (1969). Dynamical and evolutionary aspects of gradual deactivation and disintegration of short-period comets. Astron. J. 74, 1223-1234.

Sekanina, Z. (1971). A core-mantle model for cometary nuclei and asteroids of possible cometary origin. In Physical Studies of Minor Planets, Proc. IAU Colloq. No. 12, ed. by T. Gehrels, NASA SP-267, pp. 423-428.

Sekanina, Z. (1972a). A model for the nucleus of Encke's Comet. In The Motion. Evolution of Orbits, and Origin of Comets, Proc. IAU Symp. No. 45, ed. by G. A. Chebotarev, E. I. Kazimirchak-Polonskaya, and B. G. Marsden, D. Reidel Publ. Co., Dordrecht, Holland, pp. 301-307.

Sekanina, Z. (1972b). Rotation effects in the nongravitational parameters of comets. In The Motion, Evolution of Orbits, and Origin of Comets, Proc. IAU Symp. No. 45, ed. by G. A. Chebotarev, E. I. Kazimirchak-Polonskaya, and B. G. Marsden, D. Reidel Publ. Co., Dordrecht, Holland, pp. 294-300.

Sekanina, Z. (1973). Existence of icy comet tails at large distances from the sun. Astrophys. Lett. 14, 175-180.

Sekanina, Z., and Miller, F. D. (1973). Comet Bennett 1970 II. Science 179, 565-567.

Traub, W. A., and Carleton, N. P. (1974). A search for H_2O and CH_4 in Comet Kohoutek. Icarus (in press).

Van Biesbroeck, G. (1914). Beobachtungen der vier Herbstkometen des Jahres 1913. Astron. Nachr. 197, 85-88.

Van Biesbroeck, G. (1930a). Observations of comets at the Yerkes Observatory. Astron. J. 40, 51-60.

Van Biesbroeck, G. (1930b). The return of Comet 1913 III (Neujmin) in 1931. Astron. J. 40, 77-79.

Van Biesbroeck, G. (1933). Observations of comets at the Yerkes Observatory. Astron. J. 42, 25-32.

Van Biesbroeck, G. (1950). Observations of comets. Astron. J. 55, 53-60.

Veverka, J. (1973). The photometric properties of natural snow and of snow-covered planets. Icarus 20, 304-310.

Walker, M. F. (1958). Observations of Comets Bakharev-Macfarlaine-Krienke, 1955f, and Baade, 1954h. Publ. Astron. Soc. Pacific 70, 191-196.

Whipple, F. L. (1950). A comet model. I. The acceleration of Comet Encke. Astrophys. J. 111, 375-394.

Whipple, F. L. (1962). On the distribution of semimajor axes among comet orbits. Astron. J. 67, 1-9.

DISCUSSION

J. C. Brandt: How do you regenerate the surface without regenerating the intermediate layers of the snow?

Z. Sekanina: The proposed mechanism regenerates snow supplies not only at the surface but also beneath it (though not necessarily in proportion) by transporting vapor via diffusion from deeper layers. This process is stimulated primarily by a decrease in the concentration of snow near the surface resulting from intense surface evaporation around perihelion, and facilitated by the presumably porous structure of the cometary solid material. Furthermore, as the comet approaches aphelion, the surface cools off more rapidly than subsurface layers, thus giving rise to a rather substantial temperature inversion which, in turn, assists the mass transport to the surface and increases the rate of recondensation of water vapor on the surface. On a long-term scale, this mechanism leads to a complete depletion of snow reservoir in the nucleus, thus turning an active comet into a defunct object.

Now, besides, you can show that at large heliocentric distances before the aphelion point is reached, you would have an inversion of temperature. The surface is cooler than the interior, because the heating of the surface for in earlier times before aphelion propogates in a form of heat rate inside and, because the comet in the meantime gets farther away from the sun, there is less energy coming to surface. You can actually, numerically show that at several meters under the surface there is a higher temperature.

In other words, when surface is cooler and there is a transport of vapor to the surface, there is a good chance of condensation on the surface because of the lower temperature.

H. Keller: I have a question concerning the observations of the nucleus at the larger heliocentric distances.

I wonder whether there is a possibility for some systematic effect due to the fact that the geocentric distances, is also increasing when the heliocentric distance is increasing on the comet, an effect which maybe would be similar to the f-ratio effect of instruments. This may be a question for Dr. Roemer, and I would —

E. Roemer: Specifically with respect to P/Encke, some part of the systematic difference between the absolute "nuclear" magnitude derived from preperihelion observation as against that derived from postperihelion observations could easily derive from observational circumstances. Because of the orientation of the inclined orbit, P/Encke goes south very fast after perihelion passage and as a consequence is not observable for the Northern Hemisphere for a number of months, and even then, at very low altitude. Although I normally correct the "nuclear" magnitude estimates for extinction in blue light of 0.3 mag/air mass, that correction likely is inadquate for observation made at very large air mass.

More generally, I prefer to use those "nuclear" magnitudes that refer to a reasonably sharply separated nuclear condensation on an individual basis to form an idea of the limits on the radius of the nucleus defined photometrically. Although the available evidence seems to confirm that use of a $1/\Delta^2$ dependence is appropriate in deriving a "reduced" magnitude, error could arise in use of the "absolute" magnitude for calculation of the radius of the nucleus. The reason is that the unresolved contamination of the "nuclear" magnitude by light from the inner coma will generally be greater when the comet is closer to the sun. A dependence of the brightness on a higher inverse power of the heliocentric distance than the second would be the consequence. It would then become unclear how closely the absolute "nuclear" magnitude might be related to the absolute magnitude that referred only to light reflected from a monolithic nucleus.

Opik suggested some years ago that the geocentric distance dependence of the brightness is better represented by $1/\Delta$ than by $1/\Delta^2$. Meisel (1970 Astron J. 75, 252), as well as a graduate student of mine, Charles Snell, (MS thesis, U Arizona, 1971) have failed to find support for this proposal.

E. Ney: I'd like to make a remark about comet Bradfield.

Between April 7 and 9, to call your attention to it—I mentioned it yesterday in my talk, but I don't think people paid much attention—in two days, this comet changed very abruptly, by three magnitudes at long-wave infrared wave lengths. It just went out; it went down three magnitudes.

In a big diaphragm, Mintler found that it dropped two magnitudes in the visible in a 4-minute diaphragm.

Now, I'm not an experienced comet observer, but I looked at quite a lot of them this year; and I saw at the time the dust went away on Comet Bradfield it certainly changed its appearance. There was a thin coma, but there was a definite stellar image in the center.

I'd like to call your attention to that case, where the dust disappeared. It may be a case to measure a nucleus right.

OMIT

THE NUCLEUS: PANEL DISCUSSION

C. R. O'Dell

My approach to the nature and origin of the nucleus is strongly influenced by the quantitative data on amounts of dust and gas being released near perihelion. Calibrated spectra and photoelectric photometry (Gebel 1970, O'Dell 1971, Stokes 1972) have shown that the morphological division of Oort and Schmidt into dust-rich and dust-poor seems to be correct. More accurately, I can say that we have observed a wide variation in the ratio of scattered light continuum to molecular emission. This may or may not reflect a large variation of the dust to gas ratio in the nucleus. In fact, the apparently dustiest comets may have smallest dust to gas ratio at the nucleus! This is because the process of accelerating the particles out from the nucleus by means of viscous gas flow depends sensitively on the amount of gas leaving (Finson and Probstein 1968). The comet with weak scattered light is probably one that is unable to lift the particles from the nucleus, leaving a residual surface of particles. Since small particles can be lifted more easily, the remaining surface would selectively become one of large particles, forming an insulating layer of low albedo with internal degasification occuring at an even slow

rate. This in turn would diminish the particle loss rate, with a rapid convergence to a particle cover and nucleus. This model would explain the variation from continuum strong to continuum poor in the Oort-Schmidt new and old comets, in addition to the intrinsically low luminosity and photometric radius of old comet nuclei.

In a young strong continuum comet, if one assumes that a cosmic abundance of gases applies and proceeds from observations of reasonably well understood molecules such as C_2 (O'Dell 1973), one can calculate that the total mass of particles and gas leaving the coma is nearly unity. Since the gas escapes much more easily than the dust, this means that particulate matter probably dominates the nuclear composition, even in the initial state as a comet enters the inner solar system. In the old comets, the preferential loss of gas would leave an even greater particle dominance. For this reason, I believe that we must look on the nucleus as a gasey dustball rather than as a dusty snowball.

Of course, what we are discussing is the particles that succeed in leaving the nucleus, for only they are observable. Under appropriate conditions, one can eject particles nearly a millimeter in size (Gary and O'Dell 1974, Sekanina 1974); but, most of the ejected mass

is in the small particles. We do not directly measure these small particles' parameters, but only the combination $\rho d/Q_{rp}$, where ρ is the particle density, d the diameter and Q_{rp} the radiation pressure scattering efficiency. This value cuts-off at $\rho d/Q_{rp} \simeq 5 \times 10^{-5}$ (O'Dell 1974), which may indicate a true minimum size but is more likely due to the result of Q_{rp} becoming small for particles much smaller than the wavelength of sunlight.

Starting from the position that comet nuclei must be very dusty, I have examined the three types of models that can be constructed by particles. These are listed in Table 1:

Table 1
Models of Comet Nuclei

Name	Gravitational Binding	Proponent
Very Loose	Not Bound	Lyttleton (1953)
Loose	Bound	Richter (1954)
Solid	Very Strong	Whipple (1950

Each model has its advocate and the models differ primarily in the amount of gravitational binding that is assumed. The Lyttleton (1953) model of a comet being a host of particles, not gravitationally bound to one another, but sharing a common orbit has been most successfully

criticized by Whipple (1963), who argues convincingly that this model does not apply to observed comets. The second model involves a swarm of particles gravitationally bound together, and bears many resemblances to a globular cluster. The strongest arguments against this model are theoretical. Both Shatzman (1952) and O'Dell (1973) have calculated the effects of perturbations on and collisions within the swarm of hypothesized particles. It is shown that those clouds of particles that are sufficiently dense to survive solar tidal torques have physical collision rates so high as to cause them to collapse down to solid bodies during infall from large heliocentric distances. This means that the three models can also be referred to as the inconsistent, the impossible, and the unavoidable. The unavoidable model that I envision is not the classical Whipple nucleus of dominant ices near the surface, but one composed mostly of very small particles, together with large particles built up of them, and initially a comparable amount of frozen gases. Such a model is quite consistent with the low tensile strength of the nucleus as inferred from the phenomenon of splitting, the low density and fragility of comet related meteors and the evolutionary change of the coma that characterizes long and short period comets.

It is interesting to consider the possible origin of such a solid nucleus, composed of many small particles (O'Dell 1973). Due to the volatile nature of the trapped gases, I argue for formation at large heliocentric distances, which raises the possibility that the frozen gases are not from the original pre-solar nebula but may be a frost acquired by the small particles prior to collapse into a gravitationally bound system. The one known source of small particles in the present solar system is in the zodiacal light cloud. Through the effects of radiation pressure (Harwit 1963), selectively the small particle component can be forced into highly eccentric orbits, with aphelion distances in the hypothesized Oort Cloud. Since the zodiacal cloud must continuously be replenished, this means that there must be a continuous flow of particles to very large heliocentric distances. If this is the source of particles eventually forming comet nuclei, it requires trapping into these outer orbits and forces to initiate collapse into single, gravitionally bound clouds, neither of which are now understood.

REFERENCES

Finson, M.L., and Probstein, R.F. (1968). "A Theory of Dust Comets. I. Model and Equations." Astrophys. J., 154, 327.

Gary, G.A., and O'Dell, C.R. (1974). "Interpretation of the Anti-Tail of Comet Kohoutek as a Particle Flow Phenomenon." Icarus, 23, 519.

Gebel, W.L. (1970). "Spectrophotometry of Comets 1967n, 1968b, and 1968c." Astrophys. J., 161, 765.

Harwit, M. (1963). "Origins of the Zodiacal Dust Cloud." J. of Geophysical Research, 68, 2171.

Lyttleton, R.A. (1953). "The Comets and Their Origin." Univ. Press, Cambridge.

O'Dell, C.R. (1971). "Spectrophotometry of Comet 1969g (Tago-Sato-Kosaka)." Astrophys. J., 164, 511.

O'Dell, C.R. (1973). "A New Model for Cometary Nuclei." Icarus, 19, 137.

O'Dell, C.R. (1974). "Particle Sizes in Comet Bennett (1970II)." Icarus, 21, 96.

Richter, N.B. (1954). "Statistik und Physik der Kometen." Johann Ambrosius Barth Verlag, Leipzig.

Schatzmann, E. (1952). "La Physique des Comètes." Quatriene Colloque International d'Astrophysique à Liege, p. 313.

Sekanina, Z. (1974). "On the Nature of the Anti-Tail of Comet Kohoutek (1973f). I. A Working Model." Icarus, 23, 502.

Stokes, G. M. (1972). "The Scattered Light Continuum of Comet Bennett 1969i." Astrophys. J., 177, 829.

Whipple, F. L. (1950). "A Comet Model. I. The Acceleration of Comet Encke." Astrophys. J., 111, 375.

Whipple, F.L. (1963). "Moon, Meteorites and Comets." (B.M. Middlehurst and G.P. Kuiper, eds.). Univ. of Chicago Press, Chicago.

DISCUSSION

M. Dubin: On the Schatzman arguments of compacting, does Schatzman take into account either or both, the charge on the bodies as they approach the Sun, either comparable to gravity or the angle momentum of the ensemble as they approach the sun?

C. R. O'Dell: Neither.

M. Dubin: In other words, there are two contra-forces that may make the impossible less impossible, more likely to happen?

C. R. O'Dell: No. The time scale is so strong in the sense of saying they must compact that the force, the angular momentum, would have to be very high or the electrostatic repulsion by the neutral particles would have to be quite high.

Actually, I've done the calculations too, you know, the language barrier strikes again. You do a calculation and then you find out that it's been done but published in French, and you finally face up and you make the translation you did the same thing.

Most of the compaction occurs at such large distances that charges on particles should be small. The angular momentum effect still would remain, though.

J. C. Brandt: Is there an inconsistency with your picture by presupposing the dust to make comets whereas Whipple's model says that comets make dust, for example the zodiacal light?

F. L. Whipple: I don't think we're inconsistent on that.

B. Donn: The compaction was early in the history, and this is now. Fred has them releasing dust now.

C. R. O'Dell: They didn't hear the question in the back.

F. L. Whipple: The question was whether comets make dust or dust makes comets, and I think the point is that in the zodiacal light you meant that the comets now break up into dust, didn't you? I hope.

C. R. O'Dell: That certainly fit by the calculation. On the other hand, I'm not convinced that by the numbers that you've proven the zodiacal light particles all come on as debris from comets.

J. C. Brandt: Where does it come from, then?

C. R. O'Dell: I don't know. All I know is it exists.

G. Wetherill: As I understand from the things McCrosky has told me, the large Taurids, Perseids, and Leoniels seen by the Praire network have finite strength and densities of about 2. While they ablate more readily than the Lost City chondrite their densities indicate considerable compaction.

F. L. Whipple: It's still a moot question, how dense they are whether it's four-tenths or two?

G. Wetherill: The conclusion that there is evidence for their being very weak, dusty aggregates, I don't understand.

F. L. Whipple: They're extremely fragile. That is proven by the way they break up. They break up much faster than they should.

G. Wetherill: There are things that break up more easily as well.

D. J. Malaise: Monte Carlo computations by Dr. Everhart shed in my mind some doubts about the Oort's model for the origin of comets; that is we are observing the tail of a continuous diffusion of a huge number of comets formed at the origin of the solar system in the inner part of the primitive nebula.

The process you just described is a nice way to solve the problem because it is based on things which we know that exist (the dust in the vicinity of the sun) and on process we know that are working (radiation pressure). This gives us a cloud of dust in the position of Oort's original cloud of comets. The question now is how do you build comets from this dust cloud. Did you put any figure on the expected density and in homogeneity? Anyhow I don't think this question should stop you developing further this model by simply assuming that comets are formed in the cloud. After all we see stars forming in interstellar clouds without knowing exactly how to explain the beginning of the contraction process.

C. R. O'Dell: This key issue is what produces the cloud of these particles. It demands somehow you could form such a cloud, either through interaction with the interstellar gas remember, these conditions are interstellar rather than solar system or by perturbations of other objects, such as large objects gravitationally perturbed or passing stars. However, in any event it does take the formation of an initial cloud, and the collapse time of that cloud one can calculate.

A cloud sufficiently dense to survive tidal distortion does have sufficiently short freefall time to collapse within the in-fall time into inner solar system.

So what's needed is an intitial formation into a cloud.

D. J. Malaise: This makes me very happy, because it solved the biggest problem I had in Oort's Theory, that is, you had to bring them out and then to bring them in.

F. L. Whipple: That's what worried us all these years.

D. J. Malaise: Because when it is collapsed the radiation force is much less, of course. And, as far as the cloud formation goes, we don't have to worry about this because clouds are formed, anyhow.

OMIT

THE NUCLEUS: PANEL DISCUSSION

W. F. Huebner

Almost all information about the physics of the nucleus is based on deductions from observations of the coma and tails. It is well to keep in mind the hierarchy of events on which these deductions are based:

1. The material properties of the constituents of the nucleus and the detailed physical and chemical structure of the nucleus form the basis for the behavior of coma and tails.

2. Interaction of solar radiation with the surface of the nucleus determines the overall temporal development of the coma.

3. The subsequent interaction of solar radiation and solar wind with the coma determine the gross features of the tails.

4. Short term fluctuations primarily in the solar wind (and associated magnetic field) cause disturbances of comparable duration observable mostly in the tail but also in the coma.

In a large number of cases (particularly if the coma is involved) it is difficult to isolate the cause of the disturbances, i.e., whether the observed effect is due to a fluctuation in the solar wind or due to an inhomogenity in the structure of the nucleus. The further removed an observed effect is in the hierarchy of events, the more difficult it is to relate it to the nucleus. Our concepts about the nucleus should therefore be based primarily on those observations which can be linked to the nucleus in the most direct manner.

With this in mind let us follow an "average, new" comet on its way around the sun and note how the observed phenomena reflect on the properties of the nucleus. At a heliocentric distance comparable to the orbit of Jupiter the comet is a diffuse object. The diffuseness can be explained by the evaporation of highly volatile material, for example a frosty deposit accumulated during the long time that the comet spent in Oort's cloud. Embedded in this material may be grains of dust or water ice. The thickness of the shell must be small compared to the size of the nucleus but thick enough to drag dust or icy grains into the coma. In most cases there is no observable ion tail or spectrum; this indicates that the volatile material most likely is not composed primarily of CO. Spin of the nucleus reduces gravitational attraction and therefore aids in the development of a diffuse coma.

As the comet approaches the orbit of Mars the coma develops more fully, dust and particularly ice-covered grains are dragged into the coma and the spectroscopic radicals become observable. The surface of the nucleus begins to warm up and the more volatile components mixed with the less volatile frozen gases (e.g., H_2O) must be preferentially vaporized. Between Mars and Earth solar wind and solar radiation ionize part of the molecular coma. Through interaction with the solar wind the ions are transported to form an ion tail. The solar radiation also interacts with the grains in the coma and by the process of radiation pressure they form a dust tail. Dissociation of molecules and radicals in the coma gives rise to the observable ultraviolet coma which consists primarily of hydrogen and hydroxyl radicals. The thin layer of depleted volatiles on the surface of the nucleus schematically indicated in Fig. 1-A

by cross hatching will now begin to vaporize more actively. As the heat slowly penetrates into the nucleus additional volatile material dispersed in the less volatile frozen gases will be brought to the surface and vaporize. Any pockets of volatiles which were on the surface have of course been depleted (Fig. 1-B). As the comet moves to still smaller heliocentric distances, say to about one half astronomical unit, the frozen gases (primarily water ice and some mixed-in more volatile compounds) continue to be vaporized from the surface of the nucleus. This vaporization occurs rather uniformly. The data collected by Ulich and Conklin (1974) on methylcyanide shows no significant Doppler shifts. Methylcyanide is a relatively volatile compound with a latent heat of vaporization of $L \approx 8$ kcal/mol (in relation to water with $L \approx 13$ kcal/mol). Heat is transported relatively slowly for some small distance into the nucleus. As the comet moves further on its orbit around the sun this heat vaporizes pockets of more volatile gases trapped under the surface. These pockets of volatiles are now engulfed in a bath of somewhat warmer (say, ~150°K) less volatile components of the frozen nucleus. At this temperature the volatiles can build up a pressure which is several orders of magnitude higher than the vapor pressure of the surrounding, less volatile frozen gases. If these pockets are not too deep under the surface (~1 m) then the gases will be released rather explosively from the fluffy structure of the nucleus. For an adiabatic explosion the front of the escape velocity wave (Lelevier, 1965) is

$$v = \frac{2c}{\gamma - 1} \quad , \qquad (1)$$

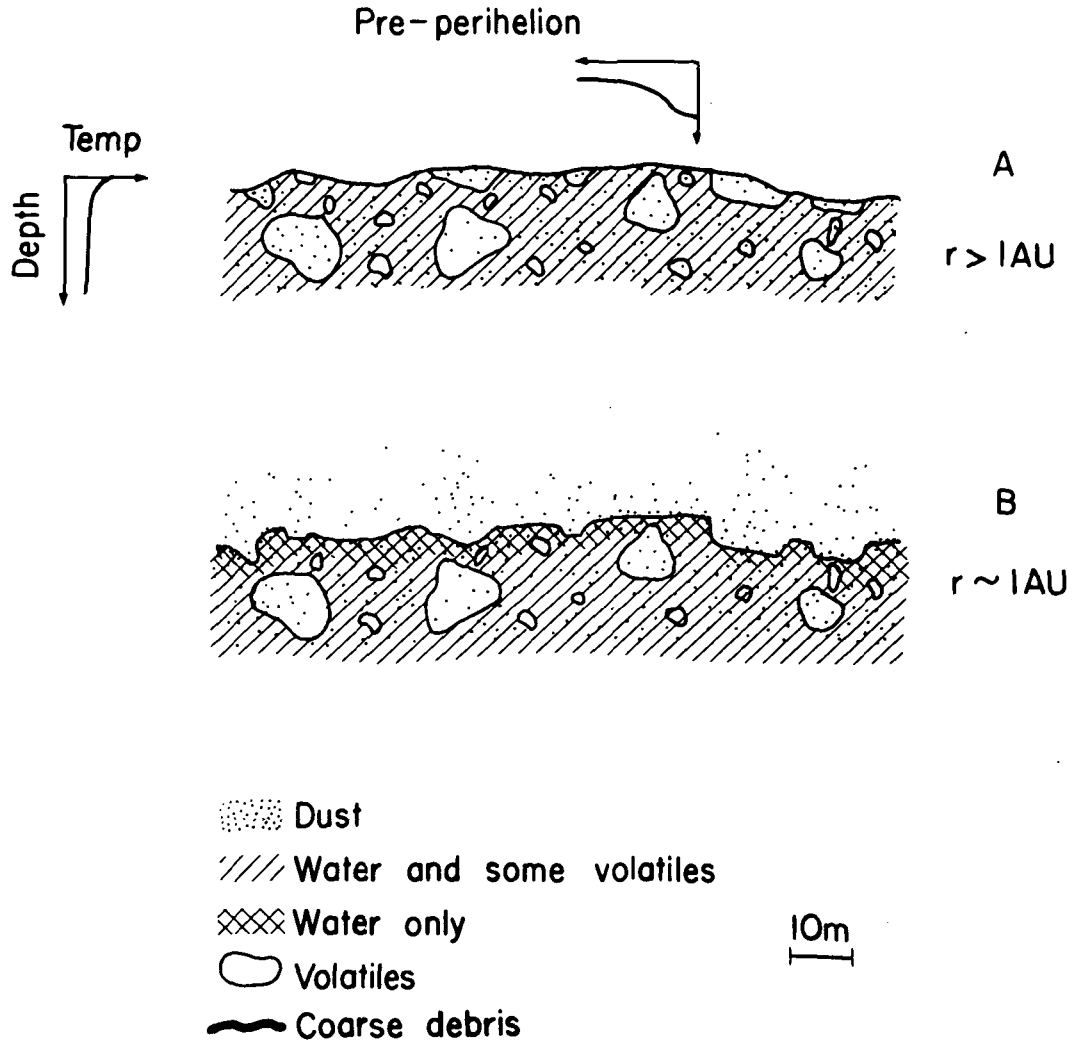

Fig. 1-A. A portion of a cross section near the surface of the heterogeneous model of a comet nucleus. At some heliocentric distance r > 1 A.U. the outgassing of the volatile components begins. The temperature profile on the left indicates a rise of the equilibrium temperature at the nuclear surface.

Fig. 1-B. At r ~ 1 A.U. volatiles have been depleted from the surface, heat begins to penetrate.

where c is the speed of sound which is approximately the thermal velocity of the gas. If the gas causing the outburst consists of polyatomic molecules then its polytropic index is $\gamma = 1.1$ to 1.3. For an average value of $\gamma = 1.2$ the front of the escape velocity is therefore approximately ten times the speed of sound or approximately ten times the thermal velocity of the gas. This is in agreement with the observed Doppler shifts of HCN and CH_3CN as observed by Buhl, et al. (1974). If the surface is uneven then the outbursts can occur in almost any direction from the sunward hemisphere of the nucleus (Fig. 1-C). After the pressure in a pocket has been relieved the vent may close again until the pressure has built up to its critical value and another puff of volatile gas is issued, similar to the action of a water droplet emersed in nearly boiling oil in a frying pan. Under these conditions the surface of the nucleus may approach Shul'man's spotty model of the nucleus. The rather limited observations available at this time indicate that for larger pockets the escape of gas occurs for a few hours but less than 24 hours. From the column density of radio observations and the measured Doppler shifts one obtains for the size of the larger pockets a diameter of the order of a few times 10 m.

The peak of the temperature distribution continues to travel into the nucleus even after perihelion. Therefore outbursts can still be detected even after the comet is receding from the sun (Fig. 1-D). Interpretation of the radio observations (particularly of HCN) indicate that the structure of the nucleus is inhomogeneous on a scale of about 10 m. As the comet recedes further from the sun the temperature distribution in the nucleus flattens out and outbursts become more rare

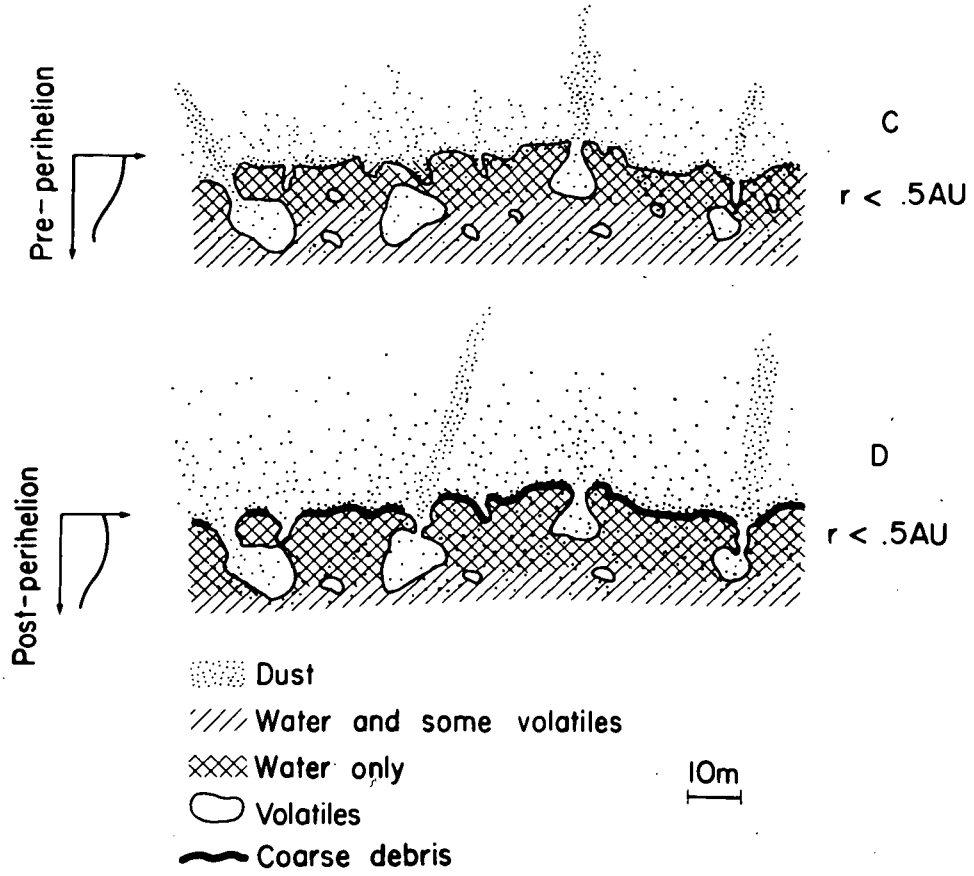

Fig. 1-C. At r < 0.5 A.U. heat has penetrated to pockets of volatiles and causes them to erupt in jets.

Fig. 1-D. After perihelion, but still at small heliocentric distances (r < 0.5 A.U.) the temperature profile broadens and heat still penetrates somewhat deeper, but the temperature begins to decrease at the surface. A few more pockets of volatiles explode. Coarse-grained dust (indicated by a black surface contour) accumulates. At still later times only the frozen gases remaining on the surface receive sufficient heat from incident radiation to vaporize. This causes the observed dimming of the comet when its brightness is compared to that at the same heliocentric distance before perihelion.

and finally cease. Vaporization then occurs entirely from the surface which has been virtually depleted of volatile gases. This explains the general dimming of the comet after perihelion when its brightness is compared to that before perihelion at the same heliocentric distance.

I have given a possible interpretation of recently acquired data as it reflects upon the structure of the nucleus. Let us briefly look at the chemical abundances. With the exception of water for which there now exists considerable indirect as well as some direct evidence (Jackson, et al., 1974) all of the identified mother molecules have very strong molecular transitions in the radio range. Of the five molecules most likely to be found in a comet because of their strong transition probabilities HCN, CH_3CN, CH_3NC, H_2CO, and HNCO (see Huebner, 1971) the first two have been detected. HCN appears to be abundant to a few percent in comet Kohoutek. The abundance of methylcyanide cannot be ascertained because it appears not to be in equilibrium. The point to keep in mind is that there may be other molecules, perhaps even more abundant than HCN, but it is more difficult to detect them because of their weak line transitions. A few unidentified lines in the radio range have been reported, but these lines seem to correspond to a different class of transitions. Typically, a mother molecule exhibits a line width of 100 to a few 100 kHz. The unidentified lines are however much broader: of the order of 1 MHz. A possible explanation is that these transitions correspond to molecules or radicals which have undergone an exothermic reaction or an exothermic dissociation. It is also very likely that they are light molecules.

As indicated above much new data is becoming available: New molecules give information about the chemistry of the nucleus, Doppler shifts give us information about the structure of the nucleus, infrared observations tell us about the composition of the grains, observations of light reflected in the coma and the antitail give us information about the dynamics of grains close to the nuclear surface, and about the latent heats of the propelling gases. Spectroscopy has of course for many years given some indication about the general constituents to be expected in the frozen nucleus. The question now really is: do we interpret the data correctly? Do we have enough physical and chemical information to interpret the data? I believe that the basic data needed in comet physics is not always of the common variety. I therefore propose that serious thought be given to the establishment of a laboratory for comet physics and that an effort be made to organize the data which already is available. Of particular need, I believe, are data on physical chemistry. For example, data on vaporization; data on mixtures; data on chemical reaction rates; and data on grain scattering, to mention a few specific areas. Much work is already being done, for example, at Leningrad Kaimakov and Sharkov work on physical chemistry. Here at NASA Donn and Stief work on photochemistry. In Canada Prof. Herzberg does outstanding work on laboratory spectroscopy. At Toledo Delsemme works on clathrates. At NBS Lovas and Johnson work on radio line transitions. In Munich Michel has carried out some basic work on grains and infrared spectroscopy. And in Italy Cosmovichi works with molecular beams. Undoubtedly, there are many other laboratories at work on physics and chemistry relevant

to comet problems (which usually are also of interest to interstellar problems). But it will be necessary to stimulate some work currently in progress to make it relevant to the physics and chemistry of comets; and in other cases it will be necessary to analyze the results for their relevance to comet research.

References

Buhl, D., W. F. Huebner, and L. E. Snyder, 1974, "Detection of Molecular Microwave Transitions in the 3 mm Wavelength Range in Comet Kohoutek (1973f)." Proceedings of this conference.

Huebner, W. F., 1971, Bull. Am. Astron. Soc. 3, 500.

Jackson, W. M., T. Clark, and B. Donn, 1974, "Radio Observations of H_2O in Comet Bradfield," Proceedings of this conference.

Lelevier, R., 1965, "Lecture Notes on Hydrodynamics and Shockwaves," Lawrence Radiation Laboratory report UCRL-4333 Rev. 1.

Ulich, B. L., and E. K. Conklin, 1974, Nature 248, 121.

DISCUSSION

Z. Sekanina: There is one thing I'd like to ask both Dr. Huebner and Dr. Delsemme with respect to the expression for the escape velocity.

I understood from the papers of Dr. Delsemme that the escape velocity is basically only that of the thermal velocity, whereas you suggested you get essentially one order of magnitude larger velocity than is the thermal velocity.

W. F. Huebner: I don't think that's any conflict. When you get evaporation from the surface, you indeed get evaporation from thermal velocity. What is happening here is an explosion of the pockets of high pressure of volatile material which has a vapor pressure of the order of 100 to 1,000 times higher than that of the surrounding water.

B. Donn: I have one question about the amount of material. What the pocket implies is only a small amount of material goes out in the jet. But if we look at your slides, these displaced components of HCN seem to me to have comparable intensity as the perhaps normal one, which suggested that a lot of material is going out in these jets and therefore a lot of material is going out with high velocity. Can you put this into a consistent picture?

W. F. Huebner: I didn't show the spectrum for the CH_3CN, but in CH_3CN you do not see a quiescent state. I therefore interpret the spectrum to mean that the zero Doppler shifts are also outbursts, but in a direction perpendicular to the line of sight. And they all are about the same order of magnitude, and therefore they all correspond to exploding pockets.

B. Donn: But in that case, what's bothering Sekanina is that you have a high velocity of ejection of the material, not the nearly thermal one that we use. And this, it seems to me, presents lots of problems with all these models of the coma, if the gas is coming off with these high velocities.

W. F. Huebner: I think the fluctuations that we see are the high velocity components, and those explode in pockets. The material which was lying on the surface has already disappeared by this time. We are observing at heliocentric distances which are smaller than 0.5 AU, something like 0.3 to 0.4.

H. Keller: I think in this connection in the first 1000 to 10,000 km we should have a lot of collisions of the exploding gas. I wonder whether you can keep up this beam direction or would this effect make things more isotropic so that you wouldn't see such high velocity components, at least not this high

velocity coming out of the pockets, because the density is pretty high in the vicinity of these explosions.

W. F. Huebner: The spectra is already a few hundred kilohertz wide, and theoretically it's best to assume that by broadening it would only be about 90 kilohertz wide. I think we see some broadening effects on that.

M. Dubin: I would like to be on record as I think the water molecule is a parent molecule.

(Podashnick & Scheuerman) published in Nature recently, an interesting aspect of the phase of water, amorphous water at 140 K changes phase.

The change in phase is such as to be endothermic and to be expansive the density changes. The effect, then, is to transfer the phase change to some depth and to spall the ice.

Now, I think this has a clear connection with the Podashnick-Scheuerman type of description you've given.

W. F. Huebner: If you take the paper of Delsemme, I think the one difficulty in the paper is that it assumes the density for the amorphous water as a density of 2.3 grams/cm^3, which is rather high, and with the difficulty of understanding how it's got to be that high.

A. H. Delsemme: I just want to comment about this high density of amorphous ice. We had found high density. It has never been confirmed. I believe this high density was spurious. I still am unable to explain why we have found it, although we have observed amorphous water, of course.

So let's put it this way. I believe that the density of amorphous water is rather high, but certainly not as high as we have found. It looks to me, when I haven't looked at my results for a few weeks it looks impossible. When I go back to the dates, of course, I'm again convinced by myself, but that's another story.

Voice: Then you should tell the key point, I think.

A. H. Delsemme: No, I think—what I would like to discuss now is the chemical nature of the nucleus.

Of course, this implies the discussion of the interface of the nucleus with the coma because that's our only source of information about the nucleus. That's the vaporization that is happening at the coma level.

THE NUCLEUS: PANEL DISCUSSION

A. H. Delsemme

What I would like to discuss here is the chemical nature of the nucleus.

This implies the consideration of the vaporization of the nucleus into the coma because the coma is our only source of information on the nucleus. The nature of the parent molecules vaporizing from the nucleus has been for a long time the missing link for our understanding of the molecular processes. A major development has been brought about by the first identification of three neutral parent molecules HCN and CH_3CN identified in Comet Kohoutek, H_20 in Comet Bradfield, confirmed by H_2O^+ in Kohoutek.

The atomic resonance lines of carbon and oxygen will also play a fundamental role in our understanding of the cometary phenomena, because we will be able to make a balanced budget of all the atoms to explain the molecular abundances.

Incomplete as they are, the major feature that seems to emerge from these new results is the large depletion of hydrogen of the volatile fraction, at least as compared with a mixture of cosmic abundances. In particular, the H/O ratio points to an oxidation-reduction equilibrium, very much like that of carbonaceous chondrites.

For the first time we have rather good data on the total production rate of hydrogen, with rather good data on the oxygen forbidden line, which gives the lower limit to the total oxygen produced in a comet; finally, we have assessments on the production rates derived from the resonance lines of carbon and of oxygen.

The H/O and C/O ratios will certainly be revised in the future, and measured more accurately on bright comets. Let's assume that the present values are meaningful. They suggest a major departure from the early model of the nucleus. Instead of molecules like CH_4 and NH_3 containing large amounts of hydrogen, they suggest molecules with less hydrogen, like ethylenic, acetylenic or aromatic compounds, and hydrazine instead of ammonia. The fact that nobody has yet been able to detect CH_4 or NH_3 may not be very significant, but it goes in the same direction.

The probable presence with water, of much CO and CO_2 (suggested by C/O and by the ions CO^+ and CO_2^+) is also difficult to explain without a serious depletion in hydrogen. Of course, I do not really believe that thermodynamic equilibrium is likely to be reached. It is a trend that can be modified by different factors influencing the reaction kinetics, as exemplified by the Fischer-Tropsch (FTT) reactions proposed by Anders.

These FTT reactions were proposed in order to explain the hydrocarbons observed in carbonaceous chondrites. It may be significant that this same type of reaction would explain the parent molecules of C_2 and C_3, as being higher acetylenes.

If the cometary stuff was made in deep space where triple molecular collisions are notoriously absent and where the radiation field is a diluted mixture of two Planckian distributions, roughly, at one hundred and ten thousand degrees, it is clear that the thermodynamic equilibrium has no meaning and that the depletion of hydrogen may simply translate the fact that hydrogen cannot easily stick, for eons, on interstellar grains. However, if Herbig's ideas have any sense, comets as well as interstellar molecules could have been formed in the primeval solar nebula and other primeval stellar nebulae, and the clues we have just found about the present redox potential of the cometary nuclei may simply mean that comets were made in the confines of the solar nebula, not with a solar mixture, like Jupiter and Saturn, but with a solar mixture already much depleted of its hydrogen and its helium, like Uranus and Neptune.

OMIT

THE NUCLEUS: PANEL DISCUSSION

B. Donn

My remarks will present some views of the behavior of the nucleus and problems with their explanation.

One thing we definitely know about comets is that there has to be a permanent structure which revolves around the sun in the comets orbit. Permanent means carrying over from apparition to apparition during the lifetime of the comet. I adopt some form of the "icy nucleus" model as proposed by Whipple. This structure reasonably fits most of the known cometary features although no completely consistent model accounting for all known phenomena in a satisfactory manner has yet been described. The icy nucleus does not appear to have any major flaws. It has a real advantageous feature in that detailed models can be constructed and their behavior more or less accurately predicted, e.g. (Donn 1963; Delsemme and Miller, 1971; Sekanina 1972, 1973; Huebner, 1975).

The attempts to analyze various models in greater detail emphasize one of the great needs in cometary research, namely, more laboratory studies of simulated icy nucleus material. Only very limited work has been published in this area (Delsemme and Wenger, 1970, and Kajmakov, et al. 1972a, b).

Another important area of research concerns physical observations; luminosity, spectra and colors of comets over large intervals of

heliocentric distance extending beyond 2 A.U. Only occasional observations of this type are available. Several papers and much of the discussion at this colloquium have shown the need for such data.

The main points I wish to discuss here are rather closely related to the last item, observations at large distances, and show in more detail why such observations are so important.

For a long time it has been my belief that the presence and behavior of the C_3(4050) bands are important clues to nuclear and probably coma processes. C_3 is one of the first molecular emissions to become detectable as a comet approaches the sun. This is well shown in Plates I and II of the Atlas of Cometary Spectra (Swings and Haser, 1957). The high relative intensity of C_3 at large heliocentric distances is brought out in the Atlas. In every instance of spectra taken beyond 1.5 A.U. the C_3 emission is the second most prominent after CN(0,0). Qualitative evidence is given by Hogg (1929) (CH_x has been identified as C_3) based on all spectra taken prior to 1929. This was true for Halley's Comet in 1909 (Bobrovnikov, 1931) and also for Comet Encke (Swings, 1948 ; Swings and Haser, 1957).

The behavior of C_3 is essentially the same in comets making their first approach to the Sun and in very old Comets. The general similarity of the behavior of all molecular emissions among all categories of comets, as far as it is now known, is a strong argument for similar processes occurring throughout the life of a comet after its initial close perihelion passage.

Although several sources for C_3 have been proposed, none are generally acceptable at the present time. The formation of C_3 either requires (i) photodissociation of a complex organic molecule containing a three carbon chain, methylacetylene H_3 C - C C - H is the only laboratory source yielding C_3 in an apparently primary photochemical process (Stief, 1972),(ii) formation by collision (iii) release of C_3 radicals from the nucleus. There are difficulties with making any of these mechanisms consistent with the reduced activity and lower coma densities at large distances and the absence or relatively lower intensities of all other cometary emissions as r increases. Only the scattered solar continuum shows the same general intensity behavior. In fact, at distances greater than 3 A.U., with the exception of Comet Humason, 1962 VIII, only a solar continuum has been detected.

Spectroscopic observations of the behavior of cometary emissions at 3 A.U. and beyond using image intensifiers or large aperture interference spectrometers are essential. There is great danger in developing a theoretical explanation or model on insufficient data. Although many of the details of comet activity at large distances are uncertain, there is no doubt of the common occurrence of such activity beyond 5 A.U. as Sekanina has shown. The first problem is to account for it in a way consistent with other cometary features.

A second problem is closely related to the point just raised. Not only do comets show significant ejection of material beyond 3 A.U., but there are several indications that this ejection rate decreases

after and even during its first approach to the sun. There are direct observations such as for the recent apparition of Comet Kohoutek 1973, which showed a luminosity drop of perhaps 1 1/2 to 2 magnitudes (Jacchia, 1974) after perihelion. A very suggestive evidence for rapid fading is the sharp peak in the 1/a distribution for $1/a < 50 \times 10^{-6}$ (Oort, 1951, Whipple, 1962).

Comets in an Oort cloud have existed in interstellar space for the lifetime of the solar system, about 4×10^9 years. During this time they have been exposed to all the radiation found there. The possible chemical effect of an intense early solar wind was pointed out by Donn (1968). More recently Shul'man (1972) has called attention to the chemical effects of cosmic rays over the lifetime of a comet in producing similar results. The results of a more detailed analysis of this phenomena is given here.

For the region of the Oort cloud the extrapolated cosmic ray flux near the Earth may be represented by

$$\frac{dN}{dE} = k(E_T)^{-\gamma} \text{ particles/m}^2\text{-s-ster-MeV/nucleon} \qquad (1)$$

where E_T is the total energy = $E_{kin} + m_o c^2$ (938 MeV) γ is very near 2.5 and $k = 2.5 \times 10^8$ (Goldstein et al., 1970; Gleason and Urch 1972). Intensities of cosmic rays below about 100 MeV are not determined by these measurements because such particles are degraded from higher energy cosmic rays. It is reasonable to extrapolate over some interval and it is assumed here that the distribution law in

Equation 1 is valid to 10 MeV. As the proton flux is a factor of ten higher than the alpha particle flux, only protons are considered in the following analysis.

Radiation incident on the comet surface penetrates to a distance R(E) where E is the particle kinetic energy. Energy is lost along the path primarily by ionization (Dalgarno, 1962) which produces electrons of several tens of electron volt energy. These in turn dissociate molecules, producing chemical effects. Range and energy loss as a function of energy up to 5000 MeV for protons in water are given in Table III of Barkas and Bergen (1964). From that table the energy deposited in successive layers of thickness 20 gm/cm^2 was obtained for protons in water. Proton ranges in a wide variety of materials from quartz to propane lie within 20% of the range in water. Energy calculations for a water-ice nucleus will apply closely for the uncertain actual composition of the nulceus. Above 1400 MeV an average loss of 43 MeV per layer was used.

From the energy loss vs energy data a matrix $\Delta E_{j,n}$ was determined. This represents the energy deposited in a layer ΔD_j between mass load limits 20 (j-1) and 20j gm/cm^2 for a particle of initial energy E_n with range 20n g/cm^2. The total energy deposition for normal incidence cosmic rays was found by suitably combining this matrix with the energy distribution of equation 1. The results for an isotropic cosmic ray flux was obtained by integrating the above slant range distribution over a hemisphere. Figure 1 shows the relative energy deposition as a function of depth for protons. As the nucleus density

is about 1 g/cm^3 and probably nearly constant in the outer portion, the abscissa also represents depth in meters.

In addition to cosmic rays protons the comet nucleus in the Oort cloud will be irradiated by cosmic ray electrons, gamma rays and ultraviolet photons. Ultraviolet photons will only interact with a very thin surface layers but will subject that region to an intense irradiation. The electron flux is one tenth of the protron flux (Goldstein et al, 1970). Although the energy loss of electrons is similar to that of protons with 2000 times greater energy, the large scattering of electrons will cause the electron energy deposition to also have a high gradient. The gamma ray photon flux is about a factor of ten less than the extrapolated proton flux at 10 MeV and has a steeper slope (Peterson et al, 1974). For 10 MeV photons, 90% of the energy is absorbed within 1.5 m. The net effect of all energetic radiation is to make the curve of Figure 1 even steeper.

In order to determined the effect of the radiation during the comets stay in the Oort cloud, we need the absolute energy deposition. The unit of the ordinate corresponds to 240 MeV/cm^2 sec. There is little experimental data to cover the irradiation of a cosmic mixture. Oro (1963) irradiated a condensed mixture of methane, ammonia and water with 5 MeV electrons. An irradiation of $6x10^{16}$ MeV/gm over a two hour period converted 6% of the carbon to other species including 4% to non-volatile products. Berger (1961) exposed a condensed methane-ammonia-water mixture to 12 MeV protons and obtained a yield of 1.4

molecules formed per 100 ev. This presumably refers to energy incident rather than absorbed and an equivalence of about 100 molecule formed per 100 ev absorbed may not be unreasonable.

The energy absorbed per 20 cm layer of the nucleus in the Oort cloud can be obtained by setting unit ordinate in Figure 1 at 2.4 x 10^{19} MeV/cm^2. A comparison of this dosage with the experimental yields indicates that approximately complete conversion of the first few layers of an icy nucleus will occur during its time in the cloud. Only some percent of the nucleus below a few meters will be affected. The irradiation will tend to polymerize the simple, volatile original ices. The results would be a less volatile outer zone compared to the inner protected region.

This conclusion is in contradiction with the apparent greater activity of new comets coming from the Oort cloud. Hence, the importance of studying the spectra, especially of new comets at large distances.

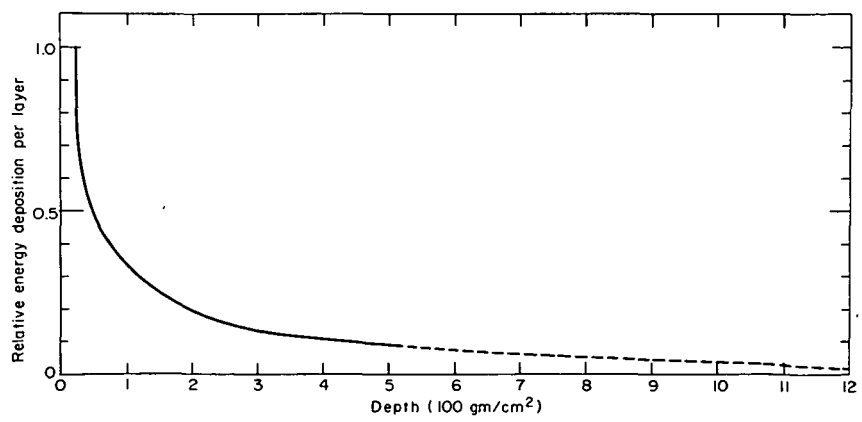

Figure 1. Relative energy deposition as a function of depth. The dashed line is based on an extropolation.

REFERENCES

Barkas, W.H. and Bergen, M.J., 1964, NBS SP 6421.

Berger, R. 1961, P.N.A.S. 47, 1434.

Bobrovnikov, N.T. 1931, Lirk Obs. Bull 17, 309.

Dalgarno, A. 1962, In Atomic and Molecular Processes, ed. D.R. Bates (N.Y. Academic) p. 623.

Delsemme, A. H. and Miller, D. C. 1971, Planet. Space Sci. 19, 1229.

Delsemme, A. M. and Wenger, P. 1970, Planetary Space Sci. 18, 717.

Donn, B. 1963, Icarus 2, 396.

Donn, B. 1968, Introduction to Space Science, ed. W. N. Hess and G. N. Mead (Gordon and Breach, N. Y.) p 501

Gleason, L.J. and Urch, I., 1971, Ast. and Space Sci. 11, 288.

Goldstein, M.L., Ramaty, R., Fisk, L.A., 1970, Phys. Rev. Let. 24, 1193.

Hogg, F.S. 1929, J.R.A.S. Can. 23, 55.

Huebner, W.F., 1975, Their Proceedings

Jacchia, L.J., 1974, Sky and Telescope 47, 216.

Kajmakov, E.A. and Sharkov, V.I., 1972a, In I.A.U. Symposium 45, The Motion Evolution of Orbits and Origin of Comets, ed. G.A. Chebotarev, E. I. Kazimirchak-Polonskaya and B.G. Marsden (Dordrecht: Reidel) p. 308

Kajmakov, E.A., Sharkov, V.I. and Zhuralev, S.S. 1972b, In I.A.U. Symposium 45, The Motion, Evolution of Orbits and Origin of Comets, ed. G.A. Chebotarev, E.I. Kazimirchak-Polonskaga and B.G. Marsden (Dordrecht, Reidel) p. 316.

Oort, J.M. 1951, B.A.N. 11, 91.

Oro, J. 1963, Nature 197, 971.

Peterson, L.E., Trombka, J.I., Metzger, A.E., Arnold, J.R., Matteson, J.I., and Reedy, R.C., 1974 in NASA SP 339 ed. F.W. Streaker and J.I. Trombka (Washington, NASA) p. 41.

Sekanina, Z. 1972, In AGU Symposium No. 45, The Motion, Evolution of Orbits and Origin of Comets, ed. G.A. Chebotareo, E.I. Kazimirchak-Polonskaya and B.G. Marsden p. 301.

Shul'man, L.M. , 1972, In IAU Symposium No. 45, The Motion, Evolution of Orbits and Origin of Comets, ed. G.A. Chebatarev, E.I. Kazimirchak-Polonskaya and B.G. Marsden (Dordrecht; Reidel) p. 265.

Stief, L.J. 1972, Nature 237, 29.

Swings, P. 1948, Ann. d'Astrophys. 11, 124.

Swings, P. and Haser, L. 1957, Atlas of Representative Cometary Spectra Liege.

Whipple, F.L. 1962, In the Moon, Meteorites and Comets, ed. B.M. Middlehurst and G.P. Kuiper (Chicago, Univ. of Chicago Press) p. 639.

DISCUSSION

A. H. Delsemme: The volatile material diffuse has ample time to diffuse away from the center into the upper layers of the model you have just described.

D. J. Malaise: I thought that the general behavior of comets is that they are more active before perhilion than after?

F. L. Whipple: That's part of Donn's paradox.

D. A. Mendis: I'd like to make one comment, and that's about the charging of the grains. The grains are charged by electrostatic charging in a stream. The charging does not necessarily disrupt the stream. One has to take into account the effect of the polarization image charge which can cause the grains to stick. The same point has to do with the more general comment on the classifications of nuclear models on loose to very loose to compact. It might also be classified as a time sequence: very young, middle-aged, and older.

G. H. Herbig: This doesn't have implications for cosmic ray irradiation, but one way of dating material, of cosmic composition, as you know, is determining a lithium to the calcium ratio in the material. This dates stars. The question is whether the material that's in comets has an older or new lithium to calcium ratio.

In the passage of Ikeya-Seki near the Sun in 1965, there was a major attempt to find out what the lithium-calcium ratio was when this Comet was very near the Sun. And, as you know, the resonance lines of potassium, calcium, sodium, nickel, copper, and iron came up in the spectrum of the coma when it was near the Sun. But lithium never appeared.

Now, this isn't as simple a thing as it is in stellar atmosphere; the fact that lithium didn't come up may be that it was bound chemically in some very tight fashion.

All I was going to say is that if you are interested in answers to questions of this sort, there's another kind of chemistry that ought to be talked about. That is the chemistry of the volatile compounds these metallic elements. If lithium is locked up preferentially, that may account for the observations. But it's a rather puzzling thing.

If things like copper appeared in the coma, why can't we see the lithium lines in resonance emission at that time?

W. Jackson: It would seem that lithium would have more volatile compounds than any of the other things that we see. If I remember correctly, I think that lithium compounds tend to be more volatile than the others.

THE NUCLEUS: PANEL DISCUSSION

Fred L. Whipple

In discussing the nucleus of comets and the role of comets in the evolution of the solar system I summarize the observation only in Table 1, the observed composition. Note that gas-phase chemistry obscures the nature of the active atoms, molecules and radicals in the nucleus.

I wish to stress the fact, so obvious from this symposium, that the comprehensive observational attack on Comet Kohoutek (1973f) has led to an enormous step forward in deciphering the comet enigma.

We may confidently assume the following basic facts and deductions about the character of cometary nuclei.

A. Comets are members of the solar system. No evidence exists for orbits of interstellar origin (Marsden and Sekanina, 1973).

B. Comets have been stored for an unknown length of time in very large orbits in the Öpik-Oort cloud out to solar distances of tens of thousands of astronomical units (Öpik, 1932, Oort, 1950). Perhaps 10^{11} comets with a total mass comparable tc that of the Earth still remain, as Oort suggested, perhaps many more.

C. The basic cometary entity is a discrete nucleous (rarely, if ever, double) of kilometer dimensions consisting of ices and clathrates, including specifically H_2O, CH_3CN, HCN, CO_2 and probably CO. Other parent molecules of the abundant H, C, N and O atoms mixed in an unknown fashion with a com-

Table 1

Observed Composition of Comets

HEAD:	H, C, C_2, C_3, CH, CN, $^{12}C^{13}C$, HCN, CH_3CN, NH, NH_2, [OI], O, OH, H_2O, Na, Ca, Cr, Co, Mn, Fe, Ni, Cu, V,
TAIL:	CH^+, CO^+, CO_2^+, N_2^+, OH^+, H_2O^+, and Continuum from particles including Silicate 10-um band.

parable amount of heavier elements as meteoric solids must occur in comets because of the observed radicals, molecules and ions, in Table 1. (Whipple, 1950, 1951. Delsemme and Swings, 1952, Swings, 1965).

D. Cometary meteoroids are fragile and of low density (McCrosky, 1955, 1958. Jacchia, 1955).

E. The comet nuclei as a whole must never have been heated much above a temperature of about 100 K for a long period of time, otherwise new comets could not show so much activity at large solar distances (Kohoutek, 1973f, for example). Possible internal heating by radioactivity and temporary external heating, by supernovae for example, are not excluded.

F. Comets were formed in regions of low temperature, probably much below 100 K.

G. Comet nuclei are generally rotating, but in no apparent systematic fashion and with unknown periods in the range from about 3^h to a few weeks, based on non-gravitational motions and the delayed jet action of the icy nucleus.

H. The nuclei, at least of three tidally split comets, show evidence of a weak internal compressive strength the order of 10^4 - 10^6 dyne cm^{-3} (Öpik, 1966) and evidence of little internal cohesive strength.

I. The surface material of active comets must be extremely friable and porous to permit the ejection by vapor pressure of solids and ices at great solar distances. The evidence for clathrates by Delsemme and Swings (1952) coupled with the probable ejection of ice grains at great solar distances (Huebner and Weigert, 1966) and the behavior of Comet 1963f support this deduction.

The following probable limits of cometary knowledge or negative conclusions appear valid:

1. Roughly a solar abundance of elements may reasonably be assumed for the original material from which comets evolved. Note Millman's (1972) evidence regarding the relative abundances of Na, Mg, Ca and Fe in cometary meteor spectra and the solar value of the $^{12}C/^{13}C$ ratio measured by Stawikowski and Greenstein (1964, C. Ikeya, 1963I) and Owen (1973, C Tago-Sato-Kosaka, 1969 IX).

2. The material in the region of comet formation (with roughly solar abundances of elements) could not have cooled slowly in quasi-equilibrium conditions from high temperatures. The significant abundances of CO, CO_2,

C.2

C_2, C_3, and now CH_3CN and HCN in comets along with the low density and friability of the cometary meteoroids indicate non-equilibrium cooling in which the carbon did not combine almost entirely into CH_4 and the meteoroids generally did not have time to aggregate into more coherent high-density solids before they agglomerated with ices.

3. The existence of an original plane of formation of comets beyond some 3000 to 5000 a.u. appears to be unknowable. The perturbations by passing stars would have so disturbed the orbits that the lack of evidence for a common plane in the motions of new comets tells nothing about the place or plane of origin (Oort, 1950) (note exception in 4 below).

4. That the comets formed concurrently with the solar system some 4.6×10^9 years ago is an assumption based on the lack of a tenable theory for more recent or current formation. The lack of evidence for a common plane of motion implies an origin remote in time or, if recent, no common plane of origin.

5. The highly variable ratio of dust to gas observed from comet to comet proves a large variation in particle-size-distribution but has not yet been shown to measure a true variation in the dust/gas mass ratio. P/Encke, for example, shows a low dust/gas ratio in its spectrum but has contributed enormously to the interplanetary meteoroid population.

THE ROLE OF COMETS IN THE ORIGIN OF THE SOLAR SYSTEM*

The above evidence points conclusively to the origin of comets by the growth and agglomeration of small particles from gas (and dust?) at very low temperatures. But where? If concurrently with the origin of the solar system (and necessarily associated with it gravitationally) two locations in space are, a priori, possible:

---

*The reader is referred to V. S. Safronov's comprehensive book "Evolution of the Protoplanetary Cloud and Formation of the Earth and Planets" (Izdatel ' stvo "Nauka, Moscow, 1969; translated into English by the Isael Program for Scientific Translation and published by NASA, 1972) for a modern development of the Kant-LaPlace concept including the important contributions by O. J. Schmidt, and a general historical background of this general concept. For less general special treatments see Kuiper (1951), Urey (1952), Levin (1958), Cameron (1962), Whipple (1964), Alfvén and Arrhenius (1970 a, b), Nobel Symposium 21 (1972) and Opik (1973). For concepts of comet or solar system origin deviating from the "classical," see Sourek (1946), Lyttleton (1948), Whipple (1948 a, b), Trulsen (1972), O'Dell (1973) and especially Cameron and other contributors to the Symposium at Nice "On the Origin of the Solar System" (1972, Edition du Central National de la Recherche Scientifique 15, Quai Anatole France, Paris).

I. In the other regions of the forming planetary system beyond proto-Saturn (Kuiper, 1951; Whipple, 1951), or

II. In interstellar clouds gratitationally associated with the forming solar system but at proto-solar distances out to a moderate fraction of a parsec, that is to say, in orbits like those in the Öpik-Oort cloud of present day comets (Whipple, 1951; McCrea, 1960; Cameron, 1962).

There can be little doubt that comets were the building blocks for the great outer planets, Uranus and Neptune. The mean densities of these planets (Ramsey, 1967) are consistent with their origin largely from the accretion of comets, assumed to consist of the compounds possible, excluding H_2, in a solar mix of elements. This process of building Uranus and Neptune is precisely analogous to building the terrestrial planets from planetesimals. Temperature was the controlling factor, being too high within the orbit of proto-Jupiter for water to freeze. For this reason Oort's (1950) suggestion that the comets formed within the Jupiter region appears unlikely because asteroids clearly formed there. Similarly, Öpik's requirement for solid H_2 in the proto-Jupiter region appears untenable. Nevertheless, Oort's idea that comets were thrown out from the inner regions of the solar system by planetary perturbations is highly significant.

Thus the possible origin of the presently observed comets in the Uranus-Neptune region rests solely on the premise that the major planets (or proto-

planets) could indeed throw the comets into stable orbits with aphelia out to some 50,000 a.u. or more. The low efficiency of the process is only restrictive in the sense that too much angular momentum may be required of the outer planets to accomplish the feat successfully. Approximately an earth mass of comets in large orbits appears to be required as an end product but a hundred earth masses may originally have been involved. Öpik (1965, 1973) is doubtful about the process unless the comets formed near Jupiter; Everhart (1973) finds it highly unlikely while Levin (1972) provides the angular momentum from proto-Uranus and proto-Neptune by forming these planets at very great solar distances (up to 200 a.u.) from a very large nebular mass and drawing them into their present orbits by the ejection of comets (mostly to infinity).

Everhart's doubts may possibly be removed if the space density of comets originally fell off rapidly with solar distance and that the supply at great distances (Marsden and Sekanina, 1973) has been replenished by those in smaller orbits, more stable against stellar perturbations. Indeed Öpik (1932) showed that stellar perturbations will systematically increase perihelion distances to remove the comets from the region of perturbation by the outer planets. The number of comets thrown into the inner solar system during the immediate post-nebula period could have been significant and may account for major crater formation on the Moon (see Hartmann, 1972) and volatiles on the terrestrial planets (Lewis, 1974).

Alternative II, of forming the comets directly in the orbits of the Öpik-Oort Cloud is highly attractive except for the difficulty of agglomerating kilometer

sized bodies in the low-density fragmented interstellar clouds. Such a possibility must be demonstrated before one can accept the tempting solution to the problem. Öpik (1973) finds the process quite impossible.

Let us now look to the comets themselves to see whether their structure can help us distinguish between the two possible regions of origin. Most conspicuous are the numerous carbon radicals, molecules and ions, not in low-temperature equilibrium with excess hydrogen. The gas, if once hot, could not have cooled slowly. Note, too, the friability and low density (0.5 to < 0.01 gm/cm^3) for meteoric "solids." Sekanina (this volume) finds evidence that for Comet Kohoutek the larger grains tend to shrink appreciably in a period of a few days. We must conclude that the ices, earthy material and clathrates were all accumulated simultaneously at very low temperatures.

More specifically, the ices, clathrates and "solids" collected together intimately in such a fashion that earthy molecules were somewhat bonded together in order to provide some degree of physical strength after the ices sublimated. Note that any sintering process to make the earthy grains coherent physically would remove the highly volatile substances necessary to provide the activity of Comet Kohoutek and other comets at great solar distances where the vapor pressure of H_2O is negligible. Thus the process of grain growth must have involved the "whisker" type of growth, commonly observed in laboratory crystals. We can confidently visualize a comet as a complex lacy structure of "whiskers" and "snowflakes" that grew atom-by-atom and molecule-by-molecule while highly

volatile molecules were trapped as clathrates.

The temperature could have been sufficiently low for such cometary growth anywhere in space beyond perhaps 30 to 50 a.u. from the center of the proto-solar-system. Levin's (1972) concept of comet growth up to 200 a.u. is entirely consistent with such growth, as is alternative II, fragmented interstellar clouds at far greater distances. Safronof and Levin's requirement of excessive material (perhaps 30 - 100 times the present-day mass of Uranus and Neptune) to provide a reasonably rapid growth rate for Uranus and Neptune confirms Öpik's vehement denial that fragmented interstellar clouds may be capable of producing comets. Careful analysis of grain growth rates under imaginative sets of assumptions as to the nature and stability of such clouds is clearly needed. Note that a comet does not appear to be an aggregate of interstellar grains if, indeed, these grains are solids covered with icy mantles. Such grains might mot cohere when exposed to solar radiation sublimating the ices and thus not provide the much larger meteoroids or the large dust particles in Comet Kohoutek.

At the present, then we have no criterion to identify the unique region in space where comets formed, if indeed, they all formed in the same general region. We need more precise knowledge concerning the identity and abundances of the more volatile parent molecules. Did CH_4, CO, Ar or Ne, for example, actually freeze out in comets? As Lewis (1972) shows, the mass percentages of such volatiles can be used as thermometers. Even the dimensions of comet

nuclei are uncertain, while we have no knowledge whatsoever of their detailed structure. Are they layered? Do they contain "pockets" of ices or "pockets" of dust? How fast do they rotate? What produces comet bursts in luminosity? What causes "new" comets to split?

Furthermore, we do not know whether comets generally or indeed any comets contain cores of asteroidal nature. It is tempting to identify many of the Apollo or Earth-orbit crossing asteroids, as "burned out" comets. Proof of a truly asteroidal core for an old comet would require a further knowledge of the chemistry and structure of the core to ascertain whether meteoric material collected first or whether radioactive heating drove out the volatiles. Such knowledge would, of course, be invaluable in ascertaining the physical and chemical circumstances of the origin. No definitive answer is likely without such data. Anders, however, presents strong evidence that even the most primitive carbonaceous chondrites (Type 1) are not of cometary origin (1974 private communication).

It is clear that far more ground-based and space-based research on comets is necessary. Comet Kohoutek has shown that a massive attack on one comet can produce extraordinary results. There are too many comets to permit an over-all observational attack on each one. Nevertheless we need to accumulate data on all observable comets. A reasonable program is to institute massive observing programs from time to time for especially selected comets while accumulating basic data for all comets.

Only space missions to comets can give us the "quantum jump" in knowledge necessary to solve the most fundamental problems of comets. Equally we need to study a few asteroids at their surfaces to understand their nature and to identify the sources of meteorites. Because meteorites have given us extraordinary insight regarding early conditions in the developing solar system, we can expect asteroid space missions to answer some basic direct questions, while "calibrating" our laboratory data on meteorites. Furthermore, the extraordinary successes in exploring the Moon and Mars have given us only limited data concerning the early phases of solar system formation because these bodies have been severely altered since they were originally agglomerated.

Space missions to comets and to asteroids are the essential next steps towards understanding how the solar system came into being. Such missions are entirely feasible in the present state of our space technology.*

---

*The following references are related to space missions to comets and asteroids:

Report of the Comet and Asteroid Mission Study Panel, NASA TM X-64677, 1972.

Alfvén, H. and Arrhenius, G. 1970. Mission to an Asteroid. Science, 167, 139.

Lüst, Reah, "Cometary Probes", Space Science Reviews, 10 (1969), 217-299.

The 1973 Report and Recommendations of the NASA Science Advisory Committee on Comets and Asteroids, NASA TM-X-71917, 1973.

Physical Studies of Minor Planets (NASA SP267) ed. T. Gehrels, NASA, 1971.

Proceedings of the Cometary Science Working Group, ed. D. L. Roberts, IIT Research Institute, 1971.

Comets, Scientific Data and Missions, ed. E. Roemer and G. P. Kuiper, Lunar and Planetary Laboratory, Univ. of Arizona, 1972.

Nobel Symposium No. 21, From Plasma to Planet, ed. Aina Elvius, Almquist and Wiksell, Stockholm, 1972.

On the Origin of the Solar System, ed. Hubert Reeves, Centre National de la Recherche Scientifique, Paris, 1972.

Comets and Asteroids, Strategy for Exploration, NASA TMX-64677, 1972.

REFERENCES

Alfvén, H. and Arrhenius, G., 1970a, Ap. & Sp. Sci., 8, 338-421.

Alfvén, H. and Arrhenius, G., 1970b, Ap. & Sp. Sci., 9, 3-33.

Cameron, A. G. W., 1962, Icarus, 1, 13-69.

Delsemme, A. H. and Swings, P., 1952, Ann. d'Astrophys., 15, 1-6.

Everhart, E., 1973, A. J., 73, 329-337.

Hartmann, W. K., 1972, Ap. & Sp. Sci., 17, 48-64.

Heubner, W. and Weigert, A., 1966, Z. f. Astrophys., 64, 185-201.

Jacchia, L. G., 1955, Ap. J., 121, 521-527.

Kuiper, G. P., 1951, Astrophysics, ed. J. A. Hynek, McGraw-Hill Co., N. Y., London, Ch. 8.

Levin, B., 1958, L'Origine de la Terre et des Planets, Moscow.

Levin, B., 1972, "On the Origin of the Solar System," a symposium at Nice, Centre National de la Recherche Scientifique, Paris.

Lewis, J. S., 1972, Icarus, 16, 240-

Lyttleton, R. A., 1948, Mon. Not. Roy. Ast. Soc., 108, 465.

Marsden, B. G. and Sekanina, Z., 1973, A. J., 78, 1118-1124.

McCrea, W. H., 1960, Proc. Roy. Soc. (London), A256, 245-266.

McCrosky, R. E., 1955, A. J., 60, 170.

McCrosky, R. E., 1958, A. J., 63, 97-106.

Millman, P. M., 1972, Nobel Symposium 21, From Plasma to Planet, ed. A. Elvius, 156-166, Almquist and Wiksell, Stockholm.

O'Dell, C. R., 1973, Icarus, 19, 137-146.

Oort, J. H., 1950, Bull. Astr. Inst. Neth., 11, 91-110.

Öpik, E., 1932, Proc. Amer. Acad. Arts and Sci., 67, 169-183.

Öpik, E. J., 1966, Irish Ast. J., 7, 141-161.

Öpik, E. J., 1965, Mem. Soc. Roy. Sci. Liege, Ser. 5, 12, 523-574.

Öpik, E. J., 1973, Ap. & Sp. Sci., 21, 307-398.

Owen, T., 1973, Ap. J., 184, 33-43.

Ramsey, W. H., 1967, Planetary and Space Sci., 15, 1609-1633.

Sourek, J., 1946, Mem. and Obs. of Czech. Ast. Soc. Prague, No. 7.

Stawikowski, A. and Greenstein, J. L., 1964, Ap. J., 140, 1280.

Swings, P., 1965, Quart. J. Roy. Ast. Soc., 6, 28-69.

Trulsen. J., 1972, Nobel Symposium 21, From Plasma to Planet, ed. A. Elvius, 179-192, Almquist and Wiksell, Stockholm.

Urey, H. C., 1952, The Planets, Their Origin and Development, 245 pp. Yale Univ. Press, New Haven.

Whipple, F. L., 1950, Ap. J., 111, 375.

Whipple, F. L., 1951, Ap. J., 113, 464-474.

Whipple, F. L., 1948a, b, a. Sci. Amer., 178, 34-45; b. Harv. Obs. Mon., No. 7, 109-142.

Whipple, F. L., 1964, Proc. Nat. Acad. Sci., 52, 565-594.

DISCUSSION

B. Donn: I think that these volatile materials were collected not atom by atom but by condensation into your whiskers and snowflakes, which then accumulate, volatile or non-volatile, until you get a comet.

F. L. Whipple: So you go with the whiskers and snowflakes?

B. Donn: Yes.

F. L. Whipple: You then accumulate them rather than to collect them all? The point is that the solids have to be intimately associated with the volatiles to make the thing break up. You can't have very big solid pieces by themselves. You have to mix them together in some fashion like that. I think the point is rather technical. We'd have to define our terms rather carefully, I believe, to see where we agree to disagree; and I don't think if we voted we'd know for sure what we were voting on.

A. H. Delsemme: I have one question. When you speak about the solar abundance, do you accept my depletion of hydrogen?

F. L. Whipple: Oh, yes, of course. I'm talking about condensables and condensable materials; therefore, you've lost volatiles. But you started, I presume—you could start with something like that. I think that's a reasonable assumption. I certainly would defend that one very strongly.

M. Dubin: The isotope ratio of oxygen in Allende does not fit that?

F. L. Whipple: I didn't know there were any disagreements in isotope ratios. Oh, you mean that's a meteorite?

B. Donn: Yes.

F. L. Whipple: Well, we're not talking about meteorites we're talking about comets.

Where were they formed? It seems that we're pretty well limited to those two regions and interstellar clouds that were probably gravitationally associated

with the solar system. It's hard to see how we can capture them unless they were originally there.

I presume capture is a possibility, but these two suggestions I made in 1950 or '51 and I still would like to know the answer. Last slide.

(Slide.)

This is a plug. Only space missions to comets and asteroids can give us this quantum jump knowledge that will lead to the solution of the most fundamental problems of the solar system. Enough of that.

Well, we have three minutes for discussion if we are going to give Dr. Mendus time for his presentation. Who wants to argue about something?

M. Dubin: What is the shape of the nucleus if you assume that all comets have an angular momentum and they condense way out in space? Would the shape be disk-like, donut-like, or spherical; and why?

F. L. Whipple: I think the answer is that whenever you accumulate things you've got an irregular body that's something like a sphere. What else can you get? There's a little angular momentum that might flatten it a bit, so maybe it's an oblate spheroid or nearly sphered with some irregularities on it. I don't know.

H. Keller: What is the importance now of clathrates as compared to ices? We seem to have both. Is it important to make a difference between ices and clathrates?

A. H. Delsemme: It's not really important. After all, I have emphasized that we shouldn't attach too much importance to this label "clathrates," because, after all, we have shown recently—I have shown with Miller—that the clathrates are, after all, limits of the absorption of gases in water ices or water snows. Therefore, if you are willing to speak about absorption, that's okay.

F. L. Whipple: I want to thank the participants for their patience in rushing through this. I want to make two last comments.

I think Dr. Huebner's suggestion of more laboratory work is extremely important, and I hope that none of you will forget about it. And I hope that NASA particularly will remember it.

ON THE ORIGIN OF COMETS

Asoka Mendis and Hannes Alfvén

1. Introduction

The cosmogony of the planetary and satellite systems consists of understanding the physio-chemical processes leading to their formation and also trying to decide at what time and over what period their formation took place. The cosmogony of the comets require answers to not only these two questions but also as to where, in relation to the solar system, the observed and inferred distributions of comets were formed.

One also recognizes that unlike in the case of the larger bodies the time scales of dynamical and physical evolution of some of these bodies are very much smaller than the age of the solar system. This leads directly to the question of the maintenance of their observed abundances and consequently to the genetic inter-relationships between the various classes of comets and also to those between comets and other bodies in the solar system. It also provokes the question whether the formation of the comets was completed long ago together with the rest of the solar system or whether the process of formation may be still continuing even though on a much diminished scale.

Attempts at answering each of these questions has produced a number of interesting ideas, but despite considerable effort by a number of authors it must be admitted that all of these questions still remain

largely unresolved, although the continuing work on the dynamical evolution of cometary orbits[1] have put important new constraints on the evolutionary path of these bodies.

So far various theories have proposed solar origins, proto-planetary origins, planetary origins and interstellar origins. They have also proposed completed past origins as well as continuing origins. Comprehensive reviews of these ideas are available elsewhere[2], [3], [4], [5]. Here we will restrict ourselves to offering a few comments pertinent to some of these problems.

2. Observed and Inferred Distributions

Up to the pressnt time about 100 individual short period ($P \lesssim 200$ yrs) and over five times as many long period comets have been discovered, and the present rate of discovery averages about 4 long period and 1 short period comet per year[5].

The differences in the orbital characteristics between these two classes are well known. The short period comets which spend almost all their time within the confines of the planetary system have mostly low inclination ($i \lesssim 25^{o}$) orbits. Only five of them are known to be retrograde. Also about 2/3 of them have aphelia close to Jupiter's orbit and are likely to be strongly influenced by that

planet. The long period comets on the other hand show a uniform distribution in inclination with about equal numbers having prograde and retrograde orbits. They are also for the most part moving in almost parabolic elliptic orbits with periods in excess of 10^6 yrs. Based on a statistical analyses of 22 long period comets whose original barycentric orbits had been accurately calculated, Oort[6] showed that the bulk of them seemed to come from a region between about 3×10^4 A. U. and 10^5 A. U. with a median value of about 5×10^4 A. U. He also noted that average planetary perturbation in $1/a \left(< \Delta \left(\frac{1}{a} \right) > \right)$ which amounted to about $\pm 5 \times 10^{-4}$ A. U.$^{-1}$ was more than an order of magnitude larger than the observed dispersion in $1/a$ near the maximum. He was thus led to conclude that the observed long period comets were "new" in the sense that they were being observed at their first passage through the inner regions of the solar system ($q \lesssim 2$ A. U.). Based on the frequency of discovery of new comets, their average period and an assumed distribution of the transverse velocity at aphelion Oort further deduced that the number of "intrinsically observable" comets in this reservoir $\left(3 \times 10^4 \lesssim Q \lesssim 10^5 \text{ A. U.} \right)$ must be in excess of about 10^{11}. Although Oort's conclusions have been strongly criticized by Lyttleton,[7] a more recent detailed analysis by Marsden and Sekanina[8] seems to confirm them,

despite the very small numbers on which the statistics are based. They have shown that for comets having perihelion distance more than 3 A. U. and which are thus likely to be free of non-gravitational forces if their volatile component is largely water ice as is now generally believed[9], the distribution of original barycentric orbits show a remarkable concentration corresponding to an aphelion distance around 5×10^4 A. U. Of course if these "new" comets are charged with a component much more volatile than water or the clathrate[10] then this result too could be largely fortuitous.

Besides these distributions one has to grant the possible existence of others. Indeed a comet having aphelion $\lesssim 2 \times 10^4$ A. U. and perihelion well outside the planetary system will be dynamically stable against both stellar and planetary perturbations, during the lifetime of the solar system. It may also be barely possible to have some comets stably trapped in certain perculiar orbits in the outer regions of the planetary system over the cosmognic time scale[11]. Furthermore it is known that there is a continuous ejection of long period comets from the solar system at the present time and the process may have proceeded on a grander scale during the formation stages of the solar system. Consequently interstellar space may be continously being populated by comets from our own solar system as well as others like our own. We shall, however, concern ourselves here mainly with the observed distributions.

3. The Origin of Long Period Comets

Believing that it was difficult to form comets in situ at such large distances ($r \approx 5 \times 10^4$ A. U.) Oort[6] suggested that they originate within the inner solar system. They were ejected out by planetary perturbations and while some would have immediately escaped the solar system in hyperbolic orbits those on elliptic orbits whose aphelia $Q, \gtrsim 10^5$ A. U. were subsequently removed by stellar perturbations over a time scale of 5×10^9 yrs, whereas those with $Q \lesssim 2 \times 10^4$ A. U. are hardly affected at all. These two values of Q define the limits of the so-called Oort's cometary reservoir. Oort further showed that while stellar perturbations will completely isotropize the velocity distribution near aphelion of comets in this region, the continual re-shuffling of the velocity distribution will continuously inject some long period comets into orbits bringing them to the vicinity of the sun to explain the observed isotropic distribution. Although Oort originally made the highly unlikely supposition that these comets, together with the minor planets resulted from the break up of a planet inside Jupiter's orbit, several other authors have subsequently suggested that these comets originate in the outer regions of the planetary system in a more reasonable way[12], [13]

The difficulty with this scheme is already apparent from Everhart's calculations[14] for the diffusion of the $1/a$ values of hypothetical comets started within the solar system (despite their incompleteness, particularly the neglect of stellar perturbations). If we, however, accept Everhart's linear law for a number of orbits vs $1/a$ and scale it for the fact that there are, say, 10^{11} comets in the region 2×10^4 AU - 10^5 AU, this seems to require an embarrassingly large number of comets within the solar system at some time ($\gtrsim 10^{16}$).

Recently Alfvén and Arrhenius[15] have developed a detailed hydromagnetic, planetesimal theory for the formation of planetary systems around a central star as well as the formation of satellite systems around a central planet. The basic steps in the process are the following: Initially gas infalling towards a spinning, magnetized central body is ionized and brought into partial corotation. Grains condensing out of this plasma fall on neutralization towards the equatorial plane and are collected there at various descrete distances from the central body due to mutual inelastic collisions to form streams of almost co-orbital particles called "jet streams". These grains then further accrete within these streams due to mutual inelastic collisions growing into larger and larger planetesimals which ultimately grow into planets and satellites, the final stages of the accretion process being gravitational.

The central problem here is the time evolution of these jet streams which have been studied recently both numerically[16] and analytically[17] with the authors drawing basically similar conclusions. In order to make the problem tractable a number of simplifying assumptions have been made in both cases. In particular, the effects of fragmentation and accretion have been neglected as are gravitational perturbations and electromagnetic effects such as the Poynting-Robertson effect. Within these limitations, however, one finds in a general way that, if collisions are sufficiently inelastic, a radial focussing or clustering would occur such that the thickness of the stream is reduced.

More recently Ip and Mendis[18] have studied the time evolution of such streams using simple mathematical models which also take into account the effects of fragmentation and accretion. Accretion here meaning not merely the coagulation effect of stream particles sticking to each other during inelastic collisions but also the continuous sweeping up of matter intersecting the streams. The treatment is in terms of the average kinetic and physical parameters of the particles and considers for simplicity a pure accretion case and a special fragmentation case wherein despite the competing effect of accretion, fragmentation continues to keep the average grain radius constant. The results of the computation are shown in the following figures. Figure 1 depicts the pure accretion model. Here Λ_o is the initial value of the ratio of the accretion time

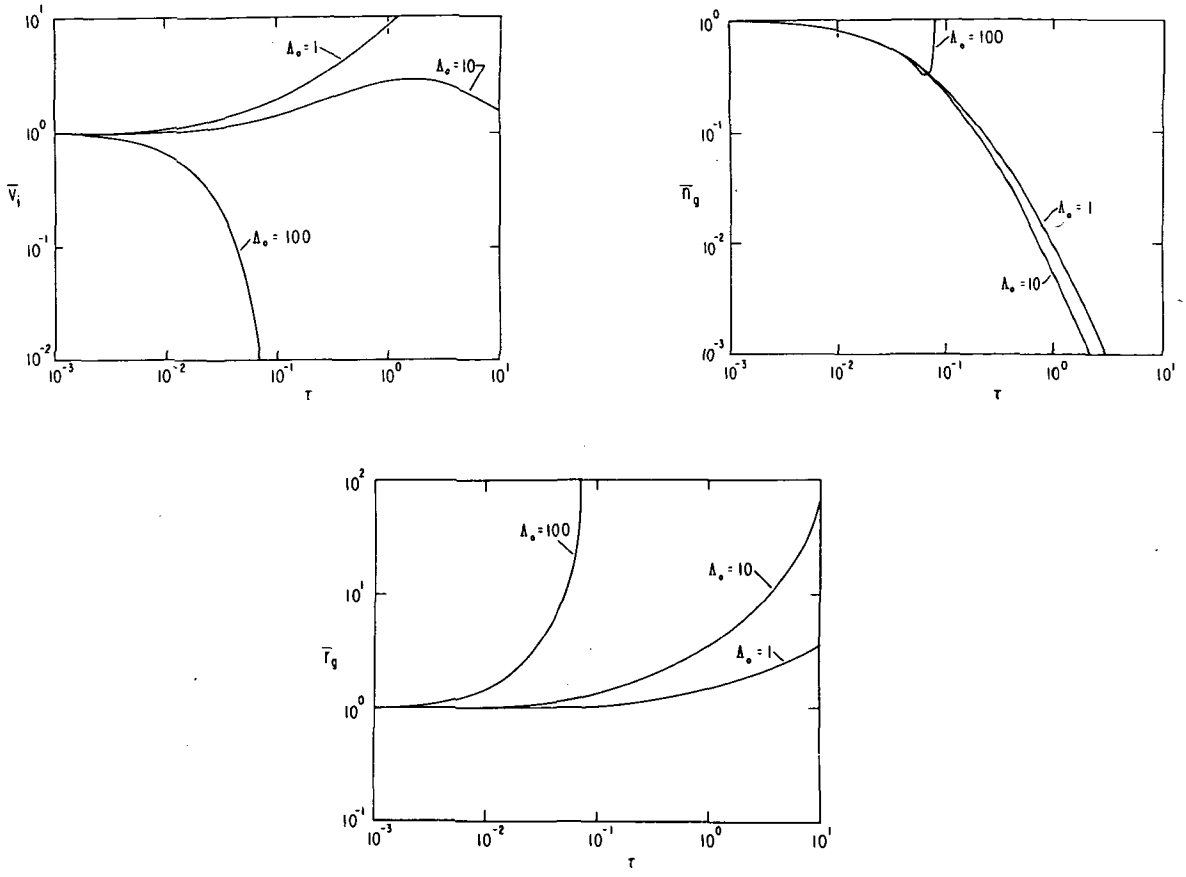

Figure 1: The variations of the normalized internal velocity, the number density and the grain radius with time, for different values of Λ_o, in the pure accretion model.

scale to the internal collision time scale, and time is measured in units of the initial accretion time scale. For $\Lambda_o = 1$ we have a gradual dispersion of the matter stream due to the thermalization effect of the accretion of the external matter. In the case of $\Lambda_o = 100$ there is a rapid focussing of the stream because the evolution of the stream is dominated by the inelastic collision process among the stream particles. An intermediate behavior is observed when $\Lambda_o = 10$, the matter stream has an initial expansion phase until $\tau \sim 1$. At this stage the thermalization effect is balanced by the internal energy dissipation by inelastic collisions, and contraction begins. It seems therefore that, in the case of a pure accretion model for interplanetary matter streams, focussing will always occur if $\Lambda_o \gtrsim 10$.

Figure 1 also shows that for $\Lambda_o \lesssim 10$ the particle density of the stream is reduced by three orders of magnitude within a period of about $3\,\tau_{A0}$ while the average radius of a grain increases by one to two orders of magnitude due to the efficiency of the coagulation process in the stream.

Figure 2 depicts the fragmentation model. The variations of $\bar{v}_i$ and therefore the thickness of the stream are similar to those of the pure accretion model. However, in the case of $\Lambda_o = 10$, the contraction of the stream occurs much faster culminating in a catastropic collapse just before $\tau \approx 2$. Due to the rapid focussing the particle density begins to increase almost instantaneously following an initial phase of gradual decrease.

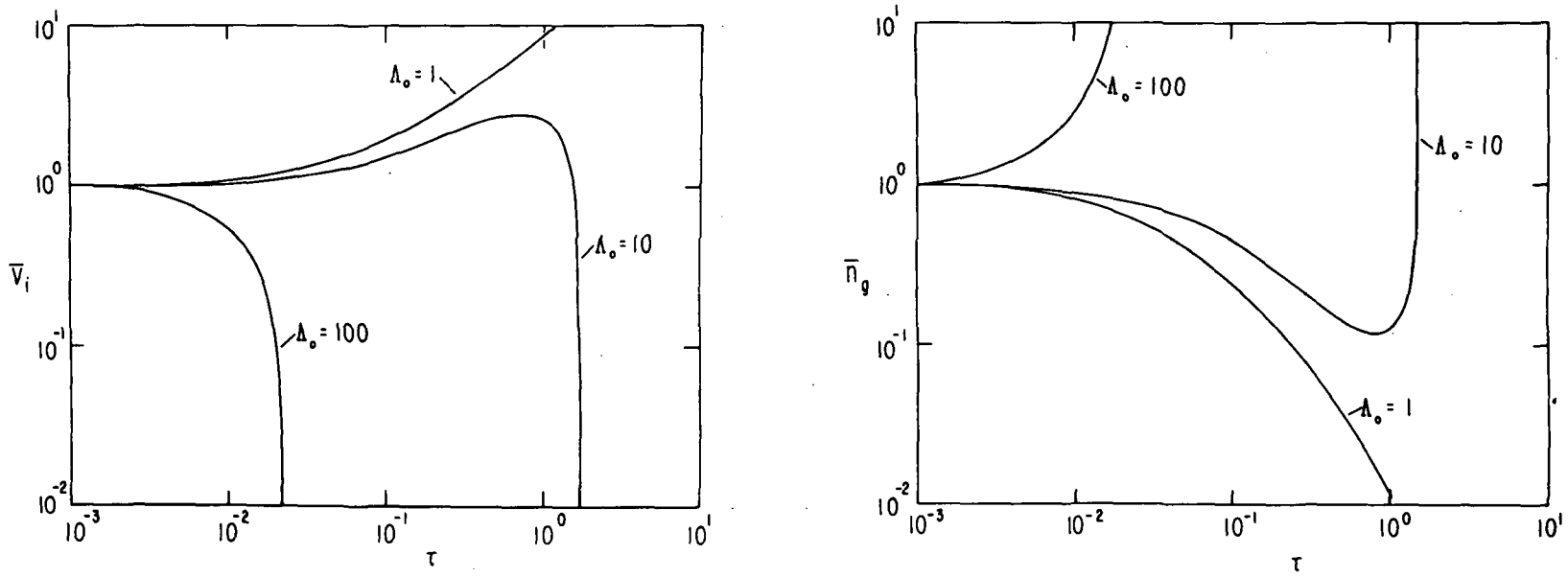

Figure 2: The variation of the normalized internal velocity and number density with time for different values of Λ_o in the fragmentation model.

In the evolution of any proto-planetary matter stream while there would be a gradual increase in the average grain size as shown by the pure accretion model, this growth would be hindered to some extent by the competing effects of fragmentation. Consequently the real situation would be intermediate to those suggested by the two models we have discussed. The general conclusion then is that any proto-planetary matter stream in which accretion and fragmentation are taking place a strong focussing would occur over a period of a few accretion time scales.

While planets and satellites will be formed in this way close to the equitorial plane of the central body, dust particles associated with the gas and having a sufficiently small charge to mass ratio not to be significantly effected by the magnetic field will fall in streams towards the sun. If we consider a spherical cluster of such dust of cometary mass ($\approx 10^{18}$ g) initially at a large heliocentric distance r_A from the sun falling in towards it in a highly elongated elliptic orbit, then if r_B is the heliocentric distance sufficiently before perihelion such that a linear approximation may be made to the portion of the orbit between A and B, it is seen that the cluster will be drawn out into a thin pencil shaped stream near B whose length $\approx \sqrt{\frac{r_A}{r_B}}\, D_A$ and whose cross-sectional diameter is $\left(\frac{r_B}{r_A}\right)^2 D_A$ Consequently the density will be increased by a factor $\left(\frac{r_A}{r_B}\right)^{3/2}$ If we take $r_A \approx 5 \times 10^4$ AU and $r_B \approx 5$ AU, and the distributed dust

density at $A \approx 2 \times 10^{-20}$ gm cm^{-3} (corresponding to a neutral gas density $\approx 10^4$ cm^{-3}), $\rho_B \approx 10^6 \rho_A \approx 2 \times 10^{-14}$ gm cm^{-3}. Since the internal collision time scale at B is given by $t_B \approx \frac{r_g \rho_g}{\rho_B v_{rel}}$, taking $r_g \approx 10\,\mu$, $\rho_g \approx 0.5$ gm cm^{-3}, $v_{rel} \approx 10^4$ cm sec^{-1}, we get $t_B \approx 2 \times 10^6$ secs $\approx$ 1 mo. Consequently a fast focussing into consolidated body of cometary size is possible during a single perihelion passage. While the isotropy of the observed distribution of long period comets is a natural consequence of this formation process, the emerging view of a comet as a lossely consolidated grainy matrix is consistent with such a formation. It also anticipates the observed compositional similarities between interstellar dust and comets.

It should be noticed that the mechanism we are proposing is essentially different from Lyttleton's gravitational lensing[19]. It is also asserted that these dust streams are unstable against the effects of internal inelastic collisions and would quickly agglomerate into one or more larger bodies.

4. The Origin of Short Period Comets

The idea that short period comets derive from long period ones that pass near one of the massive outer planets (especially Jupiter) and lose energy is nearly two centuries old being generally attributed to Laplace. This classical capture hypothesis has since been considered by several authors and worked out in detail by Newton[20] whose calculations have

been extended and refined more recently by Everhart[21]. Both authors reached the conclusion that single close encounters of long period (or more precisely parabolic) comets belonging to the observed random distribution, with planets (particularly Jupiter) cannot solve the problem of the origin of short period comets. While the capture probability remains finite although very small, the calculated post-capture distribution of these short period comets following a single close encounter with Jupiter does not in any way correspond to the observed distribution and nowhere is this discrepancy more marked than in their distribution with regard to period and inclination. In fact, these calculations perdict that about a quarter of the short period comets with perihelion $\lesssim$ 2 A. U. and period $\lesssim$ 21 yrs should have retrograde orbits although there are none observed.

Very recently Everhart[22] has made a Monte Carlo statistical study of the interaction of hypothetical random parabolic comets with the Sun-Jupiter system, following some comets up to 2000 returns. While elucidating several important points regarding the capture hypothesis it identified a so-called "capture-region" consisting of prograde comets of low inclination ($i_o \lesssim 9^o$) having perihelia close to Jupiter's orbit ($4 < q_o < 6$ A. U.) from which over 90% of the captures take place. While the calculated post-capture distributions agree rather well with observation, subsequent work by the same author[14] shows that from a purely orbital evolution point of view the source of the observed short period distribution could

equally well be situated within the confines of the solar system, in particular the Jupiter-Saturn region. Consequently such claculations have so far not succeeded in unambigiously identifying the source region of the observed short period comets. The problem of maintaining the observed short-period population against dissipation and fading require a capture rate of at least one every ten years or so. Based on the rate of capture deduced from Everhart's numerical results and the deduced rate of injection of "new" comets from the Oort cloud into the "capture region" Joss[23] concluded that the capture rate was 4-5 orders of magnitude too small to account for the observed number of short period comets. Delsemme[24] on the other hand, considering also the intermediate period distribution and assuming a concentration towards small inclination in the capture region concludes, on the basis of the number of comets reaching perihelia per unit time, that no such discrepancy exists. Besides a number of questionable assumptions and the uncertainties in the several parameters inherent in Delsemme's analysis it needs to be realized that the 10^8 "intermediate period comets" required to increase the capture rate must ultimately derive from the "new" comets entering the capture region from the Oort cloud (2×10^4 AU $\lesssim Q \lesssim$ 10^5 AU) due to stellar perturbations. Even with an orbital diffusion time scale as large as the age of the solar system one still needs an input of such comets at the rate of 1 every 50 years. Consequently we now have a problem not of accounting for the observed short period comets

but rather for the deduced abundance of "intermediate period comets" from which the short period comets are supposedly derived.

Vsekhsviatsky had earlier attempted to circumvent this difficulty by reviving the old Lagrangean idea of an eruptive origin for short period comets. In a series of papers (e.g. see ref. 25), he has successively proposed that comets are the ejecta of violent volcanic eruptions on the surfaces of planets (particularly Jupiter) and their satellites. Besides the essentially circumstantial nature of the evidence, simple considerations based on the energy requirements as well as the survival of these objects during such violent eruptions argues strongly against such a view.

This leads us to our final topic: the genetic relationship between comets and other small bodies in the solar system. The orbital associations of comets and meteor streams on the one hand and the formal similarity of the orbits of short-period comets and Apollo-type minor planets on the other, have been known for a considerable time. Both classes of objects are generally believed relics of comets. While the Apollo-type minor planets are believed to result from a complete degassing of cometary nuclei and the consequent shrinkage of their orbits due to non-gravitational forces, meteor streams are believed to result from the complete or partial disintegration of cometary nuclei.

There are at least 17 major permanent meteor streams observed to intersect the Earth's orbit, while a somewhat smaller number of temporary meteor streams too have been observed. Since meteor streams (whose typical thicknesses are $\lesssim$ 0.1 A.U) are observed only when their orbits are favorably positioned with respect to the earth's orbit, the total number within the solar system is likely to be much larger. Several of these meteor streams are known to be approximately co-orbital with comets (e.g. Perseids with P/Swift-Tuttle, October Draconids with P/Giacobini-Zinner, Leonids with P/Temple-Tuttle, Taurids with P/Encke, etc.). It is of course not unreasonable that meteor streams should be considered as the disintegration products of comets since we witness cometary erosion--i.e. the loss of gas (type I tails) and dust (type II tails) as comets approach the Sun, all the time. We have also seen on several occasions cometary disintegration; P/Biela was seen to break up into two parts in 1846. Subsequent to break up both comets moved in very close orbits and were seen at their next return in 1852 separated by about 3×10^6 km. They were never observed after that, but a temporary meteor stream (Andromedids) is now believed to be associated with their orbit. While we cannot deny a process occurring before our eyes, we need not necessarily assume that this process is irreversible. It seems worthwhile considering, in the light of the development of the theory of jet streams, whether the opposite process, viz., comets and/or Apollo-type minor planets forming in meteor streams is also possible.

A meteor stream, where we have a swarm of particles moving in Kepler orbits in a gravitational field with a small spread both in velocity and configuration space is a good physical example of an idealized "jet" stream" suggested by Alfvén and Arrhenius, and whose dynamical evolution has been disussed in section 3. Trulsen[26] has made a preliminary study of the effects of planetary perturbations on meteor streams. He considers the case of Jupiter producing a perturbation in a co-orbital eccentric jet stream of particles dispersed along the orbit. A velocity modulation is produced which causes a traveling density wave. The longitudinal focussing achieved this way is, of course, only temporary for any given group of particles and the maximum focussing achieved is only about 20. A greater compression could possibly be obtained through the interference of two such waves excited at consecutive close approaches of the meteor stream to the planet. Besides, if viscous effects of some form are present, as would be the case if an appreciable quantity of gas could be retained in the stream for a sufficient time, it may be possible to achieve a more permanent condensation which may be considered as the birth of a comet or at least an Apollo-type minor planet. The process considered above must be of a rather frequent occurrence because only a modest modulation is required to trigger it. In fact, if the modulation is too large, as would be the case if the stream approached Jupiter too closely, it is a scattering rather than a focussing that results.

Mendis[27] has considered the time scales for a number of dispersive effects including differential precession of nodes and perihelia, the dispersion of particles of different sizes due to the Poynting-Robertson effect, the longitudinal dispersion due to variation of the "effective" gravity on particles of different sizes moving in the combined gravitational and radiation fields of the Sun, and the dispersion due to the differential efficiencies of accretion of particles of different sizes. It is found, in a typical case, that all these times are comparable or larger than the time scale for agglomeration, which is typically about 9×10^4 yrs with the typical values adopted by Ip and Mendis[18] $\left(V_{10} \approx 0.5 \text{ km/s}, \; r_g \approx 10\mu, \right.$ $\left. a \approx 3 \text{ A.U.}, \; \rho_i \sim 10^{-22} \text{ g/cm}^3, \; \rho_s \sim 10^{-20} \text{ g/cm}^3 \; \Lambda_o \approx 10\right)$. The low elasticity and high sticking coefficients assumed in these calculations seem to be supported by the studies of the surface properties of lunar dust grains, dust grains sticking to the protective paint of Surveryor III and also of dust grains artificially irradiated with large doses of low energy praticles simulating solar wind conditions[28]. Furthermore if a factor is allowed for the clumpiness of these streams the focussing time scale would be further reduced, so will the retnetion of a sufficient quantity of gas. Consequently while the situation remains somewhat marginal an eventual focussing of some present day meteor streams is not excluded. The initial expansion phase noticed in our recent model computation (see figures 1 and 2) too is interesting in that it may explain the claim that "young" meteor streams are dispersing faster than can be explained by planetary perturbations or electromagnetic effects[29].

It is also shown[27] that unlike comets, meteor streams could be very efficient in accreting matter from interplanetary space due to their large "effective" cross-sections. How much could be collected of course naturally depends on the highly undertain dust density of the interplanetary space, especially in the regions beyond Jupiter. However, should this be even as much as two orders of magnitude lower than the distributed density in meteor streams a fraction of about 10^{-5} can be collected by the stream per revolution, which could account for the volatile fraction in the subsequently consolidated comet, if a significant fraction of these interplanetary grains contain such a component, perhaps in the form of clathrates.

An interesting observation in this connection concerns P/Temple-Tuttle ($P \simeq 33.2$ yr) which was first recorded as a diffuse but bright object only as recently as 1866[30] although the associated Leonids had been known for centuries earlier. An even more significant observation concerns Comet P/Swift-Tuttle ($P \simeq 120$ yr) which was bright on its first apparition (in 1862) to be easily seen with the naked eye being a 2nd magnitude object at its brightest[27]. What is surprising is its association with the Perseids meteor stream which has been observed for over twelve centuries[31]. Both these observations seem to indicate that comets may have formed in already existing meteor streams. Due to the very large times which span these observations and the uncertainty with regard to the conditions of the early observations we hesitate to draw any strong conclusions from them at this stage except to state that they seem very suggestive. It should, however, be stressed that these observations are of such an important nature that their significance merit further investigation.

If indeed the genetic relationship between comets and meteor streams is a reciprocal one with meteor streams providing not merely a sink for comets but also a source, it could very well mitigate the crucial difficulty at the present time, with regard to the observed abundance of short period comets. At a more basic level is the intriguing possibility that the comet-meteor stream complex may provide us with a cosmic laboratory where we could still observe even though on a much diminished scale the planetesimal process which led to the formation of the solar system over 4.5 million years ago.

References

(1) Everhart, E., 1974, paper read at the 25th IAU Colloquium: The Study of Comets, GCFC, Greenbelt, Maryland (Oct.-Nov. 1974).

(2) Richter, N. B., 1963, The Nature of Comets, Methuen, 145.

(3) Everhart, E., 1973, Astron. J., 78, 329.

(4) Alfvén, H., and Mendis, D. A., 1973, Nature, 246, 410.

(5) Marsden, B. G., 1974, Ann. Rev. of Astron. and Astrophys., 12, 1.

(6) Oort, J. H., 1950, Bull. Astron. Inst. Neth., 11, 91.

(7) Lyttleton, R. A., 1968, MNRAS, 139, 225. (See also Lyttleton's introduction to Richter's Nature of Comets, ref (1)).

(8) Marsden, B. G. and Sekanina, Z., 1973, Astron. J., 78, 1118.

(9) Delsemme, A. H., 1973, Space Science Rev., 15, 89.

(10) Mendis, D. A. and Ip, W-H., 1974, Nature, 249, 536.

(11) Everhart, E., 1973, Astron. J., 78, 316.

(12) Kuiper, G. P., 1951, Astrophysics, ed. J. A. Hynek, Mc Graw-Hill, N. Y., 357.

(13) Whipple, F. L., 1963, Earth, Moon and Planets, Harvard Univ. Press, Camb., Mass.

(14) Everhart, E., 1973, Astron. J., 78, 329.

(15) Alfvén, H. and Arrhenius, G., 1970, Astrophysics and Space Sci., 8, 338 (paper I); 1970, 9, 3; (paper II); 1973, 21, 117; (paper III); 1974, 29, 63 (paper IV).

(16) Trulsen, J., 1971, Physical Studies of Minor Planets, ed. T. Gehrels, 327 (NASA SP-267).

(17) Baxter, D., and Thompson, W. B., 1971, Physical Studies of Minor Planets, ed. T. Gehrels, 219 (NASA SP-267).

_____ 1973, Astrophys. J., 183, 323.

(18) Ip, W-H. and Mendis, D. A., 1974, paper read at the 55th Annual Meeting of the AGU, Washington, April 1974.

(19) Lyttleton, R. A., 1953, The Comets and their Origin, Cambridge Univ. Press.

(20) Newton, H. A., 1891, Mem. Nat. Acad. Sci., 6, 7.

(21) Everhart, E., 1969, Astron. J., 74, 735.

(22) Everhart, E., 1972, Astrophys. Letts., 10, 131.

(23) Joss, P. C., 1973, Astron. and Astrophys. 25, 271.

(24) Delsemme, A. H., 1973, Astron. and Astrophys., 29, 381.

(25) Vsekhsviatsky, S. K., 1966, Nature et Origine des Cometes, Liege, 495.

(26) Trulsen, J., 1970, Proc. IAU Symposium, No. 45, Lenningrad, 487.

(27) Mendis, D. A., 1973, Astrophys. and Space Sci., 20, 165.

(28) Bibring, J. P. and Maurette, M., 1972, paper presented at the IAU/CERN Colloquium, Nice, France, April 1972.

(29) Lindblad, B., 1971, Nobel Symposium 21; From Plasma to Planet, ed. Aina Elvius, 195.

(30) Vsekhsviatsky, S. K., 1958, Physical Characteristics of Comets, Moscow (U. S. NASA Tech. Translation F80, 1964).

(31) Lovell, A. C. B., 1954, Meteor Astronomy, Oxford Press.

OMIT

COMET FORMATION INDUCED BY THE SOLAR WIND

Fred L. Whipple and Myron Lecar

ABSTRACT

The current evidence concerning the nature of comet nuclei suggests that comets may be sizeable aggregations of interstellar grains. This is a progress report on an effort to find circumstances and processes whereby such aggregations might be formed in the solar system at distances far beyond the protoplanets during the early stages of solar-system development. Under investigation are interactions between the early solar "gale" and the surrounding interstellar gas and dust–the so-called "snowplow effect." Compression of the gas and resultant motions of the dust coupled with the pressure radiation from the Sun and nearby new stars may, under certain idealized circumstances, produce a high enough concentration of dust for gravitational instability to occur in the dust, thereby producing km-sized coherent bodies. The likelihood or probability of actual comet formation by such processes remain to be determined.

DISCUSSION

J. C. Brandt: Dr. Whipple, do you have observational methods for out flows from solar type stars at rates 10^6 to 10^8 times the present solar wind?

F. L. Whipple: Kuhi's studies of the t-Tauri stars suggest 10^6 or 10^7 times the present solar wind.

Stephen Strom believes it. Strom even likes 10^6 solar masses per year of lose for the first 10^4 or 10^5 years.

There's a lot of difference of opinion on that. George Herbig here knows as much about it as anybody in the world, but he isn't saying a word, I notice.

J. C. Brandt: That number just strikes me as high.

F. L. Whipple: 10^{18} grams/sec would be a lot. That's about 10^6 times. 10^{20} gm/sec is 10^8 times. It strikes me as high, too.

M. Oppenheimer: Interstellar masses have been observed in the circumferential material about young stellar objects. These objects contain large densities of H_2O, OH, and CO which are species observed or searched for in comets, and other species, such as CH_3OH which may exist in comets. These species are efficient cooling agents through their molecular-transitions.

The maser regions are transitory phenomena which may rapidly cool and become thermally unstable through these molecular transitions. The cooled object less its H_2 molecules is of appropriate mass to become a comet. Thus, masers are associated with regions where Dr. Whipple says comets are forming. In fact, comets may actually be old masers which have cooled off and condensed.

W. F. Huebner: Regarding Prof. Whipples talk, I would like to point out that opacities used in the past for calculations of star formation (i.e., in gravitational collapse of interstellar clouds) are internally inconsistant. They are composits of certain approximations. For example, some average grain opacity has been used up to some temperature T_1, between this temperature and some temperature T_2 an average molecular opacity has been used, and beyond T_2 and average atomic opacity has been used. No effort has been made to allow for coexistence of several phases: there are no molecules below T_1, and no grains above T_1, nor is the composition of mantles on grains consistent with condensation

of the molecular phase. It is very probable that the molecular opacities are too low because a number of molecular bands have been ignored. Just below T_1 and just above T_2 the opacity may be too low because molecules have been ignored in these regions. To give more quantitative estimates requires a detailed analysis. This is one of the problems we are working on.

F. L. Whipple: Just a quick comment on a very important problem.

In producing pseudo-gravity, one is interested in an actual true opacity; in other words, an absorption and re-radiation at longer wavelengths. Forward scattering doesn't help you much because if you forward scatter into the cloud, you don't get the pseudo-gravitation.

The general idea is that about half of the observed extinction is thought to come from absorption and re-radiation of long wavelengths. The other half is largely forward scattered and wouldn't affect it much.

So if the fraction is something like a half, I don't worry about it. That's much closer than the rest of the assumptions. But if it is one percent, then one would worry.

B. Donn: I would just like to repeat the comment Whipple made, that Herbig is staying very quiet through all of this.

(Laughter.)

COMETS, INTERSTELLAR CLOUDS AND STAR CLUSTERS

B. Donn

It is now a generally accepted concept that comets are a residue of the early history of the solar system from the time when the planets were forming. Because of the approximately 0.1% loss of material from the nucleus during perihelion passage near 1 A.U., lifetimes of short period comets are limited to 10^4-10^5 years. This requires an astronomically recent source of the comets seen at the present epoch. From the statistics of the aphelia of parabolic and long period comets, Oort (1951) proposed the existence of a comet cloud between 50,000 and 100,000 A.U. which serves as a reservoir from which presently observed comets have recently been perturbed. Although there are various difficulties with populating the cloud (Opik, 1973) and its subsequent evolution (I.A.U. Symposium 45, 1972; Everhart, 1974) it is the basis for nearly all current studies on the origin and evolution of comets.

At heliocentric distances of tens of thousands of A.U. the density of matter in a solar nebula isolated in space was much too small to allow for the accumulation of cometary size objects. Until recently, all theories of star formation or planetary origin have assumed that the Sun formed as an isolated single star. Cameron (1973) in an analysis of planetary accumulation, postulated massive fragments breaking off from the outer limits of the primordial solar nebula and revolving around it. He proposed these sub-clouds as the regions where comets could

form at distances comparable to Oort's cloud. This theory was based on his theory of the evolution of a solar mass fragment of a collapsing interstellar cloud (Cameron , 1973).

This paper develops further the proposal I made (Donn, 1973) that comet formation occurs in fragmenting interstellar clouds in which star clusters form. Evidence for continual star formation in the galaxy is now so well established that it can no longer be questioned. This evidence has been described in several places, e.g. Spitzer (1968) and is only concisely reviewed here. (1) The very luminous O and B stars are consuming their nuclear energy at a rate that will permit them to continue to maintain their present characteristics for a time of the order of 10^6 years; (2) a similar result is obtained for the ages of young clusters from the position in the Hertzsprung-Russell diagram where the stars show evolution off the zero age main sequence line; (3) expansion of OB associations yield dynamical ages of similar duration; (4) irregular variables with emission lines among spectral classes G and K, the T Tauri stars, are intimately associated with heavy obscuration, frequently in conjunction with OB stars. These objects seem to be stars that have only recently undergone gravitational contraction to the main sequence (Herbig, 1962).

Observed newly formed stars tend to occur in clusters and some theoretical analyses have indicated that all star formation occurs in large groups of a hundred to about one thousand stars (Roberts, 1957; Ebert, et al. 1969). On the other hand, Aveni and Hunter (1967) have found four early-type stars that

they could not attribute to known clusters or associations. They have proposed (Aveni and Hunter, 1969, 1972) that OB and T Tauri stars can form in condensations of 100 or less solar masses. Herbig (1970) believes that stars may form in small groups, possibly as single objects.

It is very likely that the Sun formed some 6×10^9 years ago as a member of a cluster. During that interval this cluster has presumably disintegrated. In this regard, the oldest galactic clusters (Iben, 1967) are 10×10^9 yrs for NGC 188 and 5×10^9 yrs for M67. In a developing cluster the conditions for comet formation are not restricted to within fifty A.U. of the Sun. Indeed, matter of appreciable density is distributed over a volume with dimensions of several parsecs. This is shown in photographs of gas and dust distribution for young clusters and regions showing good evidence of star formation.

Although theoretical investigations of cloud fragmentation are still in an early, controversial state, there is general agreement (Larson, 1973) on the occurring of fragmentation. Observationally, clusters do exist and their association with gas and dust is clear evidence of star formation in clusters via fragmentation. Theoretical investigations (Salpeter, 1959; Hartman, 1970) lead to mass functions varying as M^{-b} where b is between 1 and 1.5. This relation fits the star distribution near the Sun down to a few tenths solar mass (Hartmann, 1970). Beyond that point stellar luminosity functions begin to decrease although the behavior for small masses is uncertain. The smallest measured stellar mass is Ross 614B, $M_V = 16.8$,

$M = 0.07\ M_\odot$ (van de Kamp, 1971). In the Hyades, the nearest open cluster, the faintest stars have $M_V = 17$ (von Altena, 1966). Greenstein, et al. (1970) concluded that the faint end of the main sequence is bounded at $0.09\ M_\odot$. This value shows good agreement with the theoretical lower limit $0.085\ M_\odot$ (Hoxie, 1970; Straka, 1971a,b). It appears that a real minimum stellar mass of about $0.07\ M_\odot$ exists. This limit is the result of an instability to produce nuclear energy and cloud fragments of such mass may yield massive condensations. The collapse of these and small fragments does not appear to have been investigated. It is rather likely that such small masses in a cluster either intrinsically or because of nearby star formation cannot collapse to stars. However, such fragments are expected (Cameron 1973; Larson 1973). For the smallest mass clouds they will exceed the stellar mass function and almost certainly peak at smaller masses.

In the smallest fragments the density may be large enough and the temperature cold enough that volatile material condenses. This may occur homogeneously as well as on existing non-volatile grains. Under these conditions, efficient accumulation of larger solid objects could occur. In his analysis of the evolution of cloud fragments from a few solar masses to a fraction thereof, Cameron's (1973) analysis suggests that accumulation of cometary nuclei in the range 10^{14}-10^{20} gm will be a rapid process.

Within the volume of the cluster will be many regions where comets may form. Their composition will be that of the interstellar molecule population in each subcloud. The complex

molecular array in Orion is highly concentrated toward the region of the Beklin-Neugebauer infrared source. Formaldehyde has a broader distribution and carbon monoxide is still less concentrated. Water is only detectable in maser sources but its cloud distribution presumably is intermediate between carbon monoxide and formaldehyde. The composition of the nuclei formed depends upon the effectiveness of molecule formation in the region. This in turn probably depends upon the availability of energy sources (Donn and Stief, 1974). Cometary nuclei may form with variable ratios of three classes of constituents; CO, H_2O: complex organic molecules: dust. The spectra of new comets actually fall into these three classes, i.e. "new" comets in which each type of material predominates are known: continuum strongest; molecular emissions dominate or CO^+ dominates.

Some description of the possible evolution of the comet cloud can be given. Within clusters and associations the velocity dispersion is less than 3 km/sec (Blaauw, 1964). For subclouds in the proximity of a particular star, turbulence theory suggests that relative velocities will tend to be less than for the cluster as a whole. Consequently, comets forming within a fraction of a parsec of a star will have average relative velocities of perhaps 1 km/sec. The velocity dispersion within a comet cloud can be expected to be comparable or greater.

In a cluster the average distance between stars is about 0.5 pc. It is to be noted that this distance is significantly smaller than the 2.2 pc mean distance (van de Kamp, 1971) for

stars presently within 5 pc of the sun. As a result for comet formation in clusters, the stability and early evolution of the comet cloud differs from similar features of the standard Oort cloud. Comets having near zero velocity relative to the Sun and within about 0.1-0.3 pc or $20\text{-}60 \times 10^4$ A.U. would be the primary members of the cloud. Because of stellar perturbations within the cluster, resistance effects and non-gravitational effects caused by radiation or stellar winds within the cluster, comets with higher velocities or at larger distances might have become members of the Sun's cloud. Tinsley and Cameron (1974) have proposed that a large number of interstellar comets could act as sinks of heavy elements and in this way explain the slow rate of heavy element buildup in the galaxy. Greenberg (1974) has also proposed that comets may account for interstellar deficiencies of heavy elements.

The association of comets with star formation in clusters seems a natural development. This hypothesis also provides prospects for explaining the origin and evolution of the Oort cloud, the composition of comets, and relationships between cometary and interstellar molecules. It also suggests that comets allow us to study interstellar matter close to the sun. According to this hypothesis, a comet probe would be an interstellar probe as well.

REFERENCES

Aveni, A.F. and Hunter, T.H. Jr. 1967, Astron. J. 92, 1019.

Aveni, A.F. and Hunter, T.H. Jr. 1969, Astron. J. 74, 1022.

Aveni, A. F. and Hunter, T. H. Jr., 1972, Astron. J. 77, 17.

Blaauw, A. 1964, An. Rev. Astr. and Ap. 2, 213.

Cameron, A.G.W. 1973, Icarus 18, 407.

Donn, B.D. 1973, Bull. A.A.S. 5, 342.

Donn, B.D. and Stief, L.J. 1974, Bull. A.A.S. 6, 221.

Ebert, R., von Hoerner, S., and Temesvary, S. Die Entstehung von Sterner, Springer Verlag, Berlin, 1969.

Everhart, 1974, I.A.U. Coll. 52, The Study of Comets, in press.

Greenberg, J.M. 1974, Ap.J. 189, L81.

Greenstein, J., Neugebauer, G. and Beklin, E. 1970, Ap.J. 161, 519.

Hartman, 1970, "Evolution Stellaire Avant la Sequence Principle," 16 Liege Astrophysics Symp., Liege, also Mem. Soc. Roy. Sci. Liege. 15 Se, 19, 49.

Herbig, G.H. 1962, Advances in Astronomy and Astrophysics 1, 47.

Herbig, G.H. 1970, "Evolution Stellaire Avant la Sequence Principale," 16 Liege Astrophysics Symp., Liege, also Mem. Soc. Roy. Sci. Liege 5th Se, 19, 13.

Hoxie, D.T. 1970, Ap.J. 161, 1083.

IAU Symp. 1972, "The Motion, Evolution of Orbits and Origin of Comets," ed. by G.A. Chebotarev, E.I., Kazimirchak-Polonskaya, E.I., and B.G. Marsden, D. Reidel, Dordrecht, Holland.

Iben, I. Jr. 1967, Ap.J. 147, 624.

Larson, R.B. 1973, M.N. 161, 133.

Oort, J.H. 1950, B.A.N. 11, 91.

Opik, E. 1973, Astrophys. and Sp. Sci. 21, 307.

Roberts, M.S. 1957, Pub. A.S.P. 69, 59.

Salpeter, E.E. 1959, Ap.J. 129, 608.

Spitzer, L.J. Jr., Ch. 9 Stars and Stellar Systems, V. 7, ed. by L.H. Aller and B. Middlehurst, U. Chicago Press, 1968.

Straka, W.C. 1971a, Ap.J. 164, 125; b, Ap.J. 165, 109.

Tinsley, B. and Cameron, A.G.W. 1974, Astrophys. and Sp. Sci. 31, 31.

van Altena, 1966, A.J. 71, 482.

van de Kamp, P. 1971, Ann. Rev. Astr. and Ap. 9, 103.

DISCUSSION

L. Biermann: The reason for expecting many more cometary nuclei in interstellar space than in the Oort clouds of stars like our sun is a quite general one. The total energy per gram of such an object must be negative but only by a quite small amount. Irrespective of the exact place of first formation, the solar system or outside of it, but in that dense interstellar cloud in which here and there a star is being born, the probability of such an object ending up in the Oort cloud with such initial parameters that it stays there for 10^9 years is only of order some percent or less. Since this point was the subject of a contribution of mine at the 1972 Nice Colloquium on the Origin of the Solar System, I shall not elaborate it further. In closing I should say only that it is a least conceivable that a sizeable fraction of the interstellar C, N, and O atoms are tied up in such objects (not necessarily of 10^{-16} gm or more) a possibility currently being discussed in connection with the chemistry of interstellar space (M. Friesberg, 1974).

J. T. Wasson: I think that many of the arguments that you give for believing that interstellar material will give you high CH_3CN or CH — or methyl acetylene, whatever ratios, are quite correct but I'm also not convinced that you can't get them by material forming close to the sun.

I think that we don't know, first of all, anything about the temperature distribution in the early solar system: even though it undoubtedly got fairly hot in near to the sun, we don't really know how hot it must have gotten out at 30 astronomical units during, say, the collapse phase of the solar nebulae.

Secondly, we don't know that all the matter in the solar system fell in at once. It may have been a very gradual process of material being captured by the solar system from the interstellar cloud. One could certainly imagine a model where half or more of the material that ultimately ended up at ten astronomical units from the sun or every further out was in fact interstellar material that had never been hot and had never, therefore, lost the inner stellar signature that you've been talking about.

B. Donn: It is certainly true. I wouldn't insist that this is necessarily a unique distinction but we know in the interstellar medium that these complex compounds have in fact surprisingly high concentration compared, to any CO and H_2.

In the solar nebulae it is true we don't know. Most of the theoretical calculations have assumed that it is near an equilibrium calculation. It may not be. And so it may be that when you get these observations, you will not be able to make a unique determination. But I think it is one possibility.

The isotope ratios may be a little bit better but again, the same sort of thing may apply if the material falling into the solar system was again not recycled to bring about equilibrium.

J. T. Wasson: I think most of these calculations have been done by meteoriticists who believed they were talking about material that formed at about 2.8 astronomical units.

M. Oppenheimer: Along the same line, in line with Dr. Whipple's model, there's a way that comets forming at very large distances can be characterized by a signature of high temperature formation. It gets very complicated because that's sort of a region which is neither here nor there.

And also, with respect to the deuterium problem, the thing that determines the hydrogen to deuterium ratio in those molecules is the energy defect as far as the exothermicity of reactions like $HD + HCN \rightarrow H_2 + DCN$, which are a few hundred degrees, and you have to be very careful that as the densities become very high as this matter conglomerates—even if the temperature never gets a above 100 or 150, the time scales are going to become short enough so that you may wipe out the original signature, and when the hydrogen is blown out of the object that becomes a comet, that difference may just totally disappear.

So I think it is something that has to be worked out very carefully.

B. Donn: I agree. What I'm proposing here is not that this is a definite, unique phenomena but that both the observations and the whole theory of molecular formation should be looked at from this point of view to see what happens.

And of course to do these observations in comets is certainly intrinsically significant and would be very worthwhile. If one does find, for example, distinction among comets for example, different ratios, that could be a useful clue.

OMIT

LABORATORY STUDIES OF POLYATOMIC COMETARY MOLECULES AND IONS

G. Herzberg

At present only four polyatomic molecules or ions have been identified in the spectra of comets and their tails. They are C_3, CO_2^+, NH_2, and H_2O^+. The first two are linear molecules. The C_3 radical gives rise to the well-known 4050 group. It was first obtained[1] in the laboratory in an interrupted discharge through CH_4; was definitely identified by Douglas[2] as being due to C_3, and was later investigated in considerable detail in absorption[3] in the flash photolysis of CH_2N_2. The complicated vibrational structure of this spectrum was first understood when it was realized that the bending frequency in the ground state is very low (64 cm^{-1})[3,4] and that in the excited state the interaction of the vibrational angular momentum with the electronic angular momentum leads to large splittings (Renner-Teller splittings)[5].

The same kind of interaction of vibrational and electronic angular momentum occurs also in the ground state of CO_2^+ but up to now only a provisional analysis of this spectrum is available[6,7].

NH_2 and H_2O^+ are non-linear molecules. The spectrum of the first occurs in emission in oxyammonia flames and in absorption in the flash photolysis of ammonia[8,9], while the spectrum of the second was first obtained by Lew and Heiber[10] in emission in a low pressure hot cathode discharge. The spectra of NH_2 and H_2O^+ are surprisingly similar to each other, consisting of progressions of bands in the red part of the spectrum which are alternately of the Σ and Π type. While in the lower state the molecule or ion is strongly bent with an angle of 103° and 110° respectively, in the excited state both are nearly linear. Some molecular data on H_2O^+ are given in the accompanying Table 1 supplied by Dr. Lew[11].

The first H_2O^+ lines identified in the spectrum of Comet Kohoutek were the lines at 6147.6, 6158.8 and 6200.1 Å observed by Herbig[12] and Benvenuti and Wurm[13]. They belong to the 8-0 Π band of H_2O^+ and represent the transitions with lowest K and N values[14]. Further spectra by Wehinger and Wyckoff and Herbig[15] have shown some fifty further lines belonging to the 5-0, 6-0, ..., 10-0 bands. The alternation of band structure between even and odd vibrational quantum numbers of the upper state is clearly visible in these spectra. It is particularly the presence of the Δ bands near the Σ bands that makes the band structure for odd v_2 values so different. In Herbig's spectra the spin doubling in a number of "lines" is well resolved, leaving no doubt whatever in the identification of H_2O^+ in the tail of the comet.

Table 1

Rotational Constants of H_2O^+ (in cm^{-1})

$^2B_1$ Ground State (0,0,0)

A = 29.040	D_K = 0.04338
B = 12.410	D_{JK} = -0.00392
C = 8.474	D_J = 0.00087
	D_2 = -0.000767

$^2A_1$ Excited State

5799.6Å Σ(0,9,0)	B = 8.77±0.01
	D = -0.0066
5494.7Å $\left\{\begin{matrix}\Pi^+\\ \Pi^-\end{matrix}\right\}$ (0,10,0)	$\left\{\begin{matrix}B = 9.50\\ B = 8.40\end{matrix}\right.$

References

1. G. Herzberg, Ap. J. 96, 314 (1942).
2. A.E. Douglas, Ap. J. 114, 466 (1951); Can. J. Phys. 32, 319 (1954).
3. L. Gausset, G. Herzberg, A. Lagerqvist and B. Rosen, Ap. J. 142, 45 (1965).
4. A.J. Merer, Can. J. Phys. 45, 4103 (1967).
5. G. Herzberg, "Molecular Spectra and Molecular Structure. III. Electronic Spectra and Electronic Structure of Polyatomic Molecules", D. Van Nostrand Co. Inc., New York, 1966.
6. S. Mrozowski, Phys. Rev. 60, 730 (1941); 62, 270 (1942); 72, 682, 691 (1947).
7. J.W.C. Johns, Can. J. Phys. 42, 1004 (1964).
8. G. Herzberg and D.A. Ramsay, J. Chem. Phys. 20, 347 (1952).
9. K. Dressler and D.A. Ramsay, Phil. Trans. 251A, 553 (1959).
10. H. Lew and I. Heiber, J. Chem. Phys. 58, 1246 (1973).
11. H. Lew, to be published.
12. G.H. Herbig, I.A.U. Circular 2596 (1973).
13. P. Benvenuti and K. Wurm, Astron. & Astrophys. 31, 121 (1974).
14. G. Herzberg and H. Lew, Astron. & Astrophys. 31, 123 (1974).
15. P.A. Wehinger, S. Wyckoff, G.H. Herbig, G. Herzberg and H. Lew, Ap. J. 190, L43 (1974).

DISCUSSION

A. H. Delsemme: Well, I think that Dr. Herzberg has again demonstrated how fundamental his contribution has been to the understanding of the molecular spectra. We know it already.

Now, to be fair for the next talk, I think we can have a 3 to 5 minute discussion, no more. Yes?

M. Oppenheimer: First of all, are you in disagreement with what Wehinger has just said?

G. Herzberg: I am in disagreement with his point that the excitation is by photoionization. I believe that it is due to resonance fluorescence. I've had several discussions with Dr. Wehinger about this point, and I think we are perhaps converging.

I think one of the difficulties that perhaps he didn't quite appreciate, is that in the calculation of the intensities of these bands one has to use Franck-Condon factors that correspond to H_2O-plus only and not the Franck-Condon factors that are observed in the photoelectron spectrum of H_2O. When you start from the ground state say, H_2O, and go to the excited state of H_2O-plus, you get certain Franck-Condon factors. And they are definitely slightly different from those of H_2O-plus. The H_2O-plus ones are not so readily available, and this may be the reason for the discrepancy that Dr. Wehinger found between observed intensities and those calculated on the fluorescence mechanism.

M. Oppenheimer: Which is faster, the ionization of H_2O, or the excitation of H_2O-plus?

G. Herzberg: I would say that the excitation would be faster, but I'm only guessing. There are certainly people here in this group who would know that better than I do.

M. Oppenheimer: If the ionization is faster, and since H_2O was created by sublimation on the surface, then you should only see H_2O-plus created by direct ionization and never by resonance fluorescence.

G. Herzberg: Yes, but the trouble then is the H_2O^+ in the tail, far in the tail, cannot come from H_2O in the tail. It's hard to assume that neutral H_2O is concentrated in the tail.

Well, it could also be excited by photoionization the first time. What I'm saying is that in order even to account for the low temperature, it has to emit infrared radiation in order to keep the temperature down. And that requires that there is a transition to the ground state, then going up again, and so on.

Let me give another example. You know that N_2^+ is present in the comet tail, and I would predict that in N_2^+ you would find that the rational temperature, is high, for the same reason that the apparent temperature in C_2 in the coma is hot, because it can't radiate infrared radiation.

N76-21079

LABORATORY OBSERVATIONS OF THE PHOTOCHEMISTRY OF PARENT MOLECULES: A REVIEW

William M. Jackson

Introduction

Many years ago K. Wurm (1) suggested that the photodissociation of stable molecules such as H_2O, HCN, CH_4, NH_3, etc., could account for the observed cometary radicals. This postulate can be represented schematically by the following photochemical reaction,

$$R_1R_2 + h\nu \longrightarrow R_2 + R_1$$

In this particular reaction R_1R_2 represents the parent molecule, R_1 the cometary radical and R_2 may or may not be a stable molecule. The original postulate of Wurm has been largely confirmed by the satellite observations of the overwhelming abundances of cometary H and OH (2), the spectroscopic identification of H_2O^+ (3) and the radio detection of CH_3CN (4), HCN (5), and H_2O (6) in comets. All of the cometary radicals cannot be explained by CH_3CN, HCN, and H_2O which suggest the presence of other parent molecules. An important clue to the identity of other parent molecules is the observations of complex molecules in the interstellar mediums (7). Present theories on the origin of comets (8) suggest that the interstellar molecules are also likely candidates for parent molecules in comets. This review on the status of the photochemistry of parent molecules in comets will use the known interstellar molecules as a guide to the identity of parent molecules.

The photochemical investigation of any molecule should attempt to answer certain basic questions. The qualitative identification of each of the primary products should be made along with the quantitative measurement of the yields of each of these primary products. A photochemical reaction has a threshold energy E_t so that if the energy of the photon E_h used to initiate the reaction is greater than E_t, the excess energy

$\Delta E = E_h - E_t$ must be divided among the primary products. The nature of this energy partitioning, i.e. the division between translational, vibrational, rotational, and electronic energy, is extremely important in any photochemical study. All of these questions must then be answered as a function of the wavelength of the incident photon.

The importance to cometary astrophysics of the qualitative and quantitative identification of each of the primary products is obvious. However, the importance of understanding the energy partitioning among the primary products is not generally appreciated so that a few examples of how this information affects our interpretation of cometary observations will be given. The scale lengths of radicals, atoms, and parent molecules are determined from monochromatic isophotes of the emission of the radicals and ions. These scale lengths are the product of the velocity (v) and the lifetime, t, of the particular species. The velocity of neutral cometary fragment is determined by the energy partitioning among the fragments. Thus, a knowledge of this energy partitioning is essential if we are to obtain the maximum information available in the observed isophotes.

Another example of the importance of understanding energy partitioning is in the interpretation of the relative intensities of radical emission from comets in the infra-red region. Specifically, Meisel and Berg (9) has measured the infra-red emissions of the CN and OH radicals in comet Kohoutek. If an equilibrium model is used to interpret these measurements, then the calculated production rates for CN would be higher than the OH production rates. We know from the UV observations, which we understand, that the situation is just opposite. The net result is that IR radiation is greater for CN than it should be. A possible way out of this dilemma

is to explain the excess IR radiation upon the photochemical formation of vibrationally and rotationally excited CN radicals.

At this point, a few elements of caution should be injected into the discussion about applying laboratory photochemical data to comets. First, there is a large difference between the collision frequency in the laboratory and the collision frequency in comets. For example, in a typical photochemical experiment the total pressure is generally greater than 0.1 torr. At these pressures, one obtains collision frequencies of the order of 10^6 per sec. In comets the collision frequency at the nucleus when the comet is 1 AU away from the sun is of the order of 10^3 to 10^4 collisions per sec. which is three orders of magnitude less than the laboratory values. The net result is that there is a much lower probability in comets for the collisional stabilization of any excited molecules produced in the primary process.

Another process that one could expect to be more probable in comets than in the laboratory is the phenomena of two stage photolysis. Consider the following sequence of events,

$$R_1R_2 + h\nu_1 \longrightarrow R_1 + R_2$$
$$R_1 + h\nu_2 \longrightarrow R_3 + R_4$$

In the first reaction the molecule R_1R_2 is photolyzed to produce the radical R_1. Suppose the lifetime for process 1 at 1 AU is 10^4 sec., and that R_1 absorbs in the near u.v. region of the spectra so that its lifetime is 10^3 sec., then if R_3 is an observable radical or ion its net lifetime will be 10^4 sec. This type of processes is generally unimportant in the laboratory because the collision frequency is high enough so that R_1 reacts before it can undergo secondary photolysis.

Photochemical Lifetimes and the Fractional Probability for Dissociation

The total photochemical lifetime (t_T) may be defined in terms of the absorption coefficient σ_λ, the quantum yield ϕ_λ, and the intensity of the incident light I_λ by the following relationship (10),

$$t_T = \frac{1}{\int_\lambda \sigma_\lambda I_\lambda \phi_\lambda d\lambda}$$

The average intensity of solar radiation at 1 AU for 50 nm intervals between 100.0 and 400 nm is given in figure 1. This figure illustrates how sharply the solar radiation decreases below 300 nm. In fact, not only does the magnitude decrease but below 150 nm, the character shifts from a continuum to a line spectra. This has the effect that an accurate measure of the total lifefime in this region can best be obtained by using a high resolution spectra of the gas along with a high resolution spectra of the sum. Fortunately, the only really important line between 100.0 and 150.0 nm is the Lyman alpha line at 121.6 nm. This line has been removed from the rest of the spectra because of its high intensity and will be considered separately. No attempt will be made to take into consideration the light below 100 nm because except in special cases for gases, such as CO and N_2, that have high thresholds for dissociation this region has a negligible effect on the photochemical lifetime.

Knowing the absorption coefficient of the gas and assuming ϕ_λ is equal to 1 for all wavelengths, the data in figure 1 can be used to calculate the minimum photodissociation lifetime for parent molecules in comets. These results are given in table 1. The important point to note is that most molecules have lifetimes below 2 x 10^{+4} sec. at 1 AU. This is in contradiction to the earlier work of Potter and Del Duca (11) where most of the molecules had much longer lifetimes. In their work only the

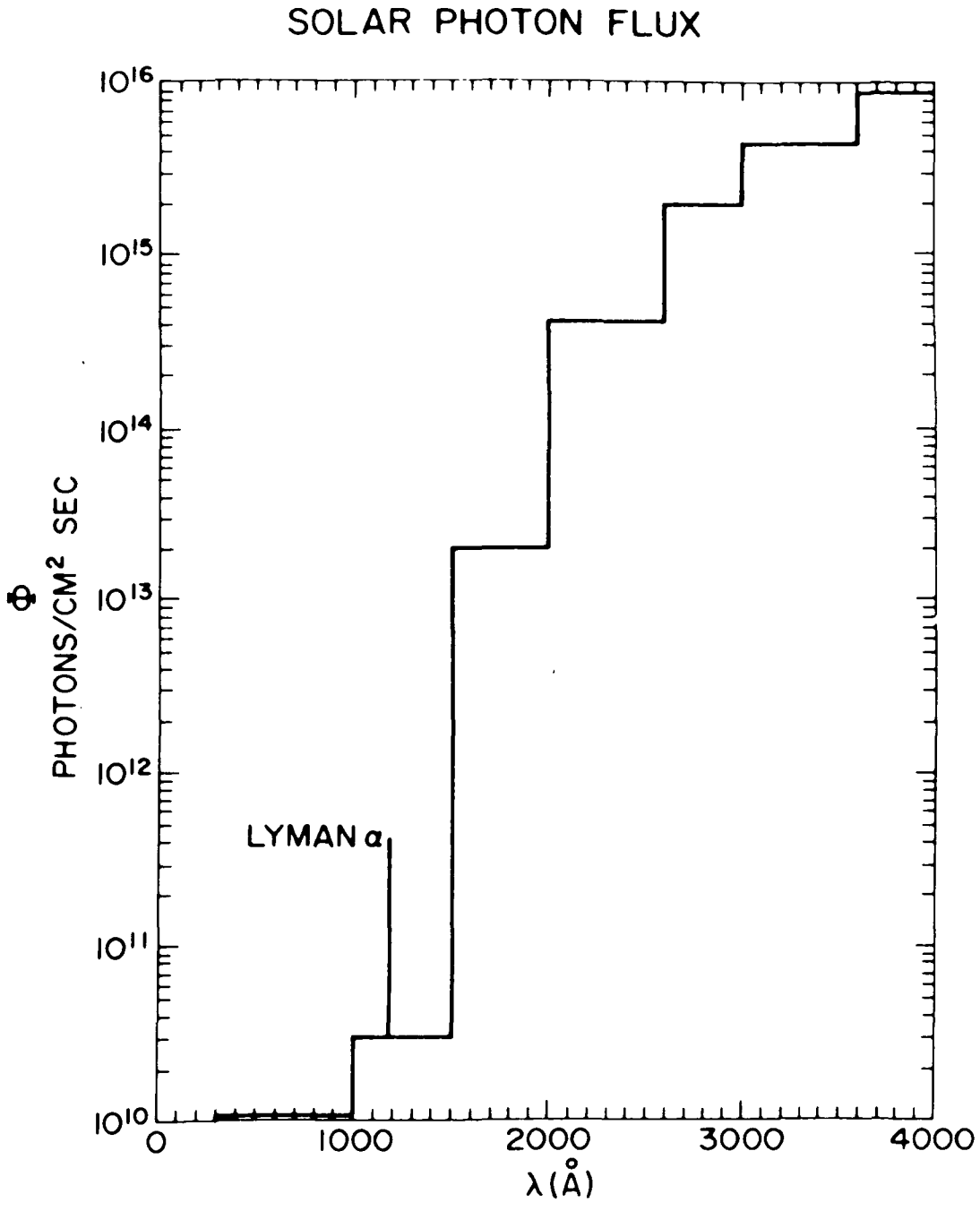

Figure 1. The Integrated Solar Flux at one Astronomical Unit.

Table 1

PHOTOCHEMICAL LIFETIME (t_r) AND PARTIAL DISSOCIATION FRACTION P_f FOR PARENT MOLECULES AT 1 A.U.

Molecule	t_r (sec.)	P_f 100-150 nm	P_f 150-200 nm	P_f 121.6 nm	P_f 200 nm	Source for Absorption Cross-Section
NH_3	2.1×10^3	0.09	0.16	0.012	0.82	J.A.R. Samson and J.A. Meyer. Geographical Corp. Rept. #TR-69-7-N "Absorption Cross-Section of Minor Constituents in Planetary Atmospheres from 105.0-210.0 nm"
H_2O	2.0×10^4	0.05	0.83	0.16	-	J.A.R. Samson, op cite.
CH_4	1.2×10^5	0.07	-	0.93	-	J.A.R. Samson, op cite.
HCN	9×10^4	0.05	0.14	0.81	-	M. Berry, Private Communication, Univ. Wisc. Chem. Dept.
C_2N_2	1.1×10^4	0.02	0.71	0.27	-	R.E. Connors, J.L. Roberts, and Karl Weiss, J. Chem. Phys. 60, 5011, 1974
HC_2CN	1.3×10^4	0.10	0.72	0.17	-	R.E. Connors, op cite.
CH_3C_2H	4.9×10^3	0.006	0.90	0.09	-	T. Nakayama and K. Watanabo, J. Chem. Phys. 40, 558, 1964
C_2H_2	5.7×10^3	0.004	0.83	0.17	-	T. Nakayama, op cite.
H_2CO	1.9×10^3	0.008	0.17		.82	J.G. Calvert and J.N. Pitts, Jr. "Photochemistry," John Wiley New York, 1966; J.E. Mentall, E.P. Gentiew, M. Krauss and D. Neumann, J. Chem. Phys., 55, 5471, 1971
CH_3CHO	1.6×10^3		0.25		0.75	J.G. Calvert, op cite. E.E. Barnes and W.T. Simpson, J. Chem. Phys., 39, 670, 1963

Table 1 (continued)

HNCO	1.3×10^4	0.01	0.56	0.19	0.24	J.W. Rabolais, J.R. McDonald and S.P. McGlynn, J. Chem. Phys., 51, 5103, 1969 H. Okabe, J. Chem. Phys., 53, 3507, 1970
CH_3OH	2.1×10^4	0.005	0.91	0.09	-	D.R. Salahub and C. Sandorf, Chem. Phys. Lett., 8, 71, 1971
$HCONH_2$	1.5×10^3	0.001	0.90	0.009	0.09	H. Basch, M.B. Robin and N.A. Kuebler, J. Chem. Phys. 49, 5007, 1968
HCOOH	7×10^3	0.004	0.81	0.08	0.11	E.E. Barnes, op cite.
CH_3NH_2	1.5×10^3	0.002	0.17	0.02	0.80	E. Tannenbaum, E.M. Coffin, and A.J. Harrison, J. Chem. Phys. 21, 311, 1953
CH_3OCH_3	8.2×10^3		1.00			J.G. Calvert, op cite.

absorption coefficient for the continuum was used in determining the lifetime and as Herzberg (12) has pointed out this ignores predissociation. The effect of predissociation has been included in table 1 by including the absorption of spectral lines.

The partial dissociation fraction (P_f) for a parent molecule can be defined as

$$P_f = \frac{\bar{\sigma}_\lambda \bar{I}_\lambda}{t_r}$$

where $\bar{\sigma}_\lambda$ is the mean absorption co-efficient over the wavelength band and $\bar{I}_\lambda$ is the mean solar flux over the same wavelength interval. This table shows that for most molecules the important photodissociation region is between 150 and 200 nm, while the region below 150 nm is relatively unimportant.

Triatomic Parent Molecules

(H_2O)

The most important parent molecule in comets is the triatomic molecule (H_2O) water. The photochemistry of H_2O is probably better understood than any other parent molecule. Table 1 shows that the principle wavelength regions for the photodissociation of H_2O are the first continuum between 150-200 nm and the Lyman alpha line of the sun at 121.6 nm. Of the two regions the first absorption band is the most important with 83% of the H_2O molecules decomposing in this region.

150.0 - 200.0 nm

The three possible primary processes in this wavelength region are:

(1) $H_2O + h\upsilon \longrightarrow H_2 + O\ (^3P)$ $\quad E_t = 5.1$ e.v.

(2) $\longrightarrow H + OH\ (x^2\Pi)$ $\quad E_t = 5.2$ e.v.

(3) $\longrightarrow H_2 + O\ (^1D)$ $\quad E_t = 7.1$ e.v.

The first primary process which produces H_2 and ground state 0 atoms is spin forbidden and is of negligible importance. The latest available evidence (13) indicates that the relative quantum yields for the production of H atoms to the quantum yield for the production of 0 atoms in this region is greater than 99 to 1. Thus, even the spin allowed processes is of negligible importance. The solar photon energy is between 5.8 and 8.3 e.v. in this region so that the products of reaction 2 have to dispose of 0.6 to 3.1 e.v. of excess energy. The work of Sthul and Welge (14, 15) shows that the OH radical produced in the vacuum ultraviolet flash photolysis of H_2O is not vibrationally or rotationally excited. All of the excess energy for reactions (2) and (3) must go into the relative translational motion of the fragments. Masanet and Vermeil (16) using a chemical method to determine the amounts of excess translational energy produced in reaction (2) have confirmed this observation.

121.6 nm

Most of the H_2O molecules that are not photodissociated in the first continuum will be dissociated by Lyman alpha. At this wavelength there is strong evidence (13) that some of the H_2O is photodissociated to yield H_2 amd $O(^1D)$ atoms. A new primary process is also observed (17) namely,

$$(4)\quad H_2O + h\nu \longrightarrow H + OH(A^2\Sigma)$$

This reaction has been known to occur for almost 30 years and the work of Carrington (17) shows that the quantum yield for the production of the $A^2\Sigma$ state of OH is $\sim .05$ at 121.6 nm. The uncertainty in the absolute measurement of the intensity are such that as much as 15% of the H_2O could dissociate to form the A state of OH. Steif (13) has shown that 89% of the H_2O dissociates to form OH plus H in the 105.0 - 145.0 nm wavelength

region along with 11% to form H_2 and $O(^1D)$. If these results are applicable at the single wavelength of 121.6 nm, then less than 17% of the total OH formed at this wavelength is in the A state. Most of the energy in reaction (4) that must be distributed among the products ends up as rotational energy in the hydroxyl radical (17) but chemical evidence (16) has been presented that the H atom produced in the photolysis at 121.6 nm are translationally hot which suggest that reaction (4) is not important. The authors of this particular study have also suggested that reaction (3) is pressure dependent and quote a lifetime for the suggested (C^1B) intermediate state of H_2O of 2×10^{-8} sec. The relative quantum yield measurements of Steif et al. were done by quenching the (O^1D) to the (O^3P) state and subsequent detection of this state using and O atom resonance fluorescence lamp. This method of necessity requires high pressures and could lead to error in the determination of the yield of (O^1D) if the product is formed by the predissociation of the (C^1B) state of H_2O.

HCN

More than 82% of the HCN will be photodissociated by the Lyman alpha radiation from the sun. At this wavelength all three of the following primary processes are energetically possible.

$$(5)\ HCN + h\nu \longrightarrow CN\ (B^2\Sigma) + H$$
$$(6)\ HCN + h\nu \longrightarrow CN\ (A^2\Pi) + H$$
$$(7)\ HCN + h\nu \longrightarrow CN\ (X^2\Sigma) + H$$

The first two processes have been observed (18) by Mele and Okabe in the photolysis of HCN at 123.6 nm. Both the A and the B state of the CN radicals were produced with a large amount of excess vibrational and rotational energies. No information exists on the quantum yields for the production of the X, A, and B states at this wavelength.

Most of the remaining HCN will be photolyzed in the 150 to 200 nm region. M. Berry (19) has recently studied the photolysis of HCN in this wavelength region where only the A and the X states can be produced. He used gain measurements of the laser lines that result from the A to X transition when HCN is photolyzed. With this technique he was able to show that the production of A state radicals is the principle primary processes. Most of these radicals were formed in the $v' = o$ with a few of them in the $v' = 1$ level. Most of the remaining energy will be converted into the translational motion of the H atom.

C_2N_2

This particular molecule has not been observed in the interstellar medium but is expected to occur since it represents the dimer of the CN radical. Most of the photodissociation (71%) of C_2N_2 occurs in the 150 to 200 nm region. The remaining amount of this dissociation occurs at L_α. The photodissociation in the 150 to 200 nm region has been extensively studied by the author (20, 21, 22) and M. Berry (19). The primary processes that are energetically possible at this wavelength are,

$$(8)\quad C_2N_2 + h\nu \longrightarrow CN(x^2\Sigma) + CN(A^2\Pi)$$

$$(9)\quad \longrightarrow 2CN(x^2\Sigma)$$

$$(10)\quad \longrightarrow 2CN(A\ ^2\Pi)$$

M. Berry states that most of the radicals are formed in the A state. The author and his co-workers (22) were able to determine how the excess energy is partitioned among the fragments. Most of the available energy, 82%, goes into the translational motion of the fragments. Of the energy that remains, 11% goes into vibrational excitation and 6% into rotational excitation.

NH_3

Ammonia has been considered a probable parent molecule for a long time. Most of the NH_3 will be photodissociated in the first absorption bands. In this wavelength region it is energetically possible to produce NH_2 in the ground (X^2B) state and in the ($\tilde{A}\ ^2A_1$) excited state. The evidence (23) is that the principle photochemical process occuring for NH_3 in this band is,

$$(11)\ NH_3 + h\nu \longrightarrow NH_2\ (X\ ^2B_1) + H(1\ ^2S)$$

even though several others are energetically possible and have been searched for (25). The quantum yield for photodissociation via reaction (11). is one throughout this wavelength region. Nothing is known about the partitioning of energy in this molecule.

C_2H_2

It has been supposed for a long time that acetylene is the source of C_2 in comets. No laboratory evidence exists (25) at the present time to support this contention. The principle wavelength region for photodissociation of acetylene is the 150-200 nm region where it is estimated that 83% of the C_2H_2 decomposes. Most of this decomposition (76%) occurs at the 153 nm peak. The principle photochemical process in this wavelength region (26) is thought to be the formation,

$$(12)\ C_2H_2 + h\nu \longrightarrow C_2H_2^*$$
$$(13)\ C_2H_2^* \longrightarrow C_2H + H$$

of a long lived excited acetylene molecule. This excited molecule then either undergoes polymerization reactions or decomposes to yield C_2H and an H atom. This reaction is 5.38 e.v. endothermic (27) and a photon at 153 nm has an energy of 8.10 e.v., which leaves 2.72 e.v. for partitioning

between the C_2H and H fragments. This is not enough energy to form electronically excited C_2H so the excess energy has to be in either internal energy of C_2H or translational motion of the H atom. No information exists at the present time relating to this question.

Earlier it was mentioned that there is no direct evidence for C_2 production from acetylene. This problem is complicated by the known participation of C_2H_2* in the photodissociation. There is an observation by Steif et. al (28) that suggests that C_2 might be a primary product, being produced via reaction 14. This postulate,

$$(14)\ C_2H_2 + h\upsilon \rightarrow C_2(x^1\Sigma_g^+) + H_2$$

is based upon the observation that substantial amounts of molecular hydrogen appear to be formed at low total pressures. It would be extremely important to try to observe the C_2 in some direct manner in the gas phase photolysis of C_2H_2 since the Swann band is one of the most prominent emissions in comets. These bands result from the fluorescent pumpting of $X^3\Pi_u$ ground state radicals. The direct production of the triplet ground state of C_2 via a molecular processes is only slightly more endothermic, 6.3 e.v. versus 6.2 e.v., than the production of the singlet state. However, the triplet processes is spin forbidden. It is possible, however, that the selection rule might be violated via an intersystem crossing to a highly vibrationally excited triplet state of C_2H_2 (30). This state then can decompose to yield the $(X^3\Pi_u)$ state of C_2. A direct observation of this radical is needed to clear up this point.

H_2CO

This molecule was one of the first fairly large molecules observed in the interstellar space (7). It is also one of the molecules that will undergo appreciable amounts of photodissociation above 200 nm since it does have

a reasonable absorption coefficient in the 250 to 350 nm meter range. As table 1 shows 99% of the formaldehyde will be decomposed in this wavelength range. The two primary photochemical processes (30) are,

$$(16)\ H_2CO + h\nu \rightarrow H_2 + CO$$
$$(17)\ H_2CO + h\nu \rightarrow H + HCO$$

The relative yields of these two reactions is a function of wavelength with the quantum yield of the molecular process 16 increasing from 0.2 to 0.8 as the wavelength decreases from 256 to 330 nm. In addition to the very short photochemical lifetime of H_2CO, an extremely interesting observation is that the molecular processes is only .06 e.v endothermic. So that from 3.8 to 4.8 e.v. of energy has to be distributed between the products. A recent theoretical treatment of this problem (31) suggests that dissociation of the formaldehyde occurs from a highly excited vibrational level of the singlet ground state. The products of this dissociation should be both vibrationally and rotationally excited but not electronically excited.

HNCO

This molecule is fairly unique since substantial decomposition occurs throughout the solar spectrum. There is a large amount of qualitative data available on the states of the photochemical products, but no work on the quantum yields or the internal energy distribution of these products appears to be available. H. Okabe (32) has summarized most of this work. In the 200 to 230 nm the two principle primary processes are,

$$(18)\ HNCO + h\nu \rightarrow NH + CO$$
$$(19)\ HNCO + h\nu \rightarrow H + NCO\ (X^2\Pi)$$

Both radical intermediates have been observed (33,34) in the flash photolysis of this compound. The particular transition of NH that was observed was the

NH ($X\ ^3\Sigma$) $\longrightarrow$ NH ($A^3\ \Sigma$) transition. Reaction 18 would violate the spin selection rule if NH was produced directly in the $X^3\ \Sigma$ state. It has been suggested that the NH in 18 is produced in the A $^1\Delta$ state which is then quickly quenched to the $X^3\ \Sigma$ state. This quenching reaction also violates the selection rule so this question deserves further study. The two processes, 18 and 19, are 3.4 and 4.9 e.v. endothermic so between 2.8 and 1.2 e.v. of energy has to be partitioned among the fragments.

In the next absorption region between 150 and 200 nm a new primary processes occurs in which the NCO fragment is electronically excited to the $A^2\ \Sigma$ state. The threshold for this processes is at 160.5 nm so that this processes is probably not too important for comets:

$$(20)\ HNCO + h\nu \longrightarrow H + NCO\ (A^2\Sigma)$$

The last important absorption region at Lyman alpha (121.6 nm). Two new primary can now occur. The first of these (21) is the excitation of the NCO to the ($B\ ^2\prod$) state. This reaction,

$$(21)\ HNCO + h\nu \longrightarrow NCO\ (B\ ^2\prod) + H$$

has been observed by Okabe (32). The other reaction that is energetically possible is the production of two triplet molecule via,

$$(22)\ HNCO + h\nu \longrightarrow NH(A\ ^3\Sigma) + CO\ (a\ ^3\prod)$$

Reactions of this type may be extremely important if the CO($a^3\prod$) is produced in rotational levels where little mixing occurs with allowed transition. In this manner the lifetime of CO against photoionization might be substantially lowered since this metastable ($a\ ^3\prod$) state can be photoionized at longer wavelengths.

CH_4

Methane has not been observed in the interstellar medium but is expected to be very abundant there and in comets. This expectation is based primarily upon the fact that this is the most thermodynamically stable

carbon compound in a hydrogen rich atmosphere. Since methane does not absorb above about 140 nm, the most important solar wavelength for photodecomposition is for Lyman Alpha at 121.6 nm. There are two important primary processes (35) in this region, one of which involves the molecular detachment of H_2, the other is the formation of atomic H. The measured values of these quantum yields are given below. No information exists on

$$(23)\ CH_4 + h\nu \rightarrow CH_2 + H_2 \quad 0.42 \leq \phi \leq 0.52$$
$$(24)\ CH_4 + h\nu \rightarrow CH_3 + H \quad 0.48 \leq \phi \leq 0.58$$

the energy partitioning among the products.

HCOOH

This is the simplest organic acid but very little is known about its photochemistry. Apparently, the only photochemical studies that have been reported (36, 37) are in the region above 200 nm which only accounts for 11% of the photodissociation if this molecule occurs in comets. The principle primary processes that have been reported in this region are,

$$(25)\ HCOOH + h\nu \rightarrow H_2 + CO_2$$
$$(26)\ HCOOH + h\nu \rightarrow H_2O + CO$$
$$(27)\ HCOOH + h\nu \rightarrow HCO + OH$$

No measurements have been made on the partitioning of energy among the products; however, the interesting point is that reactions 25 and 26 are almost thermoneutral. The reaction which forms H_2 plus CO_2 is exothermic by 0.15 e.v. while the reaction forming H_2O + CO in endothermic by 0.3 e.v. The result is that in each case large amounts of energy have to be converted into either recoil or internal energy of the products. Since formic acid has a relatively short photochemical lifetime and 81% will be decomposed in the 150 to 200 nm region, the products of 25 and 26 could have as much as 8 e.v. of energy. If this energy went into exciting a long lived

metastable state of CO, then only 6 e.v. of energy would be needed to ionize this state. The solar flux (36) that would be available for ionizing this metastable state of CO is 10^{13}. Thus, with an effective ionization, cross section of $10^{-16}cm^2$ the photoionization lifetime of metastable CO would be only 10^3 sec. This is many orders of magnitude lower than lifetime of ground state CO.

CH_3CN

The absorption coefficient of this compound has not been measured so the important photochemical region of the spectra cannot be determined. Two studies have been reported on the photochemistry of acetonitrile. The first was a classical photochemical study (37) where the following reactions were postulated:

$$(28)\ CH_3CN + h\nu \rightarrow H + CH_2CN$$
$$(29)\ CH_3CN + h\nu \rightarrow CH_3 + CN$$

In that study it was determined that at 184.9 nm the quantum yield for H production is much greater than the quantum yield of CH_3 production. At the shorter wavelength, 121.6 nm, the photodissociation leads the formation of electronically excited CN radicals via the following processes,

$$(30)\ CH_3CN + h\nu \rightarrow CH_3 + CN\ (B^2\ )$$
$$(31)\ CH_3CN + h\nu \rightarrow CH_3 + CN\ (A^2\ )$$

Reaction 30 has been observed by Okabe (38) who measured the relative fluorescence yield as a function of the wavelength of the light. M. Berry (19) has observed lasing from the $A^2\Pi$ to the $X^2\Sigma$ state in the flash photolysis of CH_3CN which indicates that reaction 31 occurs. No information is available on the partitioning of energy among the internal degrees of freedom.

NH_2CHO

Formamide has been studied (39) at 206 nm and the quantum yields of the following primary processes were determined.

$$(32)\ NH_2CHO + h\nu \rightarrow NH_2 + CO + H \quad \phi\ (206) = 0.35$$
$$(33)\ NH_2CHO + h\nu \rightarrow H + NHCHO \quad \phi\ (206) = 0.22$$
$$(34)\ NH_2CHO + h\nu \rightarrow NH_3 + CO \quad \phi\ (206) = 0.45$$

In the wavelength region above 200 nm only 9% of the formamide will be decomposed. No measurement has been reported for the vacuum ultraviolet region below 200 nm and neither have any studies been reported on energy partitioning among the fragments. An energy partitioning study in the region below 200 nm would be extremely valuable since reaction 34 probably has a lot of excess energy that must be disposed of.

CH_3OH

This molecule is dissociated primarily in the region between 150 and 200 nm. The following primary processes are thought to occur (40) with the associated quantum yields:

$$(35)\ CH_3OH + h\nu \rightarrow CH_3O + H \quad \phi = 0.75$$
$$(36)\ CH_3OH + h\nu \rightarrow CH_3 + OH \quad \phi = 0.05$$
$$(37)\ CH_3OH + h\nu \rightarrow CH_2O + H_2 \quad \phi = 0.20$$

All of these reactions are thought to be a result of this collision induced predissociation (42) of excited methanol. If this is the case throughout this region, then the photolysis of CH_3OH needs to be studied very carefully as a function of time between collisions. In comets where the time between collisions at the surface of the nucleus is of the order of a few tenths of a millisecond, processes like collision induced predissociation would be rare.

CH_3NH_2

Methylamine is dissociated mostly by light in the 200 to 250 nm region. In this region the principle primary product (43) is the formation of the methylamine radical and an H atom. There are, however, five minor primary processes in this region. The limits to their respective quantum yields (41) are given as follows:

$$(38)\ CH_3NH_2 + h\nu \rightarrow \begin{cases} CH_3NH + H & \phi = 0.75 \\ CH_2NH_2 + H & \phi = 0.07 \\ CH_3 + NH_2 & \phi = 0.05 \\ CH_3N + H_2 & \phi = 0.03 \\ CHNH_2 + H_2 & \phi = 0.02 \\ CH_2NH + H_2 & \phi = 0.05 \end{cases}$$

Nothing is known about the photochemistry in the wavelength region below 200 nm nor have any energy partitioning studies been reported.

CH_3CHO

Acetaldehyde is a homolog of formaldehyde and like formaldehyde, a molecular processes and a free radical process occurs in the photodissociation process (42) above 200 nm. The molecular process has a quantum yield (43) of

$$(39)\ CH_3CHO + h\nu \rightarrow CH_4 + CO$$

less than or equal to 0.5 and the free radical process results from the decomposition of an intermediate state. Like formaldehyde the molecular products

$$(40)\ CH_3CHO + h\nu \rightarrow CH_3CHO^* \rightarrow CH_3 + CHO$$

in reaction 39 have to carry away ~ 5 e.v. of excess energy because of the near thermoneutral character of the reaction. The free radical products are known (44) to carry away only 0.5 e.v. of rotational energy.

CH_3C_2H

Propyne has not been adequately studied in the 150 to 200 nm region which is the most important photochemical region from the cometary point of

view. The one study (45) reports only product yield and gives no mechanism. There has been a rather extensive study (46) at 123.6 nm in which an excited $C_3H_3^*$ intermediate is postulated. This intermediate then decomposes to give C_3 and H_2.

$$(41)\quad CH_3C_2H + h\upsilon \rightarrow C_3H_2^* + H_2$$

$$(42)\quad C_3H_2^* \longrightarrow C_3 + H_2$$

In comets since few collisions occur, it has been suggested by Steif (47) that propyne might be a good source for C3.

SUMMARY

The photochemistry of possible parent molecules of comets has been reviewed. The survey of the available literature suggests that a great deal of work remains. The quantum yield for many of the primary processes are unknown. Energy partitioning among the fragments has not been extensively investigated. This latter question might be extremely valuable in understanding the presence of cometary ions such as CO. Finally, a few of the studies have been performed as a function of the number of collisions that the excited molecules undergo, so that possible differences that may occur in a cometary environment may be ascertained.

REFERENCES

1. K. Wurm, Die Nature Die Kometen, Mitt. Hamburg Sternwarte, 8, 51 (1934).

2. A. D. Code, T. E. Houck, C. F. Lillie, I.A.U. Circular No. 2201, 1970.

3. P. A. Wehinger, S. Wyckoff, G. H. Herbig, G. Herzberg and H. Lew., Ap. J. 190, L43, 1974.

4. B. L. Ulich and E. K. Conklin, Nature, 248, p. 121 1974.

5. W. F. Huebner, L. E. Snyder, and D. Buhl, Icarus, 23, 580, 1974. (Special Kohoutek Issue)

6. W. M. Jackson, T. Clark and B. Donn, Proceedings of Int. Astr. Union Colloquium #25, "The Study of Comets", 1974 to be published.

7. L. Snyder, Spectroscopy, Physical Chemistry Series One, ed. A. D. Buckingham (MTP International Review of Science, Vol. 3, ed. D. A. Ramsay, Butterworths, London, 1972) chap. 6, 193.

8. B. Donn, Proceedings of I.A.U. Colloquium #25, "The Study of Comets," N.A.S.A. S.P.

9. D. D. Meisel and R. A. Berg, Icarus, 23, 454, 1974.

10. W. M. Jackson, Molecular Photochemistry, 4, 135, 1972.

11. A. Potter and B. Del Duca, Icarus, 3, 103, 1964.

12. G. Herzberg, Intern. Astron. Union. Trans. 12B, 194, 1966.

13. L. Stief, W. Payne, and B. Klenim, submitted to J. Chem. Phys., 1974.

14. F. Sthul and K. Welge, J. Chem. Phys., 46, 2440, 1967.

15. F. Sthul and K. Welge, J. Chem. Phys., 47, 332, 1967.

16. J. Masanet and C. Vermeil, J. Chem. Phys. Physiochem. Bio., 66, 1249, 1969.

17. T. Carrington, J. Chem. Phys., 41, 2012, 1964.

18. A. Mele and H. Okabe, J. Chem. Phys. 51, 4798, 1969.

19. G. A. West and M. J. Berry, J. Chem. Phys., 61, 4700, 1974.

20. W. M. Jackson, Ber. der. Busengesel. Fur Phyk Chem. 78, 190, 1974.

21. W. M. Jackson and R. J. Cody, J. Chem. Phys., 61, 4183, 1974.

22. W. M. Jackson, M. Sabiety-Dzvonik, and R. J. Cody, Bult. Am. Phys. Soc., CD-6, November, 1974.

23. K. Mantei and E. J. Bair, J. Chem. Phys., 49, 3248, 1968.

24. J. P. Simons, "Photochemistry and Spectroscopy," Wiley-Interscience, London, 1971, p. 280.

25. K. H. Becker, D. Haaks and M. Schurgers, Z. Naturforsch, 26a, 1770, 1971.

26. M. Tsukoda and S. Shida, Bull. Chem. Soc. Japan, 43, 362, 1970.

27. H. Okabe, Preprint of Paper submitted to J. Chem Physics.

28. L. J. Stief, V. J. DeCarlo and R. J. Mataloni, J. Chem. Phys., 42, p. 3113, 1965.

29. J. P. Simon, op cit, p. 180.

30. B. De Graff and Jack Calvert, J. Am. Chem. Soc., 89, 2247, 1967.

31. R. L. Jaffe, D. M. Hayes and K. Morokuma, J. Chem. Phys., 60, 5108, 1974.

32. H. Okabe, J. Chem. Phys., 53, p. 3507, 1970.

33. R. Holland, D. W. G. Styli, R. W. Nixon, and D. A. Ramsay, Nature, 182, 336, 1958.

34. R. W. Nixon, Can. J. Phys., 37, 1171, 1959.

35. J. P. Simon, Op cit, p. 279.

36. ASTM Annual Book of Standards Part 41, American Society for Testing and Materials, Philadelphia, Penna., p. 609, 1974.

37. D. E. McElcheran, M. H. J. Wijnen and D. W. R. Steacie, Can. J. Chem., 36, 321, 1958.

38. H. Okabe and V. Dibler, J. Chem. Phys., 59, 2430, 1973.

39. J. C. Boden and R. A. Back, Trans. of Fard. Soc., 66, 175, 1970.

40. J. Hagege, P. C. Roberge, and C. Vermeil, Trans. Farad. Soc., 64, 3288, 1968.

41. J. V. Michael and W. A. Noyes, Jr., J. Am. Chem. Soc., 85, 1228, 1963.

42. C. S. Parmenter and W. A. Noyes, Jr., J. Am. Chem. Soc., 85, 416, 1963.

43. A. S. Buchanan and J. A. McRae, Trans. Fard. Soc., 64, 919, 1968.

44. J. Solomon, C. Jonah, P. Chandra and R. Bersoh, J. Chem. Phys., 55, 1908, 1971.

45. A. Galli, P. Harteck and R. R. Reeves, Jr., J. Phys. Chem., 71, 2719, 1967.

46. W. A. Payne and L. J. Stief, J. Chem. Phys., 56, 3333, 1972.

47. L. Stief, Nature, 237, 29, 1972.

DISCUSSION

H. Keller: I looked also at the lifetime of H_2O by photodissociation and my lifetime is definitely higher than 2×10^4 seconds.

I figured out it would be between 7 and 10 times 10^4 seconds.

W. Jackson: We'll have to get together and see. It may be due to the fact that I used old values of the solar flux.

H. Keller: And I integrated in 25 angstroms intervals.

W. Jackson: I won't argue about the exact value. I was trying to illustrate the general principle.

W. F. Huebner: I have two quick questions.

First of all was predissociation taken into account?

W. Jackson: Yes.

W. F. Huebner: The second questions is, do you have similar numbers for ionization lifetimes?

W. Jackson: No, I don't, but in general the photon flux below a thousand angstroms drops by several orders of magnitude, and even if they have the same absorption coefficient the photoionization lifetimes are going to be several orders of magnitude longer.

M. Dubin: This is an inverse question and not the subject of your talk, but can you determine the parent molecules from the spectrum of the radicals? I mean, this is one of the objectives.

What about the inverse problem? Is it possible to determine on a kinetics basis what the parent molecule distribution will be, given the solar abundances, in the atomic form? And is anybody doing any work in this regard to give a pattern of parents based on the number of elements?

W. Jackson: The difficulty with doing that, you have to know quite a bit about the origin of comets, which means that you have to know whether you have equilibrium. Then you would have to know all the kinetic equations for the formation of the particular species.

At least, I'm not doing it. There may be some other people who are.

DISCUSSION (Continued)

C. Cosmovici: Are the results you have shown on photodissociation of parent molecules all experimental?

W. Jackson: They're all experimental results.

C. Cosmovici: That means you have detected these product molecules?

W. Jackson: That means that in one way or another the photochemists have decided that that was one of the possible parent molecules.

There are any number of ways of doing that. You can do kinetic spectroscopy, for example; analyze the products and using suitable isotopic labeling, you might use mass spectrometry; or you might use laser-induced flourescence.

To get into the many different techniques that photochemists would use would take me the rest of the week.

C. Cosmovici: No, I just wanted to know if it's possible to detect all these product molecules experimentally?

W. Jackson: It is possible to detect atoms; it is possible to detect free radicals by resonance fluorescence spectrum, using a tunable dial laser. We've shown that with CN. Welge and Braun have shown earlier that you can detect atoms, using resonance fluorescence method.

Yes, it's possible to detect them all. The most sensitive method is resonance fluorescence, of course.

C. Cosmovici: Also for complex molecules?

W. Jackson: Well, complex molecules, you would probably have to look at absorption, or you might have to get cute.

Now, there are cute ways of doing suitable isotopical labeling and look at the product distribution. You can do high intensity flash photolysis, but you have to be careful because you get secondary processes that would affect your results for photodissociation.

You might do something like flash photolysis producing, say, C_3H and then have another flash lamp to photodissociate the C_3H and look at the C_3 by resonance fluorescence, using a tunable dye laser.

C. Cosmovici: Thank you.

The second question was, we spoke about the dissociation of parent molecules, but we didn't speak about the possibility of gas reaction to form parent molecules. And I would like to ask if it is possible in a cometary coma to have chemical reactions in order to get parent molecules?

W. Jackson: That is a question, I think, Bert Donn and I addressed in the Liege symposium, 10 years ago. In fact, we had a table in which we gave what were the relative probabilities of reaction per collision.

Now, a lot of radical, radical reactions don't go on every collision. It's possible, but the region where you form most of the radicals and ions—is also the region where you have the lowest density, so you have to be careful.

I'm not going to say it's impossible. It depends upon the density distribution and so forth.

L. Stief: Just one comment in case people are concerned about all those unknowns.

Nature hasn't been very kind to us. There are two ways we normally do photochemistry. The older way was to look at products, and this was really good for the big molecules because a variety of fragments would give a variety of identifiable products.

The so-called simple molecules mess you up, because no matter what you do you get the same product. You get hydrogen, nitrogen and oxygen, even though you have ten different processes occurring. You can help this somewhat with isotopes, but you're still stuck.

Therefore, you're forced to go to more direct methods. However, you like to do photochemistry with a single line, and when you do the direct method you like to have an intense source that you can turn off quickly and make a time resolve observation.

So both sides have their problems. The products are indirect but at least are monochromatic. The direct methods are becoming monochromatic. We tend to work with wide band sources.

LASER INDUCED PHOTOLUMINESCENCE SPECTROSCOPY OF COMETARY RADICALS

W. M. Jackson and R. J. Cody and M. Sabety-Dzvonik*

A relatively new technique called Laser Induced Photoluminescence Spectroscopy has been applied to laboratory studies of cometary radicals. This technique can be used to measure properties of radicals, to determine photodissociation processes in parent molecules, and to investigate reactions of radicals in specific vibration-rotation levels. Thus far, the LIPS method has been applied to the CN radical to determine: (1) the radiative lifetime and quenching constants for the $B^2\Sigma^+$ state and (2) the photodissociative formation of CN from several parent molecules.

This experimental technique combines flash photolysis together with laser excitation of the product fragments. Figure 1 is a schematic diagram of the apparatus, and the experimental sequence of events is summarized below. The parent molecule is photodissociated:

$$RCN + h\upsilon \rightarrow R + CN.$$

After a variable time delay, the tunable dye laser is fired and excites those radicals in a specific vibration-rotation level of the ground electronic state to the B state via the $\Delta V = 0$ sequence of the Violet Band system. The reradiated light is then detected.

$$CN(X^2\Sigma^+, v'', N'') + h\upsilon(\text{laser}) \rightarrow CN^*(B^2\Sigma^+, v', N')$$

$$CN^*(B, v', N') \rightarrow CN(X, v'', N'') + h\upsilon \text{ (observed)}.$$

---

* NAS/NRC Postdoctoral Associate presently at GSFC.

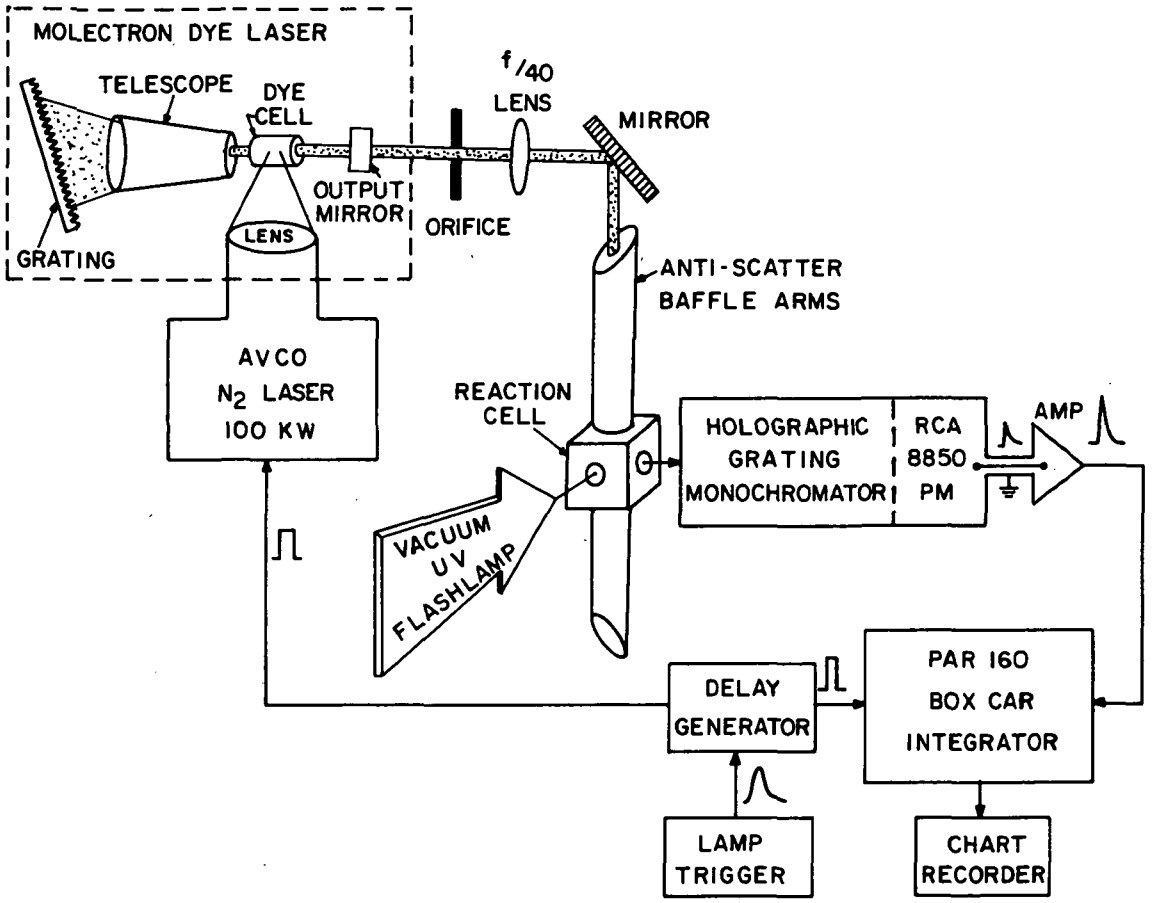

Figure 1. Diagram of Experimental Apparatus

Figure 2 shows two spectra taken for the photodissociation of cyanogen (C_2N_2). The spectral resolution is ~0.01 nm and is determined by the characteristics of the dye laser.

The LIPS method has been used to measure the radiative lifetimes of the individual rotational levels in the zeroth vibrational level of the B state of CN.[1] Using photon-counting, the decay of rotational line intensities was measured after laser excitation. A radiative lifetime of 65.6 ± 1.0 nsec was determined for the unperturbed levels, and the quenching cross-section of the B state by C_2N_2 was 41 ± 20 Å^2.

The energy partitioning between the CN radicals formed in the photodissociation of C_2N_2 was also studied. The spectrum at the top of Figure 2 is that of CN radicals which are newly formed in the X state and have suffered no more than a few collisions. The band-heads of both the 0-0 and the 1-1 bands are clearly visible which indicates rotational excitation. The lower spectrum was taken after the radicals had undergone several hundred collisions which are sufficient to thermalize the rotational levels. Analysis of the spectral line intensities by the following equation from Herzberg[2]

$$\ln\left[\frac{I_R}{\upsilon(N'+N''+1)}\right] \alpha \quad -E_R(N'') * \frac{hc}{kT_R}$$

yielded "effective" rotational temperatures (T_R) for the two lowest vibrational levels. The newly formed CN had rotational temperatures for the v''=0 level of ~1500°K and for the v''=1 level of ~950°K. The vibrational band intensity ratio, i.e. the vibration population

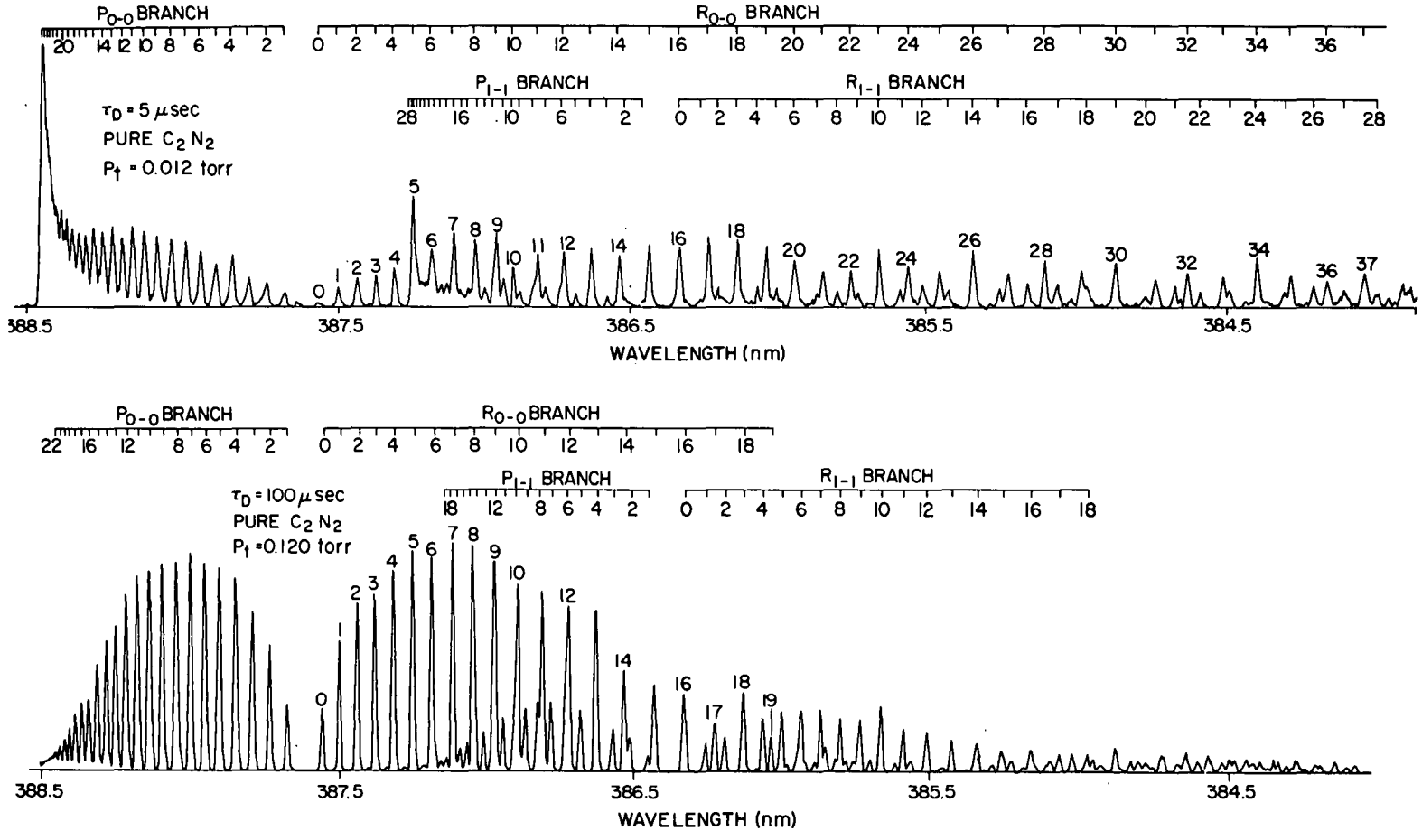

Figure 2. Spectra of CN Radicals Produced by Photodissociation of C_2N_2.

ratio, of the v"=0 to 1 levels is 2.3, which corresponds to an "effective" Boltzmann temperature of 3600°K.

The photodissociation of C_2N_2 occurs in its first strong absorption band between 150.0 and 170.0 nm above the cutoff of the sapphire window. At these photon energies there are two possible mechanisms: formation of the CN radicals (1) both in the X state or (2) one in the X and one in the A state. Results of indirect experiments indicate that the primary photochemical ratio of A to X is ~1, pointing to process (2) as predominant. When electronic, vibrational, and rotational excitation is accounted for, there remains ~ 0.67 ev of energy for translational excitation, i.e. a translational temperature of 2600°K for equal energy partitioning.

CN radicals formed in the photodissociation of dicyanoacetylene (NC-C≡C-CN) were also found to have vibrational and rotational excitation and probably translational as well. In comets if photodissociation is one of the sources of radicals, then similar rotational and translational excitation of the fragments could heat the cometary atmosphere.

REFERENCES

1. W. M. Jackson, J. Chem. Phys. 61, 4177 (1974).
2. G. Herzberg, "Molecular Spectra and Molecular Structure: Vol. I. Spectra of Diatomic Molecules", van Nostrand Reinhold Company (New York, 1950), p. 126.

THE NEUTRAL COMA OF COMETS: A REVIEW

A. H. Delsemme

I. INTRODUCTION

Most records of the first half billion years of the solar system have been wiped out from the planets and from their satellites by their evolution and their morphological differentiation. However, two sources of information seem still to be available on this early period: some meteorites give us clues on the non-volatile fraction that condensed from the primeval nebula, whereas the clues on a more volatile fraction, possibly condensed at a colder temperature, may come from the comets.

In order to study the chemical nature of this more volatile fraction, the best approach would probably be to send a space probe to a comet; waiting for this time to come, the study of the neutral coma probably is the next best approach. The study of the ion tail and of the nature of its source in the vicinity of the nucleus proposes another fascinating challenge but there, the number of unknown parameters is larger, because the ions' behavior depends also on electric and magnetic phenomena.

However, even the study of the neutral coma is not as simple as it looks, because most of the molecular processes are not yet quantitatively understood. The spectroscopy of the coma tells the story of that single step leading to the emission of light, usually a resonance-fluorescence, in a chain of several unobserved processes that we must reconstruct without enough clues.

II. PROCESSES WITHIN THE COMETARY COMA

The first step in this chain of processes is the vaporization of the nucleus, visualized as an icy conglomerate (Whipple 1950). The production rate of gas and dust is set by the vaporization rate of the nucleus

(Delsemme and Miller 1971a). The brightness law of the comet versus its heliocentric distance may be used as a crude indicator of the variation of the production rate of gas and dust; in particular, the heliocentric distance at which the coma appears, gives clues on the volatility of the snows and therefore, on their chemical nature; (Delsemme and Swings 1952); the production rates of the major constituents (like H and OH) confirm the existence of a vaporization equilibrium (Delsemme 1973a, Keller and Lillie 1975) and set the size of the nucleus as well as its albedo; (Delsemme and Rud 1973).

As the dust is dragged away by the vaporizing snows, the hydrodynamics of the gas drag provides a confirmation of the production rate of gas (Finson and Probstein 1968). Volatile grains like hail grains or snowflakes are also probably dragged away by the vaporizing gases (Delsemme and Wenger 1970, Delsemme and Miller 1970, 1971a and b).

The gas production rates are such that molecular collisions take place only in a small region surrounding the nucleus, of the order of 10^3 to 10^4 km at 1 A.U. (Delsemme 1966). The existence of this region has been confirmed by the pressure-induced changes in the fluorescence equilibrium of CN (Malaise 1970). Outside of this nuclear region, the gases are steadily lost in space by a collisionless effusion in vacuum, and each individual molecule interacts only with the flux of solar photons and of the solar wind, which is going to dissociate or ionize them, depending on their individual cross-sections.

The dissociations take place for wavelengths that are shorter than a threshold set by the binding energy of the bond to be broken: most of them are in the ultraviolet. In the same way, most of the ionization energies correspond to the extreme ultraviolet. The ultraviolet end of the solar spectrum is now rather well known; it is rather constant in the range where there is much energy available (from 4000Å to 1400Å). At lower wavelengths,

the variability of Lyman α and of the other emission lines introduces some uncertainty.

With due consideration to these variations, the solar flux can be used to predict the lifetimes of the possible parent molecules against photo-dissociation and photo-ionization. However, none of these parent molecules were known until recently; only their dissociation or ionization products. (As discussed in detail later on, the situation has suddenly changed with the discovery of H_2O, HCN and CH_3CN in comets Kohoutek and Bradfield). But the early comparison of the predicted and observed lifetimes (Potter and Del Duca 1964) had not brought about any positive identification. As a matter of fact, the "observed" lifetimes never are really observed; they are deduced by dividing the observed scale length by the assumed mean velocity of the molecules; this velocity is probably known by and large within a factor of two.

However, the fact that identifications remain difficult in most cases suggests that we have neglected a possible source of dissociation. The primary agent that we have neglected so far is the solar wind; but dissociations by charge-exchange collisions with protons or electrons leading finally to neutral molecules, are less likely than straightforward ionizations, although some are possible through a chain of several steps. Many of them are poorly known, but some have been studied (Cherednichenko 1965). The probably existence of a shock wave in the flow of the solar wind, ahead of the comet (Alfvén 1957, Biermann et al. 1967), changes the energy of those protons and electrons that are going to reach the vicinity of the nucleus, and may therefore affect their charge-exchange process with the parent molecules. These phenomena are less quantitively understood than the flux of solar photons because they are more complex. Explaining quantitatively the production rates of the ions observed in the tail meets the same difficulty for the same reasons.

Whatever the dissociation or ionization mechanism, when a radical has been produced that can be excited by the solar light, we observe its bands in emission in the cometary spectra. We usually can explain their intensities by a fluorescence mechanism, by taking into account the accurate flux of photons available in the solar spectrum at all those wavelengths that are needed for the excitation, properly corrected for the radial velocity of the comet. We have even enough high-dispersion spectra to try to explain minute differences in terms of collisional effects in the vicinity of the nucleus (Malaise 1970) or radial velocity differences from different parts of the coma (Greenstein 1958).

The only known exception is the 6300Å red line of forbidden oxygen, that had to be explained by another mechanism, (Biermann and Trefftz 1964) its excitation stemming from the dissociation of its parent molecules, and not directly from the solar light.

The decays of the observed radicals can be assessed from their photometric profiles. We have not yet succeeded in explaining all of them quantitatively, but at least we believe that we understand them qualitatively, as being further dissociated or ionized by the solar light and/or by the solar wind.

The major problem that we were facing, before Comet Kohoutek, was therefore the identification of the parent molecules, in order to bridge the gap between the vaporization of the nucleus and the presence of neutral and ionized radicals in the coma and in the tail.

III. THE IDENTIFICATION OF THE MAJOR CONSTITUENTS

Circumstantial evidence suggested that water was controlling the vaporizations (Delsemme 1973b) but no neutral parent molecule had ever been

positively identified. After comets Kohoutek and Bradfield, three of them have been found, namely H_2O (Jackson, Clark and Donn 1974, in Bradfield), HCN and CH_3CN (Ulich and Conklin (1973), Snyder, Buhl and Huebner (1974) in Kohoutek), without mentioning the spectacular identification of the H_2O^+ ion in comet Kohoutek (Herzberg and Lew 1974).

The list of the atoms or molecules that have now been observed in comets is given in Table I. There is not much doubt left that H_2O is the parent molecule which explains the bulk of H and OH, (although minor contributions to H and OH are still possible from the photodissociation of minor constituents); whereas the molecular bands of H_2O^+ do not show the bulk of water. From the photo-ionization and photo-ionization thresholds of water, which are 12.62 and 5.114 eV respectively (Herzberg 1966) some 99.9% of H_2O should photodissociate whereas some 0.1% should photo-ionize into H_2O^+, although ionization by the solar wind could multiply the share of H_2O^+ by more than one order of magnitude (Cherednichenko 1965).

However, the most significant discovery, whose importance has not yet been properly assessed, is probably the identification of the resonance lines of carbon and oxygen, in the far ultraviolet spectrum by two Aerobee rockets (Feldman et al., 1974; Opal et al., 1974). The C line at 1657Å is approximately four times stronger than the O line at 1304Å. The number of solar photons available is approximately 10 times as large at 1657Å as at 1304Å. Taking transition probabilities and lifetimes into account, Feldman et al. think that the production rate of carbon could be of the order of 0.24 that of oxygen. Assuming that all molecules containing carbon and oxygen are finally dissociated into their elements, we probably detect the total ratio of C/O of the volatile fraction lost by vaporization.

Table 1

atoms	radicals	stable molecules	
		neutral	ionized
H, O	OH, OH^+	H_2O	H_2O^+
C	C_2, C_3, CH, CH^+		CO^+ CO_2^+
	CN, NH, NH_2	HCN, CH_3CN	N_2^+
metals			

The first results coupled with the production of hydrogen seem to suggest a H/O ratio between 2 and 3,and leave little leeway outside a production rate of CO or CO_2, possibly of the same order of magnitude as, although probably somewhat smaller than that of water. As comet Kohoutek's orbital data suggest that it is likely to be a "new" comet in Oort's sense, these results should certainly not be extrapolated to older comets, that might have lost most of their CO or CO_2 excess during earlier passages through the solar system. Another factor casts some doubt on these preliminary results: in order to deduce how many fluorescence cycles take place during the lifetime of the atoms against ionization, that is, the number of photons emitted per atom produced, the lifetimes of the C and O atoms in the solar field were needed. No actual measurements were available and therefore, the lifetimes used are theoretical assessments. The present writer submits that one of the most important measurements to be done on future comets is the establishment of the brightness profile of the resonance lines of C and O (and possibly N which has not yet been observed), in order to check the actual lifetimes of these atoms, against all actual sources of ionization in the solar field. Waiting for new bright comets to be observed from space, a reassessment of the ionization lifetimes of C, N and O, using the most recent solar data being obtained by the Naval Research Laboratory, seems to be in order in the near future.

IV. THE BRIGHTNESS PROFILES OF THE NEUTRAL COMA

The brightness profiles of the neutral coma, observed in the monochromatic light of the different radicals or atoms, also remain one of the principal clues for the understanding of the nuclear region. The importance of the brightness profiles stems from the fact that in a first approximation, isophotes

of neutral radicals are always circular. Barring rare cataclysmic events, as mentioned by F. Miller (1957), the observed departures from circularity seem to be second-order phenomena that are rather well understood. In particular, a slight distortion coming from the light pressure of the sun is easy to discount. The single feature then to be explained is the average brightness profile itself, that is, the law of variation of the monochromatic brightness with radial distance from the nucleus.

The actual profiles observed, sometimes show humps or distortions that probably come from violent variations in the instantaneous production rate of gas in the nucleus. These variations probably come from corresponding fluctuations in the solar wind or in the ultraviolet flux emitted by the sun (flares), but they have never been explained quantitatively. The light curve in global light also reflects this type of variations, usually referred to as the "activity" of the comet, (whatever that means). However, there often are long periods where the activity of the comet is at a minimum, and where the brightness profiles show a smooth and regular curve (as in figure 1). There is little doubt that the outside drop of the curve, for values exceeding 10^5 km, can be interpreted in terms of the exponential decay of the light emitters into unobservable species (Delsemme and Moreau 1973). However, the production of the light emitters from unobserved species takes place in a range of the order of 10^4 km, and the length of the profile in this region is not large enough to provide a criterion in order to distinguish between different models. For instance, based on Wurm's (1943) ideas, Haser's (1957) model uses an exponential decay for the parent molecules. Malaise (1966) introduces two decays to take into account the possibility of a chain of two processes: unobservable grandparent molecules decaying into unobservable parent molecules. Based on Delsemme's (1968) ideas about a halo

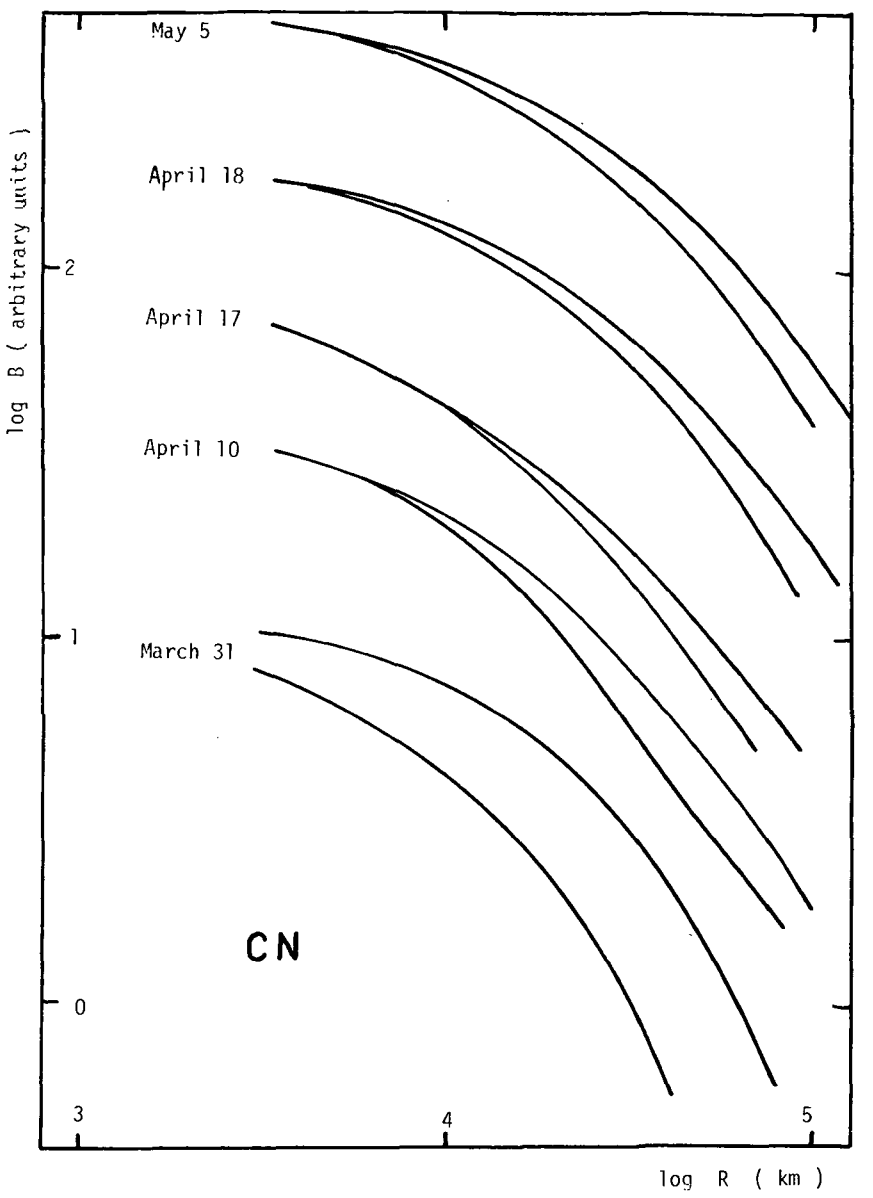

Figure 1. Example of Brightness Profiles in the monochromatic light of CN(0-0) observed in the coma of Comet Bennett (1970 II). B is the brightness in arbitrary units, R is the distance from the nucleus in kilometers; s and a label the sunward and anti-sunward profiles, respectively. The profiles have been shifted vertically from date to date, in order to avoid their superposition, (from Delsemme and Moreau, 1973).

of ice grains surrounding the nucleus, Delsemme and Miller (1971) develop a model based on the linear decay of the ice grains by vaporization. None of these models changes the theoretical profiles of the production zone, enough to allow a direct observational test. Similarly, a model assuming random velocity vectors for the radicals, instead of the oversimplified assumption of a radial velocity vector, in Haser's model, does not change appreciably the profile of the production zone (Delsemme and Miller 1971b).

Of course, the probable existence of a halo of ice grains, acting as an extended source, is based on another evidence (Delsemme and Miller 1971b). Indeed it links the photometric profiles of C_2 and of the continuum in Comet Burnham (1960 II). This halo seems to have also been observed by its emission at 3.71 cm wavelength, in Comet Kohoutek (Hobbs, et al. 1975).

However, in doubt on the best theoretical profile to be used in order to fit the observations, it is clear that it does not make any harm to use Haser's model for obtaining two parameters: an exponential scale length (near 10^5 km) describing the simple decay of the observed radicals, and another exponential scale length (near 10^4 km) describing by one single parameter the extension of the probably more complex source function of the same radicals; this simple parameter sets the size of the zone produced by the possible existence of the parents, grandparents, halo of ice grains, and all unknown phenomena of the nuclear region.

V. VARIATION OF THE SCALE LENGTHS WITH HELIOCENTRIC DISTANCE

The previous discussion justifies the systematic use of Haser's model in order to describe the brightness profiles in terms of two parameters only: the exponential scale length of the light emitter (against decay) and an exponential scale length giving the scale of the source of these light

emitters (possibly from an unobservable parent molecule, but also possibly scaling the largest of the other phenomena that may influence the size of the source, like the existence of a halo of ice grains).

However, different observers have either published photometric data without interpretation, or used different models to interpret their data. For this reason, the present writer has computed an homogeneous reduction of all the brightness profiles available in the literature, by systematically using Haser's model. The details of this reduction will be published elsewhere. It was based on 12 brightness profiles of CN from 7 different comets, and on 14 brightness profiles of C_2 from 8 different comets. The results (Delsemme 1975) are consistent with the following formula:

$$\log s\ (CN) = 5.17 \pm 0.04 + 2 \log r$$

$$\log s\ (C_2) = 4.82 \pm 0.06 + 2 \log r$$

$$\log s\ (\text{CN parent}) = 4.12 \pm 0.09 + \log r$$

$$\text{los s } (C_2 \text{ parent}) = 3.99 \pm 0.20 + \log r$$

where s is the scale length in kilometers and r the heliocentric distance in astronomical units.

These results deduced from all published data, confirm rather well the previous findings of Delsemme and Moreau (1973) on Comet Bennett. In particular, it is clear that the decay of CN as well as that of C_2 both depend on a square law of the distance to the sun, which is consistent with the usual assumption that the decay of CN and that of C_2 are both triggered by the solar flux.

Delsemme and Moreau had also found that the two scale lengths of the parents both vary less quickly than the square law, and were consistent with a proportional dependence on r. This law is inconsistent with a photodissociation of the parent into either CN or C_2, whereas the law is predicted

by the theory of the halo of ice grains.

However, despite the fact that all data available in the literature rather confirm these findings, it is proper to be very cautious here, because half of the data are based on poor resolving powers.

If the seeing disk is large, it may simulate a spurious scale length; the seeing disk, projected to the comet's distance, would give a "scale length" in proportion to the geocentric distance Δ, which for faraway comets would not be statistically very different from the heliocentric distance r. A careful discussion rejecting all the poor resolving powers, and keeping the best space resolutions only, still definitely rejects a square law and suggests a dependence on distance which is no more than a proportional law, or possibly even less, for the size of the source of C_2 as well as of CN (Delsemme 1975).

In urgent need of an estimate for OH, the present writer has recently used (Delsemme 1973c) an unpublished brightness profile established by Malaise from a spectrum of Comet Burnham (1960 II) published by Dossin et al. (1964). The range of the tracing was too short, therefore the inaccuracy was large. Fortunately, two better determinations of the scale length of OH have been obtained recently.

Here they are, reduced for 1 A.U. (the scale length s is in kilometers):

log s (OH) = 5.1 ± 0.2 (c. Kohoutek, Blamont & Festou 1974).

log s (OH) = 5.2 ± 0.2 (c. Bennett, Keller & Lillie 1974).

When this average value is used to interpret comet Burnham's profile, then the best fit is obtained with log s (OH parent) = 5.0 (reduced at 1 A.U.); this is consistent with the identification of the parent with water. This has also been verified for comets Bennett (Keller and Lillie, 1975) and Kohoutek (Blamont et al. 1975).

A profile of the [OI] red line was measured by Moreau (1972) at the request of the present writer. No deviation of the inverse law of the distance was detected up to almost 10^5 km, where the red line intensity merged into that of the atmospheric night glow. This suggests a scale length larger than 10^5 km.

It is unfortunate that no good scale lengths have ever been published for the other radicals, although some indications on their order of magnitude for C_3 and CH can be deduced from Malaise's (1966) photometric profiles of comets Burnham and Ikeya.

VI. PRODUCTION LAWS AND BRIGHTNESS LAWS

The production law is the law of dependence on heliocentric distance, of the production rate of a given molecule.

The brightness law, in the monochromatic light of a given molecule, is the law of dependence on distance of the integrated light emitted by these molecules within the coma, during their lifetime, that is after their production and before their dissociation.

Levin (1943) pointed out that the two laws must be the same, because the solar flux (which excites the fluorescence of the molecules) varies with r^{-2}, whereas the lifetime of the molecules varies with r^2 (r heliocentric distance).

Of course the variation of the lifetime extends the coma for larger heliocentric distances and the previous statement is therefore true only if we integrate the total light of the coma from the nucleus to infinity. What does this mean in practice?

The writer (Delsemme 1973c) has shown that the two laws remain the same, only if we integrate the light to a distance of at least 7 to 8 times the largest of the two scale lengths of the brightness profile. If

the integration is limited by a diaphragm smaller than this limit, if the production law is $P = P_0 r^{-n}$, then the brightness law is $B = B_0 r^{-n-\alpha}$, where α is the correction to add up to the exponent of the brightness law in order to obtain the true exponent n of the production law.

The correction α is given by Delsemme (1973c) as a function of the diaphragm radius, expressed in scale length units, with the ratio of the two scale lengths as a second parameter. This correction α varies from zero (for very large diaphragms) to an upper limit of +3.6 for diaphragms much smaller than the two scale lengths.

A consequence explaining the poor significance of the cometary light curves in global light must be mentioned first. As the reflection of the solar light by the dust makes all things even more complex, we will have to consider only the case of the non-dusty comets in order to make our point. In this case, CN + C_2 usually prevails in visible light. However, it can be seen that the light curve expressed in magnitudes as a function of the logarithm of the heliocentric distance, usually has a slope larger than the average production law of CN + C_2, for the following reason: only the center of the coma can be distinguished from the sky, therefore the sky brightness plays the role of an effective diaphragm. The fainter the comet, the smaller this effective diaphragm, and the larger the correction α to the slope of the light curve in order to establish the production law. The average production law of CN + C_2 cannot therefore be accurately deduced from the light curve. However, as $0 \leq \alpha \leq 3.6$, upper and lower limits of the exponent of the instantaneous production law can be deduced. In particular, it can be established that for large heliocentric distances, the exponent of the production law is often much larger than 2, because α cannot grow larger than 3.6, whereas $n + \alpha$ often is $>> 6$.

Standing in contrast, observations of the monochromatic brightness law, in the light of a given radical, can now be used to establish its production law, when the diaphgram used for the observations is known.

For instance, Mayer and O'Dell's (1968) observations of Comet Rudnicki can now be used for this purpose. As they were obtained with a rectangular slot of 509" x 203", the α for circular diaphragms cannot be used readily, but the present writer (Delsemme 1975) has established that, although the apparent brightness laws of CN, C_2 and C_3 are very different, their exponents are brought in the same general range, when the three corrections α are taken into account. This suggests a single production law for the three molecules, its exponent being $n = 3.6 \pm 0.2$. (The value of this exponent could be lowered somewhat if the contribution of the continuum has not been properly taken into account).

A more recent example is given by the monochromatic brightness laws observed by Code (1970) with the OAO for the hydroxyl and the hydrogen comas. Here, as $(n + \alpha) = 5.9$ for both OH and H, Delsemme (1973c) deduced $n(OH) = 2.9 \pm 0.2$ and $n(H) \geq 2.8 \pm 0.2$. Here the sign $\geq$ suggests that the neglected, but growing optical depth in Lyman α, when the comet approaches the sun, may hide a larger and larger fraction of the production rate.

Using the more recent value of the scale length of OH quoted in the previous section, a revised value $n(OH) = 2.0 \pm 0.2$ is obtained. This new value removes the apparent excellent agreement of the two production laws previously given for H and OH, although the accuracy of the results is unlikely to be good enough for the observations to become inconsistent with a single production law.

Bertaux et al. (1973) report a production law of H for Comet Bennett which is consistent with $n = 2.5 \pm 0.5$; whereas Keller (1973) finds $1.0 \leq n \leq 2.2$ from the same OGO-5 data. From the OAO-2 observations of the same comet, Keller and Lillie (1975) find $n = 2.3$ for the two production laws of H and OH. This recent determination seems to merit a much larger weight than that from the OGO-5 data.

Now, Delsemme (1973c) has stressed that if n is definitely larger than 2, then the vaporization temperature of the snows cannot be much lower than 200°K. The reason is that at steady state, the radiative term of the energy balance equation is not negligible, compared with the vaporization term, otherwise the vaporization would follow a strict inverse-square law of the heliocentric distance.

Such a high temperature of vaporization rules out all snows of gases more volatile than water, and in particular CO_2, CO, CH_4, NH_3, etc. Of course this does not rule out the solid hydrates of gases whose vaporization temperature is practically that of water. It does not rule out either other materials less volatile than water, but the production rates of OH and H seem to confirm that water is indeed the major constituent that controlled the vaporization, at least in comets Tago-Sato-Kosaka and Bennett.

The accurate value of n can be predicted by the theory, but it still depends on the ratio of the visible albedo of the nucleus to the infrared albedo near 15 microns; and it is also a function of the heliocentric distance. There is however little doubt now that water controls the vaporization. In particular, Delsemme and Rud (1973) have listed eight different arguments in support of this fact. More recently the discovery of H_2O in comet Bradfield and the identification of H_2O^+ in comet Kohoutek, both already mentioned in section III, have much strengthened their argumentation.

If the gas released by the nucleus is indeed a vaporization phenomenon, then the kinetic theory of gases gives the production rate per unit area per second, and if the size of the nucleus were known, we could predict quantitatively the observed production rates (Delsemme and Miller 1971a).

The production rates of different radicals have also been reported in the past, but most of them are obviously minor constituents, when compared with H and OH, therefore they can be neglected in the assessment of total production rates. Production rates have been reported for H or OH for comets Tago-Sato-Kosaka, Bennett and Encke. Preliminary values are known for Kohoutek. A list of the early assessments can be found in Delsemme and Rud (1973). A more recent result is found in Keller and Lillie (1975). These authors obtain for comet Bennett, reduced at 1 A.U.: 3.0×10^{29} molecules OH per sec, and 5.4×10^{29} atoms H per sec. In order to check numerically the theory of vaporization, the albedos of the nuclear snows are needed.

Delsemme and Rud (1973) have tried to disentangle the albedo A and the cross sectional area S of the nucleus, by using two determinations of AS and (1-A)S for three different comets. AS is given by the reflected light, from Roemer's assessments of the magnitude of the nucleus at large heliocentric distances; (1-A) is given by the energy absorbed in order to vaporize the observed rates of H and OH, assuming they come from water. The albedos deduced for comets Bennett and Tago-Sato-Kosaka are both very near 0.6 which is a rather high value, although consistent with a moderately dirty snow. The use of Roemer's magnitudes depends on whether they really are nuclear magnitudes, as correctly criticized by Sekanina. If a fraction of the light still coming from the coma has been included into the magnitudes used, the albedos could be diminished to 0.5 easily, but to 0.4 with great difficulty.

It appears therefore that the vaporization theory is consistent with the numerical values obtained for the production rates of H and OH, the albedos and the cross sectional area of the nucleus, for comets Bennett and Tago-Sato-Kosaka. Standing in contrast, the numerical values obtained for the production rate of H in comet Encke is not consistent with a nucleus totally covered by water snow.

VII. CONCLUSION

A very significant progress in our understanding of the production of gases by the cometary nucleus, has been brought about by the observation of the recent bright comets (Tago-Sato-Kosaka, Bennett, Encke, Kohoutek and Bradfield); and in particular, by their observations from space and by radio telescopes.

The hypothesis that water snow controls the vaporization of the nucleus of the first two comets seems verified from the general order of magnitude of the size of their nucleus and of their nuclear albedo; the largest observed production rates are H and OH which both seem to originate from the photodissociation of H_2O, as also confirmed by the scale length of the invisible parent molecule producing OH. Some of the production laws are still inconclusive, but all seem to be consistent with water, whereas some of the results seem to be totally inconsistent with any of the more volatile gases. However Comet Encke is not uniformly covered by water snow, as it produces only one tenth of the expected vaporization. Early results on comet Kohoutek suggest that the conclusions could be slightly different for some of the "new" comets in Oort's sense. If the far ultraviolet observations confirm the early assessments of the production rates of C, O and H, from their far-ultraviolet resonance lines, then at least another major constituent

competing with water has not yet been detected. Such a major constituent is suggested by the ratios C/O = 0.24 and H/O = 2.5; these ratios are probably known only within a factor of two. However, we have for the first time a suggestion of a possible redox ratio that prevailed in the cometary stuff when it was condensed from the primeval solar nebula.

NSF Grant GP 39259 is gratefully acknowledged.

REFERENCES

Alfvén, H. 1957, Tellus, 9, 92.

Bertaux, J. L., Blamont, J. E., Festou, M. 1973, Astron. Astrophys. 25, 415.

Blamont, J., Festou, M. 1974, C. R. Acad. Sci. Paris, 278, Serie B, 479.

Biermann, L., Trefftz, E. 1964, Z. Astrophys. 59, 1.

Cherednichenko, V. I. 1965a,b, in "Physics of Comets and Meteors," p. 25, and 31. V. P. Konopleva, edit. translation from Russian publ. NASA-TTF-340.

Code, A. D. 1970, I.A.U. Transact. 14B, 124.

Delsemme, A. H. 1966, Soc. Roy. Sci. Liege, 12, 77 (also Coll. Internat. Astrophys. 13, 77 (1965).

Delsemme, A. H. 1968, in "Extraterrestrial Matter," p. 304 (proceedings Argone Conference, March 1968), edit. Ch.A. Randall, publ. Northern Illinois Univ. 1969.

Delsemme, A. H. 1973a, "On the Origin of the Solar System," Nice 1972, p. 305, edit. H. Reeves; publish. CNRS, Paris.

Delsemme, A. H. 1973b, Space Sci. Rev. 15, 89.

Delsemme, A. H. 1973c, Astrophys. Letters, 14, 163.

Delsemme, A. H. 1975, (in preparation).

Delsemme, A. H., Miller, D. 1970, Planet. Space Sci. 18, 717.

Delsemme, A. H., Moreau, J. L. 1973, Astrophys. Letters 14, 181.

Delsemme, A. H., Wenger, A. 1970, Planet. Space Sci. 18, 709.

Delsemme, A. H., Miller, D. 1971a and b, Planet. Space Sci. 19, 1229 and 1259.

Delsemme, A. H., Rud. D. A. 1973, Astron. Astrophys. 28, 1.

Delsemme, A. H., Swings, P. 1952, Ann. Astrophys. 15, 1.

Feldman, P. D., Tanacs, P. Z., Fastie, W. G., Donn, B. 1974, Science 185, 705.

Finson, M. L., Probstein, R. F. 1968, Astrophys. J. 154, 327 and 353.

Greenstein, J. L. 1958, Astrophys. J. 128, 106.

Haser, L. 1957, Bull. Acad. Roy. Belgique, Cl. Sci, 43, 740.

Herzberg, G. 1966, Molecular Spectra and Molecular Structure III, p. 585, publ. Van Nostrand, New York.

Herzberg, G. and Lew, H., 1974, Astron. Astrophys. 31, 123.

Hobbs, R. W., Maran, S. P., Brandt, J. C., Webster, W. J., Krishna Swami, K. S. 1975, Astrophys. J. (in press).

Jackson, W. M., Clark, T., Donn, B. 1974, IAU Circular 2674.

Keller, H. U. 1973, Astron. Astrophys. 27, 51.

Keller, H. U., Lillie, C.F. 1975, Astron. Astrophys. (in press).

Levin, B. J. 1943, Astron. Zhu. 21, 48.

Malaise, D. 1966, Nature and Origin of Comets, p. 199, edit. Univ. Liege. (International Colloquium, Liege 1965).

Malaise, D. J. 1970, Astron. Astrophys., 5, 209.

Mayer, P., O'Dell, C. R. 1968, Astrophys. J. 153, 951.

Moreau, J. L. 1972, "A Study of Photometric Profiles in Comet Bennett," Master's Thesis, The University of Toledo, Toledo, Ohio.

Miller, F. D. 1957, Publ. Astron. Soc. Pacific 69, 82.

Opal, C. B., Carruthers, G. R., Prinz, D. K., Meier, R. R. 1974, Science 185, 702.

Potter, A. E., DelDuca, B. 1964, Icarus 3, 103.

Snyder, L., Buhl, D., Huebner, W. 1974, IAU Circular 2616.

Ulich, B. L., Conklin, B. K. 1973, IAU Circular 2607.

Whipple, F. L. 1950, Astrophysical J. 111, 375.

Wurm, K. 1943, Mitt. Hamburger Sternw. 8, 51.

DISCUSSION

W. Jackson: I'd like to make a few comments about Professor Delsemme's talk.

The velocity of the daughter may be much greater than the velocity of the parent so that determination of the lifetime of parent from photometric profiles may be extremely difficult. For example the energy of the parent, if it is moving at 1 km/sec, is 0.1 eV and the daughter may carry away a much higher energy than this. The result is that the velocity vector of the daughter is much greater than the velocity vector of the parent and more isotropic. The net result is that the flow of the daughter is now determined by its recoil velocity.

A. H. Delsemme: It doesn't bring any difficulty in fitting the photometric profile because we don't find the life times. The photometric profile gives two scale lengths—but later on, when you want to deduce from these lengths the lifetimes, you may be in trouble. But this does not bring any difficulty in the fitting of the profiles in order to assess two scale lengths.

W. Jackson: But the point is to get the lifetime. You may run into a quite a bit of difficulty, and it's likely that in some cases there will be a large amount of translational energy.

The other thing that you mentioned—I do have the lifetime of HCN. The lifetime of HCN determined by using Michael Berry's absorption coefficients and my solar fluxes, would be nine times 10^4 seconds—almost 10^5 seconds. The scale length for CN, which you gave, if I read your slide correctly, was the log of 4.1.

A. H. Delsemme: Your value is between the two values that I have in my slide, 4.1 for the CN parent and 5.2 for CN. But because of the symmetry of the expression one is not really sure which is which.

W. Jackson: Another lifetime that's much lower, if you need a lower parent—would be the lifetime for C_2N_2, which is 1.1 times 10^4 seconds, and that is very close to what you would like for the parent if the daughter is going to have the much longer lifetime.

The final thing is you put up acetylene as a possible source of C_2. Nobody has observed C_2 from acetylene, but supposing that you can get C_2 from the photodissociation of acetylene, the lifetime of acetylene at one A. U. is about 6 times 10^3 seconds, and that would be lower than any of the values that you have for beta.

A. H. Delsemme: I have not really proposed acetylene. I was listing the different possibilities as an example of our difficulties right now, and I was not, of course, using other considerations, as the spectroscopic evidence, for singlet or triplet states.

B. Donn: One thing that probably needs to be kept in mind, is that all of this analysis assumes that single observed species comes from a single parent molecule. Now when you have an array of parent molecules in a comet it's very likely that C_2 can come from a number of different molecules, and that means, then, that this interpretation becomes much more involved, but that is a characteristic of most of our cosmic problems. We don't have the nice, neat, simple features we have in the laboratory where you can relate things one to one.

M. Shimizu: I hope to present two evidences to endorse the presence of CO in cometary nuclei from the finding of comet C atom emission in UV region.

1. Dr. Jackson pointed out a difficulty of large dissociation time of CO. This is certainly important. Please see the paper of Ogawa (J. Mol. Spectr. 45 (1974) 454) on high resolution spectra of CO. He found many diffuse bands in 980-1030 Å region whose rotational analysis was completely impossible. CO could be predissociated at these bands.

2. Another information comes from Venus. Mariner 10 recently observed strong C emission on Venus. Since the composition of Venus' atmosphere is almost 100% CO_2, C might come from the dissociation of CO_2. The estimated value on the basis of such expectation is, however, more than one order of magnitude smaller than the observed one. Mariner 10 observed a strong OI 1304A line and the CO 4th positive bands. Consequently C atom appears to be formed by the dissociation of CO. In this case, too, the situation may be similar to the comet.

L. Biermann: The extent of those regions in the coma in which collisions are important is sometimes underestimated. With the gas production rates known now, for a bright comet we have approximately $10^{24}/r^2$ molecules/cm^3. For a cross-section of 10^{-15} cm^2 collisions are therefore important out to $\gtrsim 10^4$ km; for ion-molecule reactions these cross-sections are still larger (cf. L. Biermann and G. Diercksin, Origins of Life, 1974) and in consequence so is the extent of the region over which such reactions and dissociative recombinations play an important role. This of course effects also the plasma-dynamical process in the same region (cf. L. Biermann, paper in Asilomar Conference on Solar Wind, 1974, and H. U. Schmidt, review paper given at this Colloquium).

P. D. Feldman: This question of CO, which Jackson brought up on Tuesday and which Shimizu just addressed, I looked up some calculations that were made on the disassociation of CO for the Martian atmosphere by McElroy and McConnell.

They indicate that the branching ratio

$$\frac{CO + h\nu \rightarrow C + O}{CO + h\nu \rightarrow CO^+ + e} \approx 1$$

Therefore one expects roughly equal production rates of C and CO^+ from CO.

In other words, we expect to get a large number of CO^+ ions, as well as a large amount of carbon, and when I get around to presenting the paper later this morning, I'll show you how this can be tied in with the amount of carbon that was observed.

D. J. Malaise: In 1965 I made a model in which molecules were expelled from a source region with finite dimension, and then you had a chain of dissociation of one parent to the other, and we suppose that this is an observable one. And then I computed a profile.

This was ejected with a Maxwellian velocity, not with two-velocity component. And then you show the general result, which is well-known, that you get a profile with a production zone, an expansion zone with a gradient close to 1, and then a destruction zone. And whatever mechanism you invoke to produce the molecule, you always get this picture.

But in this formula, for sure, it is not symmetrical, so I don't know how Haser could get a symmetrical formula and -- well, I'm quite sure it is false, because you can prove it qualitatively here. If you had a lifetime of the mother molecule, and the lifetime of the observed radical if you change these two τ's, it is not symmetrical because you have a very short lifetime for the observed radical. So that what you observe essentially is the curve of the mother molecule alone.

So you will get this shape with the destruction of the mother, and on top of this you will be a little lower because of the destruction of the molecule you observed and -- well, this operates all along the curve, but you never get the characteristic slope here in the center. It seems to me quite clear that this has to be dissymmetrical

A. H. Delsemme: Malaise claims that Haser's formula is not symmetrical in respect to the two scale lengths. I disagree. Intuition does not help here. Apart from a factor which depends on the ratio of the scale lengths, and which only shifts the whole profile vertically when scale lengths are inverted, Haser's formula is totally symmetrical in respect to the two scale lengths. Malaise's statement that it is false that Haser's formula is symmetrical, is nonsense. The integration and its symmetry has been repeatedly checked at different times

and places by O'Dell, by Arpigny and by myself, and we all agree. The integration is trivial and Malaise can check for himself. But I know that at the first time I thought about it, I had the same reaction as you do. I thought it was impossible to explain it symmetrically. Now I am convinced that his integration is right.

(Discussion here about the term and interpretation of the expression for the profiles.)

A. H. Delsemme: Well, we disagree on this point, but it's a technical matter.

D. J. Malaise: I thought this could be settled.

A. H. Delsemme: I hope so.

(Laughter.)

B. Donn: There's a point that we're not going to be able to settle here, and it needs to be cleared up.

M. K. Wallis: You commented on Haser's model in saying that when you analyzed your profiles, they could be fitted fairly well - I think was your quote - fairly well to Haser's model.

Now, for the inner region there are various reasons we wouldn't be very confident on this exponential formula for the inner region. Professor Biermann has mentioned one, ion-molecular interactions and collisions are occurring. There may be others, like you, or Bill Jackson said, on the dissociation products of parent molecules having higher velocities, and so on.

So, one wouldn't expect Haser's model to be very good, anyway, in the inner region - inside 10^4 km. Can you not say - can we not say anything yet, or can we not provide another model - or find any important discrepancies - where it is clear that Haser's model is breaking down?

A. H. Delsemme: The fitting of theoretical curves and of the observational curves is not satisfactory anymore when we reach the region where the seeing is involved; the seeing disc, plus the convolution with the resolution of the photographic plate and the microphotometer entrance port, brings what I will call a confusion zone of the order of five arc seconds.

Within these five arc seconds the observational slope is flattened; therefore when the scale lengths are smaller than this confusion zone, not only we cannot

measure them, but we are not even sure of their existence. The scale lengths of the parent molecules may be changed or even totally hidden by the spurious scale length of the confusion zone. In my work with Moreau, we stop the fitting at this limit of 5 arc sec. We use the scale length of the parent molecule as a convenient parameter that usually improves very much the fitting of the curves, say from 5 to 20 arc sec.

H. U. Keller: I think the difficulty is not that we do get different profiles. The difficulty is just the principal interpretation of the inner part. Even if you have a very complicated process acting like a parent molecule, the profile won't be changed very much. The differences are very small, and I think they are too small to be detected by ground based observations even by accurate measurements. The discussion should be how so you reasonably explain the profiles in the inner part - what is the parent molecule or what are the processes possibly going on and how many parent molecules do we possibly have?

I think it is difficult to conclude in one way or the other on the parent molecules from those profiles which we have, whereas on the daughter molecules, it's much more certain, because the extension is larger.

In the case where the parent molecule definitely has a shorter lifetime than the daughter molecule, the total profile, itself, I am sure, won't be changed very much, even by a hydrodynamical model.

THE COMA: PANEL DISCUSSION

H. U. Keller

I would just like to make a brief summary of some of the major points in my review two days ago. The most important results from the cometary UV observations are: (1) We know now that the gas production rates of a medium bright comet is on the order of 10^{30} molecules s^{-1} based on hydrogen Lα observations and interpretations. (2) The large amounts of OH indicate that water is an abundant molecule. I do not know of any other probable parent molecule of OH. The case for water as a parent molecule is strengthened by the parallel decrease of OH and H in comet Bennett and by arguments given by Delsemme. (3) Disregarding the observed amounts of OH and O, one would not necessarily conclude that the hydrogen is a dissociation product of water. The uncertainty is due to the deduced outflow velocities of about 8 km s^{-1}. I feel this value for the velocity is pretty mysterious and not yet explained. We have yet to connect this velocity with the dissociation -- or formation -- producing the hydrogen atoms. The possibility that an appreciable amount of hydrogen does not stem from water cannot be excluded. (4) The UV observations of comet Kohoutek seem to indicate that water is not predominate over other molecules by two orders of magnitudes. The production of carbon atoms (and, therefore, of parent molecules containing carbon) seems to be nearly as great as that of water. The uncertainties of the numbers for the production rates are at least factors of two. I, personally, think it is too early to draw definite conclusions on the various abundance ratios. H, O, OH, and C may well be produced in the same

order of magnitude. But a C deficiency by an order of magnitude (or even more) is not rules out either.

We need observations of other bright comets to improve and confirm the results. I am sure we can then settle these questions and come up with firm conclusions. I do not have to stress the importance and implications of the abundance ratios for the nature of the cometary origin and development. (5) We also need improved models of the coma taking into account at least some of the complex formation processes in the inner coma, the excess dissociation energies, and the resulting velocity distributions.

THE COMA: PANEL DISCUSSION

D. Malaise

Well, I just said that I disagree with nearly all that was said in the review paper. Now I have to illustrate this point a little, so I will first write something on the board.

What we are looking for in the coma, in fact, is data about the nucleus because this is the only important part in comets, and the coma is something evanescent. So what we are trying to identify by observing the coma is essentially what I would call a "source function" - not a source. This function represents the intensity of the source in number of molecules of species M emitted per second in the direction α, ϕ and with the velocity v, per steradian and per unit velocity. It can be written : $I(t, \alpha, \phi, v, M)dtd\Omega dv$

Then, in order to identify and build up a good model of this source, we have just observation of a few fragments that we happen to see in the coma. And we just try to identify some characteristic of the source by making a model fitting. That means that we are putting a lot of ourselves, of our thought, of our dreams, between the observation and the result.

Starting from the nucleus, what we need first is hydrodynamics, then we need chemistry near the center with all the physical data which enter into it. And then we need what I would call physics when we are sufficiently far away from the center, and have to deal essentially with photo-dissociation and radiation pressure.

Now, this is an extremely complicated situation, the models on which conclusions are drawn concerning the source are utterly simple. Of course, science is not simply materializing your dreams ; it consists rather in solving contradictions.

And now I would like to illustrate some contradictions between the accepted picture and the observations. These are, by no means, exceptional cases; on the contrary, I hardly see any case that fits the simple image of photo-dissociation processes to build up the coma.

Fig. 1 is extracted from my early work (Malaise 1966). It shows the log-log diagrams of the photometric profiles of comet Burnham. Four radicals were observed on five nights. The night number and the corresponding heliocentric distance is indicated at the left of the figure. The plain lines are the profiles in the direction of the sun and the dashes are on the tail side. I have to point out here the distance scale : this comet passed very close to the earth (about .2 a.u.) so that the resolution was very good : 500 km for 1, 3 and 5 and 1000 km for 6 and 9. But we observe here only a very limited part of the inner coma, something between 1500 and 7000 km, that is well inside the production zone of the radicals.

If we consider the symmetry of the profiles, viz : the relative intensity of the sun and the tail sides, we notice large differences : CH is in general quite symmetric, CN is symmetric except on the first night; but C_2 and C_3 are very dissymmetrical and this dissymmetry varies rather fast. On the fifth night both C_2 and C_3 are 25% brighter on the sun side, while the next night both C_2 and C_3 are about 30% dimmer on the sun side. The relative variation of C_2 and C_3 is markedly parallel, while there is no correlation with the variations in the profiles of CN and CH. These large intensity variations are clearly due to variations in the number of radicals in the line of sight. This cannot of course be explained by a steady state model. It could be explained by a source whose strength, ejection velocity, angular distribution and composition (relative amount of species) varies with time. But of course it is not clear whether we have to trace back these observed variations all the way down to the source.

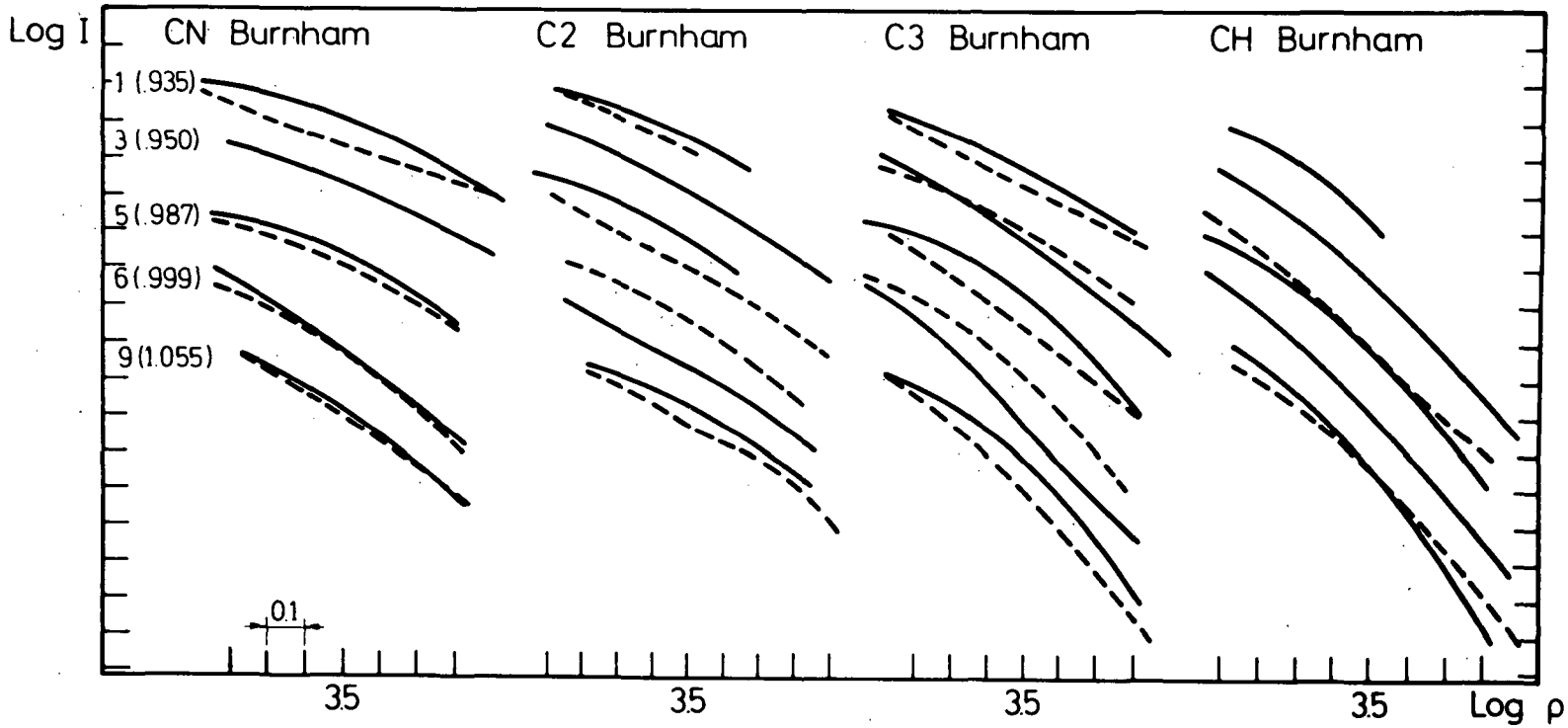

Figure 1 : Log-log photometric profiles of comet Burnham. Intensity in arbitrary units.

Another thing you may notice here is that the gradient, if you insist on finding a mean gradient in these curves, is rather constant with heliocentric distance for C_2 and CH, but for CN and C_3 it shows a trend towards increasing when the distance to the sun increases. This very fact, that you get a flatter profile when you approach the sun is at complete variance with any model where the production of the radical is by photodissociation with a source which has a constant strength. So this can be due either to the fact that we have wrong physics in the model or to the fact that we have the wrong source.

These are not small effects and I must stress that Burnham was a very quiet comet with no dust, faint tail and a nice symmetric amorphous coma.

Now I want to show you a more recent observation of profiles of Comet Bennett (fig. 2). These were done with a photo-electric photometer, six channel polychromator. That means that all six channels are taken at the same time, so that not only can I compare the bands within themselves, but the position of the bands with respect to each other are completely respected.

These are log-log graphs and you have the tail side of the comet on the top each time, and the sun side of the comet at the bottom. On the 6th the angle ψ between the radius vector and the photometric cut was 45° ; on the 9th ψ = 16° and on the 10th ψ = 17°. On the 10th the diaphragm had a diameter of 4000 km ; on the other dates it was twice as large. The ordinate scale is absolute: for the continuum it gives the intensity in ergs cm^{-2} s^{-1} A^{-1} $sterad^{-1}$ while for the bands the intensity is integrated over the band.

These are a few examples to illustrate further my point about the activity of the source : you see that the profiles are not symmetric and that practically we never observe

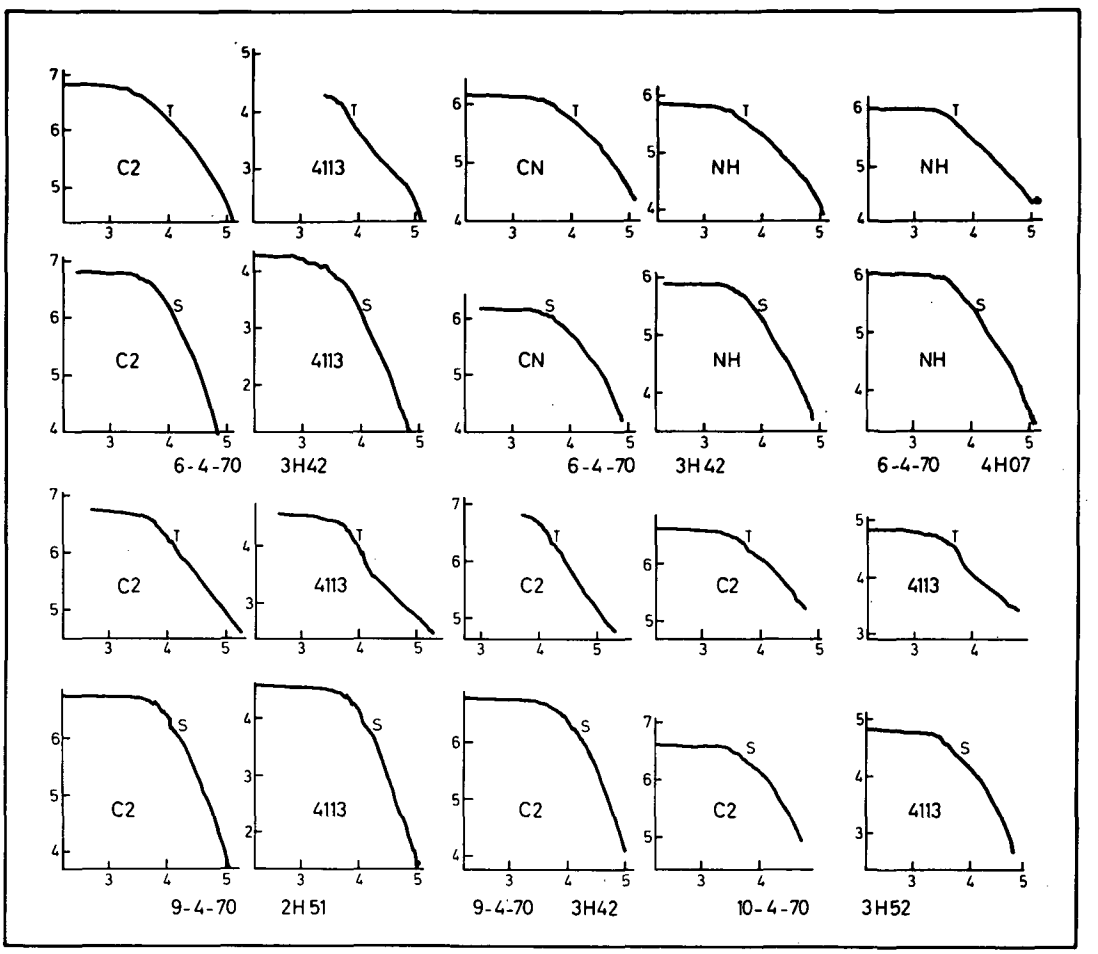

Figure 2 : Log-log photometric profiles of comet Bennett. Intensity in absolute units. T : tailward side, S : sunward side.

an expansion zone with a constant slope equal to - 1. In the model of photodissociation, this is typical for a ratio of lifetime which is not much smaller than 0.1. That means the lifetime of the parent and the lifetime of the observed radical are not more than one order of magnitude different. If we turn to the continuum, you see that on the tail side, the profile shows a typical concavity. This shape is given by no model based on a constant source of dust escaping at constant velocity : this always gives a kind of expansion zone which has a constant slope on a certain region, but the slope never increases. What we observe here, on the tail side is the formation of an envelope. On the sun side, the continuum has a steep nearly constant slope (- 3). This high gradient is also difficult to explain with a simple theory. If we compare the continuum on the 9th and on the 10th, we see that the envelope has shrunk on the tail side, but on the sun side we have now a profile typical of a molecule. This case is unique in our observations.

We notice also that the intensity of C_2 has slightly increased (1%) from the 9th at 2h.51 to the 9th at 3h.42 and then has dropped by 2.7% on the 10th at 3h.52. At the same time, the continuum has first increased by 5% on the 9th and then has kept the same value on the 10th. Observe also how the central intensity of NH varies on the 6th between 3h.42 and 4h.07 (25 min !) thereby changing completely the shape of the profile : no doubt that if one should try to deduce time of flight for these two profiles, the resulting values would have astonishingly different values which would certainly be related to nothing else other than the activity of the source. At any rate, we observe a highly variable behavior among these profiles. We nearly never observe an expansion zone in the three radicals, and when some part of the diagram has a constant slope, this slope is not 1 ; it is rather 1.25 or so and it varies from night to night. But any simple

model gives a slope equ 1 to 1.00 to the second decimal. The best one can suppose is that the intensity of the source varies with time. But if one supposes this (and one is lead to this assumption when one sees these observed profiles), all the conclusions about the time of flight and the scale length are becoming doubtful, because you can change a profile in any way, and you can simulate any time of flight just by varying the strength of the source with time.

Fig. 3 illustrates something I found with the six channel photometer. As I told you, I scan the head of the comet with a small diaphragm by scanning the telescope. Behind the diaphragm I have a concave grating and six exit slits for the bands. So the six channels correspond exactly to the same part of the comet and the displacement of the profiles with respect to each other are meaningful. The left part of fig. 3 shows the displacements of the center of luminosity of the bands for the different dates. Remember that the scans of the 6th were made at an angle of 45° while the others were made at 16 or 17° of the radius vector. The sun is to the left of the figure. You see that NH is always relatively displaced towards the sun ; the splitting of the continuum is not real ; it shows you the uncertainty in the displacements. CN and C_2 on the other hand are systematically displaced towards the tail.

The right part of fig. 3 gives more details about these displacements for the night of the 10th. Each curve corresponds to a different radical or to the continuum ; it represents the central point of the isophotes, so that the higher the point in ordinate, the brighter the isophote to which it corresponds and the lower part corresponds to low isophotes, that is to parts of the comet which are far away from the nucleus. The ordinate axis has been made to coïncide with the position of the center of luminosity of the continuum. The scale in thousand km is the distance of the corresponding isophote along each curve.

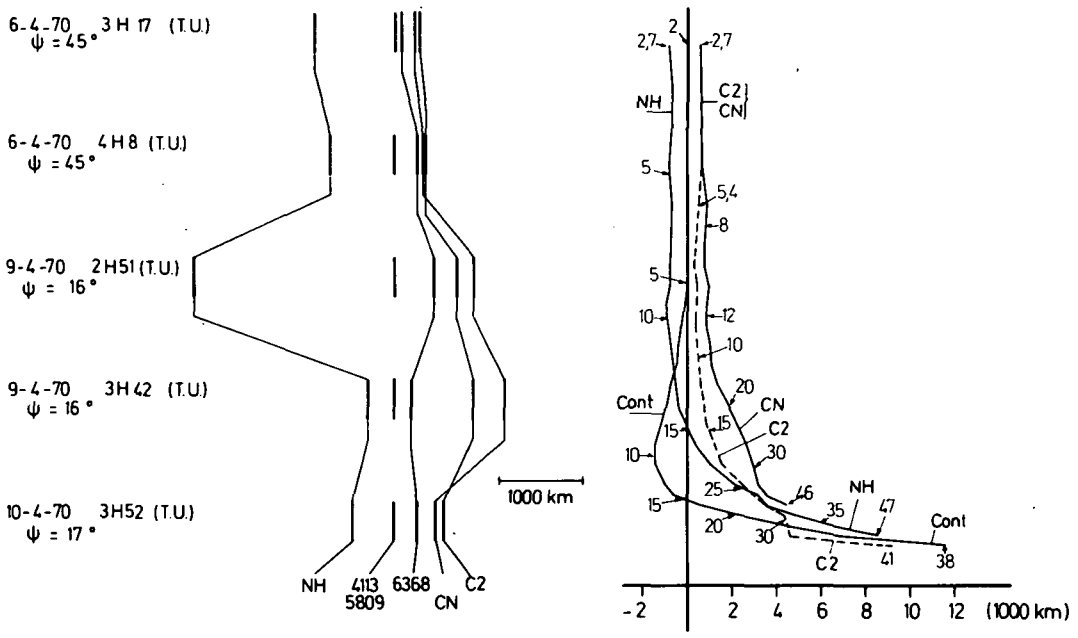

Figure 3 : a. (left) relative displacements of the center of luminosity of the radicals with respect to the continuum for comet Bennett.

b. (right) relative displacements for various isophotes (distance of isophote in thousand km indicated by arrows). Center of luminosity of the continuum has been taken as reference.

The top of the figure corresponds to the brightest part of the comet, near the center. One sees that as close as one comes to the source i.e. 2700 km for the radicals, there are displacements of the isophotes relative to the reference. For NH, this displacement is 800 km to the sun and for C_2 and CN it is 600 km to the tail. These displacements are constant to a distance of about 5000 km (C_2), 7000 km (CN) or 10.000 km (NH). Then the center of the isophote is slowly pushed back to the tail for the three radicals. Off hand, only the fourth model of Haser (Haser 1966) can account for this general behaviour. It consists of a lambertian source ejecting molecules in the direction of the sun with a velocity function which is gaussian about a mean speed v_o ; the molecules are pushed back by the radiation pressure and are finally destroyed by photodissociation or a similar process. Note that a maxwellian distribution of velocity would not fit since in this case the center of the lower isophotes is never pushed back to the tail. The gaussian case does not fit very well either since in this case an envelope is formed in the direction of the sun ; but it is possible that our profiles do not reach the envelope. In any case, if we take the initial velocity to be the same for the three radicals, we can compare the distance by which each radical has been repelled for the same isophote ; these distances should be roughly proportional to the acceleration. For the 24000km isophotes, these distances are 1890 km (CN), 2870 km (C_2) and 2950 km (NH). These figures do not fit the know values of the acceleration. At any rate, we have to infer from these observations and from the Haser model that the source coincides with the luminosity center of C_2 and CN or that it lies on the tail side of it. In the former case, the source of these two radicals should be isotrope (and not the source of dust and of NH). In the latter case, all sources should be lambertian-gaussian. In this case, it is noticeable that the displacement of the continuum is larger than that of C_2 and CN which means that the acceleration of the dust is much lower than that of the radicals.

The shape of the center of the isophotes for the dust is very special i.e. the position is constant between 2000 and 5000 km, then it is first displaced towards the sun to a maximum of 1450 km for the 10.000 km isophote ; thereafter it is swept back very rapidly to 11.500 km for the 47.000 km isophote. It is easy to see that this is related to the formation of an envelope on the tailside in the continuum, but no theory, to my knowledge, can account for this. Note also the large irregularity in the curve of C_2 and CN and the smaller one in NH.

These results are very preliminary and were given mainly to illustrate my point about the complexity of the source. I am now going to dwell on building models to try to extract as much information as possible from these profiles. My biggest frustration is that since this instrument has been in operation (1967) I have had in all less than ten hours of observing time on comets. This is due to the fact that to obtain good profiles, I need to work at the cassegrain focus of a large telescope (at least 2 m) and that the big observatories have their observing program planned six months or one year in advance. Anyhow, these observations show at the least that we have to be very careful when we speak about the symmetry of the profiles particularly when we try to fit the models.

R E F E R E N C E S

Malaise, D., 1966 XIII Coll. Liège, p. 199

Haser, L., 1966 XIII Coll. Liège, p. 233

DISCUSSION

F. L. Whipple: I mention the effect of "blanketing" and absorption near the nucleus only because it has not been mentioned so far in the discussion. Three results of several are worthy of mention here: (a) reduction in sublimation rate of the nucleus; (b) spatial effects on ionization and excitation phenomena; (c) opacity in the line-of-sight of observations. Blanketing and opacity may well account for some of Malaise's difficulties.

W. Jackson: In a paper published in ICARUS (Vol. 8, p. 270 (1968)), B. Donn and I tried to take into account the effect of optical depth on the center of luminosity of the observed radical emission. The figures in that paper are theoretical estimates for radicals and ions. In all cases there will be a displacement of the center of maximum radical density some 100 to 1000 km toward the sunward side.

Finally, I wonder if the coupling between C_2 and C_3 can be explained by the photodissociation of C_3 to yield C_2. e.g.

$$C_3 + h\nu \rightarrow C_2 + C$$

or possibly

$$R_1 C_3 H + h\nu \rightarrow R_1 + C_3 H$$

$$C_3 H + h\nu \rightarrow C_3$$

$$C_3 H + h\nu \rightarrow C_2 + CH$$

Z. Sekanina: Effects of opacity from the dust particles released following a massive outburst of gas are apparently responsible for a feature occasionally observed in tails and generally known as a "shadow of the nucleus." In some cases the screening of the nucleus might be so efficient that the vaporization from the surface virtually ceases for a while—until the surplus of particles in the atmosphere is dispersed out into space.

Voice: What was the time scale?

Z. Sekanina: That was a very short time scale. I guess it was five hours or something like that. And you simply have trouble to explain that by any other mechanism except by stopping the influx of the solar radiation to the surface.

I think this is a very effective mechanism.

A. H. Delsemme: Yes, I just wanted to mention that I had prepared a lengthy discussion on the different causes for departures of circularity of the isophotes. But I had no time to run through it in my short expose. I will submit it for publication on this occasion. I think that is the best way to handle it, because it was prepared but I didn't read it. It was too long.

But, of course, I am quite aware of all these difficulties and my discussion will cover not only the things which have been mentioned, but some other ones that have not been mentioned to date.

I would like to emphasize that Malaise's observations are very important because those are the only clues we have on the different positions of the different isophotes. We have theoretical reasons to believe that it should happen, and I am going to mention them in these notes.

But it is important to observe them. And I would like to encourage him to publish these data that were taken four years ago, in that I have already seen them two years ago in Liege.

GAS PHASE CHEMISTRY IN COMETS

M. Oppenheimer

Present theories for the formation of molecular species observed in comets predict the sublimation of parent molecules such as H_2O, CH_4, CO_2, and NH_3 from the surface of the nucleus and their subsequent photodissociation and ionization to form the observed species (Delsemme 1973). It can be shown (Oppenheimer 1975) that gas phase chemical reactions occur between these fragments which have characteristic timescales which are short compared to the timescale for significant variation in the solar flux incident on the comet. Hence, a steady-state approximation may be used for determining the densities of many species. It can also be shown (Oppenheimer 1975) that the rate of formation of many species is faster by gas phase reactions than by photoprocess. For instance, the formation of OH^+ from H_2O^+ by the reaction

$$H_2O^+ + O \rightarrow OH^+ + OH$$

with an estimated rate coefficient of 1×10^{-9} cm^3 s^{-1} proceeds more rapidly than by the process

$$H_2O^+ + h\nu \rightarrow OH^+ + H$$

if the density of atomic oxygen exceeds 10^4 cm^{-3} at heliocentric distance r = 1 AU. Hence, gas phase reactions

rapidly reshuffle parent molecules and their fragments in the coma.

The reaction sequence leading to the formation of H_2O illustrates the significance of gas phase reactions in determining the nuclear structure. Molecular hydrogen will form if the nucleus is composed of almost any hydrogen-bearing compound. If oxygen evolves from the nucleus in any form and is subsequently ionized, the reaction sequence

$$O^+ + H_2 \rightarrow OH^+ + H$$

$$OH^+ + H_2 \rightarrow H_2O^+ + H$$

$$H_2O^+ + H_2 \rightarrow H_3O^+ + H$$

$$H_3O^+ + e \rightarrow OH + H_2$$

$$\rightarrow H_2O + H$$

leads to the formation of the observed cometary species OH, OH^+, and H_2O^+ (Delsemme 1973; Wehinger et al. 1974) and H_2O (Jackson et al. 1974). Therefore, an observation of H_2O^+ and H_2O is not sufficient to indicate the composition of the nucleus. If n(i) is the density of constituent i and γ is the branching ratio between OH and H_2O formation from H_3O^+, we find at 0.6 au that

$$\frac{n(H_2O^+)}{n(H_2O)} = 3 \times 10^4/n(H_2)\gamma$$

if gas phase reactions determine the molecular densities, and

$$\frac{n(H_2O^+)}{n(H_2O)} = (n(e) + 10^{-3}n(H_2))^{-1}$$

if H_2O is sublimated from the nucleus and subsequently ionized.

Gas phase reaction sequences can be formulated which lead to substantial abundances of all molecular species observed in comets if all the necessary atoms are present in any molecular form in the nucleus (Oppenheimer 1975). However, we predict that little or no CH_4 and NH_3 form in the gas phase compared to radical fragments of these molecules.

Many of the reactions in our scheme are of the ion-molecule type and proceed at the gas kinetic rate. Others are of the neutral-neutral type and depend strongly on the particle temperatures. The rates of the latter reactions such as

$$H_2 + O \rightarrow OH + H$$

may be greatly enhanced if one of the reactants has excess kinetic or internal energy resulting from formation by photo-dissociation of a molecular parent. The energy of molecular fragments may also be enhanced if they are produced in strongly exothermic reactions.

Our conclusion is that the effects of gas phase chemical reactions must be considered in interpreting cometary spectra with regard to implications for the structure of the nucleus.

References

A.H. Delsemme 1973 Space Science Reviews 15, 89.

W.M. Jackson, T. Clark, B. Bonn 1974 I.A.U. Circ. No. 2674.

M. Oppenheimer 1975 Ap. J. 196, 251.

P.A. Wehinger, S. Wycoff, G.H. Herbig, G. Herzberg, and H. Lew 1974 Ap. J. (Letters) to be published.

DISCUSSION

A. H. Delsemme: At the 1965 Comet Colloquium in Liege, I showed that water vaporization leads to a large collisional zone within the inner coma that I called the "chemical" coma. As an illustration of what could happen in the chemical coma, I computed a simple-minded model using thermal equilibrium, and the absorption of the solar light by water as a source of heat. A water, methane plus ammonia coma model leads then to a surprisingly large amount of those parent molecules that are needed to explain the spectra. But the model succeeded in getting rid of the hydrogen excess, by using an unrealistically high temperature. It is unrealistic because the coma is not optically thick and radiates backwards to space by rotational transitions. I should have been wiser: this high temperature could have been avoided by using HCN and CO_2 instead of CH_4 and NH_3. However, I have never considered that thermal equilibrium was the final answer, and I am glad to see that people are now willing to consider this gas phase chemistry as a proper approach. The individual reactions must now be considered each individually, and the problem becomes formidable, but it is worthwhile trying. I want to encourage Dr. Oppenheimer in his difficult endeavor, by suggesting that he should follow the same way as mine, that is, getting rid of the unobserved methane and ammonia in his future models, in favor of the observed H_2O, HCN and CH_3CN, and possibly CO and CO_2 (from the observed CO^+ and CO_2^+).

E. Gerard: You say that ion-molecule reactions play an important role in comets (as they seem also in the interstellar medium), so can you give a figure of the electron density needed near the nucleus?

Do you think that such high ion densities can be found very close to the nucleus?

M. Oppenheimer: If you have sublimation rates of neutrals of 10^6 to 10^7, then you do derive ion densities which are the same as the electron density, of 10^3 or 10^4, which is in good agreement with some observations that were made years ago, there was an article by Arpigny in 1965 that mentioned that kind of number.

I haven't seen much since then. But that would be roughly the electron density.

E. Gerard: But you think it is no problem to create these ions as close to the nucleus as you are saying? They can be created very fast?

M. Oppenheimer: There is a peak in the density—this was shown by Jackson, he tells me, some nine years ago. And it is possible to create a very high abundance, not a relative abundance, but an absolute abundance of ions—at few hundred kilometers by photoionization. But they are being removed quickly, of course.

This is without considering chemistry. This is just considering the ionization rates. When you consider the chemistry, it will bring that peak down, because the ions moved.

But you can definitely create a substantial abundance of ions at small distances from the nucleus.

G. H. Herbig: I gather from your abstract that you have a predicted model of the coma, with all your predictions so that we can compare with observations.

M. Oppenheimer: No. There is an article I wrote which will be in Ap. J. in February, which has a model of the coma, based on a methane nucleus, but where all the other atoms are present in some unknown form.

But I don't want that taken seriously in terms that I really believe methane is in the nucleus. I did it to show what would happen if methane were in the nucleus. You could get everything else anyway.

So, that, I am not ready to predict what the nucleus is really made out of, because it is too early. You need more production rates. In a few years, when those production rates are available when we have a whole table of them, we can make ratios. Then I think from the gas phase chemistry you can say something more intelligent.

The only things you could say now, for instance, are what other people have said—that because, for instance, CN, C_3, C_2 appear early and in great abundance, that that suggests that some hydrocarbon is in there.

And I am ready to go along with that on the basis of what I can say from the chemistry. But more than that is hard to say.

G. H. Herbig: Do you expect appreciable numbers of negative ions, C_2-, OH-. Are you concerned about this?

M. Oppenheimer: No, because in the solar radiation field, the photo detachment rates are very, very fast. I would expect that negative ions form but they destroy very quickly. First of all, they form slowly, much slower than positive ions, and they are destroyed much more easily because of detachment in the solar field.

So that I would expect negative ions not to play a big role.

B. Donn: Your analysis suggests a number of new species for which we need the spectrum so that we can try to identify and look for them.

So, in case Dr. Herzberg is running out of work to do—.

(Laughter.)

W. I. Axford: One cannot talk in terms of a "scale length" for coma ions such as CO^+ simply because ions (and electrons) do not expand in a more-or-less simple way as do neutrals. In effect the motion of charged particles must be largely determined by the magnetic field surrounding the comet, and by the dynamical effects of the solar wind. Accordingly one can expect the distributions of coma ions to be quite complicated, and certainly not similar to that of neutrals.

The maxima density of ions is determined approximately from the fact that the maximum coma plasma pressure must be comparable to the solar wind ram pressure. This requires maximum ion density of 10^4 - 10^5 cm^{-3} depending on their temperatures.

M. Oppenheimer: There is no doubt that the ion distribution is not correct, because it is assumed the ion velocity and the neutral velocities are the same, which won't be true, especially as you get more and more towards the edge.

But, you had to start somewhere. And what it shows is that the ion scale lengths, for instance, may not be determined at all. And even the neutral scale lengths are affected. The OH scale length that was derived from the observations that were put on earlier was about 10^5 kilometers.

The OH scale length due to chemical processes is comparable to and actually shorter than that. There is a big warning here that you can't assume that the scale lengths that are observed are due to photo processes. Because the chemical processes change the scale lengths all around.

C. Cosmovici: Does the interaction between neutrals and dust particles near the nucleus become important for the formation of new molecules like in the interstellar medium?

M. Oppenheimer: The interaction between dust particles and neutrals in a strong ionizing field is much slower than the interaction between ions and neutrals.

And the dust particles may effect the distribution but at these temperatures, you don't even expect the neutrals to stick to the dust particles very well. If things are flying off, then they are not coming back and sticking.

So, in terms of what I know, I don't expect them to be as important.

D. A. Mendis: Regarding the conversion of scale lengths to lifetimes even in the case of neutrals one has to be careful especially when they are small (i.e., $\lesssim 5.10^4$ km) because of the effect of collisions. For instance if the expansion is

sonic it means that by the time an emitter goes out a distance D, it has also random walked a distance D so already a factor of two is involved.

I would also like to state that with all this talk about the importance of collisions and the gas phase chemistry it is becoming clear that we have to use a complete multiconstituent hydrodynamic model using a proper energy equation before we can get to a proper interpretation of the observations. There is no use trying to fit a Haser model to the exosphere while ignoring the nuclear region—surely what happens in the exosphere is directly related to what happens in the collision dominated region, and a proper hydrodynamic model can be applied to the entire region—including the collisionless region—if properly interpreted.

Also the effect of the attenuation of the incoming exciting radiation in the coma has to be taken into account in a consistent way.

M. Oppenheimer: In line with that point, there is an important one which I want to show.

Reactions like this which make destroy parent molecules themselves very rapidly, are generally ignored, because they have rate constants which aren't high until you get to a few thousand degrees, at which time they do get to be gas kinetic.

The trouble with that is that oxygen coming off is photo dissociated, and may have several volts of energy associated with it. And if CH_4, for instance, were a major constituent of the coma, in the first collision oxygen has, instead of being thermalized, it reacts. And "whamo," you have a reaction immediately, which removes one of these what might be a parent molecule.

So even the neutral reactions could be extremely important if we find the photo dissociation products are really hot.

B. Donn: I would like here to make a contribution of my own on this subject, which I mentioned earlier, concerning chemistry in these astronomical sources, and that is: one has to be careful in using laboratory data and applying it here, because the laboratory data is taken under fairly high densities where collisions are frequent.

There, we have a Boltzmann distribution of the vibrational and rotational energy of the participating species in addition to a Maxwellian velocity distribution, which is not true at the densities in the comet. Densities of 10^6 to 10^{12} will lead to radiation of the vibrational energy and much of the time rotational energy and you will end up with cold molecules in their ground vibrational states and frequently ground rotational states also.

Almost all of these neutral processes, and some of the ionic processes are very dependent on having vibrationally excited molecules. The reactions take place in excited states, and therefore, one needs to know what the detailed rate constants are, not for a Boltzmann distribution of energies, but for reactions from each of the energy levels, to determine how much the contribution will be made there. Dr. Oppenheimer just gave an example of nonequilibrium velocities and some consequences.

Another point is that in discussing neutral chemical processes, at temperatures of 300 degrees Kelvin or even 500 degrees as Delsemme proposed earlier for most of these processes, the rates are extremely slow. In the time scale of the solar system, you would generally not reach equilibrium.

M. Oppenheimer: Thermal equilibrium has nothing to do with this.

D. J. Malaise: When observing the variations of the photometric profiles with heliocentric distance with high space resolution, several radicals show a behavior which is at complete variance with any kind of photodissociation production.

These radicals show a flatter profile when distance to the sun decreases. In 1966 (Malaise, XIIIth Colloquium of Liege, 199; 1966) I interpreted this as an indication that the production of radicals depended on collisions. At that time, however, the total density of gas at 10^4 km from the center was thought to be in the range of 10^4 cm^{-3}. To solve this contradiction, I looked carefully to find collisional effect in the rotational structure of CN and to my surprise I found total densities in the range of 10^8 cm^{-3} for an average comet. The difficulty is that for small comets (Encke) the total density is 10^5 cm^{-3} or smaller. But the small comets produce the same radicals as the large ones.

M. Dubin: Two comments: first in regard to Malaise.

It has been shown that there are two classes of dust particles—small particles and larger particles which sublimate. The distribution of the larger particles may affect the radial dependence on the distributions of the molecules and radicals.

Secondly, Oliveso of Penn. State has been studying the possible role of small dust particles in the Earth's D and E region in relation to the ion chemistry. He has found that at the very small dust concentrations in the Earth's atmosphere the dust reaction is competitive with the ion reaction rates-as the cross section of surface ion recombination is nearly 100 per cent efficient. For comets, with a tremendously larger dust to gas ratio than the Earth's D region this type of reaction must be considered.

M. Oppenheimer: I am very skeptical about those kinds of assumptions, though, because I think that especially in the thermosphere, where the temperatures are a thousand degrees for the neutrals and greater for the ions sometimes, that they don't stick to grains. It just seems unlikely, especially in the light of the kind analysis in the interstellar medium that Salpeter did, that these effects really lead to reactions anywhere near as a efficient as the gas phase.

And I haven't seen that paper, so maybe I should shutup about it.

M. Dubin: D region—

M. Oppenheimer: Oh, the D region. There it may be a different story.

L. Biermann: I would like to congratulate Dr. Oppenheimer on his very fine work which in many details goes beyond our own work mentioned earlier (Biermann and G. Diercksan, 1974, loc. cit.). His general conclusions are essentially identical with those reached there. As to details, the rate of dissociative recombination of CO^+ is known from laboratory work since 1970 and was applied to cometary chemistry already then (cf. L. Biermann, Report of IAU Commission 15, 1970). A first value for the electron density in the coma was derived in 1964 in Dr. Trefftz's and my paper quoted by Dr. Delsemme this morning, in which the effect of the absorption of the solar ultraviolet was at least crudely allowed for.

B. Donn: After the reviews by Delsemme and Malaise, the report just presented by Oppenheimer and the discussion by several participants following these three papers and others, it is my feeling that the study of the coma is entering a new level of sophistication. The simple Haser model served for two decades as a valuable scheme for analyzing coma photometry. It now appears that both theory and observation indicate that we must be careful in deducing cometary parameters, e.g., lifetimes and sources from the Haser model. Several refinements need to be added; velocity distribution of fragments, effects of collision, chemical reactions, time variations, more complete hydrodynamic analysis including ions and other processes still to be appreciated. How to do all this is not clear.

NEUTRAL TEMPERATURE OF COMETARY ATMOSPHERES

Mikio Shimizu

The spectral analysis of the coma and type I tails of a comet gives a clue to clarify the composition of the volatiles in its nucleus. The ultraviolet observation of strong H, O, and OH emissions in comets 1969 g and i by OAO II (Code and Savage, 1972) and the recent identification of H_2O^+ in the spectrum of 1973f (Wehinger et al., 1974) have suggested that the main constituent of cometary coma is H_2O. It was also suggested from the computation of the ionization processes (Jackson and Donn, 1968) that CO and N_2 may be the second most abundant gases (some ten% by number) in comets. Other gases detected in the optical (C_2, CN, C_3...), ultraviolet (NH, CN) and radio (CH, CH_3, CN) regions appears to be minor constituents of cometary atmospheres.

Water has so large a dipole moment (~1.84 Debye) that it is a good infrared radiator. If this molecule is the main constituent of cometary comas, we may expect that the cometary atmosphere may be extremely cooled. This could be the most important factor to determine the neutral temperature of the cometary gas.

Water can emit infrared radiation through a vibrational transition at 6.3 microns and a rotational one near 50 microns. In the vibrational case, the dependence of the emission rate on temperature will mainly be determined by that of the excitation cross-section from v = 0 to v = 1 level which obeys SSH theory (Schwartz et al, 1952) since the de-excitation rate by molecular collisions is smaller than that of the spontaneous emission (non LTE condition). This rate can be written

$$R_v = 1.2 \times 10^{-22} \text{ EXP } \left(- \frac{38.3}{T^{1/3}} - \frac{2294}{T} \right) N^2 \qquad (1)$$

where T and N are the temperature and density of the cometary gas, respectively.

In the rotational case, the energy differences between adjacent levels are much smaller than those between vibrational ones and so the energy transfer from translational mode to rotational one is much easier. The molecular distribution is of Boltzmann type (LTE condition) and the total emission rate is obtained by summing each contribution over all rotational states. The rotational emission rate of a linear molecule with a dipole moment μ and a rotational constant $\bar{B}$ has been computed by Bates (1951) as

$$R_d = \frac{2^{10} \pi^4}{3} \, c \, \mu^2 \, \bar{B}^4 \left(\frac{k T}{hc \bar{B}} \right)^2 N \qquad (2)$$

The rotational constants of water are (in cm^{-1}):

$$A = 27.79, \qquad B = 14.51, \qquad C = 9.29.$$

Consequently, by taking $A = \infty$, and $\bar{B} = \sqrt{B\,C}$, an approximate form of emission rate is obtained

$$R_d = 5.5 \times 10^{-19}\, T^2\, N \tag{3}$$

A better expression for the emission rate of water may be obtained by approximating H_2O as a rigid symmetric rotor ($B = C = \bar{B}$ and $\bar{A} = A$). After some manipulation, the emission rate in this approximation R_r can be written in the form

$$R_r = \left(1 + \frac{9}{8}\frac{\bar{B}}{\bar{A}} + \frac{3}{8}\frac{\bar{B}}{\bar{A}}\right) R_d = 1.54\, R_d \tag{4}$$

Since the correction factor to the linear dipole approximation is only 50%, the improvement by using a (classical) asymmetric rotor approximation ($B \neq C$) is not very important.

It is noteworthy that the OH radical formed by the dissociation of H_2O has also a large dipole moment and that it may also contribute greatly to the cooling of cometary coma in nearly the same rate as H_2O does, particularly in its outer part. Weaker but still serious contribution may be expected for other radicals such as CN, NH, etc., too.

It may be instructive to compare the planetary upper atmospheres with cometary atmospheres here, since the gas density in the neighborhood of cometary nucleus is around 10^{12} cc, a density similar to those

at the bases of planetary upper atmospheres (although there is a difference between them in that atmospheric densities of planets decrease exponentially outwards, while those of comets vary approximately as the inverse square of the distance). For instance, the cooling in the Venus and Martian upper atmospheres is due to CO_2 15 micron band. The heating at the top of these atmospheres by the absorption of the solar ultraviolet radiation is approximately in balance with the (vibrational) cooling and their exospheric temperatures become of the order of some hundreds degrees. For much detailed discussions, some effects of dynamics (eddy diffusion on the composition of the upper atmospheres, thermal conduction from heating level to cooling one etc.) should be taken into account and the inclusion of such effects explained observed properties of planetary upper atmospheres by space probes well (Shimizu, 1973a, 1974). Consequently, if the vibrational cooling due to H_2O 6.3 micron band is the dominant cooling process in the cometary atmosphere, its neutral gas temperature at 1 AU may also be around 300 ^{o}K. However, as the formulae (1), (3), and (4) show, the rotational cooling is much stronger for H_2O. If the heating by the solar ultraviolet radiation is equated to this, the equilibrium temperature at 1 AU can be of the order of only 10 ^{o}K. The transport of heat by expansion of cometary atmosphere can easily be shown to be of the order of the vibrational cooling and to have a negligible effect as compared

with the rotational one. If the cometary coma has a 300 ^{o}K temperature it is clear that some other much stronger heating source is necessary unless H_2O is a minor constituent (~0.1%) of cometary atmospheres, which is unlikely from the recent observations. Electron impact may not be an important source, since a bow shock and other hydromagnetic structure around a comet may prevent the inflow of such a large electron energy flux as 10^3 times the ultraviolet radiation into the coma. Consequently, a possible mechanism may be a strong infrared coupling between H_2O and dust grain in the coma. It is known that the icy halo model (Delsemme and Miller, 1971) on the basis of the composition of hydrate clathrate well explains many observational features including the photo-dissociation paradox (Wurm, 1963). Recent infrared observations of comets suggest that the mean radius of cometary dust grain is around 1 micron and that its number density is about 10^7/cc, at least for the non-volatile part. Even so, the collision time between gas and dust is much longer than the typical expansion time, ~1 day (although the collisional times among gases are of the order of 10^{-1} sec, short enough to be in equilibrium). Consequently about 10^{-2} of the solar visible radiation, whose energy flux is 10^5 times larger than that in the ultraviolet region, once absorbed by the dust grain or at the surface of nucleus should be transferred to H_2O molecules in the form of

infrared radiation. Such a strong infrared coupling could naturally be expected by taking into account that the main part of the dust grain may be H_2O ice, although it is necessary to carry out a tedious radiation transfer problem to obtain the temperature of H_2O gas explicitly.

One of the advantages if this model is that it can explain the dependence of the atmospheric temperature on the distance of comet from the sun, r. Wurm (1963) suggested a relation of $T \propto 1/r$. The heating rate is proportional to N/r^2 and so, if we equate this to (3), T should be inversely proportional to r.

The most important conclusion from the above discussion is that the atmospheric temperature of comets cannot be so high as 1500 ^{o}K. This is also suspected from the analysis of high resolution CN spectrum (Malaise, 1970). It is concluded from thermochemical calculation (Delsemme, 1966) that the conversion of CH_4 and NH_3 to CO and N_2 occurs at the dissociation level whose temperature is assumed to be extremely high by the absorption of the solar ultraviolet radiation. The expansion of cometary atmosphere is attributed to this heating (Shul'man, 1972) and a detailed hydrodynamic calculation has been carried out on this assumption to support the above quasi-thermochemical equilibrium model (Wallis, 1974). However, all these discussions have

neglected the strong cooling effect of H_2O and should be reconsidered. It is now evident that CO and N_2 may be abundant in the cometary nucleus (Jackson and Donn, 1968), possibly in the form of clathrate. Our proposal in the IAU Symposium No. 52 (Shimizu, 1973b) that the cometary nuclei are composed of the dirty ice of second kind (mainly H_2O and some ten % of CO and N_2) appears to be confirmed. The similarity of cometary molecules to the interstellar molecules should more seriously be taken into account in the theory of cometary formation. Proposals for the origin of comets in interstellar space by Whipple and Lecar and by Donn at this colloquium give a physical meaning to the similarity.

It is to be noted that the ejection of various molecules from stars, both of oxygen rich type (NML Cygnus) and of carbon rich type (IRC + 10216), has been found during these years. Furthermore, CO molecules have been detected in the envelopes of T Tauri stars. This evidence might be correlated with our suggestion for the interchange of cometary substances among stars and clouds, although it is far from conclusive. A large number of interstellar comets trapping the heavy elements appears to be consistent with interstellar deficiences of these elements (Greenberg, 1974).

Addendum: Recent finding of carbon atom emission in the atmosphere of Comet 1973f (Feldman et al., Science, 185, 705, 1974) endorses the discussion in this paper and this may be a conclusive evidence for the dirty ice of second kind in the nuclei of comets.

REFERENCES

Bates, D.R., Proc. Phys. Soc. London, B 64, 805 (1951)

Clayton, R.N., Grossman, L. and Mayeda, T.K., Science 182, 485 (1973)

Code, A.D., and Savage, B.D., Science, 177, 213 (1972)

Delsemme, A.H., Soc. Roy. Sci, Liege, 12, 77 (1966)

Delsemme, A.H. and Miller, D.C., Plan. Space Sci., 19, 1229 (1971)

Greenberg, J.M., Ap.J., 189, L81 (1974)

Jackson, W.M. and Donn, B., Icarus, 8, 270 (1968)

Malaise, D.J., Astron. Astrop., 5, 209 (1970)

Schwartz, R. N., Slawsky, Z. I. and Herzfeld, K., 1952, J. Chem. Phys. 20, 1591

Shimizu, M., J. Geophys. Res., 78, 6780 (1973a)

Shimizu, M., in "Interstellar Dust and Related Topics" ed. by Greenberg J.M. and Van de Hulst, D. Reidel Publ. Comp., p405 (1973b)

Shimizu, M., J. Geophys. Res., in printing (1974)

Shul'man, L.M., in "Dinamika kometnikh atmosfer-neitralnii gaz", Chap. 3, Kiev (1972)

Wallis, M.K., Month. Not. Roy. astro. Soc., 166, 181 (1974)

Wehinger, P.A., Wyckoff, S., Herbig, G.H., Herzberg, G.H., and Lew, H., Ap. J., 190, L43, (1974)

Wurm, K., in "The Moon, Meteorites, and Comets" ed. by Middlehurst, B. M., and Kuiper, G.P., Univ. of Chicago Press, p. 573 (1963)

DISCUSSION

W. Jackson: If the comets are composed of mostly H_2O, CO and N_2, what is the order of magnitude ratio of $(CO)/(H_2O)$ and $(N_2)/(H_2O)$?

These ratios have to be low if the rate of water evaporation is to control the gas production rate of comets.

M. Shimizu: The composition of volatiles depends on the accretion process and themal history of comets. I am not discussing them. I tentatively favor clathrate theory, but the real values should be determined by observation.

M. K. Wallis: It is not clear to me that at the relevant cometary densities (10^6 - $10^8/cm^3$) and energies, the approach to equilibrium would be rapid enough. Taking H-atoms resulting from photo-dissociation of H_2O with 1-2 eV energy, cooling via rotational excitation with cross-section $10^{-15} cm^2$ and 0.01 eV loss would not dominate elastic collisional transfer of energy from the H-atom to the H_2O. So some energy seems available for increasing the thermal and outflow energies of the H_2O gas. Clearly one has to be careful about drawing definite conclusions one way or the other.

M. Shimizu: The time constant of the excitation is

$$T = \frac{1}{N \sigma v} = \frac{1}{10^8 \ 10^{-15} \ 10^5} = 10^2 \text{ sec},$$

much shorter than the expansion time 10^5 sec. So the kinetic energy of hydrogen will be transferred to water, the main constituent, and radiated in the infrared. That leads to the low atmospheric temperature.
(The detailed analysis by taking into account non LTE process and various dynamical effects will be submitted to Astrophysics and Space Science later.)

B. Donn: To try to interpret the radio observations of water in Comet Bradfield, we have worked with Dr. Krauss of the National Bureau of Standards. In a preliminary analysis he obtained a kinetic temperature of 10K in the coma in a similar process to that of Shimizu using cooling by rotational excitation of water. This is clearly an important process to take into account and a detailed analysis is necessary to determine coma temperatures and rotational excitation of molecules.

FAR ULTRAVIOLET EXCITATION PROCESSES IN COMETS

P. D. Feldman, C. B. Opal, R. R. Meier and K. R. Nicolas

Introduction

The recent observations of atomic oxygen and carbon in the far ultraviolet spectrum of Comet Kohoutek (1973f) (Feldman et al. 1974; Opal et al. 1974) have demonstrated the existence of these atomic species in the cometary coma. However, in order to identify the source of their origin, it is necessary to relate the observed ultraviolet flux to the atomic production rate. Assuming the only excitation mechanisms allowed are those produced by resonance scattering and fluorescence of solar ultraviolet radiation, the problem reduces to finding the emission rate factors (g-factors) as a function of the heliocentric comet velocity. Since the widths of the solar emission lines are smaller than the maximum heliocentric Doppler shift, given by

$$\overset{\circ}{r}_{max} = \left(\frac{M_\odot G}{q}\right)^{1/2} = 21.06\ q^{-1/2}\ \text{km sec}^{-1} \quad ,$$

where q is the perihelion distance in A.U., it is necessary to consider the detailed multiplet structure of the transition, the solar line shape and the relaxation of excited fine structure levels.

Analyses of the observed OI λ1304 and CI λ1657 A multiplets have been carried out using high resolution solar spectra obtained from the ATM solar spectrograph aboard Skylab. In addition, we have examined the possibility of observing ultraviolet fluorescence from molecules such as CO (which may be the parent molecule of atomic carbon) and H_2, as well as resonance scattering either from atomic ions for which there are strong corresponding solar lines (CII) or from atoms for which there is an accidentical wavelength coincidence (SI). The scattering of solar Lyα from atomic hydrogen has been discussed in detail by Keller (1973) and Meier (1974) and will not be considered here.

Emission Rate Factor

The emission rate factor, which is the probability that an atom or molecule will resonantly scatter a solar photon of wavelength λ into 4π sr in unit time, is given by Barth (1969) as:

$$g_\lambda = \left(\frac{\pi e^2}{mc^2}\right) \lambda^2\ f_\lambda(\pi\ F_\lambda)\ \text{photons sec}^{-1}\ \text{mol}^{-1}$$

where f_λ is the absorption oscillator strength and πF_λ

the solar flux per unit wavelength. For resonance fluorescence in molecules, the relative transition probabilities for downward transitions must also be taken into account. The emission rate per unit volume is then simply related to the density of the scattering species n_i by

$$j_\lambda = g_\lambda \, n_i \text{ photons sec}^{-1} \text{ cm}^{-3}$$

In the case of cometary emission, the large heliocentric velocity of a typical comet requires the use of the solar flux $\pi F_{\lambda'}$, where

$$\lambda' = \lambda\left(1 - \frac{\dot{r}}{c}\right) ,$$

so that $g_\lambda = g_\lambda(\dot{r}) = g_\lambda(r, q)$.

Solar Ultraviolet Fluxes

The Naval Research Laboratory solar spectrograph (S082B) on the Apollo Telescope Mount (ATM) of Skylab photographed the solar spectrum from 970 Å - 4000 Å. It provided the necessary high spectral resolution (0.06 Å) to yield data necessary for the cometary interpretation. The spectrograph slit averaged over a 2″ by 60″ area on the sun. In order to estimate the solar intensity from the total disk it was necessary to include the effects from limb brightening and from the increased contribution of active regions which introduces a variable intensity component. Spectra of these phenomena were available from the large number of observations taken within the Joint Observing Program.

Densitometry of the Kodak 104 film gave the density versus position information which was used to determine the relative intensity versus wavelength of the solar spectrum. Spectra with 40, 160, and 640 sec exposure times were used to construct a relative H-D curve for each wavelength region of interest. The conversion from density to relative intensity for each of the plates in the exposure sequences yielded a maximum variation in relative line shape of about ±15%, the random error being mostly due to grain clumping. The wavelength determination was made by using from 5 to 9 standard lines (Sandlin, 1974) within each wavelength interval. The estimated absolute error is ±0.02 A which translates into

±10% intensity error at the steepest part of the line profile.

The absolute intensity was determined independently of the ATM calibration in two ways.* The first method was to match the continuum intensity level at 1650 A with a value determined from a 1971 rocket flight (Brueckner and Nicolas, 1972). This gave an absolute intensity scale for the CI emission feature at 1656 A. The rms error is about ±30%. At shorter wavelengths the absolute scale was determined by comparing the total relative line intensities with those of OSO VI (Dupree et al. 1973). The error for this method is approximately +100%, -50%.

The total flux averaged over the solar surface and its time variation was estimated from spectra of quiet solar limb scans and of active regions. The intensity of the emission lines is fairly constant (neutral) over the solar disk. The maximum error introduced by assuming that they have neutral limb brightening is less than ±10%. The active region enhancement over the quiet region intensity is approximately a factor of 2 to 3 for CI and a factor of 10 to 20 for OI and CII. Since the area of the disk covered by active regions can be as high as 10% (De Jager 1961), the total solar flux during the solar cycle could vary by 30% for CI and up to a factor of 2 to 3 for OI or CII. Short term fluctuations (on the order of two weeks) within a solar cycle could also be of comparable magnitude.

CI λ1657 A

The carbon multiplet at 1657 A provides an excellent example of the dependence of g_λ on radial velocity. Carbon, long known as a major constituent of cometary molecules and radicals, was not detected in atomic form until the two recent rocket ultraviolet observations of Comet Kohoutek. There are six components of the multiplet, as shown in Fig. 1, resulting from the fine structure triplet nature of both the excited and ground state. An additional consideration in the evaluation of the g-factors in cometary emission is the question of relative population of ground state fine structure levels. We assume that they are initially populated according to a Boltzmann distribution characteristic of some temperature T_o of the parent molecule. However, since the coma becomes non-collisional very close to the nucleus, radiative transitions $J=2 \rightarrow J=1$ and $J=1 \rightarrow J=0$ will tend to cool the atom in a time of the

*The inflight ATM calibration is not yet finished, but will be completed and published shortly.

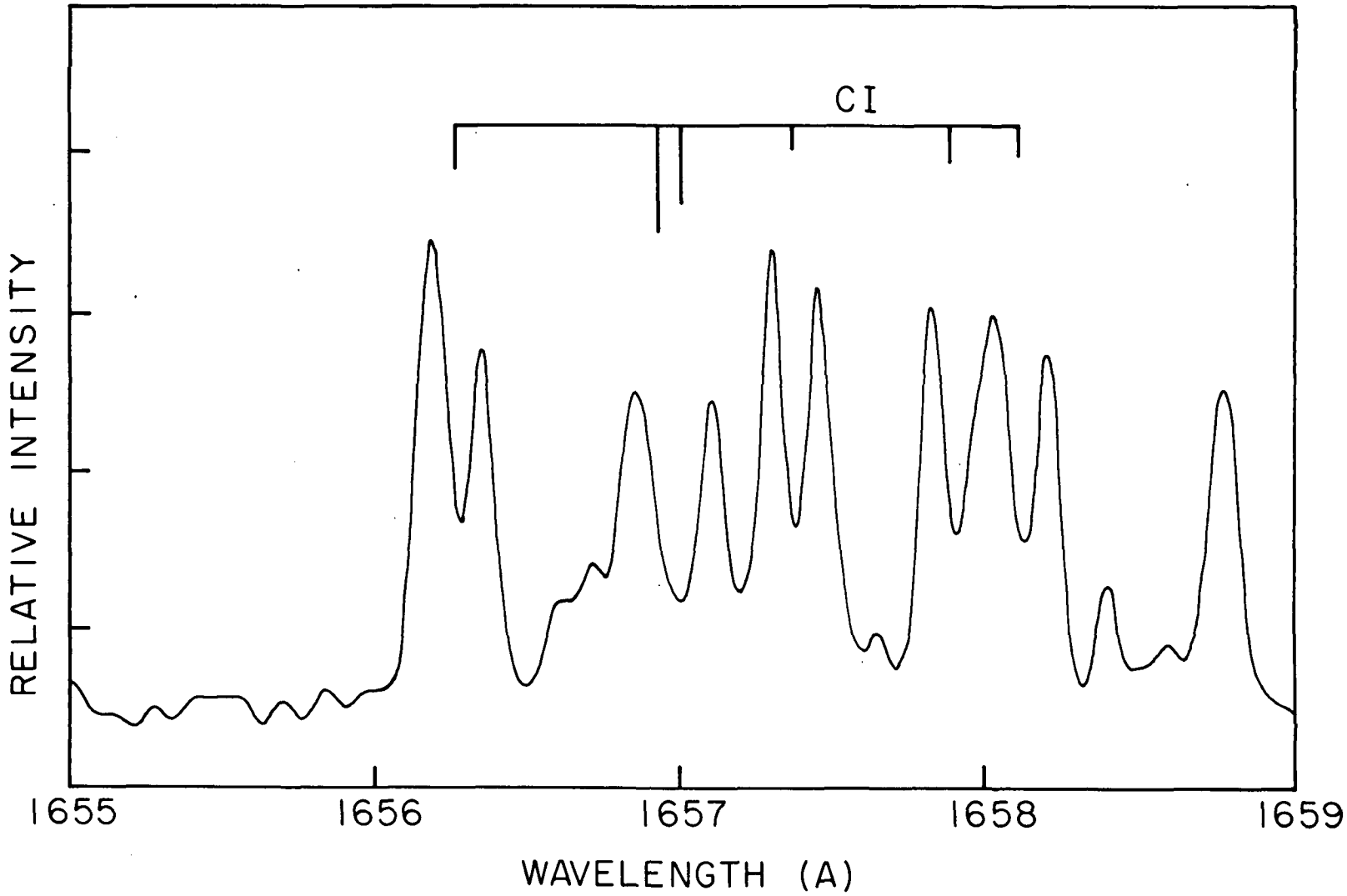

Fig. 1. High resolution spectrum ($\triangle\lambda$ = 0.06 A) of the sun in the region of the CI multiplet at 1657 A, observed 300" in from the solar limb.

order $\tau_c = A_{ij}^{-1}$, where A_{ij} is the Einstein coefficient for the transition. The effect of cooling is significant only if the A_{ij} values are greater than the photoionization rate J_i which depends on heliocentric distance as r^{-2}. For the carbon ground state, $A_{10} = 7.9 \times 10^{-8}$ sec^{-1} and $A_{21} = 2.7 \times 10^{-7}$ sec^{-1}, which are both less than the value of J_i at 1 A.U. of 4.0×10^{-6} sec^{-1} (Feldman et al. 1974). The distance at which the cooling time τ_c and ionization lifetime τ_i are equal, r_c, is given in Table I for the most important species. For cases in which $\tau_c < \tau_i$ the variation of the relative populations in time will be determined primarily by the effect of optical pumping produced by the resonance scattering of solar radiation, which as we have noted will also vary with both r and $\dot{r}$. In most cases of interest, the resonance scattering time, $\tau_s = g_\lambda^{-1}$, is less than τ_c, so that the optical pumping effect is not negligible.

To first order we regard the temperature in the coma as constant and show in Figs. 2 and 3 the variation of g_λ with $\dot{r}$ and r. All g-factors are calculated for r = 1 A.U. The values of $\dot{r}$ corresponding to the observations of Comet Kohoutek are indicated in Fig. 3. For planetary atmospheres the value of g for $\dot{r} = 0$ is to be used.

OI λ1304 A

The oxygen triplet in the solar spectrum has recently been observed with sufficient resolution to permit the evaluation of the absorption at the line center due to terrestrial oxygen in the upper atmosphere. An example of one of the lines (after correction for atmospheric absorption) is shown in Fig. 4. A Doppler shift of $\pm$0.17 A corresponding to a velocity of $\pm$40 km sec^{-1} is sufficient to completely shift the cometary absorption wavelength completely off of the solar line. Thus the observed oxygen emission (Feldman et al. 1974; Opal et al. 1974) must be due to either resonance scattering from the solar continuum, which is very weak, or another mechanism. Fig. 5 illustrates a Bowen fluorescence mechanism in which the $^3S_1$ state is populated via the ^3D-^3P transition at 1025.77 A which is nearly degenerate with the solar Ly β line of HI at 1025.72 A. The g-factors for the entire multiplet for the two processes are illustrated in Fig. 4. Resonance scattering from the solar continuum gives a g-factor of 4×10^{-8} sec^{-1} atom^{-1}, independent of wavelength. For the case of oxygen, cooling via the fine structure transitions at

Table I

COOLING AND IONIZATION TIMES

Species	τ_c (sec)	τ_i (sec at 1 A.U.)	r_c (A.U.)
OI	10^4	4.0×10^6	0.05
CI	10^7	2.5×10^5	6.3
CII	4×10^5	--	--

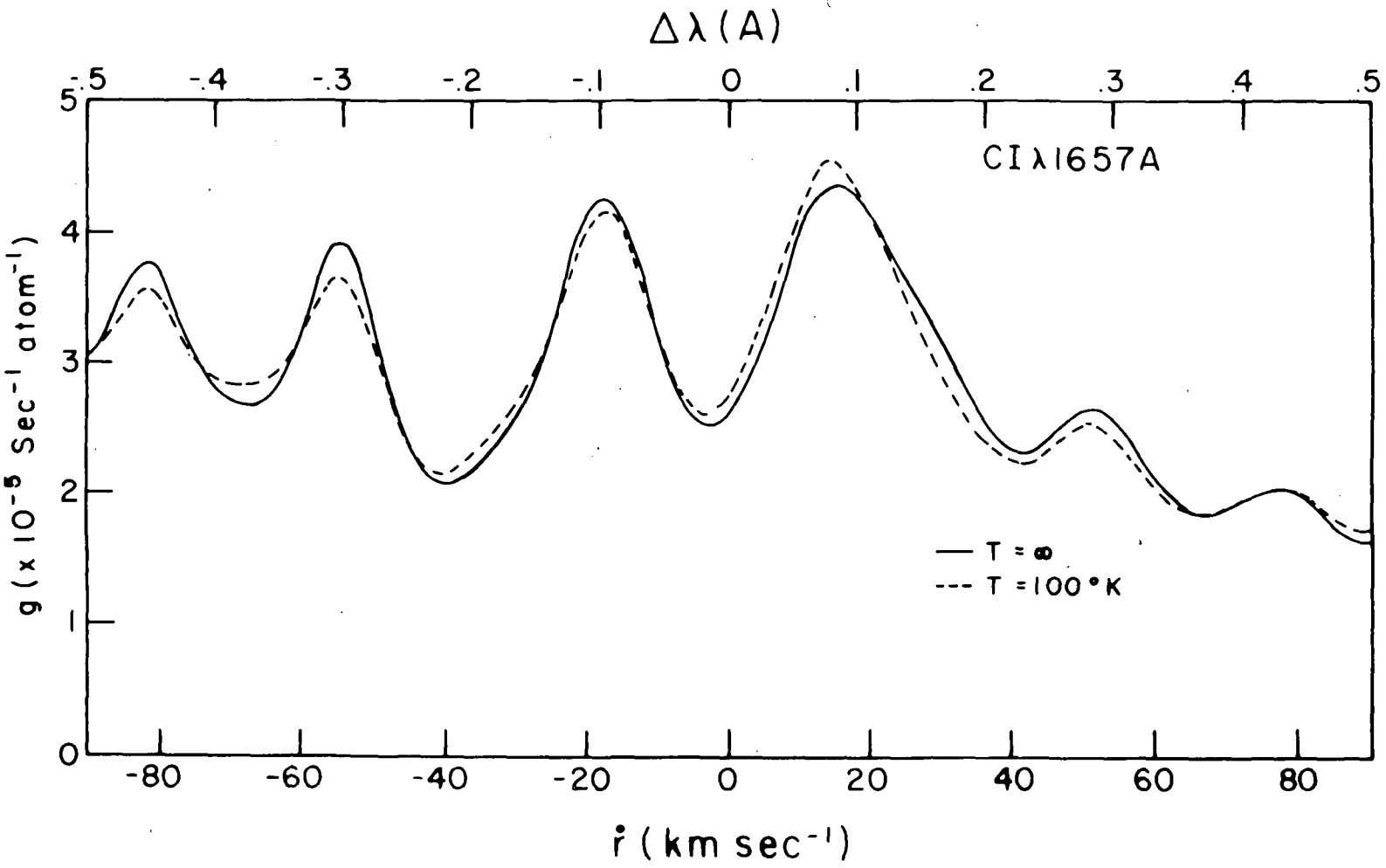

Fig. 2. Dependence of the CI 1657 A g-factor on heliocentric velocity.

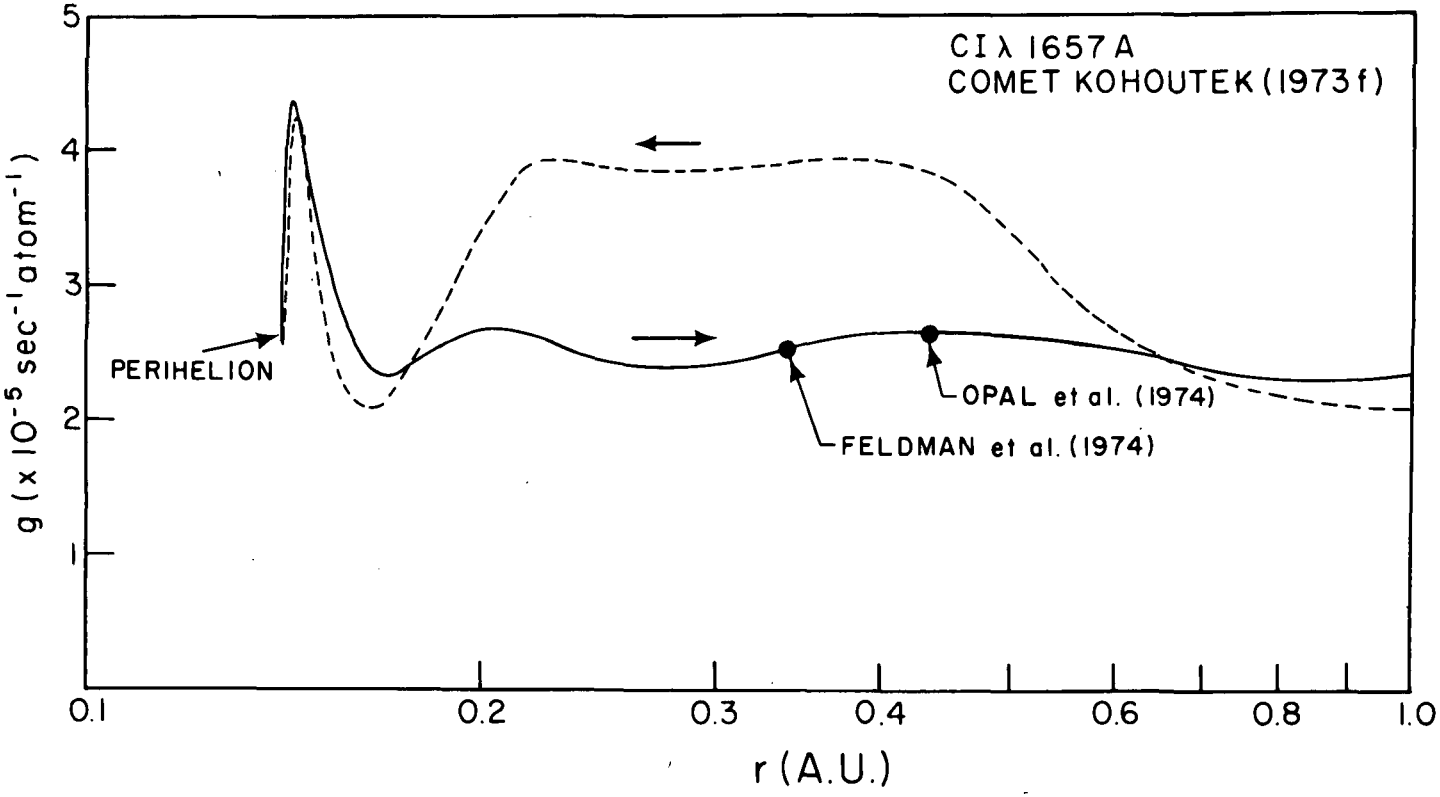

Fig. 3. Dependence of the CI 1657 A g-factor on heliocentric distance for Comet Kohoutek (1973f). The arrows indicate direction of motion.

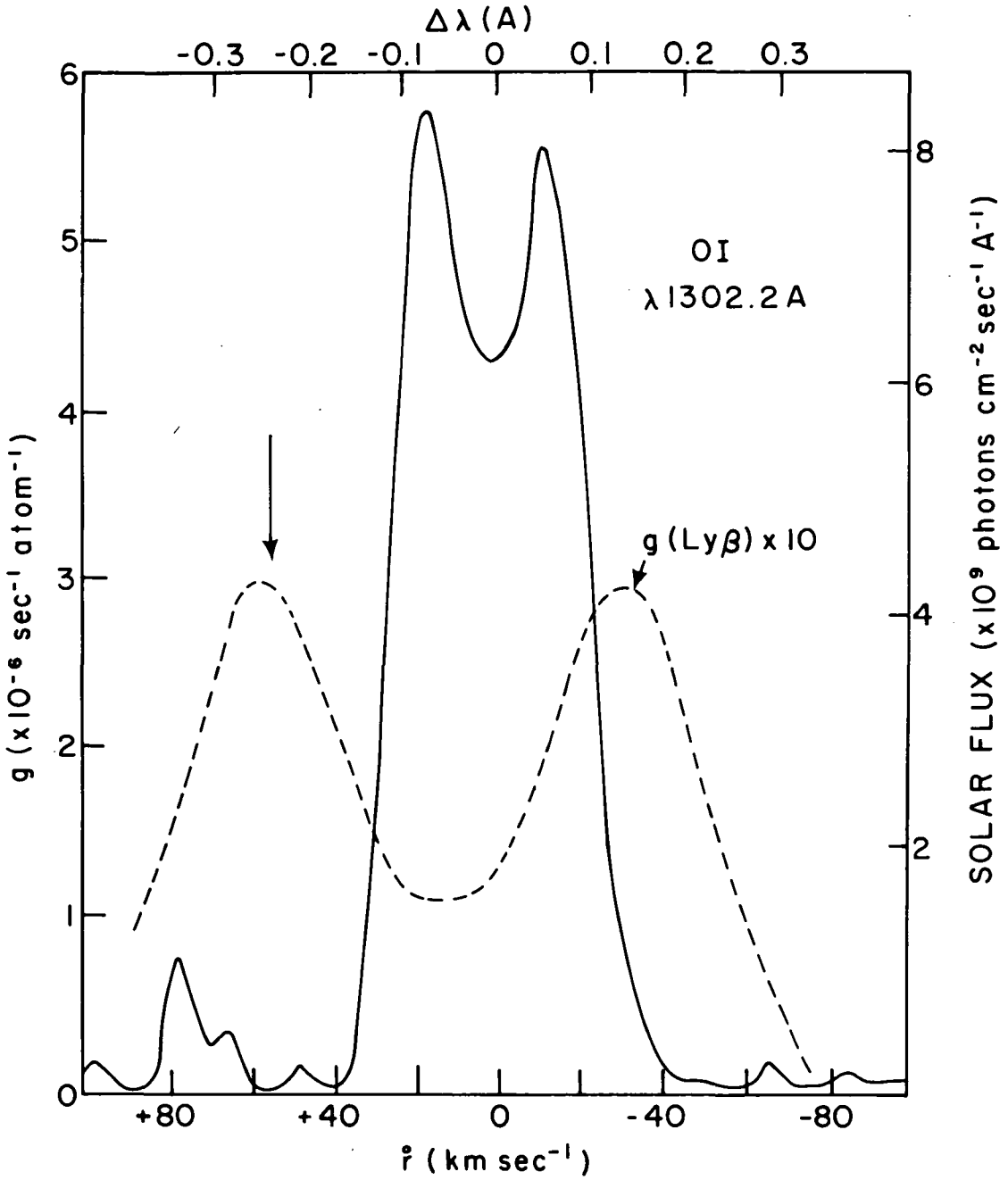

Fig. 4. High resolution profile of the solar OI 1302.2 A line. The OI g-factor is shown for both resonance scattering and fluorescence excited by solar Lyβ as a function of heliocentric velocity. The arrows correspond to the observations of Feldman et al. (1974) and Opal et al. (1974).

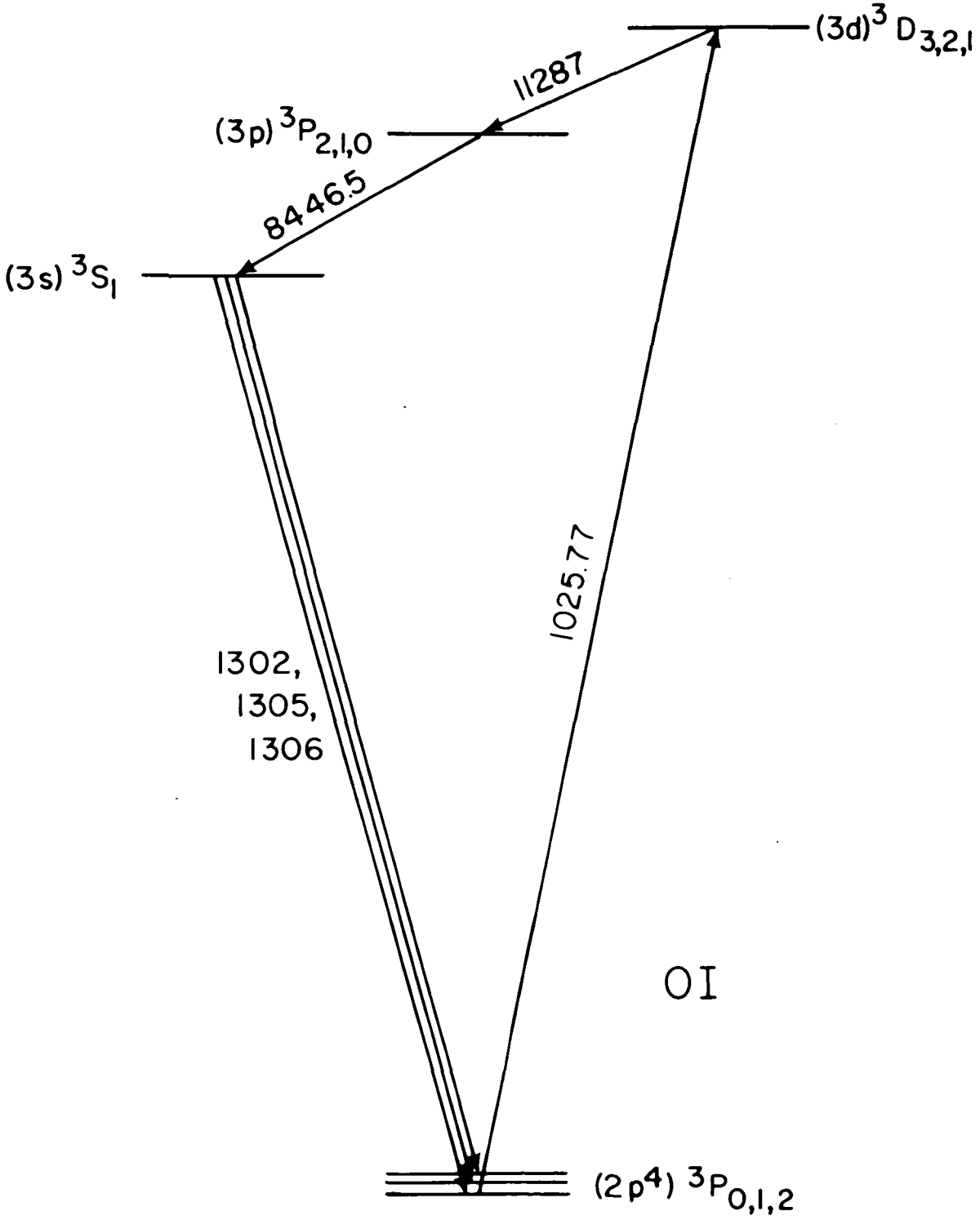

Fig. 5. Fluorescence mechanism for excitation of OI 1302 A via solar Lyβ radiation.

63μ and 147μ is quite rapid with $\tau_c < \tau_i, \tau_s$. However, for any reasonable range of equivalent temperatures, since the individual lines do not overlap, there is little variation in the total multiplet intensity. For the Bowen mechanism we assume that all of the atoms are in the lowest (J=2) level.

While the intensity due to Bowen fluorescence is more than an order of magnitude smaller than that due to direct resonance scattering, for comet velocities >40 km sec^{-1} it is the dominant source of cometary λ1304 emission. Using the Bowen g-factor, the oxygen production rate derived by Feldman et al. (1974) for Comet Kohoutek on 5.1 January 1974 was found to satisfy the requirement $Q_O = Q_{OH} = 1/2 Q_H = Q_{H_2O}$ expected if photodissociation of water is the dominant source of atomic oxygen. At smaller heliocentric velocities the comet might be expected to be extremely bright at 1304 A and in fact could provide, near perihelion, a measurement of the solar 1304 A multiplet profile free of the effects of terrestrial oxygen absorption since the cometary absorption width is small compared with the width of the solar emission profile. The role of photoelectron excitation has been neglected since it is assumed that the coma becomes collisionless at radii greater than $\approx 10^4$ km in which case the 1304 A image would appear to be less than 1 minute of arc contrary to the 10 arc min image reported by Opal et al. (1974).

Because of the steep slope in the solar line shape, corresponding to Doppler velocities of the order of ±25 km sec^{-1}, an appreciable intensity asymmetry (Greenstein, 1958) can result. To illustrate the effect of a rapidly varying solar line profile, we have computed atomic oxygen 1304 A intensities from Comet Kohoutek under somewhat idealized conditions. For resonance scattering, one must compute the probability that a photon of a given frequency and direction (from the sun) will be scattered at a new frequency in the direction of the observer. The procedure for doing this is described by Meier (1974). At each point in the atmosphere this probability function must be integrated over the solar line, the velocity distribution of oxygen, and the emitted line profile. The resulting volume emission rate must then be integrated along the line of sight to compute the column emission rate. Assuming a radial outflow density distribution and a radial maxwell-Boltzmann velocity distribution (Keller, 1973; Bertaux et al., 1973), we have computed the expected Greenstein effect. The idealized observation for the comet is taken to be at a 90° sun-comet-earth angle. Velocities of 0 and -22.5 km sec^{-1} relative to

the sun are used. The mean velocity of oxygen atoms is taken to be 1 and 2 km sec^{-1} both with a production rate of 10^{28} atoms sec^{-1} sr^{-1} and a g-factor appropriate to 1 A.U. The solar line shape in Fig. 4 was used. The line-center point of the comet rest frame is at $\dot{r}$=0 in Fig. 4. As discussed above, all atoms are assumed to be in the ground state so that although only the 1302.2 A line participates in excitation, all three lines will be present in emission.

The results of this calculation are shown in Fig. 6. The larger asymmetry found for the 2 km sec^{-1} outflow velocity is due to the broader cometary absorption coefficient overlapping a larger portion of the solar line. The $\dot{r}$ = -22.5 km sec^{-1} isophotes have both been normalized to the $\dot{r}$ = 0 case (a factor of 1.275) for purposes of comparison in the figure. Thus it is clear that the degree of asymmetry upsun and downsun can yield information about the mean velocity of the scattering gas when the solar line varies significantly over the absorption line.

CII λ1335 A

An anti-solar tail at least 5 x 10^6 km long and about 5 x 10^5 km wide was observed in the 1250-1800 A band before perihelion at r = .182 A.U. with the electrographic camera on Skylab 4 (Page, 1974). This feature should also have been observable by the rocket instruments, assuming an r^{-4} power law dependence of brightness on sun-comet distance, however the rocket images in that band of Opal *et al.* (1974) showed only a circular coma, attributed mainly to 1304 A oxygen emission, and the spectrometer of Feldman *et al.* (1974) observed down-sun of the comet for over 30 sec without detecting any emissions from the comet.

The tail observed from Skylab could be attributed to dust, a neutral species, or an ion. The dust tail hypothesis can probably be ruled out from geometrical considerations, but in any case it should have been observed by the more sensitive rocket instruments. For a neutral constituent to form the tail, it would have to be strongly influenced by radiation pressure yet have a very long lifetime, which is highly improbable at such a small sun-comet distance. The remaining candidate is an ion, with C^+ as the obvious choice, since it has a resonance multiplet in the bandpass (1335 A) and the sun

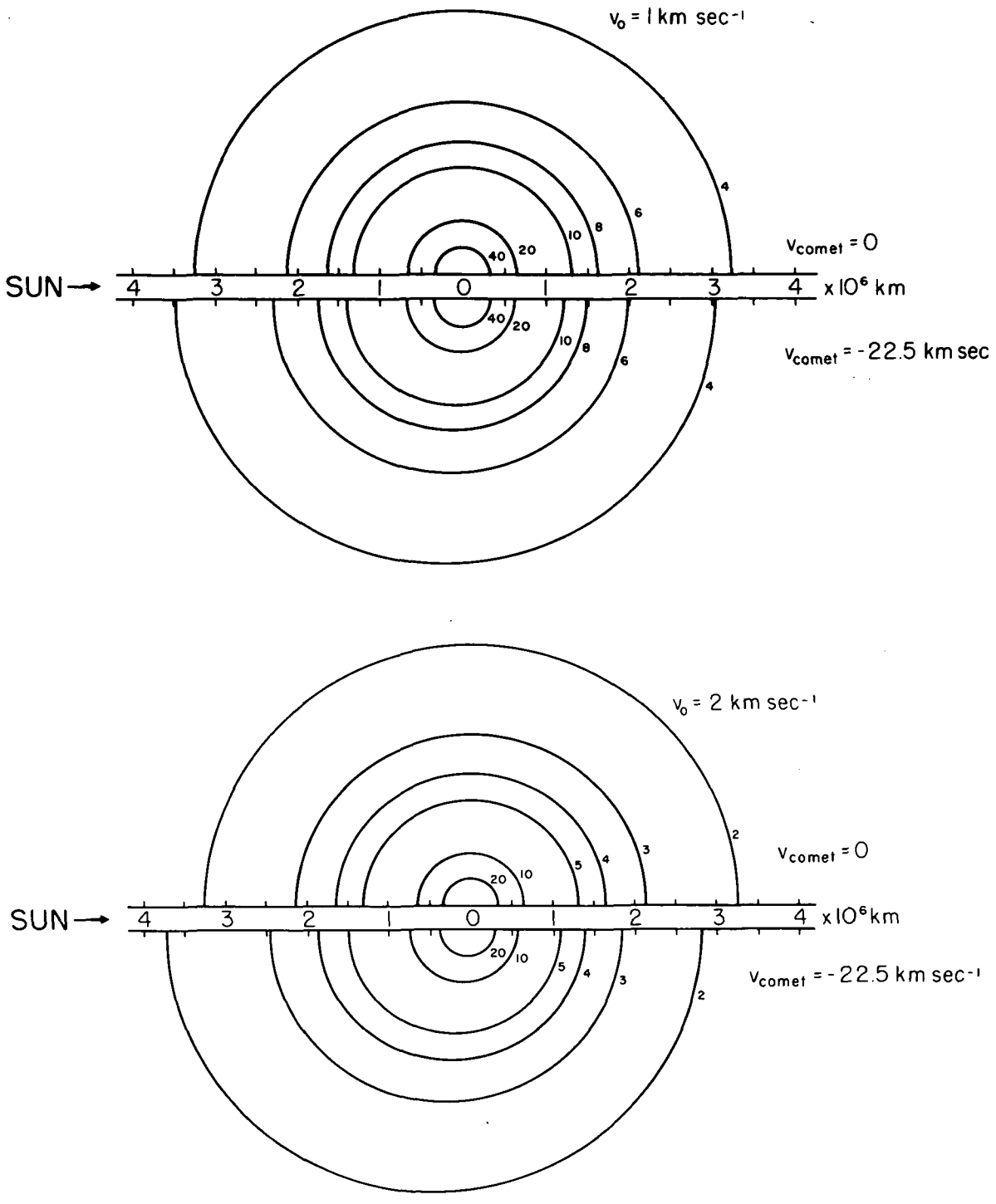

Fig. 6. Intensity contours for OI 1304 A computed for heliocentric velocities of 0 and -22.5 km sec^{-1}. The outflow velocity of oxygen atoms is 1 km sec^{-1} in (a) and 2 km sec^{-1} in (b).

emits the multiplet strongly. The fact that no ion tail was observed from the rockets after perihelion is explained by considering the motion of an ion created in a moving plasma. In the rest frame of a (perfectly conducting) plasma there is only a magnetic field, so the ion velocity consists of its original component parallel to the field plus a circular component due to its orbit around the field line. In the frame of the sun, the radial velocity of the ion will then consist of the sum of the radial velocity of the comet and a cycloidal component varying between zero and twice the radial plasma velocity (which can be as much as 10^3 km sec^{-1} outward if the ion is in the solar wind). Thus before perihelion the ions spend considerable time with a small radial velocity and can resonantly scatter the solar line. After perihelion the radial velocity of the ions can never be less than that of the comet, so at the time of the rocket observations, when the ions were always Doppler shifted completely out of the solar lines, the ionized carbon was unobservable.

CO Fourth Positive System

Fluorescence of CO in the fourth positive system ($A^1\pi - X^1\Sigma^+$) can be excited by solar radiation shortward of 1544 A. The g factors for the strongest bands are shown in Fig. 7, using oscillator strengths and branching ratios given by Mumma et al. (1971) and the continuum solar flux of Rottman (private communication; see Donnelly and Pope 1973). Since excitation is from the continuum there is no variation in the g-factors with $\dot{r}$. The g-factor for the total fourth positive emission between 1440 and 1670 A is simply the sum of all of the values shown in Fig. 7, 1.24×10^{-6} photons sec^{-1} mol^{-1}. The flux at the earth can be written as

$$F = \frac{Q \cdot g^{\tau}}{4\pi \Delta^2}$$

where Q is the production rate in molecules sec^{-1} and the product g^{τ} is independent of heliocentric distance and may conveniently be evaluated at 1 A.U. In Table II we give the values of g and τ for C, O and CO at the time of the rocket observations of Comet Kohoutek. If CO were in fact the parent of the observed carbon we would expect $Q_C = Q_O \approx \frac{1}{2} Q_{CO}$, since the CO photodissociation

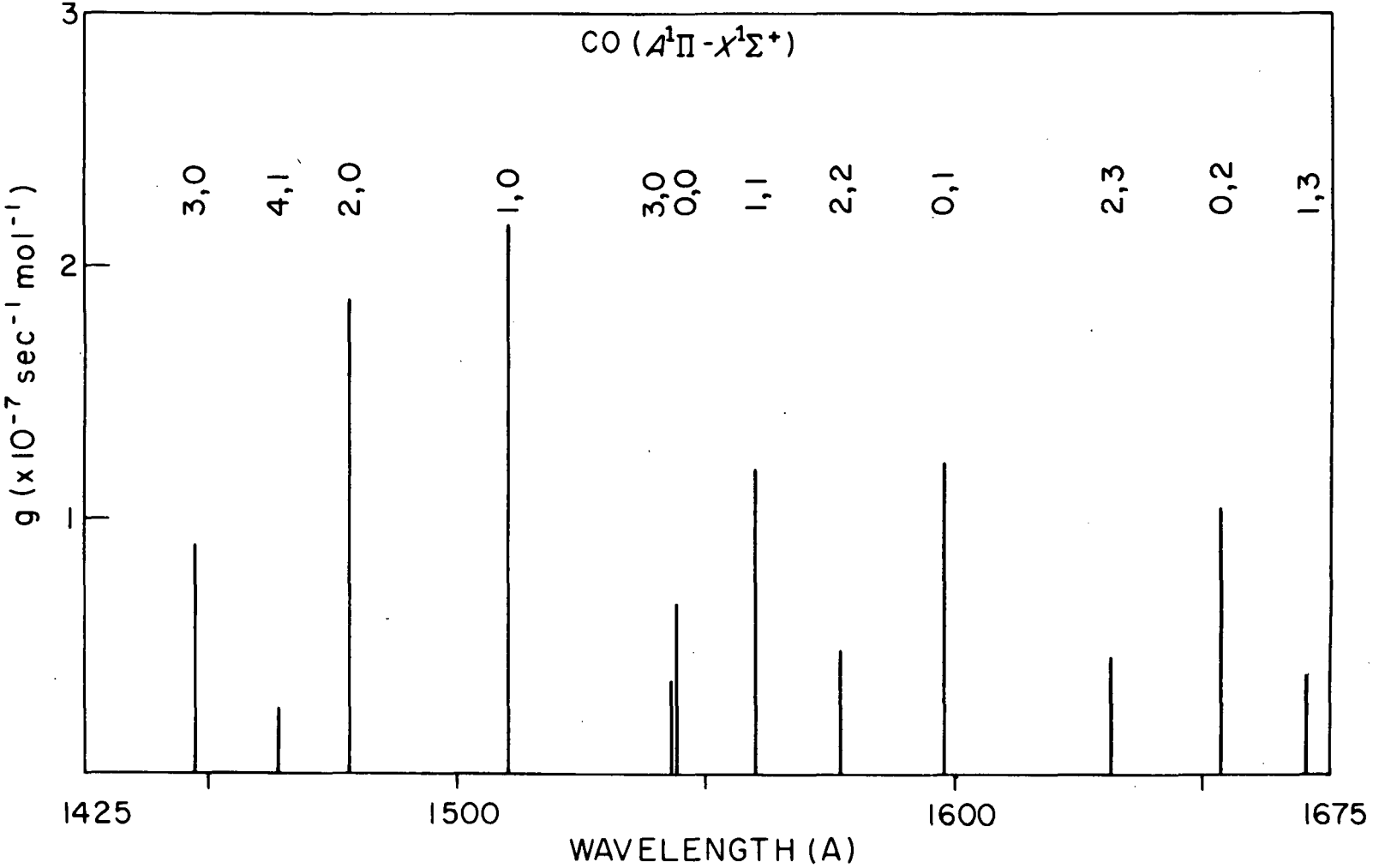

Fig. 7. g-factors for the strongest bands of the CO fourth positive system.

Table II

Excitation Parameters for $\dot{r}_\odot$ = +55 km sec^{-1}

Species	g (photons sec^{-1} mol^{-1})	τ (sec)	gτ (photons mol^{-1})	Relative Signal
CI λ 1657 A	2.5×10^{-5}	2.5×10^{5}	6.25	.49
OI λ 1304 A	3.4×10^{-7}	4.0×10^{6}	1.36	.28
CO (1440-1670 A)	1.2×10^{-6}	6.9×10^{5}	0.86	.23

(McElroy and McConnell 1971) and photoionization (Siscoe and Mukherjee 1972) rates are nearly equal. The table also gives the relative signal to be expected in this case, taking into account the response of a CsI photocathode, and it is seen that the three constituents give comparable contributions to the signal. Of course the primary source of oxygen, the photodissociation of OH, will give a larger 1304 A signal.

It should be noted that detection of the strongest CO bands was just beyond the sensitivity of both rocket instruments, but that an order of magnitude improvement in either the instrument capability of the brightness of the comet at the time of observation would have enabled us to determine whether or not CO is the parent molecule. The values of Q_i derived from the data of Feldman et al. (1974) have been revised using the g-factor discussed above, and are given in Table III. The upper limit on Q_{CO} is about a factor of 3 higher than would be expected from the derived Q_C.

The (9, 0) fourth positive band at 1301 A is nearly coincident with the OI line at 1302.17 A, raising the possibility of strong fluorescence in the $v' = 9$ progression. However, the absorption oscillator strength is smaller than that for the (1, 0) band by roughly the same amount that the solar flux in the line is greater than the continuum at 1510 A so that the absorption g-factors are of comparable magnitude. The rotational development of the band extends several A so that the overlap of the band with the relatively narrow OI line is less than 10%, as shown in Fig. 8 for T = 100°K. The maximum g-factor obtainable for any one band in this progression is $< 1.0 \times 10^{-8}$ which is considerably smaller than the values given in Fig. 7. A plot of the g-factor for the (9, 2) band at 1378 A as a function of $\hat{r}$ is shown in Fig. 9.

H_2 Lyman Band System

Solar HI Lyβ can also produce fluorescence in the $v' = 6$ progression of the Lyman band system of H_2 with the strongest emission in the (6, 13) band at 1608 A (Feldman and Fastie 1973). The P1 line lies at 1025.935 A while the wavelength of the Lyβ line center is at 1025.72 A, so that once again the g-factor is a sensitive function of $\hat{r}$. The dependence on $\hat{r}$ is the same as the dashed curve in Fig. 4, except that the velocity axis is shifted so that the peak g-factors occur at values of

Table III

SUMMARY OF RESULTS FROM AEROBEE 26.023

Species	F (photons sec^{-1} cm^{-2})	g (sec^{-1} mol^{-1})	τ (sec)	Q (sec^{-1})
OI 1304 A	120 ± 40	3.4×10^{-7}	4.0×10^{6}	2.1×10^{29}
CI 1657 A	140 ± 50	2.5×10^{-5}	2.5×10^{5}	0.5×10^{29}
OH 3090 A (0, 0)	3100 ± 100	1.2×10^{-3}	1.0×10^{5}	0.6×10^{29}
CO 1510 A (1, 0)	≤ 15	2.2×10^{-7}	6.9×10^{5}	$\leq 2.7 \times 10^{29}$

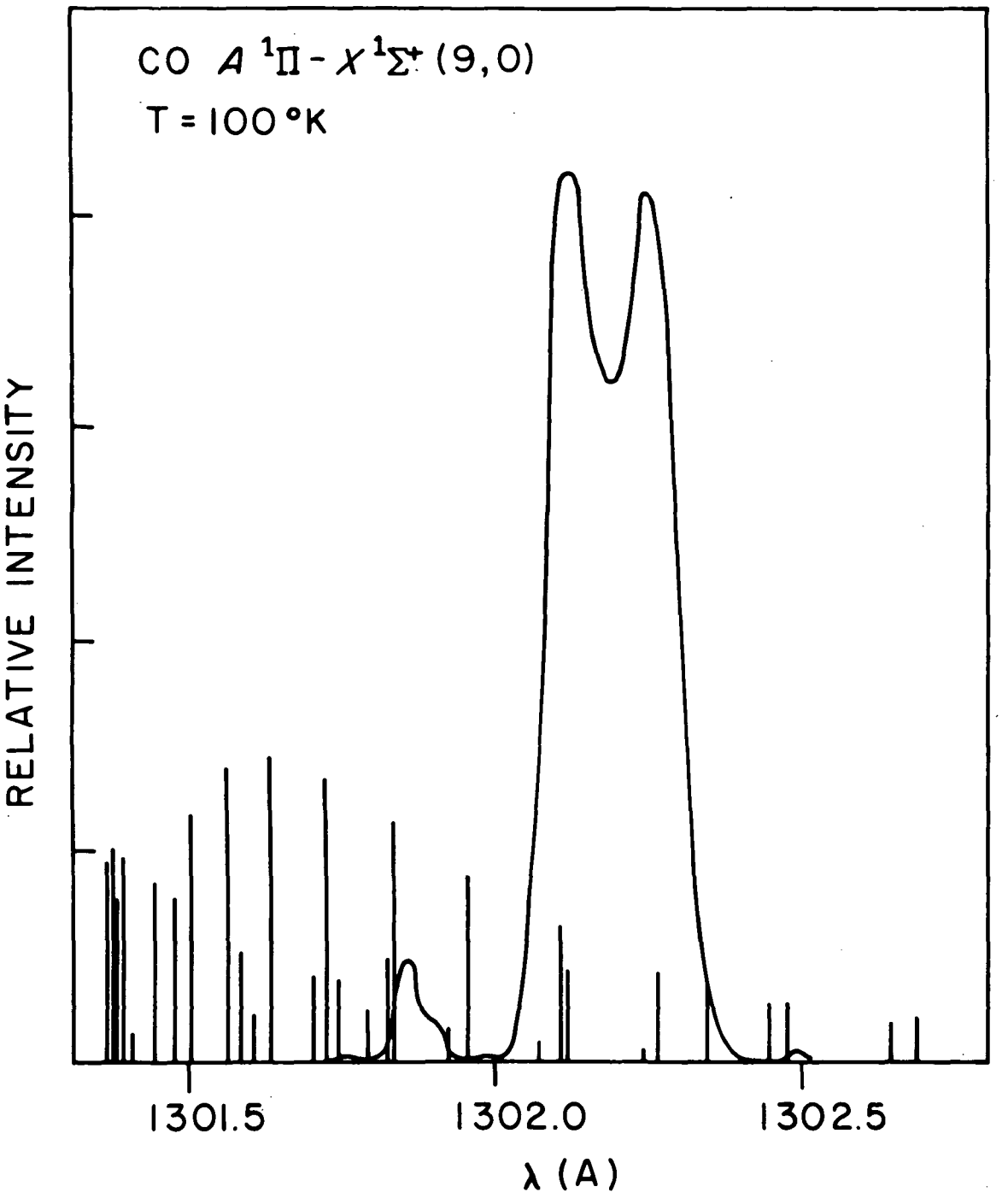

Fig. 8. Line strengths in the (9, 0) band of the CO fourth positive system showing the overlap with the solar OI 1203 A line.

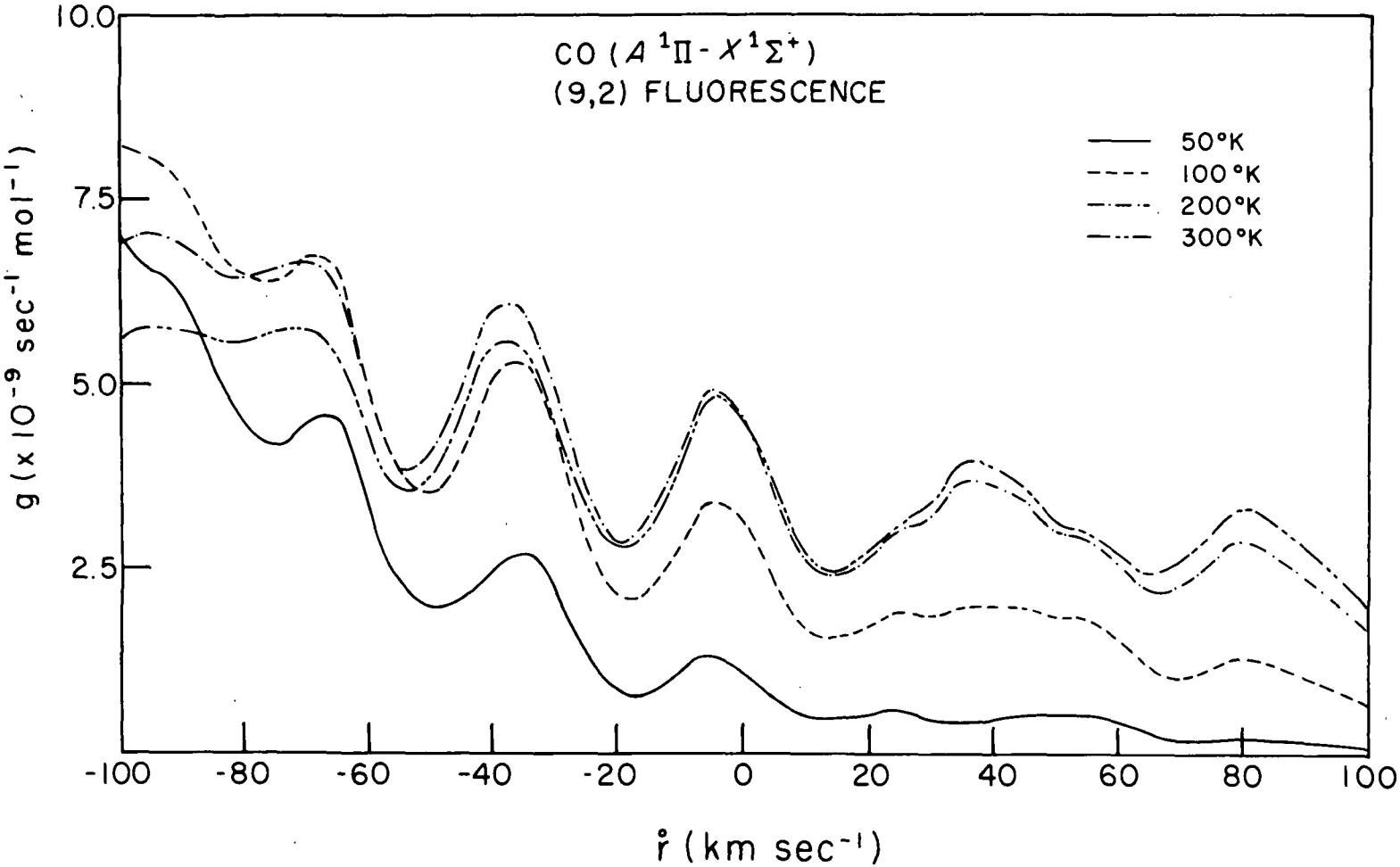

Fig. 9. Expected fluorescence in the (9, 2) band due to the overlap with the solar OI 1302 A line.

$\dot{r}$ of +15 and +110 km sec^{-1}. In this case, significant observations can be made only in the post-perihelion period. The maximum g-factor for the (6, 13) band is temperature dependent and has a value of 1.6×10^{-7} sec^{-1} mol^{-1} for T = 300°K at 1 A.U. Using this value, the data of Feldman et al. (1974) give an upper limit to the H_2 production rate an order of magnitude smaller than the production rate of atomic hydrogen.

SI λ1300 A

Finally, we consider the possibility of an accidental coincidence between a strong solar emission line and the resonance transition of a minor species. For example the sulfur multiplet near 1300 A contains a $^3P_1 - {}^3P_2$ line at 1302.34 which can resonantly scatter the OI 1302.17 A line over a wide range of heliocentric velocities. For this particular sulfur line the cooling time of the J=1 level is short ($\approx 10^3$ sec), so that resonance scattering from it is highly unlikely. However, in the general case of wavelength coincidence, the identity of the scattering species would have to be determined either by means of high resolution spectroscopy or from a measurement of intensity over a large range of values of $\dot{r}$. No unidentifiable features were found with either of the rocket spectrometers.

Future Observations

At present, the major uncertainty in the interpretation of cometary ultraviolet emission features lies in the value of the species lifetime. Many authors have evaluated photoionization and photodissociation lifetimes, but these are based largely on theoretical cross-sections. In addition, the effect of solar wind ionization is not understood since the extent of solar wind penetration into the coma is unknown. Photographs of the cometary coma in monochromatic ultraviolet radiation, similar to the Lyα photographs of Opal et al. (1974), if obtained at high enough angular resolution, should provide reliable values of the scale length and consequently of these lifetimes. Taken together with ultraviolet spectrophotometric observations of the species discussed above over a large range of heliocentric velocities and distances (presumably from an earth orbiting satellite), it should be possible to determine accurately both the total gas production rate in the comet and its dependence on heliocentric distance.

Acknowledgements

We thank Dr. R. Tousey and the NRL ATM Skylab team for permission to use the ATM results prior to publication. Mr. H. Park assisted in the calculations. The work at Johns Hopkins University was supported by NASA grant NGR-21-001-001.

References

Barth, C. A., 1969, Appl. Opt., 8, 1295.

Bertaux, J. L., Blamont, J. E., and Festou, M., 1973, Astron. Astrophys., 25, 415.

Brueckner, G. E., and Nicolas, K. R., 1972, Bull. A. A. S., 4, 378.

De Jager, C., 1961, in Vistas in Astronomy, Vol. 4 (Ed. A. Beer; London, Pergamon Press), p. 143.

Donnelly, R. F., and Pope, J. H., 1973, NOAA Rept. ERL 276-SEL 25.

Dupree, A. K., Huber, M. C. E., Noyes, R. W., Parkinson, W. H., Reeves, E. M., and Withbroe, G. L., 1973, Ap. J., 182, 321.

Feldman, P. D., and Fastie, W. G., 1973, Ap. J. (Letters), 185, L101.

Feldman, P. D., Takacs, P. Z., Fastie, W. G., and Donn, B., 1974, Science, 185, 705.

Greenstein, J. L., 1958, Ap. J., 128, 106.

Keller, H. U., 1973, Astron. Astrophys., 23, 269.

McElroy, M. B., and McConnell, J. C., 1971, J. Geophys. Res. 76, 6674.

Meier, R. R., 1974, in preparation.

Mumma, M. J., Stone, E. J., and Zipf, E. C., 1971, J. Chem. Phys., 54, 2627.

Opal, C. B., Carruthers, G. R., Prinz, D. K., and Meier, R. R., 1974, Science, 185, 702.

Page, T., 1974, paper presented at Comet Kohoutek workshop, Huntsville, Ala., June 1974.

Sandlin, G., 1974, private communication.

Siscoe, G. L., and Mukherjee, N. R., 1972, J. Geophys. Res., 77, 6042.

DISCUSSION

Voice: I just want to know if the values for production rates supersede the ones published in Science.

P. D. Feldman: Yes. They will appear in the proceedings of this conference. I don't think they are going to change. At least, we are not going to do any more work on it.

I think what is called for now are some more observations.

INTERPRETATION OF COMET SPECTRA

C. Arpigny

INTRODUCTION

This report will be devoted to a discussion of the theoretical interpretation of the spectra of comets and in this discussion we shall consider successively a number of molecules that have been studied recently : CN, CH, C_2, C_3, OH, CH^+. The first two of this list, CN and CH, have been analysed in greatest detail until now, so that we shall be rather brief on the other molecules. We shall try to indicate what kind of information can be derived from these studies concerning the conditions prevailing in cometary atmospheres and to show which fundamental data are needed in the calculation of the theoretical spectra.

Before going into the main part of the report, however, I should like to present a résumé of a paper of a general character which is concerned with the Spectral Classification of Comets and which is due to Dr. Bouška.

Up to now a few hundred spectra of several tens of comets have been obtained at different observatories over the world. On the one hand, there are high-dispersion spectra photographed with slit spectrographs attached to large telescopes, and on the other, small-dispersion spectra obtained by means of objective prisms.

It seems therefore useful to introduce a classification of the spectra of the cometary heads. It is evident that it is impossible to put into practice a classification similar to that used for stellar spectra. The classification of cometary spectra could rather be like the classification of meteoric spectra.

The cometary spectra show mostly two components :

(C) continuum which is the solar spectrum reflected on the dust particles present in the cometary coma, and

(E) emission bands (CN, C_2, C_3 and some others) connected with the intrinsic radiation of molecules in the cometary atmosphere.

The apparent intensity of these components may be weak (1), normal (2) or strong (3). In some exceptional cases continuum or emission bands may be absent (0). Consequently the classification may be as follows :

Continuum	Emission Bands	Apparent Intensity
C0	E0	absent
C1	E1	weak
C2	E2	normal
C3	E3	strong

In most cometary spectra the CN (0,0) band is dominant, in others the Swan bands of C_2; this may be expressed by the following symbols

c - cyanogen bands dominant,

s - Swan bands dominant.

The presence of the sodium doublet $D_{1,2}$ observed in cometary spectra at heliocentric distances $r \leq 1$ a.u.may be denoted by the symbol n.

Metallic lines are observed exceptionally, for instance in the spectra of Sun-grazing comets. Such spectra may be denoted by the symbol M.

The cometary spectrum depends, of course, on the comet's heliocentric distance and this distance must therefore be given in the classification of the cometary spectra.

The following examples illustrate the proposed classification :

C3E2c(0.6) Comet Arend-Roland (1957 III). Strong continuum, normal intensity of emission bands, CN (0.0) dominating; r = 0.6 a.u.

C1E2s(1.2) Comet Ikeya-Everhart (1966 IV). Weak continuum, normal intensity of emission bands, Swan bands C_2 ($\Delta v = +1$) dominating; r = 1.2 a.u.

I should like to make two very quick comments to this proposed classification scheme, which would indeed be useful for rapid communication through the IAU circulars, as well as for statistical studies of comet spectra.

First, the strength of the continuum, especially with respect to the discrete emissions, depends strongly upon the dispersion of the spectrogram used, so that it would seem desirable to specify this dispersion in the classification symbol. This point is illustrated on Figures 1 and 2, which show the region of the CN violet (0,0) band in Comet Bennett (1970 II) as observed at r ≃ 1.0 a.u. at the Haute-Provence Observatory using 12 Å/mm and 7 Å/mm reciprocal dispersions respectively. The continuum, which is strong even in this ultraviolet part of the spectrum, is nevertheless appreciably weaker relative to the discrete emissions when recorded at a higher dispersion.

The second remark is that the classification would be even more useful if it contained some information about the spectra of the ions, in particular of CO^+.

I should now apologize to those who are well acquainted with cometary spectroscopy, but it seems worthwhile, for those who are not so familiar with this subject, to start with a short summary of the basic ideas underlying the interpretation of the spectra of comets. This anyhow will set the stage for what we are going to discuss later on. A more complete presentation can be found elsewhere (Arpigny 1971).

When one examines all the possible mechanisms he can think of

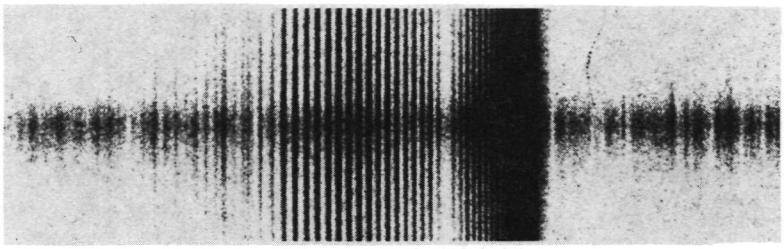

Fig. 1 - The region of the CN Violet (0,0) band in Comet Bennett (1970II) - (Haute-Provence Observatory; original reciprocal dispersion : 1.2 Å/mm).

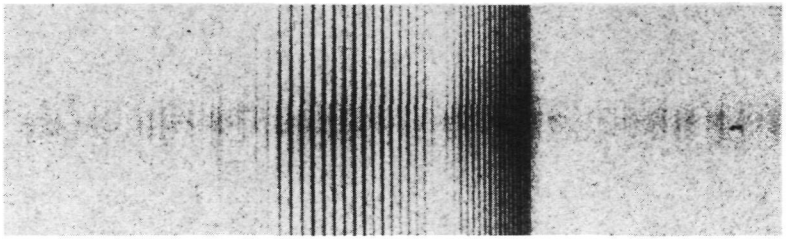

Fig. 2 - The region of the CN Violet (0,0) band in Comet Bennett (1970II) (Haute-Provence Observatory; original reciprocal dispersion : 7 Å/mm).

for exciting the electronic transitions observed in cometary spectra, he finds that the only plausible process is one of resonance-fluorescence in which solar radiation is absorbed in their resonance transitions by the cometary molecules, which re-emit right away in the same electronic systems. This is due to the very long timescales associated with the other processes, typically of the order of 10^5 to 10^6 sec or larger. The processes in question are, for instance, collisional excitation by cometary heavy particles or electrons or by solar wind particles and the long characteristic times are due either to low densities, or to the low energies available, to rather small cross-sections, or to a combination of these. By contrast, the characteristic times for absorption of solar radiation in the "optical" region are of the order of 10 to 100 sec for the molecules or atoms observed in comets near one a.u. from the sun. The corresponding relaxation time or the time for a steady state to be established is about several 100 to several 1000 sec. Now the excitation conditions, which depend upon the intensity of the solar radiation available at the various transitions and hence upon the heliocentric distance r and upon the heliocentric radial velocity dr/dt, remain essentially constant during a time of that order and we are therefore justified in assuming that stationary conditions will indeed be therefore justified in assuming that stationary conditions will indeed be reached.

CN.

As an example, we shall consider the emissions of cyanogen and we shall first simplify the situation in order to emphasize the essential features of the mechanism. Thus, we shall (a) assume that the only transitions to be considered are those in the (0,0) Violet band (b) neglect the small spin splitting in the X and B $^2\Sigma^+$ electronic states (c) consider that all the CN radicals are moving at the same velocity relative to the sun, i.e. the orbital dr/dt. According to our assumptions, we have only two kinds of electronic transitions, P and R transitions. In addition to these, pure rotational transitions in the ground state must be included. Under

steady-state conditions we equate the rates of population and of depopulation of the rotational levels and by considering the absorption-emission cycles which connect these levels it is easy to obtain at once a set of equations involving the populations, x_N, of the lower rotational levels only. For level N (≡N", rotational quantum number) we have

$$x_{N-2}\cdot(\bar{s}_R)_{N-2}(s_P)_N\, C_{00} + x_{N+1}\, A^{rot}_{N+1,N} + x_{N+2}\cdot(\bar{s}_P)_{N+2}(s_R)_N C_{00}$$

$$= x_N\{[(\bar{s}_R)_N(s_P)_{N+2} + (\bar{s}_P)_N\,(s_R)_{N-2}]\, C_{00} + A^{rot}_{N,N-1}\} \qquad (1)$$

where the C's and the A's are transition rates per molecule in the initial level; C_{00} is the overall absorption rate in the (0,0) band. $\bar{s}$ and s are the absorption and emission intensity factors, respectively, representing the appropriate rotational line strength divided by the statistical weight of the initial level of the transition. $\bar{s}$ contains in addition the residual intensity factor, i_λ, which takes account of the energy available in the solar spectrum at the excitation wavelength of the transition. For example, the first term in equation (1) is the rate of the RP fluorescence process N-2 → N' = N-1 → N($x_{N-2}(\bar{s}_R)_{N-2}\, C_{00}$ = transition rate for absorption of the R (N-2) line; $(s_P)_N$ = branching ratio for the downward P(N) transition).

Once the system represented by eq. (1) has been solved (in practice about 30 rotational levels must be included in the lower electronic state), the populations of the upper levels as well as the relative intensities of the lines can be readily computed. These populations and intensities will be governed by two effects :

(i) the first effect is the balance between the two kinds of processes:
   a) the fluorescence cycles tend to increase the rotational energy of the molecules in the electronic ground state (if we start out with all molecules in the lowest rotational level, the distribution of molecules will be spread toward higher levels via RP cycles);

b) the pure rotational transitions on the contrary tend to return molecules back to lower levels;

(ii) besides this competition, the spectral energy distribution in the exciting solar radiation plays a predominant role.

The fluorescence terms in the steady-state equations all contain C_{oo}, while the pure rotation transition terms are proportional to A^{rot} and the determining factor is the ratio between these, represented by a quantity

$$\mathcal{R} \div \frac{\mu^2 r^2}{f_{oo}}$$

μ being the permanent dipole moment of the molecule, f_{oo} the f-value of the electronic transition. The distribution of populations will go through a maximum which will occur at a smaller rotational energy, the larger $\mathcal{R}$ is. Thus, for a given molecule, with μ and f_{oo} fixed, the maximum will occur at lower rotational quantum numbers for the larger heliocentric distances. On the other hand, at a given r, the rotational "excitation temperature" will be different for the different molecules. It will be low for heteronuclear molecules, and large for homonuclear molecules like C_2 or for an atom like F_e which has a number of low-lying metastable terms. In the latter case ($\mathcal{R}$ very small) it can be shown that the excitation temperature approximates the colour temperature of the exciting solar radiation in the relevant wavelength range.

If we now consider the second effect mentioned above, i.e. the effect of the solar spectrum, we see that the very irregular character of this spectrum, with numerous Fraunhofer lines in the region of the CN Violet system for example, is responsible for the irregularities observed in the intensity profiles of the cometary emissions. This interpretation was given for the first time some 30 years ago by Swings (1941) who also pointed out that the intensity distribution would be very sensitive to the heliocentric radial velocity of the comet.

The first computations based on such a simplified ("zeroth order approximation") model were made about 10 years ago by Carrington (1962) and by myself (1964). The comparison of the observed and theoretical spectra for Comet Mrkos (1957V) showed that the general character of the distribution was rather well represented by the computations, but there were some discrepancies. In particuliar, the R(7) and R(8) lines were predicted appreciably too high. It was hoped that the situation would be improved if one included transitions in the Red system of CN in the calculations because there are fewer absorption lines in the red region of the solar spectrum and this would smooth out the distribution of populations. While this is indeed the case, one is still left with differences which can reach about 35 % for a few weak lines in the region of higher quantum numbers. Another example of simplified model calculations is given in Figure 3. This is the R branch of the CN (0,0) band in Comet Bennett (1970 II). The spectrum was computed by Aikman et al (1974) and one sees again a good general agreement, although a few significant differences are noticed between observed and theoretical spectra.

Let us note that from the value of $\mathcal{R}$ required to compute the synthetic spectra one can derive a value for the dipole moment if f_{oo} is known and we may mention in passing that the value obtained from the zeroth order approximation was used in the interpretation of the excitation of interstellar CN radicals (Field and Hitchcock 1966) at a time when no experimental determination existed for μ. This is an example where, even if the value for μ was crude, cometary spectroscopy has been of some help in connection with an outstanding astrophysical problem, which in fact was related with no less than the origin of the Universe !

We shall come back to the analysis of the rotational structure of CN, but let us first say a few words about the relative band intensities in the Red and Violet systems of this radical in comets. We consider nine vibrational levels in each of the $X\ ^2\Sigma^+$, $A\ ^2\Pi$, and

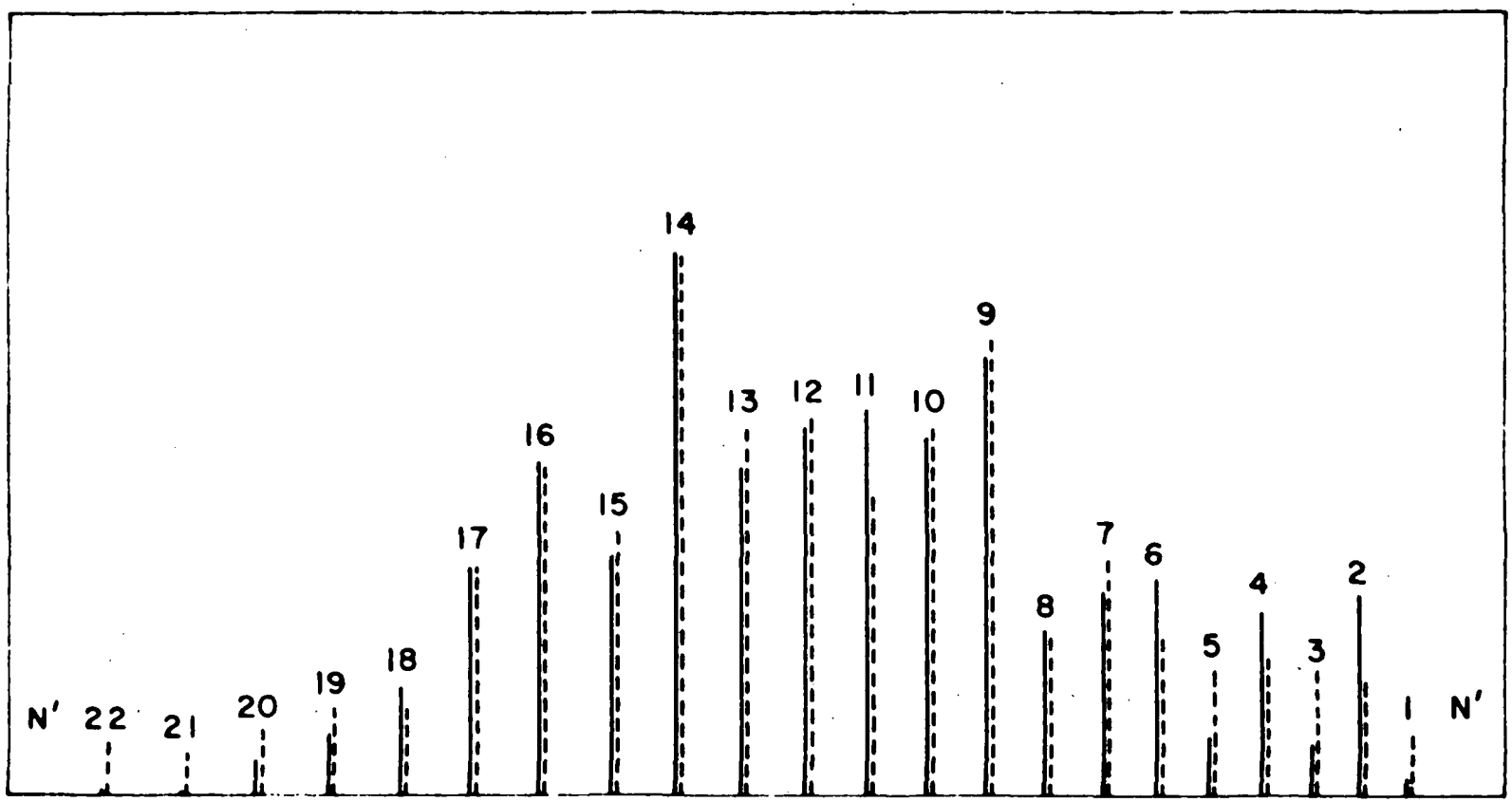

Fig. 3 - The R-branch of the CN Violet (0,0) band in Comet Bennett (1970II). Dashed lines : observed spectrum; solid lines : spectrum calculated on the basis of the simplified model assumptions (taken from Aikman et al, 1974).

B 2E+ electronic states and write steady-state equations under solar radiation excitation. Just as we have defined a quantity $\mathcal{R}$ for the rotational structure, we define here $\nu = A_{10}^{vib} / C_{00}^{\nu}$, A_{10}^{vib} being the Einstein coefficient for spontaneous emission of the vibration-rotation fundamental band and C_{00}^{ν} the absorption rate in the Violet (0,0) band. A_{10}^{vib} is not known, so that ν must be treated as a variable. Another relevant quantity is the ratio of the f-values of the Violet and Red (0,0) bands, $f_{00}^{\nu} / f_{00}^{R}$ (hereafter called FR), about which there is also some uncertainty. Some computations have been made recently by T. Danks and myself (1973) in an attempt to interpret O'Dell's and some older observations by Dufay and Swings of some CN Red and Violet bands in comets Tago-Sato-Kosaka (1969 XI) and Mrkos (1957 V), respectively. By varying ν (or ν_1, its value at r = 1 a.u.) and FR and looking for a fit with the observed intensity ratios, we find a region defined in Figure 4 by the thick-lined box inside which the fit is possible. We have here two cases corresponding to two different sets of relative f-values within the Red and Violet systems. The dot and error bar indicate the most recent experimental value for FR and we see that in one case there is no overlap while in the other there is. The thin lines indicate how the right-hand boundary of the "fitting" box is shifted for a change by 5 % and by 10 % in the observed value of R_{31}/R_{20}, the ratio of the Red (3, 1) and (2, 0) bands. The sensitivity is very high indeed. The conclusion of our study is that ν_1 is certainly > 10, i.e. $A_{10}^{vib} > 1\ sec^{-1}$, and that FR $\geq$ 15, but new, accurate measurements of several band intensity ratios in comets would be most welcome.

We now return to the rotational structure of the CN comet spectra. A number of important refinements were brought about by Malaise (1970) a few years ago, especially with respect to the model of the coma. As far as the CN molecule itself is concerned, Malaise considers radiative transitions in the (0, 0) Violet band and in several Red bands, as well as pure rotation and vibration-

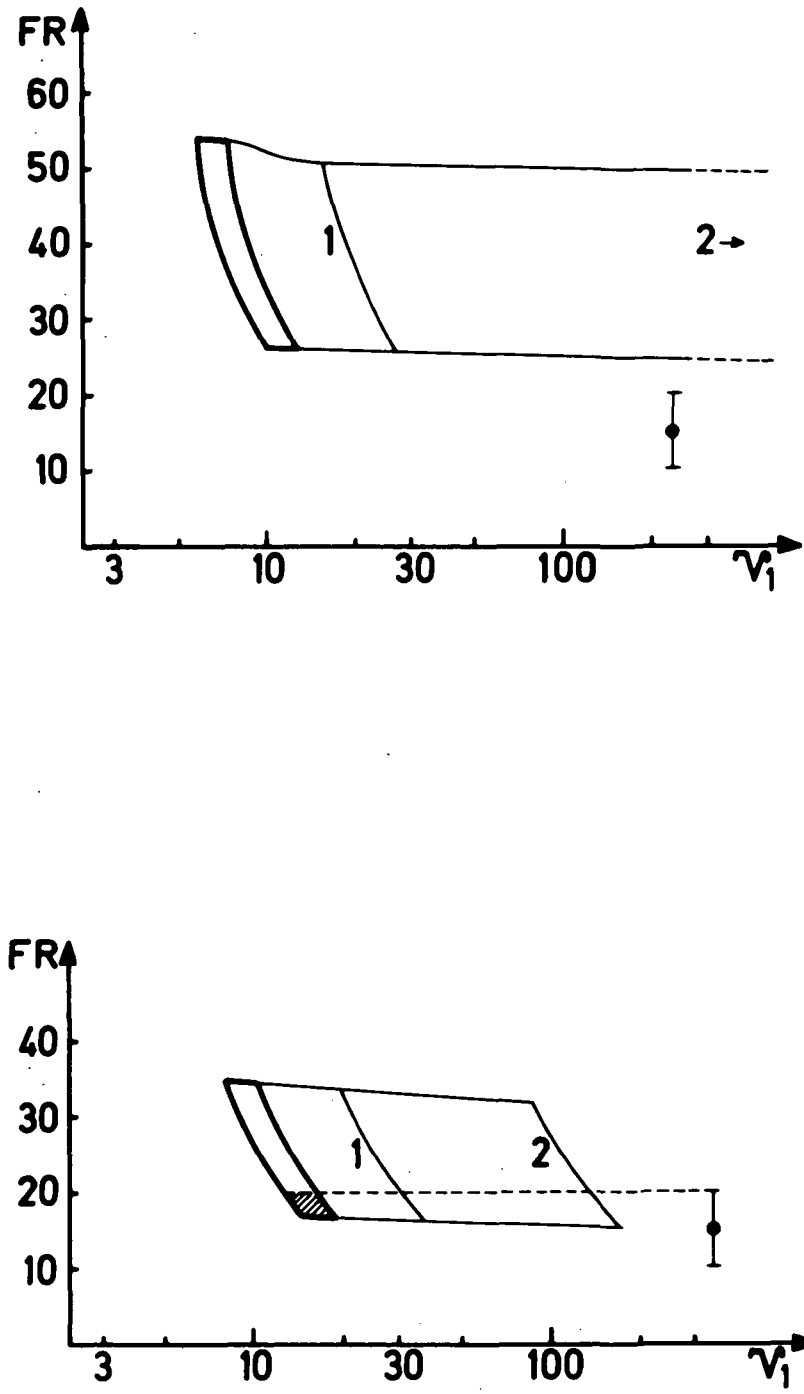

Fig. 4 - The regions of possible fit between the observed and calculated CN band intensity ratios for two different sets of relative f-values within the Red and Violet systems (see text).

rotation transitions in the ground state. He also takes account of the spin splitting, as required. Besides these radiative transitions, Malaise introduces for the first time in such calculations the effects of some collisional processes which could excite the rotational levels within the ground electronic state. Such transitions among rotational levels require much less energy and have larger cross-sections than the electronic excitations and if the densities of exciting molecules are high enough, the collisions may compete with or even dominate the radiative transitions within the ground state. One immediately realizes the considerable interest of this, because it gives a hope to estimate <u>total</u> particle densities or the densities of the main constituents of the cometary gas, as opposed to the already known densities of the observed radicals, which are minor constituents. If the collisions are predominant, the lower rotational levels of CN will be populated according to Boltzmann's law at the temperature of the colliding particles and the way in which Malaise takes account of the collisions is as follows. The population of each lower rotational level is written as a linear combination of the corresponding Boltzmann population and pure fluorescence population :

$$x = \alpha x^B + (1 - \alpha) x^F, \qquad (2)$$

where α gives a measure of the relative importance of the collisional and radiative mechanisms and is taken from the relation

$$\frac{\alpha}{1-\alpha} = \frac{\tau_F}{\tau_F} = n \bar{v} \sigma \cdot \tau_F, \qquad (3)$$

τ_F being the time necessary to reach a steady-state under fluorescence conditions (this is estimated to be a few 100 sec for CN at 1 a.u. from the sun), τ_C the collision time, n the density of exciting molecules, $\bar{v}$ the average relative velocity, and σ the cross-section for collisional excitation. Now this looks reasonable at first sight, since the expression (2) gives correct asymptotic values at the extremes of high and low densities. When n is high, the collisions

dominate, the ratio (3) will be large, hence α will be near unity and the populations will be Boltzmannian, while for low n the ratio is small, hence α will be near zero and we have essentially pure fluorescence populations. However, the validity of eq. (2) in the intermediate situations is highly questionable, as we shall see later on when we discuss the case the of the CH radical. At any rate, n and therefore α are functions of position within the comet and the calculations have to be made and eq. (2) used at a number of points. An integration is then performed along the line of sight. For this, of course, model distributions must be appropriately chosen for n (R) and n_{CN} (R), R being the distance from the centre of the comet. The former distribution is adjusted while making the computations of synthetic spectra, whereas the latter is derived from the observed radial profile of CN emissions (intensity distribution in the direction perpendicular to the dispersion). Furthermore, it can be shown that the cometary gas is optically thin in the light of CN, so that the integration reduces to a simple summation. On the other hand, the kinetic temperature of the exciting molecules (related to $\bar{v}$) is considered to be constant throughout the comet, which is only a rough approximation.

Another important effect comes in also, that is the influence of the motions of the radicals within the atmosphere of the comet. Such motions are of course expected, but their existence is actually inferred in the interpretation of the so-called Greenstein effect, which consists in differences in the relative intensities of the spectral lines in different regions of the comet, for instance on the two sides of the nucleus. The model adopted is one of uniform, isotropic expansion where the radicals move radially away from the center with velocity v_o. What counts, of course, is the component of this v_o on the direction to the sun and Malaise computes a projection factor in terms of the phase angle sun-comet-earth, assuming that the sun lies in the plane defined by the slit of the spectrograph and the line of sight. This assumption is often not

valid, however, and this does introduce in some cases significant errors in the residual intensities i_λ which enter the steady-state equations. The heliocentric radial component of v_o obviously varies with position along the line of sight and this is another reason for making an integration.

Four high-dispersion and four medium-dispersion spectra of comets obtained at the Haute-Provence Observatory were studied by Malaise. The comparison between observed and theoretical spectra shows a rather satisfactory agreement, but there are again a few lines for which the discrepancy reaches about 20 %. Two quantities come out of this kind of analysis. One is T, the kinetic temperature of the colliding molecules and the other is the expression $n_o \sigma \tau_F / \sqrt{M}$, where n_o is the total density (or a minimum value for this total density, if the exciting species is not a predominant constituent) at some reference distance from the nucleus, say at $R = 10^4$ km, while M is the reduced mass of CN and the exciting molecule. There are three comets for which Malaise finds important collisional effects, namely Seki-Lines (1962 III), Ikeya (1963 I), and P/Encke (1961 I) (α_o, the value of α at $R = 10^4$ km, equal to 0.90, 0.90 and 0.55, respectively). Assuming the gas to be made primarily of H_2O or CO for instance, and taking σ equal to the gas-kinetic cross-section, one derives (after multiplication of the second member of eq. (9) of Malaise (1970) by a correcting factor of $1/\pi$, that of eq. (11) by $2/\pi$) : $n_o \simeq 10^9$ cm^{-3} for the first two comets, and $n_o \simeq 10^8$ cm^{-3} for P/Encke. The corresponding total production rates are $Q \simeq 10^{33}$ and 10^{32} molec. sec^{-1}, respectively. These are lower limits if the production of the exciting molecules does not take place entirely in a region the dimensions of which are small compared to 10^4km. The first figure is some three orders of magnitude larger than $Q(H_2O)$ observed in Comet Bennett (1970II), which belongs to the same general class of rather bright objects as Seki-Lines and Ikeya, while the second figure exceeds by about four orders of magnitude the value of $Q(H_2O)$ derived for Comet Encke itself at a similar heliocentric distance during itsperihelion passage of 1970. One may also say that with

the above densities and production rates the total mass loss $\Delta\mathcal{M}$ of each of these comets during one revolution around the sun would be close to or even greater than its mass $\mathcal{M}$, as shown in Table 1. The $\Delta\mathcal{M}$'s computed here are based upon the Q's quoted above, parabolic orbits, and various power laws for the variation of Q with heliocentric distance $Q \div r^{-n}$, with $n = n_o + n_1\sqrt{r}$, n_o and n_1 being in each case chosen in such a way that n lies near 2 to 2.5 for r near one a.u. — cf Keller and Lillie, 1974). On the other hand, the $\mathcal{M}$'s are evaluated using the radii derived by Miss Roemer (1965) from "nuclear" magnitudes (the albedo is taken here equal to 0.1, probably on the low side of the actual value) together with a density of one $g.cm^{-3}$. The corresponding values of $\mathcal{M}$ represent upper limits to the masses of the comets, for the nuclear magnitude tends to overestimate the luminosity of the nucleus, hence its radius, because of a non-negligible contribution from a halo surrounding the nucleus, and if we have to do with separated particles rather than with just a monolithic nucleus, the total mass for a given total reflecting area will be smaller than if we assume the presence of only one single body. Clearly there is a very serious difficulty regarding the molecular densities which Malaise's results lead to. There are only two factors multiplying n_o in the expression given earlier that could possibly influence the conclusions, namely σ and τ_F.

The value adopted for σ, i.e. 2×10^{-15} cm^2, does not appear to be too small by any significant factor and on the contrary can be deemed rather good from what is known about cross-sections for translational to rotational energy transfer (Gordon et al, 1968). One might consider that the agents producing rotational excitation are charged particles. With the very large cross-section calculated by Crawford et al (1969) for excitation of CN by slow ($\approx$ 0.05 ev) electrons, in order to reach the collision rates of 0.03 to 0.3 sec^{-1} in question here one would need 10^5 such electrons per cm^3 or more, which seems rather high, although we have unfortunately no direct evidence about electrons in comets. As far as heavy ions are concerned, while it cannot be expected that the corresponding cross-sections be

Table 1.
A Comparison Between Mass Losses and Masses for Three Comets.

Comet	$\Delta\mathcal{M}(10^{16}$g.)	$\mathcal{M}(10^{16}$g.)
Seki-Lines (1962III)	$\gtrsim$100-300	$\lesssim$40
Ikeya (1963I)	$\gtrsim$ 20-30	$\lesssim$20
P/Encke (1961I)	$\gtrsim$ 5-7	$\lesssim$ 2

$\Delta\mathcal{M}$ is calculated as follows. It is assumed, for the sake of simplicity in these order of magnitude estimates, that the rate of mass loss is the same after perihelion as it was before, so that

$$\Delta\mathcal{M} = 2 \int_0^\infty Q\, dt \qquad (t = o \text{ at perihelion}).$$

Now, if Q_s is the value of Q derived from a spectrum taken at $r = r_s$ and if $n_s = n(r_s)$, we can write

$$Q = Q_s \left(\frac{r_s}{q}\right)^{n_s} \left(\frac{q}{r}\right)^n \qquad (q = \text{perihelion distance}),$$

while for a parabolic orbit we have $r = q\,(1+\beta^2)$ and $\tau = \beta+3\beta^2$, provided that $\beta = \tan(w/2)$ (w = true anomaly) and we have substituted $\tau = C^{-1}t$, with $C = (29^3)^{1/2}.(3k)^{-1}$ (k = Gaussian gravitational constant). Finally, we obtain

$$\Delta\mathcal{M} = 6CQ_s \left(\frac{r_s}{q}\right)^{n_s} \int_0^\infty (1+\beta^2)^{1-n(\beta)}\, d\beta,$$

which is readily evaluated by a numerical integration. Note that the use of a parabolic orbit is a good approximation even for Comet Encke because the contribution to the integral gets small once r becomes large compared to 1 a.u. or β large compared with $(q^{-1} - 1)^{1/2}$ (the perihelion distances of the three comets are 0.03, 0.63, and 0.34 a.u. respectively). Besides, the $\Delta\mathcal{M}$'s are essentially unchanged if it is assumed that the activity of the comets stops at some distance r_M from the sun, say 3 a.u., and the upper limit of the integral accordingly replaced by $\beta_M = (r_M/q - 1)^{1/2}$.

three or four orders of magnitude larger than the gas kinetic cross-sections, it is also unlikely that the production rate of ionized species be much larger than the production rate for the neutrals.

On the other hand, one might think that one way out of the difficulty would be to say that τ_F has been wildly underestimated. In fact, however, this relaxation time was computed for CN excited by sunlight some ten years ago (Arpigny, 1964) and the result was of the order of 10^2 sec at one a.u. from the sun, which indeed agrees with the value adopted by Malaise. Besides, it may be pointed out that if one reduced the densities considerably by artificially increasing τ_F, for instance, by several orders of magnitude, then he would be faced with another problem, namely that the collision times even further in, say at 10^3 km from the nucleus, would become large compared with the radiative lifetimes of the rotational levels, so that the concept of a Boltzmann distribution of populations would become meaningless.

Let us now make a remark illustrating another point, related to the fundamental data required for the computation of the synthetic spectra. Malaise found in particular for a spectrum of Comet Ikeya (1963I) that the reason why collisions were needed to reproduce the observed spectrum was that fluorescence alone predicted too small intensities for the lower rotational lines relative to the higher, whereas a better agreement could be obtained by introducing "mixed" populations (eq. 2) and adjusting the "rotational temperature" properly. However, it can be argued that the relative intensities of the lower rotational lines could be increased, under pure fluorescent excitation, by increasing the value of $\mathcal{R}$, i.e. of the dipole moment of CN. Indeed, the experimental value of μ is about twice the value used by Malaise. More should be said about the values of $\mathcal{R}$ and of ν adopted by this author, but such a discussion would be outside the scope of the present review.

Something should also be said about the wavelengths scales. In spite of Malaise's very careful and thorough discussion of the data on the λ's of the CN Violet lines that were available when he made

his computations, he had to use λ's which, we know now from recent analyses, were in a number of cases in error by up to 15-20 mÅ (although many lines had better λ's). This is significant because such displacements in the solar spectrum can produce appreciable changes in i_λ. The new λ's are accurate within $\approx \pm$ 2 mÅ. Furthermore, we now have separate wavelengths ($\Delta\lambda$ = 15-30 mÅ) for the components of the spin doublets (down to N = 7), which were unresolved previously. On the other hand, Malaise had to make use of solar spectra of the center of the disk which were also affected by wavelength uncertainties of the order of 5-10 mÅ. Recordings of the solar spectrum, of the integrated light from the disk, with considerably more accurate wavelengths ($|\Delta\lambda| \lesssim$ 2-3 mÅ) now exist. Use of the new data should hopefully give a satisfactory interpretation of the Greenstein effect and thus allow a good determination of the velocities of the CN radicals in the coma (The velocities given by Malaise correspond to shifts that are smaller than 10 mÅ, so that the wavelengths scales should preferably be known with a rather high accuracy !).

Finally, let us have a look at Figure 5, which shows a very beautiful spectrum of Comet Bennett (1970II) taken by Preston with the 100-inch telescope on Mount Wilson. At the reciprocal dispersion of 4.5 Å/mm the P-branch of the CN Violet (0,0) band is completely resolved. We also see a number of weak lines in between the principal lines : these belong to the (1,1) band and they should be included in a refined treatment, especially for example if one wants to make a search for isotopic lines, which also fall in between the lines of the main band. Notice a somewhat stronger line just shortward of R(14) : this is a blend of the P(2) line of the (1,1) band with a perturbed line. There are a few such perturbed lines in the R and in the P branch of the (0,0) band and their analysis in very high-dispersion comet spectra could provide some insight on the formation of CN radicals in excited states and on the rates of collisional processes.

In conclusion, it is clear that CN in comets deserves further study. The more detailed analysis of the rotational structure of the Violet (0,0) band shows a good agreement between computed and observed

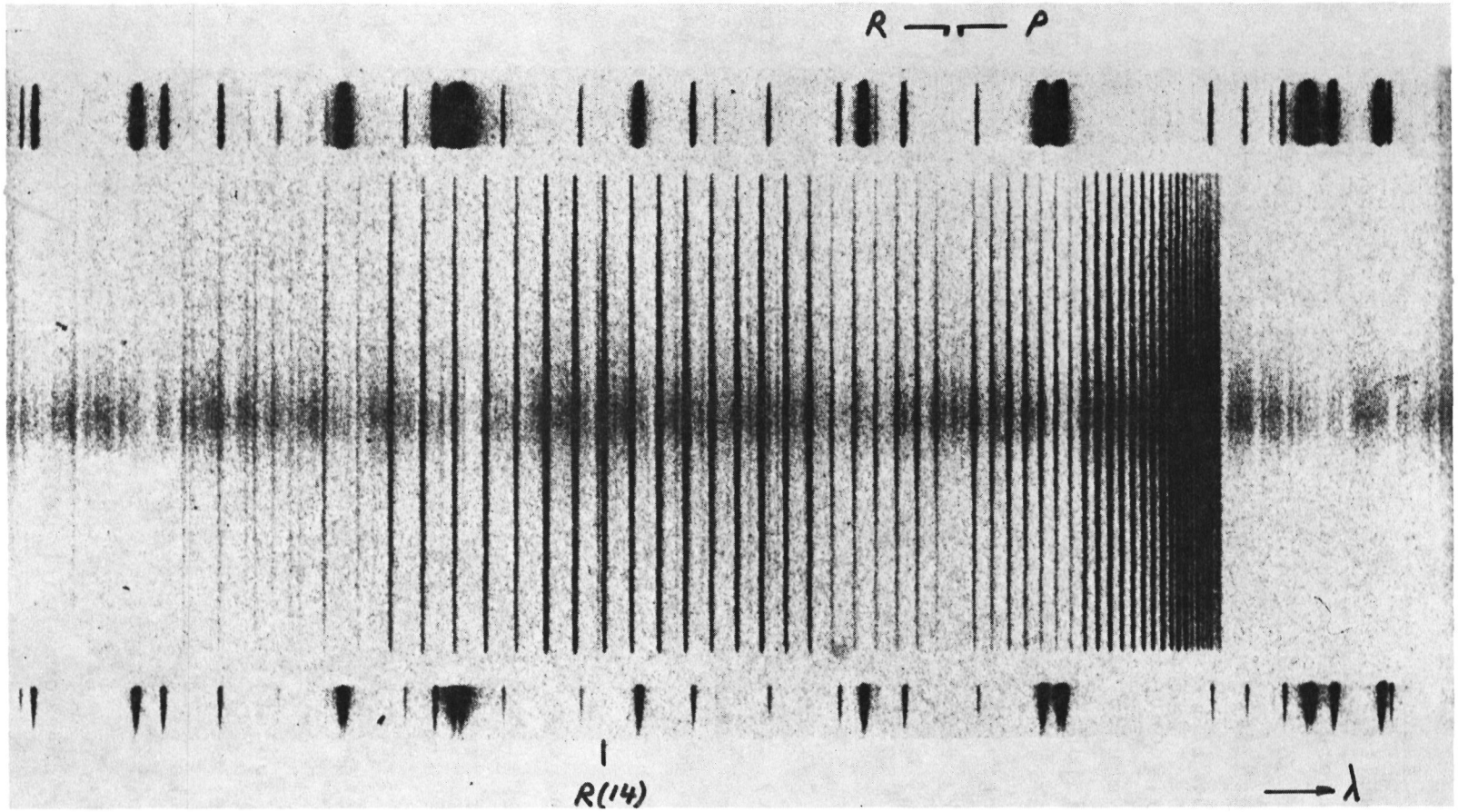

Fig. 5 - The CN Violet (0,0) band in Comet Bennett (1970II) (Mount Wilson Observatory; original dispersion : 4.5 Å/mm). Note the weak lines due to the (1,1) band in between the stronger features. The emission next to R(14) on the left is partly due to a perturbed line.

spectra, but we have seen that the zeroth order approximation already gave rather good results. This is indeed a rather awkward situation and in order to interpret the finer details and thus to assess the actual importance of collisional effects, to derive reliable information on the densities, temperatures, and velocities within cometary atmospheres, if is in fact necessary to treat the excitation mechanism rigorously, to use the most precise fundamental data available, to improve upon the model of the coma. It would even be desirable, in my opinion, to have recourse to photoelectric photometry, to avail ourselves of a higher accuracy in the observations themselves, just because the margin between the results of the simplified analysis and those of the more refined treatment is rather narrow.

CH.

We now come to the spectrum of the λ 4300 band of the CH radical, Figure 6 shows density tracings of this emission in four comets observed at the Haute-Provence Observatory (V90, V927, V964) and at the McDonald Observatory (8384C). It is seen that the whole band reduces to a few rotational lines and that the relative intensities of these lines are rather different in different spectra. The comparison between one observed spectrum and the corresponding computed spectrum based on a zeroth order approximation (Arpigny, 1965) showed a fairly good agreement, with differences of 20 to 30 % in the relative intensities of one or two lines. However, the value to be adopted for μ^2/f_{oo} in that case was about 5 times smaller than the experimental value for this ratio. I should now like to present some preliminary results obtained very recently by Miss Klutz and myself and based on a considerably more elaborate treatment.

We include fluorescence transition in the (0,0) bands of the $A\ ^2\Delta - X\ ^2\Pi$ and in the $B\ ^2\Sigma - X\ ^2\Pi$ systems of CH and take acount of the spin-doubling in the various electronic states, as well as of the Λ-doubling in the $^2\Pi$ state. On the other hand, we adopt the isothermal model for the coma, with uniform, isotropic expansion with velocity v_o. The heliocentric radial component of v_o is computed correctly, taking account of the angle between the sun-comet-earth

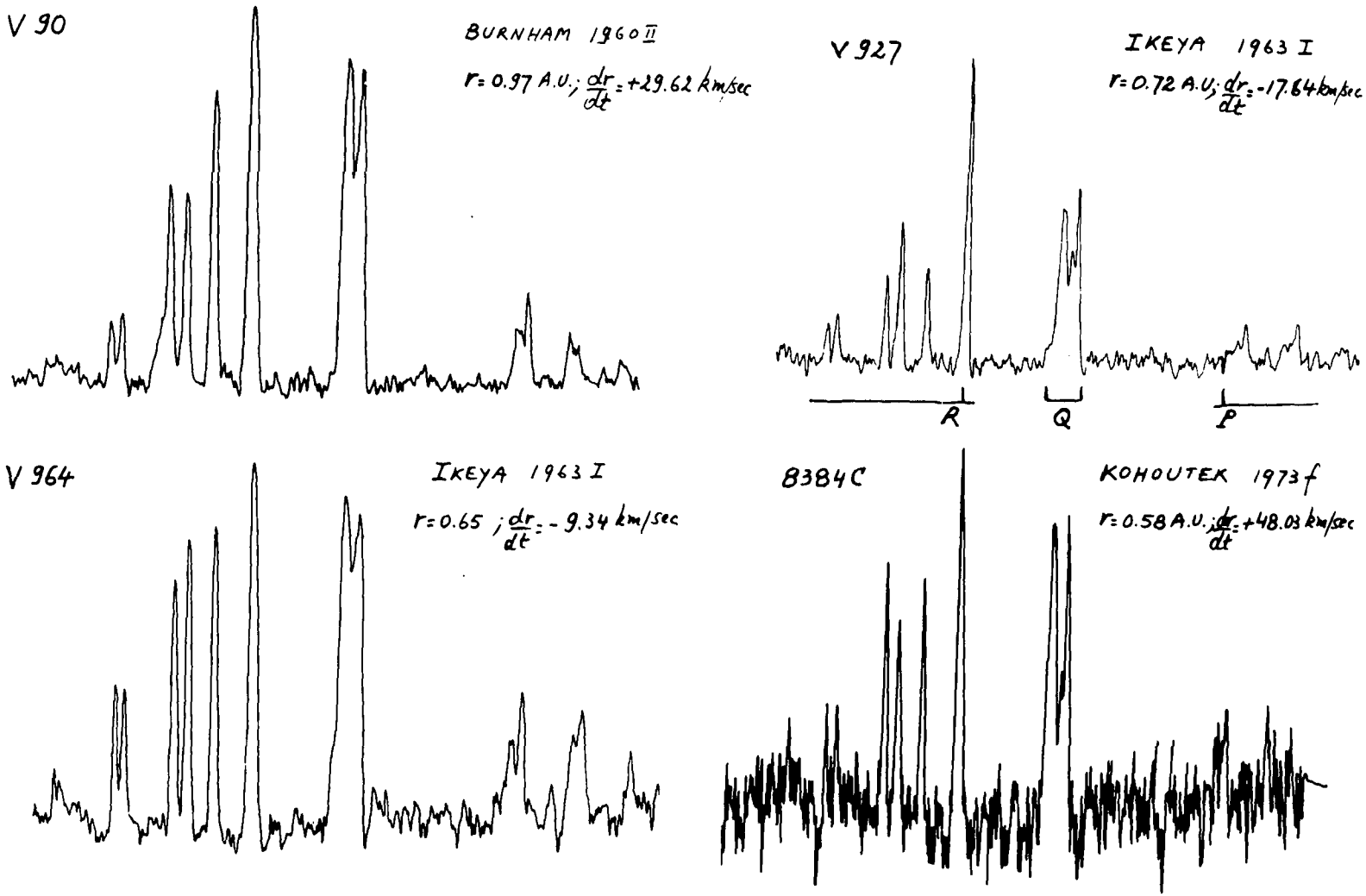

Fig. 6 - The (0,0) band of the A $^2\Delta$ - X $^2\Pi$ system of CH in four comets (density tracings).

plane and the plane defined by the line of sight and the slit of the spectrograph. The colliding particles that could excite the lower rotational levels are distributed according to $n(R) \div R^{-k}$, R being the distance from the centre of the comet and $k \leq 2$. For the same reasons as before, we have to solve steady-state equations at several points along the line of sight and we introduce the effects of the collisions right at this stage rather than using linear combinations of Boltzmann and pure fluorescence terms for the populations of the lower levels. In other words, in addition to radiative, we also have collisional matrix elements of the form $nv\sigma$. We have considered several models for the cross-sections corresponding to different selection rules and to different laws of variation with the rotational quantum number, but we have been unable to distinguish between these models from this first investigation.

The results obtained so far will be illustrated by means of the example of a spectrum (V927) of Comet Ikeya (1963I). We shall consider three kinds of situations :

(1) cases in which the radiative processes dominate in the ground electronic state,

(2) cases where the collisional processes are predominant among the lower rotational levels, or

(3) intermediate cases.

Let us first take the radiation-dominated ($\mathcal{R}$-d) case and refer to the upper part of Figure 7, where we plot the computed relative intensities of the various lines against the fundamental parameter $\mathcal{R}_1$. Then each curve is marked with two vertical bars representing the corresponding observed intensity with its error limits. A fit with the observations is obtained of course if the various $\mathcal{R}_1$ intervals so defined do overlap. As we see, this does not happen for this $\mathcal{R}$-d case, whatever $\mathcal{R}_1$ may be. The experimental values of μ and of f_{oo} yield a value of 50×10^{-6} cm^3 for $\mathcal{R}_1$, and it is clear that for this value the higher rotational lines are predicted too weak, the lower rotational lines too strong. How about the collision-dominated ($\mathcal{C}$-d) case ? This is illustrated in the lower part of

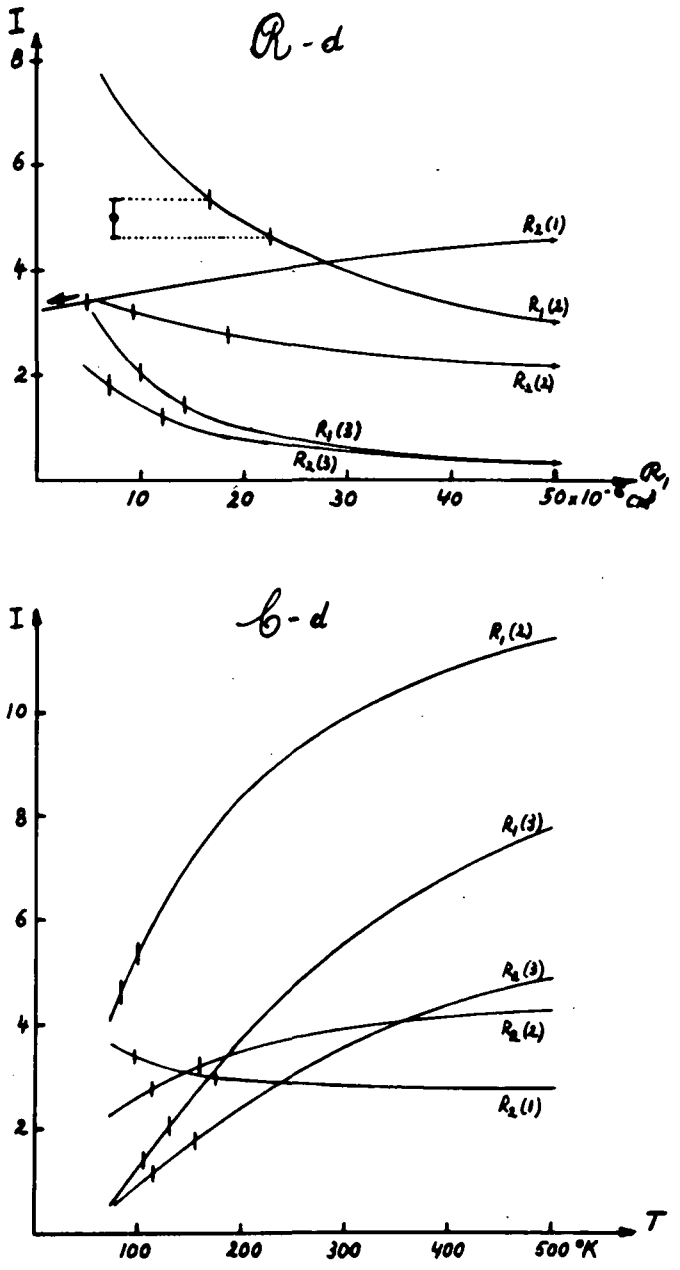

Fig. 7 - The relative intensity curves for the principal lines under radiation-dominated (top) and collision-dominated conditions (bottom). The vertical bars on each curve represent the corresponding observed intensity with its error limits. The intensities are normalized to $R_1(1) = 1$.

Figure 7 where the abscissae are the values of the kinetic temperature of the colliding molecules. Here again we find no solution. The value of T nearest to a solution would be rather low, near 100°K, but $R_1(2)$ and $R_2(3)$ are mutually exclusive and there is indeed no fit. From these extreme cases it can be concluded that n_o, the density at R = 10^4 km, must be contained in the interval from about 10^4 cm^{-3} to about 10^8 cm^{-3} (this is for gas kinetic cross-sections and H_2O exciting molecules).

Thus we are led to turn to intermediate cases. Let us take $\mathcal{R}_1$ equal to the experimental value and fix T at 600°K, for instance. In Figure 8, then, we plot the relative intensities versus log n_o and we have a solution, corresponding to $n_o \simeq 5 \times 10^4$ cm^{-3}. It is instructive to examine the spectra themselves, which are represented schematically in Figure 9, the intensity of each line being shown by a vertical line. The observed spectrum appears as solid lines, the theoretical spectrum as dotted lines, all normalized at $R_1(1)$. This is done for five values of n_o, each value being indicated at the top of the corresponding spectrum. As mentioned above, with $\mathcal{R}_1 = 50 \times 10^{-6}$ cm^{-3} the pure fluorescence predicts too weak higher rotational lines; there is a deficiency in rotational excitation energy and we supply this energy by putting in molecules at some appropriate T. With $n_o = 5 \times 10^3$ cm^{-3} we do not have enough molecules, so that the higher lines are still too faint whereas at $n_o = 5 \times 10^5$ cm^{-3} on the contrary these lines become too strong because there are too many molecules. It would seem from this that a unique solution exists, corresponding to $n_o \simeq 5 \times 10^4$ cm^{-3}. That such is not the case, however, is seen when one wonders about the value of T. It turns out that situations similar to the one we have just met with occur at temperatures in the range of roughly 400 - 800°K. What happens is shown in Figure 10. As we go from 600 to 800°K, for example, the relative intensity curves given here for two lines move in such a way that the n_o intervals still overlap so that we still get a solution. The value of n_o is well defined in each case because the

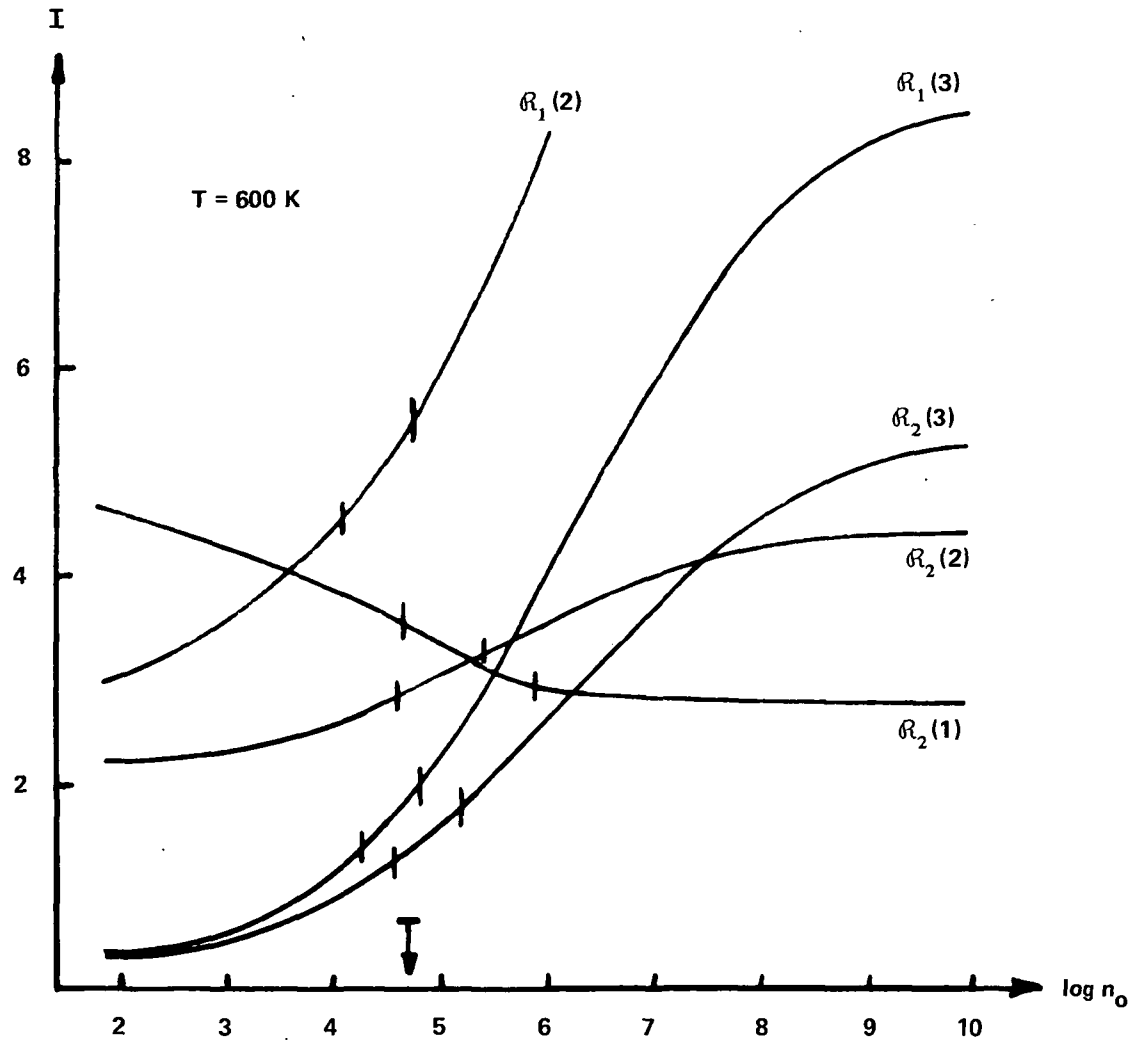

Fig. 8 - Relative intensity curves for the principal lines of CH under intermediate conditions. The vertical bars on each curve represent the corresponding observed intensity with its error limits. The intensities are normalized to $\mathcal{R}_1(1)$. The arrow indicates the approximate value of log n_o for which a fit with the observations is possible.

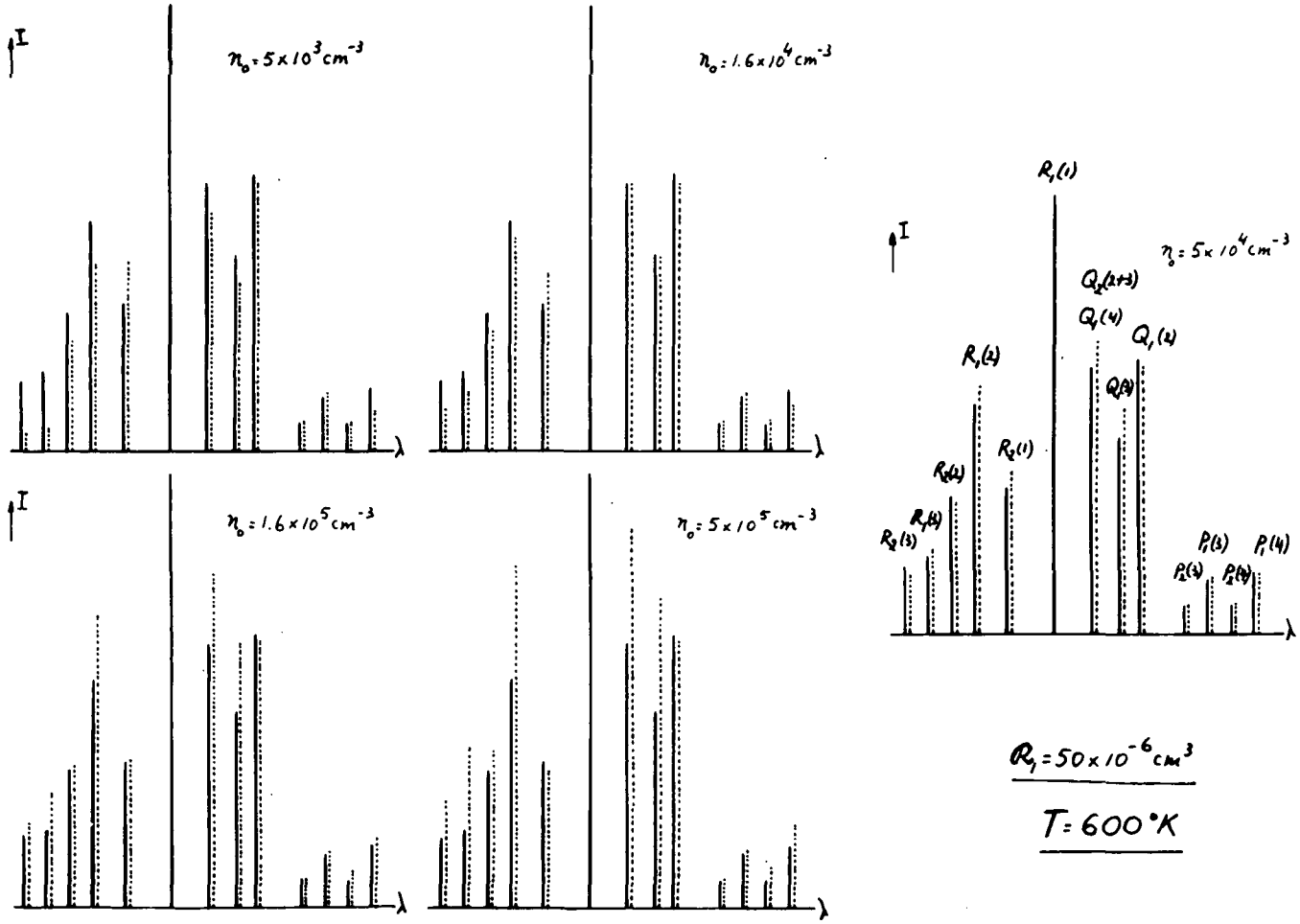

Fig. 9 - Comparison between the observed spectrum (solid lines) and corresponding spectra of CH calculated (dotted lines) for intermediate cases with various densities of exciting molecules.

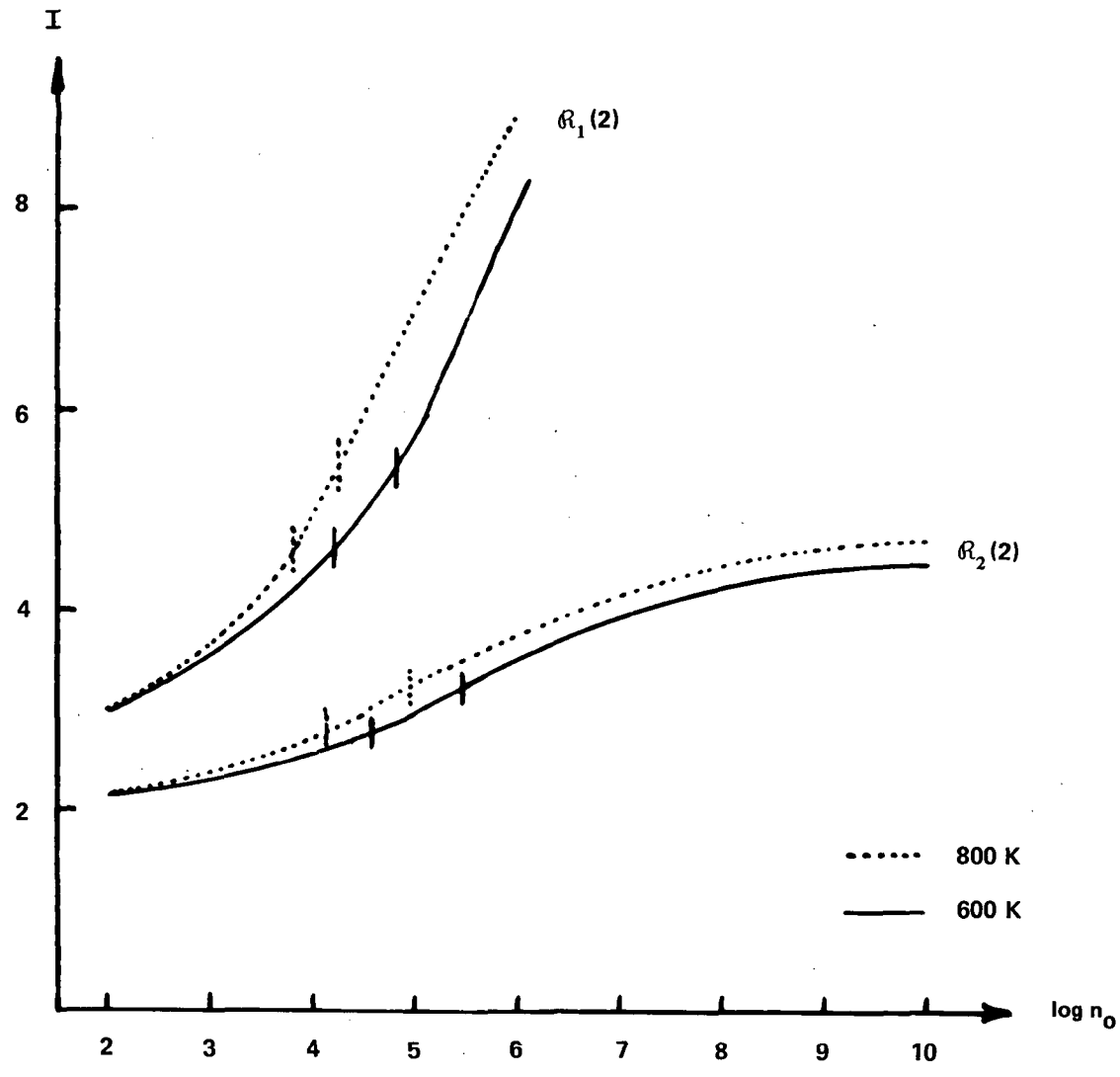

Fig.10 - Relative intensity curves for two CH lines under intermediate conditions at two different temperatures.

overlap of the intervals is small. For T = 400°K, n_o is found to be $\simeq 10^5$ cm^{-3}, while at T = 800°K it is $\simeq 2 \times 10^4$ cm^{-3}. At lower T we need more molecules to supply the missing excitation energy.

Similar situations are encountered for some other spectra of comets Burnham (1960I), Ikeya (1963I), Bennett (1970II), and Kohoutek (1973XII), which we are studying. The densities fall in the range $10^4 - 10^6$ cm^{-3} and the temperatures are ill-defined, covering a range of several hundred degrees. Here also it is felt that if very accurate observations obtained by photoelectric photometry were available, one would be in a better position to make the adjustment of the parameters and to improve the model of the cometary atmosphere. On the other hand, if the same molecules contribute to the excitation of the lower rotational levels of CH and CN for example, which seems likely, then the values for the densities and temperatures that come out from the analysis of the emissions of these (as well as of other) radicals in one given comet spectrum should obviously agree. This condition will have to be borne in mind in future studies.

We can take advantage of the fact that we are able here to calculate steady-state populations with radiative and collisional terms and at the same time to compute pure fluorescence populations as well as Boltzmann populations, in order to test the validity of a linear approximation such as that described in the discussion of CN. In other words, referring to eq. (2) we have the means of knowing x (corresponding to a given density n of exciting molecules) as well as x^B and x^F, hence we can deduce α. If eq. (2) had any general meaning, the same value should of course be obtained for α when using the populations of all the levels. This has been done for a number of values of n corresponding to $\mathcal{R}$-d, $\mathcal{C}$-d, and intermediate cases as defined above, with the result that α is anything but constant for the various rotational levels. When n is very low or very high, α is very nearly equal to zero or to one for all levels, as expected. However, it covers a very wide range (e.g.

0.10 to 1.45, or 0.20 to 1.25) when n is intermediate. This is not unexpected either, because the radiative lifetimes of the different lower rotational levels are different (in particular owing to the Swings effect), so that the ratio of the characteristic time against radiative transition to the characteristic collision time is not the same for the different levels. Similar conclusions would most probably apply to the case of CN.

Finally, let us mention that only for one spectrum, namely a spectrum of Comet Bennett (1970II) has it been possible to estimate the expansion velocity v_o of the radicals, the other spectra being rather insensitive to velocity shifts in the interval 0-1 km.sec^{-1}. In the case of this spectrum of Comet Bennett the intensity distributions on the two sides of the centre are very different from one another and it is found that v_o is equal to 1.0 $\pm$ 0.3 km. sec^{-1}.

C_2.

Now a few words about the C_2 radical. The high rotational and vibrational excitation temperatures derived from the Swan system are interpreted in terms of the resonance-fluorescence mechanism as due to the homonuclear character of this molecule, i.e. to the very small value of R_1. However, when one looks at the spectra or at the intensity distribution one meets with difficulties here also. For example, one finds appreciably different vibrational temperatures in different band sequences. Gebel (1970) compares the values observed for flux ratios like $F(\Delta v = +1)/F(\Delta v = 0)$ and $F(\Delta v = -1)/F(\Delta v = 0)$ to the corresponding theoretical values for various temperatures and finds that the former indicates relatively low T_{vib} ($\sim$ 3000°K), while the latter corresponds to higher vibrational excitation temperatures (> 6000°K). This can be attributed to an underpopulation of the upper v" levels with respect to the lower v" levels, because the $\Delta v = +1$ sequence is produced to a considerable extent by transitions from the upper v" levels, while the $\Delta v = -1$

sequence is formed mainly from the lower v" levels. No explanation has yet been given for this anomaly. An attempt by Gebel to explain this anomaly by considering pure vibration transitions, which can be shown to be very weak anyway, has failed as can be seen in Figure 11. I should like to point out in this context that a determination of the variation of the transition moment with internuclear distance for the Swan system would be most welcome for the relative f-values of the various bands are important data that come into the interpretation of these C_2 emissions.

There is also the question of the presence of the Phillips system. A few bands of this system near 8000 Å have been detected for the first time by O'Dell (1971) in Comet Tago-Sato-Kosaka (1969IX) and it should be interesting to observe them again in various comets to derive the singlet/triplet ratio for this might give some information concerning the production mechanism of C_2.

As far as the rotational lines of the Swan bands are concerned, a number of anomalies have been found. For instance, in a detailed study of dozens of lines in several high-dispersion spectra Woszczyk (1970) has found that seventy percent of the lines could be interpreted qualitatively by the resonance-fluorescence process, but that the intensities of the remaining lines remained unexplained.

The study of the C_2 emissions has yielded important information, namely estimates of the $^{12}C/^{13}C$ isotopic ratio in three comets: Ikeya (1963I) (Stawikowski and Greenstein, 1964), Tago-Sato-Kosaka (1969IX) (Owen 1973), and Kohoutek (1973XII) (Danks et al 1974, Kikuchi and Okazaki, 1975). The isotopic shift for the shortward-degraded (1,0) Swan band amounts to +8 Å, so that the isotopic band head falls well outside that of the main band. Photoelectric scans of this region near 4737 Å have been obtained for the first time on Comet Kohoutek (1973XII) by Danks, Lambert and myself with the McDonald 107-inch reflector and the Tull coudé scanner. The scans reproduced in Figure 12 have a resolution comparable with that of the previous photographic observations (≃0.4-0.5 Å). Unfortunately, the $^{12}C^{13}C$ (1,0) band is blended with NH_2 emissions. In the hope

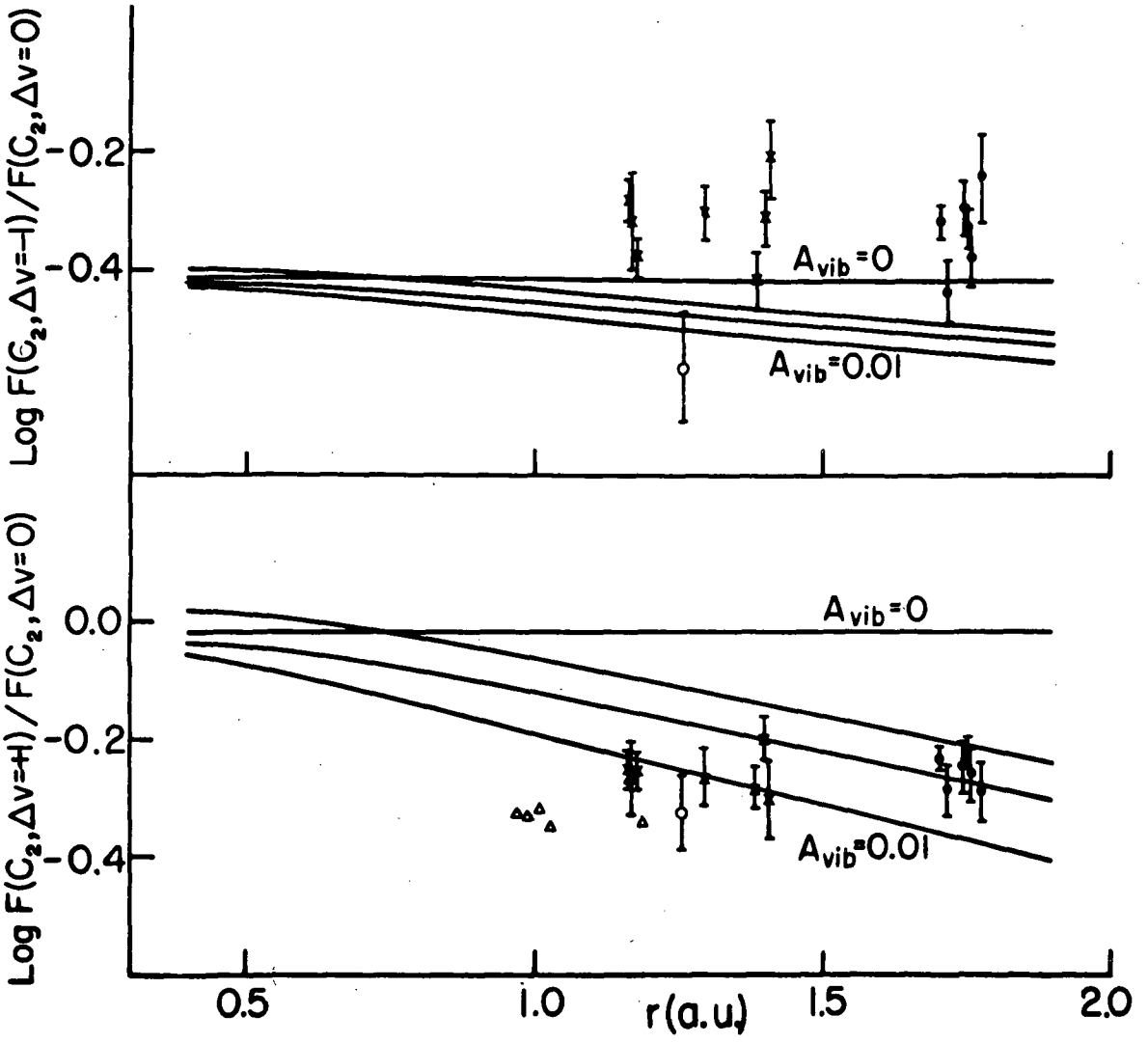

Fig.11 - Calculated (solid lines) and observed band sequences flux ratios for various comets (taken from Gebel 1970).

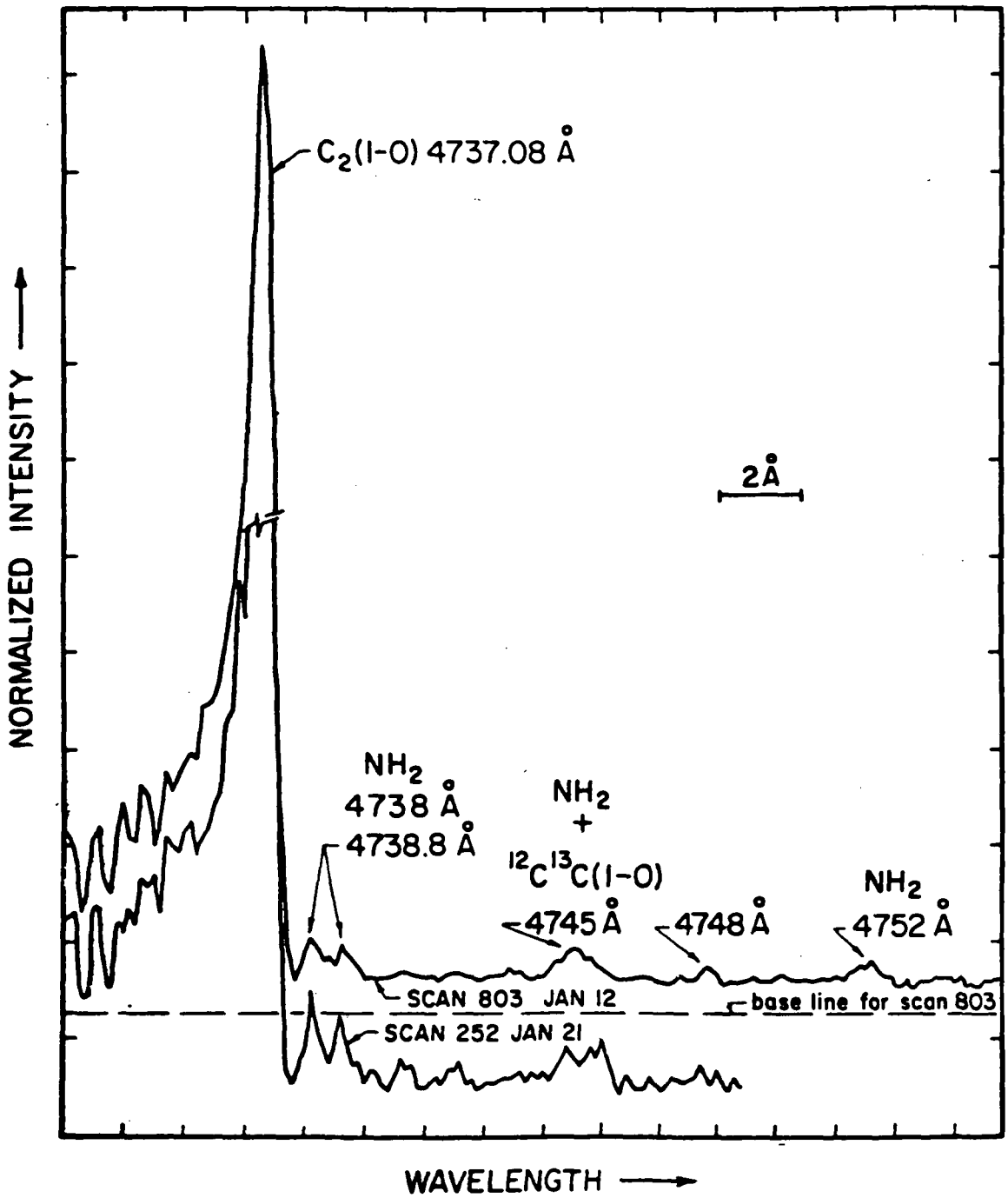

Fig.12 - Photoelectric scans of Comet Kohoutek (1973XII) at a resolution of 0.4 Å. The $^{12}C^{13}C$ + NH_2 blend is seen at 4745 Å.

of separating these emissions we have used a higher resolution ($\simeq$ 0.15 Å), which is illustrated in Figure 13 where we see that the NH_2 contribution is made of four lines. Two of these are separated from the $^{12}C^{13}C$ band, but the other two are still badly blended with this band. Thus the relative intensities of the NH_2 lines must be estimated by comparison with the laboratory spectrum and by correcting these intensities for the effect of the solar absorption lines in an approximate way. In this way we can subtract the contribution of NH_2 to the blend. An example of the comparison between observed and synthesized spectra is shown in Figure 14. Once we know how much $^{12}C^{13}C$ contributes to the blend, we derive the isotopic ratio by relating the intensity of this blend to that of the main band head. Care must be exercised in this analysis because it has been found that the overall strength of NH_2 is variable. The values obtained for the $^{12}C/^{13}C$ ratio in the comets quoted above agree within the observational errors with the terrestrial ratio of about 90. In order to be really significant this isotopic ratio should be determined in many comets, using high-resolution spectra as far as possible. This unfortunately eliminates a large number of comets, which are too faint. Nevertheless, the importance of this ratio lies in the fact that it is related to the problem of the origin of the comets and that it can tell us something about the conditions that prevailed in the regions where these bodies were formed.

C_3.

The C_3 radical in comets affords another embarrassing example. I should just like to report briefly here on the work of Sauval (Uccle Observatory) who is studying the excitation of the λ 4050 band of the $^1\Pi - {}^1\Sigma$ electronic transition in Comet Ikeya (1963I). Computations have been made under the simplified model assumptions for the $\mathcal{R}$-d and for the $\mathcal{C}$-d case and it has been found impossible to reproduce the observed intensity profile satisfactorily. The C_3 radical having no permanent dipole moment, one would expect a

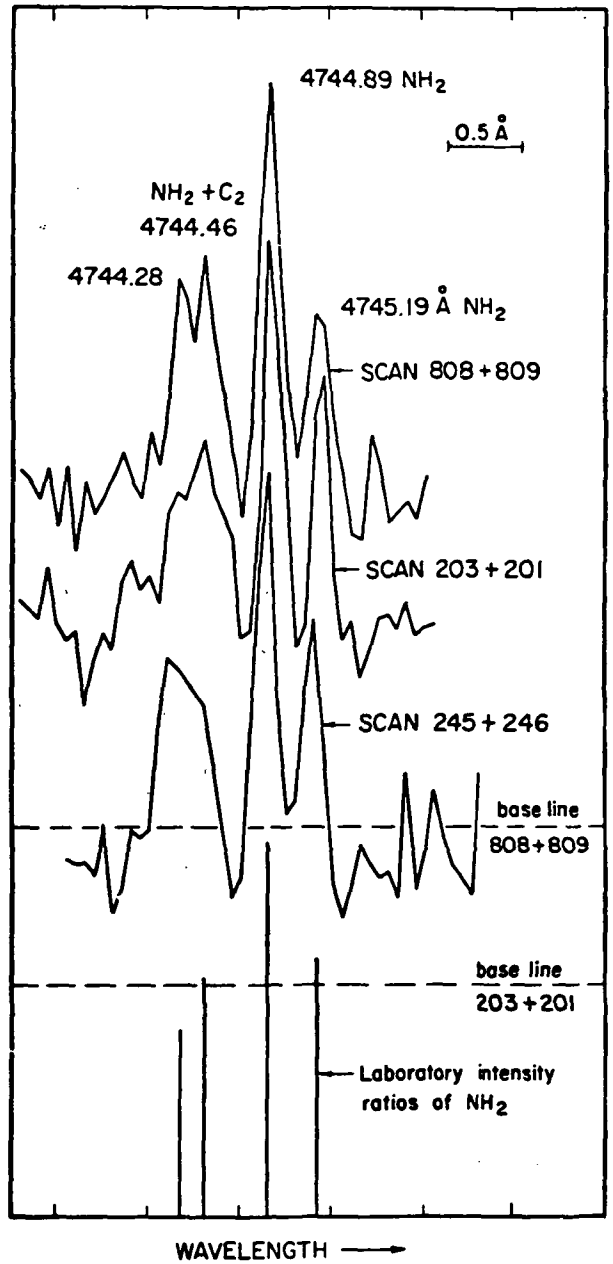

Fig.13 - High-resolution (0.15 Å) scans of the $^{12}C^{13}C$ + NH_2 4745 Å blend in Comet Kohoutek (1973XII). The similarity of the comet spectrum to the laboratory spectrum is apparent. The two NH_2 lines at the red end of the complex are completely beyond the shortward-degraded $^{12}C^{13}C$ (1,0) band head.

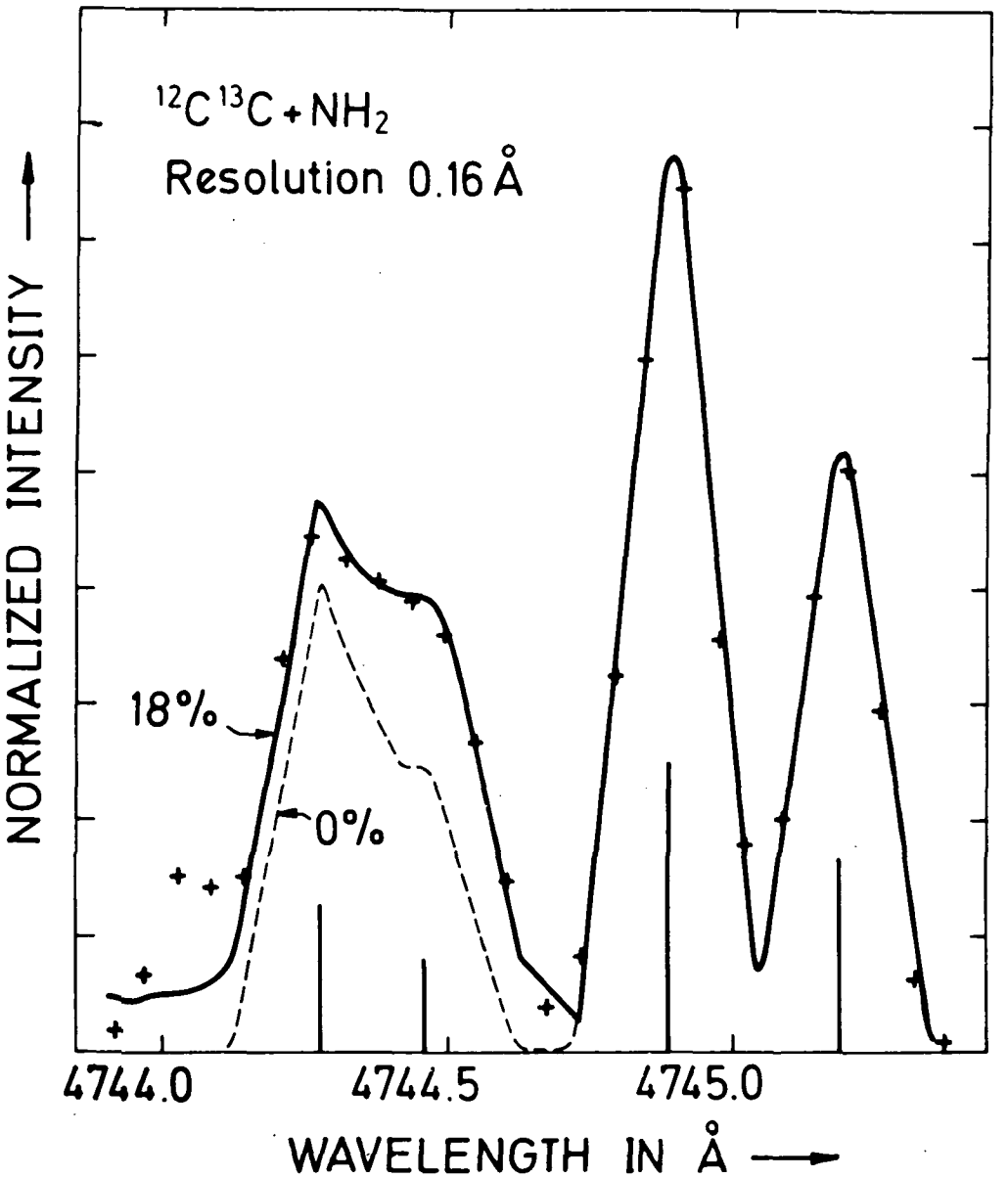

Fig.14 - Observed (crosses) and synthesized (solid line) 4745 Å blend of $^{12}C\,^{13}C + NH_2$ at high resolution. The position of the NH_2 lines as well as their adopted relative intensities are indicated; notice by comparing with the laboratory intensities shown in Fig. 13 that the λ4744.46 line was appreciably weakened by the effects of the solar absorption lines in this case. Also shown is the profile (dashed line) that would correspond to pure NH_2 emissions.

rather high excitation temperature, similar to that of C_2, if collisions are negligible. However, the observed excitation temperature is certainly smaller than 300°K. In order to obtain theoretical spectra that bear a little resemblance to the observed spectra it is necessary to adopt a value for the quadrupole moment of C_3 which is some 10^5 times larger than the quadrupole moment of the similar molecule CO_2 for instance. On the other hand, if collisions are important, then the exciting molecules must have a rather low temperature and the cross-sections for collisional excitation of C_3 must be much larger than for C_2 (the latter statement, in fact, holds not only for C_3, but also for all the other cometary radicals). Further study of the C_3 emissions in comets is certainly desirable and for this we badly need data on the transition probabilities for the various electronic, vibrational and rotational transitions.

$\underline{CH^+}$.

I have included this molecule because it is the first ion for which cometary spectra have been calculated. The work here is due to Vreux (Liège). The spectrum is very simple, being a $^1\Pi - {}^1\Sigma$ transition reduced to only a few lines of the (0,0) band. Figure 15 shows a comparison between observed and computed spectra for Comet Bennett (1970II). The observed spectrum is at the upper left and the computed spectra correspond to pure fluorescence. The agreement is rather good for $f_{00} = 8 \times 10^{-3}$ and $\mu = 1.5$ Debye, a value close to the expected value for the dipole moment of CH^+. In Figure 16 we have again the observed spectrum and now $\mathscr{C}$-d spectra for T = 100°K (upper right) and T = 150°K (lower left). These do not fit with the observed spectra and if we decreased the temperature below 100°K we should increase the ratio R(0)/R(1) and the situation would get worse. Whereas if we increased the temperature above 150°K, we should increase the ratios Q(2)/Q(1) and Q(3)/Q(2), which would also be going in the wrong direction. The conclusion to be drawn from this

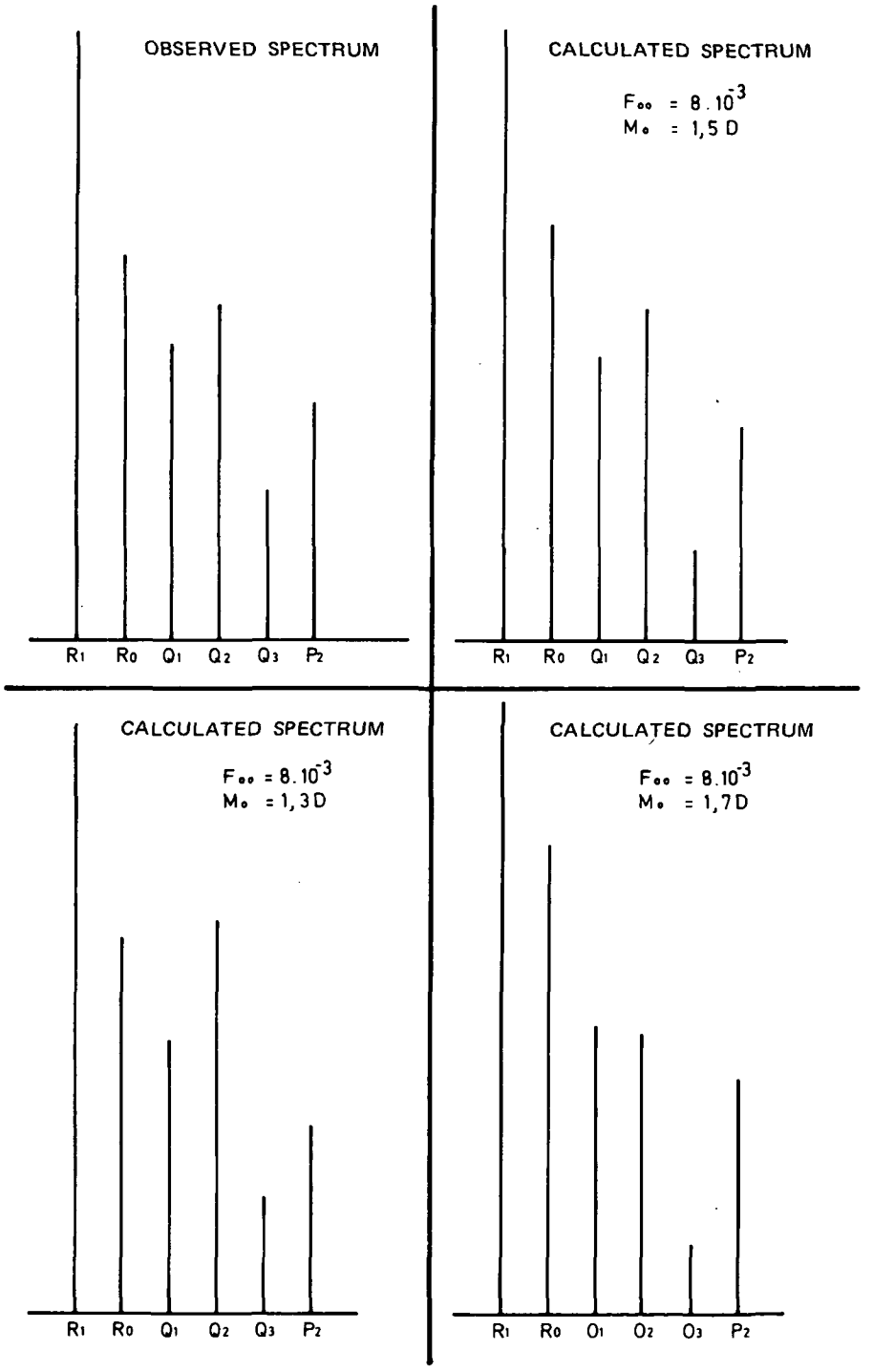

Fig.15 - Observed spectrum of CH^+ (upper left) and corresponding spectra computed under $\mathcal{R}$-d conditions. The best fit appears at the upper right.

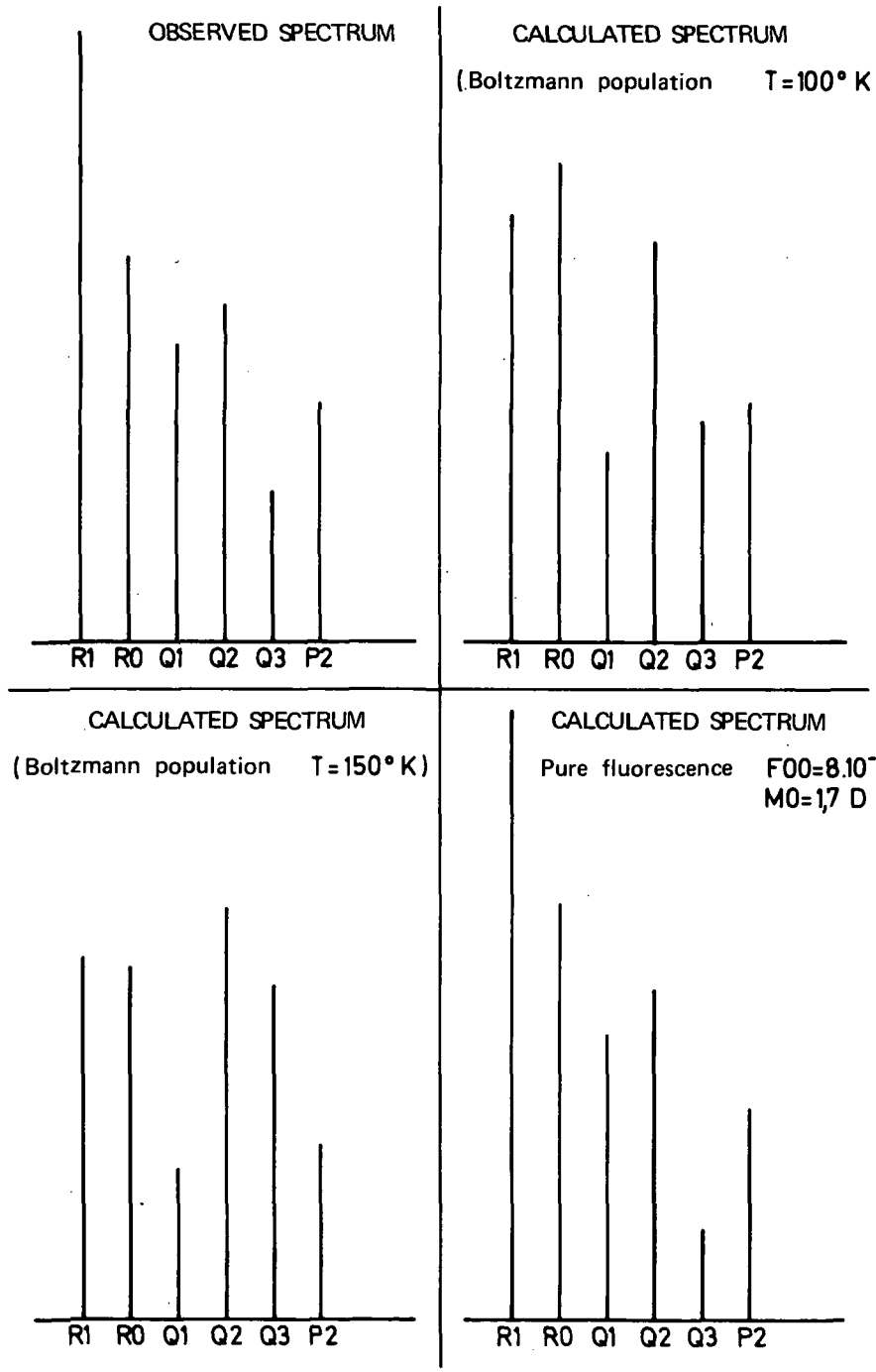

Fig.16 - Observed spectrum of CH^+ (upper left) and corresponding spectra computed under $\mathscr{C}$-d conditions (upper right and lower left). The pure fluorescence spectrum is reproduced at the lower right.

is that the density of possible colliding molecules is $\ll 10^9$ cm^{-3} at a distance of about 3 x 10^4 km from the nucleus, where the spectrum was recorded. On the other hand, it may be mentioned that there is a puzzling situation concerning the oscillator strength f_{00} for which the value found here (8 x 10^{-3}) is rather different from the experimental value derived from lifetime measurements (68 x 10^{-3}; Smith, 1971) as well as from the upper limit obtained from the negative result of a search for CH^+ lines in the solar spectrum, which gives $f_{00} \leq 1 \times 10^{-3}$ (Grevesse and Sauval, 1971). Another laboratory value reported recently (11.5 x 10^{-3}; Brzozowski et al, 1974) is closer to the "cometary" value; it is also in better agreement with a theoretical estimate (6.5 x 10^{-3}) based on calculations by Yoshimine et al (1973). This f-value is also of prime importance for the study of the interstellar medium where one needs to know the column densities of CH^+ and of CH in interstellar clouds in the discussion of the formation mechanisms of these radicals.

OH.

Let us change the subject a little and consider the OH 18 cm radio lines in comets. I shall be very brief on this since a review of this question will be presented by E. Gérard shortly. The fluorescence of the OH radical in the $A\ ^2\Sigma - X\ ^2\Pi$ system has been analysed by Mies (1974) to obtain the populations of the Λ-sublevels of the ground rotational level, in which almost all OH radicals are, and he found that the 18 cm lines can appear either in emission or in absorption according to the heliocentric radial velocity of the comets. Then Mies has proceeded to evaluate the degree of polarization of the radio and uv radiations under fluorescence conditions. For this one must compute the population distribution in the 16 magnetic hyperfine states corresponding to the ground level $^2\Pi_{3/2}$, J = 3/2. Now, provided the exciting radiation is not polarized, the populations of two of these states differing only

by the sign of the magnetic quantum number will be the same, so that the molecules will be aligned by solar pumping and this will produce some linear polarization of the radiation, the amount of polarization observed from the earth depending upon the phase angle. The maximum linear polarizations for the main radio lines (2-2 and 1-1 transitions) are -15 % and -10 % for the absorption case observed in November 1973 in Comet Kohoutek (1973XII), while for the emission observed in January 1974 the maximum linear polarizations are - 3.5 % and -0.9 %. These polarizations are too small to be detected with present-day techniques. For the uv radiation the maximum polarization is 5 % and this differs by only 1.5 % from the degree of polarization predicted for non aligned, equilibrium populations of the hyperfine states. The calculations have also shown that it was a very good approximation to ignore the details of the distribution of the radicals among the hyperfine states when computing the inversion ratio corresponding to the two Λ-sublevels of the ground level.

Let us conclude with a very brief historical note. If one were to describe the evolution of the study of comet spectra since the early days of Secchi and Huggins, he could distinguish the following periods :

- the beginning were of course characterized by the endeavour to specify the carriers of the various emissions detected in the cometary spectrum; thus the now well-known radicals and atoms were gradually identified; this pure identification phase is in fact still going on, as shown by the recent discovery of H_2O^+ and of H_2O for instance, and further efforts should be made yet to improve the identification lists;
  the qualitative interpretation period started in 1911 when K. Schwarzschild put forward the idea of fluorescence, which was taken again by Wurm in particular in the 1930's; this phase culminated in 1941 when Swings resolved the puzzle of the very irregular and unusual intensity profiles of the cometary molecular

bands by invoking the effect of the Fraunhofer lines;

- this was followed by a semi-quantitative interpretation phase marked by the works of McKellar and of Hunaerts in the 1940's and 1950's; these authors already had some success in reproducing the general characteristics of the cometary emissions, although they avoided the problem of solving the statistical equilibrium;
- the first quantitative analyses were carried out in the early 60's soon after the first high-dispersion spectra had been secured by Greenstein; these studies, which are based on the solution of the appropriate steady-state equations, require the use of a high-speed computer with a large memory;
- maybe the next phase will be called the model atmosphere period which is still in a stage of infancy; what I have tried to show here is that when we enter this certainly more rewarding phase we are forced to be rather exacting concerning the accurate knowledge of all the data which are required in the calculations because we have to do now with secondary effects which manifest themselves as rather slight departures from the results obtained with a simplified theory; the latter point also indicates that it would be desirable to base these computations on observation material of the highest quality, possibly using photoelectric photometry.

REFERENCES

Aikman, G.C.L., Balfour, W.J., and Tatum, J.B. 1974, Icarus, 21, 303.

Arpigny, C. 1964, Ann. d'Ap., 27, 393.

Arpigny, C. 1965, Nature et Origine des Comètes, 13th Liège Symposium, p. 155.

Arpigny, C. 1971, J. Phys. C5a, 32, 129.

Brzozowski, J., Elander, N., Erman, P., and Lyyra, M. 1974, Ap. J., 193, 741.

Carrington, T. 1962, Ap. J., 135, 883.

Crawford, O.H., Allison, A.C., and Dalgarno, A. 1969, Astr. & Ap., 2, 451.

Danks, A.C., and Arpigny, C. 1973, Astr. & Ap., 29, 347.

Danks, A.C., Lambert, D.L., and Arpigny, C. 1974, Ap. J., 194, 745.

Field, G.B., and Hitchcock, J.L. 1966, Ap. J., 146, 1.

Gebel, W.L. 1970, Ap. J. 161, 765.

Gordon, R.G., Klemperer, W., and Steinfeld, J.I. 1968, Ann. Rev. Phys. Chem., 19, 215.

Grevesse, N., and Sauval, J. 1971, Astr. & Ap., 14, 477.

Keller, H.V., and Lillie, C.F. 1974, Astr. & Ap., 34, 187.

Kikuchi, S., and Okazaki, A. 1975, Publ. Astr. Soc. Japan, 27, 107.

Malaise, D. 1970, Astr. & Ap., 5, 209.

Mies, F.H. 1974, Ap. J., 191, L145.

O'Dell, C.R. 1971, Ap. J., 164, 511.

Owen, T. 1973, Ap. J., 184, 33.

Roemer, E. 1965, Nature et Origine des Comètes, 13th Liège Symposium, p. 23.

Smith, W.H. 1971, J. Chem. Phys., 54, 1384.

Stawikowski, A., and Greenstein, J.L. 1964, Ap. J., 140, 1280.

Swings, P. 1941, Lick Obs. Bull., 19, 131.

Woszczyk, A. 1970, Studia Soc. Sc. Torunensis, 4, 23.

Yoshimine, M. Green, S., and Thaddeus, P. 1973, Ap. J., 183, 899.

DISCUSSION

W. Jackson: It has already been pointed out that the center of luminosity varies depending upon the particular radical one is considering. If the radical is produced by photodissociation one could expect that the maximum radical density will be displaced by a few hundred to a few thousand kilometers on the sunward side. Could the deviation that are observed in the pure resonance fluorescence model be explained by the presence of highly rotationally excited CN radicals in the v'' = 0 and v'' = 1 levels in the ($X^2\Sigma+$) state contributing to the observed fluorescence?

C. Arpigny: The answer is no, for the following reasons.

Let us assume that we start with CN radicals formed in high rotational levels, say near N = 50. The lifetime against rotational radiative de-excitation (which is inversely proportional to N^3) is about 1 sec for such high levels (cf. Arpigny, Ann. Astrophys. 27, 393, 1964; Ailman, Balfour & Tatum, Icarus 21, 303, 1974) and the radicals will go, in a time interval of the order of 100 sec, down to levels near N = 20 where the lifetime against ratational de-excitation is comparable to the characteristic time for absorption in the Violet and in the Red bands. They will thereafter fluoresce and their population distribution will tend toward the steady-state distribution, which will be reached in a matter of several hundreds of seconds (at 1 A. U.). Therefore, the memory of the initial population distribution will be lost rather quickly. (The characteristic times for the production and for the destruction of the CN radicals are assumed to be long compared to several hundred seconds).

P. Wehinger: In the paper by you and Danks concerning the CN ratios of the blue to the red system, you use a whole family of values of the oscillator strengths. It seems that laboratory determinations by Arnold and Nichols are very good, and their value is 15. I wonder why you don't just simply adopt this value.

C. Arpigny: A search through the literature on the f-values (both relative and absolute) of the CN Red and Violet bands reveals rather important differences between the results of various determinations. This is why T. Danks and I tried several sets of oscillator strengths in our calculations. On the other hand, we have not been able to interpret quite satisfactorily the existing observed band intensity ratios if we used the data given by Arnold and Nicholls for the Red and Violet Systems (J. Q. S. R. T. 12, 143, 1972 and 13, 115, 1973 - see our paper for details).

OMIT

SPECTRAL CLASSIFICATION OF COMETS

J. Bouska

ABSTRACT

Up to now a few hundred of spectra of several tens of comets have been obtained at different observatories over the whole world. On the one hand, there are high dispersion spectra photographed with slit spectrographs attached to large telescopes, and on the other, small dispersion spectra obtained by means of objective prisms. These objective prism spectra, showing the principal emission bands only, are known for a considerable number of comets, and its appearance is usually described verbally.

It seems therefore to be useful to introduce a classification of the spectra of the cometary heads. It is evident that it is impossible to put into practice a similar classification as that used for stellar spectra. The classification of cometary spectra could rather be like the classification of meteoric spectra.

The cometary spectra show mostly two components:

(C) continuum which is the solar spectrum reflected on the dust particles present in the cometary coma, and

(E) emission bands (CN, C_2, C_3 and some others) connected with the intrinsic radiation of molecules in the cometary atmosphere.

The apparent intensity of these components may be weak (1), normal (2) or strong (3). In some exceptional cases continuum or emission bands may be absent (0). Consequently, the classification may be as follows:

Continuum	Emission Bands	Apparent Intensity
C0	E0	absent
C1	E1	weak
C2	E2	normal
C3	E3	strong

In most cometary spectra the CN (0, 0) band is dominant, in others the Swan bands of C_2 (mostly the $\Delta v = +1$); this may be expressed by the following symbols:

c — cyanogen bands dominant,
s — Swan bands dominant.

The presence of the sodium doublet $D_{1,2}$ observed sometimes in cometary spectra at the heliocentric distance $r \leqslant 1$ AU may be denoted by the symbol n.

Metallic lines are observed exceptionally, for instance in the spectra of Sun-grazing comets. Such spectra may be denoted by the symbol M.

The shape of the cometary spectra depends, of course, on the comet's heliocentric distance and this distance must therefore be an inseparable component of the classification of the cometary spectra. The comet's heliocentric distance is to be added (with the sufficient accuracy of 0.1 AU) to the spectral type of cometary spectrum. The heliocentric distance $r < 0.1$ AU, for instance for Sun-grazing comets, may be denoted as 0.0.

The following examples illustrate the proposed classification:

C3E1c(1.7) Comet Kohoutek 1970 III. Very strong continuum, weak emission bands, CN (0.0) dominating. Heliocentric distance r = 1.7 AU [1].

C3E2c(0.6) Comet Arend-Roland 1957 III. Strong continuum, normal intensity of emission bands, CN (0.0) dominating; r = 0.6 AU [2].

C2E2c(1.8) Comet 1942 IV. Normal intensity of continuum and emission bands, CN (0.0) dominating; r = 1.8 AU [3].

C1E2s(1.2) Comet Ikeya-Everhart 1966 IV. Weak continuum, normal intensity of emission bands, Swan band C_2 ($\Delta v = +1$) dominating; r = 1.2 AU [4].

C1E3n(1.0) Comet Mrkos 1955 III. Weak continuum, strong emission bands, of which CN (0.0) dominates, Na-emission ($D_{1,2}$) present; r = 1.0 AU [5].

C2E0(2.7) Comet Kohoutek 1970 III. Continuous spectrum only, emission bands absent; r = 2.7 AU [6].

C3M (0.0) Comet Ikeya-Seki 1965 VIII. Very bright continuum with many metallic emission lines (iron, nickel, chromium, and also D-lines of natrium and K and H lines of ionized calcium); $r < 0.1$ AU [7].

The proposed classification may be very important not only for the short description of the cometary spectrum but it may also be very useful for communicating the shape of a cometary spectrum by means of the international astronomical telegraphic code.

REFERENCES

Bouska J., Mrkos A., Publ. Astr. Inst. Univ. Prague No. 65 = Acta Univ. Carol. Prague 12, No. 1, 65 (1971).

Bouska J., Hermann-Otavsky K., Bull. Astr. Inst. Czech. 9, 79 (1958).

Swings P., Haser L., Atlas of Representative Cometary Spectra, Plate XXa-5. Liege (1956).

Bouska J., Bull. Astr. Inst. Czech. 19, 179 (1968).

Bouska J., Astronom. Nachr. 284, 161 (1958).

Kohoutek L., I. A. U. Circ. No. 2256 (1970).

Marsden B. G., Sky Telescope 30, 332 (1965).

OMIT

POLARIZATION OF OH RADIATION

Frederick H. Mies

ABSTRACT

The ground $^2\pi_{3/2}$ state of OH consists of 2 A-doubled levels which are separated by about 1666 MHz. The upper (parity = +1) and lower (parity = -1) levels each have eight hyperfine sublevels which consist of a three-fold degenerate F=1 and five-fold degenerate F=2 energy state, and transitions between these levels give rise to the OH-18-cm radiowave spectrum. Of the four possible transitions the F=2 → 2 and F=1 → 1 transitions are most intense and are the source of the 1667 MHz and 1665 MHz signals observed from comet Kohoutek (Biraud, *et al* (1973), Turner (1973)). The peak antenna temperature $\Delta T_b/T_b$ for these lines are approximately proportional to the ratio $i = (N^+-N^-)/(N^++N^-)$ where $N^\pm$ are the total concentrations of $^2\pi_{3/2}$, J = 3/2 molecules in the indicated parity state. In the optically thin, collisionless atmosphere of a comet these populations are determined predominantly by the fluorescent scattering of solar u.v. radiation by 12 absorption lines of the $OH(A^2\Sigma^+ \leftarrow X^2\pi)$ transition. The steady state distribution is only a function of the *relative* solar flux at these 12 absorption wavelengths. The molecules are pumped into a large set of $^2\pi$ states, which then rapidly cascade by infrared transitions back to either the + or - levels of the ground state. Because of the Doppler shift of the absorption spectrum relative to the solar Franhaufer spectrum, the ratio i is a sensitive function of the heliocentric velocity V_h of the comet, and the radio signals can be seen either in absorption or stimulated emission relative to the galactic background temperature T_b, depending on whether the levels are anti-inverted, $i < o$, or inverted, $i > o$.

Biraud, Bourgois, Crovisier, Fillit, Gerard, and Kazes (1974) have published a beautiful paper in which they propose this mechanism, calculate i as a function of V_h, and indeed find excellent agreement with their observations of comet Kohoutek. Similar calculations were made by Mies (1974) for $V_h = \pm 41$ Km/sec. and both studies are in quantitative agreement. There is little doubt that optical pumping is predominantly responsible for the OH-18-cm signal. However, both sets of calculations have ignored the effects of the hyperfine levels by using averaged rate constants for the parity states. We shall study the role of the hyperfine levels in this paper. As we shall see their dominant effect is to produce a small degree of linear polarization of both the radio wave and the fluorescent signals, and otherwise they have very little influence on the resultant spectra.

The incident solar radiation is unidirectional and defines a useful axis of quantization for the magnetic quantum number $-F \leqslant M_F \leqslant +F$ associated with a given parity and F. The fluorescent pumping rate out of the 16 hyperfine levels of the ground state is dependent on these quantum numbers, and a total of 576 $^2\pi$ vibrational-rotational-hyperfine levels are either pumped directly, or reached by intermediate cascade. However, if the incident solar radiation is *unpolarized* then the pumping rates only depend on the *magnitude* of M_F, and not the sign of M_F, and the resultant ground state probability distribution $p^\pm(F,M_F)$ generally will be aligned, but cannot be oriented. Thus any radiation processes observed at an angle Θ_f relative to the incident axis may be linearly polarized in the sun-comet-earth plane, but, since $p^\pm(F,M_F) = p^\pm(F,-M_F)$, the radiation cannot be circularly polarized.

The ultimate determination of $p^\pm(F,M_F)$ can be reduced to a simple seven-fold multiplication of a (164x164) stochastic matrix. The resultant distributions for $V_h = \pm 41$ Km/sec.

are summarized in Table 1. Also tabulated is the average of the quantity $3M_F - F(F+1)$ for each parity and F state. This is proportional to the induced magnetic quadrupole moment and is a measure of the degree of alignment. (For a microcanonical distribution of M_F-states, this quantity is zero and the radiowave signal is unpolarized.) The ratio i is calculated to be -0.463 and +0.451 for V_h = -41 and +41 Km/sec. respectively. This is almost identical to the values -0.465 and -0.453 obtained in previous calculations using absorption rates averaged and summed over initial and final hyperfine states.

The calculated properties of the OH-18-cm signals from comet Kohoutek on 29 November 1973 and 25 January 1974 are presented in Table 2. As predicted, the signals were observed (Biraud, et al (1974)) first in absorption and then in emission on these respective dates. Unsuccessful attempts were made to observe circular polarization of the radiation, which is consistent with our theoretical predictions that only linear polarization should be present. However, the measurements are only accurate to about 20 per cent and we cannot be sure that circular polarization is completely absent.

The maximum linear polarization P_{max} of the radiowave signals occurs at the angle $\Theta_f = 90° \cdot P_{max}$ for the absorption of the $2 \rightarrow 2$ and $1 \rightarrow 1$ lines on 29 November 1973 is -15 per cent and -10 per cent respectively while the comparable emission lines in January 1974 only have maximum polarizations of -3.5 per cent and -0.9 per cent. However, the actual angle of observation from the earth was 135.5° in November and 112.1° in January and the expected polarizations are reduced to -6.7 per cent and -4.7 per cent in November and -3.0 per cent and -0.8 per cent in January. Obviously such small polarizations are beyond present detection techniques, and we must conclude that the influence of the non-equilibrium hyperfine distributions predicted in Table 1 cannot easily be observed.

The ratio of the 1667 to 1665 MHz total line intensities is also influenced by the non-equilibrium distribution of hyperfine populations, but the values 1.854 and 1.805 for November and January respectively deviate only slightly from the maximum theoretical ratio of 1.802 predicted for an equilibrium population, and are certainly beyond detectability. This is also true of the polarization of the u.v. fluorescence spectrum. The largest degree of polarization is about 5.0 per cent, which could conceivably be detected. However, even an equilibrated, unaligned distribution of hyperfine levels will result in linearly polarized scattered light, and the non-equilibrium effects only change the degree of polarization by at most about 1.5 per cent.

The calculations we have made of the fluorescent pumping model are based on the following four assumptions:

(1) The fluorescent pumping rate, and the infrared cascading rates are fast compared to any other processes such as collisions or infrared pumping which can influence the population of the -doubled levels of the ground state.

(2) The incident u.v. radiation is unpolarized.

(3) The OH gas is optically thin to the solar radiation.

(4) The OH gas is not exposed to any magnetic or electronic fields. The observations pretty well substantiate assumption (1) since any other mechanism for the inversion or anti-inversion of the -doubled levels would not be dependent on the heliocentric velocity of the comet. The quantitative agreement we have obtained previously with the observed fluorescent spectrum of OH from comet Kohoutek (Mies (1974)) suggests that assumption (3) is satisfied. However, a valid quantitative test of all

the assumptions could best be obtained by accurate measurement of the polarization of the radiowave signals. Substantial deviations from the predictions are expected if any of the assumptions are violated.

References

Biraud, F., Bourgois, G., Crovisier, J., Fillit, R., Gerard, E. and Kazes, I., 1973, IAU Circular No. 2607, December 10.

Biraud, F., Bourgois, G., Crovisier, J., Fillit, R., Gerard, E. and Kazes, I., 1974, Astron, and Astrophys. 34, 163.

Mies, F. H., 1974, Ap. J. 191, L145.

Turner, B. E., 1973, IAU Circular No. 2610, December 18.

Table 1

Calculated Distribution of Hyperfine Levels

STATE				V_h = -41 Km/sec		V_h = +41 Km/sec	
Energy (MHz)	Parity	F	$\lvert M_F \rvert$[a]	Relative[a] Population	$\langle 3M_F - F(F+1) \rangle$[b]	Relative Population	$\langle 3M_F - F(F+1) \rangle$
	+	2	2	0.03470		0.08548	
	+	2	1	0.03294		0.09356	
	+	2	0	0.03234		0.09635	
1720.53	+	2	sum	0.16763	+0.1465	0.45441	-0.2501
	+	1	1	0.03520		0.08944	
	+	1	0	0.03049		0.09199	
1665.40	+	1	sum	0.10089	+0.0933	0. 7087	-0.0189
	+	Total		0.26853[c]	+0.1265	0.72528[d]	-0.1638
	-	2	2	0.07758		0.03272	
	-	2	1	0.09863		0.03527	
	-	2	0	0.10683	-0.6573	0.03611	
53.17	-	2	sum	0.45925		0.17210	-0.2069
	-	1	1	0.08495		0.03403	
0.00	-	1	0	0.10232		0.03456	
	-	1	sum	0.27223	-0.1276	0.10262	-0.0104
	-	Total		0.73147[c]	-0.4602	0.27472[d]	-0.1335

[a] Populations are the same for both F, $+M_F$ and F, $-M_F$ levels.

[b] The averaged value of this quantity is proportional to the induced magnetic quadrupole moment, and is a measure of the degree of alignment in the particular state.

[c] The ratio i = -0.4629 and indicates an anti-inversion of the Λ-doubled levels.

[d] The ratio i = +0.4506 and indicates an inversion of the Λ-doubled levels.

Table 2

Predicted Properties of OH-18-cm Radiation from Comet Kohoutek

		29 November 1973 (V_h = -41 Km/sec)		25 January 1974 (V_h = +41 Km/sec)	
		$F^+ = 2$	$F^+ = 1$	$F^+ = 2$	$F^+ = 1$
$F^- = 2$	$\Delta T_1/C$[a]	-0.28693	-0.02652	+0.25994	+0.02825
	β[b]	-0.1280	+0.1467	-0.0338	-0.0169
	P_{max}[c]	-0.1468	+0.1280	-0.0350	-0.0172
	P_{obs}[d]	-0.0671	+0.0672	-0.0299	-0.0148
	ν_o(MHz)	1667.36	1612.23	1667.36	1612.23
$F^- = 1$	$\Delta T_1/C$	-0.02811	-0.15197	+0.02740	+0.14105
	β	+0.0264	-0.0908	+0.0514	-0.0090
	P_{max}	+0.0257	-0.0998	+0.0489	-0.0090
	P_{obs}	+0.0128	-0.0467	+0.0423	-0.0078
	ν_o(MHz)	1720.53	1665.40	1720.53	1665.40

(a) ΔT_1 is the change in antenna temperature for radiation polarized perpendicular to the sun-comet-earth plane. The quantity C is equal to the following: $C = 1.127 \times 10^{-9} (\nu_o/1667) N_c\, g(\nu)\, T_b$ (°K), where N_c is the total column density (cm^{-2}) of ground state OH, $g(\nu)$ is a normalized shape function such that $\int g(\nu)d\nu = 1$, and T_b is the background blackbody temperature which is assumed to be large compared to the fine structure splitting, i.e., $T_b \gg 0.08°K$.

(b) ΔT_{11} for radiation polarized parallel to the sun-comet-earth plane is dependent of the angle of observation Θ_f relative to the axis of the incident solar radiation, $\Delta T_{11} = \Delta T_1 (1+2\beta\sin^2\Theta_f)$. The degree of polarization, $P = (\Delta T_{11}-\Delta T_1)/(\Delta T_{11}+\Delta T_1)$, is then related to the parameter β as follows: $P(\Theta_f) = \beta\sin^2\Theta_f/(1+\beta\sin^2\Theta_f)$.

(c) The maximum polarization occurs as $\Theta_f = 90°$, where $P_{max} = \beta/(1+\beta)$.

(d) P_{obs} is the degree of polarization expected on the date of observation. The observation angle $\Theta_f = 135.5°$ on 29 November 1973 and Θ_f 112.1° on 25 January 1974.

N76-21086

ANALYSIS OF NH SPECTRUM

M. Krauss

INTRODUCTION

The $A^3\Pi - X^3\Sigma^-$ transition of NH is a common feature of cometary spectra. Since the NH molecule is likely to be formed by photodissociation of molecules such as ammonia or hydrazine, identifying the final states of the photolysis would shed light on the identity of the parent. Stief and DeCarlo[1] noted that the photolysis of ammonia at 123.6 nm results in emission at 324.0 nm in the $c^1\Pi - a^1\Delta$ system. They suggested that in the absence of collisions in the coma, the $NH(a^1\Delta)$ should accumulate if ammonia is the source of NH radicals. The absence of the singlet system in this view would suggest another parent molecule than ammonia as the source of the NH radical. However, the pumping rate of the UV transitions in a comet is also very small. This note will show that the transition rate for the $a^1\Delta - X^3\Sigma^-$ transition is sufficiently fast to deplete any $a^1\Delta$ concentration formed in the original photolysis process.

This analysis focused on experimental spectra obtained by Lane and Stockton[2] observing the comet Kohoutek. The fluorescence pumping of the NH molecule is calculated for November 29, 1973 and January 25, 1974 using the model of radiative equilibrium which assumes no collisions[3]. Lane and Stockton observed the usual strong 336 nm triplet system but also noted a peak near 325.8 nm which can be assigned to the $c^1\Pi - a^1\Delta$ band system. The radiative equilibrium model will be used to examine this possible assignment.

Radiative Transition Probability ($a^1\Delta - X^3\Sigma^-$)

Since this transition is a singlet-triplet intercombination, the largest contribution to the transition probability is likely to be a spin-orbit induced electric-dipole transition, $a^1\Delta_2 - X^3\Sigma_1^-$, where the subscript represents the Ω value. These states can be expanded,
(1) $\phi(^3\Sigma_1^-) = \psi(^3\Sigma_1^-) + a_1\psi(^3\Pi_1) + a_2\psi(^1\Pi_1)$ and (2) $\phi(^1\Delta_2) = \psi(^1\Delta_2) + b_1\psi(^3\Pi_2)$, since the spin-orbit interaction mixes states of the same value of Ω. The dominant

molecular orbital configurations for $^3\Sigma_1$, $^3\Pi_2$. $^1\Delta_2$. and $^1\Pi_1$ states are, respectively,

$$\psi(^3\Sigma_1^-): \quad 1\sigma^2 2\sigma^2 3\sigma^2 \ \pi^+\alpha \ \pi^-\alpha$$

$$\psi(^3\Pi_2): \quad 1\sigma^2 2\sigma^2 3\sigma\alpha \ \pi^{+2} \ \pi^-\alpha$$

$$\psi(^1\Delta_2): \quad 1\sigma^2 2\sigma^2 3\sigma^2 \ \pi^{+2}$$

$$\psi(^1\Pi_1): \quad \frac{1}{\sqrt{\ }}[1\sigma^2 2\sigma^2 3\sigma\alpha \ \pi^{+2}\pi^-\beta - 1\sigma^2 2\sigma^2 3\sigma\beta \ \pi^{+2} \ \pi^-\alpha].$$

The significant electric dipole interactions are between the $\psi(^3\Sigma_1^-)$ and $\psi(^3\Pi_2)$ states and the $\psi(^1\Pi_1)$ and $\psi(^1\Delta_2)$ states. The one-electron transition moment integral for both interactions is formally the same, $<3\sigma \ 1 \ \vec{r} \ 1\pi>$. For valence states the orbitals do not vary greatly among the states and they will be assumed to be in variant for these valence states. The transition moment integral will be determined empirically from the known transition probability for the $A^3\Pi - X^3\Sigma^-$ transition[3] since the square of the integral is proportional to the probability divided by the cube of the transition energy.

The mixing coefficients in eq. 1 and 2 are also determined empirically. Diagonal spin-orbit matrix elements have been calculated for NH both empirically and by ab initio methods[5]. It will be assumed here that off-diagonal matrix elements can be calculated with the same hamiltonian. Accepting the value of 73 cm^{-1} for spin-orbit constant used by Lefebvre-Brion and Moser, the constants a_1, a_2, and b_1 are estimated to be $-1.2\cdot10^{-3}$, $0.8\cdot10^{-3}$, and $3.0\cdot10^{-3}$, respectively.

Since the spin-orbit induced mixing coefficients are of the order of 10^{-3}, the transition probability for the intra-multiplet transition will be about 10^{-6} of the usual electric-dipole allowed transition. In the present case even with the much smaller energy difference between the $^1\Delta$ and $^3\Sigma^-$ states, the transition probability is found to be 5 S^{-1}. In order to gauge the significance of this value an estimate of the pumping rate is obtained for the comet-Kohoutek in the next section.

Calculation of the Fluorescence Pumping

Dixon[6] has determined accurate line positions and assignments for the A-X transition. The radiative equilibrium equations were solved considering only the N" = 0 and 1 rotational states. Solar fluxes were estimated from the unpublished preliminary edition of the Kitt Peak Solar Atlas normalized to the mean intensities tabulated by Allen[7]. There are three important lines that excite the N" = 0 level, the $R_1(0)$, $^RQ_{21}(0)$, and $^RP_{31}(0)$. There are strong Fraunhofer lines at the wavelengths which pump the first two on November 29, 1973. As a result the predicted fluorescent spectra on November 29, 1973 is a composite of lines pumped from both the N" = 0 and 1 states, while on January 25, 1974, the spectrum is dominated by lines pumped from N" = 0. The radiative equilibrium maintains significant population in only the N" = 0 and 1 rotational states of the $X^3\Sigma^-$ ground electronic state with the relative populations for N" = 0 equal to 0.7 on November 29 and 0.9 on January 25.

There is semi-quantitative agreement on the relative intensities of the fluorescent spectra for both observing days. Quantitative disagreements between the calculated and observed spectra can be attributed to uncertainties in the evaluation of the solar flux and the inability to resolve a number of blends. Fluorescent pumping from cold $X^3\Sigma^-$ ground state is certainly the preponderant source for the observed fluorescence. For November 29 the total fluorescent rate is only about $1.2 \cdot 10^{-3}$ S^{-1} while on January 25 it is about $3.6 \cdot 10^{-3}$ S^{-1}. The V" = 0 to V" = 1 vibrational transition is estimated to be pumped at a rate of $2 \cdot 10^{-4}$ S^{-1} by the solar flux near 3μ. The electronic pumping in the A-X system is quite weak and the possibility of vibrational pumping should be considered if a quantitative spectrum was required.

The pumping rate in the $c^1\pi$-$a^1\Delta$ system will be of the same order of magnitude as found for the A-X system. The electronic transition probabilities are comparable

for the A-X and c-a systems[4] while the solar flux is diminishing as the singlet transition is at shorter wavelength. Lane has noted a peak at about 325.8 nm which can be assigned to the $P_2(0)$ transition in the c-a system using the line list reported by Pearse[8]. The radiative equilibrium model would predict that rotationally cold $a^1\Delta$ would exhibit a very simple fluorescence spectra with predominant peaks 325.8 nm and 326.2 nm. The $P_3(1)$ peak at 326.2 nm should have an intensity about 1/3 of the peak at 325.8 nm. Since the 325.8 nm peak is weak, the $P_3(1)$ peak, if present, would be barely above the noise and the present data cannot be used to confirm the assignment of the c-a system.

Discussion

Photochemical dissociation of NH_3 is known to produce NH in the singlet state with high quantum yield. The radiative transition probability for the $a^1\Delta - X^3\Sigma^-$ system is estimated to be 5 S^{-1}. The transition probability for the $b^1\Sigma^+ - X^3\Sigma^-$ system would be comparable. There is no evidence in the NH spectra of the wide distribution in V and J expected in the initial photochemical dissociation event. The NH is apparently quite cold as expected from the radiation equilibrium model. All the NH would then radiate to the $X^3\Sigma^-$ ground electronic state unless another mechanism were found to excite the molecule. The spin-orbit induced electric-dipole transition probability is 10^3 larger than the fluorescence pumping. Such a great discrepancy far exceeds the likely errors in estimating inter-multiplet transition probabilities. The photochemical origin of the NH radical is not to be uncovered by examining the fluorescence spectra.

ACKNOWLEDGEMENT: The author was encouraged by Dr. A. L. Lane and Dr. B. Donn to consider this analysis. He thanks Dr. C. Arpigny for correcting an earlier version of this note.

REFERENCES

1. L. J. Stief and V. J. DeCarlo, (1965), Nature 205, 889.

2. A. L. Lane and A. N. Stockton, to be published.

3. C. Arpigny, (1965), Ann. Rev. Astron. Astrophys. 3, 351.

4. W. H. Smith, (1969), J. Chem. Phys. 51, 520.

5. H. Lefebvre-Brion and C. M. Moser, (1967), J. Chem. Phys. 46, 819.

6. R. N. Dixon, (1959), Can. J. Phys. 37, 1171.

7. C. W. Allen, (1973), "Astrophysical Quantities (London, Athlone Press), 3rd edition.

8. R. W. B. Pearse, (1933), Proc. Roy. Soc. A143, 112.

OMIT

OH OBSERVATION OF COMET KOHOUTEK (1973f) AT 18 CM WAVELENGTH*

F. Biraud, G. Bourgois, J. Crovisier, R. Fillit, E. Gérard and I. Kazes

ABSTRACT

The main lines of OH at 18 cm wavelength were observed in Comet Kohoutek (1973f) from December 1973 through February 1974 with the Nancay radio telescope. They were detected in absorption in early December and reappeared in emission around mid-January. In a preliminary approach these results are interpreted in terms of U.V. pumping by the sum when the Fraunhofer spectrum is taken into account.

*See Astron. and Astrophys. 34, 163(1974) for the complete text.

DISCUSSION

W. F. Heubner: What was the full width at half amplitude?

E. Gerard: Four kilometers per second; plus or minus one. (OH obs. at 18 cm.)

Voice: Would you tell more about Turner's observations that were made at the same time?

E. Gerard: Yes.

Voice: Could you compare the column densities?

E. Gerard: The problem is that he made a different interpretation, right, because he didn't assume there was some kind of maser going on there. So, he ended up with a very high column density. It was around 10^{14} per centimeters squared. Now, I will bet you it is off by almost two orders of magnitude, when we see what the column densities are that Arpigny has been talking about.

If you take Turner's numbers and interpret them in terms of the maser mechanism the column density averaged over the Green Bank beam is $1.4\ 10^{12}$ which is just okay: We find for the first period $3.3\ 10^{12}$ and for the second $4.1\ 10^{12}$.

The problem is that we have been fighting hard to make purely radio astronomy measurements of the OH cloud without mixing up with the optical people. We try to, reconcile it afterwards and it fits all right.

D. J. Malaise: Referring to your last slide, comparison of the computation based on the fluorescence process and your observation, it was striking how nice it fitted, but you mentioned that this signal disappeared just before perihelion, and I take it that really the signal should have been there. Its absence is real, bars are small, correct?

E. Gerard: Yes.

D. J. Malaise: So, of course, it might be a shrinking of the OH region with the higher dilution, but anyhow, it means that the total amount of OH just got down.

E. Gerard: Yes. Definitely.

D. J. Malaise: OH disappeared in the head in some way. So, this is a very important point of—

M. Dubin: On the same point as Malaise, I have some of the information from the Page and others' measurement of Lyman alpha versus time, the total hydrogen. And they observed what appears to be an increase in the hydrogen emission in the period from the 3rd of December through about December 15th, and then a major decrease.

Now, supposedly there is a relationship with the hydroxyl density and it is rather important to find out if in addition to the masering, whether there is a change in the total hydroxyl in the comet.

E. Gerard: So, you are saying it went down around the 16th, or sometime like that?

M. Dubin: Yes.

E. Gerard: The H signal?

M. Dubin: Yes. Lyman alpha.

Voice: We have an increase and a decrease following it, and it is not a monotonic function with radial distance, which appears to be confirmed in your measurements in your last slide.

E. Gerard: Provided you believe in the maser gain stuff.

COOLING AND RECOMBINATION PROCESSES IN COMETARY PLASMA

M. K. Wallis and R. S. B. Ong

1. INTRODUCTION

It has long been recognized that collisional cooling and recombination processes are likely to be important in the inner cometary coma, in a 10^4km radius region for the larger comets (Biermann & Trefftz 1964) Cherednichenko (1970) laid stress on dissociative recombination processes, as possibly playing a role in the production of observed ions and radicals. Oppenheimer, in his spirited contribution to this conference, emphasized that a variety of ion-molecule interactions occur relatively rapidly and probably take part in the production of known cometary radicals.

In this paper, we focus our attention on the ion-electron plasma in comets and examine in the first place the cooling processes which result from its interactions with the neutral coma. For the plasma is generally very energetic (1-100eV) and must be cooled if it is to reach moderate densities and promote efficient particle-particle interactions. For example, solar wind electrons have 10-15eV energy, they experience some adiabatic heating (factor 2 or 3) in passing through the coma, they may gain around 10eV in passing through a collision-free, resistive shock and perhaps suffer additional heating via plasma turbulence effects. Photo-ionization processes may release other energetic electrons — He 584Å photons could give electrons with about 10eV (Biermann & Trefftz 1964), although most have less than 5eV.

New cometary ions produced at 10^5-10^6km in the far coma probably gain most of the streaming energy of the solar wind, through being accelerated in the $\underline{E}$ and $\underline{B}$ fields up to perhaps several thousand eV (Wallis 1973a). How quickly these ions are lost from the incoming solar wind plasma largely determines the ion pressure.

Cooling processes have general relevance for plasma behaviour in comets, in describing the overall plasma flow through the coma and in cometary plasma formation. Specific problems that have received attention and require a careful description of the cooling rate are that the visible ion structures cannot consist of hot and therefore low density plasma; that cool molecular-ion plasma is rapidly destroyed by dissociative recombination; and that energetic photo-electrons would exert a high pressure in the inner coma and prevent penetration by the solar wind. We develop a continuous description of the cooling effects in order to look at such problems.

In this preliminary examination, we shall consider a cometary coma composed predominantly of H_2O and its decomposition products (Wallis 1973b). For specific estimates, we use a comet of the size of comet Bennett 1970 II, with a production rate $Q = 10^{29}$ H_2O molecules $ster^{-1}s^{-1}$ at 0.7a.u. heliocentric distance. The coma density depends a little on assumptions about the expansion velocity V; this factor is relatively

unimportant, but for concreteness and consistency, we suppose V increases with distance due to photo-dissociative heating (Wallis 1974), so that the density at radius R is

$$N = \frac{Q}{VR^2} \text{ where } \frac{Q}{V} \simeq \begin{cases} 4\times10^{23}\,\text{cm}^{-1} & \text{at } R>3\times10^{4}\,\text{km} \\ 10^{24}\,\text{cm}^{-1} & \text{at } R = 10^{3}\text{-}10^{4}\,\text{km}. \end{cases} \quad (1)$$

2. COOLING PROCESSES

Descriptions of electron cooling are given in planet ionosphere studies (Henry & McElroy 1968, Sawada et al. 1972, Olivero et al. 1972), energy loss rates in O, CO, H_2O etc. being computed on a continuous slowing-down approximation. Data for e-OH collisions are incomplete* and we suppose it comparable to CO above 7eV, while similar to H_2O with rotational transitions dominant at lower energies (Shimizu 1974). Ionization data for H_2O, OH and O have been summarized by Wallis (1973b).

Solar wind protons and energetic cometary ions are lost from the plasma primarily in charge exchange processes with neutral gas, having cross-sections $\sigma = 1\text{-}3\times10^{-15}\,\text{cm}^2$ at 10^3-10^4eV.

Electrons are cooled in a variety of processes at rates varying with energy as shown in Fig.1. The functions shown are a continuous approximation to the discrete energy losses actually occurring which is useful in calculations (Olivero et al.1972). The approximation exaggerates the width of the 'holes' in the CO cooling

---

* But see I.V. Sushanin 1973 Problemi kosmich.fiziki 8, 88

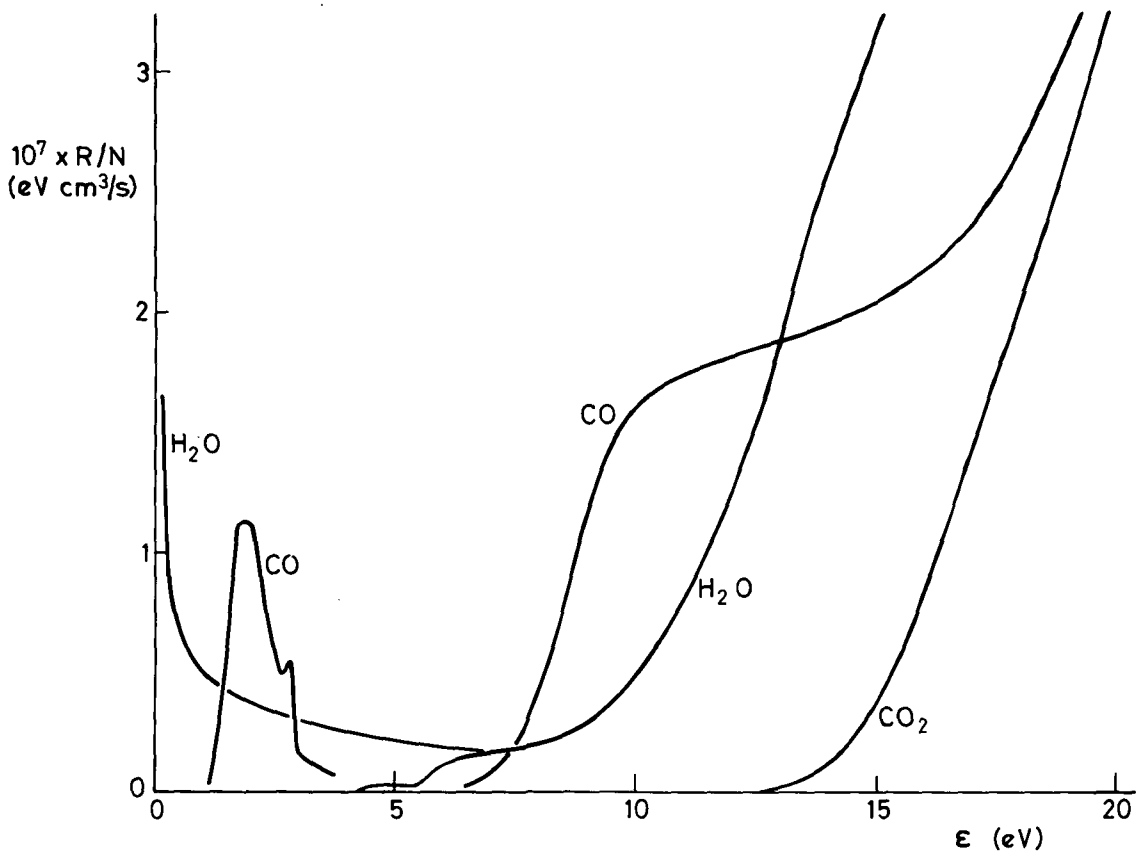

Fig. 1. Cooling rates for inelastic collisions of electrons with energy ε in molecular gases, on the continuous slowing-down approximation. The theoretical cooling rate via rotational excitations of OH is similar to that of H_2O (section to the left), but both are uncertain to a factor 3. The structured, low energy part of the CO curve is due to vibrational excitations.

function, where this becomes small or even zero. But after making allowance for the redistribution of energy between the electrons, which has to be done anyway, the inaccuracy due to the continuous approximation becomes small. For electron collisions with H_2O, rotational excitations dominate below 5eV and as each energy jump is small, the continuous approximation is good even for single electrons. The cooling rate, calculated on the rigid rotor approximation for electrons of energy ε exceeding $\Delta\varepsilon \simeq 0.025$eV has the form (personal communication from M.Shimizu)

$$d\varepsilon/dt \simeq N\sigma_{rot} v_e \Delta\varepsilon = -a\varepsilon^{-\frac{1}{2}}N, \; a \simeq 5\times10^{-8}\,eV^{3/2}cm^3s^{-1}. \quad (2)$$

Above 5eV, electronic excitations and ionizations become important (Fig.1) and the cooling rate increases steeply in 6-20eV as

$$d\varepsilon/dt \simeq -a'(\varepsilon-3eV)^2N, \; a' = 2\times10^{-9}\ eV^{-1}cm^3s^{-1}. \quad (3)$$

The time for cooling to the minimum energy $\Delta\varepsilon$ depends little on the initial energy if above 10eV:

$$t_{cool}^{-1} \simeq N\{\frac{1}{a}\int_{\Delta\varepsilon}^{6}\varepsilon^{\frac{1}{2}}d\varepsilon + \frac{1}{a'}\int_{6}^{\infty}\frac{d\varepsilon}{(\varepsilon-3)^2}\}^{-1} \simeq 3\times10^{-9}N\ cm^3s^{-1}. \quad (4)$$

For electrons in CO, the cooling function is significantly structured (Fig.1), particularly because of the sharply-peaked vibrational excitations below 5eV. It is more meaningful to calculate the average

cooling rate over a Boltzmann distribution, which turns out to be approximately linear above $\frac{1}{2}$eV:

$$d\bar{\varepsilon}/dt \simeq -b\bar{\varepsilon}N, \quad b = 1\text{-}1.5\times10^{-8}\,cm^3s^{-1}. \qquad (5)$$

Expression (5) is only applicable if thermalization processes are rapid enough. The thermalization rate due to Coulomb collisions is

$$t_c^{-1} = cn\varepsilon^{-3/2}, \quad c = 8\times10^{-5}\ eV^{3/2}cm^3s^{-1}, \qquad (6)$$

which has to exceed the cooling rate of (5):

$$t_c^{-1} > bN \quad or \quad n/N > b\varepsilon^{3/2}/c. \qquad (7)$$

In practice, condition (7) is not fulfilled for 5eV electrons at densities found in the inner coma (Table 1). Plasma instabilities will therefore play a role in thermalization. For a highly anisotropic velocity distribution, the thermalization rate is a fraction of the plasma frequency (Davidson 1972)

$$t_\sim^{-1} \simeq 0.1\omega_{pe} \simeq dn^{\frac{1}{2}}, \quad d = 10cm^{3/2}s^{-1}. \qquad (8)$$

For the densities of Table 1, $t_\sim^{-1}$ exceeds bN by more than a factor 10. A more detailed treatment would modify (8) to include the damping effect of electron-molecule collisions, but this is estimated to be significant only inside 10^3km radius. The conclusion is that the anisotropy in electron energies will generate plasma turbulence, which produces some thermalization and limits the growth of anisotropy:

Table 1

Major ionization and recombination paths.

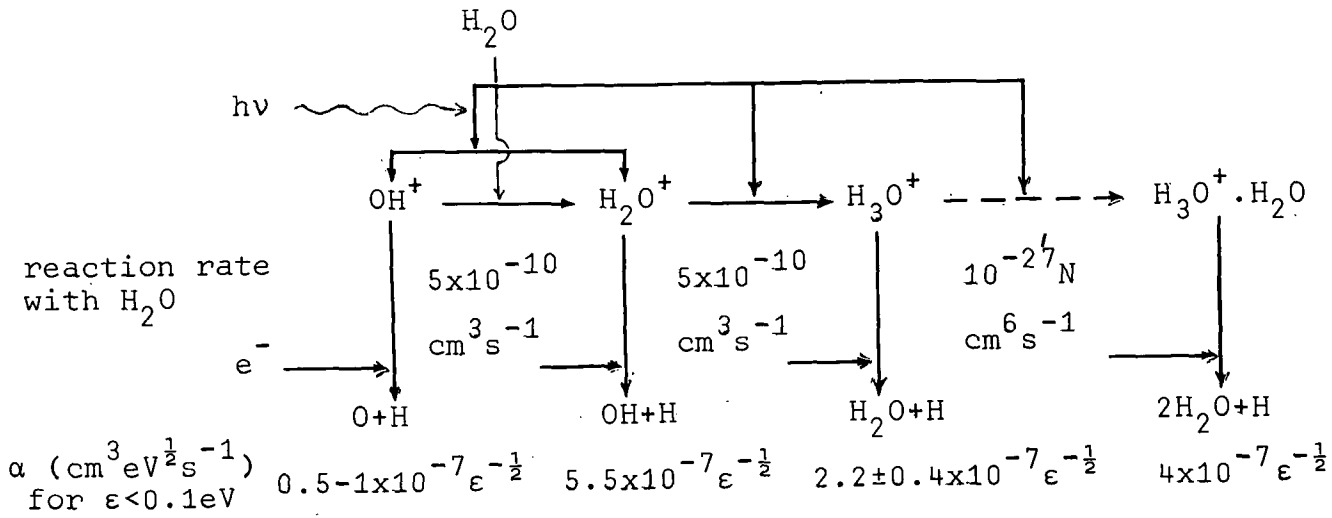

The data is culled from Banks & Kockarts (1973), Cherednichenko (1970) and Leu et al. (1973). For electron energies exceeding 0.1eV, the dissociative recombination coefficients α may decrease as sharply as ε^{-2}. At the relevant cometary densities, the 3-body collisions producing $H_2O^+ . nH_2O$ are negligible.

expression (5) should remain an adequate approximation to the cooling rate.

The electron cooling functions (2) and (3) do not tend to give large anisotropies. Plasma instabilities are less likely to be important in thermalization and the unaveraged cooling rates should be appropriate.

3. IONOSPHERE OF THE H_2O COMET.

Suppose conditions in the inner coma are quasi-stationary with photo-ionizations being balanced by recombinations, changes due to the outward expansion being comparatively slow. Photo-ionization releases a spectrum of electrons, mainly below 5eV, which cool through vibrational excitations of the H_2O as (2) and subsequently recombine dissociatively. The ions may undergo ion-molecule interactions before recombining as shown in Table 1, but this makes little difference to estimates of plasma density.

The H_2O photo-ionization cross-section (Metzger & Cook 1964, Wantanabe & Jursa 1964) varies little over 12.6-18.3eV, so the electron energy spectrum in 0-5.7eV is close to the (shifted) solar spectrum:

$$P(\varepsilon) \simeq N\tau^{-1}\, j(1+\varepsilon/\varepsilon_*)^{-j-1},\ \varepsilon_* = 12.6\text{eV}. \qquad (9)$$

Here we have used a power law approximation to the solar spectrum (e.g. Shul'man 1972) with index $j \simeq 8.7$. With the continuous description of the cooling (2), the

electron distribution function for energies above thermal where recombination is negligible is

$$f(\varepsilon) = \frac{\varepsilon^{\frac{1}{2}}}{aN} \int_{\varepsilon} P(\varepsilon')d\varepsilon' \simeq \frac{1}{a\tau}\,\varepsilon^{\frac{1}{2}}\left(1 + \frac{\varepsilon}{\varepsilon_*}\right)^{-j}. \qquad (10)$$

The solar 584Å photons contribute a further 10% by number to $P(\varepsilon)$ probably mainly in dissociative ionizations releasing electrons of 2-3eV energy, so are relatively unimportant. The 304Å and other far UV photons contribute fewer and more energetic electrons, which are very rapidly cooled according to (3) so are also unimportant. It is thus adequate to use expression (10) for the hot electrons, whose total number density and pressure do not exceed

$$\int_0^\infty f(\varepsilon)\,d\varepsilon \leq \frac{\varepsilon_*^{3/2}}{j-1} \int_0^{\pi/2} \cos^{2k-4}\theta d\theta/a\tau \simeq 40/\mathrm{cm}^3$$

$$\int_0^\infty \varepsilon f(\varepsilon)\,d\varepsilon \leq \frac{\varepsilon_*}{2j-3} \int_0^\infty f(\varepsilon)\,d\varepsilon \simeq 35\ \mathrm{eV/cm}^3. \qquad (11)$$

The numerical estimates apply for the ionization time $\tau = 10^6$s (at 0.7a.u). They are uncertain by a factor 2 or more because of uncertainty in the constant a, taken from (2).

Let us suppose for simplicity that recombination processes occur relatively slowly, so that recombination occurs only subsequent to cooling to thermal energies. This is valid if the density of thermal electrons is far greater than the density of energetic ones by (11).

Neglecting transport effects, the steady state balance of ionization and recombination rates is then

$$N/\tau = \alpha n^2$$

where α is the relevant dissociative recombination coefficient of Table 1. Thus the density of thermal electrons is

$$n = (N/\alpha\tau)^{\frac{1}{2}} \simeq 0.5\text{-}1.5\ N^{\frac{1}{2}}\ cm^{3/2}. \qquad (12)$$

Specific values of n(for $\alpha = 2.5\times10^{-7}\Delta\varepsilon^{-\frac{1}{2}}cm^3eV^{\frac{1}{2}}s^{-1}$) are given in Table 2, and clearly exceed the density (11) of the energetic electrons inside 10^5km radius. The lifetime of an ion before recombination is $(\alpha n)^{-1} = \tau(n/N)$, which is far shorter than an e-folding time for changes due to the flow, R/2.3V, so ion transport effects are indeed negligible. It can also be confirmed that electron thermal conductivity is adequately limited by e-H_2O collisions.

In the inner coma, this ionospheric plasma is closely coupled to the neutral gas and streams radially outwards with it. Outside some radius of the order of

$$Q\sigma/V \simeq 3\times10^4\text{km}, \qquad (13)$$

ion-molecule collisions become infrequent and the plasma can behave as a separate fluid with a smaller mean free path fixed by gyro-radius or collective plasma effects. A tangential discontinuity might exist between the ionospheric plasma and the plasma of solar wind origin (Wallis 1973b, Schmidt 1974). The ionospheric ions and

electrons would exert a pressure of the order of their stagnation pressure

$$P(stag) = \int \varepsilon\, f(\varepsilon)\, d\varepsilon + n(\Delta\varepsilon + kT_i + m_i V^2). \qquad (14)$$

The first term representing the suprathermal electrons is given by (11) and, on equating T_i to the neutral gas temperature T, the values of P(stag) given in Table 2 are found.

This quantity P(stag) is to be compared with the solar wind stagnation pressure, which is of order 10^4eV cm^{-3} at 0.7a.u. This would place the ionosphere discontinuity and stagnation flow region within 10^3km sunward of the comet, impossibly far inside the decoupling radius (13). If the dissociative heating and and enhanced expansion velocity of the present model coma are discounted, the values of P(stag) would be lower and the concept of a plasma contact discontinuity still more dubious.

4. PLASMA FLOW THROUGH THE COMET COMA.

As long as the ionospheric plasma pressure is low (section 3), the solar wind plasma can flow on into the inner coma. We consider that it picks up new cometary ions and loses those neutralized in charge exchange processes in interactions with the neutral coma (Wallis 1973a). There is no sudden change at the scale coupling radius $Q\sigma/V$ (13), and we can expect the flow to penetrate far inside this position. We are interested

Table 2

Parameters in an H_2O coma.

R (km)	V (km/s)	T (°K)	$kT+mV^2$ (eV)	N (cm^{-3})	n (cm^{-3})	P_{stag} (eV/cm^3)
10^2	0.55	350	0.08	$2x10^{10}$	$1.1x10^5$	$1.2x10^4$
10^3	0.8	750	0.18	$1.3x10^8$	$8.6x10^3$	$1.8x10^3$
10^4	1.5	2800	0.67	$7x10^5$	$6.3x10^2$	$4.7x10^2$
10^5	2.6	(650)	1.27	$4x10^3$	50	100

Source strength $Q = 10^{29}$ molecules $ster^{-1}s^{-1}$. The neutral gas expansion velocity V, density N and temperature T are taken from the heated coma model of Wallis (1974), but T at 10^5km is uncertain. The plasma density n and stagnation pressure are calculated for solar radiation conditions at 0.7 a.u. heliocentric distance.

here in how rapidly the plasma can cool and condense.

There is no flow solution yet available for this strongly interacting and strongly cooled plasma flow, so we shall in making definite estimates assume that the plasma velocity in the incoming flow sunwards of the comet is

$$u = R/\tau_f, \qquad \tau_f \simeq 10^3 s, \tag{15}$$

τ_f being an empirical flow time scale which fits in with the outer flow solutions in the $1\text{-}5\times10^5$km region (Wallis 1973a,b). The assumption (15) is not critically important: if in error, the distance scale that we derive is simply distorted.

The cometary ions are rather energetic: they take up most of the streaming energy of the decelerating flow and have gyration velocities of the order of the flow velocity $v_* = R_*/\tau$ at the place where they become ions. They are lost primarily through charge exchange, so their distribution function $g(v_*)$ satisfies

$$\frac{dg}{dt} = -u\frac{dg}{dR} \simeq -\frac{Q\sigma}{VR^2} v_* g. \tag{16}$$

This equation neglects increases in ion energies due to continuing adiabatic compression. The solution to (16) using (15) and taking V as constant is

$$g(v_*) \sim \exp \ell_i^2 (R_*^{-2} - R^{-2}), \tag{17}$$

where

$$\ell_i = \ell_i(v_*) = \{\tfrac{1}{2}\tau_f \sigma(v_*) v_* Q/V\}^{1/2}.$$

The number is reduced by a factor e by the position $R = \ell_i$ and a further factor e by $R = 0.7\ \ell_i$. Numerically ℓ_i is 3×10^4km for initial ions of 600km/s velocity and $\ell_i = 2\times10^4$km for the 50km/s ions formed at 5×10^4km. The solar wind protons have thermal speeds of the order of 50-100km/s, so the corresponding disappearance scale is $\ell_p = 2\text{-}2.5\times10^4$km.

The electrons in the inflowing plasma also cool rapidly due to various ionization and excitation processes. We suppose the cooling rates of (2) and (5) are representative in the mainly O and OH coma in $10^4\text{-}10^5$km. The electron energy is perhaps ε_0=50eV at $R_0 = 10^5$km and decreases as

$$\bar{\varepsilon}/\varepsilon_0 = \exp - \ell_e{}^2(R^{-2} - R_0{}^{-2}), \quad \bar{\varepsilon} > 6\text{eV}, \qquad (18)$$

according to (5) with (15), the scale radius being

$$\ell_e = \{\tfrac{1}{2}\, b\tau_f\, Q/V\}^{1/2} \simeq 2\times10^4\text{km}. \qquad (19)$$

The mean energy reaches 6eV at $R_1 \simeq 1.5\times10^4$km and would be 1eV at 10^4km by formula (18), but even faster cooling according to expression (2) is appropriate:

$$(6\text{eV})^{3/2} - \bar{\varepsilon}^{3/2} \simeq \frac{3}{4}\frac{Q}{V}\, a\tau_f\, (R^{-2} - R_1{}^{-2}). \qquad (20)$$

The electrons become fully cooled, it follows, at the position

$$\{R_1{}^{-2} + (6\text{eV})^{3/2}\, 4V/3Qa\tau_f\}^{-\frac{1}{2}} \simeq 1.0\times10^4\text{km}. \qquad (21)$$

So in the absence of heating mechanisms, such as plasma

turbulence transferring energy from the ions, the electrons cool explosively fast between positions ℓ_e — $\frac{1}{2}\ell_e$.

If plasma is to flow from the coma out laterally into tail rays, it is clear that the same scale radii are important. For example, suppose that flow occurs at constant radius and speed (the pressure gradient balancing the effective friction).

We replace d/dt in (16) by $R\tau^{-1}$ d/ds and obtain

$$g \sim \exp - \tfrac{1}{2}\ell_i^{\,2}(s-s_0)/R^3.$$

With flow distance $s-s_0 = \pi R/2$, we see that most of the ions would be lost if $R \lesssim \ell_i$. Similarly, the electrons would be strongly cooled if the lateral flow takes place at $R \lesssim \ell_e$. Coincidentally, these ion and electron scales are very similar in magnitude.

5. DISCUSSION

Solar plasma plus accumulated cometary ions and electrons is affected very strongly as it flows into the coma from 2×10^4 to 10^4km (this value for the comet with Q = 10^{29} H_2O molecules $ster^{-1}s^{-1}$. The scale distance $\sim Q^{1/2}$.) The electrons are rapidly cooled and all but some 10% of the ions undergo charge exchange. This behaviour is not sensitive to our assumption (15) for the flow velocity, since it occurs explosively quickly. We conclude that this $1\text{-}2\times10^4$km region is effectively a transition region over which the outer plasma carrying the energy and ion flux of the solar

wind changes continuously to plasma created and energised by the solar radiation. The purely cometary ionospheric plasma, flowing outwards with the expanding gas coma, would have stagnation pressure only 10% or less of that of the solar wind at the transition position — it can hardly affect the flow there. Although a stagnation region must occur in the plasma flow at some smaller radius, there will be no "tangential discontinuity" between plasmas of different nature or velocity.

An important characteristic of the ionospheric plasma is that the photo-electrons can cool rapidly to thermal energies before recombining. Rotational excitations of H_2O or OH are effective in the case considered. However, if the coma consisted for example of pure CO, the cooling mechanism would be more complex (section 2), with plasma turbulence trying to thermalize an anisotropic distribution of electron energies. The corresponding plasma pressure and density might be higher and significantly affect the transition flow. But in the H_2O comet, the conclusion is clear, that the pressure of the ionospheric plasma is unimportant.

We have assumed a model coma heated by photo-dissociations of H_2O, this model having a higher expansion velocity and temperature and larger ionospheric stagnation pressure. If there is no such heating, the

plasma pressure would be lower. Shimizu (1974) has questioned the reality of the heating in the H_2O coma, on the grounds that rotational excitations rapidly remove the energy of the H-atoms. Indeed, the energy transfer from 1-2eV H-atoms to the rotational mode appears to be comparable to the elastic transfer to translational energy (σ_{rot} is higher by a factor 10, but the energy transferred is about 0.025eV rather than 0.2-0.4eV). This indicates that part of the photo-dissociation energy is available for heating and increasing the expansion velocity of the coma. The conclusion that the coma temperature is very low (Shimizu 1974) depends on the achievement of thermodynamic equilibrium between the rotational levels of H_2O, and is inapplicable at the relevant coma densities (Table 2) of $10^8 cm^{-3}$, or less.

The plasma interaction with the coma gas imposes strong limits on the place of origin of cometary ions which are to form tail rays. For plasma moving at around 10km/s velocity within the ℓ_i, $\ell_e \simeq 2 \times 10^4$km scale is frictionally decelerated, strongly cooled and liable to recombination long before it can flow away. It appears impossible for plasma to emerge from inside 10^4km radius to form tail rays and streamers. In the transition region at 1.5-2.5km radius, the plasma can be cooled to give increased density and still flow away before recombination occurs. As such plasma

expands adiabatically into tail rays, the recombination rate per unit mass changes as

$$\rho\alpha \sim \rho T^{-k} \sim \rho^{-k(\gamma-1)+1}, \qquad (22)$$

decreasing with ρ for $k \simeq \frac{1}{2}$ (Table 1). Recombination decreases in importance, despite the adiabatic cooling.

This confirms assumptions of the earlier analysis of a tail ray (Wallis 1967) as a jet of plasma, initially cold but not undergoing recombination, ejected into the solar wind plasma where it is conductively heated and frictionally accelerated. The particular transport coefficients assumed were based on the transverse instabilities of velocity anisotropics in an unmagnetised plasma, on which much work has been done recently (Davidson 1972). As the magnetic fluctuations were found to exceed the expected intensity of any large-scale field, the unmagnetised ion-ion instability is indeed appropriate, but the postulated electron-ion instability may be eliminated by electron gyro-radius effects. The order-of-magnitude linear growth rate is, however, unchanged. Moreover, the demonstration that the non-linear process limiting the instability growth is ion trapping (Davidson 1972), confirms the earlier assumption (Wallis 1967) equating the growth rate to an effective collision or "bounce" frequency. So we consider that the earlier results need little modification. They imply, we recall, that there was substantial extra mass over and

above the observed CO^+ in the tail rays examined - this might well be C^+, O^+ or OH^+.

Values of the CO^+ density in the coma at 10^4km radius have been given by Arpigny (1965) as 400cm^{-3} in comet Bester (at 1.0a.u.) and 600-1000cm^{-3} in comet Humason (2.6a.u). These are the same order as the ionospheric density (Table 2), although with the lower ionization rate at 2.6a.u., the CO production rate would have to be higher than 10^{29}ster^{-1}s^{-1}. Alternatively the transport effects of ions being swept in by the solar wind flow can enable higher densities to be reached. It is noteworthy that 'envelope' and jet structures were observed in comet Bennett at 1-3x10^4km ahead of the nucleus (Wallis 1973b). The appearance of structures at this position corresponds well with the present argument that cooling is important in allowing condensation of the plasma swept in with the solar wind. However, the mechanism for producing structures rather than continuous flow is not yet explained.

When ion-electron recombination is the dominant loss process, a recombination instability exists (D'Angelo 1967) if the coefficient $\alpha \sim T^{-k}$ varies rapidly,

$$- k (\gamma_e - 1) + 2 < - 1 . \qquad (23)$$

If electron energies were as high as thermal energies 0.25eV at 10^4km (Table 2), the index may be as high as $k = 2$ (Leu et al. 1973), and the plasma might thus be

unstable to compressional waves along the magnetic field ($\gamma_e = 3$). However, the energy transfer due to rotational excitations would exceed that due to recombinations by a factor

$$6 \times 10^{-8}\ \varepsilon^{-\frac{1}{2}}\ N / 3 \times 10^{-7}\ \varepsilon^{\frac{1}{2}} n,$$

approximately 500 at 10^4km (Table 2). The recombination instability might still operate far out in the coma and perhaps lead to the formation of 'knots' and other irregularities in tail rays. But some other process must underlie the formation of envelopes, probably a combination of dynamical with ionization and cooling effects.

M.K. Wallis acknowledges financial support from the U.K.A.E.A. Culham Laboratory and R.S.B.Ong acknowledges a U.K. Science Research Council Visiting Fellowship and Grant AF-AFOSR-72-2224.

References

P.M. Banks, G.Kockarts 1973 'Aeronomy', Section 10.7, New York.

L. Biermann, E. Trefftz 1964 Zs.f.Astrophysik 59 1.

V.I. Cherednichenko 1970 Problemi kosmich.fiziki 5, 95.

N. D'Angelo 1967 Phys.Fluids 10 719.

R.C. Davidson 1972 'Methods in non-linear plasma theory', chapters 4 and 9, Acad.Press.

R.J.W. Henry, M.B. McElroy 1968 in 'Atmospheres of Venus and Mars' p.251, ed. J.C. Brandt & M.B. McElroy, Gordon & Breach.

M.T. Leu, M.A. Biondi, R. Johnson 1973 Phys.Rev.A 7 292.

P.H. Metzger, G.R. Cook 1964 J.Chem.Phys. 41 642.

J.J. Olivero, R.W. Stagat, A.E.S. Green 1972 J.Geophys.Res. 77 4797.

T. Sawada, D.L. Sellin, A.E.S. Green 1972 J.Geophys.Res. 77 4819.

T. Sawada, D.J. Strickland, A.E.S. Green 1972 J.Geophys.Res. 77 4812.

H.U. Schmidt 1974 This conference.

M. Shimizu 1974 This conference.

L.M. Shul'man 1972 'Dinamika kometnikh atmosfer', Ch.III Naukovo Dumka, Kiev.

M.K. Wallis 1967 Planet.Space Sci. 15 137.
1973a Planet.Space Sci. 21 1647.
1973b Astron.Astrophys. 29 29.
1974 Mon.Not.R.Astr.Soc. 166 181

K. Wantanabe, A.S. Jursa 1964 J.Chem.Phys. 41 1650.

DISCUSSION

H. Keller: The outflow velocity used by Wallis is $\sim 3\text{-}4\,km^{-1}$ (for H_2O, OH..) on the argument of heating by dissociative excess energies whereas some observations show only $\sim 1\,km\ s^{-1}$ (that means no heating of the neutral component). Observations are necessary.

H. U. Schmidt: There may be a misunderstanding. In my discussion I assumed a negligible contribution to the temperature from the electrons, so that the pressure on the contact surface comes from the expansion of the remaining ions with 1 or 3 km/sec. I think your calculations are extremely valuable for another purpose, too, i.e., the electrical conductivity which can be obtained is important in the same context.

M. K. Wallis: Well, I agree that I've ignored things like electron conductivity. One can take the view that conductivity is high along the field lines. I would rather take the view that the plasma is rather turbulent and the conductivity on the field lines is not going to be that much different from conductivity across the field lines. I agree this is speculation and that it is something that needs to be looked into at some stage.

When you use conservation procedures like this, then you've got to be on your guard against that. But the ion pressure, I thought I understood you to say earlier that the momentum contribution of the outflowing ions, was unimportant. It was more the magnetic stresses which were bigger in effecting the pressure.

I don't have an outside and inside. There were two models. One is flowing in, straight in to the comet and the other one is looking at the plasma density in the inner region when you don't have any addition of plasma flow in It's just from the photoelectron plasma.

Now, these two regions have to be matched, of course, and you will have some ion pressure. But I'm cooling my electrons down so fast that I'm going to recombine the ions.

Now, it may be if you add that in it doesn't — that you get a bigger contribution. I'm not clear on that. We'll have to see.

THE WIND-SOCK THEORY OF COMET TAILS

John C. Brandt and Edward D. Rothe

I. Introduction

Type I or ionic comet tails on the average make an angle of a few degrees at the nucleus with the prolonged radius vector in the direction opposite to the comet's orbital motion. This fact was explained by Biermann (1951) as the aberration angle caused by the comet's motion in the outflowing solar wind plasma, and, as is well known, led to the discovery of the solar wind itself. Mathematically, the direction of the tail $\vec{T}$ is given by the vector equation

$$\vec{T} = \vec{w} - \vec{V} \tag{1}$$

where $\vec{w}$ is the solar wind velocity and $\vec{V}$ is the comet's orbital velocity. Equation (1) or simplified forms of it have been used extensively to derive properties of the solar wind (Belton and Brandt 1966; Brandt 1967; Brandt, Harrington and Roosen 1973). The solar wind properties derived from ionic comet tails agree with directly determined properties in all cases where comparison is possible and, hence, the validity of equation (1) has been established. If the solar wind determines the gross shape of the entire plasma tail, what is this shape and how can it be calculated?

There are at least three conceptually distinct approaches to calculating the shapes on ionic comet tails.

(1) The Mechanical or Bessel-Bredichin Theory. The details of this approach first treated by Bessel (1836) are widely known. A constant acceleration is assumed to act on the tail material, and in the calculations, this is included by using a reduced solar gravity. Bredichin defined Type I comet tails as syndynes with extra repulsive force $(1 - \mu) \approx 18$. Unfortunately, syndynes are tangent to the prolonged radius vector at the nucleus which is contrary to the observations. The tail curvature given by a syndyne with $(1 - \mu) \approx 18$ is probably not correct either and we return to this point below.

(2) The Smoke Theory. Here, the force on the tail material is given by a momentum transfer depending on the relative velocity of the solar wind with respect to the tail material (see Belton 1965, Appendix 1). Hence, if $\vec{r}'$ is the velocity of the tail material, we would need to include a force of the form

$$F\ (w - \vec{r}') \qquad (2)$$

and calculate the speed of the tail material $\vec{r}'$ at all points. Our understanding of the solar wind interaction with plasma tails is insufficient to permit accurate calculation of the forces required on the smoke theory. This difficulty obviously applies to an entire class of theories requiring specific forces. Fortunately, knowledge of specific forces may not be necessary.

(3) Wind-Sock Theory. Here we do not need the forces accelerating the material along the tail. The magnetic field along the tail is used to channel the tail plasma and the location of the magnetic field lines in the tail is determined by the local momentum field in the solar wind. The magnetic field acts as a transparent wind sock. This viewpoint implies that the field lines are trapped in the cometary plasma around the nucleus long enough for them effectively to be fastened to the comet's head. The first explicit statement of this concept known to us was by Alfvén (1957) who wrote:

> "The tail should no more be considered as gas moving freely in space. Instead the tail is a real part of the comet, fastened to the head by magnetic field lines."

II. Theory

The gross shape of an ionic comet tail on the wind-sock theory assuming constant solar wind speed can be calculated by applying the equation $\vec{T} = \vec{w} - \vec{v}$ pointwise along the tail. The basic geometry in the plane of the comet's orbit is shown in Figure 1. By projecting the components of solar wind velocity into the cometocentric coordinate system, we obtain the basic equation for the wind-sock theory, viz.,

$$\frac{dy}{dx} = \frac{-V \sin \gamma - w_r \sin \alpha + w_\phi \cos \alpha \cos i'/\cos b}{w_r \cos \alpha - V \cos \gamma + w_\phi \sin \alpha \cos i'/\cos b}$$

Many of the quantities used are illustrated in Figure 1. In addition, w_r and w_ϕ are the radial and azimuthal components of the solar wind

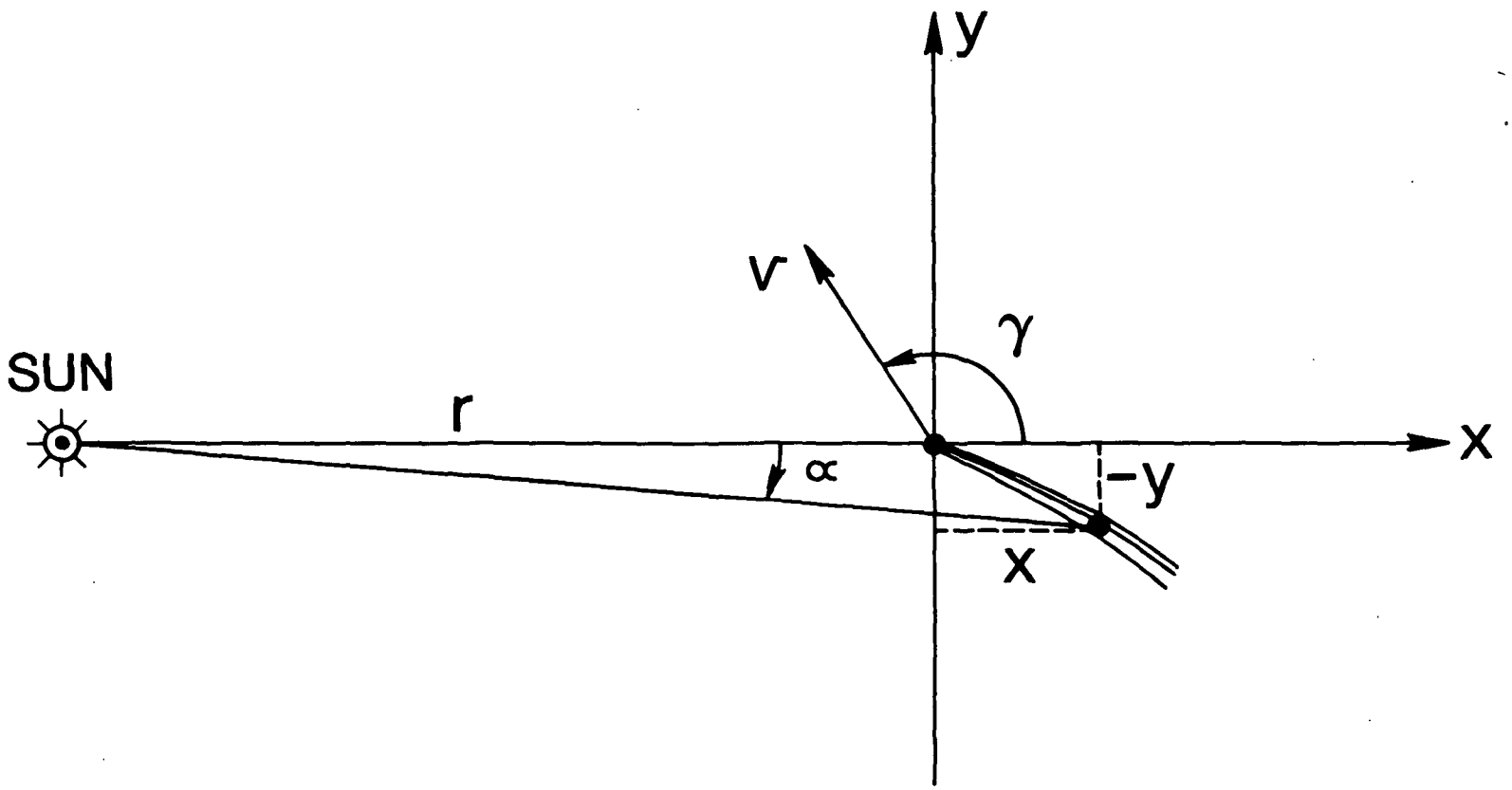

Figure 1. The geometry for the wind-sock theory of ionic comet tails in the plane of the comet's orbit.

velocity. The angles i' and b are the inclination of the orbit with respect to the solar equator and the heliographic latitude, respectively. If necessary, this equation could easily be generalized to three dimensions; in this case, the direction cosines at each point (dx, dy, dz) would be similarly determined.

A simple analytical result can be obtained on the basis of some reasonable approximations. For a comet away from the sun (i.e., non-sungrazers) and near perihelion, $\alpha \ll 1$ and $w_r \gg \cos \gamma$, respectively, are good approximations. Then, equation (3) can be written

$$\frac{dy}{dx} = \frac{-V \sin \gamma - w_r \alpha + w_\phi \cos i'/\cos b}{w_r} \tag{4}$$

Equation (4) can be used to evaluate the coefficients in a Taylor's series. If we let

$$-y = A + Bx + Cx^2 + Dx^3 + \ldots , \tag{5}$$

we find

$$\begin{aligned} A &= 0 \\ B &= \left[\frac{V \sin \gamma - w_\phi \cos i'/\cos b}{w_r - V \cos \gamma}\right] \\ C &= +\frac{B}{2r} \\ D &= \frac{-B}{6r^2} \end{aligned} \tag{6}$$

If we write

$$X = x/r$$
$$Y = y/r \tag{7}$$

where r is the comet's heliocentric distance, our final equation becomes

$$-Y = BX + \frac{B}{2} x^2 + \ldots \tag{8}$$

for $X \leq 0.3$, the cubic term is 1.3% or less compared to the sum of the first two terms.

The Taylor's series solution can be obtained without the approximations used to write equation (4) and is

$$-Y = BX + \left[\frac{w_r^2 + \left(\frac{w_\phi \cos i'}{\cos b} \right)^2 - V \left(\frac{w_\phi \sin \gamma \cos i'}{\cos b} + w_r \cos \gamma \right)}{(w_r - V \cos \gamma)^2} \right] \frac{Bx^2}{2} + \ldots \tag{9}$$

For most cases, the term in brackets in equation (9) is close to 1 and equation (9) reduces to equation (8). In doubtful cases, equation (9) provides a check on the applicability of the simple solution.

Our approximate (but rather accurate solution) for steady solar wind conditions depends only on the quantity B which is the tangent of the aberration angle at the nucleus used in the earlier work. The calculated tails are nearly straight near the head, but show curvature well away from the head. The curvature arises from the geometrical divergence of the radial direction in a spherical coordinate system.

III. Applications

First, we briefly reexamine the historical question of Bredichin's identification of the Type I tails with syndynes from the mechanical theory for $(1 - \mu) \approx 18$. We have checked back to some of Bredichin's (1884) original work in which the observations (for the Great Comet of 1882) were given. They show little or no tail curvature and we have no difficulty fitting the wind-sock theory with modern solar wind parameters (Figure 2). Bredichin's fit with $(1 - \mu) \approx 18$ would not be bad in an rms sense, even though the aberration angle at the nucleus was in error on the average by $\approx 5^{o}$ and the curvature was too large. Visual observations of very bright comets in the 19th century may be a valuable untapped source of solar wind data.

The wind-sock theory can also be applied to the geomagnetic tail (Figure 3). Behannon's (1970) observations gave an aberration angle of $3^{o}.1$ and this is closely approximated by the solar wind parameters chosen. Figure 3 shows that observations would be required at tenths of A.U. from Earth to detect the effects of the tail curvature; such observations are unlikely in the near future. A comparison of an accurate computer integration of equation (3) with the Taylor's Series result of equation (8) is also shown.

Figure 4 shows a photograph of Comet Kohoutek taken at the Joint Observatory for Cometary Research (JOCR) on January 19, 1974. We would anticipate no difficulty in explaining the gross shape of the main ion tail on the basis of steady solar wind conditions. However, it is important to note that our model may require comparison with averages

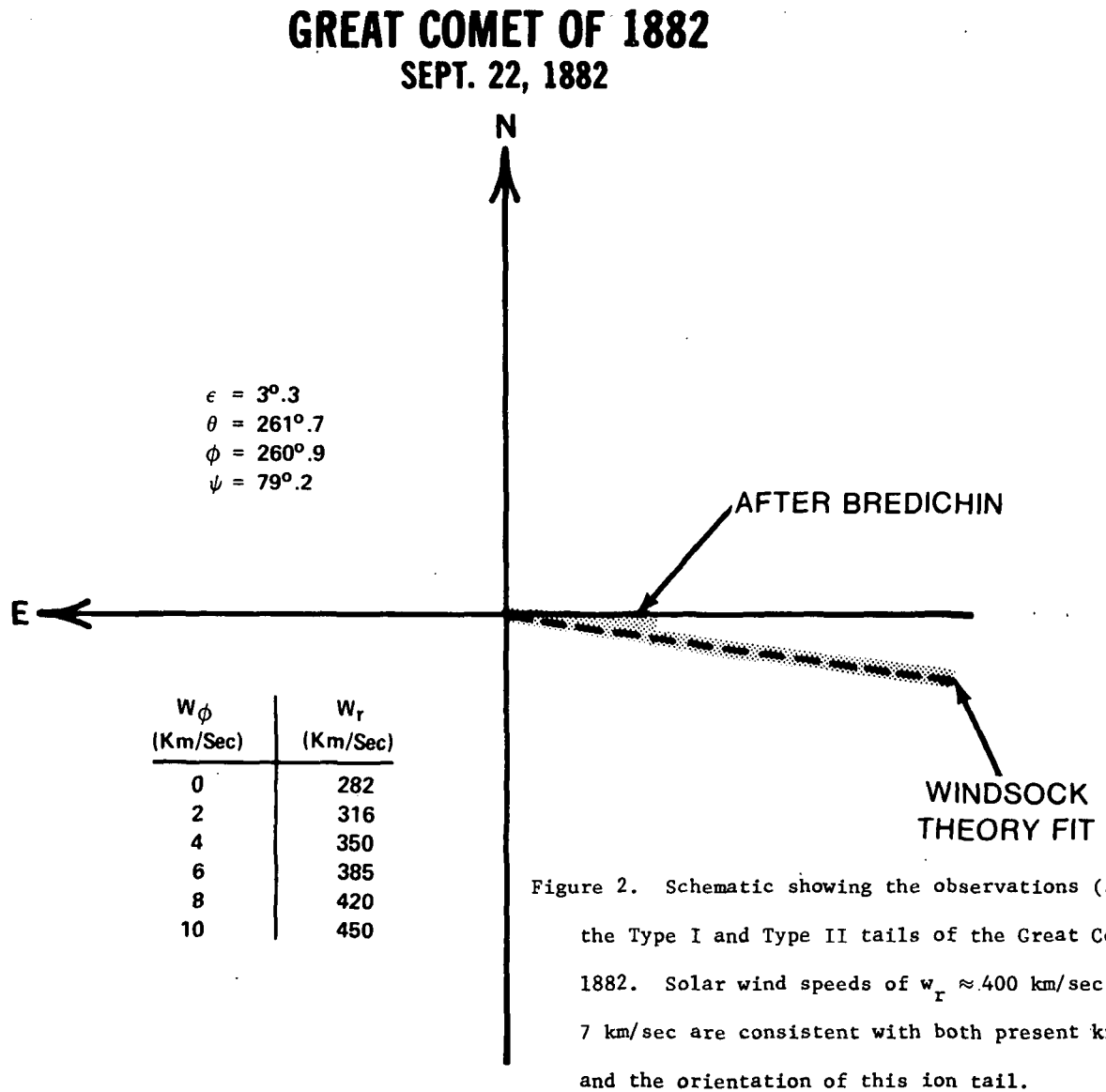

W_ϕ (Km/Sec)	W_r (Km/Sec)
0	282
2	316
4	350
6	385
8	420
10	450

Figure 2. Schematic showing the observations (shaded) of the Type I and Type II tails of the Great Comet of 1882. Solar wind speeds of $w_r \approx 400$ km/sec and $w_\phi \approx 7$ km/sec are consistent with both present knowledge and the orientation of this ion tail.

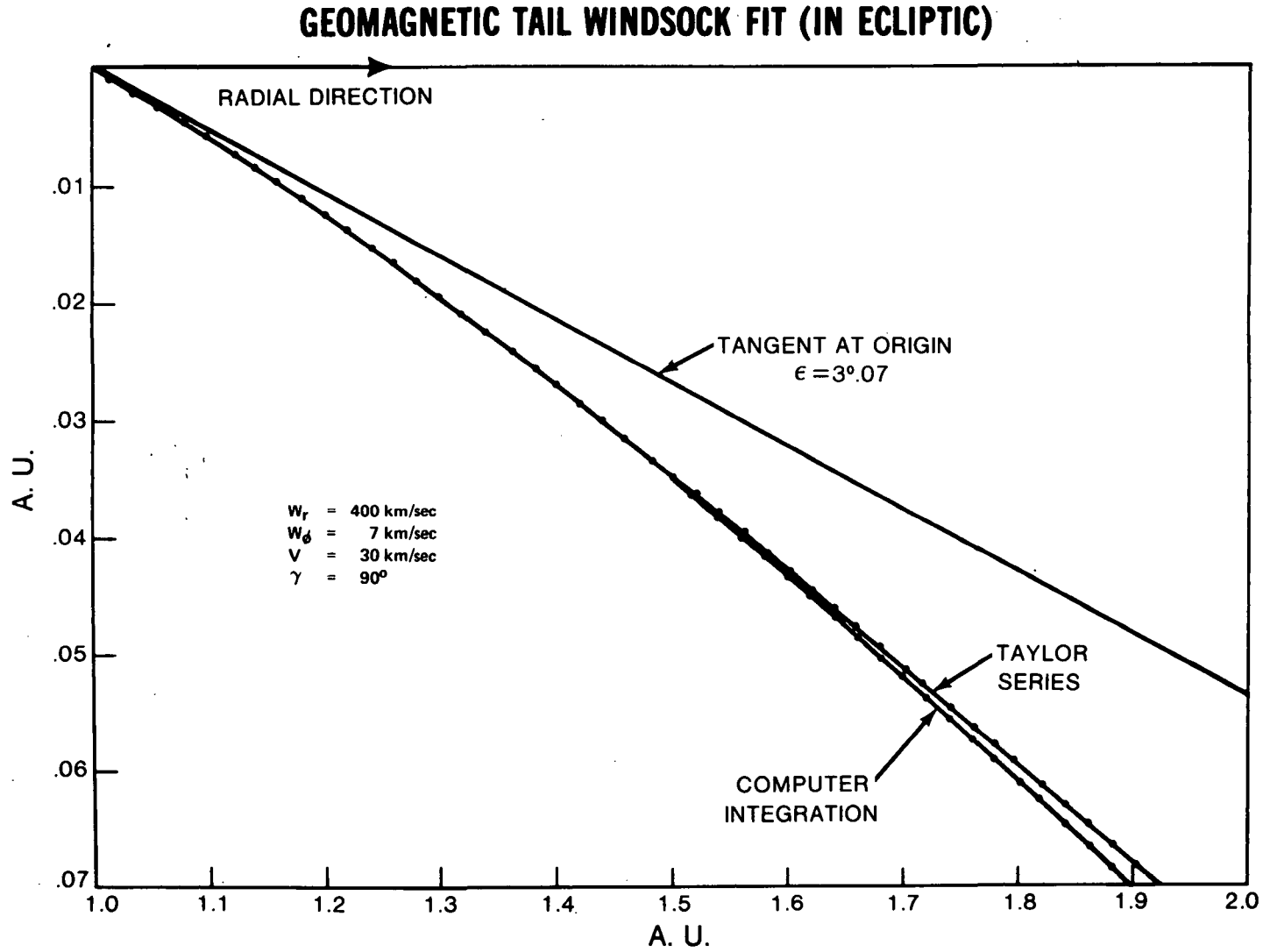

Figure 3. Application of the wind-sock theory to the geomagnetic tail as discussed in the text.

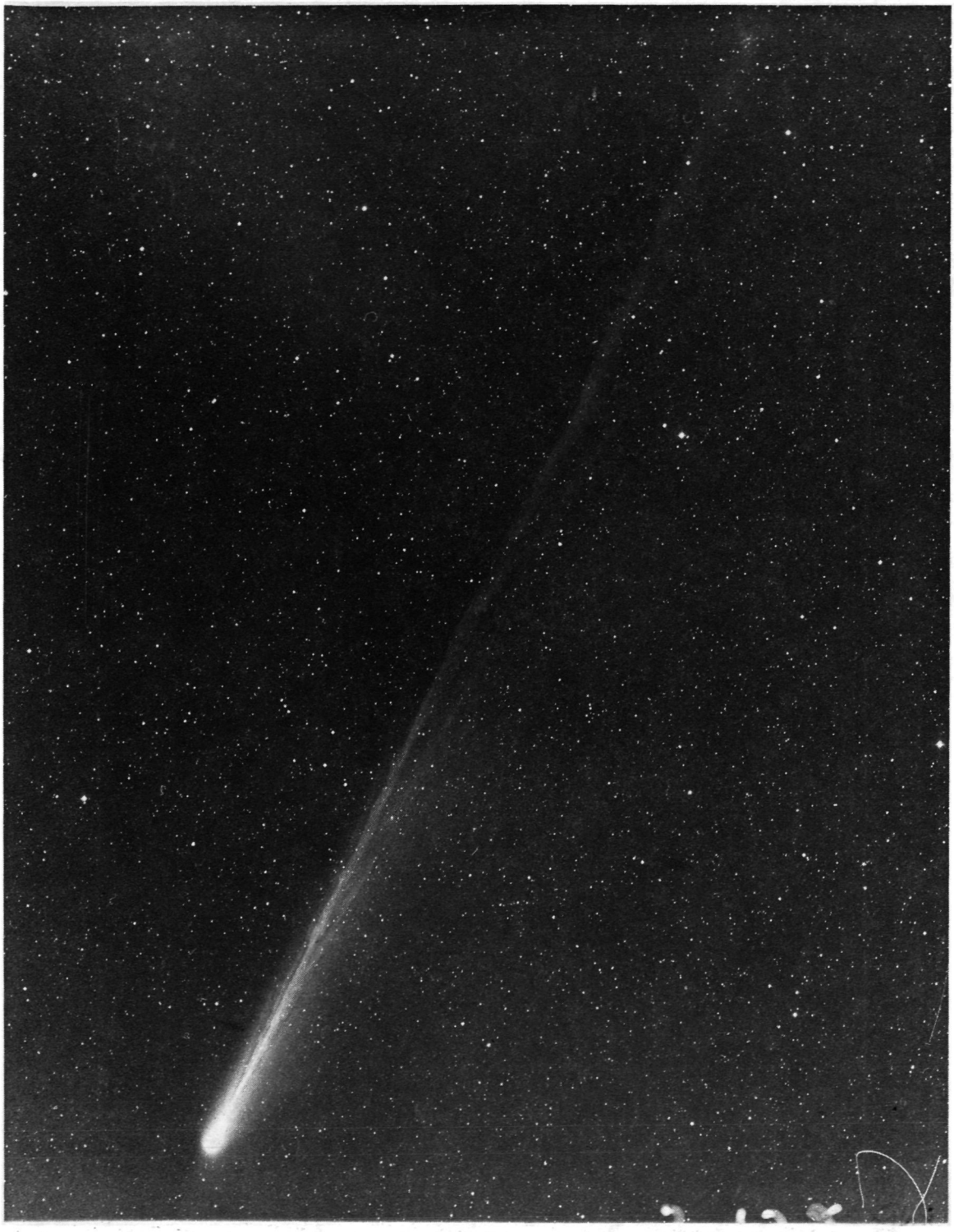

Figure 4. JOCR photograph of Comet Kohoutek on January 19, 1974.

of observations if sufficiently steady solar wind conditions are not found. For example, Comet Kohoutek on January 20, 1974 (Figure 5) showed a large disturbance in the shape of the main tail. Our solution with $B \approx 0.36$ would be a reasonable fit to the tail shape except for the disturbance as is shown schematically in Figure 6. The disturbance could be caused by a high-speed solar wind stream. Note that the quiet conditions for $B = 0.36$ are somewhat unusual; a large negative value of w_ϕ is necessary to produce a reasonable w_r value. We suspect that changes in solar wind conditions produce changes in gross plasma tail shapes and that study of tail shapes may provide information on velocity structures in the solar wind.

IV. Conclusions

We have presented a simple version of the wind-sock theory of ionic comet tails. The simple model is consistent with all facts known to us. There are straightforward improvements that can be made for the case of steady solar wind conditions (e.g., inclusion of effects due to the tail's magnetic field). Consideration of the non-steady case are also of considerable interest.

Figure 5. JOCR photograph of Comet Kohoutek on January 20, 1974.

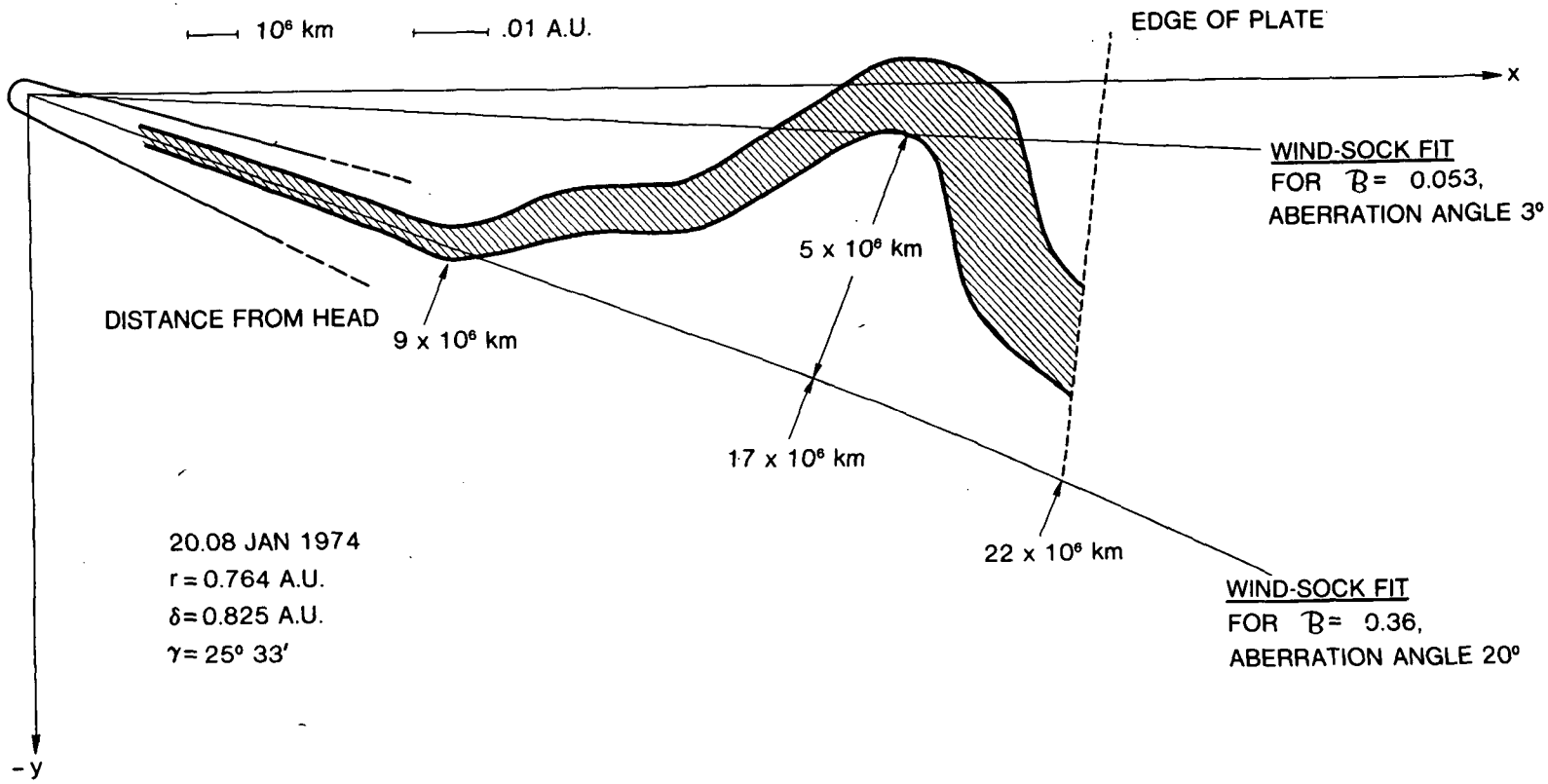

Figure 6. Schematic representation of Comet Kohoutek on January 20, 1974 (Figure 5) as seen in the plane of the comet's orbit.

References

Alfvén, H. 1957, Tellus, 9, 92.

Behannon, K. W. 1970, J. Geophys. Res., 75, 743.

Belton, M. J. S. 1965, A. J., 70, 451.

Belton, M. J. S., and Brandt, J. C. 1966, Ap. J. Suppl., 13, 125 (No. 117).

Bessel, W. 1836, A.N., 13, 185.

Biermann, L. 1951, Zs. f. Ap., 29, 274.

Brandt, J. C. 1967, Ap. J., 147, 201.

Brandt, J. C., Harrington, R. S., and Roosen, R. G. 1973, Ap. J., 184, 27.

Bredichin, Th. 1884, Ann. Moscou Obs., 10, 7.

DISCUSSION

B. Jambor: If I understand you correctly your Bredikhin approach to the problem fails because you do not get enough curvature in the tail; I would be curious to know what a more precise approach like the Finson-Probstein, not relying on approximations of series expansion, would yield.

J. C. Brandt: Yes. You know, I took that solely because for years that has been the definition of a Type 1 tail. These Type 1 and Type 2 appear in Bredikhin's papers, and I was curious as to how this got started.

D. J. Malaise: The windsock model has the nice feature that you can compute the shape of the tail. Has it not the drawback that you have to drop the assumption that the tail lies in the orbital plane of the comet. Even small departures from the orbital plane makes the computation of the true direction of the tail quite indeterminate in some projection situations.

J. C. Brandt: Now clearly, you can create such a comet. The Comet Mrkos was one such thing. It was at 90 degrees inclination, and that's going to be a problem. But with any care at all, it's not a problem.

K. Jockers: Your windsock model is the model of a tail which can withstand any tension along its axis but has to be in lateral momentum equilibrium. The small curvature of the tails is caused by a diverging but stationary solar wind flow field. How can this model be applied to an evidently non-stationary situation as on Jan. 20?

J. C. Brandt: I think, if you stop and think about it, that you can make qualitative statements about what happened.

K. Jockers: You know, that windsock has to respond to the changing non-stationary situation and that is completely different than that line you have calculated.

J. C. Brandt: It is not necessarily completely different from the line, but it may be. But if you know how to calculate that, why don't you let me know and we'll do it.

PROGRESS IN OUR UNDERSTANDING OF COMETARY DUST TAILS

Zdenek Sekanina

I. INTRODUCTION

It is almost generally accepted that the essentially structureless and often significantly curved tails of comets are composed of sunlight-scattering solid particles of various sizes, ejected from the comet's nucleus by evaporating gases. Much less agreement has so far been achieved as to the character, composition, and size distribution of the particles.

The original version of the theory of cometary tails (Section II) followed the pattern of comparing a simple theoretical model with comet drawings based on visual observations, while modern versions (Sections III through VIII) utilize small-scale photographs of comets instead. Other techniques, complementing the photographic study of dust tails, include spectroscopy, broad-band photoelectric photometry, colorimetry, infrared photometry, and polarimetry. Major problems for these other techniques are the large extent of a cometary tail and its low surface brightness, which drops rapidly with increasing distance from the nucleus. Consequently, such observations often refer only to the brightest part of a tail, adjacent to the nucleus and/or coma, rather than to the tail as a whole.

Since the philosophy, covering the advantages as well as the limitations, of the various techniques employed is discussed in other review papers at this Colloquium, we shall avoid describing it here. We shall refer, however, to the results obtained by any technique in which the data are relevant to the theory of dust tails.

II. THE MECHANICAL THEORY

The birth of the mechanical theory dates back to the 1835 apparition of periodic Comet Halley. The theory's fundamentals were worked out by Bessel (1836) in his attempt to explain the comet's observed structure. He derived equations of motion for particles ejected from a cometary nucleus and driven away from the sun by a repulsive force. This force, believed by Bessel to be caused by ether, was assumed to vary in inverse proportion to the square of heliocentric distance. It was not until more than 60 years later that the repulsive force was identified as solar radiation pressure (Arrhenius 1900; Schwarzschild 1901); this interpretation is now generally accepted.

Meanwhile, the mechanical theory was being improved by Bredikhin (Jaegermann 1903). He replaced Bessel's approximate equations of particle motion (expressed in terms of a power expansion, with the time elapsed since ejection used as the variable) by precise formulas for hyperbolic motion. The two, now very common terms describing dust tails – syndyne (or syndyname) and synchrone (or isochrone) – are also due to Bredikhin.

A syndyne is defined as the locus of particles leaving a cometary nucleus continuously and subject to radiation pressure of a particular magnitude. Each syndyne is thus determined by the acceleration $1 - \mu$ exerted by radiation pressure on the particles. When expressed in units of the solar gravitational attraction, $1 - \mu$ is related to the particle's radius a (cm) and its density ρ (g cm^{-3}) as follows:

$$1 - \mu = \frac{0.585 \times 10^{-4} Q_{rp}}{a\rho} \quad , \qquad (1)$$

where Q_{rp} is the scattering efficiency of the particle for radiation pressure.

A synchrone is defined as the locus of particles subject to radiation pressure of all magnitudes and ejected from the nucleus at the same moment. Each synchrone is therefore determined by the instance of ejection, or by its "age" τ, i.e., by the time elapsed between ejection and observation.

The shape of a synchrone or a syndyne also depends slightly on the initial (ejection) velocity of the particles. However, since ejection velocities are relatively low (only a fraction of 1 km sec^{-1}), the synchrones and syndynes used in modern methods usually refer to an assumed zero ejection velocity, and the effect of the actual velocity is taken care of in a different way. On the assumption of a zero velocity of ejection, synchrones and syndynes can be calculated from the orbital elements of the comet once the values of τ and $1 - \mu$ are specified.

Bredikhin considered most tails to be syndynes. He determined $1 - \mu$ for a rather large number of comets and eventually organized his results into a classification of cometary tails. His type I tails are now identified with the plasma tails, and type II (and type III) tails, with the dust tails.

The mechanical theory was originally intended to cover all comet tails. However, the theory completely failed to explain the complicated structure of type I tails on comet photographs and was eventually replaced by Biermann's (1951) hypothesis of interaction between the comet plasma and the solar wind.

By the 1960s, serious doubts were expressed as to the validity of the mechanical theory even for type II tails: Most dust tails appeared to match neither a synchrone

nor a syndyne; the tails were often found to point approximately midway between the prolonged radius vector and the orbit behind the comet; a dark band, observed to part tails of several comets into two branches, and described often as a "shadow of the nucleus," was much of a mystery, as was the occasional appearance of sunward-oriented tails; and the "synchronic" bands did not behave as they were supposed to according to the theory. Thus, the mechanical theory appeared to face a very bleak future.

III. THE FINSON-PROBSTEIN APPROACH

Eight years ago, Finson and Probstein (1966) published their preliminary model of dust comets. The motion of dust particles in the tail was treated as a hypersonic, collision-free, source flow. The particles, assumed to be subject to radiation pressure of a constant magnitude ($1 - \mu = \text{const}$), were allowed to leave the nucleus isotropically and continuously, though at variable rates. The emission process was described as the radial acceleration of dust outward from the nucleus by drag forces of the expanding gas in the circumnuclear region, where the dust and gas can be considered a two-phase, "dusty-gas" continuum and the problem can be solved by a fluid-dynamics approach. The ejection velocity of the dust particles is thus described as the terminal velocity from the point of view of fluid dynamics, but it becomes the initial velocity from the viewpoint of tail dynamics after the interaction between gas and dust has terminated. In their 1966 paper, Finson and Probstein approximated the ejection velocity by a Maxwellian distribution.

Their improved model (Finson and Probstein 1968a) has become the most powerful method of analyzing the dust tails of comets. It differs from the earlier version in

two ways: It relaxes the postulation of a constant $1 - \mu$, thus accounting for a particle-size distribution; and it replaces the assumption of a Maxwellian distribution in particle ejection velocities by a functional dependence of velocity on particle size and density, following Probstein's (1968) fluid-dynamics approach. In this model, the terminal velocity of dust particles also depends on the ratio of the mass-flow rate of dust to the mass-flow rate of gas, on the nuclear radius, and on the properties of the gas.

With the three parametric functions – the size-density distribution of particles, their emission rate as a function of time, and their ejection velocity – established, the Finson-Probstein model determines the distribution of the surface density of particles in the tail, that is, the theoretical photometric profile of the tail.

In practice, the crucial – and the most intricate – part of the Finson-Probstein method is to reach the best possible agreement between the observed photometric profile of the comet's tail and a theoretical surface-density distribution by means of varying the three parametric functions by trial and error (Fig. 1). For a particular combination of these three functions, the corresponding surface-density distribution can be obtained either by calculating contributions from particles of various sizes ejected at times held constant and then integrating the results over all ejection times (synchrone approach) or by calculating contributions from particles of constant dimensions ejected at various times and then integrating over all particle sizes (syndyne approach).

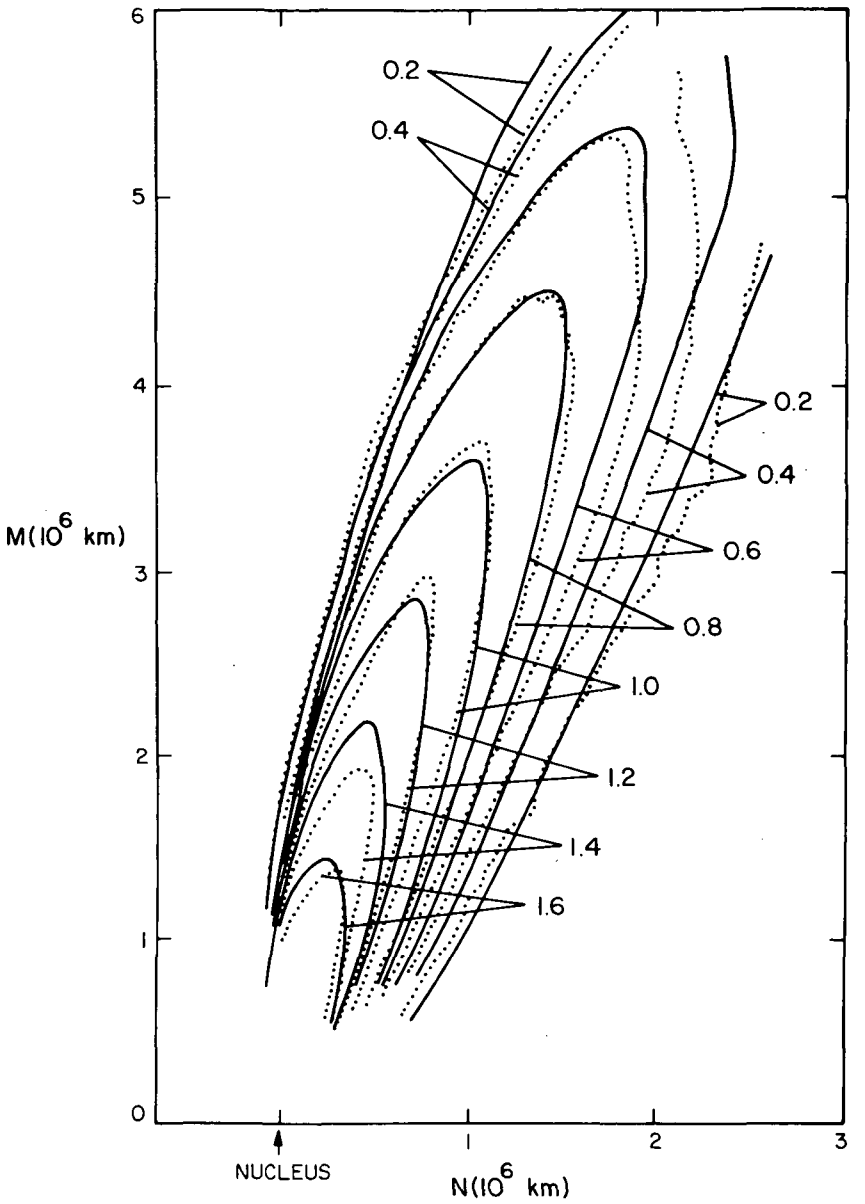

Fig. 1. Comparison of observed isophotes (dotted curves) with the theoretical density distribution (solid curves) for a photograph of Comet Bennett 1970 II taken on March 18, 1970. The numbers at individual pairs of curves indicate the logarithm of the relative surface density; M is the direction of the radius vector projected on the photographic plane; N is perpendicular to M in the direction of increasing right ascension (to the right). From Sekanina and Miller (1973).

In its full complexity, the Finson-Probstein model has so far been applied only to Comets Arend-Roland 1957 III (Finson and Probstein 1968b), Bennett 1970 II (Sekanina and Miller 1973), and, except for the absolute rate of the dust output, Seki-Lines 1962 III (Jambor 1973).

Some of the results found by Finson and Probstein for Arend-Roland and by Sekanina and Miller for Bennett are rather similar. The mass-flow rate of dust comes out to be of the order of 10^7 g sec^{-1}; the ratio of the mass-flow rate of dust to that of gas is about 1 for Arend-Roland and near 0.5 for Bennett. The corresponding production rate of the gas is of the same order of magnitude as that obtained by independent methods and suggests evaporation controlled by water snow. For Comet Bennett, direct measurements of the H and OH clouds around the nucleus give the production rate, which is in excellent agreement with the Sekanina-Miller result (Keller and Lillie 1974). Sekanina and Miller also solved for the radius of the nucleus of Comet Bennett and obtained 2.6 km.

The results for the particle sizes of the three comets differ. The optically important particle diameter (defined as the root-mean-square value of the particle-size distribution), at an assumed density of 1 g cm^{-3}, is 2.1 μm for Comet Bennett, 5.6 μm for Arend-Roland, and 14 μm for Seki-Lines. Since Finson and Probstein used the scattering efficiency for radiation pressure $Q_{rp} = 1$, whereas Sekanina and Miller assumed $Q_{rp} = 1.5$, the discrepancy between Arend-Roland and Bennett is actually even more substantial than indicated by the above figures. Indeed, Finson and Probstein

terminated the $1 - \mu$ distribution at 0.55, while Sekanina and Miller found a fairly significant fraction of particles to have $1 - \mu \gg 1$. Jambor used a different type of distribution function, but its sharp peak at $1 - \mu = 0.005$ demonstrates the abundance in Seki-Lines of very large particles, consistently reflected in the optically important size.

As a whole, the Finson-Probstein method appears to give very reliable, astrophysically significant information about the dust and gas released from cometary nuclei. The practical application of the model, however, requires utmost caution and care. Since pure dust comets are rare, it is imperative that on photographs taken for dust-tail studies, the plasma tail be suppressed as much as possible. This can rather successfully be done by using red sensitive plates (such as 103aE, 103aF, or the new 098-02) combined with appropriate filters that cut off the shorter wavelengths (such as a Schott RG1). A few inconveniences inherent in the problem cannot be removed by this method, primarily those concerning the size-density distribution. First of all, no way exists to separate the particle size from its density and from the scattering efficiency for radiation pressure. Furthermore, the $1 - \mu$ distribution is essentially indeterminate for $1 - \mu \rightarrow 0$, i.e., for very large particles. These particles do not contribute appreciably to the photometric profile of regular dust tails. This indeterminacy may have a significant effect on the estimate of the mass-output rate of dust from the comet, but not on the optically important size. By contrast, the upper end of the $1 - \mu$ distribution is well established from the fit. Unfortunately, as long as no information is available on the optical properties of dust particles from independent studies, the sizes of the smallest particles are also poorly determined, not only

because of the effect of density, but also because at $1 - \mu \gtrsim 1$, the scattering efficiency Q_{rp} varies rather considerably within very narrow limits of particle sizes, the character of variations being a strong function of the particles' composition. And finally, the mass-flow rates of dust and gas are linearly proportional to the adopted Q_{rp} and inversely proportional to the reflectivity of the dust particles; the nuclear radius is also inversely proportional to the adopted particle reflectivity.

IV. THE ICY TAILS OF DISTANT COMETS

A noteworthy controversy developed after Osterbrock (1958) published the results of his photographic observations of two comets with perihelia near 4 a.u., Baade 1955 VI and Haro-Chavira 1956 I. A careful analysis of the orientations of their tail axes resulted in Osterbrock's conclusion that the nearly straight, structureless tails pointed approximately midway between the prolonged radius vector and the orbit behind the comet. This allegedly peculiar property of the tails was considered incompatible with the mechanical theory, and substantial modifications were proposed, the least vulnerable of them having been Belton's (1965, 1966) concept of the type II tails as a mixture of electrically charged dust particles and electrons whose motions were controlled by interplanetary plasma.

The importance of Osterbrock's discovery was emphasized by Roemer's (1962) remark that the "characteristic" tails displayed by Baade and Haro-Chavira are rather common among comets of large perihelion distances, and by Belton's (1965) finding that all type II tails show essentially the same orientation property regardless of heliocentric distance.

Noticing the general similarity between the straight tails of distant comets and the theoretical synchrones, I recently undertook a study of the two comets, using a synchrone approach (considered but rejected in the past!) rather than the traditional syndyne approach (Sekanina 1973a). Application of the synchrone approach by no means implies that the tails of the distant comets are assumed to have been formed by ejection at a unique instant, since that approach can also be used advantageously to study the time span of continuous emission. My study showed that the tail dynamics were perfectly consistent with the mechanical theory, so that no additional forces – other than solar gravitational attraction and solar radiation pressure – need be considered to explain the strongly nonradial orientation of the tails. The calculations showed that the material ejected into the tail of Comet Baade was released from the nucleus essentially continuously from some 1500 to 200 days before perihelion, and the material ejected into the tail of Comet Haro-Chavira, from about 2000 to 300 days before perihelion (Fig. 2). The "age" of the tails is thus of the order of 1500 days, and the corresponding emission distances range between 5 and 15 a.u. from the sun! A slight curvature of the tails, noticed by Osterbrock, is due to the distribution of emission in time, with earlier emissions reaching farther away from the nucleus. It is believed that the activity continued even after the apparent cutoff time (i.e., 200 to 300 days before perihelion), though perhaps at a lower level, but that particles from the more recent emissions were still confined to the coma.

Analysis of the visible lengths of the two tails indicated that particles emitted from the comets must have been subjected to extremely low accelerations, not exceeding 1% of the solar gravitational attraction, and that therefore they were rather heavy particles, at least 0.01 cm in size. The implied significant deficit or, perhaps, total

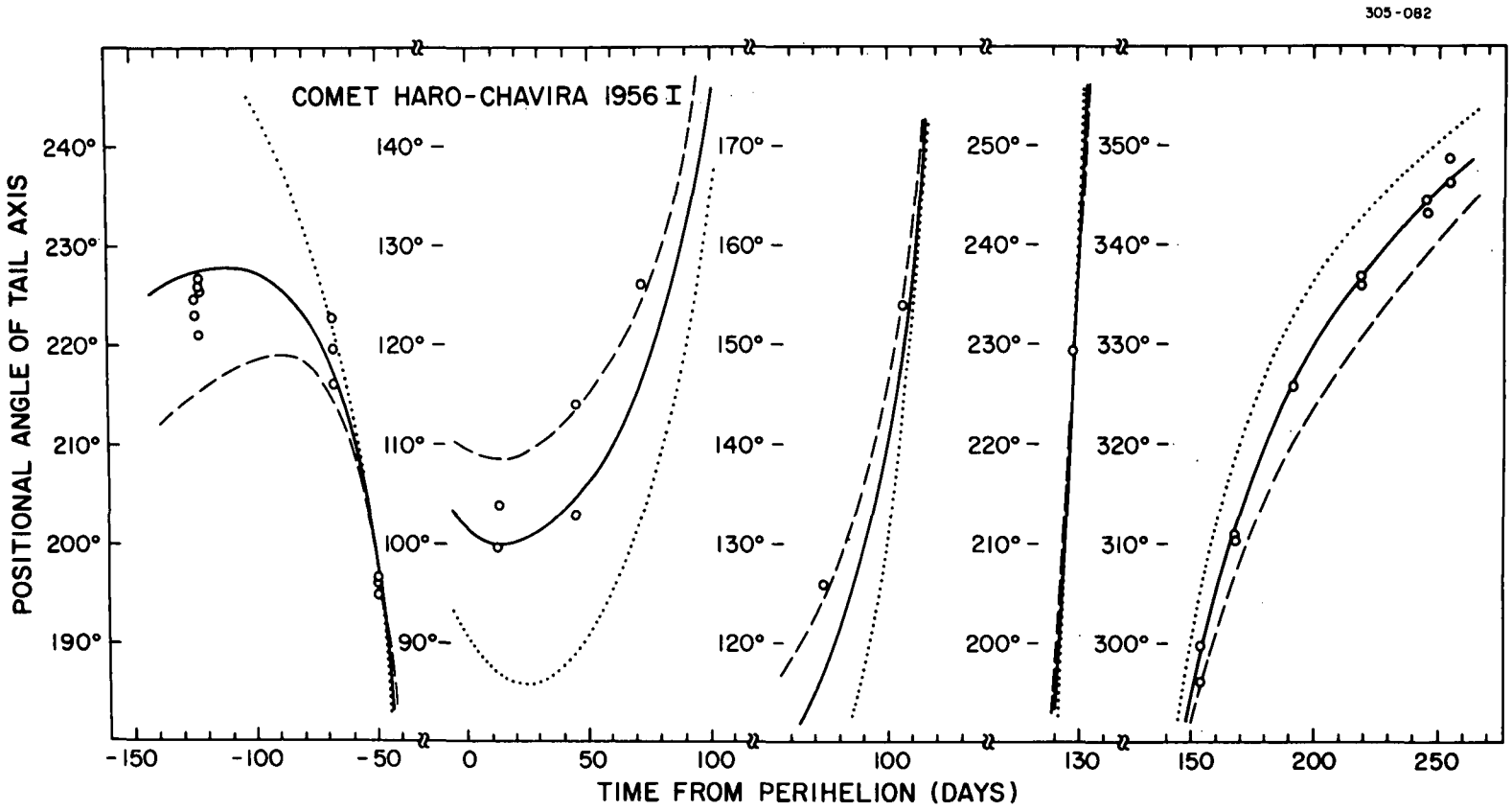

Fig. 2. Orientation of the tail of Comet Haro-Chavira 1956 I versus time. Circles: observations; dashed curve: synchrone corresponding to the emission time 2000 days before perihelion; solid curve: synchrone emitted 500 days before perihelion; dotted curve: synchrone emitted 200 days before perihelion.

lack of particles smaller than ≈0.01 cm in size contradicts all known comet-related particle-size distributions, except for the distribution of grains of solid hydrate of methane, studied in the laboratory by Delsemme and Wenger (1970). It should be pointed out that our lines of evidence cannot actually distinguish solid-hydrate grains from pure water-snow or frost grains of the same size-density distribution, and that the solid hydrates are preferred primarily for the reasons given by Delsemme and his collaborators (Delsemme and Miller 1970, 1971a, b; Delsemme and Wenger 1970). Since the dissociation of solid hydrates is determined by the evaporation of the icy lattice, the vaporization lifetimes of water-frost and solid-hydrate grains are practically identical; they were shown to be virtually infinite at heliocentric distances over 4 a.u. and can be rather long (for high-reflectivity grains) even at distances near 2 a.u. from the sun.

Examination of tail-orientation data of all comets with perihelia beyond 2.2 a.u. (Sekanina 1974a) largely confirms the conclusions from the study of Comets Baade and Haro-Chavira. The tail age, however, appears to be correlated with the perihelion distance, becoming shorter for comets with perihelia between 2.2 and ~3 a.u. (Fig. 3). This effect is attributed to an increase in the vaporization rate of water snow at heliocentric distances below 3 a.u., and therefore to a higher disintegration rate of icy grains or grains of solid hydrates.

The dynamical evidence thus appears to point unambiguously to the conclusion that the "characteristic" tails of the distant comets are indeed composed of water-frost or solid-hydrate grains. A small body of available spectroscopic evidence is also consistent with this hypothesis: Large-q comets – with the notable exception of Comet

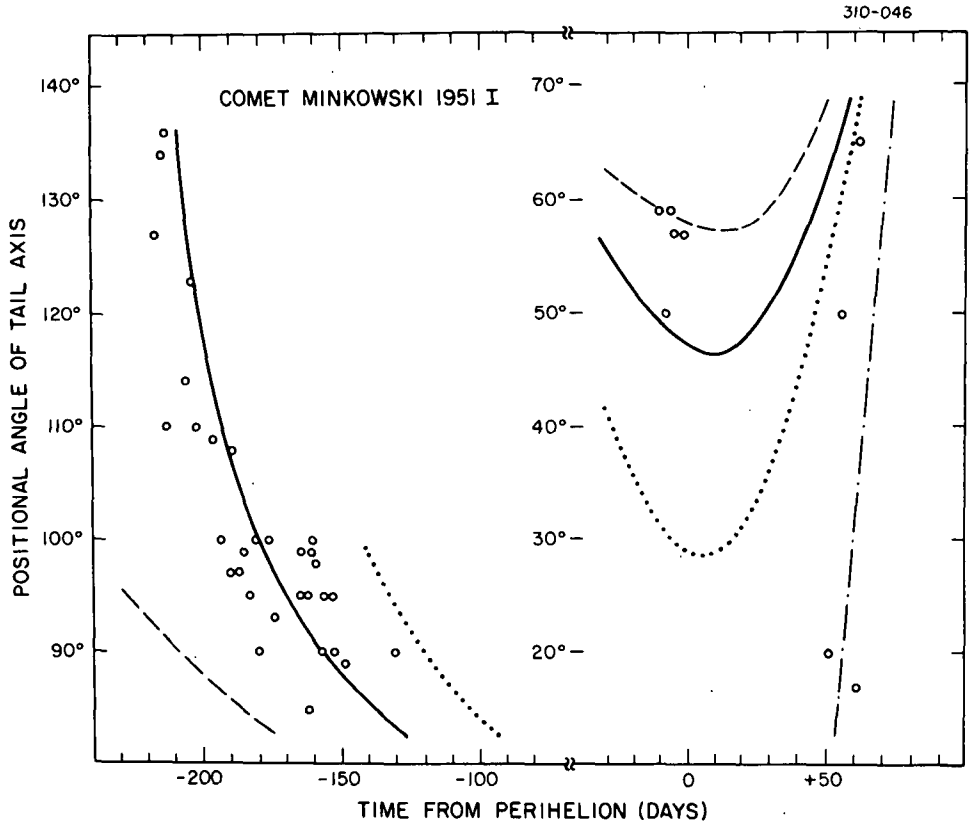

Fig. 3. Orientation of the tail of Comet Minkowski 1951 I versus time. Circles: observations; dashed curve: synchrone corresponding to the emission time 500 days before perihelion; solid curve: synchrone emitted 250 days before perihelion; dotted curve: synchrone emitted 150 days before perihelion; dotted-and-dashed curve: synchrone emitted at perihelion.

Humason 1962 VIII – have continua much stronger than molecular emissions, and in some comets, emissions are missing entirely. Obviously, the light of distant comets is mostly due to reflection of solar light. Spectrophotometric evidence, though inconclusive, possibly suggests that the grains might be "dirty," i.e., contaminated by impurities of fine dust. The concept of such dirty grains would explain the observed discrepancy between the size distribution of solid material in comet tails at large heliocentric distances and that at moderate to small distances: Micron and submicron dust particles bound to icy grains far from the sun are set free at moderate heliocentric distances when the grains start disintegrating by evaporation. Recent observations of Comet Kohoutek 1973f at nearly 2 a.u. from the sun by Rieke and Lee (1974) give some support to this hypothesis.

The proposed icy-tail hypothesis is also reasonably compatible with some other observed properties of the distant comets, such as the following: nearly parallel-sided tails, a sharply bounded envelope around the nuclear condensation, a high correlation between the appearance of the "characteristic" tail and the large perihelion distance, and occasional fan activity (Roemer 1962). However, an important implication of the hypothesis is that substances considerably more volatile than water snow are also required to be present in cometary nuclei in appreciable amounts in order to supply the necessary momentum to lift the icy grains of the inferred sizes into the tail at large distances from the sun.

It is appropriate to note here that the presence of icy grains in the coma at moderate heliocentric distances had been anticipated by Delsemme and Miller (1971a). They showed that the brightness gradient of a photometric profile of the continuum in

the coma, which progressively increases with distance from the nucleus to very large values [such as observed by O'Dell (1961) for Comet 1960 II], implies the existence of a halo of decaying icy grains. At distances comparable to the earth–sun distance, the vaporization lifetime of such grains is rather short; they evaporate completely while they are still within the coma.

V. SPLIT TAILS

A rather peculiar feature was detected both visually and photographically in the tails of quite a few comets. It can generally be described as a dark gap or band extending from the nucleus essentially along the tail's axis far into the tail, thus giving the impression that the tail is divided into two branches. The feature is often nicknamed the "shadow of the nucleus" in the literature, although such an interpretation is physically entirely unacceptable.

Brief examination of the reported appearances of split tails suggests that they were observed only in comets with small perihelion distances and, as a rule, after perihelion. The feature seems to be associated with dust tails, although a few cases of split plasma tails are not completely ruled out. Among the comets displaying a split tail, the best known are 1858 VI, 1882 II, 1910 I, 1962 III, and 1973f.

Until recently, the cause of a split tail had not been clear. Jambor's (1973) study of Comet Seki–Lines 1962 III gave a very straightforward and simple answer: The synchrones, corresponding in this case to particle emissions some 11 to 16 hours after perihelion, were missing – practically no dust was produced during the 5 hours.

The split tail is thus understood, but the cause for the missing synchrones must be explained. Jambor considered the possibility of complete evaporation of small particles and a reduction in size of the large ones due to intense solar heating. While not denying the presence of particle evaporation at such small heliocentric distances (Section VIII), we note that it is not selective, unless we are willing to accept that the particles emitted during the 5 hours were completely different in composition from those emitted at other times, notably earlier. In other words, this interpretation fails to explain why the particles that had been emitted before the critical interval of the 5 hours – and therefore were exposed to solar heating for a longer period of time – did not evaporate, too. In fact, the dust emission rate, derived from the presence of particles in the tail, shows a sharp peak right at perihelion, 11 hours before the sudden drop in the production commenced.

My guess is that the inferred drop in the rate of particle release from the nucleus of Seki-Lines is real. Subsequent to a sharp peak in the production rate of the dust (which itself must presumably have been triggered by an outburst in the nucleus), the sudden drop in the dust output should be associated with a rapid decrease in the vaporization flux from the comet's surface. The implied sink in the impinging energy is apparently caused by a high opacity for solar radiation of the dusty atmosphere, oversaturated by particles from the preceding flareup. Now, as the vaporization flux from the surface drops, an imbalance arises in the atmosphere between the high escape rate of the particles into space and the very low input rate of fresh dust from the underexposed nucleus. Consequently, the atmosphere is rapidly cleared out of the excess of dust particles, its opacity therefore drops, and the vaporization flux and production of dust from the nucleus increase to restore the equilibrium levels again.

A self-regulation mechanism of this type, turned on by a precipitous growth in the production rate of dust, might also have been operative in Comet Bennett. Although no shadow of the nucleus was reported for this comet, Sekanina and Miller (1973) found that a steep continuous increase in the emission rate of dust culminated in a sudden drop by a factor of 2, between 17 and 10 days before perihelion. On the other hand, Finson and Probstein (1968b), who detected an outburst in Arend-Roland about 6 days before perihelion, found no evidence for any subsequent drop much below the pre-explosion level of the dust emission flux.

VI. ANOMALOUS TAILS OF COMETS (ANTITAILS)

Significant lagging of early emissions behind the radius vector, combined with a special sun–earth–comet configuration, can account for an occasional appearance, primarily after perihelion, of a flat, sunward, "anomalous" tail (antitail). Physically and dynamically, there is nothing anomalous about these tails. However, they contain only large particles (usually in the range 0.01 to 0.1 cm in size – see below), whose low velocities relative to the nucleus prevent them from getting dispersed far away from the comet even after long flight times. These particles are comparable in size to meteoroids that produce radio meteors.

A great deal of information on anomalous tails can be learned from the distribution and structural details of synchrones. Actually, analysis of a synchrone diagram is sufficient for the understanding of the nature and basic properties of the anomalous tails (Sekanina 1974b).

An example of a synchrone diagram for Comet Arend-Roland is exhibited in Fig. 4, in which the projection of synchrones (and syndynes) onto the sky is complemented by their projection in the orbit plane of the comet unforeshortened by perspective. The arrow pointing to the earth's position on the right-hand side indicates that, to a terrestrial observer, all synchrones older than about 30 days project in the general direction of the sun, while the younger ones project in the other direction. This, indeed, is the picture shown on the left-hand side. A direct comparison of the latter diagram with photographs taken at approximately the same time reveals that the main body of the anomalous tail was formed by preperihelion emissions only. From diagrams similar to the one shown on the left of Fig. 4, Finson and Probstein (1968b) estimated that the antitail of this comet was made up of material emitted 5 to 9 weeks before perihelion.

The left panel of Fig. 4 indicates a considerable pileup of very old synchrones, as well as some crowding of very young ones. This effect is largely due to projection, but, as demonstrated by the orbit-plane view, real variations in the density of synchrones do occur – in particular, old synchrones indeed tend to pile up on top of each other. Also, they actually turn to the sunward side, so that the term "sunward" does not necessarily refer only to the tail's projected property. The pileup of synchrones toward the earliest ejection times readily explains another peculiarity of the sunward tail: its sharp edge on the side toward the radius vector and its fuzzy edge on the outer side.

In contrast to the crowding of synchrones of extreme ages, synchrones of intermediate age (i.e., those in Fig. 4 pointing essentially toward the earth) are greatly thinned out by projection. This is why the tail in the sky looks as if it is split into main and sunward branches.

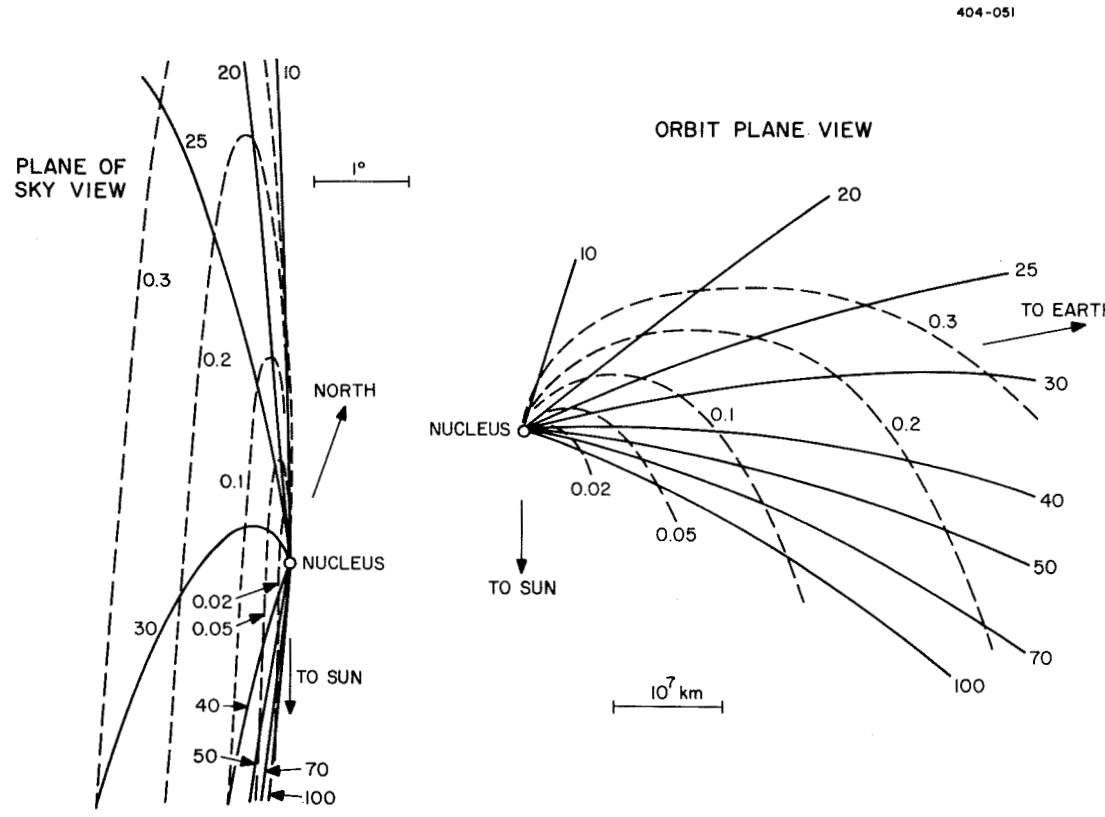

Fig. 4. A synchrone/syndyne diagram for the dust tail of Comet Arend-Roland 1957 III on April 28.0 UT, 1957, as projected onto the plane of sky (left) and as viewed in the orbit plane (right). Solid curves are synchrones, defined by their age (in days); dashed curves are syndynes, defined by the acceleration ratio of radiation pressure to solar gravity, $1 - \mu$.

The exceptionally narrow width of the sunward spike of Comet Arend-Roland during the earth's passage through the comet's nodal line indicates an ejection velocity normal to the orbit plane of less than 3 m sec^{-1}. Although the outward component of the ejection velocity should have been somewhat greater, it could not amount to more than a few percent of the relative velocity acquired by the particles from their acceleration by radiation pressure.

Finally, we note from Fig. 4 that the visible portion of the anomalous tail consists of particles significantly heavier than those in the main tail, with particle size increasing toward both the sharp edge and the nucleus. Whereas the optically important particles of the regular tail of Comet Arend-Roland, according to Finson and Probstein (1968b), were about 6 μm in diameter (at an assumed density of 1 g cm^{-3}), the anomalous tail contained particles of submillimeter and perhaps even millimeter size.

The behavior of the anomalous tail of Arend-Roland is rather representative of this type of tail in general. The conditions under which antitails can be observed from the earth can be formulated as follows:

(1) The earth must be in or at least fairly near the orbit plane of the comet to allow the edgewise or near-edgewise perspective. The "in" condition is absolutely necessary for the appearance of the narrow ray. If only the "near" condition is satisfied, the anomalous tail cannot point exactly sunward. For a comet of arbitrary inclination, this condition can be satisfied only for several days twice a year, but for a low-inclination comet, the near condition can hold for quite an extensive period of time.

(2) The earth (or, more precisely, its projected position onto the comet's orbit plane) must be located either within the sector defined by the prolonged radius vector and the synchrone of the earliest detectable emission (position E_1 in Fig. 5) or within the sector defined by the above two directions turned 180° (E_2). In the former case, the tail points in the general direction of the earth, the earth's atmosphere actually being bombarded by the comet's debris; and in the latter, it points away from the earth. If the earth is very near the prolonged radius vector (E_3) or very near the sunward direction (E_4), the comet is likely to display only a sunward tail, since the very young emissions – the only ones that project away from the sun, as seen from the earth – may not yet be well developed into a regular tail and their actual length is drastically shortened by projection.

(3) The preceding point also implies that the probability of seeing an anomalous tail from the earth increases statistically with the sector angle, which is identical to the lag angle of the apparent-onset synchrone. Since the lag angle increases with the true anomaly of the time of observation, the probability of seeing an anomalous tail is very small before perihelion but enhances considerably after perihelion.

(4) Finally, it is, of course, essential that a reasonably high level of dust-emission activity, particularly in the range of heavy particles, have been reached by the comet a sufficiently long time before perihelion.

Except for point (4), the conditions are geometrical in character. Consequently, if there are indications that the last point is likely to be satisfied (a "dusty" comet), the appearance of the anomalous tail can be rather straightforwardly predicted (Sekanina 1974b).

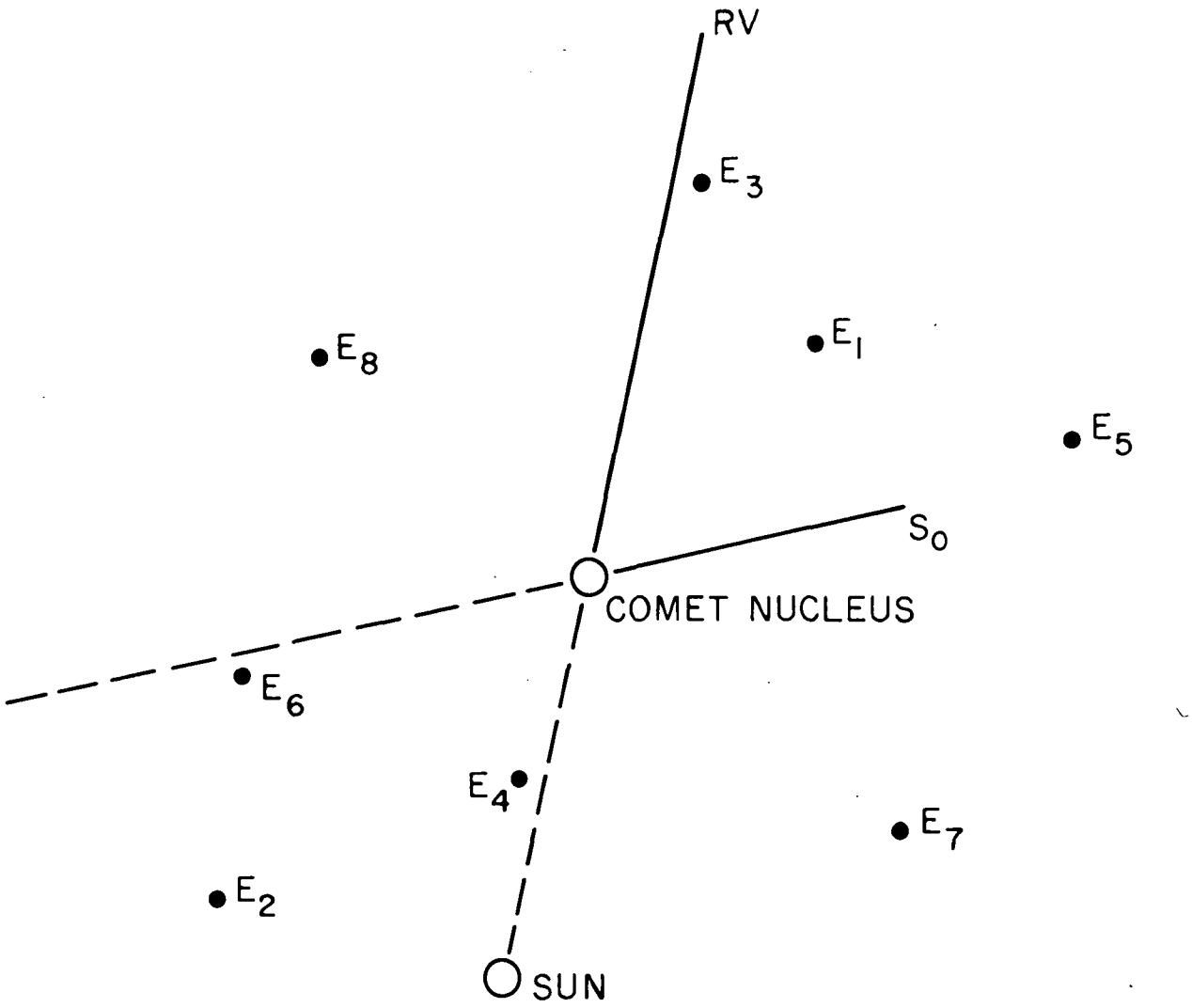

Fig. 5. Visibility conditions for an anomalous tail. Dust particles fill a flat sector between the synchrone S_0 (drawn schematically as a straight line) of the earliest detectable dust emission and the radius vector RV. When the earth is in the general area of E_1 or E_2, the comet displays, in projection onto the sky, a regular tail as well as a sunward tail. When the earth is near E_3 or E_4, the comet may display only a sunward tail. When the earth is around E_5 or E_6, the sunward tail may become difficult to detect. No sunward tail can be seen when the earth is in the general area of E_7 or E_8.

Historically, the term anomalous tail was not always used to describe the type of phenomena we deal with here. Harding (1824) and Olbers (1824) were probably the first to use the term, but Bredikhin (Jaegermann 1903) distinguished two types of anomalous tails. The tails of interest to us were called pseudo-anomalous by him; he considered "genuine" anomalous tails to be composed of heavy particles, moving toward the sun and subjected to no repulsive force. He concluded that such particle formations must move ahead of the comet and inside its orbit. Interpreting the descriptions of some of the reported sunward extensions as genuine anomalous tails, Bredikhin derived particle-ejection velocities of the order of 1 km sec^{-1}. For heavy particles subjected to no repulsive acceleration, such velocities are at least 2 orders of magnitude too high. There is no way to escape the conclusion that Bredikhin's assumptions were, in this respect, incorrect. It appears that his genuine anomalous tails can readily be identified either with gas jets or with unidirectional emissions of fine dust particles that have ejection velocities comparable to the thermal velocity of sublimating gases but that are subjected to substantial repulsive accelerations due to radiation pressure.

By contrast, anomalous tails as we define them behave in complete agreement with the equations of motion of relatively heavy particles. Yet it is the initial ejection velocity, and not the repulsive force, that can be neglected at only a minor loss of accuracy. These antitails are rather massive formations and might pose a real hazard for space missions to comets. Fortunately, since their dynamics are now well understood, it is not difficult, in principle, to avoid such a hazard. An antitail is essentially a two-dimensional formation located in the comet's orbit plane, so spacecraft are safe when kept away from the orbit plane. Hazards from the antitail could also be avoided

when spacecraft are guided slightly ahead of the comet and inside its trajectory. Finally, the known short-period comets, to which early space missions are planned, currently appear not to display anomalous tails (Section VII).

VII. STATISTICS OF APPEARANCES OF ANOMALOUS TAILS

The geometrical visibility conditions for anomalous tails were used to list the comets that should have displayed a sunward tail around the time of the earth's passage through the orbit plane (Sekanina, unpublished). A computer program executing the conditions has been applied to an updated card file of the Catalogue of Cometary Orbits (courtesy of B. G. Marsden), starting with the comets of 1737. Excluded were comets observed at elongations exceeding 135° and distances larger than 2 a.u. from the sun.

Forty-six comets with revolution periods exceeding 200 years were found to have had favorable visibility conditions (satisfied within, or not more than 5 days outside, the period of observation), when dust production was allowed to commence at 2 a.u. from the sun on the incoming branch of the orbit. When this condition was relaxed to 4 a.u., the number of eligible comets increased to 69. An extensive search of the literature revealed, however, that a sunward tail was actually observed only in the following eight comets: 1823 (Harding 1824; Olbers 1824; von Biela 1824; Hansen 1824), 1844 III (Waterston 1845; Maclear 1845), 1895 IV (Fric and Fric 1896), 1937 IV (Jeffers and Adams 1938; Van Biesbroeck 1938), 1954 VIII (Van Biesbroeck 1957; Waterfield 1954; Kresák and Vozárová 1954), 1957 III (many observations; see, e.g., Whipple 1957a, b; Larsson-Leander 1957) 1961 V (several observations; see, e.g., Porter 1962) and 1969 IX (Miller et al. 1971).

In all eight cases, the earth passed through the nodal line after the comet's perihelion, the time lag being 4 to 54 days. Comets 1957 III and 1961 V were the only ones whose tails pointed at the critical time in the general direction of the earth; the others were directed away.

Five of the eight comets - 1823, 1844 III, 1957 III, 1961 V, and 1969 IX - exhibited a double-tail appearance with the antitail no brighter than the main tail. In the case of 1954 VIII, only a sunward tail was observed by Van Biesbroeck and Waterfield, but a "faint prolongation" away from the sun, in addition to the brighter antitail, was reported by Kresák and Vozárová. The other two comets, 1895 IV and 1937 IV, displayed only a sunward tail. Three of the eight events were affected by unfavorable circumstances: The moon interfered in the case of 1844 III, while 1954 VIII and 1961 V were not discovered until about 2 days after the earth's passage through the node. Comet 1961 V was also at a very small angular distance from the sun.

The presence of the antitail is correlated, to some extent, with orbital evidence. Except for 1937 IV, all the comets had perihelion distances less than 0.7 a.u. Four seem to have come from the Oort (1950) cloud (1895 IV, 1937 IV, 1954 VIII, and 1957 III), while 1969 IX is a "fairly new" comet in the Oort-Schmidt (1951) terminology. The original orbit of 1823 is indeterminate, whereas 1844 III and 1961 V appear to be the only two "old" comets (in the Oort-Schmidt sense). Comet Kohoutek 1973f was not among the candidates, because the antitail conditions were not satisfied during the earth's passage through the nodal line on December 10, 1973. The "near" condition was not examined at all.

Of the candidates for which no antitails were reported, at least two dozen were observed extensively enough during the critical period around the nodal passage that we can be reasonably sure that the absence of the antitail indeed indicates insufficient

or no production of heavy particles from these comets at large distances Among others, this group covers two sun grazers (1843 I and 1963 V) plus Comets 1840 IV, 1853 II, 1858 VI, 1861 II, 1881 III, 1931 III, 1941 II, 1959 IV, 1963 I, and 1963 III. Many of them have revolution periods in the general range of several hundred to several thousand years, which appears to suggest that antitails, by and large, are not displayed by old comets. Observations during the critical periods for at least a dozen comets were severely affected by moonlight, and the rest of the condidates were poorly observed for other reasons.

A similar list of candidates was produced for short-period comets (with revolution periods shorter than 200 years). The list shows that if the short-period comets were currently emitting large amounts of heavy particles, anomalous tails should have been plentiful. With an assumed onset of dust production at 2 a.u. before perihelion, 20 more-than-one-apparition and 3 one-apparition comets should have displayed anomalous tails, 8 of the 20 on two or more occasions. If the condition is relaxed to 4 a.u., the figures become 28, 6, and 17, respectively. If, on the other hand, the condition is severed and dust production is assumed to commence at perihelion, 11 more-than-one-apparition comets should have displayed anomalous tails – 2 of them on two occasions – and no one-apparition comets.

Since most short-period comets have low inclinations, excellent prospects exist, statistically, for favorable visibility conditions for detecting antitails outside the critical times of nodal passages as well (the "near" condition in Section VI). As with the nearly parabolic comets, such configurations were not examined.

An extensive search in the literature for observations of antitails of short-period comets gave a completely negative result. Well-established associations of meteor streams with many short-period comets appear difficult to reconcile with the absence of anomalous tails. While it is possible that an element of proper timing is all that is responsible for the contradiction, more work remains to be done on this problem.

VIII. THE ANTITAIL OF COMET KOHOUTEK 1973f, AND THE "SYNCHRONIC" BANDS: EVIDENCE FOR VAPORIZATION AND FRAGMENTATION OF COMETARY PARTICLES?

The antitail of Comet Kohoutek, the first that was predicted (Sekanina 1973b), is currently under intensive study. A number of ground-based observations, including the first infrared measurements of an antitail (Ney 1974), were complemented by remarkable observations from outer space (Gibson 1974). At least two preliminary models have so far been proposed (Gary and O'Dell 1974; Sekanina 1974c).

My working model, based on the Finson-Probstein theory for the case of small emission velocities, has been fitted to semiquantitative descriptions of the antitail by various observers, including the Skylab III astronauts. The model shows that the main body of the antitail was made up entirely of material shed by the comet before perihelion. The particles ranged mostly between 0.1 and 1 mm in size, and their differential mass distribution, $m^{-s}\,dm$, was tentatively approximated by $s \simeq 1.4$. This value of the population index s is substantially lower than the commonly accepted $s \gtrsim 2$, derived from various radio-meteor studies, and implies a rather strong relative excess of heavy particles, in which practically all the mass of the antitail was concentrated. The excess of large particles has been interpreted as an indication of a severe evaporation effect. Indeed, a cloud of particles of specific composition, ejected from

a cometary nucleus and later undergoing evaporation as a result of exposure to intense solar heating, will have its particle-size distribution substantially modified. Because evaporation reduces the radii of the particles in such a cloud by the same amount, Δa, independent of their dimensions, particles with original radii, a, smaller than Δa do, of course, sublimate out completely. Larger particles, whose original size distribution was governed by a law of the type $a^{-u}\,da$ ($u = \text{const}$), are reduced in size to $b = a - \Delta a$, and the logarithmic slope t of their postexposure distribution varies with b and is related to its preexposure equivalent u by

$$t(b) = \frac{u}{1 + (\Delta a/b)} \quad . \tag{2}$$

Since $t = 3s - 2$, the observed (i.e., postperihelion and, therefore, postexposure) particle-size distribution in the antitail has $t \simeq 2.2$ for $b \approx 0.1$ to 1 mm. Taking, further, a population index of $2 \lesssim s_0 \lesssim 7/3$ and, hence, $4 \lesssim u \lesssim 5$ for the original (preexposure) particle distribution, we find $0.8 \lesssim \Delta a/b \lesssim 1.3$. Thus, a rough assessment of the evaporation effect suggests that the total loss in radius of the particles in the antitail of Comet Kohoutek appears to be comparable to typical postexposure particle sizes, i.e., some 0.1 to 1 mm.

This approximate result has now been checked by Sekanina et al. (1975). From the progressively increasing gradient of the radial photometric profiles of the antitail, it is found that t is, indeed, variable and fits Eq. (2). After substituting from Eq. (1), Eq. (2) can be written in the form

$$\frac{1}{t} = \frac{1}{u} + Q\,(1 - \mu) \quad , \tag{3}$$

where Q is a constant determined by u and Δa. The plot of 1/t versus $1 - \mu$, reproduced here in Fig. 6, gives 1/u and Q as the ordinate at $1 - \mu = 0$ and the slope of the fitted straight line, respectively. The numerical results of Sekanina et al. put the evaporation loss in particle diameter at about 0.12 mm and give $u \simeq 4.8$, i.e., the original population index of the particle mass distribution $s_0 \simeq 2.3$. The derived evaporation loss rate implies an apparent latent heat of vaporization of the particle material (defined as the product of the actual latent heat and of the fourth root of the ratio between the particles' emissivity for reradiation and their absorptivity for solar radiation) of about 46 kcal $mole^{-1}$, very close to the estimate of the preliminary study (Sekanina 1974c). However, an uncertainty remains in the above determinations because the effect of evaporation on the particles' motions, i.e., the change in the magnitude of radiation pressure, has not been taken into account. The improved model of the antitail therefore requires a study of non-Keplerian motions of dust particles (variable $1 - \mu$).

While dust tails are usually structureless, this was certainly not the case with such comets as 1858 VI, 1901 I, 1910 I, 1957 V, and 1965 VIII. Well-developed systems of several nearly parallel bright bands, streaking across the broad, strongly curved "background" tail, are particularly clearly seen on the photographs of 1910 I and 1957 V (Lampland 1912; McClure and Liller 1958).

Bredikhin (Jaegermann 1903) noticed that the bands essentially coincide in orientation with synchrones and concluded that they are the result of discrete ejections into the tail of a large number of dust particles of various sizes. The bands became known generally as "synchronic" bands.

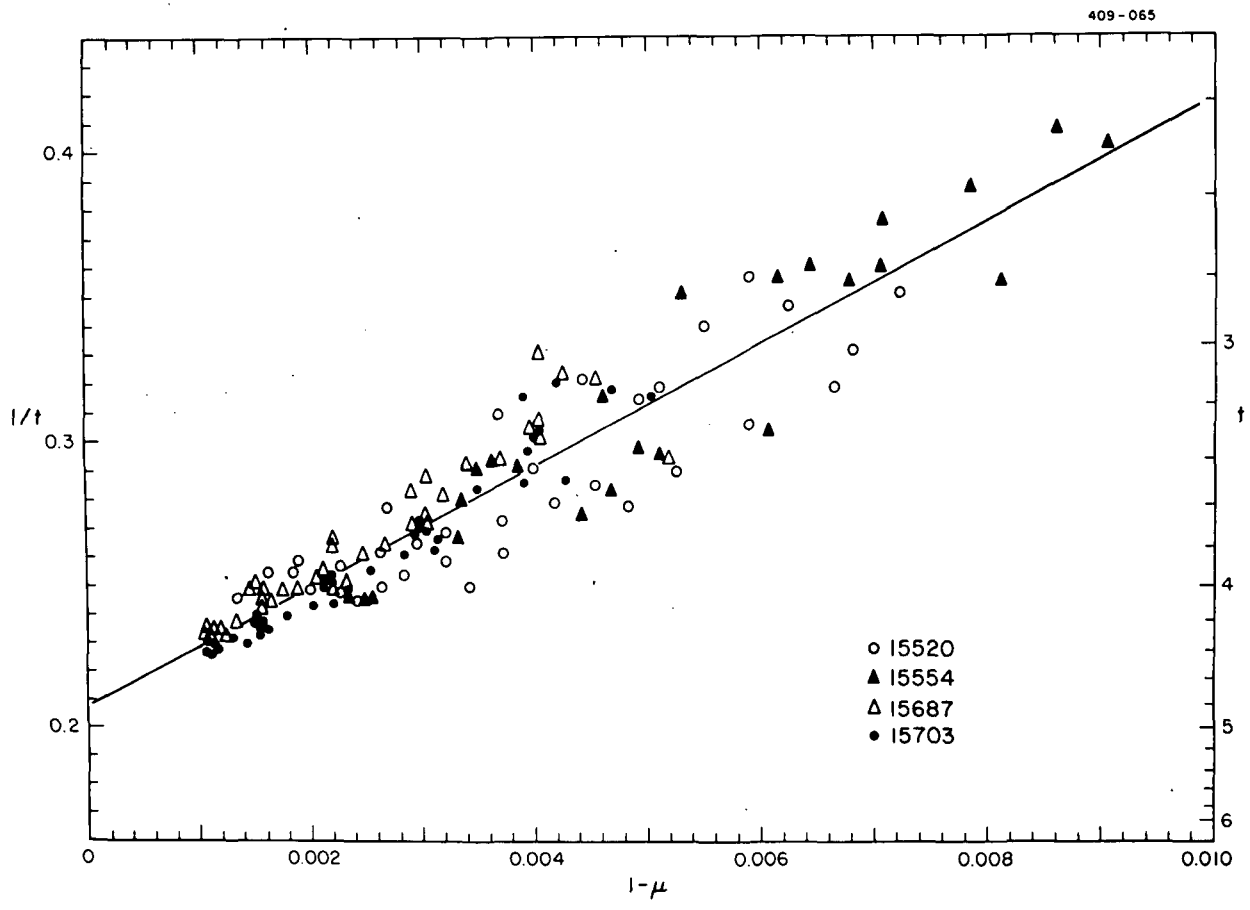

Fig. 6. Plot of particle acceleration 1 - μ versus the logarithmic gradient t of the size distribution of vaporizing particles in the antitail of Comet Kohoutek 1973f. The four types of symbols indicate the plates from which the data were derived. From Sekanina et al. (1974).

Vsekhsvyatsky (1959), however, pointed out that available photographs of the synchronic bands demonstrate a systematic deviation between the orientation of the bands and that of the theoretical synchrones. The bands always make a smaller angle with the prolonged radius vector and, when extended to intersect the radius vector, often meet on the sunward side of the nucleus (which the theoretical synchrones never do). Although Vsekhsvyatsky gave three more arguments against the interpretation of the synchronic bands in terms of discrete ejections of dust, we find the orientation problem to be the strongest point of his criticism and the only crucial objection to the laws of the mechanical theory.

The way the bands deviate from the respective synchrones gives the impression that each particle in the band is subjected to a repulsive acceleration $1 - \mu$ that gradually increases toward the far end of the band. If correct, this hypothesis implies the presence of vaporizing particles.

Some properties of vaporizing dust particles were studied by Huebner (1970). He showed that the vaporization rate of materials with high latent heats of vaporization increases very steeply with decreasing heliocentric distances; he suggested that, as a result of grain vaporization, a dust tail of a sun-grazing comet might completely disappear shortly before perihelion, with atoms ionized to form a plasma tail. Jambor (1973) pointed out that, indeed, the whole visible tail of the sun-grazing Comet Ikeya-Seki 1965 VIII, on a plate taken 9 days after perihelion, was due to emissions subsequent to perihelion. Similarly, I have found that the tail of another sun grazer, 1887 I, was a synchrone ejected 5.5 hours after perihelion (Sekanina 1973c). Spectroscopic data were also interpreted in terms of vaporizing particles (Spinrad and Miner 1968).

Obviously, plenty of circumstantial evidence exists for the presence of appreciably vaporizing dust particles in the tails of comets with small perihelion distances. However, nothing appears to have been done – to my knowledge – on actual calculations of the trajectories of such vaporizing particles. The analytical approach is clearly unfeasible because of the complex form in which the central force varies with time (caused by the variable vaporization rate of the particles). I recently developed a numerical method of computing the motion of a vaporizing particle, based on an iterative adjustment of the particle's orbital elements to its changing dimensions (and, therefore, to its acceleration). Since the particle's motion is restricted to the comet's orbit plane, the particle's orbit differs from that of the comet in only four elements: the eccentricity e, the semimajor axis a, the perihelion angle α (i.e., the angle subtended by the lines of apsides of the particle's and the comet's orbits), and a time constant (such as the moment of perihelion passage T).

A particle of known size, density, and scattering efficiency for radiation pressure is assumed to be ejected at a zero initial velocity from the nucleus at a time t_0. The repulsive acceleration $(1 - \mu)_0$ by radiation pressure is determined by Eq. (1). The four elements of the particle's orbit at t_0 are then calculated from $(1 - \mu)_0$ and from the comet's orbital elements by applying the two conditions of coincidence between the radial (distance from the sun) as well as transverse (true anomaly) coordinates of the particle and those of the comet at t_0, plus the similar two conditions of coincidence of their velocity components at t_0. With these elements, e_0, a_0, α_0, and T_0 [and with $(1 - \mu)_0$], the particle's motion is run until a time t_1. Simultaneously, the loss in the radius of the particle due to its evaporation between t_0 and t_1 is derived from the equations of an adopted physical model [see Eq. (4) below, for example],

and the new acceleration $(1 - \mu)_1$ is calculated from Eq. (1). Four conditions of coincidence in position and velocity at t_1 plus $(1 - \mu)_0$ and $(1 - \mu)_1$ then serve to determine new orbital elements of the particle at $t_1 - e_1$, a_1, a_1, and T_1 — from the preceding elements. The particle's motion is then run to a time t_2, etc., until the time of observation. The iteration intervals, $t_{i+1} - t_i$, must, of course, be kept very short to prevent an accumulation of errors. In practice, it is advisable to adjust the step in time by simultaneously checking the sequence of steps in $1 - \mu$, to avoid a large step in either quantity. The method is programed to work for both short-period and nearly parabolic comets; it also allows $1 - \mu > 1$ (negative attraction).

Although calculations of this type have just commenced, we can present, in Fig. 7, the first positive (though very preliminary) result of analysis of one of the synchronic bands in the tail of Comet Mrkos 1957 V. The orientation of band No. 3 (Vsekhsvyatsky 1959) is compared in the figure with the best matching nonvaporization synchrone (of age 8 days) and with a much more nearly coinciding vaporization synchrone (age 12 days), the latter corresponding to particles with a vaporization rate controlled by the law

$$Z = A \exp [1.80 \times L(1 - \sqrt{r})] \quad , \tag{4}$$

where $A = 10^{-17}$ g cm^{-2} sec^{-1} and the apparent latent heat of vaporization L = 30 kcal mole^{-1}.

The first results of our dynamical experimenting with vaporizing particles have proved rather successful. However, since vaporization implies a gradual loss of luminosity on account of the decreasing scattering

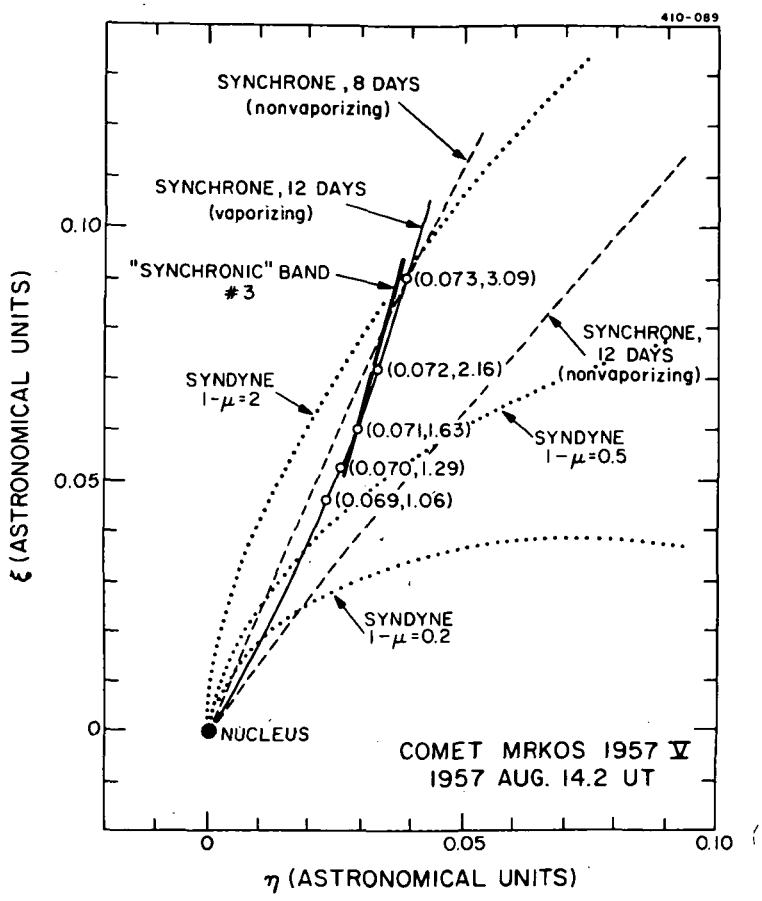

Fig. 7. Motions of vaporizing dust particles in the tail of Comet Mrkos 1957 V. The orientation of the observed "synchronic" band #3 (thick line) on a plate exposed by A. McClure (Vsekhsvyatsky 1959) is compared with a synchrone, 12 days old, of vaporizing dust particles (thin solid curve) of apparent latent heat of vaporization of 30 kcal mole^{-1}. The projection is in the orbit plane. The $+\xi$ axis points away from the sun, and the $+\eta$ axis, behind the comet. The five open circles indicate the locations of particles of specified repulsive accelerations $1 - \mu$ at the times of ejection (first figure in parentheses) and observation (second figure). Note that the observed extent of the band corresponds to a very narrow interval of $1 - \mu$ at ejection (of about 0.003). Note also that the synchrone of the vaporizing particles is concave toward the prolonged radius vector, while the synchrones of nonvaporizing particles (dashed curves) are convex. A few syndynes of nonvaporizing particles (dotted curves) are also plotted.

(or reflecting) power of the particles, the interpretation of the synchronic bands in terms of vaporizing particles is problematic from the photometric viewpoint: a synchronic band is much brighter than the ambient "background" tail, while the space between the band and the nucleus is usually almost nonluminous, as though the band emanated from "nothing". To explain both the dynamical and photometric effects, we are in need of a mechanism that would provide an increase in the acceleration (i.e., a drop in the particle size) as well as an increase in the brightness (i.e., an increase in the total scattering or reflecting surface) of the particles in the bands. The mechanism that does just that is fragmentation. Simple calculation shows that fragmentation of a particle into N fragments of equal size would increase the $1-\mu$ of the fragments as well as their total scattering surface, compared to the corresponding figures for the parent particle, by a factor of $N^{1/3}$, i.e., in proportion to the ratio between the linear dimensions of the parent and those of a fragment.

In practice, of course, the fragments have a certain size distribution; the limiting values of $1-\mu$ of the fragments define the length of the band. The position of the band in the tail at any particular moment depends on three quantities, namely, the time of ejection of the parent particles, their size and the time of fragmentation. However, since the band's position is defined only by two parameters, the three quantities cannot all be unequivocally determined from the band's single observation. The orientation of the band (i.e., its slope $d\eta/d\xi$ in Fig. 9), however, is primarily a function of the time of fragmentation, which thus can be fixed fairly precisely. As an example, we list in Table I six sets of parameters of the synchronic band No. 3 in

Fig. 9, all of which fit equally well (perfectly) its observed position. Note that while the time of fragmentation comes out indeed practically the same in each of the six cases of Table I, the time of ejection is highly correlated with $(1-\mu)_{par}$, the $1-\mu$ value of the parent particles. Only an upper limit can be established for $(1-\mu)_{par}$ from the obvious condition that the dimensions of the parent particle must be larger than those of any of its fragments. Of course, this also sets a limit on the time of ejection. In the case of the synchronic band No. 3 $(1-\mu)_{par} < 0.75$, and the ejection must have taken place earlier than 3.6 days after perihelion (i.e., before August 5.0 UT, 1957; by contrast the fragmentation occurred on about August 9.1 UT).

Since the range of the particle sizes of the fragments, assessed from the range of their $1-\mu$ values, is rather narrow, the number of fragments per parent particle does not significantly depend on their size-distribution law. However, it does depend crucially on the variations, with the particle size, in the scattering efficiency for radiation pressure, which are practically unknown, because neither the composition nor the shape of the fragments are known. It is therefore believed that only order-of-magnitude estimates can be given for the number of fragments per parent particle, such as those listed in Table I.

The outlined hypothesis of particle fragmentation in cometary tails adopts that a particular synchronic band is composed of fragments, whose parent particles had a certain $1-\mu$ acceleration, were simultaneously ejected from the nucleus and later, also at the same time, crumbled into fragments. If the first condition is relaxed to allow a multiple-peak distribution of sizes of

Table I

Synchronic band No. 3 in the tail of Comet Mrkos, interpreted in terms of particle fragmentation

(Time of observation: 12.7 days after perihelion)

	Time of ejection of parent particles from comet (days from perihelion)					
	+3	+2	0	-3	-7	-12
Age of parent particles (days)	9.7	10.7	12.7	15.7	19.7	24.7
1-μ of parent particles	0.55	0.35	0.17	0.077	0.040	0.026
Diameter of parent particles (microns) at density 1 g cm^{-3} and scattering efficiency $Q_{rp}=1$	2.1	3.3	6.9	15	29	45
Time of fragmentation (days from perihelion)	+7.6	+7.6	+7.6	+7.6	+7.7	+7.8
Age of parent particles at time of fragmentation (days)	4.6	5.6	7.6	10.6	14.7	19.8
Age of fragments (days)	5.1	5.1	5.1	5.1	5.0	4.9
Range in 1-μ of fragments	1.0 - 3.6	1.3 - 3.9	1.7 - 4.3	2.1 - 4.6	2.4 - 5.1	2.7 - 5.4
Estimated number of fragments per parent particle	$10^1 - 10^2$	$10^2 - 10^3$	$10^3 - 10^4$	$10^4 - 10^5$	$10^5 - 10^6$	$10^6 - 10^7$

the parent particles, the result is a system of practically parallel synchronic bands. Such a property of band systems has actually been observed in the tails of a few comets. It permits to improve the determinacy of the three fragmentation parameters and so does the identification of the same synchronic bands on photographs taken on two or more consecutive days.

One can also think of multiple fragmentation of cometary particles. Mathematically this case is tractable with the same ease as the problem of simple fragmentation, and I have a computer program handling the corresponding particle dynamics. At present, however, there does not seem to be any clear observational evidence for multiple fragmentation of particles in the cometary tails.

Incidental to the problem of the motions of particles subject to vaporization and/or fragmentation is that the term syndyne becomes ambiguous or meaningless and should not be used unless it is redefined.

IX. REMARKS ON RELATED RESEARCH. FUTURE WORK

The preceding sections have demonstrated that the explanation of all the major features observed in the dust tails of comets is within the reach of the mechanical theory, in spite of the fact that the original ideas of Bessel and Bredikhin required considerable revisions. We wish to stress, however, that while we claim that no additional forces — other than solar gravitational attraction and solar radiation pressure — need be considered to explain the observed motions of dust particles in cometary tails (after their lifting into the coma by molecular drag), we do not deny that the particles are also subject to other, though much smaller, forces. Credence should be given at this point to at least two studies that appear to show a potential presence of detectable forces in the dust tails ignored by the mechanical theory. Belton (1965, 1966) noted that in comets where both prominent plasma and dust tails are present, their orientations near the nucleus appear to coincide, thus perhaps suggesting that an important interaction

may occur between the dust and plasma in certain cases. Along a different line of reasoning, Harwit and Vanýsek (1971) suggested that an alignment of the angular-momentum axes of dust grains may result in cometary tails from bombardment by solar protons and in cometary heads from the drag by outgoing gas from the nucleus. An indication of such a phenomenon was indeed detected by Clarke (1971) in his polarization measurements of Bennett 1970 II.

Unfortunately, many fundamental properties of the dust tails are still known with only a rather unsatisfactory precision, the uncertainties in particle size and composition being perhaps the most severe. In spite of the accomplishments of the Finson-Probstein method, we do not know what the particles are made of. Numerous investigations were undertaken in the past to attack the problem from another direction, often by comparing the distribution of energy in the continuous spectrum of a comet's head or tail with theoretical curves for light scattering by small particles based on the Mie theory (e.g., Liller 1960; Remy-Battiau 1964). O'Dell (1974) compared the results of three different methods of particle-size determination applied to Comet Bennett, yet he found an uncertainty of at least a half an order of magnitude in the value of the minimum particle size.

Infrared observations represent another line of attack. Maas et al. (1970) found that the infrared radiation from Comet Bennett indicated effective temperatures significantly higher than the expected blackbody temperature in the 2- to 20-μm region and that a strong emission feature existed near 10 μm, which was interpreted as due to silicate grains. Extending his multichannel photometry between 0.55 and 18 μm to Comets 1973f, 1974b, and P/Encke, Ney (1974) recently confirmed the excessive

temperature [detected also by Becklin and Westphal (1966) in Comet Ikeya-Seki 1965 VIII] as well as the silicate signature. He was also able to set a lower limit (from the absence of Rayleigh scattering) and an upper limit (from the opacity of silicate material) to the average particle size: 0.2 and 2 μm, respectively. However, the antitail of 1973f showed neither excessive temperatures nor any silicate signature, and Ney concluded – in complete agreement with my independent finding (Sekanina 1974c) – that the antitail particles must have been definitely larger than 10 μm in diameter.

The field where infrared data would be of invaluable assistance to the theory is the study of the tails of distant comets. Present infrared techniques may not yet be sensitive enough to pick up the faint images of the comets at large heliocentric distances, but Rieke and Lee's (1974) observations, in the wavelength range 10 to 20 μm, of Comet Kohoutek at distances of almost 2 a.u. hold out hopes for the future. Further progress in the study of icy grains in the tails also depends on better knowledge of the optical properties of snows. At present, laboratory data on water snow are rather fragmentary, and those on other snows of interest – such as solid hydrates – are virtually nonexistent.

More work is needed on the anomalous tails of short-period comets, as well as on the apparent absence of a correlation between them and meteor streams. We would consider the possibility of predicting future favorable visibility conditions for antitails of short-period comets to facilitate a reasonably efficient observational program, if interest is expressed in pursuing such a search. In any case, we plan to make routine predictions of expected antitail appearances for bright, nearly parabolic comets.

The nature and properties of vaporizing dust particles in cometary tails probably constitute the most intricate problem ahead. Work is in progress on the antitail of Kohoutek 1973f and on the synchronic bands in Mrkos 1957 V – the two instances where the presence of vaporizing particles now appears to show up rather convincingly. A comparative study of the antitails of Comets Kohoutek and Arend-Roland is intended for the near future. The two best comets for a systematic study of the synchronic bands – in addition to 1957 V – are 1965 VIII and 1910 I. Concerning the latter, a discrepancy exists between Orlov's (1945) and Vsekhsvyatsky's (1959) comparison fits of the synchronic bands, and this needs clarification.

A purely mechanical approach is also used by Jambor (1974) to point out that there might be problems in reconciling existing models of the zodiacal cloud with the mechanism of dust contribution from short-period comets, in terms of both the amount of dust that can be supplied and particle sizes. A more comprehensive study is clearly necessary.

ACKNOWLEDGMENT

This work was supported by Grant NGR 09-015-159 from the National Aeronautics and Space Administration.

REFERENCES

Arrhenius, S. A. (1900). Ueber die Ursache der Nordlichter. Phys. Zeitschr. 2, 81-110.

Becklin, E. E., and Westphal, J. A. (1966). Infrared observations of Comet 1965f. Astrophys. J. 145, 445-453.

Belton, M. J. S. (1965). Some characteristics of type II comet tails and the problem of the distant comets. Astron. J. 70, 451-465.

Belton, M. J. S. (1966). The dynamics of type II comet tails. In Nature et Origine des Comètes, Proc. Coll. Int. Univ. Liège, pp. 317-321.

Bessel, F. W. (1836). Beobachtungen über die physische Beschaffenheit des Halley'schen Kometen und dadurch veranlasste Bemerkungen. Astron. Nachr. 13, 185-232.

Biermann, L. (1951). Kometenschweife und solare Korpuskularstrahlung. Zeitschr. Astrophys. 29, 274-286.

Clarke, D. (1971). Polarization measurements of the head of Comet Bennett (1969i). Astron. Astrophys. 14, 90-94.

Delsemme, A. H., and Miller, D. C. (1970). Physico-chemical phenomena in comets. II. Gas adsorption in the snows of the nucleus. Planet. Space Sci. 18, 717-730.

Delsemme, A. H., and Miller, D. C. (1971a). Physico-chemical phenomena in comets. III. The continuum of Comet Burnham (1960 II). Planet. Space Sci. 19, 1229-1257.

Delsemme, A. H., and Miller, D. C. (1971b). Physico-chemical phenomena in comets. IV. The C_2 emission of Comet Burnham (1960 II). Planet. Space Sci. 19, 1259-1274.

Delsemme, A. H., and Wenger, A. (1970). Physico-chemical phenomena in comets. I. Experimental study of snows in a cometary environment. Planet. Space Sci. 18, 709-715.

Finson, M. L., and Probstein, R. F. (1966). The fluid dynamics of comet dust tails. AIAA Paper No. 66-32. (Presented at the 3rd Aerospace Sciences Meeting, Jan. 24-26, 1966, New York.)

Finson, M. L., and Probstein, R. F. (1968a). A theory of dust comets. I. Model and equations. Astrophys. J. 154, 327-352.

Finson, M. L., and Probstein, R. F. (1968b). A theory of dust comets. II. Results for Comet Arend-Roland. Astrophys. J. 154, 353-380.

Fric̆, J., and Fric̆, J. (1896). Photographische Aufnahmen von Cometen. Astron. Nachr. 140, 63-64.

Gary, G. A., and O'Dell, C. R. (1974). Interpretation of the anti-tail of Comet Kohoutek as a particle flow phenomenon. Icarus (in press).

Gibson, E. G. (1974). Comet Kohoutek drawings from Skylab. Sky and Tel. 48, 207-212.

Hansen, P. A. (1824). Meridian-Beobachtungen des Cometen in Altona. Astron. Nachr. 2, 491-492.

Harding, C. L. (1824). Astronomische Nachrichten, Beobachtungen des diesjährigen Kometen, etc. Berliner Astron. Jahrbuch für 1827, pp. 131-135.

Harwit, M., and Vanýsek, V. (1971). Alignment of dust particles in comet tails. Bull. Astron. Inst. Czech. 22, 18-21.

Huebner, W. F. (1970). Dust from cometary nuclei. Astron. Astrophys. 5, 286-297.

Jaegermann, R. (1903). Prof. Dr. Th. Bredichin's Mechanische Untersuchungen über Cometenformen. St. Petersburg.

Jambor, B. J. (1973). The split tail of Comet Seki-Lines. Astrophys. J. 185, 727-734.

Jambor, B. J. (1974). History of the dust released by comets. These Proceedings.

Jeffers, H. M., and Adams, B. (1938). Observations of comets and asteroids. Lick Obs. Bull. 18, 163-166.

Keller, H. U., and Lillie, C. F. (1974). The scale length of OH and the production rates of H and OH in Comet Bennett (1970 II). Astron. Astrophys. 34, 187-196.

Kresák, L., and Vozárová, M. (1954). Comet Vozárová (1954f). IAU Circ. No. 1467.

Lampland, C. O. (1912). Comet a 1910. Lowell Obs. Bull. 2, 34-55.

Larsson-Leander, G. (1957). The anomalous tail of Comet Arend-Roland. Observatory 77, 132-135.

Liller, W. (1960). The nature of the grains in the tails of Comets 1956h and 1957d. Astrophys. J. 132, 867-882.

Maas, R., Ney, E. P., and Woolf, N. J. (1970). The 10-micron emission peak of Comet Bennett 1969i. Astrophys. J. (Lett.) 160, L101-L104.

Maclear, T. (1845). Great comet of 1844-5. Observations made at the Royal Observatory, Cape of Good Hope. Mon. Not. Roy. Astron. Soc. 6, 234-237.

McClure, A., and Liller, W. (1958). Rayed structure in the tail of Comet Mrkos, 1957d. Publ. Astron. Soc. Pacific 70, 404-406.

Miller, F. D., Blanco, V. M., and Gomez, A. (1971). A secondary tail of Comet Tago-Sato-Kosaka (1969g). Publ. Astron. Soc. Pacific 83, 216-217.

Ney, E. P. (1974). Multi band photometry of Comets Kohoutek, Bennett, Bradfield and Encke. Icarus (in press).

O'Dell, C. R. (1961). Emission-band and continuum photometry of Comet Burnham, 1959k. Publ. Astron. Soc. Pacific 73, 35-42.

O'Dell, C. R. (1974). Particle sizes in Comet Bennett (1970 II). Icarus 21, 96-99.

Olbers, H. W. M. (1824). (Extract from a letter.) Astron. Nachr. 3, 5-10.

Oort, J. H. (1950). The structure of the cloud of comets surrounding the solar system, and a hypothesis concerning its origin. Bull. Astron. Inst. Neth. 11, 91-110.

Oort, J. H., and Schmidt, M. (1951). Differences between new and old comets. Bull. Astron. Inst. Neth. 11, 259-269.

Orlov, S. V. (1945). Synchrones in comet tails (in Russian). Astron. J. (USSR) 22, 202-214.

Osterbrock, D. E. (1958). A study of two comet tails. Astrophys. J. 128, 95-105.

Porter, J. G. (1962). Comets (1961). Quart. J. Roy. Astron. Soc. 3, 167-178.

Probstein, R. F. (1968). The dusty gasdynamics of comet heads. In Problems of Hydrodynamics and Continuum Mechanics, Soc. Industr. Appl. Math., Philadelphia, p. 568.

Remy-Battiau, L. (1964). Étude du spectre continu des têtes de comètes. I. Diffusion de la lumière solaire par des particules diélectriques. Acad. Roy. Belg. Bull. Cl. Sci. (Sér. 5) 50, 74-89.

Rieke, G. H., and Lee, T. A. (1974). Photometry of Comet Kohoutek (1973f). Nature 248, 737-740.

Roemer, E. (1962). Activity of comets at large heliocentric distance. Publ. Astron. Soc. Pacific 74, 351-365.

Schwarzschild, K. (1901). Der Druck des Lichtes auf kleine Kugeln und die Arrhenius'sche Theorie des Cometenschweife. Sitz. Bayer. Akad. Wiss. München 1901, pp. 293-327.

Sekanina, Z. (1973a). Existence of icy comet tails at large distances from the sun. Astrophys. Lett. 14, 175-180.

Sekanina, Z. (1973b). Dynamical and photometric investigation of cometary type II tails. NASA Grant NGR 09-015-159, Semiannual Progress Report No. 4, pp. 41-47; see also note in IAU Circ. No. 2580.

Sekanina, Z. (1973c). Dynamical and photometric investigation of cometary type II tails. NASA Grant NGR 09-015-159, Semiannual Progress Report No. 3, pp. 7-21.

Sekanina, Z. (1974a). A study of the icy tails of the distant comets. Submitted to Icarus.

Sekanina, Z. (1974b). The prediction of anomalous tails of comets. Sky and Tel. 47, 374-377.

Sekanina, Z. (1974c). On the nature of the anti-tail of Comet Kohoutek 1973f. I. A working model. Icarus (in press).

Sekanina, Z., and Miller, F. D. (1973). Comet Bennett 1970 II. Science 179, 565-567.

Sekanina, Z., Miller, F. D., and Waterfield, R. L. (1975). On the nature of the anti-tail of Comet Kohoutek 1973f. II. Comparison of the working model with ground-based photographic observations. To be submitted to Icarus.

Spinrad, H., and Miner, E. D. (1968). Sodium velocity field in Comet 1965f. Astrophys. J. 153, 355-366.

Van Biesbroeck, G. (1938). Observations of comets at the Yerkes Observatory. Astron. J. 47, 157-163.

Van Biesbroeck, G. (1957). Observations of comets. Astron. J. 62, 191-197.

von Biela, W. (1824). (Extract from a letter.) Astron. Nachr. 3, 27-30.

Vsekhsvyatsky, S. K. (1959). On the nature of "synchronic" formations in comets' tails. Soviet Astron. 3, 490-498.

Waterfield, R. L. (1954). Comet Vozárová (1954f). IAU Circ. No. 1467.

Waterston, J. J. (1845). (Extract from a letter.) Mon. Not. Roy. Astron. Soc. 6, 207-209.

Whipple, F. L. (1957a). The sunward tail of Comet Arend-Roland. Nature 179, 1240.

Whipple, F. L. (1957b). Comments on the sunward tail of Comet Arend-Roland. Sky and Tel. 16, 426-428.

DISCUSSION

P. M. Millman: In reference to Dr. Sekanina's suggestion that the tensile strength of the dust in comet tails may break down at certain sizes in their evaporization, it should be noted that evidence from various types of observation of the interplanetary medium suggests that there is a tendency for micrometeoroids to break into certain preferred sizes in various size regimes.

Z. Sekanina: I'm of course glad to hear that.

E. Gerard: Did you study what the effect of the rotation of the nucleus may be if you have anisotropic dust emission and could this affect the dust tail curvature?

Z. Sekanina: I don't want to go into details, but the basically correct answer is that it would not affect the curvature.

D. A. Mendis: A modification of the mechanical theory could be produced by the charging of the grains. With small grains in the typical environment of the tail it is not difficult to charge them to large potentials and if magnetic fields in the tail are of the order of 100—1000γ it may be possible to explain the helical features seen in the dust tail of comet Ikeya-Seki.

Z. Sekanina: This is, of course, one of the objections that has been raised in the past. My reply to that is, if you come up with a quantitative picture and you get better agreement than I get with other sources, I am going to accept it. So far, nobody has come up with a sufficiently precise quantitative picture.

B. Jambor: I am anxious to see the applicability of the "vaporizing particle" variation of the Finson-Probstein theory shown by Dr. Sekanina to Comet Ikeya-Seki. In this case the features appear only far away in the tail in the zone where particles of $1-\mu > 1$ are found, showing that only small particles are involved, the larger ones do not seem to vaporize. Vaporization and reduction of radius should be accompanied by charging and therefore plasma effects are to be expected. If no such effects are observed, one should almost necessarily ask: "why?"

Z. Sekanina: Yes. There is a complete lack of sufficiently precise theory that explain the observations by including other forces. If this problem were overcome, I would be willing to accept such a theory but so far, nothing great has happened.

W. F. Huebner: What is the significance of the value of 0.585 for the density? Is this an effective value, or are you assuming spherical particles?

Z. Sekanina: This number is only a mathematical exercise. We generally work with 1 minus mu, and if we want to talk about particle radii, we have to assume the density. Of course, in the case of vaporization we are very lucky because what we actually get is the change in the size multiplied by the density, so that a only problem would arise only if the density of the particle changes. I use $Q_{RP}=1$ everywhere in the calculation and I use latent heat of vaporization=30 Kcal/mole.

W. F. Huebner: If the dust particles vaporize under the effect of solar radiation, then the released atoms may get ionized, either by radiation or by charge exchange. The Los Alamos Vela satellite group can look at the ionic charge-to-mass ratio, e.g., they have detected various isotopes of iron coming from the solar abundances. Is there any possibility of looking for released cometary ions in the Vela satellite data; what date might be the most appropriate to look for?

Z. Sekanina: The dates would be specific for various comets.

H. Keller: The orbital positions of satellites were checked by M. Dryer at NOAA Boulder to determine whether they were favorable for detection of cometary ion in Kohoutek. They were not.

Does Comet Ikeya-Seki also show evaporation of dust?

The observations of the fast increase in the tail length of Kohoutek after perihelion by the astronauts on Skylab may support the evaporation of particles, since large values of $1-\mu$ ($\geqslant 10$) were necessary as explanation (not taking evaporation into account).

Z. Sekanina: Yes. I haven't done the quantitative analysis but I know that this may be the case.

E. Grün: I do not agree with Dr. Sekanina's statement that the probability of detecting particles by in-situ dust experiments is very low. Trajectories of dust particles can always be found — by varying the emission time and the size of particles — such that these particles are at the same place in space as the in-situ detector during its penetration through the orbital plane of the comet. The probability of detection is really dependent on how abundant these particles are. Our group will continue looking for more evidence of dust-particles released from comets using our dust detector on Helios A.

Z. Sekanina: I haven't done a quantitative analysis but I think it's a good idea to try this experiment.

HISTORY OF THE DUST RELEASED BY COMETS

B. J. Jambor

INTRODUCTION

The origin of the Zodiacal cloud has been attributed to an influx of cometary debris which maintains a stable meteoritic complex (Whipple, 1955). Objections to a cometary origin of the Zodiacal cloud were presented by Harwit (1963) without denting the cometary theory (Whipple, 1967). Since then, the Finson-Probstein theory of dust production has been applied successfully to dusty comets. As a consequence size distributions of dust particles have been deduced for Arend Roland, 1957 III, (Finson and Probstein, 1968), Seki-Lines, 1962 III, (Jambor, 1973), Bennett, 1970 II, (Sekanina and Miller, 1973) and Kohoutek, 1973 f. (Jambor unpublished). Only careful consideration of the size distribution of the dust from periodic comets can resolve the problem of the origin of the Zodiacal cloud.. The following reexamines the production and history of the dust released from periodic comets using the Finson-Probstein theory and compares it to the size distribution of dust deduced from the above mentioned comets.

History of the Dust Released by Comets

Practically none of the dust released by new comets with near parabolic orbits stays in the inner parts of the solar system. The dust acquires hyperbolic orbits and is lost. Of the periodic comets with period less than 200 years we know that some are responsible for regular meteor showers. One can calculate the minimum size a dust grain released with zero initial velocity by an elliptical comet must have to have a non-parabolic or non-hyperbolic orbit and thus stay in the solar system. It can be shown that the eccentricity of the dust grain is

$$e_d = \left[1 + \frac{2p(1-\mu)}{\mu^2 r_c(t_c - \tau)} + \frac{e^2 - 1}{\mu^2}\right]^{\frac{1}{2}}$$

where p is the semi-latus rectum, e, the eccentricity of the comet, $r_c(t_c - \tau)$ is the distance of the nucleus from the sun at the time of release. If we set $e_d^2 = 1$, i.e., parabolic orbit, we have the condition:

$$2p(1-\mu) = (1 - e^2)\, r_c(t_c - \tau)$$

or

$$1 - \mu = \frac{r_c(t_c - \tau)}{2a}$$

where a is the semi major axis of the comet. To obtain an order of magnitude estimate, let us assume the dust is released mostly during the perihelion passage. We then obtain

$$1 - \mu = \frac{a(1 - e)}{2a} = \frac{1 - e}{2}$$

as the condition for escape. Table I shows the sizes of grains released by some important periodic comets. The average minimum size is 13.4 μm for ice and 5.3 μm for silicates. No particle smaller than this has a good chance of staying in the inner solar system. It can be shown that for parabolic or hyperbolic orbits, no single collision with a planet can perturb the orbit into an elliptical one (Everhart 1974).

Table I

Comet	Meteor Shower	Limit of $1 - \mu$	
1948 XII	α Cap	0.093	$1 - \mu$ average is
1852 III Biela	Andromeda	0.123	then: 8.86×10^{-2}
Encke	Taurids	0.076	$pd/Qr_p = 1.34 \times 10^{-3}$
Giacobini-Zinner	Draco	0.135	Ice: 13.4 μm
Halley		0.016	Silicates: 5.36 μm

Minimum size of the dust released by Periodic Comets which stays in the Interplanetary Medium.

The study of the dust released by some recent comets shows that the size distribution peaks at about one micron with distribution widths much larger for comets that come close to the sun, 1962 III, 1973 f, than for those that have perihelia at larger distances like comets, 1957 III and 1970 II. The former can release larger grains due to the more intense heating and subsequent faster release of gas, whereas the latter have proportionately fewer of these grains, of size 10 micrometers and above. Since periodic comets do not come very close to the sun, we can assume that their size distribution of grains is like those of comets 1957 III and 1970 II. In this case, only a very small fraction, about one tenth of the total at the most, of the grains released have the size required to stay in the Zodiacal cloud. If we take an extremely wide zeroth order logarithmic distribution of sizes, Kerker (1969), more characteristic of 1962 III and 1973 f, the area corresponding to the sizes which can be permanent members

of the Zodiacal cloud is only about one-third of the total. This is shown in figure 1. This says that periodic comets contribute only a fraction of their dust to the cloud. In this context the Zodiacal cloud would be made up of particles larger than say 5 μm. This is in agreement with the determination of sizes from line shapes in the Zodiacal light spectrum (James and Smeethe, 1970). Results from scattering models are less conclusive (Giese, 1973). These scattering models, based on Mie calculations suffer from the contribution of many angles of scattering and distribution of sizes which all wash out fine structure and colors. Only in the Gegenschein region and very close to the corona are the contributions from angles few in number. Due to the difficulty of sorting out noise factors contributing to the low value of brightness of the Gegenschein, it appears that the best hopes of conclusive measurements of sizes of interplanetary dust lie with direct collection far from the earth or careful investigation of the F and K corona regions.

Mass Injection from Comets

Despite the loss of small particles, if enough large ones are ejected, comets can contribute to the Zodiacal cloud. The contribution of the comets to the Zodiacal cloud has been assessed from the point of view of mass supply compared to mass loss, (Whipple 1967). In this approach we must clearly distinguish between the particles which contribute to the continuum of the coma and tail and those that influence the total mass. The light scattering depends on the number density of particles of size comparable to the wavelength of light, it favors the small particles of 0.5 micron size. Given any size distribution of particles $g(\rho_d d)$ expressed in terms of the diameter d and density ρ_d, the most representative mass is given by (Finson and Probstein, 1968)

$$\pi \langle (\rho_d d)^3 \rangle \, / 6 \, \rho_d^{\,2}$$

where the expression between brackets is the third moment of the distribution function:

$$\langle (\rho_d d)^3 \rangle = \int_0^\infty (\rho_d d)^3 \, g(\rho_d d) \, d(\rho_d d) \, .$$

The mass contribution is not very sensitive to the smaller particles but weighted

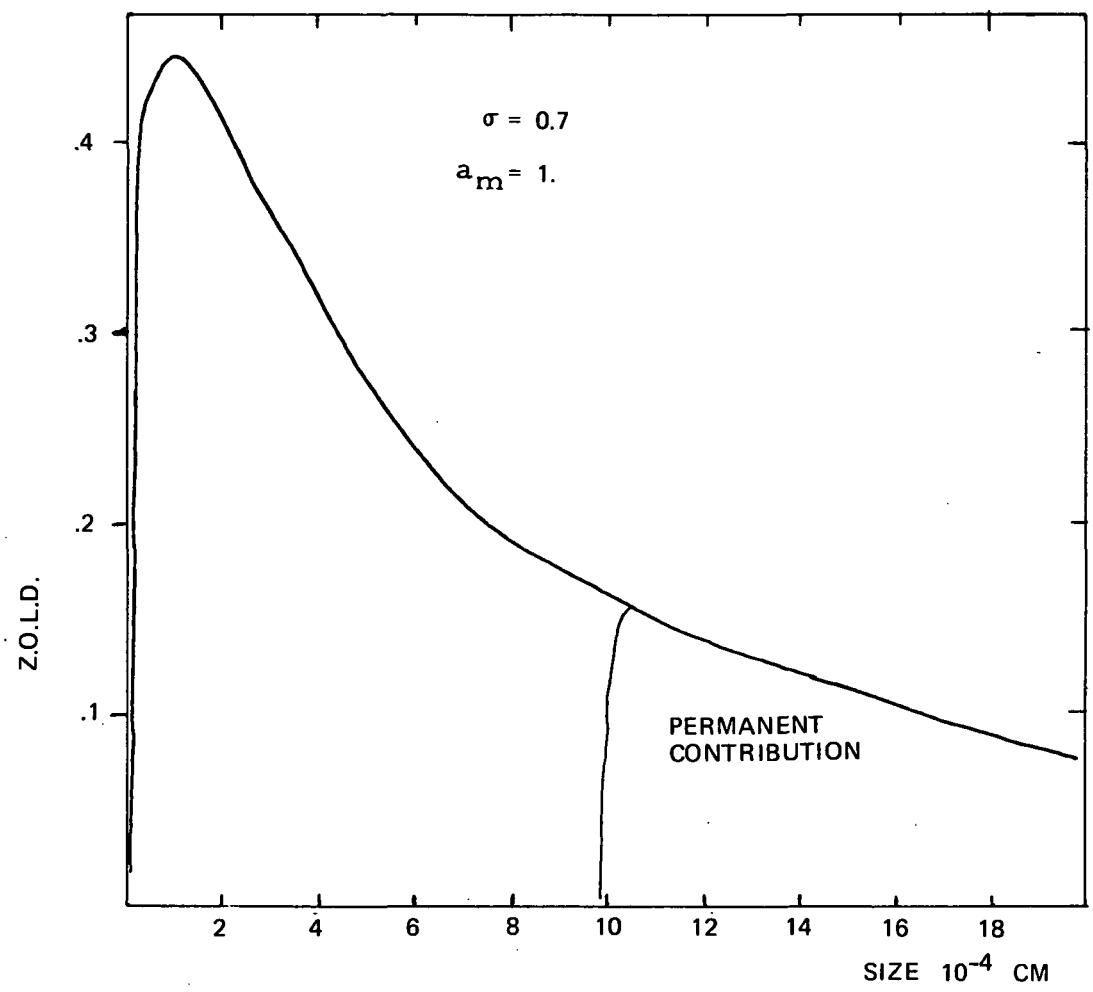

Figure 1 - A zeroth order logarithmic distribution (Z.O.L.D) with modal size a_m = 1 μm and scatter parameter σ = 0.7.

towards the lower part of the distribution where larger particles are found. It is, therefore, not correct to base mass injection rates on calculations based on visual estimates of absolute magnitude. In the first place, the separation between emission and continuum must be done carefully, since bright comets can have low dust content. Secondly, considering the dust continuum only, a size distribution must be carefully calculated taking into account the dynamics of the particles, as revealed by the shape of the tail, which delineates the maximum and minimum sizes, together with the brightness distribution. On the basis of such size distributions which determine the true ratio of large to small particles produced by the comet, mass production can be obtained. One can, therefore, not deduce a necessarily large mass injection from a bright visual display, nor can one estimate the previous brightness of a comet like Encke from the relics found in meteor streams. The presence of large particles detected as meteors coming from Encke does not necessarily mean an abundance of large particles high enough to replenish the Zodiacal cloud by itself.

Conclusion

We can eliminate all of the bright new comets from the ranks of the contributors to the Zodiacal cloud. Among the periodic comets, all particles of size much smaller than 10 μm are lost also. This leaves only the large particles as possible candidates. The situation at the present time does not allow us to draw any definite conclusions about the extent of the contribution of periodic comets. The amount of large particles released by Encke is not known. Only a careful analysis of the dust content of this comet can give the answer.

REFERENCES

Everhart, E (1974). The Evolution of Comet Orbits, These proceedings.

Finson, M. L. and Probstein, R. F. (1968). A Theory of Dust Comets, Ap. J., 154, 327.

Giese, R. H., (1973). Space Research XIII, 1165-1171, Akademie-Verlag, Berlin.

Harwit, M. (1963). Origins of the Zodiacal Dust Cloud. J.G.R., 68, 2171-2180.

Jambor, B.J. (1973). The Split Tail of Comet Seki-Lines. Ap. J. 185. 727-734.

James, J. F., and Smeethe, M. J. (1970), Nature 227, 588-589.

Kerker, M. (1969). The Scattering of Light. Academic Press, N.Y., 351.

Sekanina, Z. and Miller, F.D. (1973). Comet Bennett 1970 II. Science 179, 565-567.

Whipple, F. L. (1955). Ap. J. 121, 750.

Whipple, F. L. (1967). On Maintaining the Meteoritic Complex. In "The Zodiacal Light and the Interplanetary Medium". (J. L. Weinberg ed) 409-425.

PARTICLES FROM COMET KOHOUTEK DETECTED BY THE MICROMETEOROID EXPERIMENT ON HEOS 2

H.-J. Hoffmann, H. Fechtig, E. Grün and J. Kissel

INTRODUCTION

The HEOS 2 satellite was launched into a highly eccentric orbit around the earth on January 31, 1972 and re-entered the earth's atmosphere after a successful mission on August 2, 1974. Due to the orbit (apogee: 240 000 km, perigee: 300 - 5000 km) the satellite spent most of the time in the interplanetary region where the influence of the earth's gravitation field is negligible with regard to its effect on interplanetary dust particles.

The micrometeoroid experiment on board measured the mass and the speed of dust particles by the plasma produced during their impact on the sensor. The field of view was a cone with a semi-angle of 60°. The detector was mounted with the axis of symmetry parallel to the spin axis of the spacecraft. By an active reorientation system the viewing direction of the detector could be turned in any direction perpendicular to the earth-sun line. A detailed description of the detector has been given earlier (Dietzel et al., 1973) (Hoffmann et al., 1975).

About 54 days before the end of the mission the earth and hence the satellite passed through the orbital plane of comet Kohoutek. Prior to this event a study of the orbital mechanics of the earth, the comet and its dust showed that it should be possible within the given attitude constraints

of the spacecraft to encounter dust released from the comet.

Particles, ejected from a comet which moves on a parabolic orbit, can be detected by an earth orbiting satellite only during the transit of the earth through the orbital plane of the comet, provided that the comet's node is on or within the earth orbit. In the latter case merely particles with orbits further outwards are able to encounter the earth. This applies to particles subject to the repulsive force of radiation pressure after being released from the comet nucleus. With β denoting the ratio of the force of radiation pressure to that of gravity, particles with an appropriate $\beta > 0$ can encounter the earth orbit. Due to the radiation pressure the particles lag behind the comet and can only be detected if the comet passes its node before the transit of the earth through the orbital plane of the comet. Thus, in principle, solely particles with a specific value of $\beta = \beta_o$ and a specific heliocentric release distance $r_R = r_{Ro}$ are able to encounter the earth.

During the emission process the outstreaming gas from the comet nucleus adds a velocity distribution to the initial speed of the particles given by the comet's speed at the release time. This effect will permit particles from a certain range of heliocentric distances around r_{Ro} and with values of β around β_o to encounter the earth. As demonstrated in figure 1, in the case of comet Kohoutek,

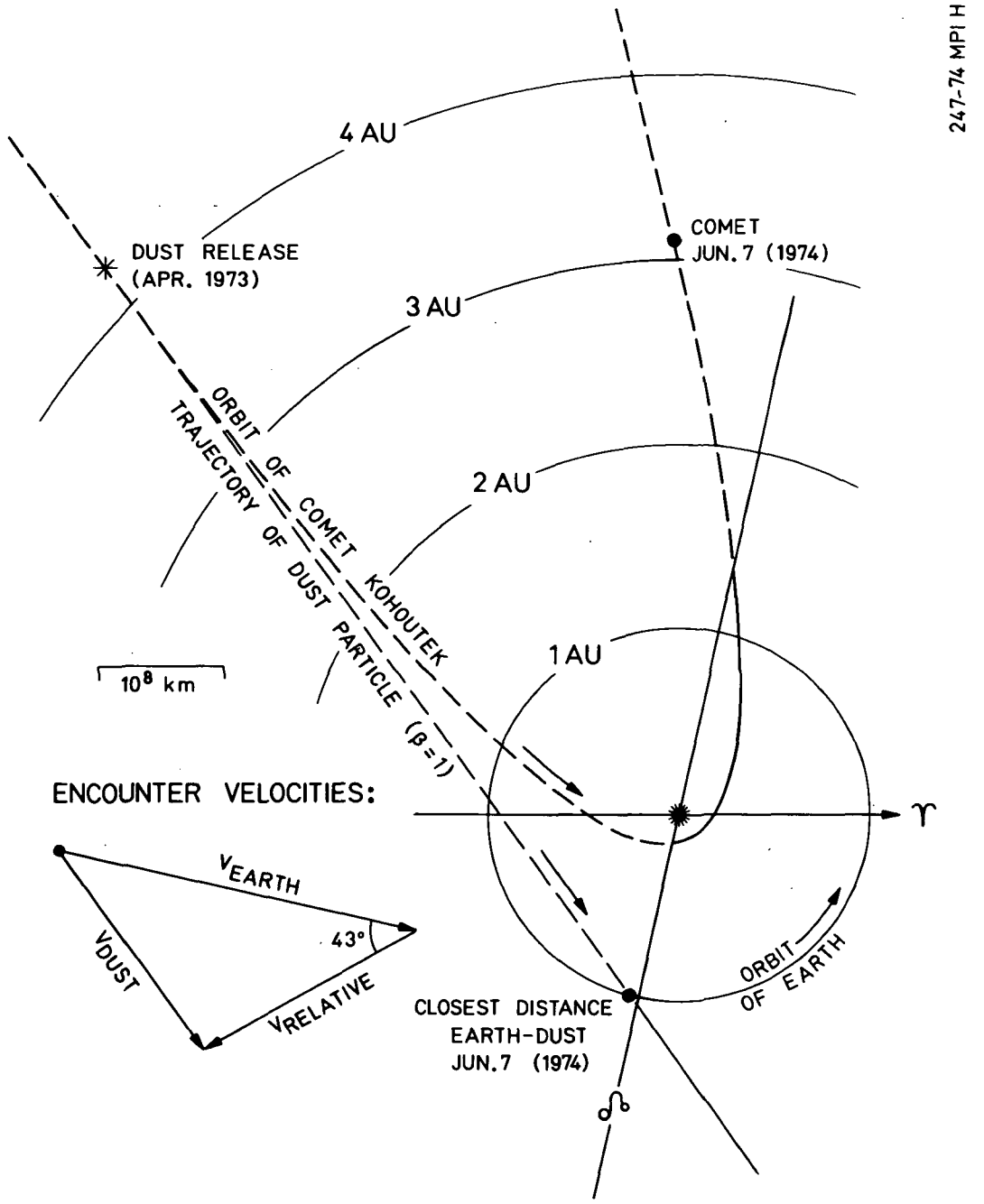

Fig. 1: Trajectory of dust particle ($\beta = 1$) released from comet Kohoutek at a heliocentric distance of $r_R = 4.3$ AU passing the earth close to the comet's line of nodes and velocity diagram during encounter (to the left).

particles with $\beta \approx 1$ released at a heliocentric distance $r_R \approx 4.3$ AU could encounter the earth. Their heliocentric speed at the release point is approximately 20 km/sec. With $\beta = 1$ the net force acting on the particle is zero, so their speed remains constant and they move on a straight line tangentially to the comet's orbit. Close to their ascending node they are overtaken by the earth. Their geocentric speed is 19 km/sec with the apparent radiant 43° away from the earth's apex towards the sun; hence the best viewing direction of the detector within the given attitude constraints is towards the earth's apex. The particles then would encounter the detector at an angle of incidence of approximately 40° which is well within the detector's field of view.

During the transit of the earth through the orbital plane of the comet, the rate of particles with speeds of approximately 19 km/sec should increase compared to the normal rate before and after the transit while viewing towards the earth's apex for particles with $\beta \approx 1$. Since the inclination of the comet's orbit is fairly low ($i = 14.3^{\circ}$) it would be possible to detect these particles for a time-period of approximately two months around the transit.

MEASUREMENTS AND DISCUSSION

Due to refurbishing of telemetry stations the detector could not be reorientated before May 16, 1974. At that time the rates were already significantly increased, but the remaining period until the mission end was sufficient to observe the decrease of the rate towards the "normal" value. The normal rates were taken from the two periods in 1972 from day 90-140 and in 1973 from day 29-214 when the detector also was viewing towards the earth's apex.

In figure 2a and 2b the average particle rate is shown as a function of the particle speed and mass, respectively, presenting the data from the transit period (period T) on the right and those under normal conditions (period N) on the left part of the figures. The rates refer to the randomly distributed particles with known speed from the interplanetary region (Hoffmann et al., 1975) and the appropriate effective measuring time T_{EFF} taking into account the data coverage.

As demonstrated in figure 2a the rates of particles with speeds less than 15 km/sec are equal within the statistical error for both periods, whereas during period T a significant excess of particles is observed in the speed interval from 15-20 km/sec where the cometary particles were expected. Accordingly, in figure 2b during period T the mass distribution raises in the mass range from 10^{-13} to 10^{-11}g over the normal mass distribution (background). In figure 2c both criteria established in figure 2a and 2b have been combined, showing the history

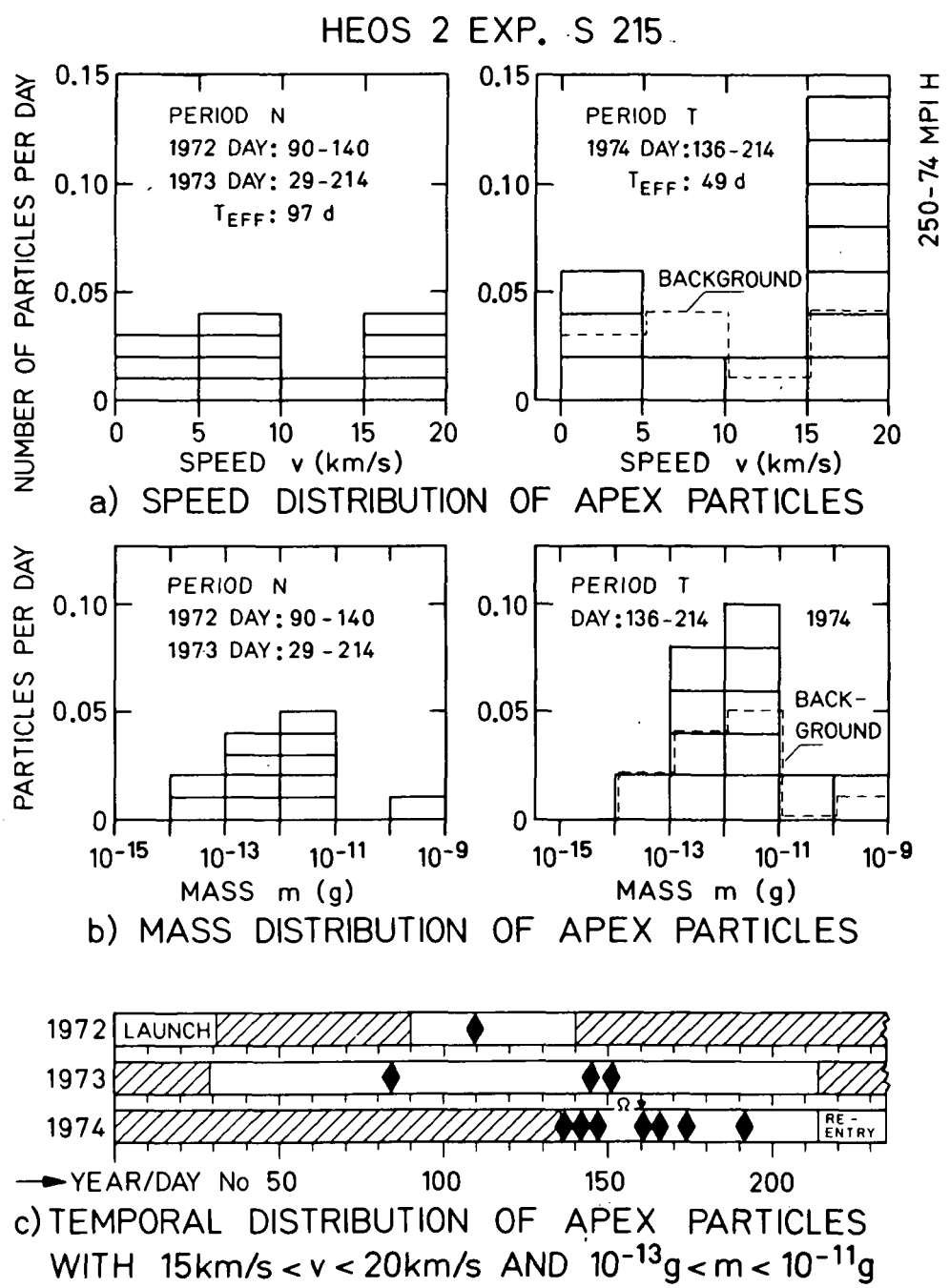

Fig. 2: Data from the HEOS 2 micrometeoroid experiment S-215 while facing the earth's apex during the transit of the earth through the orbital plane of comet Kohoutek (period T) and under normal conditions (period N).

exclusively of particles matching the relevant mass and speed intervals. The rate of these "cometary candidates" from period T is higher approximately by a factor of 3.5 than the rate of the background particles from period N. For the sake of completeness it may be mentioned that the rate of these particles during periods when the detector was facing directions different from the earth's apex is of the same magnitude or less than during period N.

Though the number of particles is small, the probability that 7 particles instead of the average of 2 in the relevant speed interval (see fig. 2a) and 9 instead of the average of 4 in the relevant mass interval (see fig. 2b) may be random is approximately 10^{-4}. Therefore, an additional particle source during period T is very likely.

Apart from comet Kohoutek no other sources such as the earth (Bigg and Thompson, 1969), the moon (Alexander et al., 1973; Hoffmann et al., 1975), meteor showers or other comets fulfil all conditions required by the measurements listed below:

a) time interval of enhanced particle rate between May 16 and June 23, 1974 equivalent to ecliptic longitudes from 235^{o} - 273^{o},

b) mass range of particles: 10^{-13} - 10^{-11} g,

c) speed range of particles: 15 - 20 km/sec

d) apparent radiants of particles: cone around the earth's apex with semi-angle of 60°.

Particles with the required speed, originating in the earth, can be excluded because their trajectories cannot enter the sensor while it is facing the earth's apex. A lunar origin can be ruled out since the same argument holds for 5 out of 7 candidates. Meteor showers as sources are unlikely for two reasons because 1) no increased particle rate has been observed in the preceding year (1973) and 2) the radiants of the showers occuring in the relevant time interval (Daytime Arietids, Daytime ζ Perseids and Daytime β Taurids) do not match the required cone of directions (Whipple and Hawkins, 1959). As the nodes of all major comets (apart from comet Kohoutek) observed in 1973 and 1974 , such as comet Bradfield (1974b) (IAU Circular No. 2636), do not fit in the required interval of ecliptic longitudes or have perihelion distances of more than 1 AU, they cannot supply these particles either. Therefore, the authors believe that the excess of particles during the transit of the earth through the orbital plane of comet Kohoutek is due to dust particles ejected from this comet.

The direct measurements of the individual mass and speed of the particles supply new knowledge about cometary dust

which supplements the data derived from photometric studies (Finson and Probstein, 1968, Sekanina and Miller, 1973 and Sekanina, 1975). A direct measurement of cometary dust by a collection experiment during the transit of the earth through the orbit plane of comet Giacobini Zinner has been reported by Hemenway (1973).

INTERPRETATION

For further evaluation of the measured data, orbit calculations have been performed for particles ejected from comet Kohoutek encountering the earth at a time of observation t_o around the date of the earth's transit through the orbital plane of the comet on day 160 in 1974.

Figure 3 shows an instant picture of the particles' positions as a function 1) of the magnitude of β (syndyne) and 2) of the release time t_R (synchrone) and the corresponding heliocentric distance r_R, respectively, at t_o = day 160 (1974). The additional velocity distribution arising from the gas streaming away from the comet nucleus has been neglected in this picture. Due to the additional velocity component Δv, particles with values of β different from 1.00 have a chance to encounter the earth as long as their Δv is sufficient to cover the missing distance to the earth during the time interval $\Delta t = t_o - t_R$. The magnitude of Δv is presented in figure 4. It shows the minimum

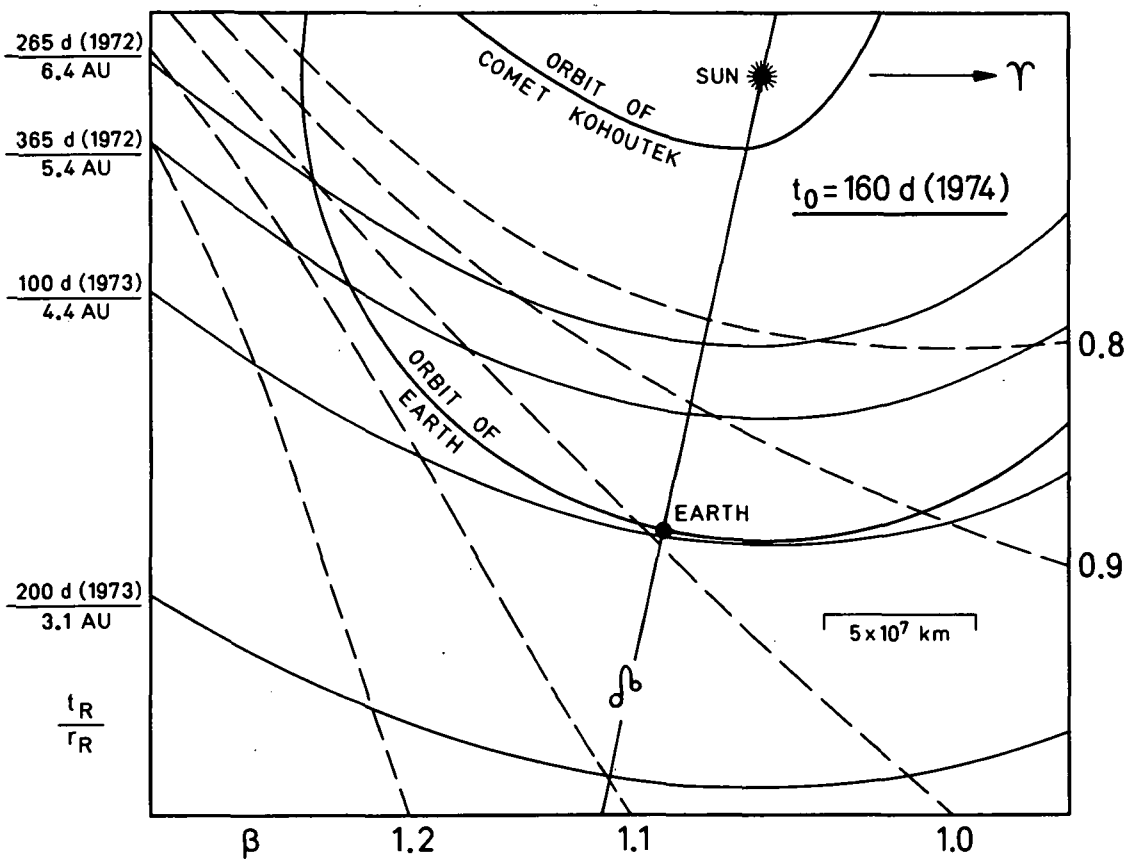

Fig. 3: Position of particles from comet Kohoutek for constant values of 1) β (syndyne: broken lines) and 2) release times t_R (synchrone: solid lines) or the corresponding heliocentric distances r_R during the transit of the earth through the orbital plane of the comet at t_0 = day 160, 1974.

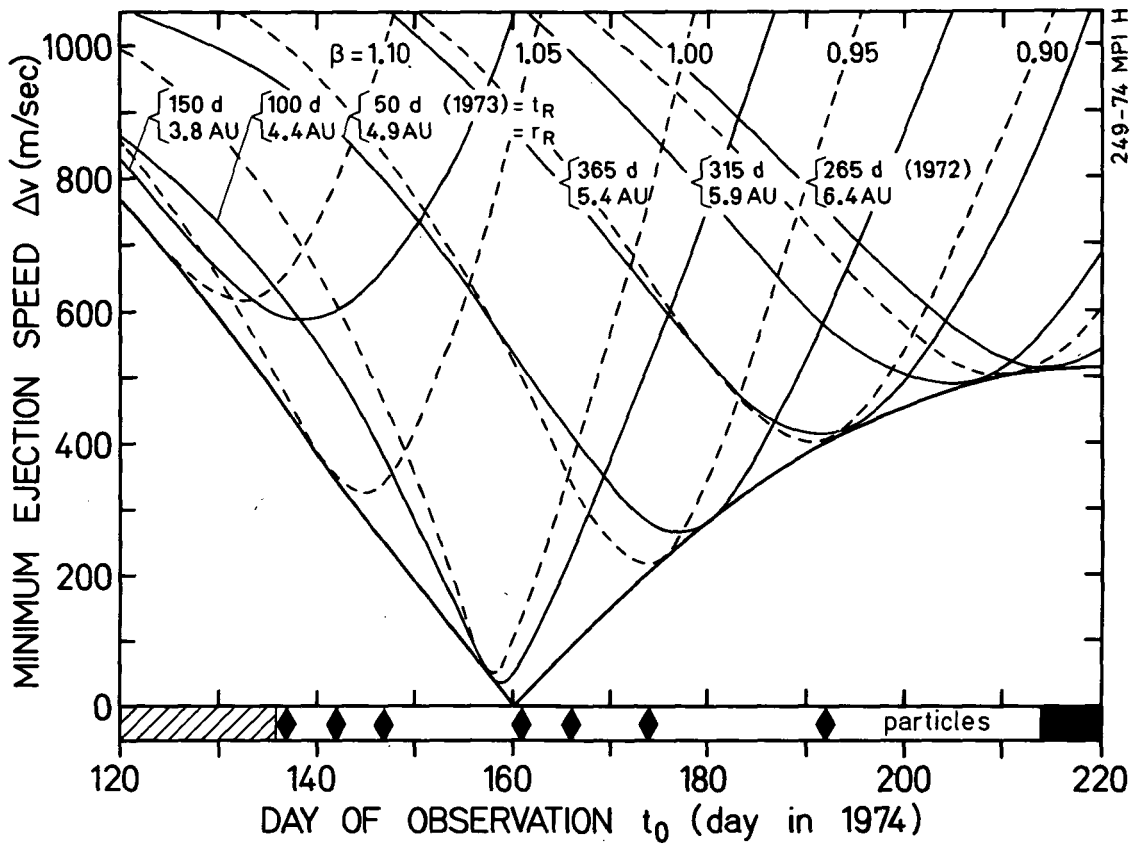

Fig. 4: Minimum ejection speed Δv for constant values of 1) β (broken lines), 2) release times t_R or the corresponding heliocentric distances r_R (solid lines) and envelope (fat line) as a function of the observation time t_0 and temporal distribution of the cometary particles.

ejection speed Δv required to reach the earth as a function of the time of observation t_o and the parameters β and r_R or t_R. The envelope (fat line) indicates the absolute minimum speed at the various days of observation. Using the time history of the candidates (on the bottom of the figure) ejection speeds can be derived.

If the candidate from day 192 (1974) is a descendent of comet Kohoutek it must have been released with $\Delta v \gtrsim 400$ m/sec. On the other hand, Δv cannot be much larger because otherwise further particles should have also been observed at later times. Particles arriving at the earth at day 137 (1974) must have been released with $\Delta v \gtrsim 450$ m/sec. However, in this case Δv may be more than 450 m/sec because the rise of the candidates' rate apparently occurred before day 136 which would require a higher ejection speed. Thus, from figure 4 can be deduced that the parameters of the observed candidates range from $\beta \approx .90$ at $r_R \approx 5.4$ AU with $\Delta v \approx 400$ m/sec to $\beta \approx 1.10$ at $r_R \approx 3.8$ AU and $\Delta v \gtrsim 450$ m/sec.

ACKNOWLEDGEMENT

This project was supported by the "Bundesministerium für Forschung und Technologie". We also acknowledge the excellent cooperation with ESTEC and ESOC.

REFERENCES

Alexander W.M., Arthur C.W., Bohn J.L. and Smith J.C. (1973) "Four Years of Dust Particle Measurements in Cislunar and Selenocentric Space from Lunar Explorer 35 and OGO 3". Space Research XIII, Akademieverlag Berlin, 1035

Bigg E.K. and Thompson W.J. (1969) "Daytime Photograph of a Group of Meteor Trails". Nature 222, 156

Dietzel H., Eichhorn G., Fechtig H., Grün E., Hoffmann H.-J. and Kissel J. (1973) "The HEOS 2 and Helios Micrometeoroid Experiments". J. of Phys. E: Sci. Instrum 6, 209

Finson M.L. and Probstein R.F. (1968) "A Theory of Dust Comets. II Results for Comet Arend-Roland". Astrophys. J. 154, 353

Hemenway C.L. (1973) "Collections of Cosmic Dust" paper presented at "Whipple Memorial Symposium", Cambridge, Massachusetts

Hoffmann H.-J., Fechtig H., Grün E. and Kissel J. (1975) "First Results of the Micrometeoroid Experiment S-215 on the HEOS 2 Satellite". Planet. Space Sci. 23, 215

Sekanina Z. (1975) "Progress in Our Understanding of Cometary Dust Tails". Proceedings of IAU Colloquium No. 25

Sekanina Z. and Miller F.D. (1973) "Comet Bennett 1970 II". Science 179, 565

Whipple F.L. and Hawkins G.S. (1959) "Meteors". Handbuch der Physik, Vol. 52, ed. S. Flügge, Springer-Verlag Berlin, Göttingen, Heidelberg, 519

PHYSICAL PROPERTIES OF INTERPLANETARY GRAINS

D. E. Brownlee, F. Horz, D. A. Tomandl and P. W. Hodge

I. INTRODUCTION

This paper presents physical properties of interplanetary dust determined by in-situ techniques. It is probable that, like millimeter-sized meteoroids (Jacchia, et al. 1967), most interplanetary dust is cometary matter. Although a cometary origin for interplanetary dust is widely accepted (Whipple 1967) (Millman, 1972) there is currently no unambiguous proof of this hypothesis. The results presented here must be interpreted accordingly. It must also be remembered that even if interplanetary particles are cometary, they might possibly be altered in the interplanetary medium by collisions and by thermal effects during close perihelion passages, so the dust particles may not be representative of unaltered cometary material.

Over the past 5 years it has become possible to make relatively direct measurements of some physical properties of interplanetary dust. Morphological analysis of micrometeorite craters found on lunar rocks and returned spacecraft experiments has provided an opportunity to measure the properties on an unbiased sample of interplanetary particles, and the collection of genuine micrometeorites in the stratosphere has made it possible to do detailed laboratory investigation on them.

II. MICROMETEORITE CRATERS

The hypervelocity (>3 km s^{-1}) impact of an interplanetary dust grain onto a surface results in the almost total vaporization of the particle and in the production of a crater. Through laboratory simulation experiments and the analysis of craters on lunar rocks, criteria have been developed that enable reliable identification of such impact sites (Hartung et al., 1972). Laboratory calibration experiments (Vedder and Mandeville, 1974) make it possible to correlate crater morphological parameters with certain physical properties of the impacting projectiles.

a.) Shape and Density

Vedder and Mandeville's (1974) calibrations demonstrate that the circularities and depth/diameter ratios of micron-sized micrometeorite craters are determined in part by the shapes and densities of impacting meteoroids. By measurement of circularities and depth/diameter ratios for a large number of lunar microcraters, it was concluded that micron-sized meteoroids are roughly equidimensional and they have densities compatible with stony meteorites (Brownlee et al., 1973)(Horz et al., 1975). The high degree of circularity of lunar craters is strong evidence that grossly nonspherical shapes like platelets and rods are practically non-existent in the interplanetary medium. The measured depth/diameter ratios indicate meteoroid densities greater than 1 g cm^{-3} and less than 7 g cm^{-3}. Strict interpretation of the data implies a mean meteoroid density between 2 and 4 g cm^{-3}. Recent measurements of depths of craters on small lunar glass spherules by Smith et al. (1974) indicate three groupings of depth/diameter ratios corresponding to

projectile densities of 8 g cm^{-3}, 3 g cm^{-3} and 1-2 g cm^{-3}. These measurements disagree with our measurements in that an abundance of particles as dense as metallic iron are reported. The existence of dense particles is currently a matter of dispute, but both groups agree that particles of extreme low density (<1 g cm^{-3}) do not exist. This result is in direct contradiction with the traditional concept of fluffy cometary meteoroids.

b.) Chemistry

In simulation experiments where micron-sized iron projectiles are impacted onto silicate targets, there normally is a detectable particle residue lining the crater floor. In hundreds of lunar craters examined, however, only one crater has been found which is reported to contain residue (Fechtig et al., 1975). In this case, Fe-Ni mounds were found inside a 0.5 mm crater. The lack of residue in the majority of lunar craters in silicates can be construed as evidence that metallic iron micrometeorites are rare and that whatever the composition of normal meteoroids is, it is totally vaporized upon impact onto silicate surfaces.

The impact processes in metal targets are somewhat different from those for silicates, as shown by the observation that for a given impact energy, craters in metals are nearly an order of magnitude more voluminous then craters in silicates. Conditions in metal targets are apparently more suitable for residue retention, as seems to be shown by the fact that the two craters found in the aluminum cover of S228 Skylab IV experiment both contained significant meteoroid residue (Brownlee et al., 1975). For the two Skylab craters it was estimated that ~10% of each meteoroid survived as residue. Microprobe analysis showed that the larger crater (110μm diameter)(Figure 1) contained elemental abundances essentially identical with chondritic meteorites (Figure 2) and that the small crater

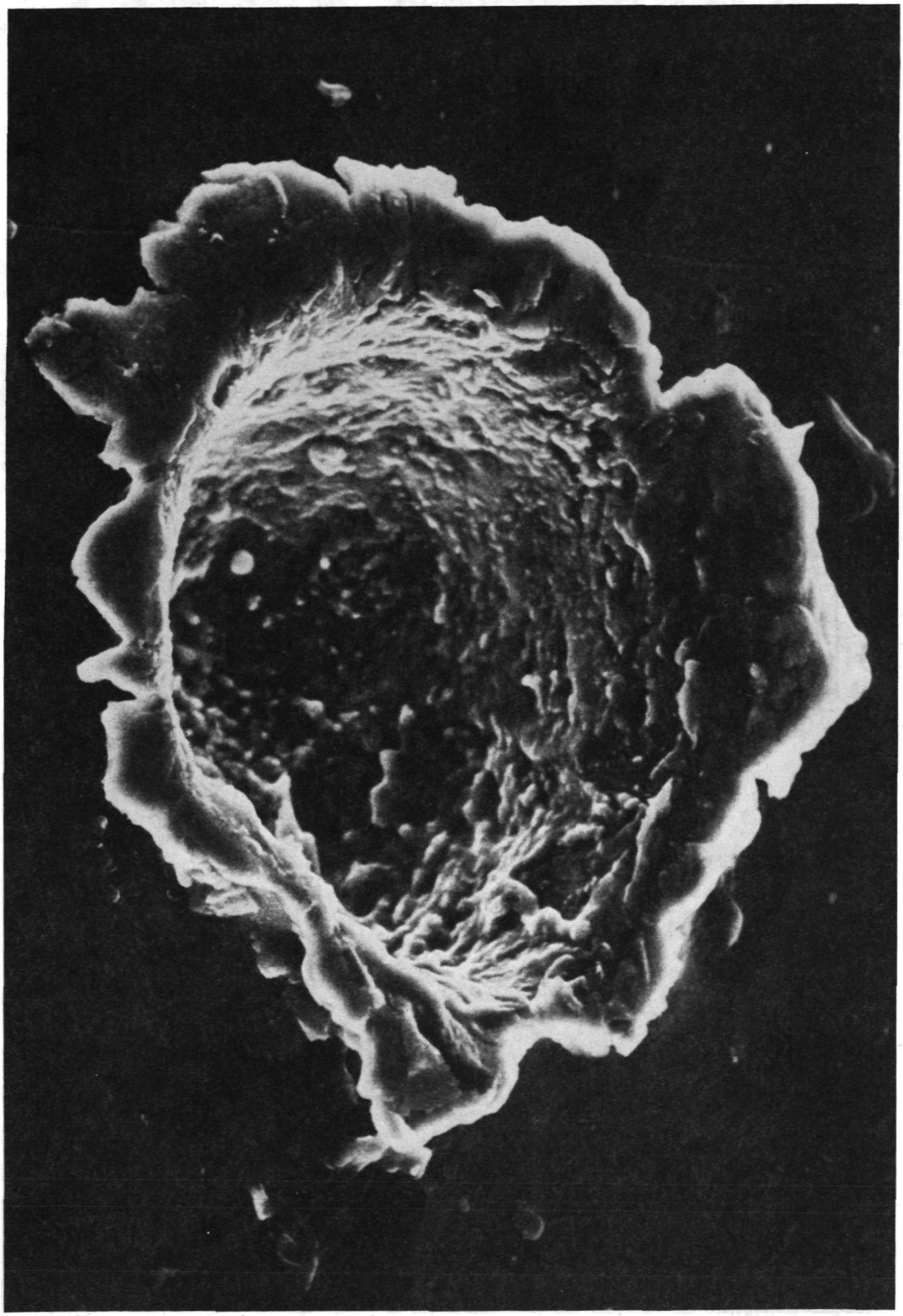

Figure 1 110μm diameter microcrater from Skylab IV.

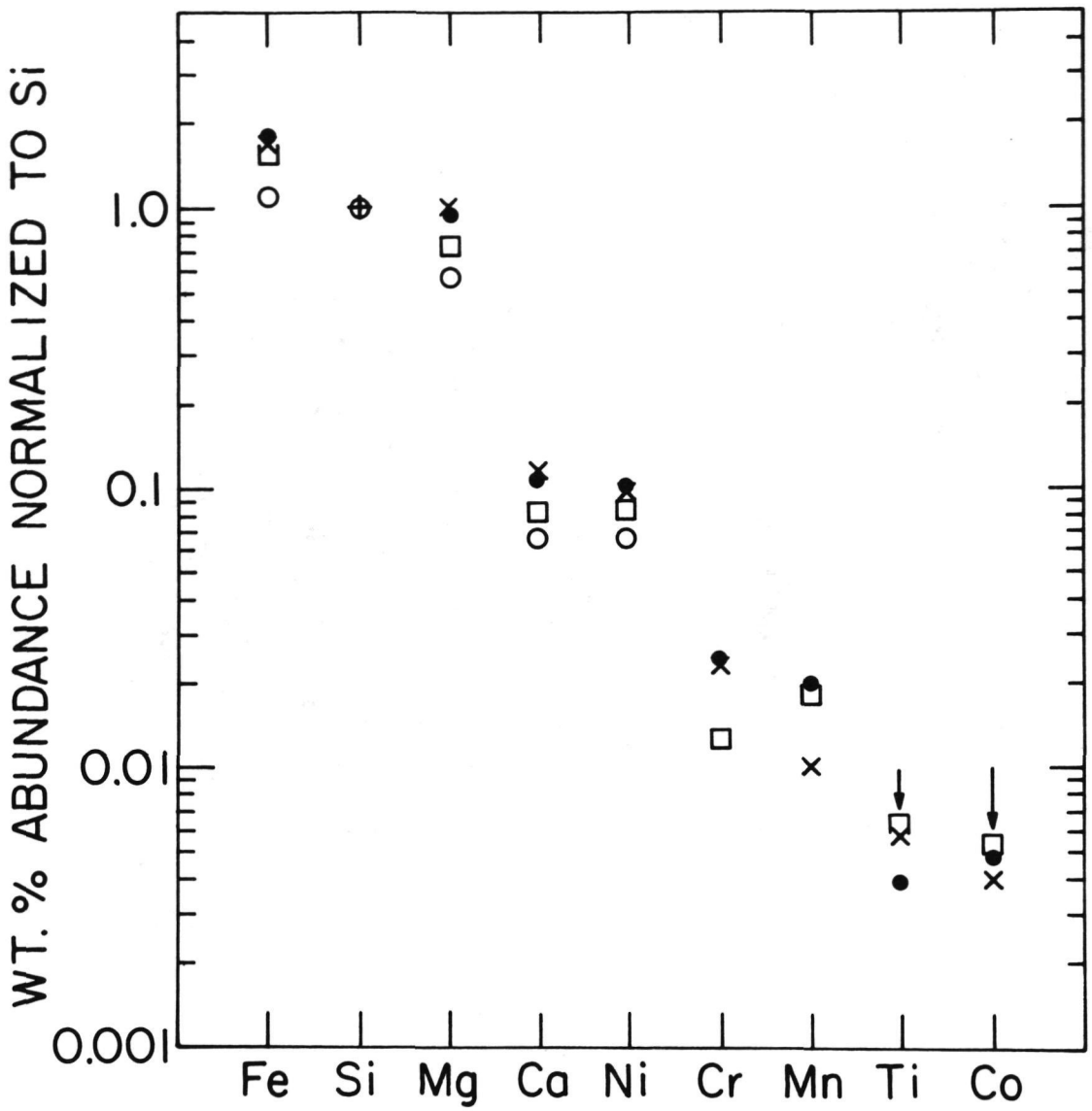

Figure 2 Microprobe analysis of meteoroid residue in the 110μm Skylab IV crater. The open squares and open circles represent independent microprobe analyses of 30μ spots on the crater floor. Filled circles and crosses, respectively, are C1 and C3 meteorite averages (Mason, 1971). Sulfur was analyzed in a separate probe run and was found to be qualitatively similar to the Fe, Mg, Si group.

(30μm) contained residue of an iron sulfide meteoroid with minor amounts of Ni and Mg. Because no known mineral contains chondritic abundances, the close agreement of the 110μm crater residue indicates that the impacting meteoroid was an aggregate of grains. For the bulk particle composition to be so close to chondritic the average grain sizes in the aggregate must have been considerably smaller than the 30μm diameter particle that produced the crater.

III. MICROMETEORITES

Small interplanetary particles, because of their large surface area/mass ratios, can survive high velocity entry into the atmosphere (Whipple, 1951). The micrometeorite flux is extremely low, but our measurements indicate that, for particle sizes larger than 10μm, extraterrestrial particles are the dominant particulate in the stratosphere. We have collected particles by inertial deposition from a high velocity air stream onto clean, oil-coated collection surfaces. The collection technique is successful because it is clean and because it samples enormous volumes of air. We have had two successful sampling flights at 34 km with a balloon sampler (Brownlee et al., 1973) and 3 long-duration sampling runs at 20 km with an impactor mounted on a NASA U-2 aircraft. The five flights have cumulatively sampled 6×10^4 m^3 of ambient air. Collected particles range in size from 2μm to 20μm. All five collections produced similar densities and types of particles.

Disregarding particles which are primarily aluminum oxide (a common stratospheric contaminant), 50% of the collected particles with diameters >5μm are with iron sulfides with some Ni or are particles with abundances of Fe, Si, Mg, Ca, Ni and S consistent with chondritic meteorites. We have collected

and analyzed 50 chrondritic particles and 26 iron-sulfur-nickel (FSN) particles. The measured stratospheric flux of both types is 4×10^{-6} part. m^{-2} s^{-1} for diameters $\geq$ 6μm.

The particles are analyzed qualitatively using energy dispersive X-ray techniques in the SEM. The FSN particle compositions are consistent with troilite (or pyrrhotite) containing 1-5% Ni. These particles (see Figure 4) contain no other detectable elements and the Ni has never been found to be higher than 5%. The chondritic particles agree remarkably well with chondritic meteorites (Figure 3), with Mg, Si, and Fe relative abundances usually within a factor of 2 of chondritic values. Most of these particles contain sulfur at approximately the 5 wt % level, and Ca and Ni at the 1% level, but no higher. With long integration times minor amounts of Cr and Mn usually also can be detected. In the optical microscope the particles are very black, suggesting the existence of an appreciable carbon content. We do not see particles with near-chondritic compositions that have anomalously high abundances of non-cosmically abundant elements, (i.e. Al, Ca, Na, K, Cu, Ti, etc.).

One particle has been ground in half, polished and analyzed quantitatively with standard microprobe techniques. This particle, because of its spherical shape, its depletion of sulfur and the existence of small magnetite grains, similar to those seen in meteorite fusion crusts (Blanchard and Cunningham, 1974), is believed to be a meteor ablation droplet. Considering the fact that the particle is only 12μm in diameter, the agreement with chondritic abundances is remarkable (see Table I).

That a large fraction of the collected particles have chondritic abundance patterns is very strong evidence that the particles are bona-fide micrometeorites and not contamination artifacts. A close match

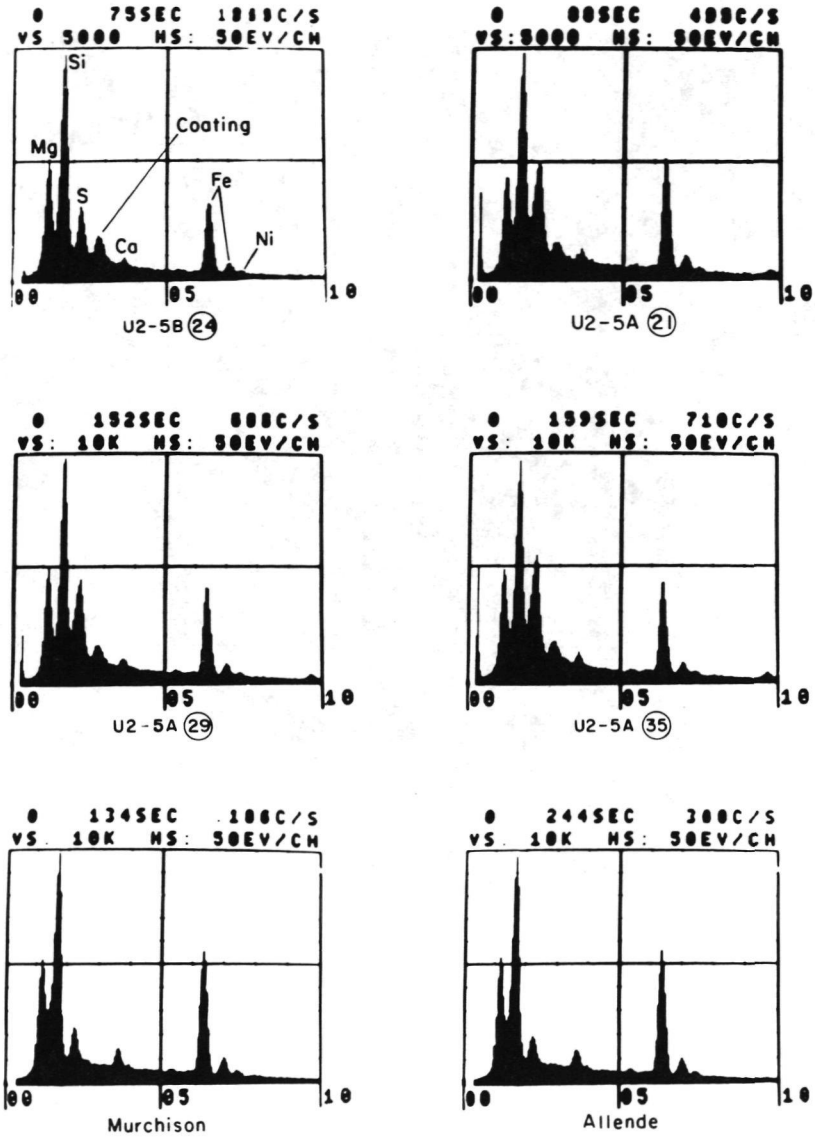

Figure 3 Energy dispersive X-ray spectra of 4 chondritic micrometeorites collected at 20 km altitude, compared with representative spectra of the Murchison and Allende carbonaceous chondrites. Each spectrum is a plot of the number of detected X-ray photons vs. photon energy (Kev). The line marked "coating" is Pd. The gold line is coincident with Sulfur and makes the U2-5A sulfur peaks appear ~25% higher than they should be. The small peak near 10 Kev in the U2-A particles is a gold L line.

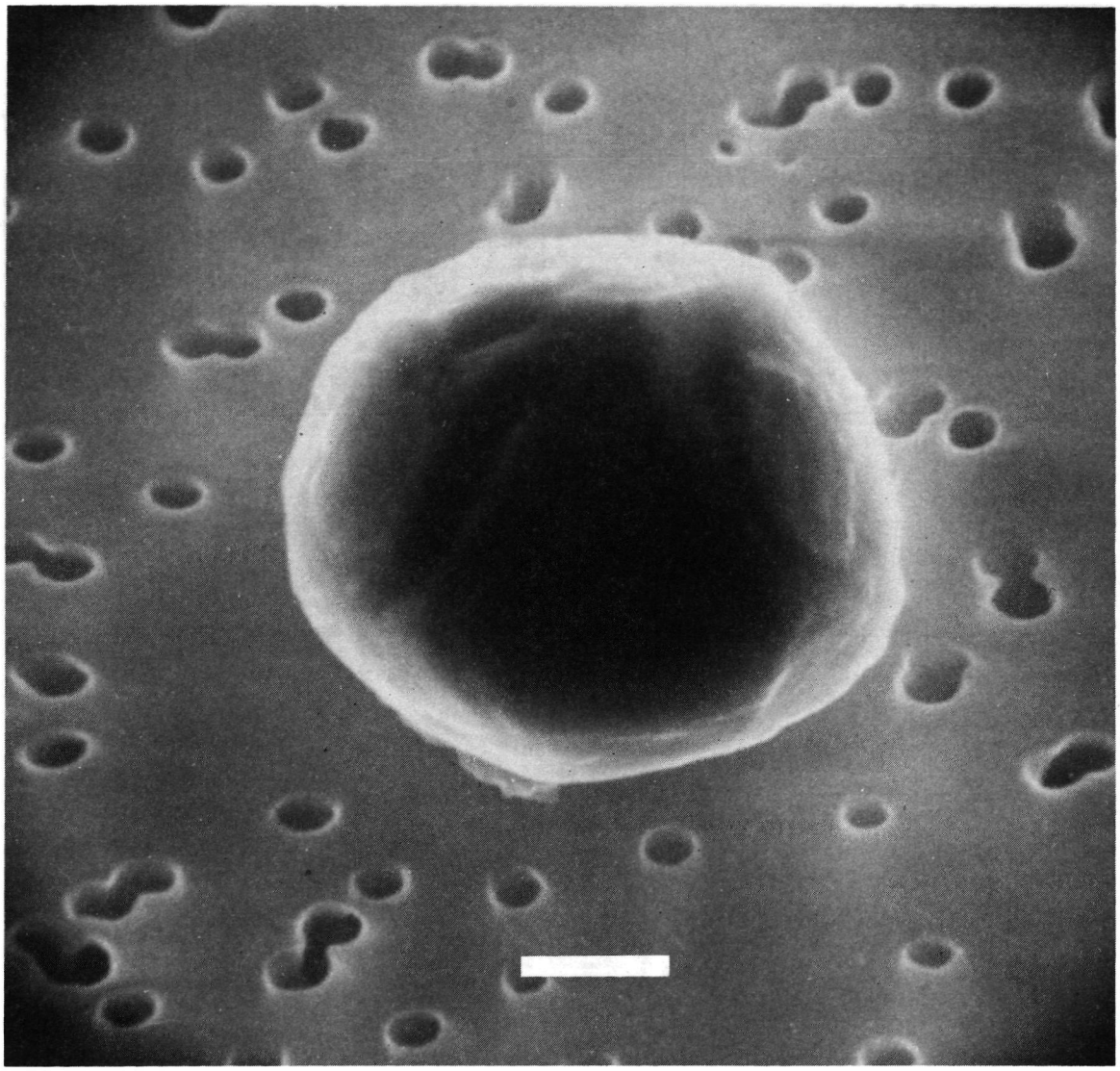

Figure 4 SEM picture of U2-5B (3), a iron-sulfur-nickel micrometeorite collected with a U2 aircraft at 20 Km. This particle is a single crystal which makes it unique among the collected FSN particles. Most of the FSN particles are spheres. The iron:nickel ratio is 11:1 weight percent. Scale bar = 1μm.

TABLE 1

Microprobe analysis of the 12μ diameter spherical micrometeorite VM II A-4 -- a probable meteor ablation debris.

	VMII A-4	C3 Chondrite Average (Mason Handbook)
SiO_2	33.05	33.20
TiO_2	.35	.14
Al_2O_3	4.47	2.59
Cr_2O_3	.35	.51
FeO	10.75	32.36
Fe_2O_3*	13.80	---
NiO	2.30	1.78
MgO	28.58	24.00
CaO	3.60	2.38
Na_2O	< .027	.47
S	< .15	2.19
total	97.25**	

*The partition of Fe between FeO and Fe_2O is based on the optical microscope estimate that ∿20% of the polished section is magnetite.

**The low total may be due to the presence of carbon. Carbon is present in the fusion crusts of some carbonaceous chondrites.

with chondritic abundances for Fe, Mg, Si, S, Ca and Ni is a highly diagnostic identification criterion. We know of no single natural or man-made material from the earth or from the moon with similar abundances. Over 50% of the FSN particles are spheres and it is possible that they are meteor ablation debris. Only 10% of the chondritic particles are spheres. The non-spherical chondritic particles have structural textures and sulfur abundances that suggest that they are particles which have not been thermally altered by passage through the atmosphere. Except for the spheres, all of the chondritic particles are aggregates of very small grains. Typical grain sizes are in the range 1000 A - 10,000 A (Figures 5-8). There appears to be a filling material between many of the grains and the major visible difference from particle to particle appears to be in the abundance of the filling material. The particles with very little filling between grains have porosities which would give the particles bulk densities on the order of 1 g cm^{-3}. Typical particles have sufficient filling material to give bulk densities on the order of 2 g cm^{-3} or higher.

IV. DISCUSSION

As a stereotype interplanetary dust particle, for optical scattering calculations, we suggest a model meteoroid which is roughly spherical and has a density of 2 g cm^{-3}. The model particle has chondritic elemental abundances. Like C 1 chondrites the model also contains a high content ($\gtrsim$ 4%) of finely dispersed carbon which has a dominating effect on optical properties.

Both particle collections and microcrater analyses indicate that micron-sized interplanetary particles have densities greater than 1 g cm^{-3}.

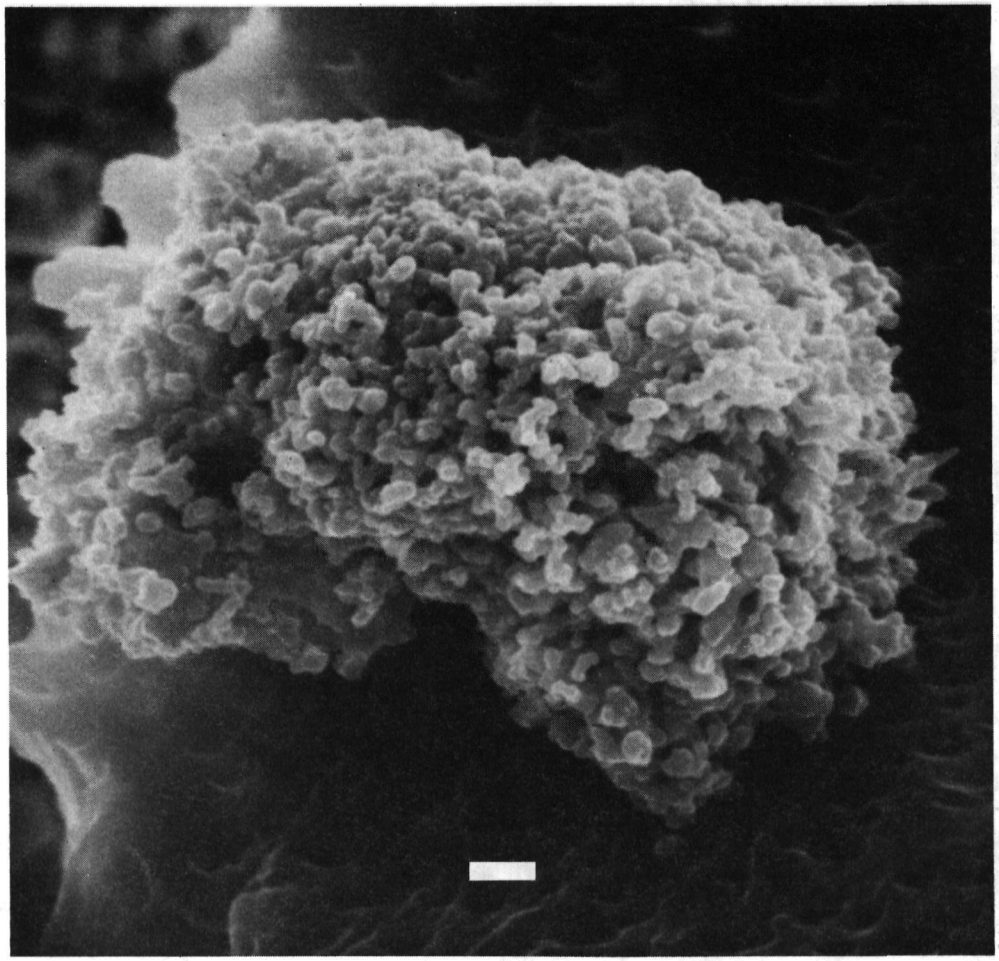

Figure 5 Chondritic micrometeorite U2-5A (21). This is the highest porosity micrometeorite collected by the balloon or U2 collection program. Scale bar = 1μm.

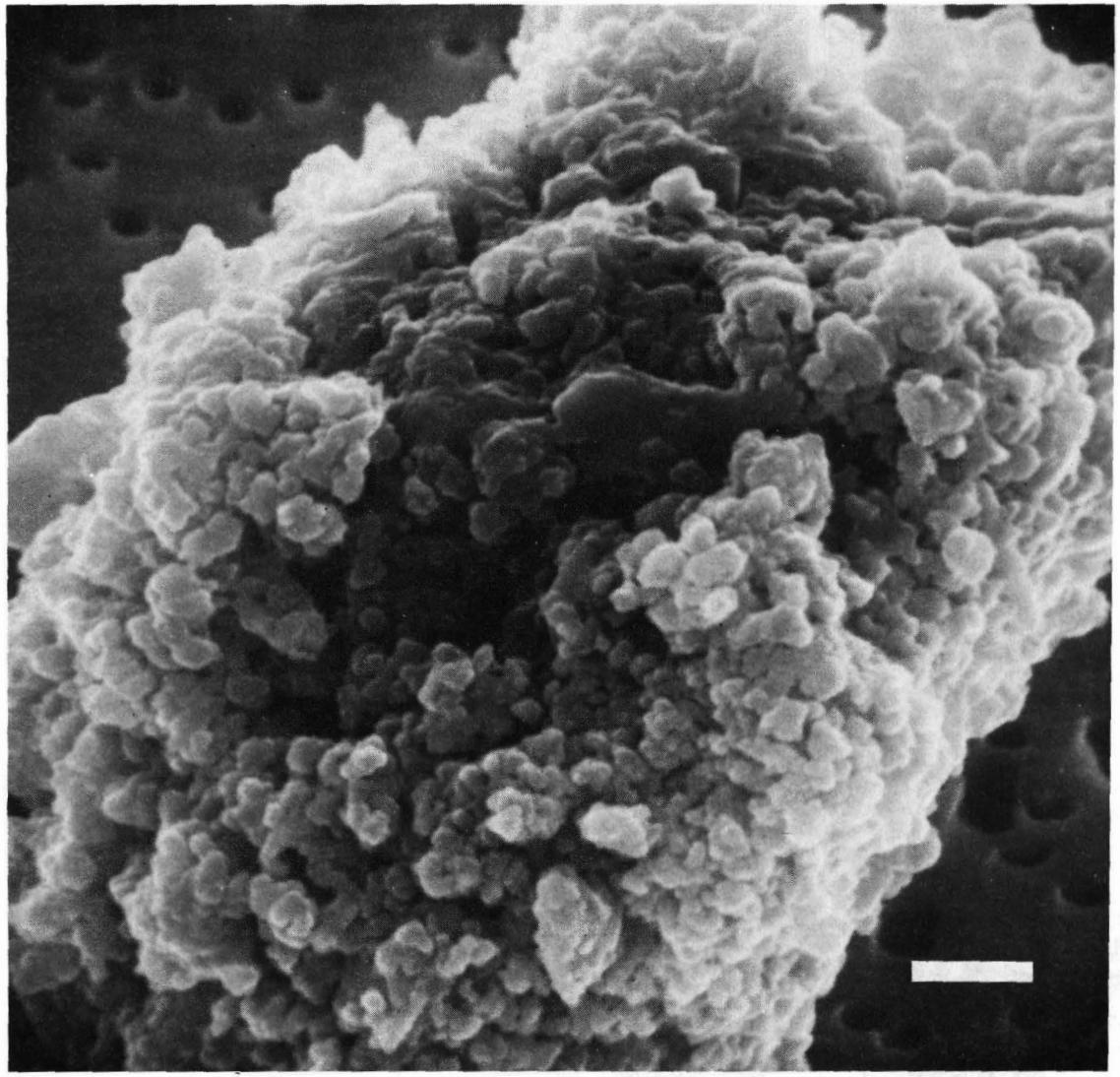

Figure 6 Chondritic micrometeorite U2-5A (35). Scale bar = 1μm.

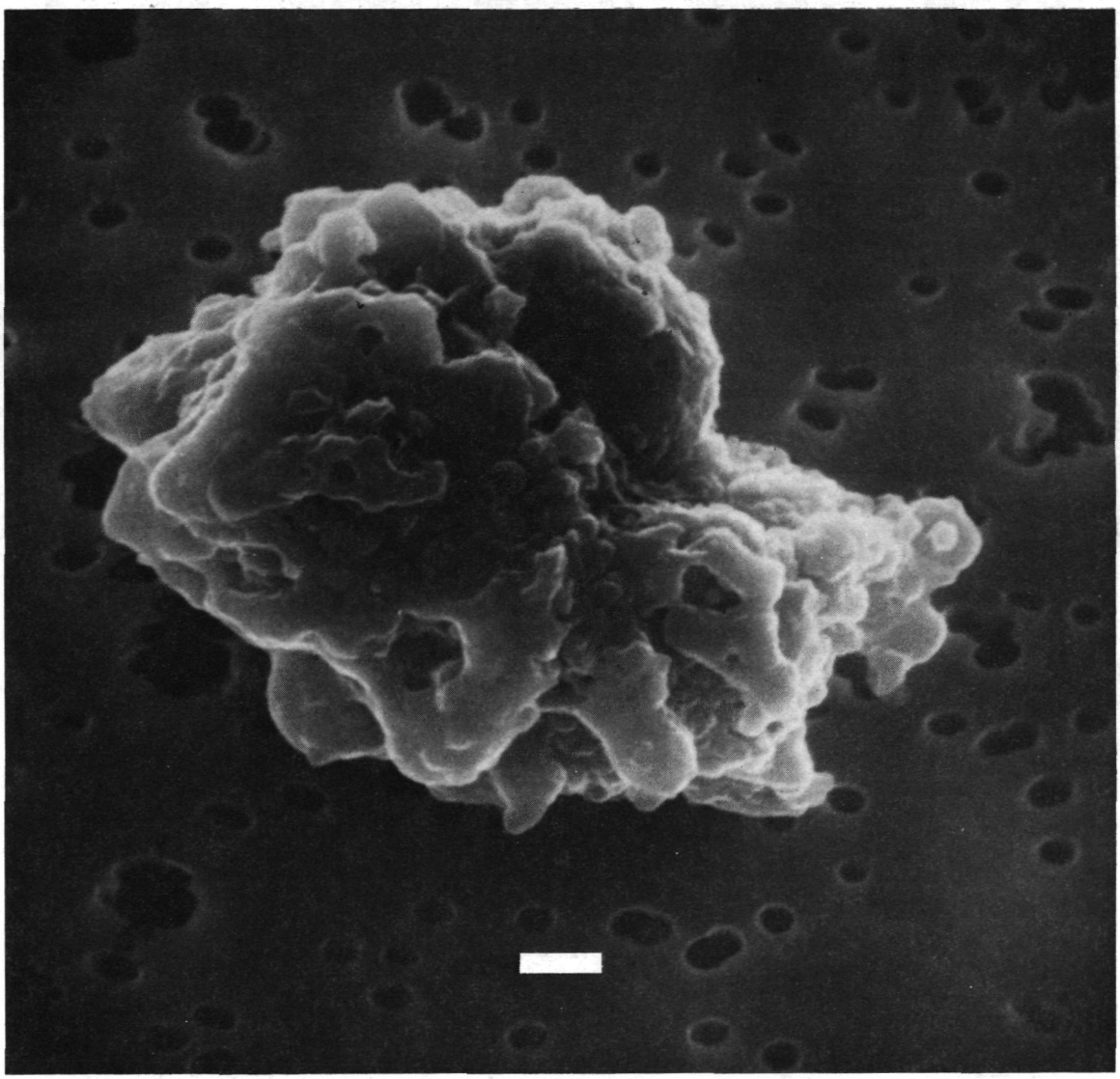

Figure 7 Chondritic micrometeorite U2-5A (29). This particle has an aggregate structure but contains a large amount of inter-grain filling material resulting in a rather low porosity. Scal bar = 1μm.

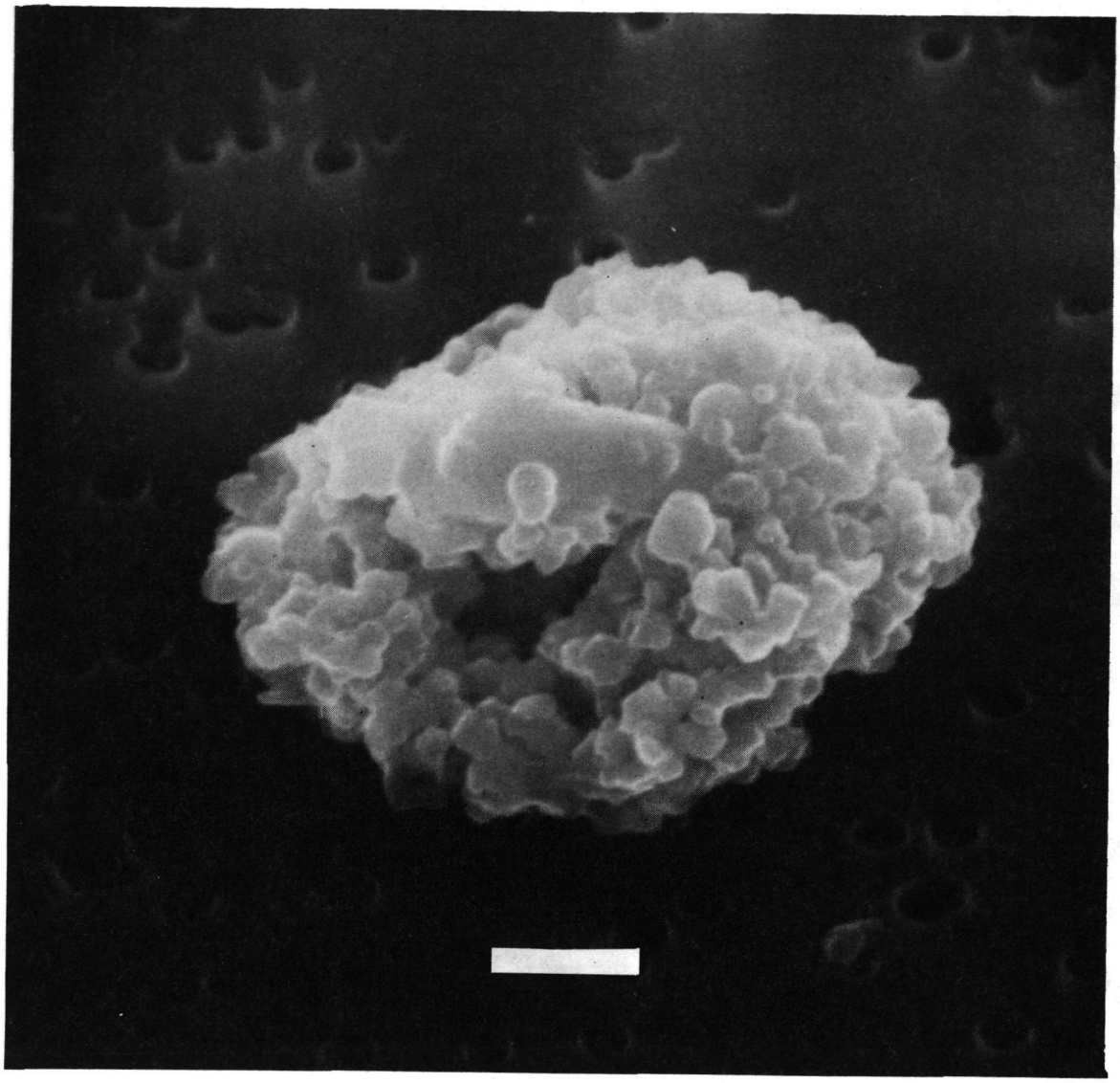

Figure 8 Chondritic micrometeorite U2-5B (24). This particle contains a moderate amount of filling material and the structure is rather typical of the chondritic micrometeorites. Scale bar = 1μm.

Consideration of both data sources suggests that typical particles have densities between 1 g cm^{-3} and 4 g cm^{-3}. Although the collection data might be affected by selection effects, the crater data is not. The laboratory calibrations very closely simulate the actual impact conditions on lunar rocks and it is believed that the density lower limit derived from crater data is quite reliable. These results indicate that the widely-accepted hypothesis that interplanetary grains have extremely low densities is incorrect. If a cometary origin of micrometeoroids as well as the reported mean densities of 0.3 g cm^{-3} for the somewhat larger cometary meteors are correct, then our results indicate a structure of cometary matter such that high porosity does not exist in particles smaller than about 50μm.

Our observations indicate that the majority of interplanetary dust grains are rather equidimensional aggregates of sub-micron grains with bulk elemental abundances very similar to primitive meteorites. Analysis of meteor spectra (Millman, 1972) (Harvey, 1973), measurement of ion enrichment in the mesosphere during some meteor showers (Goldberg and Aikin, 1973) and the characterization of the micrometeoritic component in lunar soils (Anders et al., 1973) also indicate that the majority of small interplanetary particles have abundances similar to primitive chondritic meteorites. In addition, our results indicate that a smaller but significant fraction of interplanetary particles are iron sulfides which contain a few percent nickel. It is significant that both FSN-like particles and fine grained aggregate particles with chondritic compositions could be produced by crushing primitive meteorites to a 10μm particle size. Iron sulfides with a few percent Ni are common in C2 and C3 meteorites and the matrix of all carbonaceous chondrites is similar to the chondritic particles. Analyses of 5μm square areas on polished surfaces of Orgueil

(C1), Murchison (CM2) and Allende (CV3) show abundance dispersions very similar to those observed in the 50 chondritic particles collected from the stratosphere.

The similarity between interplanetary dust and meteorites is probably not a consequence of a common origin but rather a result of their both being accretional aggregates of small particles which condensed from a gas of cosmic composition. It is generally accepted that primitive meteorites are aggregates of particles which formed in the solar nebula within 5 AU of the sun. If the particles analyzed in this study are cometary then it is possible that they formed at much greater distances from the sun, either by accretion of condensates from the solar nebula or by accretion of pre-existing interstellar grains. It may be feasable to investigate these possibilities by detailed investigations of chondritic micrometeorites. Primitive meteorites contain a variety of inclusions (chondrules, calcium aluminum inclusions, olivine, glass, etc.) some of which may have been produced only in the inner parts of the solar nebulae and would not be expected to be incorporated in bodies formed further out. Searches for meteoritic-like inclusions plus comparitive mineralogical (via electron and X-ray diffraction techniques) and morphological studies of micrometeorites may be capable of determining whether or not micrometeorite and meteorite parent bodies formed in the same region of the solar system.

Preliminary investigation of grain shapes in interplanetary dust indicates that they are not similar to common grain shapes in carbonaceous chondrites. The constituent grains in micrometeorites are fairly equidimensional while grains in most carbonaceous chondrites are typically platelet shaped. The only mineralogical information obtained to date, for an unablated particle, is an X-ray diffraction pattern obtained for

the largest particle collected. The pattern shows the definite existence of magnetite. Magnetite is a low temperature mineral, in meteorites, and is only found in abundance in type 1 carbonaceous chondrites.

Existing microanalysis techniques are very powerful. It is anticipated that further SEM and transmission electron microscope studies on micrometeorites will result in a rather detailed knowledge of their mineralogy and structure. This information is potentially capable of providing rather fundamental insights into the processes that formed cometary bodies.

REFERENCES

Anders, E., Ganapathy, R., Krähenbühl, U., and Morgan, J.W. 1973, Meteoritic Material on the Moon, The Moon, 8, 3.

Blanchard, M.B., and Cunningham, G.G. 1974, Meteor Ablation Studies: Olivine, J. Geophys. Res., 79, 3973.

Brownlee, D.E., Hodge, P.W. and Bucher, W. 1973, The Physical Nature of Interplanetary Dust as Inferred by Particles Collected at 35 km, in Evolutionary and Physical Properties of Meteoroids, IAU Colloquium 13., ed., C.L. Hemenway, P.M. Millman and A.F. Cook, (NASA SP-319), p. 291.

Brownlee, D.E., Horz, F., Vedder, J.F., Gault, D.E. and Hartung, J.B. 1973, Some physical properties of micrometeoroids, Proc. Fourth Lunar Sci. Conf., Geochim. Cosmochim. Acta, Suppl. 4, Vol. 3, 3197.

Brownlee, D.E., Tomandl, D.A., Hodge, P.W., and Horz, F. 1975, Elemental abundances in interplanetary dust, Nature, (in press).

Fechtig, H., Gentner, W., Hartung, J.B., Nagel, K., Neukum, G., Schneider, E., and Storzer, D. 1975, Microcraters on Lunar Samples, Proc. of the Soviet-American Conference on Cosmochemistry of the Moon and the Planets, in press.

Goldberg, R.A. and Aikin, A.C. 1973, Comet Encke: meteor metallic ion identification by mass spectrometer, Science, 180, 294.

Hartung, J.B., Horz, F., and Gault, D.E. 1972, Lunar microcraters and interplanetary dust, Proc. Third Lunar Sci. Conf., Geochim. Cosmochim. Acta, Suppl. 3, Vol. 3, (MIT Press), 2735.

Harvey, G.A. 1973, Elemental abundance for meteors by spectroscopy, J. Geophys. Res., 78, 3913.

Horz, F., Brownlee, D.E., Fechtig, H., Hartung, J.B., Morrison, D.A., Neukum, G., Schneider, E., and Vedder, J.F. 1975, Lunar Microcraters, implications for the micrometeoroid complex, Planet. Space Sci., in press.

Jacchia, L.G., Verninani, F., and Briggs, R.E. 1967, An analysis of the atmospheric trajectories of 413 precisely reduced photographic meteors, Smithsonian Contr. to Astrophysics, 10.

Mason, B. 1971, Handbook of elemental Abundances in Meteorites, (Gordon and Breach, New York).

Millman, P.M. 1972, Cometary meteoroids, in Nobel Symposium 21: From Plasma to planet. ed. A. Elvius, (Wiley) p. 157.

Smith, D., Adams, N.G., and Khan, H.A. 1974, Flux and composition of micrometeoroids in the diameter range 1-10μm. Nature, 252, 101.

Vedder, J.F. and Mandeville, J.-C. 1974, Microcraters formed in glass by projectiles of various densities, J. Geophys. Res., 79, 3247.

Whipple, F.L. 1951, The theory of micrometeorites, Part II: In a hetrothermal atmosphere, Proc. Nat. Acad. Sci., 37, 19.

Whipple, F.L. 1967, On maintaining the meteoritic complex, in The Zodiacal Light and Interplanetary Medium, ed. J.L. Weinberg, NASA SP-150.

DISCUSSION

F. L. Whipple: My only comment is that the classical diameter of interstellar grains is 2000Å!

S. Auer: How could you collect a highly porous and fragile looking particle without destroying it?

D. Brownlee: It was collected from an aircraft at a small relative velocity of 600 ft/s.

S. Auer: What is your argument that this particle has an extraterrestrial origin?

D. Brownlee: The only argument is the similarity between its composition and the composition of carbonaceous chondrites. Terrestrial particles should have a different composition.

ORBITAL ERROR ANALYSIS FOR COMET ENCKE, 1980

D. K. Yeomans

Several recent studies have been undertaken to optimize mission strategies and to select appropriate instrumentation for in situ studies of short period comets (Farquhar et al, 1974; Bender, 1974; Newburn, 1973; Meissinger, 1972; Roberts, 1971). Although some studies have contrasted the physical characteristics of several proposed target comets, few have comprehensively studied the orbital history and ephemeris uncertainties of target comets. In general, the navigational accuracy of cometary flyby probes is almost entirely dependent upon the target comet's position uncertainty at the time of intercept. Although cometary error analyses are necessary for realistic mission planning, such analyses cannot be conducted in the standard fashion. Comets are affected by nongravitational forces (Marsden et al, 1973), they occasionally exhibit slight discontinuities in their orbital motions, and at least one comet (Biela) has completely disintegrated (Marsden and Sekanina, 1971). Each comet is an individual. Comets have steadfastly resisted recent attempts at classification. Hence, it seems clear that, for each comet of interest in mission planning, a separate in-depth error analysis study must be undertaken to realisticly determine the target comet's ephemeris uncertainty at the time of intercept. Such studies should consider a number of criteria in order to assure accurate ephemerides for prospective cometary targets. Using the 1980 apparition of comet Encke as an example, these criteria are outlined below.

CRITERIA FOR ACCURATE COMETARY EPHEMERIDES

1. The target comet should have good observability during the apparition of the proposed intercept.

   Ground based observations made prior to an intercept of a comet are critically important for reducing cometary ephemeris uncertainties. How-

ever, for many cometary mission opportunities, recovery of the target comet prior to spacecraft launch is not necessary. Provided the target comet is recovered early enough, spacecraft thrusters are fully capable of removing a priori cometary ephemeris errors with midcourse maneuvers. Fortunately, for target comets that are recovered approximately three months prior to intercept, ephemeris corrections up to 0.3 days can be removed with midcourse maneuvers (Farquhar, 1975). For well observed short period comets, modern ephemeris predictions have never required a correction of this size. Naturally, the recovery of a comet, particularly an erratic comet, prior to launch would minimize spacecraft energy expenditures.

At a particular time, a comet's uncertainty in position can be represented by an error ellipsoid whose semi-major axes (σ_r, σ_n, σ_T) are directed in a radial Sun-comet direction ($\hat{r}$), normal to the orbit plane ($\hat{n} = \hat{r} \times \hat{v}$) and transverse to the orbit plane ($\hat{T} = \hat{n} \times \hat{r}$). In the absence of observations, the error ellipsoid will evolve dynamically. In general, the a priori error ellipsoid component σ_r will reach a maximum value for a true anomaly (ν) of $\pm$ 90 degrees, when the radial velocity is a maximum. The transverse velocity is a maximum at perihelion ($\nu = 0^o$) so that the a priori transverse component (σ_T) is a maximum there. Hence, an ideal observing schedule would include observations made at a phase angle of 90^o when the comet's $\nu = \pm 90^o$, as well as observations made at phase angles of 0^o, 180^o when the comet is at perihelion ($\nu = 0^o$). In a sense, this ideal observing schedule would allow a direct "view" of the largest radial and transverse error components. In addition to observations made at optimum phase angles, the observer-comet distance (range) at the time of the observation is important in reducing a comet's ephemeris uncertainty. For a particular angular position error, the linear position error perpendicular to the line-of-sight is directly proportional to the range. Also, as the range decreases, the relative parallactic displace-

ment increases; in general, the accuracy of a cometary orbit will be enhanced if the relative Earth-comet motion is large.

Figure 1 clearly shows the excellent observability of comet Encke during its 1980 apparition. Comet Encke will be easily visible to Earth based observers for approximately four months prior to perihelion. From July through October (positions 1 - 4 on figure 1), the comet's range decreases from 2.4 to 0.3 A.U. The minimum range is 0.28 A.U. on October 29, 1980 when the relative Earth-comet motion is large. The late October observations are made at a phase angle near 90^{o}. Since the true anomaly at this time is approximately -90^{o}, the radial component of the comet's error ellipsoid is aligned nearly perpendicular to the line-of-sight. Hence the late October and early November observations are critical for minimizing the radial position error of comet Encke in 1980.

2. The target comet should have a good observational history.

Accurate orbit determination is dependent upon the number, quality and distribution of observations. The most accurate orbits are computed using consistent observations spread uniformly over a large range of a comet's true anomaly. An accurate determination of a comet's mean motion and nongravitational parameters requires a linkage of at least three apparitions. The resultant "observed minus computed" residuals in the right ascension and declination provide an indication of an orbit's accuracy. In general, the time intervals used in orbit determination are long enough to accurately determine the nongravitational parameters and short enough so that the unmodeled time dependence in the nongravitational accelerations cannot degrade the residuals. An orbit is considered successful only if there are no systematic trends in the residuals. Although the mean of the absolute values of the residuals is usually somewhat higher for the right ascension, they are close enough so that the measurement errors in right ascension and

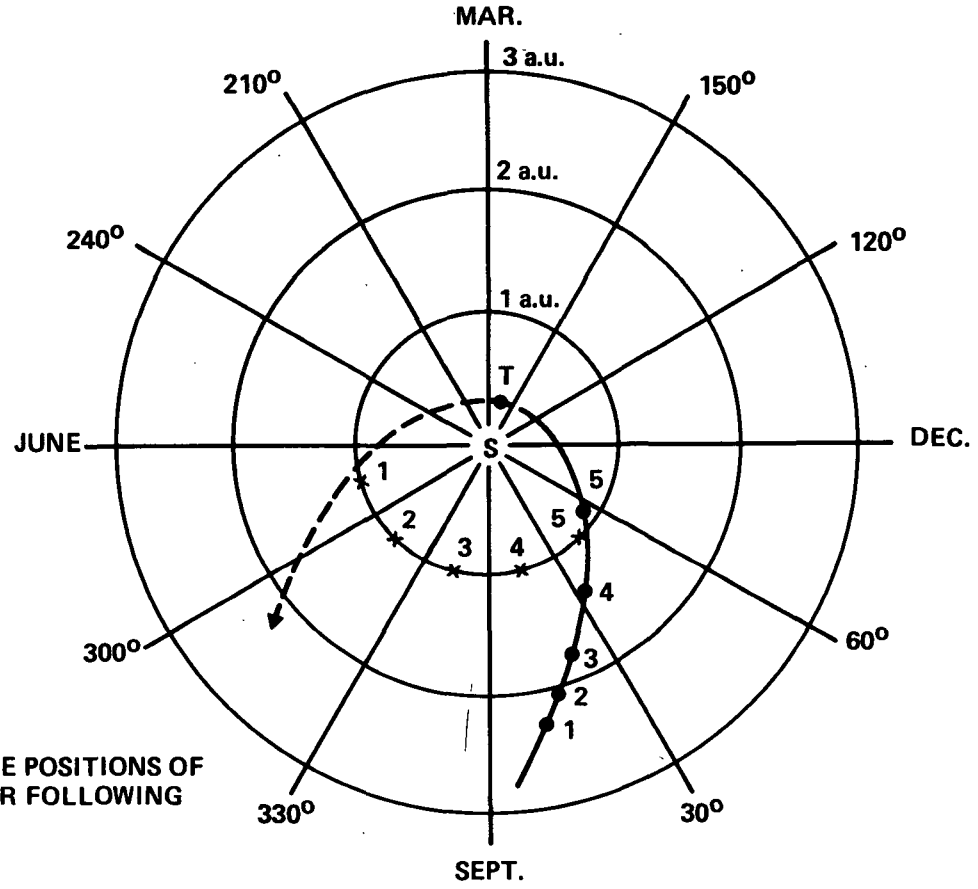

NUMBERS 1–5 INDICATE POSITIONS OF EARTH AND COMET FOR FOLLOWING DATES

1. 1980 JULY 9
2. 1980 AUG. 8
3. 1980 SEPT. 7
4. 1980 OCT. 7
5. 1980 NOV. 6

T: PERIHELION OF COMET (1980 DEC. 6)
X: POSITIONS OF EARTH
●: POSITIONS OF COMET

Figure 1. Earth-Comet Encke Relative Geometry in 1980

declination can be considered equal. These residuals are primarily due to position errors in the comparison stars, deviations of the comet's center of light from its center of mass, and modeling errors in the nongravitational accelerations. For twentieth century observations of periodic comets, the means of the absolute values of the residuals range from one to four arc seconds.

Among short period comets, the observational history of comet Encke is unexcelled. Since 1819, comet Encke has only been missed at one apparition (1944). It is the only short period comet passing within the Earth's orbit that has been seen at aphelion (Roemer, 1972). Marsden and Sekanina (1974) have analyzed the orbital motion of comet Encke from its discovery in 1786 until 1971. Differential corrections were generally made over 13 year intervals and, for recent apparitions, the means of the absolute values of the residuals were in the range 1.5-3 arc seconds.

STATISTICAL ERROR ANALYSIS FOR COMET ENCKE (1980)

A statistical covariance error analysis was undertaken to determine the evolution of comet Encke's error ellipsoid during the 1980 apparition. The computer program took into account planetary perturbations and considered the errors inherent in the values for the nongravitational parameters and initial conditions. The partial derivatives utilized in the conditional equations matrices and the state transition matrices were computed numerically.

Marsden and Sekanina (1974) have shown that five apparitions of comet Encke can be linked before the secular decrease in the nongravitational parameters begins to degrade the residuals. For the present analysis, the 5 returns to perihelion (1967-1980) are represented by forty actual observations from August 2, 1967 through October 24, 1973 and by 28 additional, postulated observations from October 24, 1973 through November 16, 1980. One observation was processed at each of the 1978 and 1979 opposition dates and the 1980 recovery of the comet was

assumed to occur on July 9. The postulated observation schedule was determined after considering the relative Sun-Earth-comet positions, the available hours of dark observing time as well as the apparent nuclear and total magnitudes for various dates.

The error analysis was initialized in 1967 and the initial a priori 8 x 8 covariance matrix was essentially infinite. Each set of observations was batch processed and the updated covariance was propagated forward in time via the state transition matrix to the date of each observation. The time history of the comet's error ellipsoid is presented in Table 1. The first column represents the dates in 1980

Table 1
Error Ellipse Components for Comet Encke (1980)

Date 1980-81	A priori errors* (in km)			1980 observations Processed** (in km)						
	σ_r	σ_n	σ_T	σ_r	σ_n	σ_T	Δ (a.u.)	r	θ (deg.)	Comments
July 9	4168	2130	3239	3352	1926	2471	2.43	2.33	72	Comet recovered
19	4338	2084	3275	2917	1737	2012	2.21	2.23	78	
29	4521	2036	3327	2572	1567	1683	1.98	2.13	84	
Aug. 8	4718	1985	3399	2271	1406	1426	1.76	2.03	90	
18	4933	1936	3494	1992	1249	1213	1.53	1.92	96	
28	5169	1894	3617	1644	1146	1026	1.31	1.81	101	
Sept. 7	5429	1876	3769	1469	945	836	1.10	1.69	107	
17	5717	1921	3952	1217	799	710	0.89	1.56	111	
27	6040	2117	4146	968	658	564	0.69	1.43	114	
Oct. 7	6403	2604	4301	724	524	427	0.51	1.28	112	
17	6811	3480	4347	504	400	313	0.36	1.13	103	
27	7258	4612	4407	387	308	264	0.28	0.97	77	
Nov. 6	7699	5595	5229	391	269	273	0.32	0.80	45	true anomaly = -90° on Nov. 15
16	7893	5683	8023	416	249	359	0.47	0.62	29	last comet observation
26	6628	4481	12910	401	234	579	0.70	0.44	23	
Dec. 6	399	3477	16833	171	243	874	1.00	0.34	20	perihelion on Dec. 6.6
16	6663	3445	13010	315	289	827	1.30	0.42	15	
26	7880	3452	8789	418	359	688	1.52	0.60	11	true anomaly = +90° on Dec. 27
Jan. 5	7627	2946	6527	433	412	632	1.73	0.78	10	
15	7143	2150	5388	426	445	642	1.90	0.95	11	
25	6663	1432	4706	414	481	677	2.05	1.11	12	

*A priori, one-sigma errors (km) in the radial, normal and transverse directions. Last observation processed was mid-September, 1979.

**Evolution of one-sigma errors (km) if one ground based observation is processed at 10 day intervals from July 9 to November 16. Measurement noise = 3 arc seconds.

on which one simulated ground based observation was made. The next six columns represent the 1-σ position errors (km) for the radial Sun-comet direction ($\hat{r}$), the direction normal to the comet's orbital plane ($\hat{n}$), and the transverse direction defined by the cross product of the first two unit vectors ($\hat{T} = \hat{n} \times \hat{r}$). The columns headed by Δ, r and θ represent the Earth-comet distance in A. U., the Sun-comet distance in A. U. and the Sun-Earth-comet angle in degrees. The a priori errors represent the forward propagation of the covariance matrix obtained by processing all observations from 1967-1979. Columns 5, 6, and 7 reflect the effect of each 1980 observation on the comet's error ellipsoid. The final ground based observation on November 16 reduces the σ_r, σ_n, and σ_T components to 416, 249, and 359 km. In the absence of further observations, the error components evolve dynamically; their magnitudes at any given time are due primarily to the comet's position in its orbit. The exclusion of the first few recovery observations in 1980 or the exclusion of the 1978 and 1979 opposition observations has a negligible effect upon the position errors in 1980. However, by taking 1980 observation at 5-day intervals between July 9 and November 16, the errors on December 6th are reduced to 155, 186, and 660 km (σ_r, σ_n, σ_T). These results underscore the fact that, while observation made during past apparitions define the mean motion and the nongravitational parameters, it is the 1980 observations that contribute most strongly to the reduction of comet Encke's ephemeris uncertainty. The importance of the 1980 observations is due primarily to the proximity of comet Encke and the Earth during October and November, 1980.

The present error analysis of comet Encke assumes a 1-σ observational error of 3 arc seconds for both the right ascension and declination. The 3 arc second value is consistent with the mean residuals obtained from various orbit determinations for past apparitions of comet Encke. Due to comet Encke's relatively high nuclear activity, the appropriate error value is somewhat higher

than for most other short period comets. The assumed error for each observation is the same value, and the observations themselves are assumed to be uncorrelated. This being the case, the only nonzero elements ($1/\sigma^2$) of the weighting matrix (W) are equal in value and aligned on the principal diagonal. If F denotes the conditional equation matrix, the normal matrix F^TWF can be reduced to $1/\sigma^2$ (F^TF) and the simplified covariance matrix becomes $\sigma^2(F^TF)^{-1}$. Thus the covariance matrix is linear with respect to observational errors. For example, although the current analysis has been undertaken using an observational error of $\sigma = 3$ arc seconds, one only has to multiply the error component entries in Table 1 by 2/3 to obtain the results for $\sigma = 2$ arc seconds.

CHECKS UPON STATISTICAL ERROR ANALYSIS FOR COMET ENCKE (1980)

A less rigorous statistical error analysis of the 1980 apparition of comet Encke has been carried out by Bynes and Boain (1974). For comparable cases, their results agree with the present analysis. However, a statistical error analysis is only as good as its underlying assumptions. For the most part, the statistical error analysis outlined in the preceeding section was based upon simulated or hypothesized observations. In an effort to check the statistical results, it seems prudent to analyze results obtained using actual observations of comet Encke.

The observations of comet Encke from 1937-1973 have been used in five separate differential corrections. Within the given mean errors, comparable orbits agree with those determined by Marsden and Sekanina (1974). The entries in Tables 2 and 3 represent an attempt to compare observed and predicted times of perihelion passage (Table 2) and perihelion distances (Table 3). In each table, the first column represents the observed time interval over which a particular differential correction was made. Columns 2-12 give the times of perihelion passage (Table 2) and perihelion distances (Table 3) for each particular interval. For example, in Table 2, line 1, columns 2-6 give the observed times of perihelion

Table-2
Comet Encke
Observed and Predicted Times of Perihelion Passage

Observed Interval	1947 Nov.	1951 March	1954 July	1957 Oct.	1961 Feb.	1964 June	1967 Sept.	1971 Jan.	1974 Apr.	1977 Aug.	1980 Dec.	1984 Mar.
1947-1961	26.32771	16.20639	2.51788	19.84902	5.59452	3.48639	22.04696	9.95477				
1951-1964		16.20842	2.51807	19.84869	5.59494	3.48951	22.05469	9.96845	28.97037			
1954-1967			2.51998	19.84886	5.59500	3.49099	22.05903	9.97727	28.98501	16.97977		
1957-1971				19.84937	5.59419	3.49046	22.06044	9.98221	28.99491	16.99603	6.55148	
1961-1974					5.59477	3.48950	22.05935	9.98232	28.99754	17.00248	6.56310	27.65721

Table 3
Comet Encke
Observed and Predicted Perihelion Distances (in A.U.)

Observed Interval	1947 Nov.	1951 March	1954 July	1957 Oct.	1961 Feb.	1964 June	1967 Sept.	1971 Jan.	1974 Apr.	1977 Aug.	1980 Dec.	1984 March
1947-1961	0.3410319	0.3380089	0.3384086	0.3381187	0.3390047	0.3392511	0.3381997	0.3388910				
1951-1964		0.3380127	0.3384123	0.3381221	0.3390085	0.3392561	0.3382050	0.3388965	0.3381216			
1954-1967			0.3384116	0.3381211	0.3390075	0.3392548	0.3382038	0.3388953	0.3381204	0.3406577		
1957-1971				0.3381260	0.3390125	0.3392600	0.3382089	0.3389005	0.3381256	0.3406628	0.3399416	
1961-1974					0.3390115	0.3392593	0.3382082	0.3388998	0.3381250	0.3406622	0.3399411	0.3410024

passage for 1947, 1951, 1954, 1957, and 1961 while the remaining times of perihelion passage (columns 7-9) are predicted (extrapolated) beyond the range of observations (1947-1961). Carrying this example further, the first predicted time of perihelion passage (1964 June 3.48639) is compared with the entry directly below it (1964 June 3.48951) which is the observed, or actual, time of perihelion passage in 1964. Strictly speaking, any of the 4 times listed below the 1964 June 3.48639 date is an observed time of perihelion passage in 1964; they all are within their respective observation intervals. By comparing each predicted time of perihelion passage with the observed times of perihelion passage, a systematic correction is noted whereby the predicted and observed times of perihelion passage can be brought into agreement. This empirical correction and its standard deviation is

$$\bar{\Delta}T = +0.00423 \pm 0.00094 \text{ days}$$

This empirical correction ($\bar{\Delta}T$) is required to allow for the decrease in $|A_2|$. In other words, by not mathematically modeling this decrease in $|A_2|$, each predicted time of perihelion passage is underestimated by 0.004 days. In a similar fashion, the empirical corrections to the time of perihelion passage required for predicting 2 and 3 apparitions ahead are +0.013 and +0.03 days respectively. These empirical corrections for predicting 1, 2, and 3 apparitions ahead (+0.004, +0.013, +0.03 days) are similar to the values (+0.005, +0.015, +0.03 days) obtained by Marsden and Sekanina (1974). We can take $\bar{\Delta}T$ as an approximate upper limit to the a priori uncertainty in the transverse position error at perihelion. The comet's velocity at perihelion is approximately 6×10^6 km/day so that, at perihelion, $\bar{\Delta}T$ corresponds to a linear, transverse, position error of 25,380 km. However, the majority of this error is due to the unmodeled secular decrease in the transverse nongravitational acceleration. An empirical $\bar{\Delta}T$ correction can be added to the predicted time of perihelion passage to greatly reduce this error so that the standard deviation of $\bar{\Delta}T$ can

be utilized as an approximate lower bound to the a priori, transverse position error at perihelion. At perihelion, this standard deviation (0.00094 days) corresponds to an approximate linear, transverse position error of 5,640 km. In a sense, the upper and lower limits on σ_T at perihelion are "observed" because they are based upon past prediction accuracies of comet Encke's times of perihelion passage (Table 2). From Table 1, the statistical, a priori, transverse, position error at perihelion (1980 December 6) is 16,833 km., a result that is bounded by the aforementioned "observed" upper and lower limits.

Unlike the $\bar{\Delta}T$ corrections, the corrections (Δq) required to bring predicted perihelion distances into agreement with the observed perihelion distances for comet Encke are not predictable. However an estimate of the "observed" upper and lower limit can be determined from the maximum and minimum values of Δq (determined from Table 3). These values are $(8.9\text{-}0.6) \times 10^{-6}$ A.U. or 1335-90 km. These "observed" errors bound the statistical, a priori radial, position error at perihelion (399 km from Table 1).

From the statistical error analysis, the radial and transverse position errors after all 1980 observations have been processed are $\sigma_r = 171$ km and $\sigma_T = 874$ km for 1980 December 6 (see Table 1). These position errors correspond to an error in perihelion distance of 1.1×10^{-6} A.U. and an error in perihelion passage time of 1.5×10^{-4} days. These results are compatible with the standard deviations associated with the differential corrections to the perihelion distance and perihelion passage time. For example, the orbital solution over the 1961-1973 observations yields a standard deviation of 0.94×10^{-6} A.U. and 1.07×10^{-4} days for the differential corrections to the perihelion distance and perihelion passage time.

SUMMARY

Since the ephemeris uncertainties of proposed target comets determine the navigational accuracy of cometary flyby space probes, each proposed target comet should be thoroughly investigated to determine its position error at encounter. Before a particular comet is selected as a flyby target, the following criteria should be considered in determining its ephemeris uncertainty:

1. A target comet should have good observability during the apparition of the proposed intercept. The following conditions aid in minimizing a comet's positional uncertainty at encounter:
   a. Perhaps more than any other condition, observations made at small range values substantially reduce the target comet's error ellipsoid.
   b. Ideal observations would include those made at a phase angle of 90°, when a comet's true anomaly is $\pm 90^{\circ}$ and those made at phase angles of 0° and 180°, when the comet's true anomaly is 0°.
   c. If the comet is observable at the proper time, a large parallactic displacement between the Earth and the target comet prior to encounter would allow a reduction in all three error ellipsoid axes.
2. A target comet should have a good observational history. Several well observed and consecutive apparitions allow an accurate determination of a comet's mean motion and nongravitational parameters.

Using these criteria, along with statistical and empirical error analyses, it has been demonstrated that the 1980 apparition of comet Encke is an excellent opportunity for a cometary flyby space probe. For this particular apparition, a flyby to within 1,000 km. of comet Encke seems possible without the use of sophisticated and expensive on-board navigation instrumentation.

REFERENCES

Byrnes, D. V., and Boain, R. J. (1974). "An Integrated Approach to Comet Mission Navigation Utilizing Astronomical Observations of the Target Body," American Institute of Astronautics and Aeronautics (AIAA) paper No. 74-849.

Bender, D. F. (1974). "Encke Ballistic Flybys in 1980," AIAA paper No. 74-782.

Farquhar, R., McCarthy, D. K., Muhonen, D. P., and Yeomans, D. K. (1974). "Mission Design for a Ballistic Slow Flyby of Comet Encke 1980," NASA TN D-7726.

Farquhar, R. (1975). "Mission Strategy for Cometary Exploration in the 1980's," this colloquium.

Marsden, B. G. and Sekanina, Z. (1971). Astron. J. 76, 1135.

Marsden, B. G. and Sekanina, Z. (1974). Astron. J. 79, 413.

Marsden, B. G., Sekanina, Z., and Yeomans, D. K. (1973). Astron. J. 78, 211.

Meissinger, H. F. (1972). "Study of a Comet Rendezvous Mission," TRW Technical Report 20513-6006-R0-00.

Newburn, R. L. (ed.) (1973). "Science Rationale and Instrument Package for a Slow Flyby of Comet Encke", J. P. L. Document 760-90.

Roberts, D. L. (ed.) (1971). "Proceedings of the Cometary Science Working Group. Yerkes Observatory, June, 1971," IIT Research Institute Document.

Roemer, E. (1972). Mercury Nov./Dec., 1972, p. 19.

OMIT

A SURVEY OF POSSIBLE MISSIONS TO THE PERIODIC COMETS IN THE INTERVAL 1974-2010

D. F. Bender

ABSTRACT

In order to survey the mission possibilities for the short period comets two catalogues are developed. In the first the physical and pertinent orbital characteristics are given for 65 short period comets. Since missions for short period comets are for the most part expected to utilize arrivals near perihelion at a time when the comet is comparatively active, the second catalogue is one containing the predicted perihelia for each of the 65 comets between 1974 and 2010. Included is enough geometry to indicate feasibility of Earth-based observation and sighting within 100 days of perihelion.

Mission selection criteria and trajectory requirements are discussed with the aim of providing the background for catagorizing the possibilities. The comets are then divided essentially on the basis of size and activity into three groups of interest from the data in the first catalogue: primary, secondary and low interest.

The perihelia are separated into two groups of interest: satisfactory and not satisfactory, essentially on the basis of Earth-comet distance.

Thus there are obtained three tables of targets for missions to the short period comets, the first of which, for primary interest comets with satisfactory perihelia, contains 57 cases and is the main shopping list for these missions. There are 43 cases in the second table for the secondary interest comets and 42 in the third for the low interest comets. The final table presented lists chronologically the 51 perihelia for which the comet is predicted to pass within .75 AU of the Earth.

EXPECTED SCIENTIFIC RESULTS ON BALLISTIC SPACECRAFT MISSIONS TO COMET ENCKE DURING THE 1980 APPARITION*

Michael J. Mumma

INTRODUCTION

This paper summarizes three proposed ballistic spacecraft missions to intercept P/Encke during the 1980 apparition, establishes a baseline physical activity model for P/Encke, and assesses the performance of the neutral mass spectrometer and of the imaging experiment on each intercept mission.[1]

Many of the most fundamental questions about comets are unlikely ever to be answered by ground-based or near-earth observations alone, and a direct intercept of a comet by an appropriately instrumented spacecraft is required in order to directly study the comet and its interaction with the solar wind.[2-5]

There is general agreement on the most obvious scientific goals of such a mission but, until now, a quantitative estimate of the possibilities of achieving these goals had not been made. Because of the long lead times required by deep space missions, the next good opportunity for intercepting a short-period comet occurs in 1980, for Encke's comet. Encke's comet has been studied from the ground for more than 150 years and from space recently, and sufficient data now are available to enable making reasonably accurate estimates of the expected scientific value of a direct intercept of this comet.

The problem of assessing the relative scientific merit of various ballistic flyby missions to Comet Encke requires: (1) a determination of the physical activity model for the comet, (2) a careful study of the ephemeris errors[6] and a determination of the consequent miss-distances for various missions, (3) a determination of the flyby velocities, and (4) knowledge of the sensitivities of particular instruments which could be carried on the cometary spacecraft. Each point will be addressed

* These results are condensed from the Final Report of the Encke Mission Engineering Panel, NASA Technical Memorandum TMX-72542. Panel members were: D. Herman (Chairman), M. Mumma (co-chairman), R. Farquhar, L. Friedman, J. Moore, B. Swenson, R. Jackson, and J. Beckman.

in this paper and the results will be used to establish physically realistic estimates of the expected scientific results of the various missions.

The scientific goals have been discussed at length by various earlier groups and can be divided into the following areas: (1) studies of the nucleus, (2) studies of dust and of the neutral and ionized gaseous components, and (3) study of the solar wind interaction with the comet through in-situ measurements of the electromagnetic fields and the particles. Two experiments are found to be particularly sensitive to the mission mode, i.e. the experiment for taking images of the nucleus, and the neutral mass spectrometer experiment for measurement of parent molecules in the inner coma. The quality of the data obtained with these two experiments depends principally on three factors: (1) the heliocentric distance at the time of intercept (determines the comet's activity and the crossing-angle of the spacecraft trajectory with the sun-comet line), (2) the spacecraft velocity relative to the comet (determines the time duration of the encounter), and (3) the targeting accuracy and minimum distance of approach to the nucleus (determines the amount of time spent within the icy halo and in regions of relatively high gas densities).

MISSION PARAMETERS

The orbital characteristics of Comet Encke are shown in Fig. 1.[7] The flyby velocity and crossing-angle are shown for various spacecraft launch dates and heliocentric intercept distances in Fig. 2 and 3. The three missions studied correspond to intercepts at 0.34 AU (Encke's perihelion), at 0.53 AU, and at 0.8 AU. These heliocentric distances were suggested by: (1) the cometary activity model (most active near perihelion), (2) the need for low flyby velocities (lowest near perihelion),

ORBITAL ELEMENTS (EQUINOX 1950.0)

EPOCH	1980 NOV. 17.0
T	1980 DEC. 6.57610
q	0.3399411 AU
e	0.8467578
Ω	334.19764°
ω	185.97967°
i	11.94599°

EPOCH	1984 APR. 10.0
T	1984 MAR. 27.68721
q	0.3410024 AU
e	0.8463305
Ω	334.18436°
ω	185.99329°
i	11.92738°

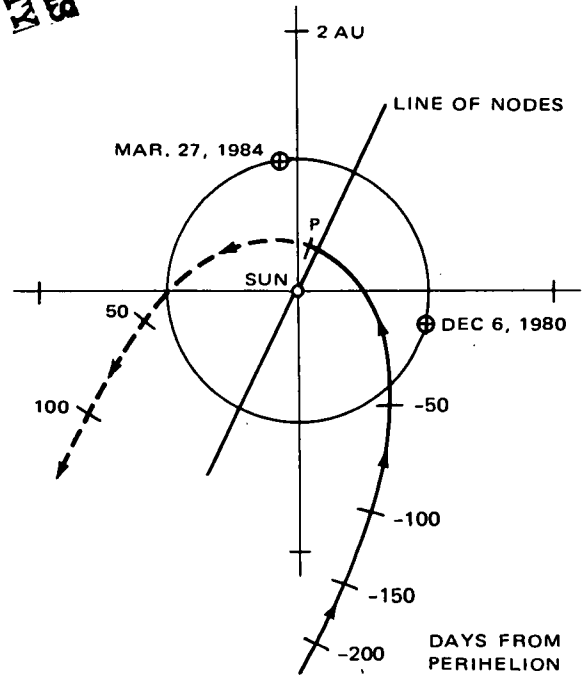

ABOVE ECLIPTIC

BELOW ECLIPTIC

⊕ EARTH AT ENCKE PERIHELIA

FIG. 1 - Orbital Characteristics of P/Encke

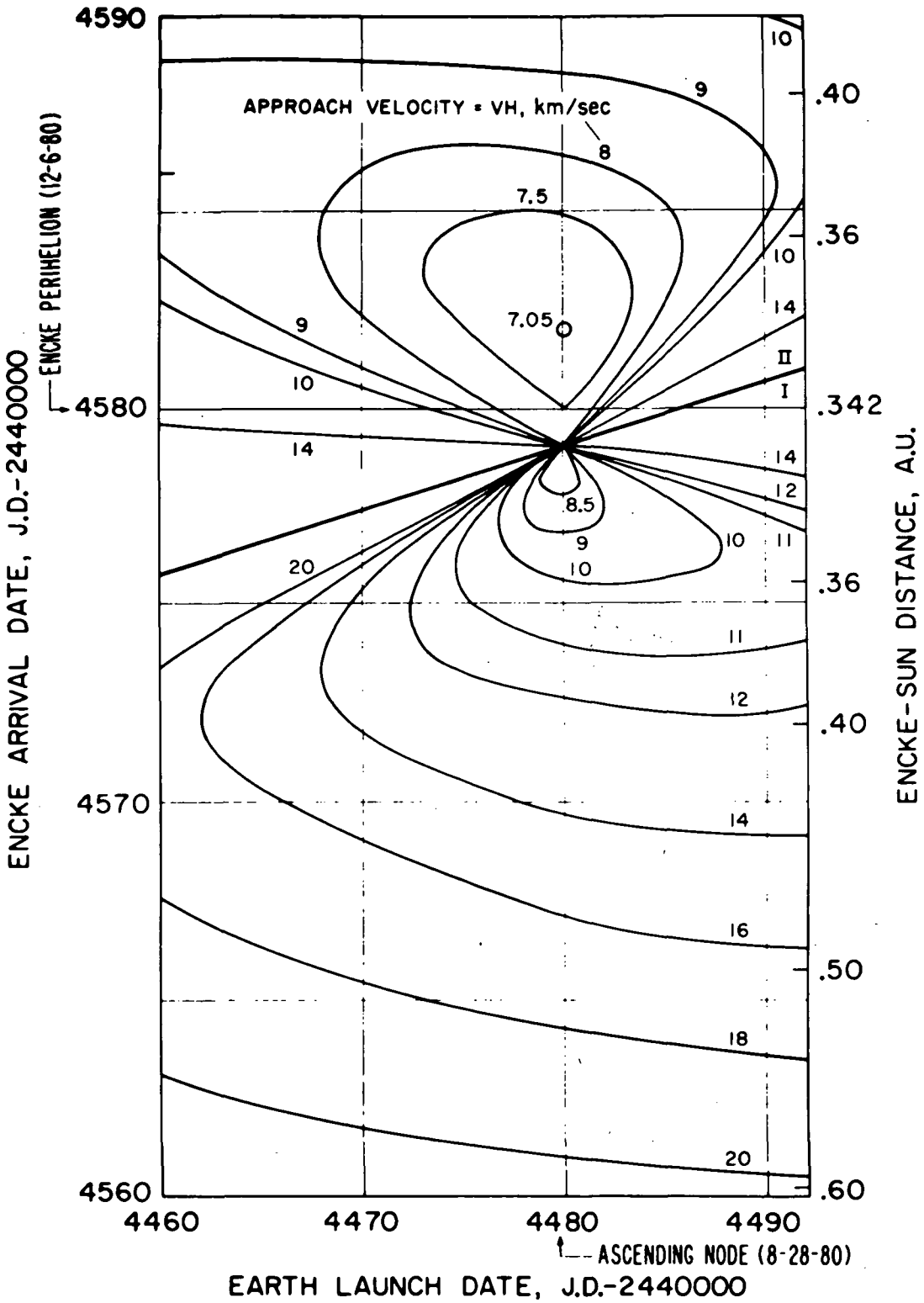

FIG. 2 - Spacecraft Velocity Relative to P/Encke (Flyby Velocity)

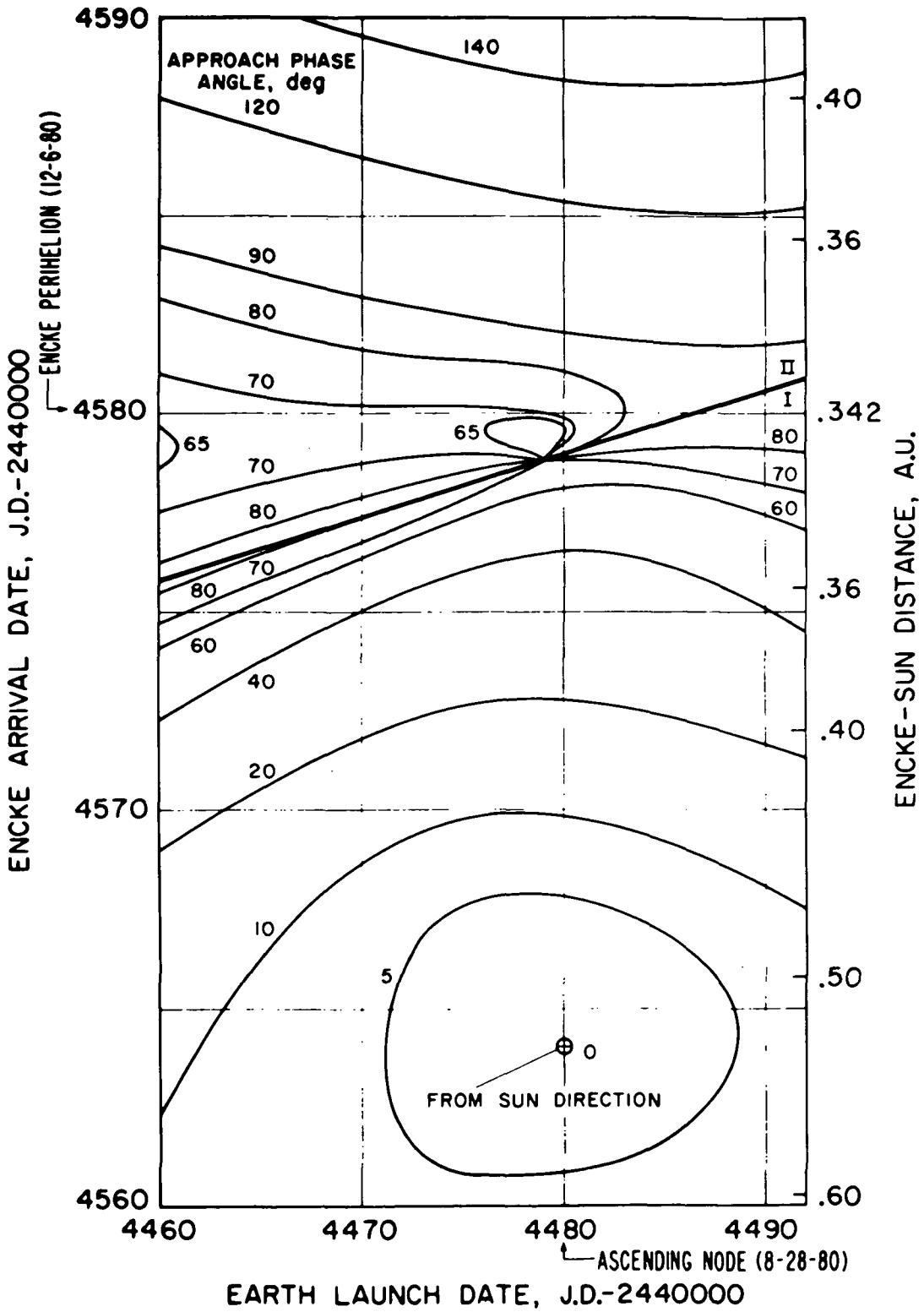

FIG. 3 - Crossing-Angle vs. Launch Date and R(AU) at Intercept

(3) the encounter geometry which determines the regions of the comet traversed by the spacecraft (the crossing-angle is zero at 0.53 AU), and (4) launch vehicle delivery characteristics and budgetary considertions (spacecraft orbits for cometary intercepts smaller than $\sim$ 0.53 AU require the very expensive Titan-Centaur launch vehicle whereas intercepts at R $\gtrsim$ .53 AU can be achieved using the relatively less expensive Atlas-Centaur launch vehicle). The nominal values of specific mission parameters such as heliocentric distance at the time of intercept (R), earth-comet distance at intercept (Δ), relative flyby velocity, etc. are shown in Table I. The achievable miss distances (impact parameters, to the atomic physicists) will be discussed later.

The spacecraft trajectories with respect to the sun-comet line are shown in Fig. 4. The crossing-geometries at closest approach are quite different for the perihelion intercept (P+2), where the crossing -angle is in the range 70^{o} - 90^{o}, and for the P-15 and P-30 intercepts where the crossing-angle is $< 20^{o}$. Also, the trajectory at P+2 has a curious 'fish-hook' shape which allows two bow-shock crossings and two traversals of the coma. However, a separate probe would be required for making measurements in the tail. The tail-probe could be launched on the same rocket with the coma-probe and would follow a trajectory similar to that of the coma probe but displaced tail-ward from the nucleus by as much as several tens of thousands of kilometers. The crossing of the tail at high angles suggests that filaments will be traversed in times short compared with temporal variations in the comet's activity so that spatial-temporal effects could be separated. The geometry at closest approach for such an intercept is shown in Fig. 5. The opportunity for simultaneous correlative measurements during cometary

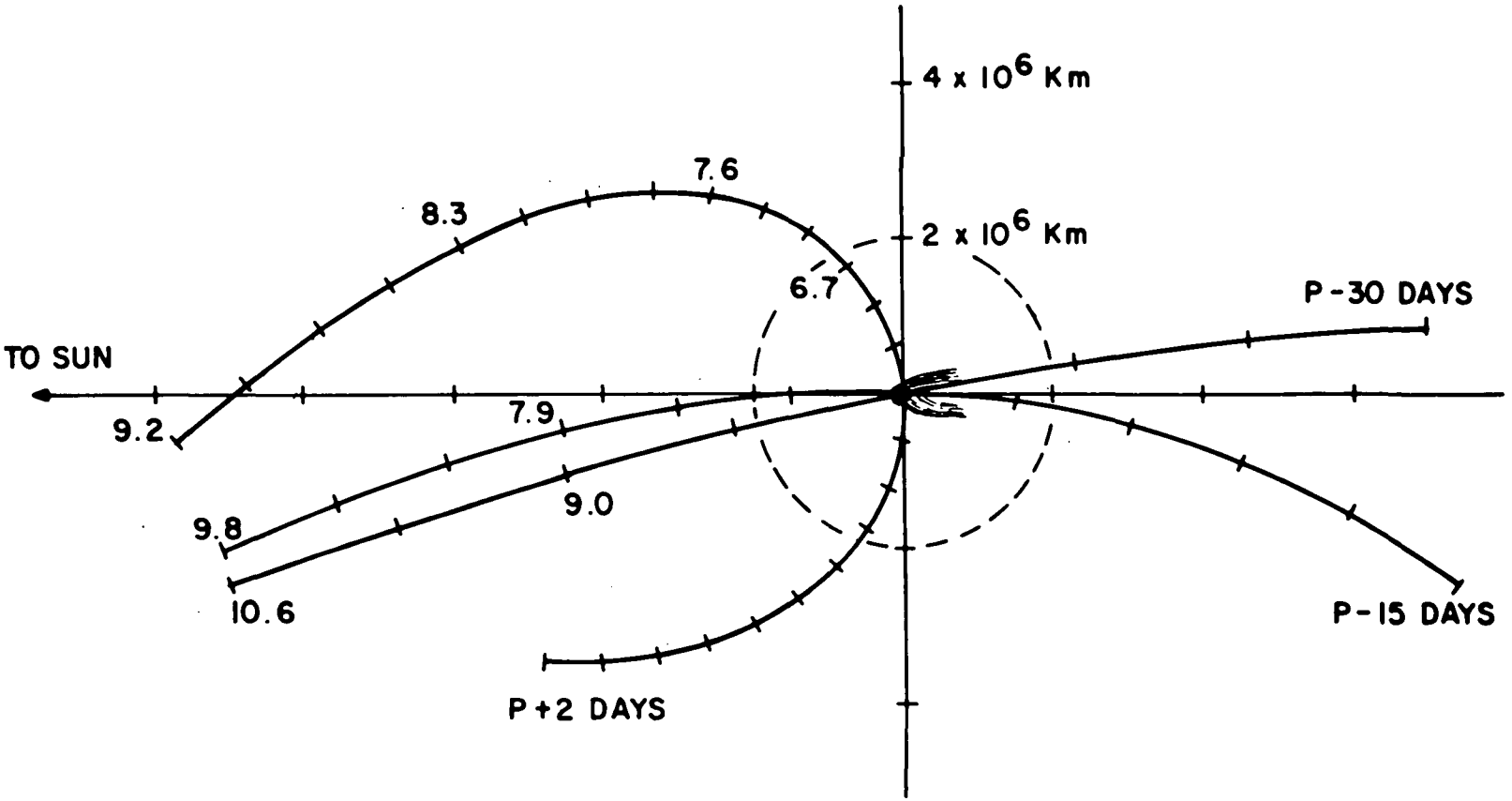

FIG. 4 ENCOUNTER GEOMETRY

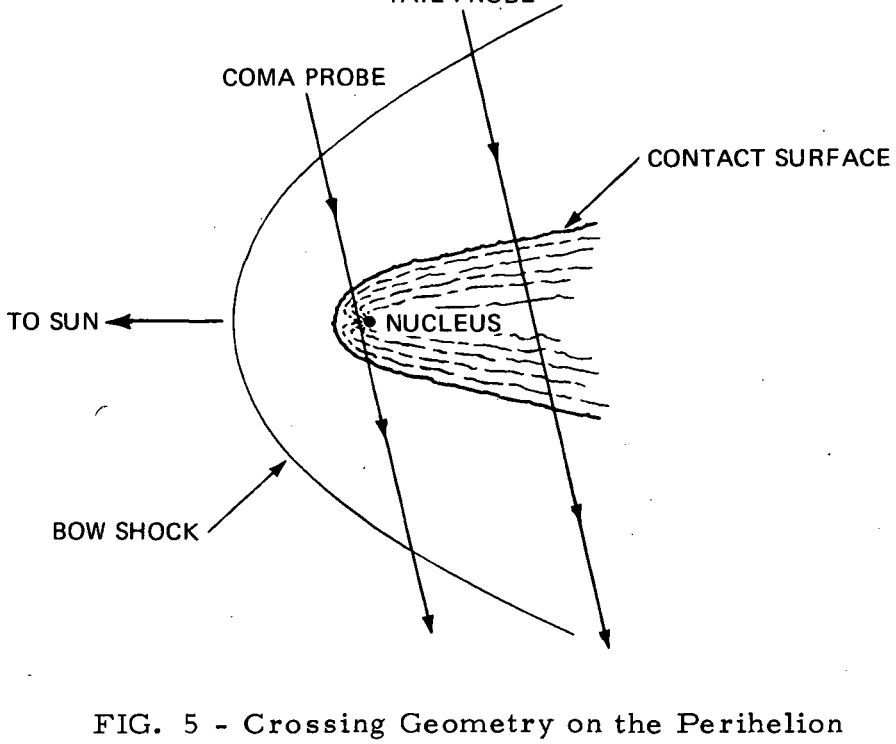

FIG. 5 - Crossing Geometry on the Perihelion Intercept

NOMINAL MISSION PARAMETERS

MISSION:	1	2	3
R(AU)	.34	.53	.80
DATE	P+2 *	P-15	P-30
Δ(AU)	1.1	.58	.34
$C_3(KM^2/S^2)$ **	94	72	43
FLYBY SPEED (KM/SEC)	8	18	26
THERMAL LOAD	8.7	3.6	1.6
MISS DISTANCE	VARIABLE		

* Two days after perihelion passage (P).

** Required launch injection energy.

encounter and also in the interplanetary cruise mode is obvious. On the other hand, during either the P-15 or P-30 intercept missions both coma and tail would be traversed by a single spacecraft. The thermal environment (insolation) is less severe at these greater heliocentric distances, but the comet's activity is reduced and the relative spacecraft velocity is larger, affording less measurement time.

The targeting strategy is affected to some extent by the need to pass on the sunward side of the nucleus to ensure good quality images (Fig. 6). The spacecraft may be targeted on the nucleus (case B) for the P-15 and P-30 intercepts, but it should be targeted sunward of the nucleus in the P+2 mission (case C). If the estimated impact hazard from dust particles were to demonstrate the existence of an 'exclusion-zone' which the spacecraft should not enter, the targeting strategy would be as shown in case A.

Median miss distances were determined from the three-standard-deviation (3-σ) error ellipses by calculating the probability density lying between R and R + dR, i.e. P(R)dR in Fig. 6. The starting point was the set of a-priori ephemeris errors (Yeomans[6]) which are unusually small because the non-gravitational effects on Encke's motion (particularly A_2) are quite small (Fig. 7). The a-priori ephemeris errors for 1980 were improved by assuming ground-based observations prior to launch and before intercept. The (3-σ) targeting error ellipses were then calculated and the median miss distances were determined for various combinations of targeting strategies, and for the absence or presence of on-board navigation (Table II). The median miss distances (3-σ) were found to be ~100 Km with successful on-board navigation and ~ 500 Km without it, assuming no exclusion zone.

CASE 1: TARGETING STRATEGY ASSUMING AN EXCLUSION ZONE OF RADIUS R_{EZ}. $R_\oplus$ = 0.34; 0.53; 0.8 AU

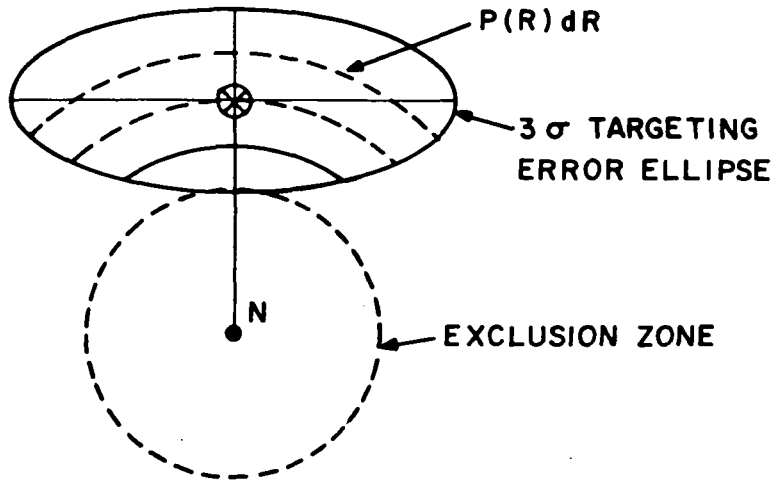

CASE 2: TARGETING STRATEGY WHEN APPROACHING FROM SUN ALONG THE SUN - COMET LINE. R_{EZ} = 0

$R_\oplus$ = 0.8 ; 0.53 AU

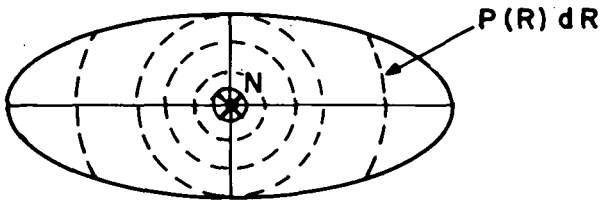

CASE 3: TARGETING STRATEGY WHEN APPROACHING AT RIGHT ANGLES TO THE SUN-COMET LINE. R_{EZ} = 0

$R_\oplus$ = 0.34 AU

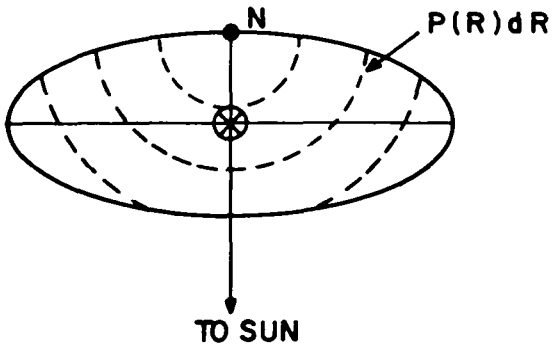

FIG. 6 - Targeting Strategy

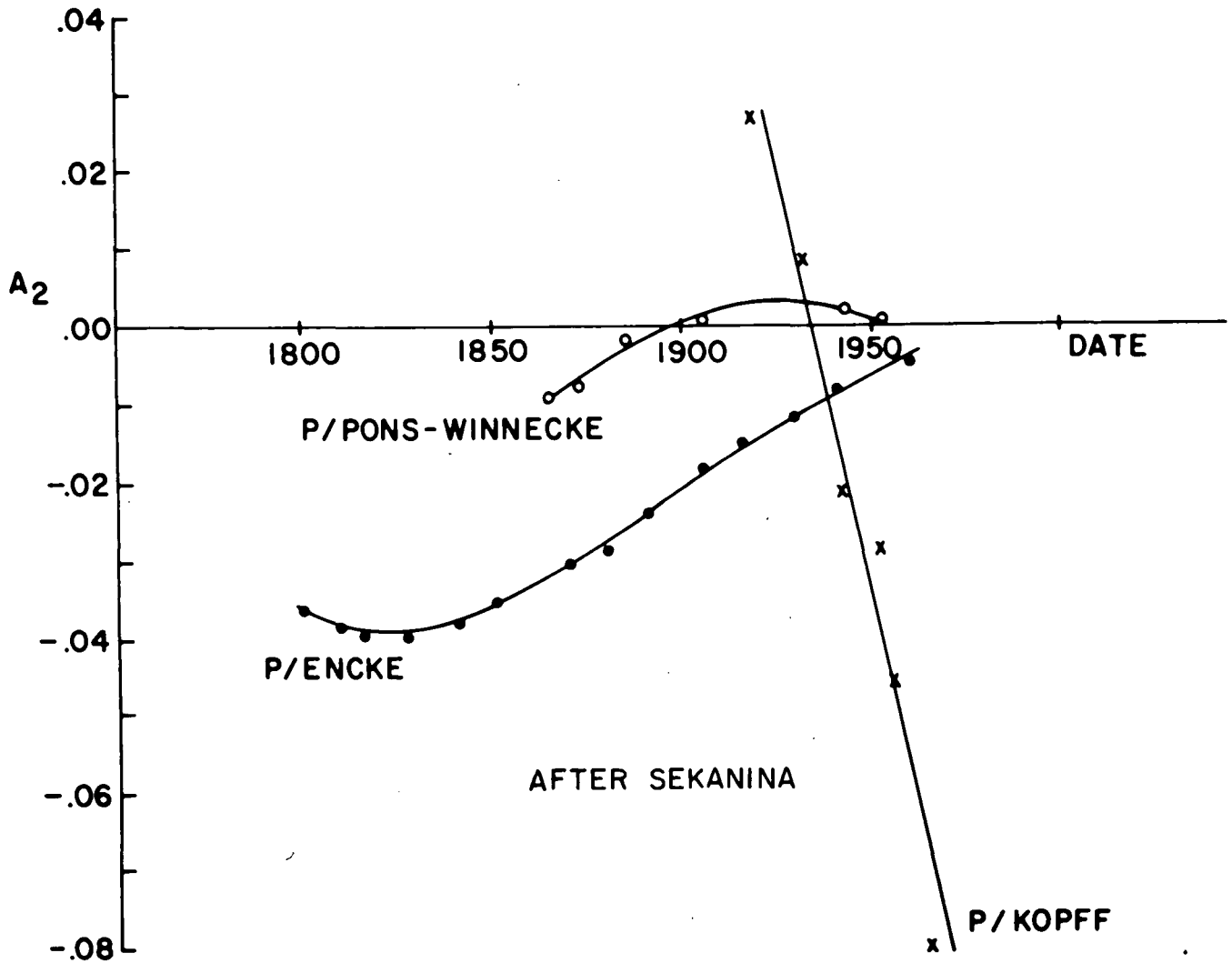

FIG. 7 - Secular Changes in Transverse Nongravitational Acceleration of Several Short Period Comets

TABLE II: MEDIAN MISS DISTANCE VS. INTERCEPT CONDITIONS

R(A.U.)	ON-BOARD NAVIGATION	MEDIAN MISS DISTANCE (Km) $R^{*}_{EZ}=0$		$R_{EZ}=400$ KM	
0.34	Yes	95	Case A**	471	Case C
	No	510		865	
0.53	Yes	98	Case B	566	
	No	403		1017	
0.80	Yes	62		515	
	No	302		996	

* Radius (Km) of possible Exclusion Zone.

** Targeting strategy, see Fig. 4.

These miss distances are quite realistic and show that the spacecraft would definitely pass through the region where ice grains may cause the parent molecule densities to fall below the values predicted by the point source model. Thus, the measured density profiles along the flight path potentially could yield information on any departures from the point source model in this region. Further estimates of the expected science return require establishing a physical model for the comet.

PHYSICAL ACTIVITY MODEL

The combined observations of Beyer[8] and Bortle[9] show that P/Encke has shown some apparent secular decrease in intensity over the past three decades but that it regularly brightens in the same way as it approaches perihelion (Fig. 8). Encke's visual brightness is composed primarily of gas emission (C_2, C_3, CN) and the scattered solar continuum is very weak.[10] Thus, the total magnitudes measured by Beyer and others are primarily gas emissions and can be expected to approach a limiting brightness law of R^{-2} at sufficiently small R. This is so because the total abundance of a certain gas in the coma is proportional to $Q(1\ AU)R^{-2} \times \tau(1\ AU)R^2 \sim Q(1)\ \tau(1) \sim$ constant, while the fluorescence intensity is proportional to the local insolation times the number of molecules in the coma, or R^{-2}. Second order effects (Swings effect, Greenstein effect) due to doppler shifts, structure in the solar spectrum, etc. play some role for a specific emission, but should average out when the entire set of visible gas emissions is seen. At larger R, the index will first increase but should again approach 2 as reflection from the

nucleus limits the brightness. The index at intermediate R can be quite large ($\sim$ 8.8 for P/Encke at 1.1 AU, Fig. 8). Inspection of Fig. 8 shows that Encke's brightness is fitted reasonably well by an n = 2 law for .34 $\leq$ R $\leq$ 0.80 AU and so we take as our first model assumption:

$$Q_{GAS} \propto R^{-2} \quad .34 \leq R \leq .80 \text{ AU.} \tag{1}$$

Bertaux et al.[11] have measured the Lyman-alpha emission rate and derived the H-atom production rate from the observed brightness at R = 0.7 AU. They concluded that if the observed H were all produced by dissociation of H_2O, the total production rate of H_2O would be

$$Q_{H_2O} = 3\text{x}10^{27} \text{ molecules/sec at 0.7 AU.} \tag{2}$$

We take (2) as our second model assumption. This value for Q_{H_2O} is $\sim$ 100 times smaller than the rates for comets Bennett or Kohoutek.

Ney has shown (earlier paper, this Proceeding) that the thermal infrared emission from P/Encke is $\sim$100 times smaller than that from Comets Bennett or Kohoutek: therefore, we conclude that the gas/dust production rates are nearly the same for these bright new comets and for Encke, a short-period 'old' comet. The lack of visual continuum for Encke relative to Bennett or Kohoutek suggests a very much lower dust albedo for Encke and/or that icy grains contribute most of the visual continuum for Bennett and Kohoutek but are absent in the case of Encke. Our third model assumption is: Encke's dust grains do not possess ice-mantles and so a point-source model for neutral parent

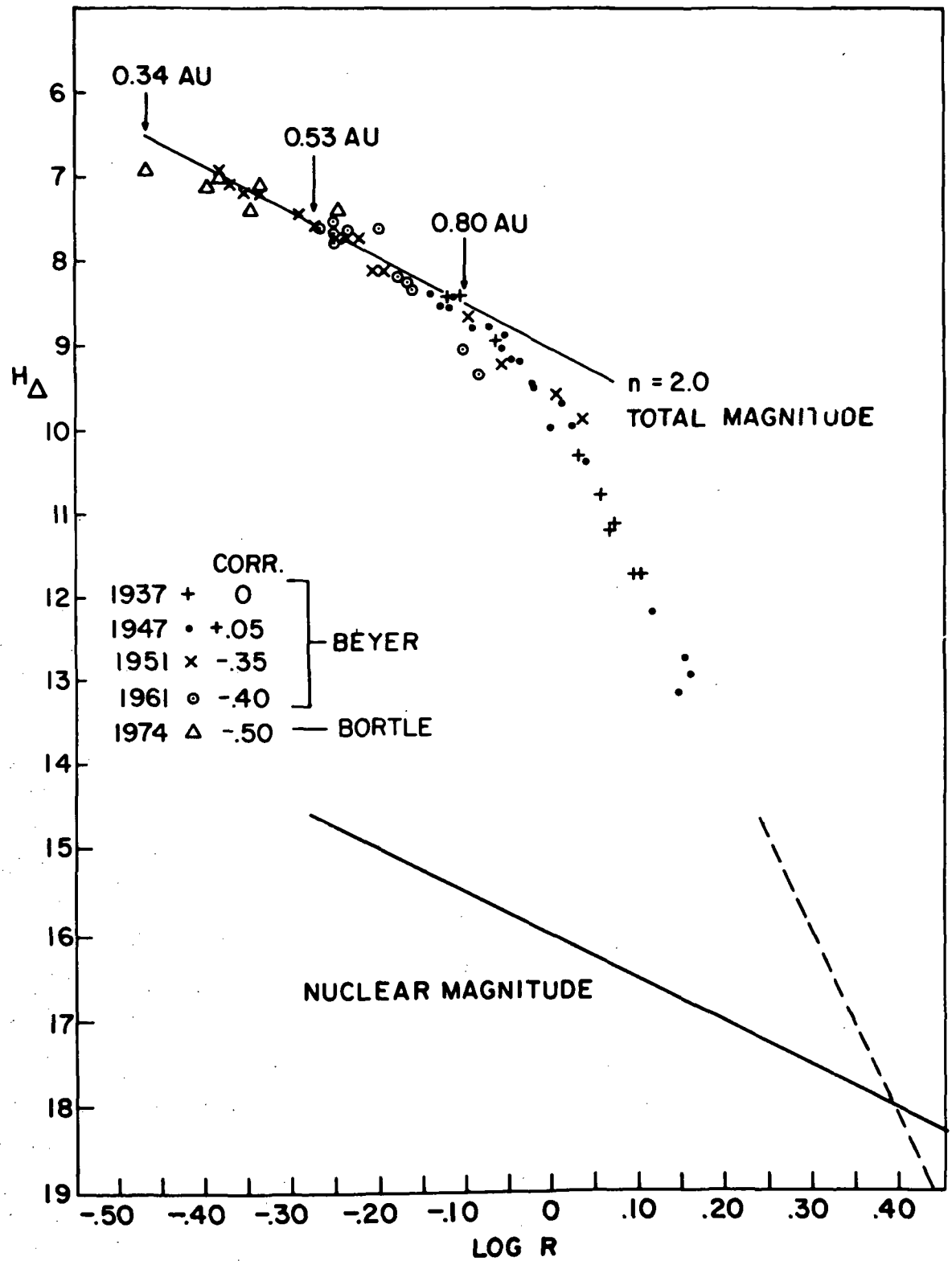

FIG. 8 - P/Encke:Brightness vs Heliocentric Distance

molecular densities is reasonable. As we shall see, the spacecraft neutral mass spectrometer experiment will be capable of verifying the validity of this assumption. For convenience, a uniform radial flow velocity (v_T) of 1 km/second was assumed. This leads to possible underestimates of the densities close to the nucleus where the flow velocity may be smaller, but it is an error on the side of caution.

The H_2O densities in the coma were calculated from the point source model. The total H_2O production rate was normalized to the observed rate at R = 0.7 AU (eqn. 2) and was scaled to other heliocentric distances by R^{-2}, which is valid for the range of R covered by these missions (eqn. 1). A destruction lifetime of τ_1 was taken to be 20 hours, corresponding to a scale length of 7×10^4 km at 1 AU. The simplified flow model is then expressed as:

$$n(D,R) = \frac{n_o(1Km,\ 1AU)}{R^2\ D^2} \exp\left(-\frac{(D-1)}{V_T\ \tau_1 R^2}\right), \qquad (3)$$

where D is the distance to the nucleus, and

$$n_o(1Km, 1AU) = 1.17 \times 10^{11}\ cm^{-3}. \qquad (4)$$

The modelled H_2O densities are shown in Fig. 9. The solid curves include photo-dissociation of the H_2O parent and the dashed portion shows how the densities would fall off in the absence of dissociation.

A lower limit to the radius of P/Encke can be established by assuming that all of the solar radiation incident on the nucleus is effective in vaporizing the H_2O produced at 0.7 AU. This leads to

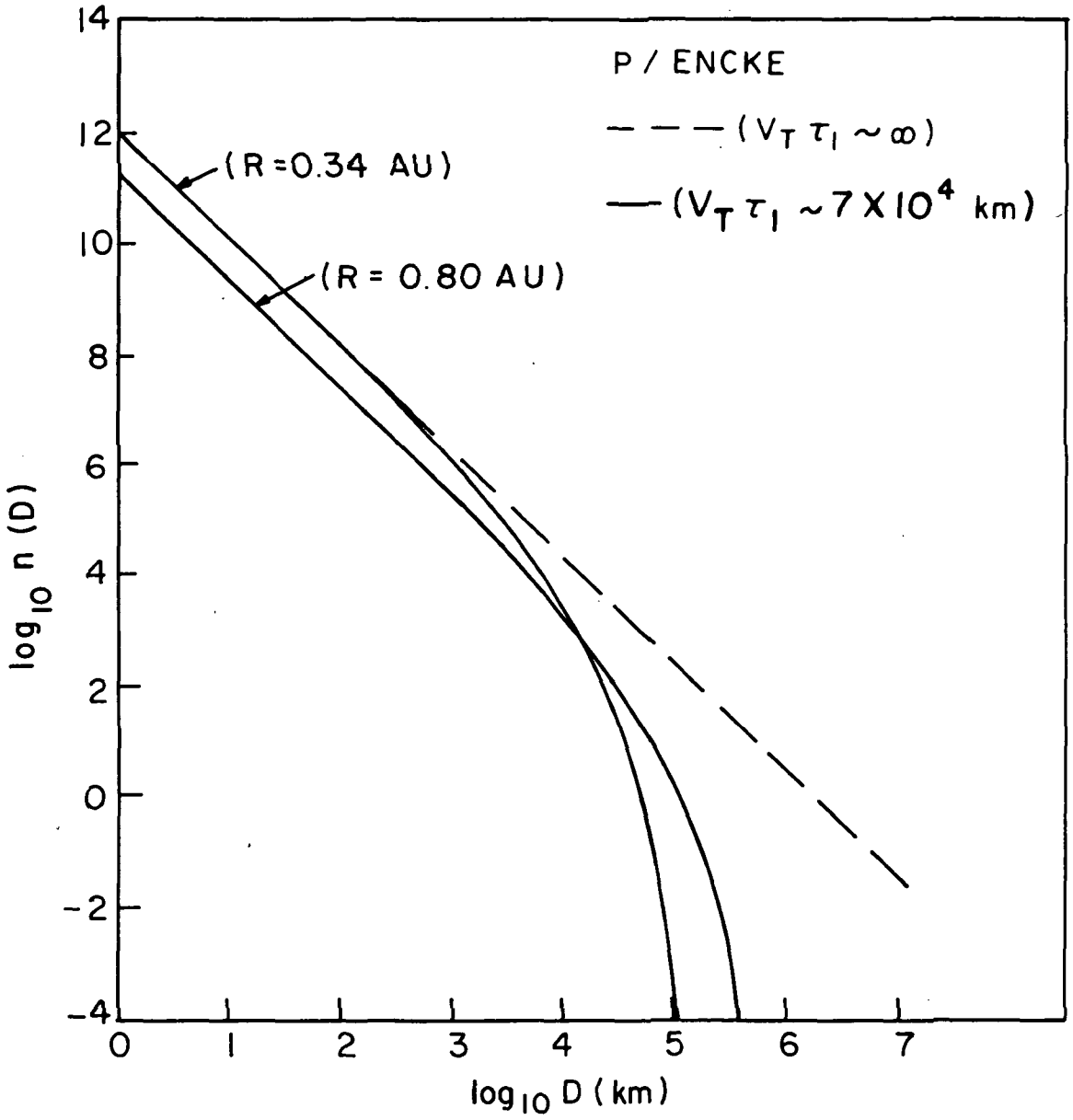

FIG. 9 - H_2O Density vs Distance From The Nucleus

$R > 0.17$ Km. Other estimates can be derived from the observed near-aphelion values of pR^2 which range from 0.7 to 0.2.[12] Extreme estimates for the albedo (0.6-0.03) yield $0.6 \lesssim R \lesssim 4.8$ Km, while nominal albedos of $\sim 0.1 \rightarrow 0.2$ yield $R \sim 2$ Km. For the purpose of assessing the quality of images returned by the imaging experiment we take as our fourth model assumption:

$$R = 1 \text{ Km.} \tag{5}$$

Marsden's recommended nuclear magnitude law[13] was adopted, which implicitly assumes an asteroidal phase law for the nuclear albedo, i.e.

$$N_{mag} = 16.0 + 5 \log\Delta + 5 \log R + .03\,\beta, \tag{6}$$

where β is the phase angle (sun-nucleus-observer).[13] The dust distribution was modelled after Finson-Probstein but an upper limit cutoff of $\sim$ 1 cm diameter in the size distribution was introduced based upon the maximum gas flow rates at perihelion.[14] The baseline physical activity model is summarized in Table III.

EXPECTED SCIENCE RESULTS: PARENT MOLECULES

Neutral mass spectrometers of the electron-impact-ionizer class can be divided into two types depending on whether the molecules to be studied are allowed to impact on surfaces in the ionizer region. In the so-called 'fly-through mass spectrometer' the gas streams through the ionizing region and on into the analyzing region without experiencing wall collisions which (at the relatively high impact velocities $\gtrsim$ 8 Km/sec) could dissociate and modify the neutral parent molecules. In the so-called 'stagnation

TABLE III

BASELINE PHYSICAL MODEL FOR P/ENCKE

- $R_N > 0.17$ KM; $R_{NOM} = 1$ KM
- $N_{MAG} = 16.0 + 5 \text{ LOG } \Delta + 5 \text{ LOG } R + .03\beta$
- $T_{MAG} = 8.9 + 5 \text{ LOG } \Delta + 5 \text{ LOG } R$, IN 1937
  $T_{MAG} \geq 10.3 + 5 \text{ LOG } \Delta + 5 \text{ LOG } R$, IN 1980
  $.34 \leq R \leq .80$
- $Q_{H_2O} \leq 3 \times 10^{27} \text{ SEC}^{-1}$ AT 0.7 AU
- COLLISIONLESS FLOW MODEL ASSUMED FOR GAS DENSITIES
- DUST DISTRIBUTION MODELED ON FINSON-PROBSTEIN RESULTS FOR P/AREND-ROLAND

mass spectrometer[1], the neutral gases ram into a chamber, collide with walls (becoming thermalized in the process), and eventually effuse out of an orifice. The density in the chamber is higher than the external density by the ratio $V_{SC}/V_{thermal}$ or by $\sim 20 \rightarrow 65$ for the missions considered here and the instrumental sensitivity is enhanced accordingly. However some of the parent molecules are likely to dissociate on impacting the wall surfaces since their kinetic energies exceed their bond dissociation limits. Furthermore, it is impossible to separate the ion signals due to parent molecules from those due to outgassing of the spacecraft materials or from dissociated fragments resulting from wall collisions. The fly-through mass spectrometer does not experience these problems but it has lower sensitivity. The state-of-the-art sensitivity (E) for a Nier-type instrument is $\gtrsim$ 1 ion count/sec per 1000 neutral parent molecules/cm^3 (A.O. Nier, private communication). The instantaneous counting rate (dN/dt) on a particular mass peak would be

$$\frac{dN_i}{dt} = E\, n_i \tag{7}$$

where n_i is the local number density for the ith parent molecular species. If the fraction of time spent on the ith mass peak is G(%), the duty cycle, and the spacecraft velocity relative to the comet is V_{SC}, then the counting rate per unit kilometer of flight path is:

$$\frac{dN}{dl} = \frac{dN}{dt}\frac{dt}{dl} = \frac{GEn_i}{V_{sc}} . \tag{8}$$

The fly-by geometry during close approach is shown in Fig. 10. The integrated number of ion counts in going from L_1 to L_2 can be written (combining eqn. 8 and eqn. 3)

$$\frac{dN}{dl} = \frac{GEQ(R)\exp[-(L^2+D_m^2)^{1/2}/v_T\tau_1 R^2]}{4\pi(L^2+D_m^2)\quad V_{SC}\ V_T} = C1(L^2+D_m^2)^{-1}\exp[-C2(L^2+D_m^2)^{1/2}] \qquad (9)$$

or

$$N_{\bar{L},R} = C1\int_{L_1}^{L_2} \frac{Q(R)\exp[-C2(L^2+D_m^2)^{1/2}]}{(L^2 + D_m^2)}\,dL \qquad (10)$$

$$N_{\bar{L},R} = F(D,\ R,\ D_m,\ \tau_1,\ Q_1).$$

This calculation was carried out for the various combinations of physical data shown in Table IV, resulting in a total of 48 possible cases. The initial value of L_1 for each case was 32,000 Km. The integration was performed until the error in the number of ion counts ($N^{1/2}$) equalled $\Delta D/\bar{D}$. An 'x' was plotted in the center of the first interval, and the procedure was begun again at L_2. The first measurement to fall below 10% statistical error ($\sqrt{2}\ N^{1/2}$) is marked with a vertical line, and the error of the measurement at closest approach is given (Fig. 11). The curves shown in Fig. 11 are for intercepts at R = 0.34 AU, 0.53 AU, and 0.80 AU reading from top to bottom. These curves show what can be reasonably expected for measurements of H_2O assuming no exclusion zone, improvement of targeting using on-board navigation, a duty cycle of 100% and a lifetime for H_2O of 20 hours at 1 AU. The absence of on-board navigation and introduction of an exclusion zone would increase the miss

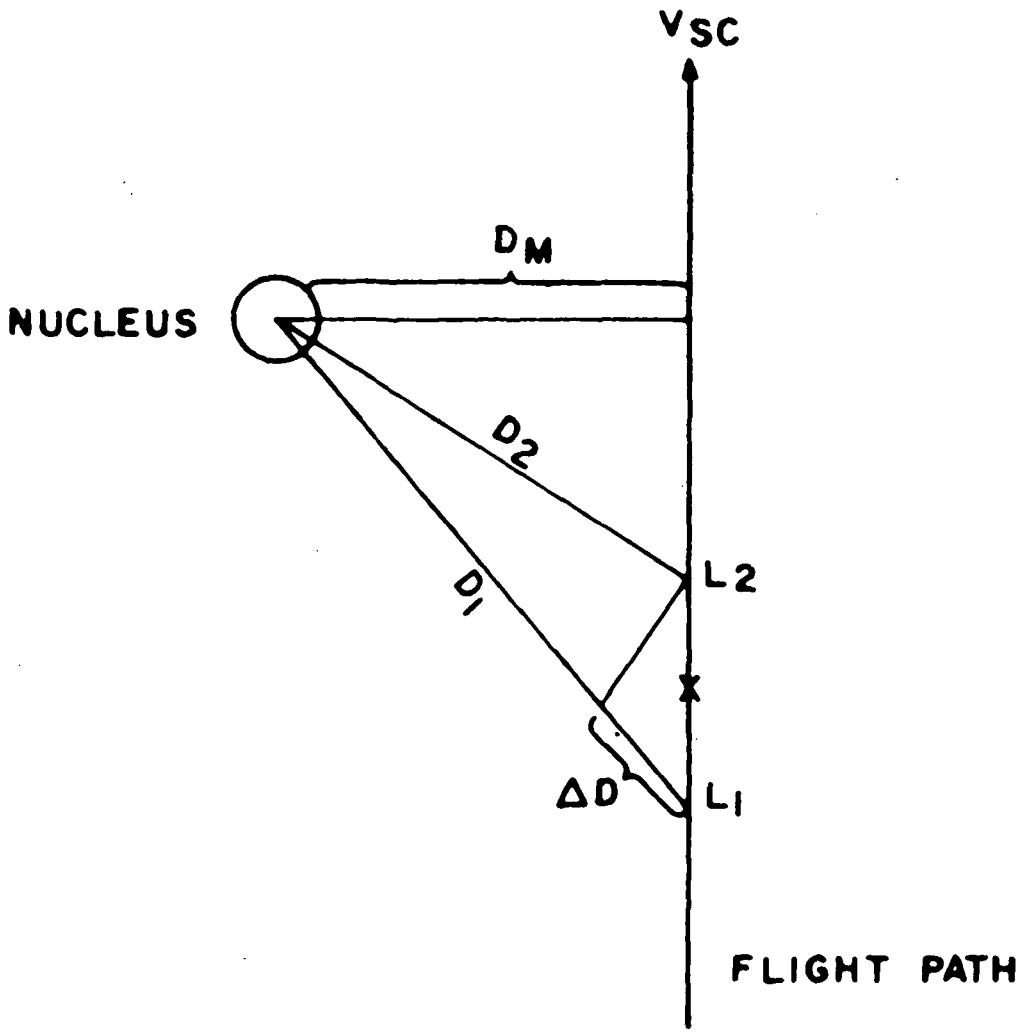

Fig. 10 - Flyby Geometry at Encounter

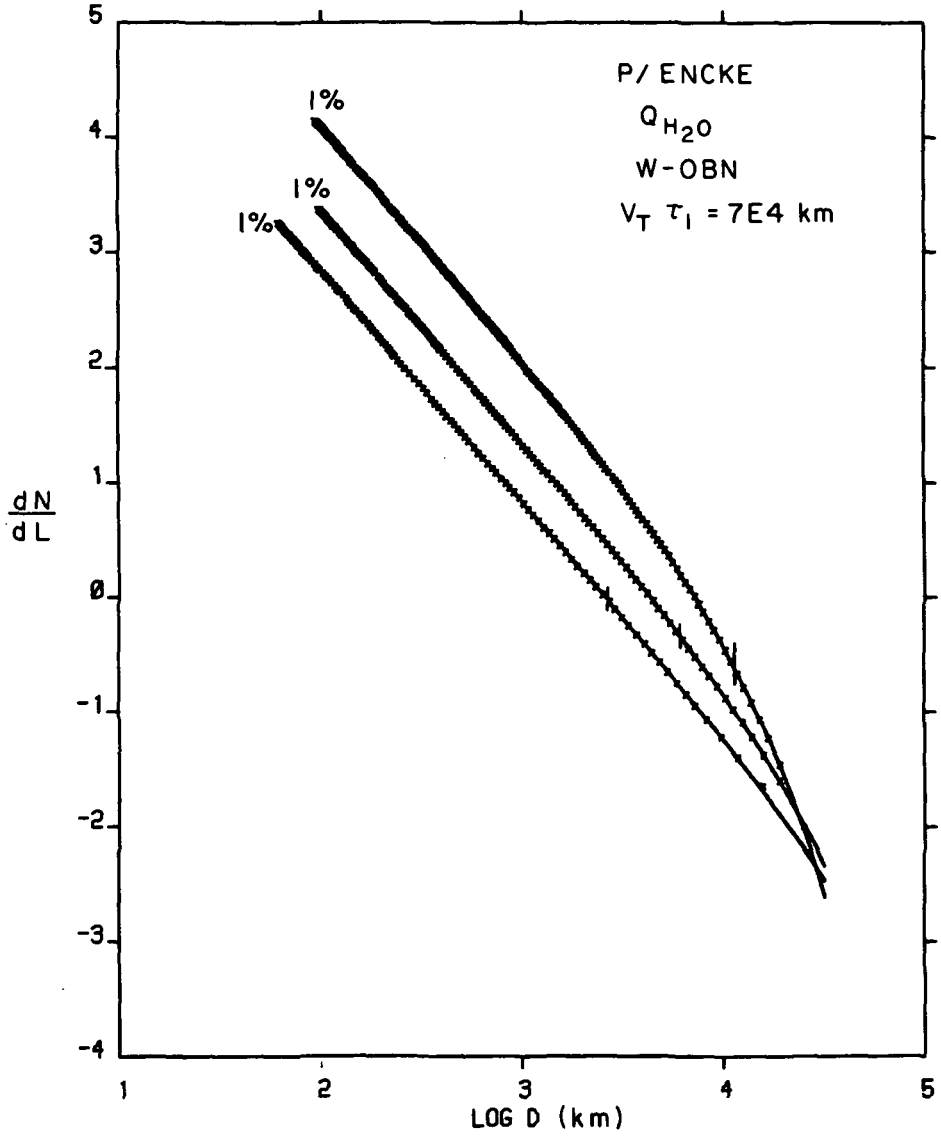

FIG. 11 - Neutral Mass Spectrometer Results: H_2O

TABLE IV

BASELINE DATA FOR NEUTRAL MASS SPECTROMETER EXPERIMENT MODELS

	MISSION 1 0.34 AU	MISSION 2 0.53 AU	MISSION 3 0.80 AU
C1: Q_{H_2O}	1.26E8	2.31E7	7.0E6
1% Q_{H_2O}	1.26E6	2.31E5	7.0E4
C_2: τ_1 = 7E4 sec	1.23E-4	5.08E-5	2.23E-5
τ_1 = 3.5E3 sec	2.46E-3	1.01E-3	4.44E-4
D_m(Km): R_{EZ} = 0, with OBN	95	98	62
R_{EZ} = 0, without OBN	510	403	302
R_{EZ} = 400 Km, with OBN	471	566	515
R_{EZ} = 400 Km, without OBN	865	1017	996

distances to ~ 1000 Km. If the densities were to fall well below the point source model within 1000 Km of the nucleus, i.e. within a hypothetical icy halo, the existence of same could be verified in the former cases. On the perihelion encounter, the curvature of the density profiles at large distances would also be measureable and the lifetime (scale-length) of H_2O could be determined.

The expected measurements of H_2O at 1% duty cycle (or of a trace molecule with 1% abundance relative to H_2O and a 100% duty cycle measurement) are shown in Fig. 12. This "best case" assumes that on-board navigation is available and that there is no exclusion zone. The flyby distances are then ~ 100 Km but only the perihelion intercept gives reasonable assurance of measuring the trace molecules before entering a hyopthetical icy halo.

From this study, we conclude that the density profiles of H_2O can be measured with high precision over a significant range of distances within the coma on all three missions, but that only the perihelion encounter will enable a determination of the lifetime of the H_2O molecule. Measurements of trace molecules with 1% abundance relative to H_2O will be possible only on the perihelion encounter. These results are based on best estimates of real instrumental sensitivities, well modelled flyby distances, and a reasonable physical activity model for Comet Encke. They show that the neutral mass spectrometer science return is best at perihelion, as intuitively expected.

EXPECTED SCIENCE RESULTS: IMAGING EXPERIMENT

A detailed study of the quality of television images of the nucleus has been carried out by T. Thorpe (JPL) for the Encke Panel. The baseline

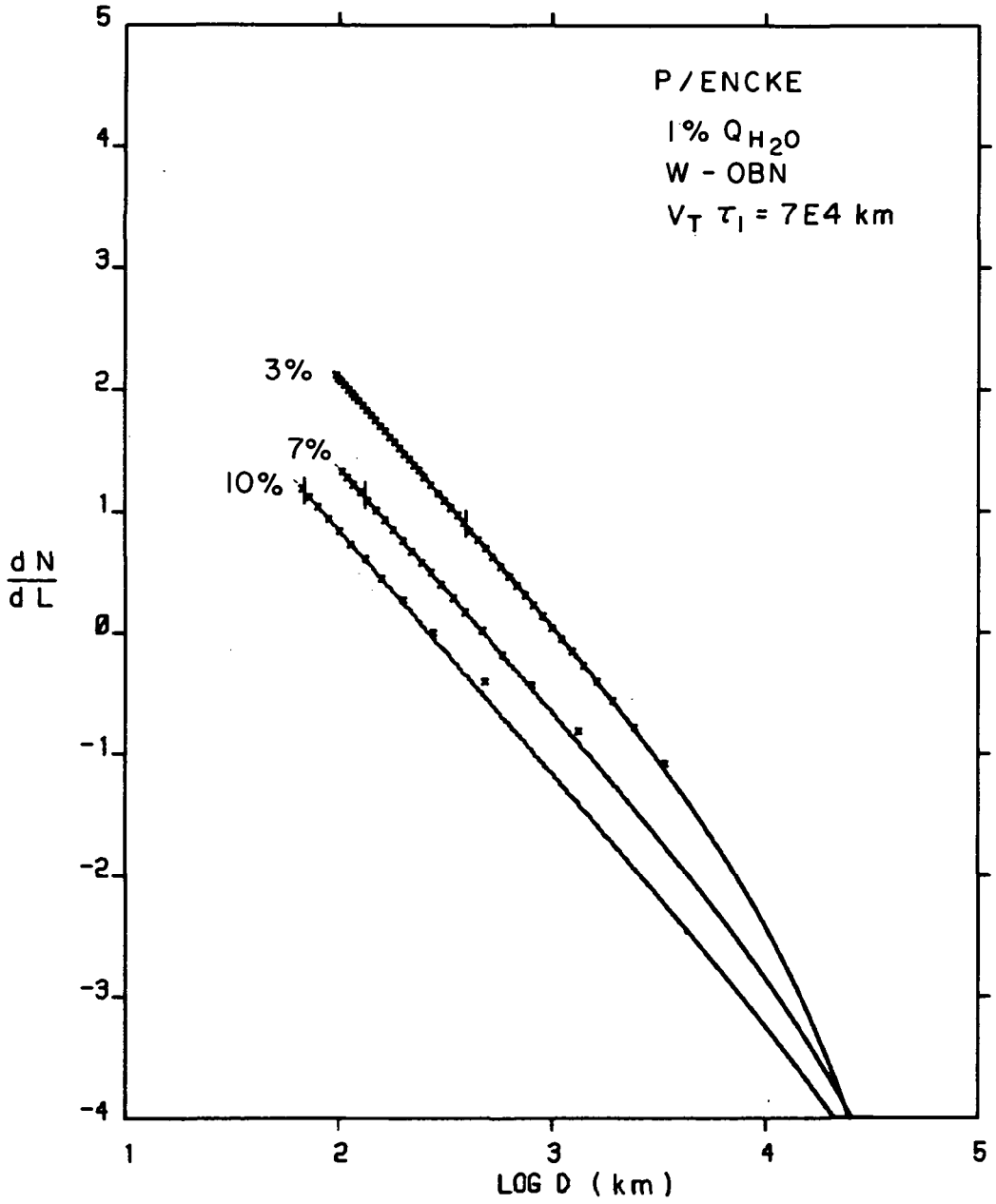

FIG. 12 - Neutral Mass Spectrometer Results: Trace Molecules

model already discussed was used together with the sensitivity data for the Mariner 10 vidicon camera to estimate exposure times, smear rates, linear dimensions of one picture element (pixel) for various frames, number of pictures returned, and the time in days-before-encounter for the first resolution of the nucleus. The assumed nuclear brightness law (eqn. 6) affects the apparent nuclear brightness, as seen by the spacecraft, through the heliocentric distance (as R^{-2}), through the nucleus-spacecraft distance (Δ), and through the phase angle (β). The phase angle is nearly equal to ninety degrees for the intercepts at 0.8 AU and 0.53 AU but can be chosen to be nearly zero degrees for the perihelion encounter (see Fig. 4 and Fig. 6). Thus the apparent nuclear brightness is nearly 2.7 magnitudes brighter for the perihelion encounter on the basis of the phase angle alone. The R^{-2} factor makes the magnitude at 0.34 AU another 1.86 magnitudes brighter than at 0.8 AU, for an overall apparent brightness improvement of 4.56 magnitudes, or a factor of 66. Shorter exposure times may be used on the perihelion encounter, leading to reduced image smear from spacecraft motion during the exposure. Also, the smear is further reduced at perihelion because the spacecraft relative velocity is smaller by a factor of three (8.6/26). Thus image smear introduced by spacecraft motion is reduced by a factor of nearly 200 on the perihelion encounter compared with the 0.8 AU encounter. This also means that for a fixed exposure time, the smear on the perihelion encounter images would be three times smaller but the signal-to-noise ratio would be 66 times greater than on the 0.8 AU encounter. The results of the imaging study are shown in Table V.

TABLE V

EXPECTED RESULTS OF IMAGING EXPERIMENT ON ENCKE'S NUCLEUS

PARAMETER	R(AU)	R_{EZ} = 0*		R_{EZ} = 400*	
		OPTICAL NAVIGATION	NO OPTICAL NAVIGATION	OPTICAL NAVIGATION	NO OPTICAL NAVIGATION
1. Encounter duration (Image ≥ 24 pixels): (seconds)	0.34 AU	606 sec	592 sec	593 sec	568 sec
	0.53 AU	289	284	282	266
	0.80 AU	194	193	190	179
2. Number of pictures possible at 20 sec/frame (Image ≥ 25 pixels)	0.34	30	29	29	28
	0.53	14	14	14	13
	0.80	10	10	10	9
3. Encounter Image Resolution at 0° phase (10% albedo)**	0.34	6 m	29 m	27 m	49 m
4. Encounter Image Resolution at 90° phase (10% albedo) **	0.53	79	54	55	66
	0.80	260	240	230	153
5. Angular Encounter Rate (deg./sec)	0.34	5°/sec	0.9°/sec	1.0°/sec	0.6°/sec
	0.53	10.2	2.5	1.8	1.0
	0.80	23.9	4.9	2.9	1.5
6. Linear Image Size at encounter (2 Km nucleus)	0.34	700 pixels	131 pixels	141 pixels	77 pixels
	0.53	680	166	118	66
	0.80	1080	221	130	67

* See Table II for the corresponding flyby distances.

** Midscale Exposure, see ref 1(a), Appendix IV.

Slew rates of 5-10°/sec are mechanically difficult to implement, whereas rates of 1°/sec can probably be achieved. Thus the best image resolution for 0.34 AU is ~ 27 m resolution; for 0.53 AU it is ~ 66 m resolution; and for 0.8 AU it is ≳ 153 m resolution. The number of pictures attained is greatest during the perihelion encounter, the signal-to-noise ratio on those frames will be much greater, and the spatial resolution is best on the perihelion encounter.

CONCLUSION

A simple physical activity model has been derived from published data on Encke's comet and has been combined with data provided by realistic mission analyses, and with actual instrumental performance figures to arrive at a quantitative appraisal of the expected scientific results returned by the two most mission-sensitive experiments on a ballistic flyby mission. The expected results have been determined for three specific ballistic intercepts, occurring at heliocentric distances of 0.34 AU, 0.53 AU, and 0.80 AU, respectively. The conclusions confirm the intuitive informed guess: the optimum intercept should occur as near to the perihelion as possible. This is so not only because the comet activity is greatest there, but also because the spacecraft velocity is lowest there. A perihelion intercept would definitely enable measurements of H_2O beginning at ~ 20,000 Km from the nucleus and extending in to ~ 100 Km from it at high accuracy. Trace molecules with 1% abundance relative to H_2O could be measured from ~ 1000 Km in to ~ 100 Km if a 100% duty cycle mass spectrometer with state-of-the-art sensitivity were used. The distances for 'first detections' could be increased by ~ 3 if the ionization efficiency were improved ten-fold.

Approximately 60 or more photographs of the nucleus could be taken with high signal-to-noise ratio on the perihelion encounter, and the resolution of the best frame would be ~ 27 meters. A 2 kilometer diameter nucleus would thus be photographed with ~ 74 resolution elements (~ 141 pixels) across its diameter, and if circular would show ~ 4300 resolution elements across its disk (at 0^{o} phase angle). This represents the first quantitative assessment of the scientific results which could be obtained on a cometary mission and shows conclusively that such a mission is capable of answering many of the fundamental questions of cometary research.

REFERENCES

1. More detailed information can be found in the following reports:

   a) "Ballistic Intercept Missions to Comet Encke", Final Report of the Comet Encke Ballistic Missions Engineering Panel, NASA TMX-72542 (1975);

   b) "Cometary Probe to Encke, 1980", Report on the Mission Definition Study, ESRO MS(74)35 (1974);

   c) "Mission Design for a Ballistic Slow Flyby of Comet Encke, 1980", R.W. Farquhar, D.K. McCarthy, D.P. Muhonen, and D.K. Yeomans, NASA TN D-7726 (1974);

   d) "Study of 1980 Comet Encke - Asteroid Missions Using a Spin-Stabilized Spacecraft", W.J. Bursnall, E.G. Howard, W.R. McMininy, R.G. Shaffer, and J.M. Van Pelt, NASA-CR-114670 (Summary) and NASA-CR-114671 (Technical Report) (1973);

   e) "Study of Ballistic Mode Comet Encke Mission Opportunities", G.R. Hollenback and J.M. van Pelt, NASA CR-137524 (1974);

   f) "Science Aspects of a 1980 Flyby of Comet Encke with a Pioneer Spacecraft", L.D. Jaffe, C. Elachi, C.E. Giffin, W. Huntress, R.L. Newburne, R.H. Parker, F.W. Taylor, and T.E. Thorpe, JPL Report 760-96 (1974);

   g) "Imaging on Ballistic Missions to Comet Encke", L.D. Jaffe, D. Bender, R.O. Hughes, B.R. Mackiewicz, and T. E. Thorpe, JPL Report 760-112 (1974); and

   h) "A Study of the Solar Electric Slow Flyby of Comet Encke in 1980", K. L. Atkins et al., JPL Report 760-90 (Rev. A) (1974).

2. cf. "Cometary Spectra", P. Swings, Quart J. Roy. Astron. Soc. 6, 28 (1959).

3. "Cometary Probes", Rh. Lust, Space Science Rev. 10, 217 (1969).

4. "Comets - Scientific Data and Missions", Proceedings of the Tucson Comet Conf., ed. G. P. Kuiper and E. Roemer, Pub. by Lunar and Planetary Lab., Univ. of Ariz. (1972).

5. "Proceedings of the Cometary Science Working Group - Yerkes Observatory (June 1971)", ed. D. L. Roberts, pub. by ITT Research Institute (Dec. 1971).

6. The a-priori ephemeris errors have been discussed by D. Yeomans in an earlier paper of these proceedings.

7. Orbital elements after D. Yeomans (private communication, 1974).

8. 1937: M. Beyer, "Physische Beobachtungen von Kometen IV", Astron. Nachr. 265, 37 (1938).

   1947: M. Beyer, "Physische Beobachtungen von Kometen VII, ibid. 278, 217 (1950).

   1951: M. Beyer, "Physische Beobachtungen von Kometen IX", ibid. 282, 145 (1955).

   1961: M. Beyer, "Physische Beobachtungen von Kometen XII, ibid. 286, 219 (1962).

9. J. E. Bortle, IAUC 2667 (1974); ibid. 2670 (1974).

10. Cf: "Atlas of Representative Cometary Spectra", ed. P. Swings and L. Haser; Technical Report, University of Liege Astrophysical Institute, Liege, Belgium (1955);

    "Photoelectric Photometry of Comets", W. Liller, Astron. J. 66, 372 (1961); and D. Malaise, J. Observ. 44, 144 (1961).

11. "Interpretation of Hydrogen Lyman-alpha Observations of Comets Bennett and Encke", J.L. Bertaux, J. E. Blamont and M. Festou, Astron. and Astrophys. 25, 415 (1973).

12. cf. E. Roemer and R.E. Lloyd, Astron. J. 71, 443 (1966);
E. Roemer, IAUC 2435;
R.E. McCroskey and C.W. Shao, IAUC 2446;
E. Roemer, IAUC 2446; and
E. Roemer, IAUC 2586.

13. B. G. Marsden, "Periodic Comet Encke", IAUC 2547 (1973).

14. This part of the study was performed by W. C. Wells, R. S. Benson, A. D. Anderson, and G. Gal (Lockheed Missiles and Space Company) and appears as Appendix III to ref. 1(a).

DISCUSSION

Z. Sekanina: To clear up the question as to what is the current production rate of large dust particles from P/Encke, I suggest that more attention be paid in the future to a possibility of detecting an antitail of this comet. Favorable visibility conditions for such an antitail can be predicted.

M. Dubin: A report of dust relating to Comet Encke was made by Alexander, et al., from measurements of "particle " impacts in Mariner 64. They reported a short-period high flux of particle impact signatures during the brief period when the Mariner spacecraft traversed the orbit plane of Comet Encke.

M. Mumma: Ney's infrared results combined with Bertaux's measurement of the H-atom production rate show that Encke's gas-to-dust production ratio is nearly the same as that for bright comets, i.e., the observed infrared dust brightnesses were ~100 times smaller for Encke and the gas production rates were also ~100 times smaller. On the other hand, Liller has shown that the ratio of continuum to gas emission in the visible is at least 5 times smaller for Encke than for bright new comets, i.e., the product of visual grain albedo and total projected grain area is much smaller for Encke than for bright comets. Assuming similar visual albedos implies that the grain temperature would have to be considerably higher for Encke in order to explain the observed infrared flux. Whipple has suggested for many years that Encke's particle size distribution may be relatively depleted of small particles but have abundant large particles. Thus the observations would seem to be consistent with an abundant large particle flux from Encke.

E. Ney: Our observations on Encke showed a thermal emission continuum at 2 microns to ten microns. This continuum certainly shows that Encke has dust, but the brightness was 100 times dimmer than Bradfield & Kohoutek — down by the same ratio as the Lyman α brightness. It should be pointed out that in passing through the average coma of Encke only about 10 particles per square centimeter would be encountered.

M. Mumma: Wells, et al., have studied Encke's dust distribution and have determined the expected impact rate on a spacecraft during each of the three intercept missions proposed for the 1980 apparition. Their conclusions agree roughly with your estimate.

L. Biermann: I thought our previous discussion had suggested small rather than large grain size as the cause of the high temperature of a grain.

DISCUSSION (Continued)

M. Mumma: An alternate explanation is that the visual albedo is much smaller for Encke's grains than for those of a bright new comet. This would explain both the infrared and visible observations without requiring a temperature excess for Encke's grains, in fact the mean temperature of Encke's grains could be lower than Bennett's or Kohoutek's consistent with larger grain sizes. A corollary is that the visual continuum of Bennett and Kohoutek be contributed primarily by icy grains or ice mantled silicate grains (high albedo) whereas Encke's visual continuum be contributed mainly by grains which do not have an ice mantle and thus have lower albedos. The infrared continuum would be contributed by stripped grains in each case.

MISSION STRATEGY FOR COMETARY EXPLORATION IN THE 1980's

Robert W. Farquhar

I. INTRODUCTION

Ballistic intercept missions to comets have been strongly endorsed as the best way to initiate a program of cometary exploration (Roberts, 1971). This mission mode is the simplest and least expensive, and can provide a large science return. Currently, a near-perihelion intercept of Encke's comet in 1980 is receiving serious consideration for the initial cometary mission. Assuming that the 1980 Encke mission will be carried out as planned, a question that should be considered is: what is the next logical step in an evolutionary sequence of cometary missions? Two possibilities are:

- Investigate a particular comet in detail. That is, perform a rendezvous mission.

- Study the physical characteristics of several types of comets. This goal could be achieved by carrying out a series of intercept missions to comets that have exhibited diverse behavior.

A rendezvous mission is the ultimate goal of a cometary exploration program. However, it is felt that the most effective strategy would be to accomplish the intercept missions before attempting a rendezvous mission. Some of the arguments in support of this position are:

- Because physical characteristics can vary substantially between different comets, a number of precursor flyby missions will be needed to optimize the selection of a rendezvous target. The precursor missions will also lead to a better definition of the science objectives for the rendezvous mission.

- Exceptional opportunities for intercept missions to comets Halley and Giacobini-Zinner will be available in 1985. It is hard to imagine a cometary survey that would not include these unique targets.

- Fiscal constraints will be easier to satisfy if the comet survey plan is adopted. The 1985 mission set, which is described below, could be accomplished with a common spacecraft design and minimal launch-vehicle costs. On the other hand, a rendezvous mission will require the development of a solar-electric propulsion module or a high-energy chemical stage.

The main purpose of this paper is to present a specific plan for a sequence of cometary intercept missions in the 1980's. Each mission will be described in detail, and the supporting role of ground-based cometary observations will also be discussed.

II. SCIENCE OBJECTIVES

A brief summary of the scientific objectives for a cometary intercept mission is given here. For the comets' nuclear and coma region, the principal scientific objectives are to:

- Determine the existence and nature of the cometary nucleus. If it does exist as a single coherent body, determine its size, shape, albedo, rotation rate, and surface features. Study the material ejection dynamics, and attempt to confirm the postulated existence of a halo of ice grains surrounding the nucleus.

- Describe the structure, composition, and motions of the cometary atmosphere. Establish the abundance, spatial distribution, kinematic behavior, and production rate of all those particles that are present in the coma with a particular emphasis on spatial resolution within the inner coma. The identity of the stable parent molecules must be known in order to understand how the unstable species (radicals) are formed.

- Determine the nature of the solar-wind, comet interaction. Two radically different types of interactions have been proposed. One model postulates a bow shock and contact surface analogous to those of the earth and its magnetosphere. The other suggests that the transition from supersonic to subsonic flow is continuous, is over a very broad region, and occurs without a bow shock.

- Study the basic mechanisms which produce ions and radicals. To fully understand the ionization processes, it will be necessary to measure the ion density, electron density, and energy distribution of charged particles within the coma. A survey of high-frequency electric and magnetic field fluctuations is also essential to determine the importance of particle-wave interactions.

- Determine the extent of the coma constituents as a function of heliocentric distance. Spectrophotometric measurements during the approach and departure phases will yield invaluable data on the time variation of the coma's structure including its hydrogen halo. The principal advantages of a comet probe for spectrophotometric experiments are higher intensities and spatial resolution.

- Survey the characteristics of dust grains. The size distribution, velocity distribution, and composition of dust particles are of particular interest.

Correlative measurements in the coma and tail regions are needed to fully understand cometary phenomena. In addition to the latter two items listed above, which should be extended to cover the tail region, there are two specific aims for tail experiments:

- Determine the physical origin of the ion tail. This includes the determination of where and how the tail materials become ionized and the flux of charged particles through the tail. The electron distribution should be determined. Direct measurements of mass per unit charge or energy per unit charge are also required.

- Study the properties of the plasma and magnetic field. Possibly establish whether or not the stylized variations of the tail structures (a) are associated with an imbedded magnetic field entrapped from the interplanetary medium, (b) are related to waves along the contact surface, or (c) are structures imbedded within the multiple neutral sheets that may exist in the cometary tail.

Experimental payloads for cometary space probes would include an imaging system, neutral and ion mass spectrometers, UV spectrometer, dust detector, impact ionization mass spectrometer, magnetometer, plasma analyzer, and an electron analyzer. Further details of possible experimental payloads can be found in the literature (e.g., Roberts, 1971; NASA, 1973).

III. TARGET SELECTION CRITERIA

Many factors are involved in forming a cometary mission sequence. From a scientific viewpoint, the two most important guidelines are:

- The mission set should be made up of different types of comets. For example, both gaseous and dusty comets should be represented. A comet that has displayed physical characteristics associated with long-period comets should also be included (Halley is the logical choice).

- Comets with a long history of prior observations are preferred. Spectroscopic measurements are particularly useful.

Application of these standards leads to a drastic reduction in the number of candidate comets. The list of good mission opportunities is further reduced by

programmatic considerations. For instance, to allow sufficient time for design feedback, a time span of at least three years is needed between the first and second cometary mission.

In addition to the scientific and programmatic criteria just mentioned, there are several mission-related characteristics that are also significant. The most important parameters for cometary intercept missions are:

1. Relative velocity at encounter. A small "flyby speed" will maximize the time available for in situ measurements of the cometary atmosphere, reduce smear in imaging experiments, and minimize the probability of neutral-molecule impact fragmentation.

2. Targeting errors at encounter. A sufficiently small miss distance is essential for adequate science return from the imaging and mass spectrometer experiments.

3. Launch energy requirement (C_3). Total mission cost is directly related to the launch energy requirement. Small values of C_3 permit the use of smaller and less-expensive launch vehicles.

4. Heliocentric distrance at encounter. Comets are generally more active at smaller heliocentric distances.

5. Geocentric distance at encounter. Data rates are higher for smaller earth distances.

6. Encounter geometry. Cross-sectional mapping of the cometary atmosphere is preferred.

7. Earth-based sighting conditions before and during encounter. Adequate dark time is required to ensure effective ground-based observational support. Recovery should occur at least three months before encounter.

Because of a widespread misconception concerning the recovery requirement, a short explanation is in order. Several authors (e.g., Kresak, 1973) have stated that a pre-launch recovery and orbit improvement is needed to minimize midcourse propulsion requirements. However, it is easy to show that a midcourse correction of less than 100 m/sec applied three months before encounter will compensate for a priori errors in the comet's perihelion passage time of as much as 0.3 days. Therefore, a recovery three months before encounter appears to be acceptable.

IV. MISSION SEQUENCE

Using the selection criteria from the previous section, it soon becomes obvious that really good cometary mission opportunities are quite rare. Fortunately, outstanding opportunities exist for missions to Encke in 1980 and Giacobini-Zinner and Halley in 1985. In terms of scientific interest, prior observations, and diversity of physical behavior this group of comets is an optimum set. Furthermore, in most instances, the mission parameters are also satisfactory.

A. Encke, 1980

As mentioned earlier, there is general agreement that the first mission to a comet should be a near-perihelion intercept of Encke's comet in 1980. This mission was originally proposed by Farquhar and Ness (1972), and has recently been endorsed by the Space Science Board of the National Academy of Sciences. The principal features of the 1980 Encke mission are given below. For a more-comprehensive discussion, see Farquhar et al. (1974).

A short summary of Encke's physical characteristics is given in Table 1. The orbit of comet Encke is depicted in Figures 1 and 2. Note that Encke's perihelion is almost coincident with its descending node. The bipolar plot of Figure 2 shows Encke's motion with respect to a fixed sun-earth line for each apparition. With this plot, it is easy to verify that 1980 is a very good year for pre-perihelion observations of Encke.

The nominal mission profile is shown in Figure 3. A near-perihelion intercept was chosen because gas densities are highest in this region and the flyby speed is minimized here. Note that the launch occurs when the earth is almost coincident with Encke's nodal line. It is this condition that makes it possible for the spacecraft to follow a transfer trajectory in essentially the same plane as Encke's orbit, thereby reducing the out-of-plane component of the relative velocity vector. In Table 2, it can be seen that the flyby speed at encounter will be less than 9km/sec throughout a 10-day launch window.

Another aspect of the near-perihelion intercept strategy is that the spacecraft's orbital period almost exactly equals one-sixth Encke's period ($T_{ENCKE} \sim 6\ T_{S/C}$). Therefore, as shown in Table 2, only a small retargeting maneuver is needed to achieve a second encounter with Encke in 1984.*

*A double encounter could also be accomplished by targeting for an intercept at P-19 days. In this case $T_{ENCKE} \sim 5\ T_{S/C}$, but the flyby speed would be about 21 km/sec.

Table 1

Comet Encke Summary

Observational History: Encke has been observed at more apparitions than any other comet. Since its discovery in 1786, it has been seen during fifty returns to perihelion, with only one apparition (1944) being missed after 1819. Due to Encke's 3.3-year period and its small perihelion distance, favorable geometric conditions for Northern-Hemisphere observers occur at 10-year intervals. Encke generally brightens perceptibly about six weeks before perihelion, and by the time it reaches perihelion, it often has enough brilliance to be classed as a naked-eye object. Indeed, 14 naked-eye observations of Encke have been recorded. A rapid decrease in brightness usually occurs about six to seven weeks after perihelion. Typical post-perihelion brightness estimates appear to be one magnitude fainter than pre-perihelion estimates for the same heliocentric distance.

Nuclear Region and Coma: Encke frequently displays a sharp nuclear condensation as it approaches perihelion. However, an unusual feature that seems to be unique to Encke is the eccentric location of the nuclear region at the antisolar apex of a fan-shaped coma. The observable coma diameter is approximately 10^5 km. Encke's spectrum is strong in CN, C_2, and C_3, but is especially faint in the continuum. Recently, a large hydrogen cloud surrounding Encke was detected by a Lyman-Alpha photometer on-board the OGO-5 satellite. The size of Encke's nucleus is still uncertain, but observations of Encke near aphelion ($\sim$4.1 AU) suggest a nuclear radius of 2-3 km.

Tail: A narrow type-I tail starts to develop about thirty days before perihelion. Typical observed tail lengths for Encke are $\sim 2 \times 10^6$ km.

Dust: The faintness of a continuum in Encke's spectrum and the non-observability of a dust tail indicates that Encke's dust content is rather low. However, larger dust grains would not contribute appreciably to these observations and could be present. This seems likely because the Taurid meteor showers are associated with Encke's comet. The absence of fragmentation in the Taurid meteors argues for a rigid structure.

Nongravitational Effects on Orbital Motion: The comprehensive analysis of Marsden and Sekanina (1974) has shown that the transverse component of the nongravitational acceleration reached a maximum value around the year 1825, and has since decreased in magnitude by about a factor of ten. At present, the nongravitational effect on Encke's motion is quite small.

ORBITAL ELEMENTS (EQUINOX 1950.0)

EPOCH	1980 NOV. 17.0
T	1980 DEC. 6.57610
q	0.3399411 AU
e	0.8467578
Ω	334.19764°
ω	185.97967°
i	11.94599°

EPOCH	1984 APR. 10.0
T	1984 MAR. 27.68721
q	0.3410024 AU
e	0.8463305
Ω	334.18436°
ω	185.99329°
i	11.92738°

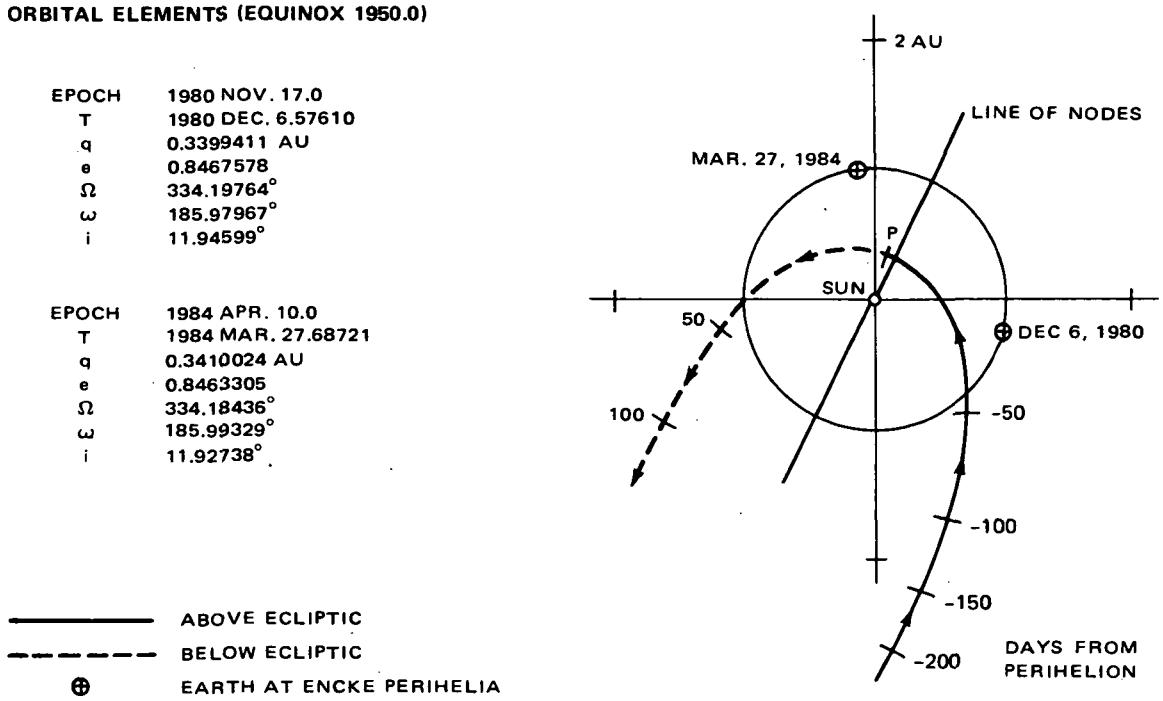

Figure 1. Orbit of Comet Encke

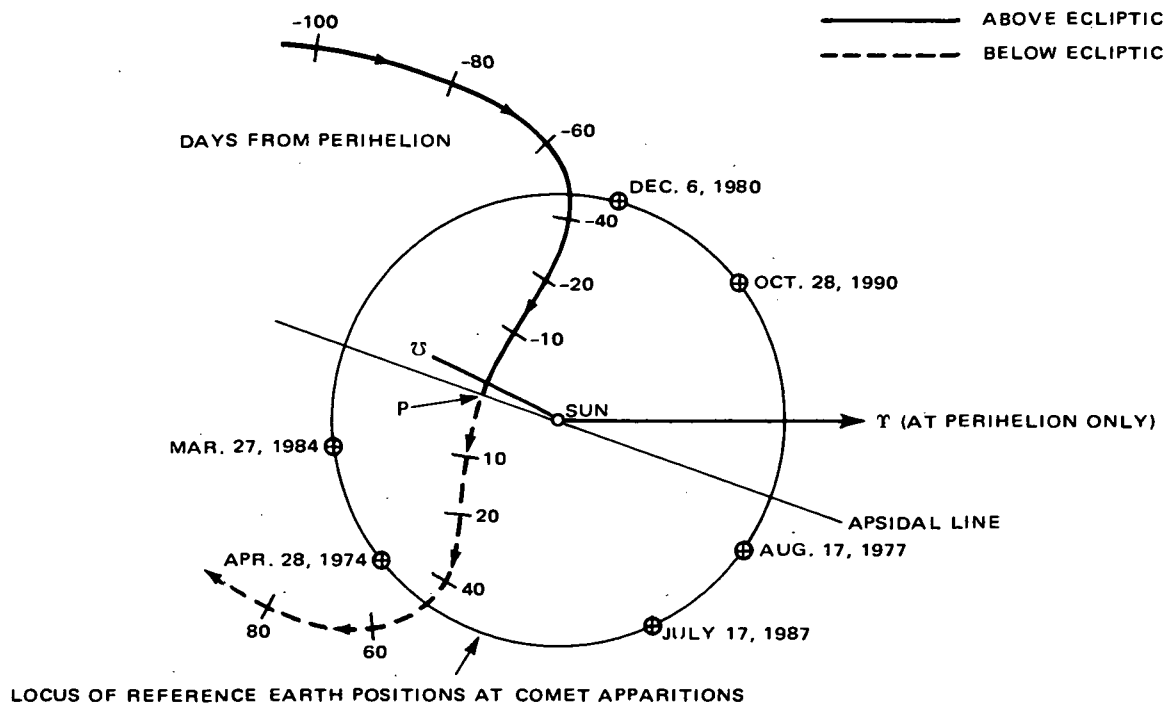

Figure 2. Orbit of Comet Encke in Bipolar Coordinates

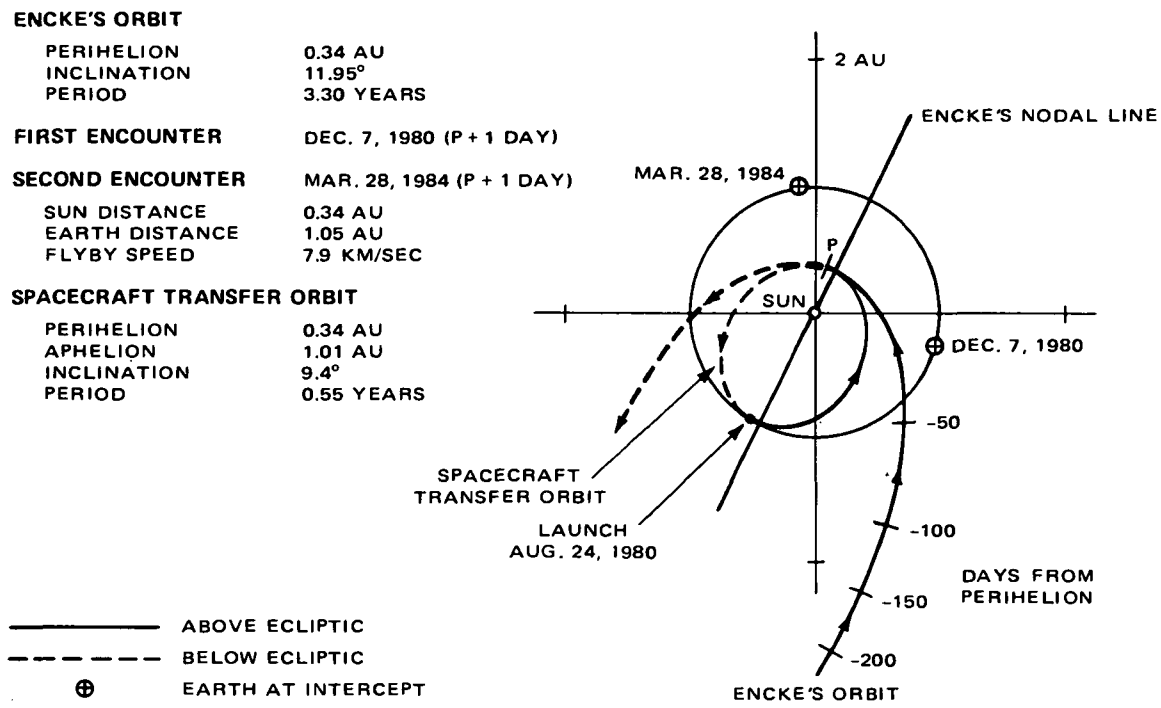

Figure 3. Encke Double Encounter, 1980-84

Table 2

Encke Mission Parameters for 10-Day Launch Window

	Nominal	Variation
Encounter Parameters		
Intercept Date	Dec. 7, 1980	Dec. 4 → 8, 1980
Sun Distance (AU)	0.34	0.34
Earth Distance (AU)	1.05	0.95 → 1.08
Phase Angle (Degrees)	77	53 → 86
Flyby Speed (km/sec)	7.9	7.6 → 8.9
Launch Parameters		
Launch Date	Aug. 24, 1980	Aug. 20 → 30, 1980*
Launch Energy-C_3 (km^2/sec^2)	89	87 → 92
Declination of Launch Asymptote (Deg.)	-0.9	-2.6 → 1.8
Payload System Weight (kg) (Titan-3E/Centaur)	845	760 → 900
Retargeting Maneuver for 2nd Encounter		
ΔV Requirement (m/sec)	130	120 → 162

*No Launch on August 27, 1980

The spacecraft trajectory near encounter is shown in Figure 4. Note the favorable geometry for spectrophotometric measurements of the coma/tail region before and after encounter. Mission plans call for a simultaneous intercept with two spacecraft (both probes are carried on the same launch vehicle). One probe will pass close to the nucleus on its sunward side, while the other traverses the tail region. The geometry for the dual-probe encounter is illustrated in Figure 5. The dual-probe scheme extends the mapping of Encke's structure to its longitudinal axis and prevents possible confusion between spatial and temporal variations.

The opportunity for a slow flyby of Encke near its perihelion in 1980 is truly exceptional. A comparable situation will not occur again until the year 2013.

B. Giacobini-Zinner and Borrelly, 1985-87

The second mission of the proposed sequence will be an intercept of Giacobini-Zinner in 1985. This mission is a perfect complement to the 1980 Encke encounter, and is further enhanced by the possibility of intercepting another comet (Borrelly in 1987) with the same spacecraft. The additional cometary encounter is attained by employing a novel earth-swingby technique that is described below.

Physical characteristics of Giacobini-Zinner are summarized in Table 3. A comparison of Tables 1 and 3 reveals sharp differences in the physical behavior of comets Encke and Giacobini-Zinner. Although scientific interest in Borrelly has not been as great as in Encke and Giacobini-Zinner, the information contained in Table 4 indicates that Borrelly is a well-observed comet.

The orbits of Giacobini-Zinner and Borrelly are given in Figures 6 and 7. From the bipolar plots, it can be seen that the geometry for earth-based observations of both comets will be quite good at these apparitions. It should also be noted that Giacobini-Zinner will be almost stationary with respect to the sun-earth line for approximately 100 days around its perihelion.

The mission profile for the Giacobini-Zinner intercept is shown in Figure 8. An encounter at the comet's descending node has been chosen to minimize the launch-energy requirement. By launching on March 10, 1985, the spacecraft will be placed into a trajectory that returns to the earth's vicinity after the Giacobini-Zinner intercept. As shown in Figure 9, this trajectory will be slightly modified by an earth swingby maneuver on March 10, 1986, and then more drastically changed by a second earth passage on August 20, 1987. After the second earth swingby, the spacecraft will be on its way towards an encounter with Borrelly on December 25, 1987. Mission parameters for the Borrelly encounter are listed in Figure 10. It is noteworthy that both encounters will take place fairly

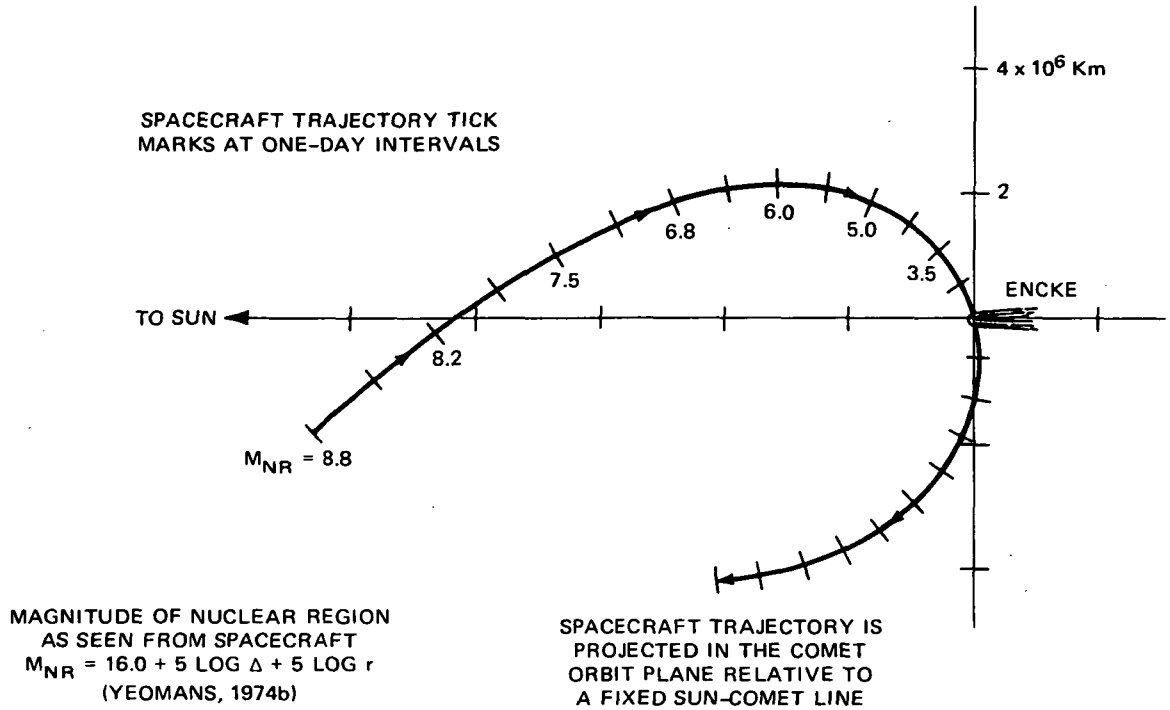

Figure 4. Encke Encounter Geometry

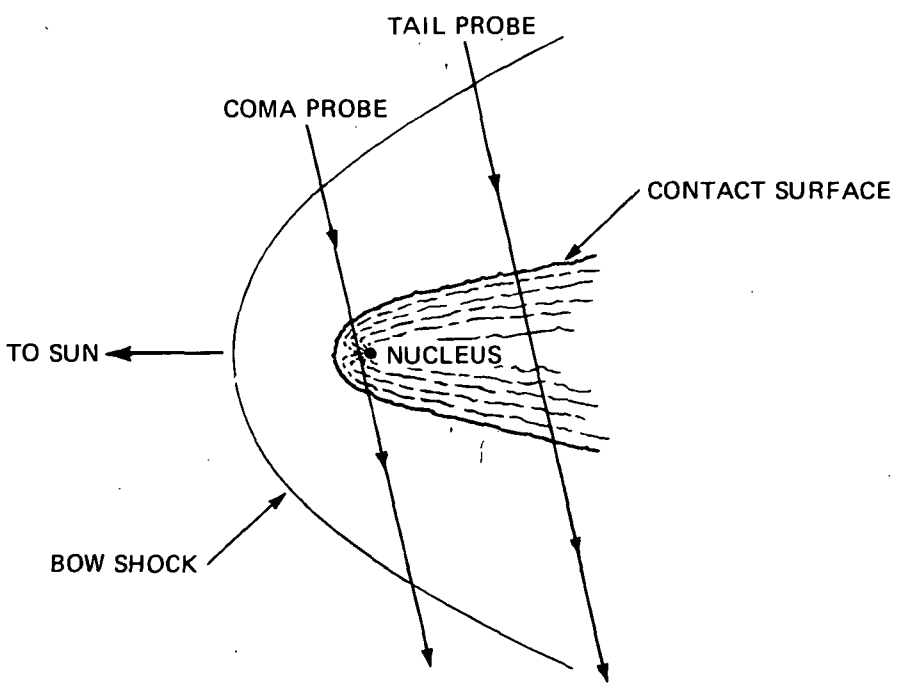

Figure 5. Dual-Probe Encounter Geometry

Table 3

Comet Giacobini-Zinner Summary

Observational History: Giacobini-Zinner has been observed at nine apparitions since its discovery in 1900. Because of unfavorable orbital geometry it was poorly observed at two apparitions (1940, 1966) and missed completely in 1907, 1920, and 1953. However, numerous observations of its behavior near perihelion were obtained in 1946, 1959, and 1972 when it passed relatively close to the earth. Giacobini-Zinner is one of the brightest periodic comets when it is near perihelion. It is noteworthy that the absolute luminosity of this comet appears to be constant or even increasing with time. Irregular brightness variations over periods of a few days have been reported.

Nuclear Region and Coma: A well-defined nuclear condensation develops near perihelion. Observations in 1972 suggest that Giacobini-Zinner possesses an inner and outer coma. The observable diameter of the outer coma is $\sim 5 \times 10^4$ km, while the diameter of the inner coma is about 2×10^4 km. The spectrum of Giacobini-Zinner shows a strong continuum which indicates a large dust component. The abundances of CN and C_2 radicals have been compared with Encke, and it was found that while the abundance of CN was approximately equal in both comets, the abundance of C_2 was greater for Encke.

Tail: A narrow straight tail begins to develop about three months prior to perihelion. Near perihelion, the observed tail length is $\sim 5 \times 10^5$ km. A dust tail has also been reported.

Dust: Giacobini-Zinner is quite dusty for a short-period comet. Its dust density is estimated to be about 50 times greater than Encke's but is probably 1000 times smaller than Halley's. The Giacobinid (or Draconid) meteor showers that are associated with Giacobini-Zinner have probably been the most spectacular meteor displays of the present century. These showers were particularly strong in 1933 and 1946. Studies by Jacchia et al. (1950) of the 1946 shower indicate that the Giacobinid meteors are abnormally fragile as compared with meteors from other showers.

Nongravitational Effects on Orbital Motion: A rigorous investigation by Yeomans (1971) has shown that Giacobini-Zinner's nongravitational forces have increased with time over the 1900-1965 interval. (This unusual characteristic is shared with Biela's comet which disappeared in 1852). The orbital motion of Giacobini-Zinner is somewhat erratic as indicated by the 1972 observations which imply that the nongravitational forces have decreased or stopped altogether. An apparent discontinuity in the comet's motion between 1959 and 1965 should also be noted.

Table 4

Comet Borrelly Summary

Observational History: Borrelly has been observed at nine apparitions since its discovery in 1904. Excellent orbital geometry during its first four apparitions (1905, 1911, 1918, 1925) produced a large number of observations. However, a perturbation by Jupiter in 1936 changed Borrelly's period, and the geometric conditions for near-perihelion observations have been poor ever since that time. Borrelly was not observed at all in 1939 and 1946. Fortunately, another perturbation by Jupiter in 1972 has again changed Borrelly's period so that favorable orbital geometry will be available in 1981 and 1987. From the numerous early observations, it has been well-established that Borrelly is quite active for a comet with a perihelion distance of about 1.4 AU.

Nuclear Region and Coma: A bright nuclear condensation has always been observed when favorable geometric conditions have existed. The observable coma diameter is $\sim 5 \times 10^4$ km. No spectroscopic observations have been reported.

Tail: A narrow bright tail has been observed during six of the apparitions, and generally persists for several months. Observed tail lengths are $\sim 5 \times 10^5$ km.

Dust: No data available.

Nongravitational Effects on Orbital Motion: The nongravitational forces affecting the motion of Borrelly have been investigated by Yeomans (1971). It was found that although Borrelly is affected by substantial nongraviational forces, the transverse component of the nongravitational acceleration has remained constant over the entire 70-year observational interval.

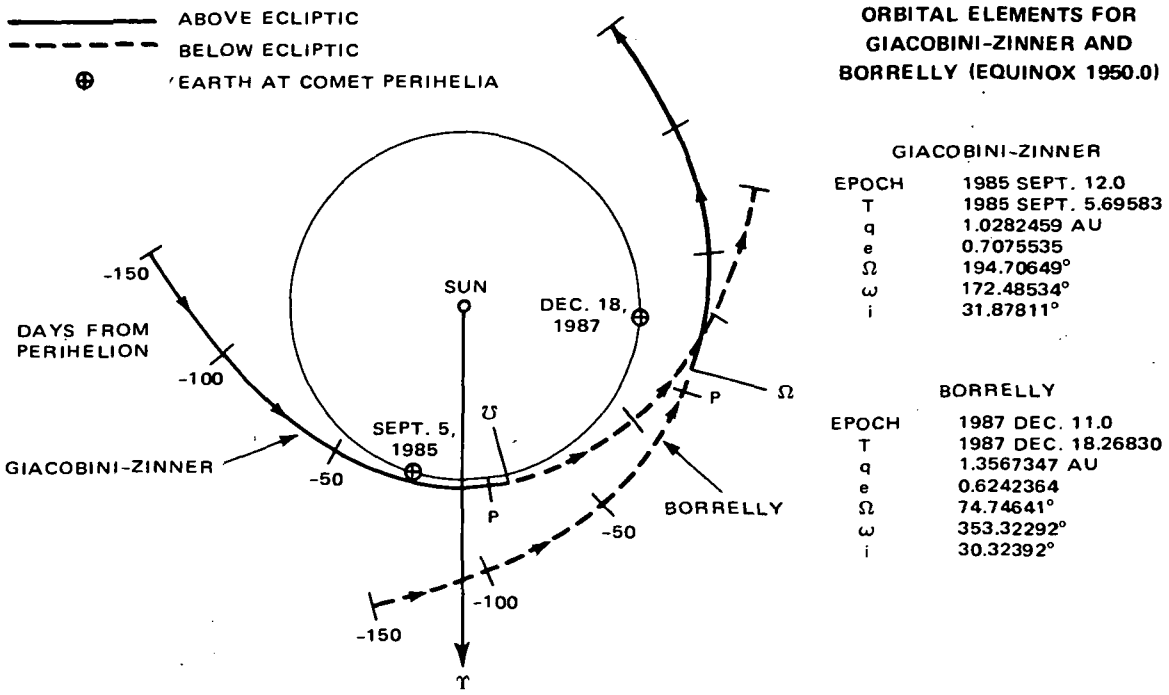

Figure 6. Orbits of Comets Giacobini-Zinner and Borrelly

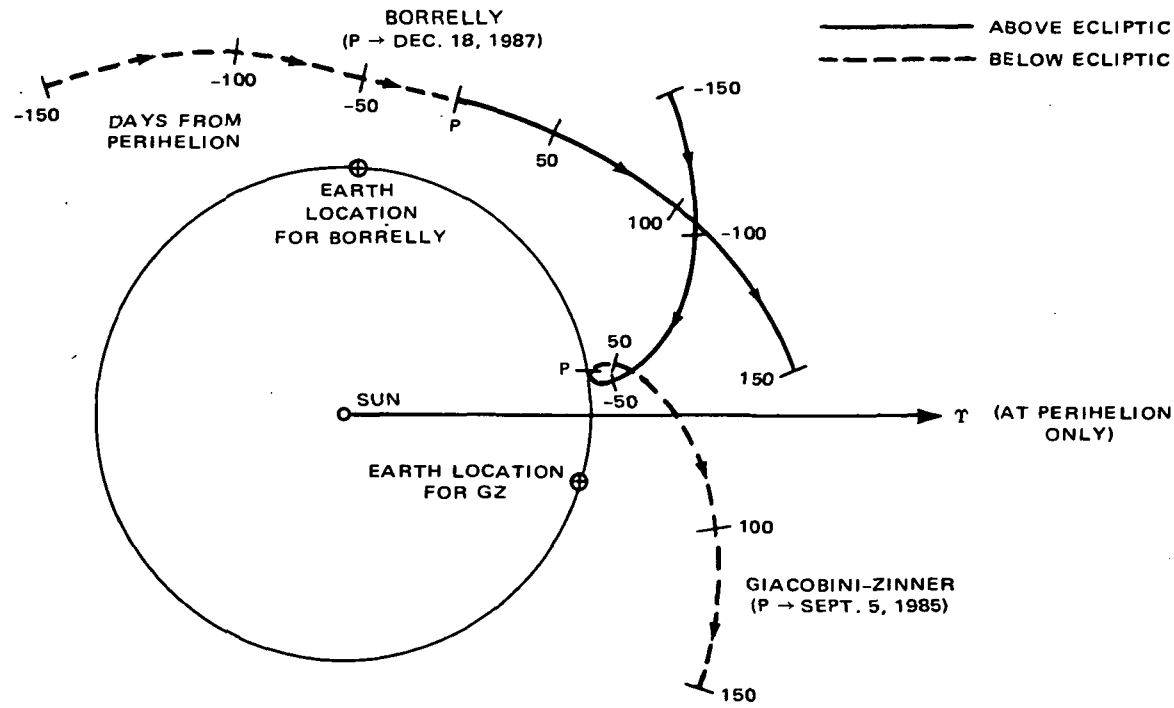

Figure 7. Orbits of Comets Giacobini-Zinner and Borrelly in Bipolar Coordinates

ENCOUNTER PARAMETERS

INTERCEPT DATE	SEPT. 11, 1985 (P + 6 DAYS)
SUN DISTANCE	1.03 AU
EARTH DISTANCE	0.46 AU
PHASE ANGLE	88.0°
FLYBY SPEED	20.6 KM/SEC

LAUNCH PARAMETERS

LAUNCH ENERGY - C_3	12.3 KM^2/SEC^2
DECLINATION OF LAUNCH ASYMPTOTE	-3.9°

SPACECRAFT TRANSFER ORBIT

PERIHELION	0.90 AU
APHELION	1.10 AU
INCLINATION	0.002°
PERIOD	1.00 YEARS

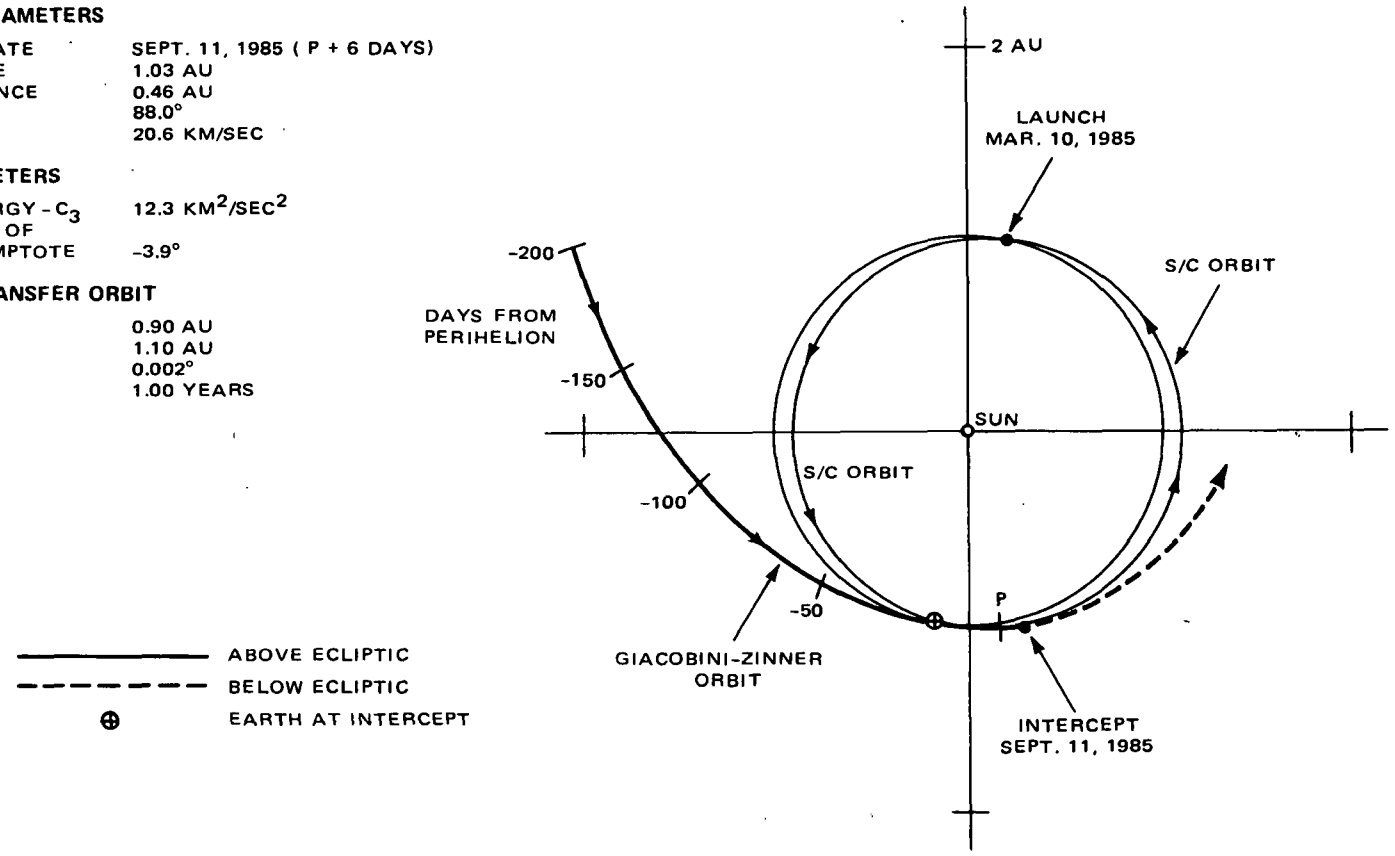

Figure 8. Mission to Giacobini-Zinner, 1985

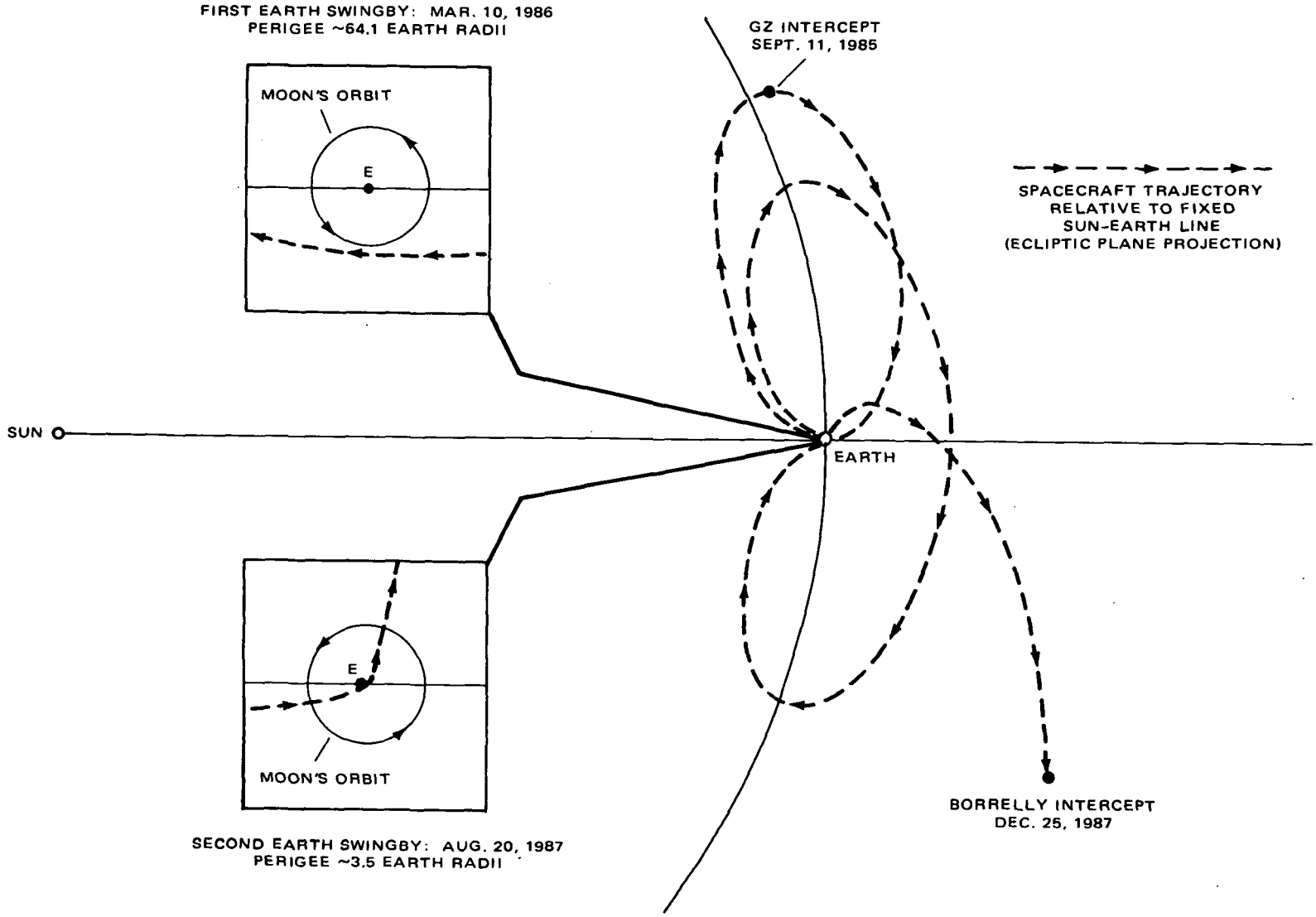

Figure 9. Nominal Mission Profile GZ → Borrelly, 1985-87

ENCOUNTER PARAMETERS

INTERCEPT DATE	DEC. 25, 1987 (P + 7 DAYS)
SUN DISTANCE	1.36 AU
EARTH DISTANCE	0.53 AU
PHASE ANGLE	74.7°
FLYBY SPEED	17.3 KM/SEC

SPACECRAFT TRANSFER ORBIT

PERIHELION	1.01 AU
APHELION	1.62 AU
INCLINATION	0.7°
PERIOD	1.51 YEARS

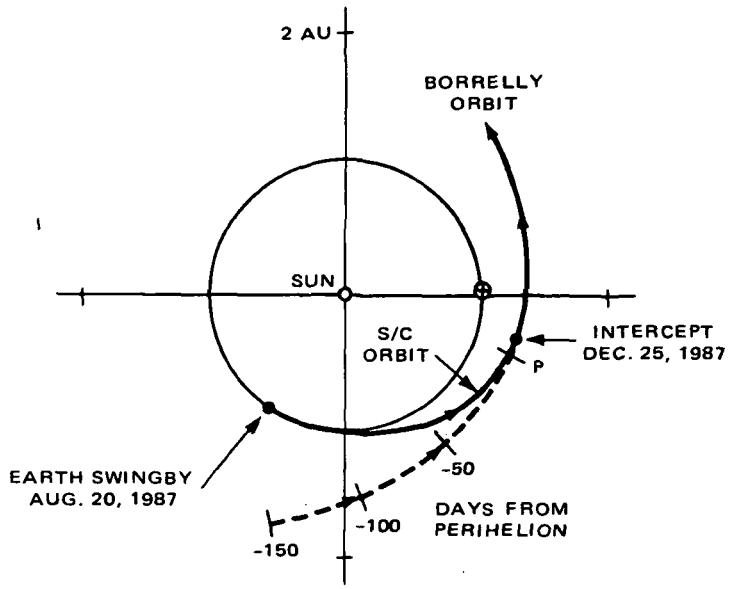

ABOVE ECLIPTIC

BELOW ECLIPTIC

⊕ EARTH AT INTERCEPT

Figure 10. Borrelly Encounter, 1987

close to the earth (~0.5 AU) and will also be near the cometary perihelia. Further details of this attractive multi-comet mission have been treated by Farquhar et al. (1975).

C. Halley, 1985-86

At present Halley is the only dramatically bright comet whose return can be accurately predicted. Unfortunately, flyby speeds for ballistic intercept missions to this comet will be very fast (>50 km/sec) due to Halley's retrograde orbit. However, because Halley is an extremely large comet, the time available for in situ measurements will be comparable to slow flybys of smaller comets. Of course, the fast flyby speed will create major problems for neutral mass-spectrometer measurements, but other experiments should not experience serious difficulties. Again, because Halley is a huge comet, it is uniquely suited for experiments concerning large-scale cometary phenomena.

Halley's physical characteristics are discussed in Table 5 and its orbit has been plotted in Figure 11. Nominal mission parameters are summarized in Figure 11 and Table 6. The exceptionally favorable orbital geometry in 1985-86 makes

Table 5

Comet Halley Summary

Observational History: Halley's comet has been seen at every apparition since at least 86 B.C., making twenty-seven appearances in all. It is a spectacular object displaying physical characteristics of a typical long-period comet, and was observed extensively during its 1910 apparition. Its exceptional brightness is indicated by the fact that naked-eye observations were recorded over a four-month interval at this apparition. Brightness estimates taken from the 1910 data imply that Halley's absolute luminosity is nearly two magnitudes brighter after perihelion.

Nuclear Region and Coma: Halley's very bright nuclear region has been estimated to be several thousand kilometers in diameter. The failure to observe a solid nucleus when Halley transitted the sun on May 18, 1910 gives an upper bound of 50 km to any solid nucleus for this comet. Diameters for the visible coma near 1 AU in the post-perihelion phase are $\sim 5 \times 10^4$ km for the inner coma and $\sim 3 \times 10^5$ km for the outer coma. The spectrum of the coma region is almost entirely CN and C_2 superimposed on a continuous background. Jets and streamers invariably showed CN specta. A number of transient phenomena were observed in the inner coma region. Explosive activity was particularly well established in April, May, and June 1910. Temporary secondary nuclei were observed to coalesce with the primary nucleus after a few hours or days.

Tail: Two well-developed tails were seen in 1910. One was primarily gaseous (CO^+), and the other was mainly dust. Near its maximum, the observed tail length was ~ 0.35 AU. Several tail condensations ("knots") were also observed.

Dust: Halley is a very dusty comet. Dust densities are probably 1000 times greater than those found in dusty short-period comets.

Nongravitational Effects on Orbital Motion: A rigorous examination of Halley's nongravitation accelerations has not been completed as yet. However, it is known that the nongravitational effects amount to an average lengthening of Halley's period by 4.1 days at each apparition (Kiang, 1972).

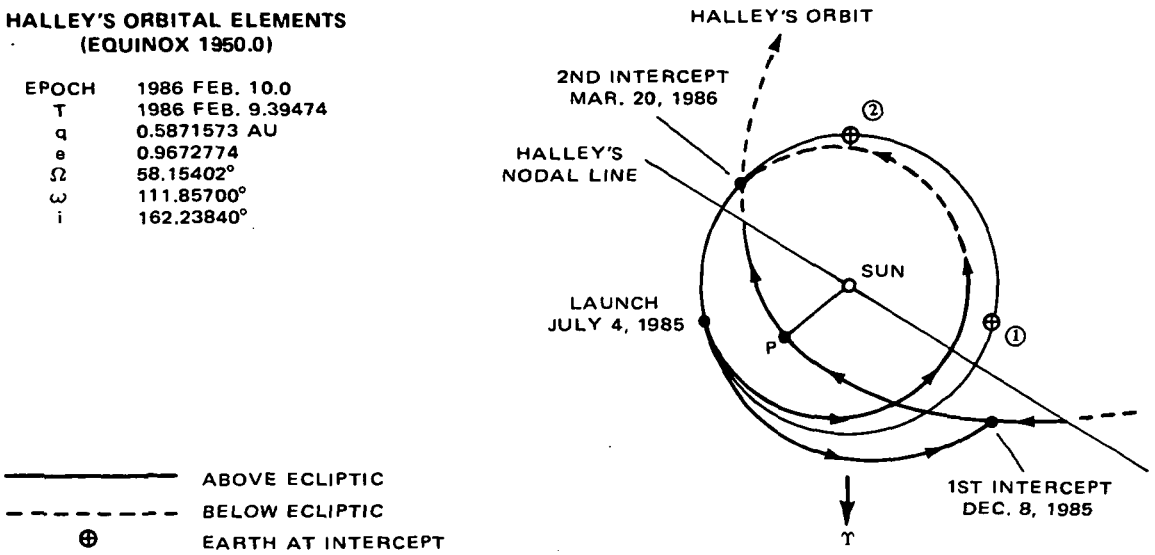

Figure 11. Dual Launch to Halley's Comet

Table 6

Nominal Parameters for Halley Mission*

	Pre-Perihelion Intercept (P -63 Days)	Post-Perihelion Intercept (P +39 Days)
Encounter Parameters		
Intercept Date	Dec. 8, 1985	Mar. 20, 1986
Sun Distance (AU)	1.37	1.00
Earth Distance (AU)	0.71	0.80
Phase Angle (Degrees)	57.7	112.2
Flyby Speed (km/sec)	55.3	64.5
Launch Parameters		
Launch Energy-C_3 (km^2/sec^2)	14.5	9.1
Declination of Launch Asymptote (Degrees)	33.5	54.3
Spacecraft Transfer Orbit		
Perihelion (AU)	1.01	0.81
Aphelion (AU)	1.44	1.03
Inclination (Degrees)	4.6	4.7
Period (Years)	1.40	0.88

*These parameters are fairly constant within a 10-day launch window. For example, throughout this period, the launch energy is <15.1 km^2/sec^2 for the pre-perihelion intercept and <9.4 km^2/sec^2 for the post-perihelion intercept.

it possible to intercept Halley before and after its perihelion passage (Michielsen, 1968). A common launch date has been selected for both the pre-perihelion and post-perihelion intercept trajectories to take advantage of the multi-payload launch capability of the "space shuttle" which should be operational in the early 1980's. The basic mission plan is to use a single shuttle launch to place two cometary spacecraft with attached solid rocket motors into a low earth parking orbit. Each solid rocket motor (fuel weight <2000kg) will be capable of injecting a 500-kg spacecraft into the specified Halley intercept trajectory.

Due to a lower flyby speed and a more favorable encounter geometry (see Figure 12), imaging science will be emphasized during the pre-perihelion intercept. Less dust obscuration of Halley's nucleus is also anticipated. Preliminary results from the pre-perihelion encounter will probably be used to optimize the targeting strategy for the post-perihelion encounter which will take place about 100 days later.

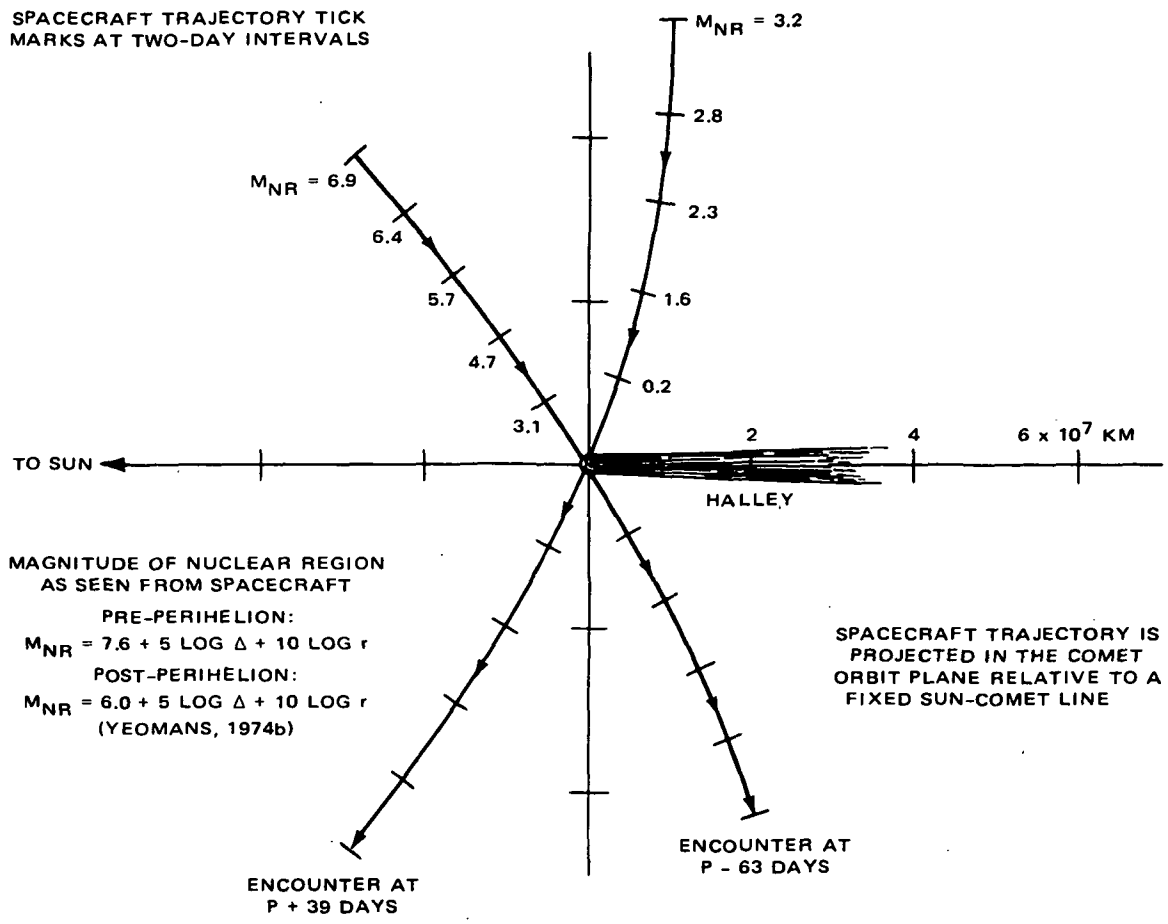

Figure 12. Halley Encounter Geometry

Correlative measurements in the coma and tail regions as well as dust experiments will have priority during the post-perihelion encounter. It is planned to release one or more small tail probes from the main spacecraft to effect a simultaneous multi-probe encounter (cf. Figure 5). Conditions for spectrophotometric measurements will probably be better during the post-perihelion encounter because Halley is expected to brighten considerably after perihelion.

V. GROUND-BASED OBSERVATIONAL SUPPORT AND TARGETING ERRORS

Observational support from earth-based telescopes can contribute significantly to the success of a cometary intercept mission. Space probe results will be complemented and better understood if ground-based measurements of the physical behavior of the target comet are recorded throughout the comet's apparition. Spectral coverage is especially desirable. For a large comet like Halley, photographs of the coma and tail regions, with a time resolution that is fast enough to track the motions of tail condensations, should be obtained.

Sighting conditions for all of the cometary encounters that were mentioned in the previous section are listed in Table 7. Notice the excellent conditions for northern-hemisphere observations of Giacobini-Zinner, Borrelly, and Halley (pre-perihelion). Post-perihelion observations of Halley must be obtained at southern-hemisphere sites, but adequate dark time is available. The lack of prime dark time at the Encke encounter is not surprising because it is always difficult to observe Encke near its perihelion.

Of major importance, are the astrometric measurements which will be needed to reduce cometary ephemeris errors. At least one measurement every ten days from recovery to encounter will suffice, but more-frequent measurements are recommended. To be useful during the mission, these measurements should be processed within a few days time.

Cometary ephemeris inaccuracies are the principal source of spacecraft targeting errors at encounter. Using simulated cometary observations, targeting errors for all the proposed encounters have been determined and the results are presented in Table 8. Analyses and assumptions used to obtain the error ellipses given in Table 8 are discussed in various papers (Farquhar et al., 1974, 1975; Yeomans, 1974a; Yeomans and Laubscher, 1975). Computations of the error ellipses for Encke, Giacobini-Zinner, and Borrelly have assumed that only earth-based measurements will be used to reduce the cometary ephemeris errors. If smaller errors are desired, it will be necessary to augment the earth-based measurements with measurements taken from the spacecraft (on-board navigation). It is clear that on-board navigation will be required for the Halley encounters. However, with the possible exception of Encke 1984, the targeting errors for the remaining cases are quite acceptable.

Table 7

Ground-Based Observations

Comet Encounter	Estimated Recovery Date	Site Latitude	Prime Dark Hours*		
			E -50 Days	Encounter	E +50 Days
Encke Dec. 7, 1980	July 9, 1980 Magnitude = 20.5 r = 2.43 AU Δ = 2.33 AU	35°N	6.0	—	—
		35°S	—	—	—
Encke Mar. 28, 1984	Oct. 5, 1983 Magnitude = 19.1 r = 2.54 AU Δ = 1.55 AU	35°N	—	—	—
		35°S	—	—	2.5
Giacobini-Zinner Sept. 11, 1985	Apr. 19, 1985 Magnitude = 18.2 r = 2.03 AU Δ = 1.76 AU	35°N	6.0	2.7	1.6
		35°S	—	0.2	3.8
Borrelly Dec. 25, 1987	Aug. 10, 1987 Magnitude = 16.7 r = 1.97 AU Δ = 1.42 AU	35°N	10.5	6.3	5.0
		35°S	—	2.4	—
Halley Dec. 8, 1985	Feb. 14, 1985 Magnitude = 17.7 r = 4.87 AU Δ = 4.43 AU	35°N	5.5	5.0	—
		35°S	2.0	2.0	—
Halley Mar. 20, 1986	Same as above	35°N	—	—	2.2
		35°S	—	1.9	5.6

*The comet is more than 25 degrees above the observer's horizon and the sun is simultaneously below the horizon by more than 18 degrees.

Table 8

Targeting Errors

Comet Encounter		Targeting Error Ellipse (1-σ)*		Miss Distance** (km)	
		Semi-Major Axis (km)	Semi-Minor Axis (km)	Nominal	Maximum
Encke Dec. 7, 1980		574	141	582	824
Encke Mar. 28, 1984		1712	154	608	1817
Giacobini-Zinner Sept. 11, 1985		427	250	800	1050
Borrelly Dec. 25, 1987		894	360	1020	1380
Halley Dec. 8, 1985	Without On-Board Navigation	3537	1297	2894	4570
	With On-Board Navigation†	1614	350	1000	1872
Halley Mar. 20, 1986	Without On-Board Navigation	10254	2349	4998	11410
	With On-Board Navigation†	637	421	1142	1563

*The error ellipse is located in the impact plane which is normal to the relative-velocity vector at encounter.

**An exclusion zone with a radius of 300 km has been assumed.

†A measurement noise of 10 arcseconds (1-σ) was assumed. Measurements are taken once every 12 hours from E-10 days to E-3 days.

The spacecraft miss distance at encounter is a function of the targeting strategy as well as the size of the cometary error ellipse. As shown in Figure 13, the nominal aim point has been chosen to guarantee that the spacecraft will not enter an exclusion zone around the nucleus even when targeting errors reach 2-σ levels. The exclusion zone has been specified to prevent possible damage to the spacecraft from large dust grains in the vicinity of the nucleus. To minimize the miss distance, the error ellipse should be oriented so that its minor axis passes through the nucleus.

VI. CONCLUDING REMARKS

The proposed mission sequence is outlined in Table 9. Notice that only three launches are required for the six cometary encounters. Additional features of this mission sequence are:

- Physical characteristics of the target comets cover a wide range of cometary behavior.
- The observational history of the target comets is extensive.
- There is ample time following the 1980 Encke encounter to incorporate the knowledge gained from the first mission into the design of an optimum science payload for the 1985 missions.

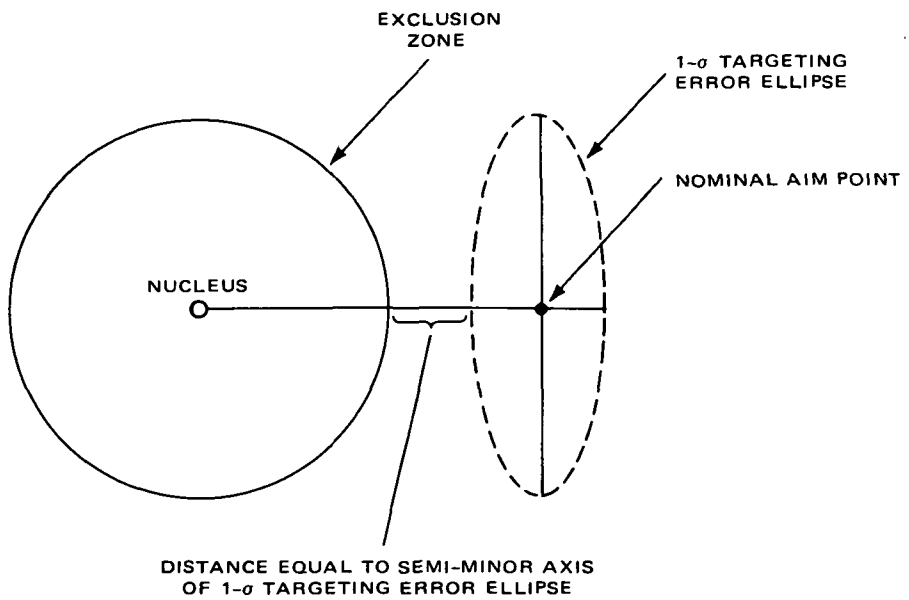

Figure 13. Targeting Geometry in Impact Plane

Table 9

Proposed Mission Sequence

Launch	Encounter	Flyby Speed (km/sec)
August 1980 Titan-3E/Centaur	Encke → Dec. 7, 1980 Encke → Mar. 28, 1984	7.9 7.9
March 1985 Shuttle/Solid Stage	Giacobini-Zinner → Sept. 11, 1985 Borrelly → Dec. 25, 1987	20.6 17.3
July 1985 Shuttle/Solid Stage (2)	Halley Pre-Perihelion → Dec. 8, 1985 Halley Post-Perihelion → Mar. 20, 1986	55.3 64.5

- Because of favorable earth-comet orbital geometry for Encke 1980, Giacobini-Zinner 1985, and Borrelly 1987, cometary ephemeris errors can be reduced to very small values with earth-based measurements alone. In other words, mission success will not be dependent on an on-board navigation system.

- Excellent earth-based sighting conditions exist for the entire 1985 mission set. All of the target comets are very bright.

- The 1985 mission set could be carried out at a relatively small cost. A common design could be used for the required spacecraft (three in all) because the operating range for all of these missions will be between 0.8 and 1.4 AU from the sun (~0.5 to 1.5 solar constants). Furthermore, the launch-vehicle costs will also be rather modest. Only two shuttle flights (or equivalently, three Delta-3914 launch vehicles) will be needed.

Finally, I wish to make a special plea for early consideration of the very-rare Halley mission opportunity by appropriate science advisory groups. The appearance of this famous comet in 1985-86 will generate considerable scientific and public interest. Therefore, it is imperative that serious planning for sending space probes to Halley begin in the near future.

REFERENCES

Farquhar, R. W., and N. F. Ness (1972), Two Early Missions to the Comets, Astronaut. & Aeronaut. 10, 32-37.

Farquhar, R. W., D. K. McCarthy, D. P. Muhonen, and D. K. Yeomans (1974), Mission Design for a Ballistic Slow Flyby of Comet Encke 1980, NASA TN D-7726.

Farquhar, R. W., F. I. Mann, D. P. Muhonen, and D. K. Yeomans (1975), Multi-Comet Intercept Missions Via Earth Swingby, NASA Report (in preparation).

Jacchia, L. G., Z. Kopal, and P. M. Millman (1950), A Photographic Study of the Draconid Meteor Shower of 1946, Astrophys. J. 111, 104-133.

Kiang, T. (1972), The Past Orbit of Halley's Comet, Mem. Roy. Astron. Soc. 76, 27-66.

Kresak, L. (1973), Short-Period Comets at Large Heliocentric Distances. Bull. Astron. Inst. Czech. 24, 264-283.

Marsden, B. G., and Z. Sekanina (1974), Comets and Nongravitational Forces. VI. Periodic Comet Encke 1786-1971, Astron. J. 79, 413-419.

Michielsen, H. F. (1968), A Rendezvous with Halley's Comet in 1985-1986, J. Spacecr. Rockets 5, 328-334.

NASA (1973), The 1973 Report and Recommendations of the NASA Science Advisory Committee on Comets and Asteroids, NASA TM X-71917.

Roberts, D. L., ed. (1971), Proceedings of the Cometary Science Working Group, Yerkes Observatory, June 1971.

Yeomans, D. K. (1971), Nongravitational Forces Affecting the Motions of Periodic Comets Giacobini-Zinner and Borrelly, Astron. J. 76, 83-86.

Yeomans, D. K. (1974a), Orbital Error Analysis for Comet Encke 1980, Proceedings of IAU Colloquium No. 25, Oct.-Nov. 1974.

Yeomans, D. K. (1974b), Magnitude Laws of Nuclear Regions for Seven Short-Period Comets, Computer Sci. Corp. Internal Document.

Yeomans, D. K., and R. E. Laubscher (1975), Orbital and Physical Data For Selected Periodic Comets, NASA Report (in preparation).

SCIENCE ASPECTS OF 1980 BALLISTIC MISSIONS TO COMET ENCKE, USING MARINER AND PIONEER SPACECRAFT

L. D. Jaffe, C. Elachi, C. E. Giffin, W. Huntress, R. L. Newburn, R. H. Parker, F. W. Taylor and T. E. Thorpe

Introduction

This paper considers science aspects of a 1980 spacecraft reconnaissance of Comet Encke. The mission discussed is a ballistic flyby (more exactly, a fly-through) of P/Encke, using either a spin-stabilized spacecraft, without despin of instruments, or a 3-axis-stabilized spacecraft. Celestial mechanics and imaging aspects of such a mission have been considered in more detail by Bender (1) and by Jaffe et al (2), respectively. Engineering designs[1] (3, 4) and more detailed accounts of science aspects[2,3] are given in other documents. A different approach to an Encke ballistic flyby has been suggested by Farquahar et al (5). Yeomans (6) has considered ephemeris uncertainties associated with such missions.

Objectives and Observables

Science objectives that appear appropriate to this mission are:

To determine the existence of a cometary nucleus and, if it exists, its dimensions and albedo.

To determine the primary composition and concentration of neutral gases and ions in the coma and tail.

---

1. J. W. Moore et al, "A 1980 Mariner Encke Ballistic Mission Study." Not yet issued, Jet Propulsion Laboratory, California Institute of Technology, Pasadena (internal document).

2. L. D. Jaffe, C. Elachi, C. E. Giffin, W. Huntress, R. L. Newburn, R. H. Parker, F. W. Taylor, T. E. Thorpe, "Science Aspects of a 1980 Flyby of Comet Encke with a Pioneer Spacecraft," Doc. 760-96, Jet Propulsion Lab., California Institute of Technology, Pasadena, 1974 (internal document).

3. L. D. Jaffe, D. Bender, R. O. Hughes, B. R. Markiewicz, and T. E. Thorpe, "Imaging on Ballistic Missions to Comet Encke," Doc. 760-112, Jet Propulsion Lab., California Institute of Technology, Pasadena, 1974 (internal document).

To determine the composition and concentration of solid particles in the coma and tail.

To determine the nature of the interaction of the coma and tail with the solar wind.

These objectives have been discussed by the Comet and Asteroid Mission Study Panel[4] and by Clay et al[5].

With a mission of this kind, it does not appear practical to determine detailed topography of the nucleus, or its temperature, mass, or spin, or to measure the temperature of an icy halo, if one exists[1,2]. With a spinning spacecraft (camera not despun), it is impractical to assure imaging at 100-m feature resolution, but there is some chance of a very few pictures at this resolution, depending on luck in not suffering a destructive dust hit when very close to the (postulated) nucleus[2,3] (2). With a 3-axis-stabilized spacecraft (or despun camera on a spinning spacecraft), feature resolution significantly better than 100-m should be possible[1,3] (2).

Trajectory and Encounter Geometry

It is felt that encounter should be prior to perihelion passage of Encke, at 0.4-0.9 AU from the sun. Encounters later in the apparition would have the disadvantages of a major decrease in coma size and a probable decrease in comet activity. Important in this regard is evidence (7)

---

4. Comet and Asteroid Mission Study Panel, "Comets and Asteroids: A Strategy for Exploration," NASA TM X-64677, National Aeronautics and Space Administration, Washington, D. C., 1972.

5. D. Clay, C. Elachi, C. E. Giffin, W. Huntress, L. D. Jaffe, R. L. Newburn, R. H. Parker, P. W. Schaper. F. W. Taylor, T. E. Thorpe, B. Tsuritani, "Science Rationale and Instrument Package for a Slow Flyby of Comet Encke," Doc. 760-90, Jet Propulsion Lab., California Institute of Technology, Pasadena, 1973 (internal document).

that the activity of Encke has often dropped significantly before. perihelion passage. Thus, an encounter at or after perihelion. seems likely to result in obtaining significantly less extra-nuclear data than one some days before perihelion. This consideration is quite independent of the engineering factor that the launch energy required for the spacecraft is lower for an earlier encounter than for one at or soon after perihelion (1).

Examination of the celestial mechanics (1, 3) suggests desirability of a launch in August 1980, when the Earth is close to the plane of Encke's orbit (Fig. 1). Encounter options near 0.4, 0.55, and 0.8 AU from the sun have been specifically examined: The dates are 8, 16, and 30 days prior to Encke perihelion (which will be on 7 Dec. 1980), and the spacecraft velocities relative to the comet at encounter[1,3] (1, 2) are 12, 18 and 27 km/s. The approach is from almost directly sunward of the comet (Fig. 2).

The spacecraft should fly through the shock front (sunward of the coma), the coma, the tail, and, if possible, the contact surface (if one exists) between the solar wind and the ionized cometary gas. Imaging of the nucleus should be from the sunward hemisphere and from as close as is reasonably safe, to improve resolution. Mass spectroscopy should be carried out as close to the nucleus as is reasonably safe - if possible, within 500-1000 km - to assure that the concentration of some minor constituents is measurable. The minimum distance of safe approach is presumably limited by the hazard of cometary dust impacts on the spacecraft. A preliminary calculation using the most conservative of several Encke models suggested by Taylor et al (8) indicated that the hazard is tolerable with a minimum distance of 500 km.

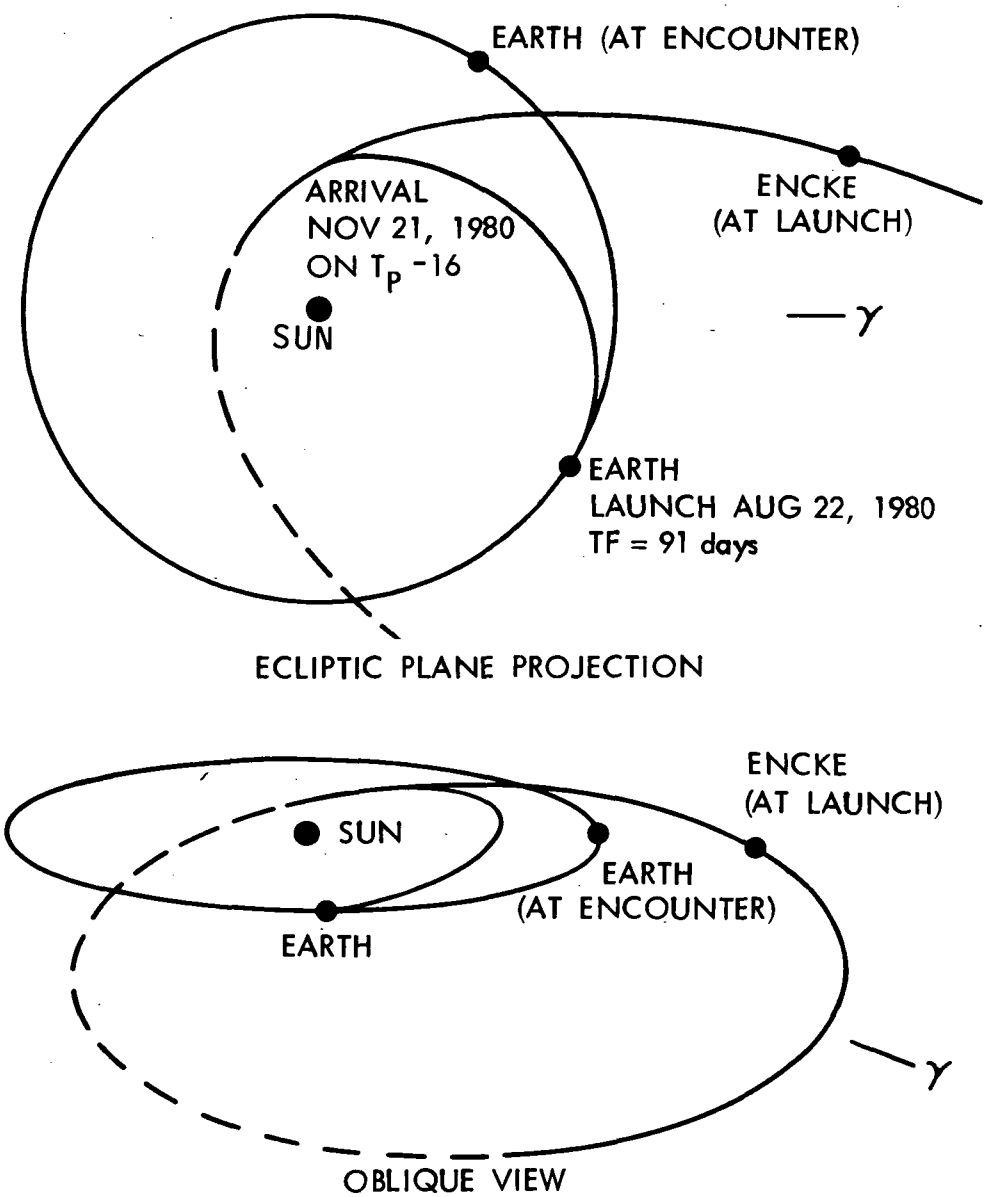

Fig. 1. Encke orbit with typical spacecraft trajectory. After Bender (1).

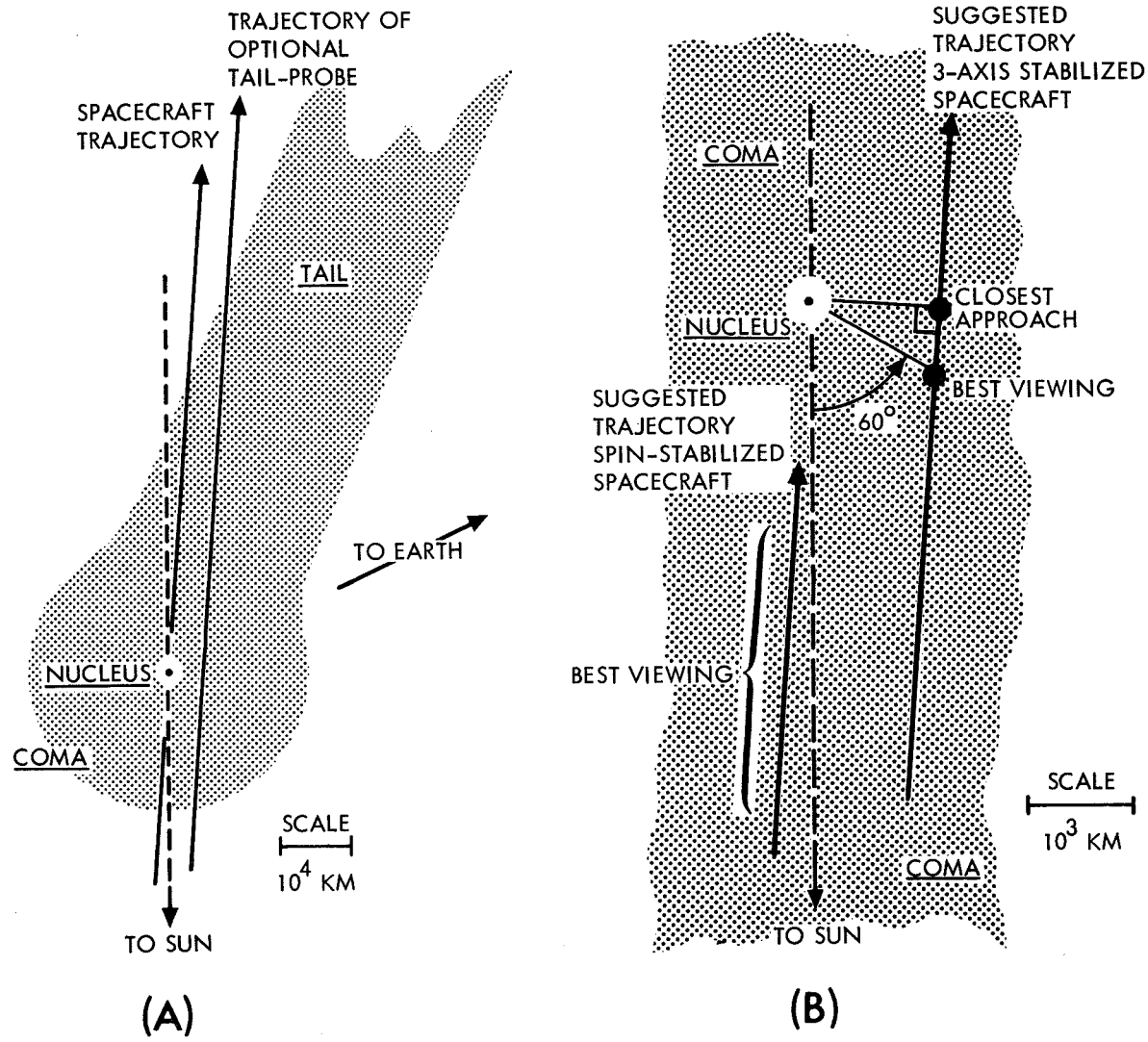

Fig. 2. Suggested encounter geometries. (B) is an enlargement of (A). Nucleus is not to scale.

A number of targeting options have been considered[1,2,3] (2). For a spin-stabilized spacecraft, it is recommended that targeting be directly at the nucleus (not expecting to hit it). Pictures of the nucleus would be taken as the spacecraft approaches to within 2000-5000 km. This targeting minimizes the slewing rate required for pointing any given distance, thus simplifying pointing and improving resolution of the television camera and of other instruments using near-optical wavelengths. Closed-loop pointing control should not be required[3] (2); indeed suitable pointing systems have not yet been developed for operation from a spinning mount. The trajectory chosen provides data closest to the nucleus for mass spectrometry and other in-situ measurements. It may involve relatively high hazard from cometary dust during closest approach. Therefore, a probe separated before encounter and transmitting data directly to Earth may be worthwhile to obtain data on the tail in case the spacecraft is damaged; this probe could fly by several thousand kilometers from the nucleus, where the risk is relatively low (Fig. 2). Even without the tail probe, the risk to the spacecraft is probably acceptable, on the basis of current information[1].

For a 3-axis-stabilized spacecraft, targeting to a nominal flyby distance of about 700 km is suggested. This is close enough to provide reasonable chance of observing parent molecules and of detecting minor constituents by mass spectroscopy, but far enough to keep the hazard from dust quite low. A 60° phase angle will give good discrimination of nucleus surface features; with this geometry it will be attained at about 800 km range and provide, with the cameras recommended, optical resolution considerably better than 100 m. Closed-loop nucleus optical sensing and

tracking will be needed to keep the cameras properly pointed at close ranges; such systems have already been flown successfully on Mariners 6 and 7. The spacecraft passes through a position where the phase angle is 0^{o} as it approaches the nucleus; this provides a phase angle range of 0^{o} to 90^{o} or greater for photometry. With a pre-selected target point biased away from the nucleus, it is relatively simple to design the spacecraft scan-platform so that its field-of-view can include the nucleus at encounter[1,3] (2).

The uncertainties in the ephemeris of P/Encke (6) are such that, for either of these targeting options, sightings of the comet from aboard the spacecraft will be needed during approach, with a terminal maneuver calculated from these sightings[3] (2). The science imaging devices suggested below should also be satisfactory for optical navigation, furnishing images of the nucleus against a star background starting at least four days before encounter.

If a spinning spacecraft is used, performance of several instruments is considerably enhanced if the spin axis orientation is approximately along the relative velocity vector during approach. (This is approximately equivalent to: directly away from the sun.) Optical axes can then be pointed very close to the spin axis, reducing the rate of image motion across the sensors. This greatly increases the effective sensitivity of optical and U.V. instruments during approach, as compared, for instance, with a spin axis orientation perpendicular to the ecliptic or toward the Earth. With the latter arrangement, it may be difficult to obtain enough sensitivity to sight the nucleus against a star background at sufficient range for a terminal maneuver[1,2] (2). A low spin rate during approach is also desirable to improve sensitivity; a higher spin rate at close

approach may be worthwhile to increase scan rates and therefore information rates. Science return could be increased by despinning a camera or a science platform, but this technique seems inconsistent with the simplicity that generally characterizes a spin-stabilized spacecraft; such an alternative is considered in Ref. (3). Typical payloads are suggested in Table 1. For a spinning spacecraft, two imaging devices are suggested: (a) a framing camera with a charged-coupled device as the sensor and a 50 cm focal length f/1.5 telescope, to view the nucleus, and, (b) a spin-scan imaging photometer to view the coma. The framing camera would have at least 200 X 200 picture elements and include image motion compensation. For a 3-axis-stabilized spacecraft, two vidicon cameras are suggested, one with a 50-cm focal length f/2.35 telescope, the other with a 150 cm focal length f/8.34 telescope. These would be modified from existing Mariner 9 and 10 cameras by providing a commandable part-frame (250-line) imaging mode, reducing the frame interval to 30 s per camera or 15 s for the pair. Use of a tape recorder is considered undesirable, since stored data would be lost if the spacecraft were damaged near closest approach. Thus, it is suggested that all data be transmitted in real time, over a communications link (considered practical) of 120 kb/s for the 3-axis spacecraft and 20 kb/s for the spin-stabilized[1,2,3] (2). Detailed characteristics of the imaging devices are considered in Ref (2); appropriate spectral filters for coma, tail, and nucleus should be included.

A UV spectrometer should be carried on either spinning or non-spinning spacecraft. For the non-spinning, a water vapor profiler (pressure-modulated IR radiometer) to measure H_2O in the coma is also suggested. A neutral-gas mass spectrometer with retarding potential, and an ion mass spectrometer,

TABLE I

TYPICAL SPACECRAFT PAYLOAD

Instrument	Mass kg	Power w	Average data rate at encounter, b/s	Typical technology base
For 3-axis-stabilized payload only				
2 vidicon cameras				
Wide-angle (50-cm focal length, f/2.35)	38	33	108,000	Mariner 9 camera B
Narrow-angle (150-cm focal length, f/8.34)				Mariner 10
Infrared water-vapor profiler	3	2	10	Nimbus G pressure-modulated radiometer
For spin-stabilized payload only				
Charge-coupled-device framing camera (50-cm focal length, f/1.5, 200 X 200 elements)	19	13	13,000	New
Imaging photometer	4	3	205	Pioneer 10
For both 3-axis and spin-stabilized payloads				
Ultraviolet spectrometer	3	3	500	Venus Pioneer
Neutral gas mass spectrometer with retarding-potential ion mass spectrometer	5	9	250	Venus Pioneer
Impact-ionization time-of-flight mass spectrometer	4	8	100*	Helios
Optical particle detector	5	3	100*	Pioneer 10
Micrometeoroid penetration detector	2	1	400*	Pioneer 10
Magnetometer	2	3	200	Pioneer 10
Plasma probe	5	5	200	ALSEP
Langmuir probe	3(2)†	5(3)†	350(200)†	OGO-6
Plasma wave detector	5	5	300	OGO-6
Total, 3-axis-stabilized	75	77	110,000	
Total, spin-stabilized	56	56	15,000	
For flyby probe only (optional add-on for spin-stabilized)				
Mass spectrometer	5	9	45	Venus Pioneer**
Magnetometer	2	3	25	Pioneer 10
Plasma probe	5	5	25	ALSEP
Langmuir probe	2	3	25	OGO-6
Total, optional flyby probe	14	20	120	

*Peak rates are higher; must be buffered.

†Values in parentheses are for spin-stabilized.

**New if velocity selector is included.

or a combined neutral/ion instrument is recommended for either spacecraft type. Retarding potential is needed for neutrals both to discriminate against material originating from the spacecraft (such as attitude-control gas) and to prevent contributions from cometary species which have impacted chamber walls at velocities that caused dissociation[1,2].

An impact-ionization time-of-flight mass spectrometer would analyze impacting cometary dust particles. An optical dust detector and a micrometeoroid (penetration) detector would be worthwhile. For charged-particle and field measurements, a magnetometer, plasma probe, Langmuir probe, and plasma wave detector are proposed. Characteristics of the non-imaging instruments are suggested in other documents[1,2]. The mass of the typical payload would be 55-75 kg, its power consumption 55-80 w.

An optional separable tail-probe might carry a mass spectrometer (perhaps with velocity selector[6]), magnetometer, plasma probe and Langmuir probe, with power consumption of 20 w, and a total bit rate for the tail-probe of 128 b/s.

Certain other instruments warrant further consideration. For example, a gas-cell type of Lyman-alpha photometer might give D/H ratios if it can be established that the H atoms are thermalized rapidly enough to provide a narrow line-width. Perhaps higher-energy charged particles should be measured.

Some attention need be paid to compatibility of instruments. The spacecraft magnetometer would probably be mounted on a boom. This might not be practical for a small tail-probe and the effect of mass-spectrometer fields on the magnetometer would have to be considered.

---

6. M. Neugebauer, A. Bratenahl, D. R. Clay, B. E. Goldstein, T. W. Unti, H. D. Wahlquist, "A Preliminary Study of Cometary Plasma Spectrometers." In preparation.

Imaging for navigation purposes would start four to ten days before encounter. The terminal maneuver, to bring the spacecraft near the nucleus, would occur 1.5 to 2 days before encounter. If no nucleus were identified by two days prior to encounter, the terminal maneuver should be targeted at the maximum brightness of coma or halo, and a search sequence started; this search should detect (though not resolve) particles as small as 1 m in diameter at ranges of 10,000 km or more[3]. An encounter science sequence would normally start after the terminal maneuver. The period of maximum science operations would last only about one hour. If a separable tail probe is used, its instruments should operate until about ten hours after closest approach, to provide data through the tail.

The spin-stabilized spacecraft, with 3-sigma errors in navigation and pointing, would be expected to provide pictures at a range of 5000 km. The corresponding pixel size would be 250 m and the imaging resolution 600 m. With 1-sigma errors, pictures should be obtainable to 1700 km range, with a pixel size of 80 m and imaging resolution of 200 m. The 3-axis spacecraft, with pointing control, should provide pictures at a range of 800 km or less, with a pixel size of 25 m and 8 m for the two cameras and corresponding image resolution of about 60 and 30 m. These resolution figures take into account smear during exposure. Over 600 pictures with a 4-km nucleus subtending 10 pixels or more, and at phase angle less than 130^{o}, should be obtained with the 3-axis spacecraft and an 0.4 AU encounter, without using a tape recorder. With either spacecraft, the proposed gas mass spectrometer would provide[1,2], at an 0.4 AU encounter, a spatial resolution of 120 km for individual neutral and ion species and of 12 km for total number densities at detection thresholds of 5000 neutrals/cm^3 and 0.002 ions/cm^3.

This work was supported by the National Aeronautics and Space Administration under Contract NAS 7-100.

References

1. D. Bender, "Encke Ballistic Flybys in 1980," AIAA Paper 74-782, AIAA, New York, 1974.

2. L. D. Jaffe, D. Bender, R. O. Hughes, B. R. Markiewicz and T. E. Thorpe, "Imaging on Ballistic Missions to Comet Encke," AIAA Paper 75-87, AIAA, New York, 1975.

3. W. Bursnall, "Ballistic Mission to the Comet Encke in 1980 - A New Phase of Solar System Exploration," Proc. 11th Space Congress, Canaveral Council of Technical Societies, Cocoa Beach, Florida, 1974.

4. K. T. Nock and C. M. Yeates, "Early Mariner Comet Flyby," AIAA Paper 75-198, AIAA, New York, 1975.

5. R. W. Farquahar, D. K. McCarthy, D. P. Muhonen and D. K. Yeomans, "Mission Design for a Ballistic Slow Flyby of Comet Encke 1980," NASA TN D-7726, National Aeronautics and Space Administration, Washington, 1974.

6. D. K. Yeomans, "Orbital Error Analysis for Comet Encke," this volume, 1975.

7. Z. Sekanina, "A Continuing Controversy: Has the Cometary Nucleus Been Resolved?", this volume, 1975.

8. F. W. Taylor, C. M. Michaux, R. L. Newburn, Jr., "A Model of the Physical Properties of Comet Encke," Tech. Rept. 32-1590, Jet Propulsion Lab., California Institute of Technology, Pasadena, 1973.

DISCUSSION

F. L. Whipple: This week's symposium has substantiated in detail our objectives for cometary missions as developed over the last few years but with one important new addition: the urgent need for more data about the chemical and physical conditions in the region very close to the nucleus (say 100—400 km). Gas-phase chemistry now appears to be critical among the cometary processes. Hence we should attempt to go as close to the nucleus as is reasonably safe.

L. Jaffe: This would involve a 'gap' in the imaging at closest approach due to a problem in slewing the camera rapidly. Also, the data transmission should then be in real-time so as to prevent loss of data if the spacecraft were destroyed by dust impact.

L. Biermann: I would like to reemphasize that the plasma experiments on a cometary mission enable us to study an example of the applicability of magneto-hydrodynamics as we understand it to an object which is quite different from the solar wind itself.

Plasma physics is applied to many problems in astrophysics, and only very rarely do we have occasion to test the theory by direct in-situ measurements. So I believe one should not just ask is there or is there not a contact surface, but rather is our present setup of magneto-hydrodynamics adequate or not in giving at least a rough representation of the situation which we really find.

SCIENTIFIC POSSIBILITIES OF A SOLAR ELECTRIC POWERED RENDEZVOUS WITH COMET ENCKE

Ray L. Newburn, Jr., C. Elachi, F. P. Fanale, C. E. Giffin, L. D. Jaffe, R. H. Parker, F. W. Taylor and T. E. Thorpe

INTRODUCTION

The present observational problem of understanding the nature and origin of comets is analogous to that we would face in attempting to understand a planet and its atmosphere if we possessed only data on its ionosphere and exosphere. Virtually everything we can observe remotely is a part of the rapidly escaping gas and dust atmosphere of the comet.

In situ studies of the coma and tails of a comet and their interactions with the interplanetary medium can readily be achieved by so-called fast ($V_{relative} > 5$ km s^{-1}) flybys, as has been detailed in other papers at this colloquium. The flyby can also settle any lingering doubts about the reality of a compact nucleus in comets. Any pretense to real knowledge of the structure, composition, and activity of the comet itself, however, depends upon an ability to study the nucleus for some days at a range such that it fills a large solid angle as seen from the spacecraft. Studies of the mineralogical, chemical, and isotopic makeup of cometary solids, studies of great importance in solar system cosmology, can be made upon the dust flowing from it, but only if the relative velocity of the dust is sufficiently low to allow its capture, intact, for analysis. Details of the chemical and physical processes in the inner coma also are likely to remain poorly understood until given extended, careful study. These requirements define clearly the need for a true rendezvous with a cometary nucleus, an approach to a few tens of kilometers at essentially zero velocity for an extended period. This report summarizes the study of such a mission carried out at the Jet Propulsion Laboratory early in 1974.

MISSION ANALYSIS

The selection of target comets and the vehicles for their study have been the subject of numerous reports. In every such report P/Encke has been high on the target list, usually highest. Some of the reasons for this have been summarized by Atkins and Moore (1). The study reported here assumed a 1984 encounter with P/Encke, but it is equally applicable to a 1990 encounter, and the qualitative conclusions are applicable to other potential targets such as P/Temple 2 or P/d'Arrest. Unfortunately they are NOT applicable to P/Halley, rendezvous with that prestigous object requiring a swing-by of Jupiter and six to eight years flight time (2).

The only technology currently available which makes it possible to rendezvous with comets is solar electric propulsion. Rendezvous by means of a multiple impulse ballistic trajectory is possible in principle, but such a rendezvous with P/Encke, for example, requires 4-5 km s^{-1} of midcourse propulsion capability with propellants that can be stored for several years (3). No such hardware exists or is planned.

Trajectories for a solar electric propelled flight to rendezvous with P/Encke typically have aphelia of $2\frac{1}{2}$ to 4 AU and flight times of $2\frac{1}{2}$ to 3 years (4). Encounter was assumed to be 40 days before perihelion (at just under 1 AU heliocentric distance) in this study, although earlier rendezvous is possible. Scientific requirements, which follow, indicated a minimum period of 20 days near the nucleus was needed, and this presents no design difficulties. In fact it is believed that survival through perihelion is possible in a low-power, non-thrusting mode, with another period of 20 or more days of scientific study of the nucleus beginning about 20 days after perihelion.

The approach to the nucleus of an SEP spacecraft is a very gradual thing. The maximum acceleration that such a craft can develop is $\sim 4 \times 10^{-4}$ ms^{-2}. The approach to the nucleus is roughly from the direction of the Sun in comet centered reference. In heliocentric reference, the spacecraft is nearer the Sun than the comet but moving toward it more slowly. The spacecraft accelerates to the same velocity as the comet just as the comet finally reaches the same heliocentric distance as the spacecraft. At no time is the spacecraft in the comet tail during approach, and since the available acceleration is so low, excursions into the tail are not practical unless the nucleus is to receive only cursory study. It was assumed in this study that in fact Encke's tail had been studied on a prior flyby and that the rendezvous would be devoted to study of the fundamental problems of the composition and structure of the nucleus itself.

Terminal guidance will be based upon information gained by optical imaging beginning at least 50 days before encounter. Two thousand kilometers from the nucleus an X-band radar will begin to furnish range and velocity information for the final day of approach. Closest approach might be $\sim$10 km at a relative velocity certainly <5 ms^{-1}. An ordinary radar altimeter would measure the velocity to 1-2 ms^{-1}. Coherent radar could reduce this to <0.1 ms^{-1}.

The mission strategy at this point becomes somewhat uncertain because of lack of knowledge of P/Encke itself. If Encke has a nominal mass of 10^{16}g attracting the spacecraft and an outflow of $2\pi x10^{27}$ molecules of H_2O per second repelling it, as implied by the measurements of Bertaux, et al. at 0.7 AU (5), then the net force should be attractive, and it might be possible to go into an orbit of some 5 days period. At best this would be a rather irregular orbit, since the gas flow must vary from day to night side of the nucleus and may be quite non-uniform even on the day side. Also the spacecraft cross-section presented to the outflowing gas will vary greatly, since the majority of that cross-section is solar panels which remain oriented toward the Sun. Certainly the spacecraft could be flown in a series of essentially linear trajectories past the nucleus, with a course reversal at the maximum acceptable range. It might even be possible to "hover" over the nucleus, if its mass is at least 10^{16} grams. (At 10^{16} grams the gravitational acceleration would be only $6.7x10^{-6}$ ms^{-2} at 10 km distance, but this is within the throttling capability of a single continuously operating solar electric thruster on a typical rendezvous spacecraft.) A closest approach of 10 km is certainly practical, as is some form of maneuvering designed to keep the spacecraft within a few hundred kilometers of the nucleus.

No landed probe was considered seriously in this study, primarily because of the obvious increase in cost it would entail. Such a probe could be built, but considerable delicacy of control might be needed to land it, since the escape velocity from the nucleus is probably about 1 ms^{-1}. In situ analysis or sample return were considered to be follow-on missions whose design (and even need) would be determined by the rendezvous flight.

SCIENTIFIC OBJECTIVES AND INSTRUMENTATION

The primary objective of the first comet rendezvous must be a detailed study of the structure, composition, and activity of the nucleus. The secondary objective is to understand the chemical and physical processes occurring in the icy halo or innermost coma, the region within 1000 km of the nucleus. Another objective may be additional study of the interaction of the comet with the solar wind as the spacecraft traverses the coma, assuming it can be made sufficiently electromagnetically quiet with the thrusters operating or that they can be turned-off at times.

Imaging

The primary information about the nucleus (size, shape, rotation, axial inclination, topography, spatial variation of albedo, color, photometric function, polarization) that can be obtained by means of remote sensing will come from the imaging system. The possibilities can best be illustrated by two systems. The existing Mariner 9 Camera B with 50 cm $f/2.35$ optics would offer a scale of 0.3m per pixel (picture element) at a distance of 10 km from the nuclear surface. At 0.7 AU heliocentric distance, unfiltered, there would be less than one picture element of smear for a signal to noise ratio of 50, even at 90° phase for a reflectivity of only 2% at a transverse velocity of 4 ms^{-1}. Realistically, the imaging detector of choice in the mid-80's is unlikely to be the selenium vidicon (of Mariner 9 use). The most likely detector for use in that period is a charge-coupled device (CCD) having a 750x750 element array within a format 2.3x2.3 cm. With a 100 cm focal length $f/5$ telescope, the resolution on the nucleus would be the same as for the Mariner 9 system. In spite of the increased focal length at the same aperture, the CCD detector has enough sensitivity to give slightly less smear than the vidicon under the same conditions and has better linearity for improved photometric accuracy. It is also lighter, cheaper, and simpler. The CCD is therefore accepted as the probable flight instrument, but existing hardware could perform the mission.

Complete coverage of a 4 km diameter nucleus would require about 1000 exposures with either camera. The 1000 exposures could be taken one every 84 seconds (the standard cycle time of existing cameras) and transmitted in about 50 seconds with 8 bit per pixel encoding. Complete "photographic" coverage would be taken in one day in a hovering mode, if the nucleus rotates in about one day, with adequate communications available for the other scientific experiments without storing any data on tape. Since coverage in more than one color or polarization and at more than one phase angle is certainly desirable, and since several complete surveys to look for changes with heliocentric distance would be valuable, a minimum mission duration of about 20 days is needed.

Radar

Radar is absolutely necessary for at least one extremely important scientific purpose, namely scaling all of the observations. Radar is the best way to determine the distance from spacecraft to nucleus on a rendezvous mission. Besides range

(and rate) data, the radar will measure the surface dielectric constant and the surface roughness. It may also make possible a mass determination as discussed separately. The radar could be designed to undertake other measurements such as detection of ejected debris and nuclear rotation, but it would be difficult to detect debris smaller than 20 cm, which is roughly the upper limit expected from Encke, or a rotation period slower than a few hours, so even limited complication probably is not warranted.

The system contemplated is an X-band radar transmitting peak power of 5 Kw (average power 5w) with a 50 cm antenna mounted on a scan platform with the other pointed instruments. This should permit simple detection of the nucleus at a range of about 2000 km. The signal to noise ratio would be 17 db at 500 km, which is probably the maximum distance from the nucleus that the spacecraft might attain after once having rendezvoused, no matter what maneuvering strategy is used.

Mass Determination

Mass is one structural parameter of great importance that is not easy to determine. A coherent radar can measure the radial velocity of the spacecraft relative to the comet to an accuracy better than 10^{-1} ms^{-1}. With the thrusters off, this would allow a measurement of the acceleration of gravity plus aerodynamic drag. The aerodynamic forces can be minimized by operating near the sunrise limb of the nucleus where evaporation of volatiles from the comet will be a minimum as will be the spacecraft cross-section as seen from the comet. (At sunrise the solar panels, which constitute 90% of the maximum spacecraft cross-section, are edge-on to the comet.) Perhaps the drag can be modeled and calibrated, if the flow field is not too irregular. At worst a lower limit to the mass can be determined. A possible complication is a nucleus of highly irregular shape.

The radar would be operated in a coherent mode only within about 50 km of the nucleus and only for the express purpose of mass determination. An extra electronic module weighing less than 5 kg and perhaps 15w of power would be the only requirements added to the standard radar.

No consideration was given to a gravity gradiometer because of the complications introduced by the complex non-gravitational forces. This possibility should be investigated further.

IR Radiometer

A quantitative understanding of the physical processes occurring on the surface of the nucleus will require several thermal maps of the nucleus at different heliocentric distances. Use of multiple spectral intervals is needed to provide the highest sensitivity over a range of temperatures and to measure the wavelength dependence of the emissivity of the nuclear material. The temperatures themselves are an important parameter in determining the exact nature of the surface activity, the energetics of the release of volatiles, as well as giving an indication of volatile composition. Temperature variation with phase angle and heliocentric distance will provide a measure of thermal inertia of the surface layer.

The Viking Infrared Thermal Mapper (IRTM) is suitable for this job virtually without change. A minor electronic change to allow for the possibility of higher temperatures than those expected on Mars is all that would be absolutely required, although new fabrication techniques giving lower mass would probably be utilized as well and are reflected in the summary table. This instrument would have a spatial resolution of 50m at a distance of 10 km from the surface. The spectral ranges are 0.3-3.0 μm, 6.0-8.0 μm, 8.0-9.5 μm, 9.5-13.0 μm, and 18.0-24.0 μm. The accuracy of measurements would be better than 1K for targets warmer than 150K, most of the uncertainty being in the radiometric calibration.

IR Spectrometer

Frozen condensates such as H_2O, CH_4, NH_3, CO_2, etc. have very characteristic reflection spectra in the near infrared. Although it is assumed that volatile composition will be well determined by mass spectrometry, the uniformity of their condensed phase distribution on the nuclear surface might well give important hints about the process by which that nucleus was formed. Further, should Encke exhibit some bare core, as Delsemme and Rud suggest may be the case (6), then these scans could be compared to the various asteroid and meteorite types. Therefore a filter wedge spectrometer is included in the instrument complement.

The instrument proposed here is a new design, though having features in common with the Nimbus 4 filter wedge spectrometer. An $f/3.5$ telescope of 15 cm aperture supplies energy to a continuously variable annular filter wedge. The filter is made in three pieces with three detectors, a PbS detector covering 0.6-3.0 μm, a

PbSe detector covering 3.0-3.5 μm, and a HgCdTe detector covering 3.4-6.0 μm. All are held at 180K by radiation cooling. The spectral resolution $\Delta\lambda/\lambda$ is about 1%. The field of view is 3 mrad, thus giving 30m resolution at 10 km. Under the worst possible assumptions of 2% reflectivity at 1.0 AU heliocentric distance, the signal to noise ratio is still 200 for a 10 second integration at 3.5 μm.

Mass Spectrometer

It is anticipated that a neutral mass spectrometer will still be one of the key experiments on the rendezvous mission. Although an earlier flyby also will have carried such an instrument, it is likely that any parent molecules or intermediate species with scale lengths less than 500 km or abundances less than 10^{-3} of water at best barely will have been detected. Many new parent species and most accurate abundances will remain to be determined. Since there is strong evidence for molecular and ionic interactions deep in cometary comae, it may also be desirable to operate for a time with the ionizing electron beam off to measure ambient ion densities in the inner coma.

Mass spectrometer operation during a rendezvous has many advantages. Relatively high gas densities and long integration times are most important. Days rather than seconds are available. Very near the nucleus, ions and radicals should be at a minimum, which will reduce instrumental interactions with the medium. There will be no molecular fragmentation from high velocity impacts. A rendezvous spacecraft has degassed in interplanetary space for almost three years. Xenon gas from the attitude control jets and mercury (fuel) and molybdenum (grid material) from the thrusters should cause no problem even if the spectrometer inlet is not perfectly "shadowed".

A double focusing magnetic sector type mass spectrometer, embodying an integrating electro-optical detector sampling all masses simultaneously, is recommended for the mission. A mass resolution of 100 over the mass range 1-100 amu is easily attained. It will certainly be possible to detect species present at a density of 100 cm^{-3}, and a 10% measurement of such a species could be made in a tenth of a day or less. This is an abundance only about 10^{-8} that of water at 10 km from the nucleus and 0.7 AU heliocentric distance. Ion sensitivities of 0.1 cm^{-3} are available.

Solids Analysis

A proper analysis of cometary solids is the most difficult experiment proposed here, but it could also prove the most valuable. If comets originate within the solar system, as there is increasing evidence may be the case (7,8,9), then cometary solids should be the least altered primitive solid material man is likely to have a chance to investigate which originated in the outer parts of the solar nebula. Obviously isotopic, chemical, and mineralogical analyses are all desireable.

Since the relative velocity of spacecraft and solids must be less than that of the outflowing cometary gas relative to the nucleus (a few hundred meters per second), several techniques appear feasible for capture of the solids, including mechanical trapping in foils and porous targets or by electrostatic trapping. Experimental work will be needed to define the best technique, taking into account the requirement that the captured material must then be transferred to the analytical apparatus.

For this mission it is suggested that the analyzer consist of a scanning electron microscope, an alpha-particle analyzer (including proton detectors), and an energy-dispersive X-ray analyzer. The X-rays for the last instrument would be produced by the electrons from the microscope and by the alphas from the α-particle instrument. These instruments in an integrated package will produce an elemental analysis of light and heavy elements at any point in the field of view, images of continuously variable magnification from 50x to 40,000x with great depth of field and an average analysis of all the collected material. Mineralogical identifications are routinely made from such data.

This complete analysis package remains to be developed. Commercial scanning electron microscopes are available in almost the size and weight needed, but these have never been packaged for spaceflight. X-ray and α-particle instruments have flown but not in the form needed. Since the first flight of this package probably is still 12-15 years in the future, an orderly development would seem no problem, but the development should not be put off too long.

Optical Particle Detector

The amount of non-volatile material in comets is known far less well than the volatile abundance. Abundance and size distribution of dust (smaller than $\sim$40 μm) can be estimated from the behavior of dust tails (10,11,12), but P/Encke itself has never exhibited a dust tail. The existence of larger debris can be inferred

from radar observations of shower meteors associated with known comets (the β-Taurids with Encke), but it is not necessarily true that the average activity of many past apparitions as represented in the meteor stream is characteristic of activity today. Direct observations are needed. A satisfactory experiment can be expected on the precursor flyby, but it seems worthwhile to measure the solid particle flux over a period of time, both pre- and post-perihelion if possible, and to look for association of particles with particular areas of the nuclear surface, assuming the latter is not completely homogeneous. The priority of this experiment is lower than those described previously, however.

On a rendezvous mission, dust will be impacting the spacecraft continuously at very low velocity. While probably not directly damaging, some concern must be taken to maintain clean optical surfaces on several experiments, and direct measurement of the dust flux might even be associated with the required rate of "window washing". Model calculations indicate that the impact of larger particles (>1 mm) should be no greater than about one per hour per square meter, and some form of optical particle detector will be required to give good statistics.

The concept of remote optical detection of small particles was brought to fruition by Soberman and coworkers in "Sisyphus" (13). In principle "Sisyphus" can determine range, velocity, and the reflectivity-cross section product for each particle which moves into its field of view. Operational problems with the first flight units were not intrinsic to Soberman's basic idea, and practical units can be flown. Rejection filtering against the brightest cometary emission features can be used to reduce the background "noise" of the cometary environment. Looking away from the nucleus, a range to radius ratio of 10^5 should be practical, allowing detection of a 2 mm diameter particle at a distance of 100m or a 2 cm particle at 1 km. Detailed design and operational strategy of this instrument will depend heavily on prior experience gained in the fast flyby.

Magnetometer and Plasma Probe

As noted earlier, the rendezvous mission is designed to study the immediate environment of the nucleus. It will cross the shock front and contact surface (if such exist) on approach to the comet at relatively low velocity, however, 400m s^{-1} at $2x10^5$ km and 125m s^{-1} at $2x10^4$ km. This will offer an opportunity to map any relatively abrupt plasma discontinuities in more detail than can be achieved in a fast flyby at 8 to 26 km s^{-1} velocity. In fact, current models

indicate a contact surface may only be 100 km from the nucleus of Encke, too close for a flyby to penetrate. Further, some comets have shown high amounts of ionization apparently extending virtually to the nucleus (14). While P/Encke is certainly no Comet Humason, some simple, reliable means of determining ion densities clear into the nucleus in search for anomalous (non-photo) ionization seems warranted, and where there is organized motion of ions there are fields. Finally, although it may appear that any intrinsic magnetic field associated with a cometary nucleus is improbable, an attempt to set a limit on such a field is not totally without merit, considering our lack of "real" knowledge of the nature of comets. Type I carbonaceous chondrites are magnetic.

A magnetometer and a plasma probe offer simple, reliable measurements of field strength and ion density for a relatively modest mass allotment. Both instruments may be limited to some extent by having to function on an operating solar electric propelled vehicle. It probably will not be practical to go below a field strength stability of $\pm 0.1\gamma$ with a mast of practical length carrying the magnetometer. Ions near the lower end of the plasma probe's 5 ev - 3 kev range may have their paths deviated by the thruster plume, although the spacecraft remains electrically neutral. This will be particularly true when the plume directly opposes the plasma flow. In the event that something interesting is found, it would be possible to turn off the thrusters for a few hours, of course. While additional instruments might prove useful, we felt their inclusion to be an unwarranted expenditure of mass and money on this second generation mission designed primarily for study of the cometary nucleus. Information from the precursor flyby could easily change this conclusion.

CONCLUSIONS

We have considered the minimum scientific instrumentation likely to result in as complete an understanding of the composition, structure, and activity of a cometary nucleus as is possible without landing on it. That payload is summarized in Table I. The payload will also give useful results on secondary goals of a better understanding of physical processes in the inner and outer coma. Studies of composition, by means of an actual landing on the surface, details of the internal structure of the nucleus, and sample return were considered beyond the scope of this mission.

Table I. Summary of a Baseline Payload for P/Encke Rendezvous

Instrument	Weight (kg)	Power (watts)
Imaging	18	15
Radar	10.5	average 45
Coherent Radar	5*	15*
IR Radiometer	9.3	average 10.5
IR Spectrometer	9	6
Mass Spectrometer	5.3	10
Solids Analysis Package	20 ?	50 ?
Optical Particle Detector	5	3
Magnetometer	2+	3
Plasma Probe	5	6
	89.1	163.5

* requirements in addition to those listed under Radar, if there is to be a nuclear mass determination

+ not including weight of the mast

The payload of Table I seems well within the capability of a solar electric propulsion system in the 15-20 kw (at 1 AU) class (4), and there is no other obvious solution to the problem of its delivery. The material presented here is a brief summary of one aspect of cometary mission studies undertaken by the authors and other staff members of the Jet Propulsion Laboratory during the past two years. We hope that this work will help to provide a better understanding of the great scientific potential of a rendezvous mission in the field of cometary studies.

REFERENCES

(1) Atkins, K. L. and J. W. Moore, Cometary Exploration: A Case for Encke, AIAA Paper No. 73-596, Denver, Colo., July, 1973.

(2) Friedlander, A. L., Halley's Comet Flythrough and Rendezvous Missions via Solar Electric Propulsion, Report No. T-28, IIT Research Inst., Chicago, May 1971.

(3) Hollenbeck, G. R., and J. M. Van Pelt, Study of Ballistic Mode Comet Encke Mission Opportunities, NASA CR-137524, Martin Marietta Corp., Denver, Colo., Aug. 1974.

(4) Sauer, C. G. Jr., Trajectory Analysis and Performance for SEP Comet Encke Missions, AIAA Paper No. 73-1059, Lake Tahoe, Nev., Nov. 1973.

(5) Bertaux, J. L., J. E. Blamont, and M. Festou, Interpretation of Hydrogen Lyman-Alpha Observations of Comets, Astron. & Astrophys. 25, 415-430, 1973.

(6) Delsemme, A. H., and D. A. Rud, Albedos and Cross-sections for the Nuclei of Comets 1969 IX, 1970 II, and 1971 I, Astron. & Astrophys. 28, 1-6, 1973.

(7) Marsden, B. G., and Z. Sekanina, On the Distribution of "Original" Orbits of Comets of Large Perihelion Distance, Astron. J. 78, 1118-1124, 1973.

(8) Everhart, E., Examination of Several Ideas of Comet Origins, Astron. J. 78, 329-337, 1973.

(9) Delsemme, A. H., Origin of the Short-period Comets, Astron. & Astrophys. 29, 377-381, 1973.

(10) Finson, M. L. and R. F. Probstein, A Theory of Dust Comets. I. Model and Equations, Astrophys. J. 154, 327-352, 1968.

(11) Finson, M. L. and R. F. Probstein, A Theory of Dust Comets, II. Results for Comet Arend-Roland, Astrophys. J. 154, 353-380, 1968.

(12) Sekanina, Z. and F. D. Miller, Comet Bennett 1970 II, Science 179, 565-567, 1973.

(13) Grenda, R. N., W. A. Shaffer, and R. K. Soberman, Sisyphus - A New Concept in the Measurement of Meteoric Flux, XIXth International Astronautical Congress, Vol. I - Spacecraft Systems, pp 245-258, Pergamon, 1970.

(14) Greenstein, J. L., The Spectrum of Comet Humason (1961e), Astrophys. J. 136, 688-690, 1962.

DISCUSSION

J. C. Brandt: Can we afford the "grandiose" mission you have presented?

R. L. Newburn: I think we can afford it, if we can afford a space program. I think this is important enough in the time frame we are now considering that yes, we can now afford it.

W. F. Huebner: If large refractory grains are expected in the coma of Encke, then snow-grains will also be present which make seeing very difficult.

R. L. Newburn: We may get a good mass determination for the small material coming off by noting how often we have to operate our windshield washers on the imaging system.

M. Mumma: Wells et al., have studied the 'blizzard' problem for the 1980 flyby missions of Comet Encke. They found that the Mie-scattered sunlight from dust in the field-of-view was ~ 3 orders of magnitude fainter than the nuclear surface brightness. The scattering by ice particles was found to be at worst equal to the dust brightness. They concluded that the ratio of nuclear brightness to background brightness was at $\gtrsim 100/1$, hence 'blizzard' would not adversely affect the imagery experiment.

C. Cosmovici: Did you consider the opportunity to guide the spacecraft to an asteroid after a flyby or a rendezvous mission?

R. L. Newburn: I do not know of any studies that have been made for the post-encounter trajectory, but one or two asteroids can be flown-by on the pre-encounter trajectory. This is because a very slow encounter requires a trajectory that takes you well into the asteroid belt on the way to the encounter with the comet.

D. Bender: In answer to the possibility of asteroid encounters on a comet mission one must allow 200-300 day intervals between the encounters because of the trajectory changes required. On the Encke Rendezvous Mission (~ 960 days) two asteroid encounters are possible. The flyby speeds are 10-15 km/s.

NATIONAL AERONAUTICS AND SPACE ADMINISTRATION
WASHINGTON, D.C. 20546

OFFICIAL BUSINESS
PENALTY FOR PRIVATE USE $300

SPECIAL FOURTH-CLASS RATE
BOOK

POSTAGE AND FEES PAID
NATIONAL AERONAUTICS AND
SPACE ADMINISTRATION
451

U.S.MAIL

POSTMASTER: If Undeliverable (Section 158 Postal Manual) Do Not Return

"The aeronautical and space activities of the United States shall be conducted so as to contribute . . . to the expansion of human knowledge of phenomena in the atmosphere and space. The Administration shall provide for the widest practicable and appropriate dissemination of information concerning its activities and the results thereof."

—NATIONAL AERONAUTICS AND SPACE ACT OF 1958

NASA SCIENTIFIC AND TECHNICAL PUBLICATIONS

TECHNICAL REPORTS: Scientific and technical information considered important, complete, and a lasting contribution to existing knowledge.

TECHNICAL NOTES: Information less broad in scope but nevertheless of importance as a contribution to existing knowledge.

TECHNICAL MEMORANDUMS: Information receiving limited distribution because of preliminary data, security classification, or other reasons. Also includes conference proceedings with either limited or unlimited distribution.

CONTRACTOR REPORTS: Scientific and technical information generated under a NASA contract or grant and considered an important contribution to existing knowledge.

TECHNICAL TRANSLATIONS: Information published in a foreign language considered to merit NASA distribution in English.

SPECIAL PUBLICATIONS: Information derived from or of value to NASA activities. Publications include final reports of major projects, monographs, data compilations, handbooks, sourcebooks, and special bibliographies.

TECHNOLOGY UTILIZATION PUBLICATIONS: Information on technology used by NASA that may be of particular interest in commercial and other non-aerospace applications. Publications include Tech Briefs, Technology Utilization Reports and Technology Surveys.

Details on the availability of these publications may be obtained from:

SCIENTIFIC AND TECHNICAL INFORMATION OFFICE

NATIONAL AERONAUTICS AND SPACE ADMINISTRATION

Washington, D.C. 20546